UNIVERSIDAD DE LA RIOJA

TESIS DOCTORAL

Título
Design, Synthesis and Biological Evaluation of Therapeutic $B^{2,2}$-Sulfamidate-Containing Peptides
Autor/es
Nuria Mazo Arribas
Director/es
Jesús Héctor Busto Sancirián y Gonzalo Jiménez Osés
Facultad
Facultad de Ciencia y Tecnología
Titulación
Departamento
Química
Curso Académico

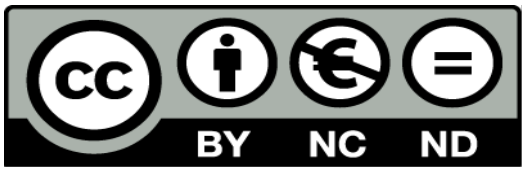

FACULTAD DE CIENCIA Y TECNOLOGÍA

DEPARTAMENTO DE QUÍMICA
ÁREA DE QUÍMICA ORGÁNICA

UNIVERSIDAD DE LA RIOJA

TESIS DOCTORAL

DESIGN, SYNTHESIS, AND BIOLOGICAL EVALUATION OF THERAPEUTIC $\beta^{2,2}$-SULFAMIDATE-CONTAINING PEPTIDES

Memoria presentada en la Universidad de La Rioja
para optar al grado de Doctor en Química por

Nuria Mazo Arribas

Marzo 2019

JESÚS HÉCTOR BUSTO SANCIRIÁN, Profesor titular de Química Orgánica del Departamento de Química de la Universidad de la Rioja y

GONZALO JIMÉNEZ OSÉS, Investigador principal Ramón y Cajal del grupo de Química Computacional de CIC bioGUNE e investigador colaborador del Departamento de Química de la Universidad de La Rioja.

CERTIFICAN:

Que la memoria ***"Design, synthesis, and biological evaluation of therapeutic $\beta^{2,2}$-sulfamidate-containing peptides"*** *ha sido realizada por la Licenciada* ***Nuria Mazo Arribas*** *en el Departamento de Química de la Universidad de La Rioja bajo su inmediata dirección y reúne las condiciones exigidas para optar al grado de Doctor en Química.*

Logroño, marzo 2019

Los directores,

J. Héctor Busto Sancirián

Gonzalo Jiménez-Osés

A mis padres, mi hermano, a Claudio D. y a toda mi familia.
En especial a mis abuelos Pablo† Sagrario† y Damiana†

"Una vez descartado lo imposible, lo que queda, por improbable que parezca, debe ser la verdad" Sir Arthur Conan Doyle

Han pasado ya muchos años desde que entré a este grupo de investigación, el cual es ya como mi segunda familia. A lo largo de estos años he aprendido muchas cosas tanto a nivel profesional como personal y por ello he de agradecer a todas y cada una de las personas que han pasado y se encuentran actualmente en el grupo.

En primer lugar, me gustaría agradecer a mis directores de Tesis. A ***Héctor***, por haberme dado la oportunidad de entrar en este grupo de investigación. A ***Gonzalo***, por creer en mí en todo momento, y por todo su apoyo y dirección durante mi formación. Por supuesto también al resto de todos los jefes ***Alberto***, ***Pere***, ***Paco*** y ***Mari Mar***, por todos sus buenos consejos y por hacerme ver desde mis inicios en la carrera lo bonita que puede llegar a ser la química.

También he de agradecer a todos mis compañeros de laboratorio, los cuales hacen que el trabajo sea más ameno. A ***Claudio D.,*** por estar siempre a mi lado y por su paciencia y apoyo en todo el momento, incluso en los malos, desde el primer día. A ***Iris,*** por todos los buenos ratos que hemos pasado desde nuestros inicios en la licenciatura. A ***Emilio***, entrenador *pokemon*, por su humor tan particular. A ***Xhenti***, la mejor estudiante *riojana* que ha tenido el QuiBi. A ***Pablo*** y ***Paula***, mis pequeños *padawans*, por contagiar su alegría hasta en los días duros. A ***Alicia***, por su gran entusiasmo y alegría. A ***Guille***, el gran *científico* del grupo. A ***Marta***, por sus interminables chistes en cualquier inesperado momento.

A las viejas glorias, ***Charlie***, ***Eva***, ***Nuria***, ***Victor S.***, ***Victor R.***, ***Lara***, ***Mada*** y ***Fer***, y en especial a ***Iván***, mi mentor y gran compañero de sulfamidatos.

A nuestros vecinos ***fotoquímicos***, los ***aurones*** y los ***platineros***. A los miembros del Servicio de Laboratorios, ***Ernesto***, ***Nines***, ***Jorge***, ***Amaya***, ***Montse***... que hacen que todo funcione correctamente.

I would like to thank all the members of the van der Donk's group with whom I was very comfortable, especially with ***Imran*** and ***Silvia***, form whom I learned so much. I would also like to thank ***Wilfred*** for giving me the opportunity to research in his lab and live this experience.

A mis padres, ***Miguel Ángel*** y ***María Ángeles***, cuyos esfuerzos han hecho posible que ambos hijos podamos optar a un mejor futuro. A mi hermano, ***Eduardo***, que como buen hermano mayor me ha inspirado en todos los pasos que doy en mi vida. A mi cuñada, ***Laura***, por esas magdalenas que le levantan el ánimo a cualquiera. Así como al resto de mi familia y amigos.

Por último, me gustaría agradecer a Universidad de La Rioja, por la beca FPI-UR 2016, por la ayuda para realizar la estancia breve en centros de investigación internacionales y por las ayudas a tesis doctorales (ATUR), así como al Ministerio de Economía y competitividad por los distintos proyectos (CTQ2012-36365, CTQ2015-67727-R, UNLR13-4E-1931, CTQ2015-70524-R y RYC-2013-14706).

Abstract

This Doctoral Thesis is focused on the synthesis of several hybrid α/$\beta^{2,2}$-peptides, in which the β-amino acid is a cyclic α-methylisoserine sulfamidate. This cyclic sulfamidate is able to undergo ring-opening reactions with several nucleophiles affording $\beta^{2,2}$-amino acid derivatives, and such reaction had only been tested within a small-molecule context. Therefore, a complete study of the behavior of this substrate in increasingly complex peptide contexts has been performed throughout this Thesis.

First, the factors affecting reactivity and chemoselectivity (S_N2 vs. E2) of the α-methylisoserine sulfamidate depending on its substitution pattern, is addressed in *chapter 3* combining experimental and computational studies.

In *chapter 4*, the coupling of α-amino acids at both *N*- and *C*- termini of the sulfamidate is explored in homogeneous phase, obtaining a library of α/$\beta^{2,2}$-hybrid di- and tripeptides. Positively charged α/$\beta^{2,2}$-hybrid peptides were then synthetized through a ring-opening reaction using pyridine as a nucleophile. The conformational analysis of these derivatives showed the occurrence of intramolecular aromatic interactions between the pyridinium moiety and aromatic side chains in solution.

The optimization of the challenging incorporation of our tertiary α-methylisoserine sulfamidate in longer peptides using the solid phase peptide synthesis (SPPS) strategy is described in *chapter 5*. Using this methodology, a new class of amyloid fibrillation inhibitors was developed. The conformational study of these candidates suggested that peptides

incorporating cyclic $\beta^{2,2}$-sulfamidates adopt a novel and rigid folded conformation both in the gas phase and in solution, which is crucial for molecular recognition. This fact was confirmed by the decrease in $\beta_{1\text{-}40}$-amyloid aggregation observed in the presence of these inhibitors.

Throughout *chapter 6*, the ring-opening reaction of the tertiary sulfamidate within a peptide context is described. This reaction can be performed in either homogeneous or solid phases, obtaining a new library of hybrid $\alpha/\beta^{2,2}$-peptides. Additionally, this sulfamidate is explored for the first time as a new class of cleavable linker with potential chemical and biological applications, taking advantage of the liability observed at the *N*-terminus under very mild conditions.

A new methodology to synthesize cyclic peptides *via* intramolecular ring-opening reaction of cyclic α-methylisoserine sulfamidates is described in *chapter 7*. This methodology allows obtaining full-length unnatural analogs of antimicrobial lantipeptides such as cytolysin S, CylLS.

Finally, a brief summary of my international short-term research stay at Wilfred van de Donk's group (University of Illinois at Urbana-Champaign, USA) is presented in *chapter 8*.

Resumen

Esta Tesis Doctoral está centrada en la síntesis de diferentes α/$\beta^{2,2}$-péptidos híbridos, en los cuales el β-aminoácido es o deriva del sulfamidato cíclico derivado de α-metilisoserina. Este sulfamidato cíclico es capaz de sufrir reacciones de apertura de ciclo con diferentes nucleófilos, obteniendo derivados de $\beta^{2,2}$-aminoácidos. Sin embargo, esta reacción sólo había sido ensayada en el sulfamidato aislado. Por lo tanto, en esta Tesis se presenta un estudio completo de este sustrato en contextos peptídicos de complejidad creciente.

En primer lugar, se discute en el *capítulo 3* el control de la reactividad y quimioselectividad (S_N2 vs. E2) del sulfamidato derivado de α-metilisoserina en función de sus distintos patrones de sustitución, combinando estudios experimentales y cálculos teóricos.

En el *capítulo 4*, se acoplan α-aminoácidos en ambos extremos del sulfamidato en fase homogénea, obteniendo una librería de di- y tri- α/$\beta^{2,2}$-péptidos híbridos. Éstos son sometidos a reacciones de apertura con piridina como nucleófilo con el fin de obtener α/$\beta^{2,2}$-péptidos cargados positivamente. El correspondiente estudio conformacional demuestra que existen interacciones aromáticas no covalentes entre el anillo de piridinio y las cadenas laterales aromáticas.

En el *capítulo 5* se describe la optimización de la incorporación del sulfamidato terciario en péptidos de mayor tamaño usando un soporte sólido. Mediante esta metodología, se obtiene una nueva clase de inhibidores de la

fibrilación de la proteína β-amiloide, que incorporan el sulfamidato derivado de α-metilisoerina. El estudio conformacional de estos candidatos tanto en disolución como en fase gas sugiere que los péptidos que incorporan el sulfamidato cíclico adoptan una nueva conformación rígida y plegada en torno al sulfamidato, la cual es crucial para el reconocimiento molecular. Este hecho fue confirmado observándose un decrecimiento en la agregación de la proteína $\beta_{1\text{-}40}$-amiloide en presencia de estos inhibidores.

A lo largo del *capítulo 6*, se discute la reacción de apertura del sulfamidato cíclico en un contexto peptídico. Esta reacción puede ser llevada tanto en fase homogénea como en fase sólida, obteniendo una nueva librería de $\alpha/\beta^{2,2}$-péptidos híbridos. Además, este sulfamidato es evaluado por primera vez como una nueva clase de *linker* lábil con potencial químico y biológico, aprovechando la especial reactividad observada en el extremo *N*-terminal.

En el *capítulo 7* se describe una nueva metodología para sintetizar péptidos cíclicos mediante aperturas intramoleculares del sulfamidato cíclico terciario. Esta metodología permite así obtener análogos no naturales de lantipéptidos antimicrobianos tales como la citolisina S, $CylL_S$.

Finalmente, se describen brevemente los resultados obtenidos durante mi estancia en el grupo de investigación del profesor Wilfred van der Donk, en la Universidad de Illinois en Urbana-Champaign (EEUU) en el *capítulo 8*.

INDEX

Abbreviations

$[\alpha]^{20}{}_{D}$	specific rotation
^{13}C NMR	carbon-13 nuclear magnetic resonance
^{1}H NMR	proton nuclear magnetic resonance
Å	angstrom
Abu	2-aminobutyric acid
Ac	acetyl
AD	Alzheimer disease
AMBER	Assisted Model Building with Energy Refinement
APP	amyloid percursor peptide
arom	aromatic
Aβ or βA	β-amyloid
Bn	benzyl
Boc	*tert*-butoxycarbonyl
BSBP	β-sheet breaker peptide
cat.	catalyst
CD	circular dichroism
COSY	^{1}H-^{1}H correlated spectroscopy
Coum	7-mercapto-4-methylcoumarine
$CylL_L$	Cytolysin L
$CylL_S$	Cytolysin S
d	doublet, days
D	deuterium
DBU	1,8-diazabicyclo[5.4.0]undec-7-ene
DCM	dichloromethane
dd	doublet of doublets

DFT	density functional theory
Dha	dehydroalanine
Dhb	dehydrobutyrine
DIC	*N*,*N*'-diisopropylcarbodiimide
DIEA/DIPEA	*N*,*N*-diisopropylethylamine
MD	Molecular Dynamics
DMF	*N*,*N*-dimethylformamide
DMSO	dimethylsulfoxide
MD-tar	Molecular Dynamics with weighted time-average restrains
Dns	Dansyl or [5-(dimethylamino)naphthalen-1-yl](dioxido)-λ6-sulfanyl
DODT	3,6-dioxa-1,8-octanedithiol
E	electronic energy
E2	biomolecular elimination reaction
Ed.	editorial
equiv.	equivalents
ESI	electrospray ionization
ESI-MS	electrospray ionization-mass spectroscopy
TEA	triethylamine
Exp	experimental
Fmoc	9-fluorenylmethyloxycarbonyl
Freq.	frequency
G	Gibbs free energy
GAFF	General Amber Force Field
GalNAc	*N*-acetyl-galactosamine
H	enthalpy

HATU	1-[bis(dimethylamino)methylene]-1*H*-1,2,3-triazolo-[4,5]bipyridinium-3-oxide hexafluorophosphate
HBTU	*N*,*N*,*N*',*N*'-tetramethyl-O-(1*H*-benzotriazol-1-yl)uronium hexafluorophosphate
HMBC	heteronuclear multiple bond correlation
HOAt	7-aza-1-hydroxybenzotriazole
HOBt	1-hydroxybenzotriazole
HPLC	high performance liquid chromatography
HRMS	high resolution mass spectroscopy
HSQC	^{1}H-^{13}C heteronuclear single quantum correlation
Hz	hertz
IR	infrared
IRID	infrared double resonance ion-dip
J	coupling constant
K	kelvin
k	kinetic constant
Lan	lanthionine
LDA	lithium diisopropylamide
m	multiplet
M	molarity, molar
MALDI-TOF	Matrix assisted laser desorption/ionization-time of flight
Me	methyl
MeLan	methyllanthionine
MM	Molecular Mechanics
MOM	methoxymethyl
mRNA	messenger ribonucleic acid
MW-SPPS	Microwave assisted solid phase peptide synthesis
NBO	Natural Bond Orbital

NEM	*N*-ethylmaleimide
NMR	Nuclear Magnetic Resonance
NOE/NOESY	Nuclear Overhauser effect spectroscopy
Ns	nosyl or (4-nitrophenyl)sulfonyl
Nu	nucleophile
ºC	Celsius degree
Oxyma Pure®	Ethyl cyano(hydroxyimino)acetate
PBS	phosphate buffered saline
PDB	protein data bank
PG	protecting group
Ph	phenyl
Py	pyridine
PyBOP	Benzotriazol-1-yl-oxytripyrrolidino phosphonium hexafluorophosphate
quant.	quantitative
R	substituent
r.t.	room temperature
RiPP	ribosomally synthesized and post-translationally modified peptide
RP-HPLC	reverse-phase HPLC
s	singlet
S	entropy
S_N2	bimolecular nucleophilic substitution
S_Ni	intramolecular nucleophilic substitution
SPE	solid phase extraction
SPPS	solid phase peptide synthesis
Sulfa or Sul	sulfamidate

t	triplet
TBAF	tetra-*n*-butylammonium fluoride
TBTU	2-(*H*-benzotriazole-1-yl)-1,1,3,3-tetramethylaminium tetrafluoroborate
^{t}Bu	*tert*-butyl
TFA	trifluoroacetic acid
Tf	trifluoromethanesulfonyl
THF	tetrahydrofurane
ThT	thioflavin-T
TIS	triisopropylsilane
TLC	thin layer chromatography
TMS	tetramethylsilane or trimethylsilyl
TS	transition state
UV-Vis	ultraviolet-visible
z	charge
ZPE	zero-point energy
ΔE	relative electronic energy
ΔG	relative Gibbs free energy
ΔH	relative enthalpy
αMeβAla	α-methyl-β-alanine
δ	chemical shift
ε	dielectric permittivity
ϕ	Phi (dihedral angle)
λ_{em}	emission wavelength
λ_{exc}	excitation wavelength
θ	Theta (dihedral angle)

VI

ψ	Psi (dihedral angle)
ω	Omega (dihedral angle)

Amino acids	Three-letter code	One-letter code	Name
	Ala	A	Alanine
	Arg	R	Arginine
	Asn	N	Asparagine
	Asp	D	Aspartic Acid
	Cys	C	Cysteine
	Gln	Q	Glutamine
	Glu	E	Glutamic Acid
	Gly	G	Glycine
	His	H	Histidine
	Ile	I	Isoleucine
	Leu	L	Leucine
	Lys	K	Lysine
	Met	M	Methionine
	Phe	F	Phenylalanine
	Pro	P	Proline
	Ser	S	Serine
	Thr	T	Threonine
	Trp	W	Tryptophan
	Tyr	Y	Tyrosine
	Val	V	Valine
	--	J	Sulfamidate

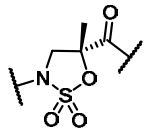

Sulfamidate (J)

Chapter 1.
Introduction

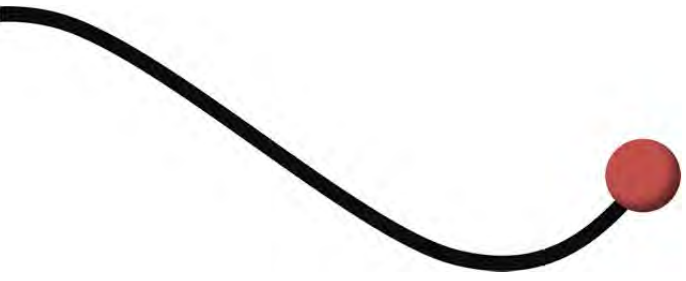

Proteins are macromolecules consisting of one or more chains of amino acid residues, which play an important role in the development of living organisms.[1] They are involved in multiple biological processes, such as catalytic metabolic reactions, DNA replication and molecule transport. These diverse biological functions are determined by the three-dimensional structure of the protein, which in turn is defined by the sequence of amino acids encoded by DNA. The complexity of these structures change from small and simple peptides to complicated folded and highly organized clusters (**Figure 1.1**).

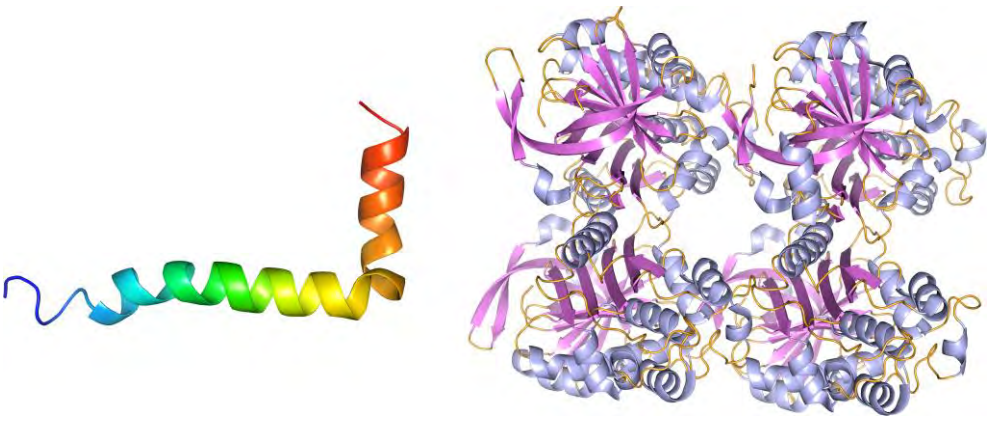

Figure 1.1. Structures of native amyloid peptide (PDB code 1IYT, left) and *S*-ovalbumin (PDB code 1UHG, right)**.**

During the biosynthesis of proteins, some residues can be chemically modified by post-translational modifications,[2] which alter their physical and chemical properties. These modifications enact the appropriate folding, stability, activity and function of proteins and can occur on the amino acid sidechain or at the protein *C*- or *N*-termini. Examples of these modifications are glycosylation, to form glycoproteins; dehydration and thioether

cyclization, to form lanthipeptides; or the formation of disulfide bonds, to stabilize a specific folding pattern (**Figure 1.2**).

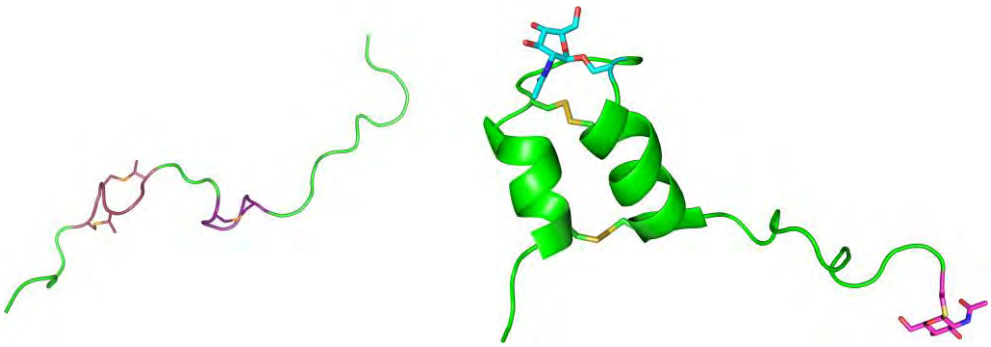

Figure 1.2. Structures of the lanthipeptide epilancin 15X (PDB code 1W9N, left) and glycocin F (PDB code 2KUY, right).

In order to study the relationship between function and structure displayed by proteins, scientists often draw upon analogous molecules that are able to mimic either the structure or the function of the putative protein. These analogs may serve as mere objects of study or may regulate a specific property, being used as drugs or diagnostic agents. The most common protein modifications can be classified in five groups.[3] *Mutation* refers to the alteration of the amino acid sequence. *Truncation* and *augmentation* involve the elimination and addition of one or more residues to the sequence, respectively. The incorporation of non-peptidic moieties (carbohydrates, fluorophores, synthetic polymers…) bound to the side chains or protein termini is called *decoration*. Finally, in *hybridization*, one or more proteinogenic residues are modified by non-proteinogenic moieties (**Figure 1.3**).

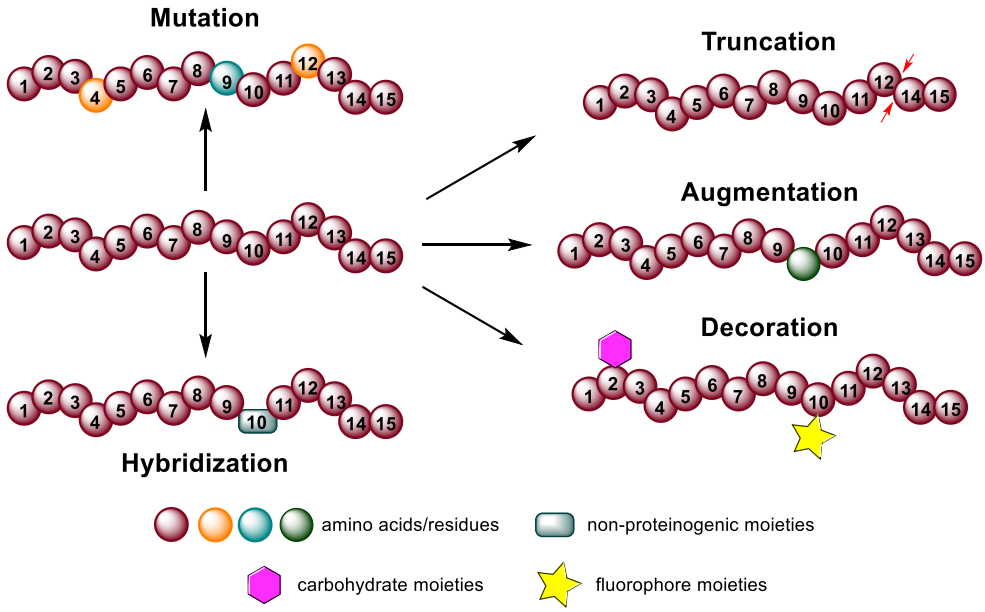

Figure 1.3. Types of protein/peptide modification.

Hybridization is the most modern modification and involves altering the polypeptide backbone without affecting the identity or the sequence of side chains relative to the putative protein. This strategy involves replacing α-amino acid residues by other similar subunits. For instance, depsipeptides,[4–7] in which one or more amide bonds have been replaced by ester bonds, have shown to behave as enzyme inhibitors[8] and to exhibit antimicrobial[9] and antiviral[10] properties. On the other hand, azapeptides have served as leads for creating receptor ligands, probes, pro-drugs and enzyme inhibitors, as well as a clinically approved drugs.[11,12] Other instances are β-amino acid residues, which form homo-β-peptides when every residue is a β-amino acid, or so-called mixed or hybrid α/β-peptides when incorporated in α-peptides (**Figure 1.4**). These hybrid peptides open the door to a new conformational space and comprise an active field of research with interesting and diverse applications in biochemistry.

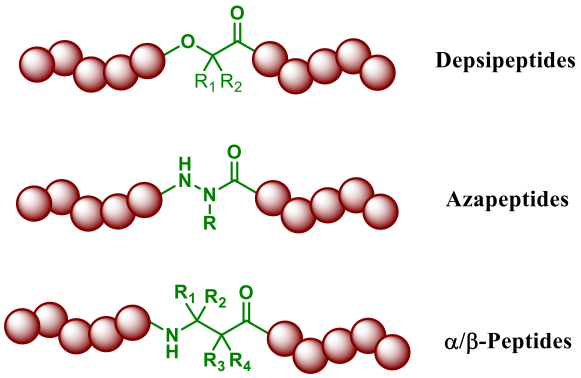

Figure 1.4. Structures of desipeptides, azapeptides and α/β-peptides.

1.1 Homo-β-peptides

β-Amino acids are found in Nature as discrete molecules and are rarely present in proteins or peptides. These residues have the amino group located at the beta carbon (Cβ) of their backbone, that is, in the second carbon after the carboxylic group. β-Amino acids may have substituents on carbon 2 (Cα), carbon 3 (Cβ) or both, being named β^2-, β^3- and $\beta^{2,3}$-amino acids respectively and providing a greater richness of derivatives than their α counter parts (**Figure 1.5**).

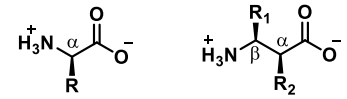

Figure 1.5. General structures of a α-amino acids (left) and β-amino acids (right).

β-Alanine, is the most common β-amino acid. This structure is present in pantothenic acid (vitamin B5), which is necessary for the formation of coenzyme A, and carnosine, a dipeptide found in brain and muscular tissues in high concentrations (**Figure 1.6**).

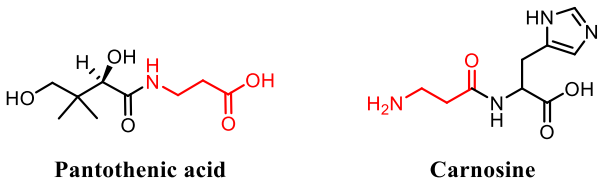

Figure 1.6. Pantothenic acid and carnosine structures with the β-alanine motif highlighted in red.

In Nature, there are some enzymes (aminomutases) able to transform aromatic α-amino acids into β-amino acids with assistance of certain cofactors. One of these cofactors is the electrophilic 4-methylideneimidazole-5-one (MIO) moiety,[13–17] which is post-translationally formed in the active site by the self-condensation of an Ala-Ser-Gly triad (**Figure 1.7**).

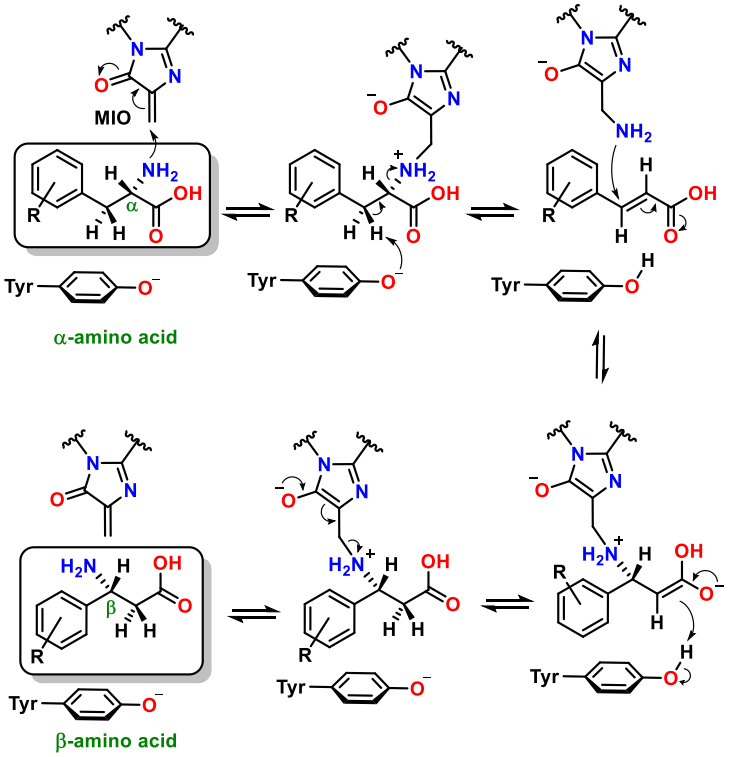

Figure 1.7. Proposed catalytic mechanism for the enzymatic conversion of α-amino acids into β-amino acids promoted by cofactor MIO.[13]

β-Amino acids have lately attracted a great deal of interest in the field of pharmacology since they are frequently found in natural bioactive products, such as the anticancer agent Taxol®.[18–20] The α-hydroxy-β-amino acid substructure is also present in compounds that inhibit the activity of proteases. In this sense, apstatin[21] and bestatine[22,23] behave as aminoprotease inhibitors, and allophenylnorstatin has inhibitory activity against VIH protease, which has special interest in the treatment of AIDS (**Figure 1.8**).[24,25]

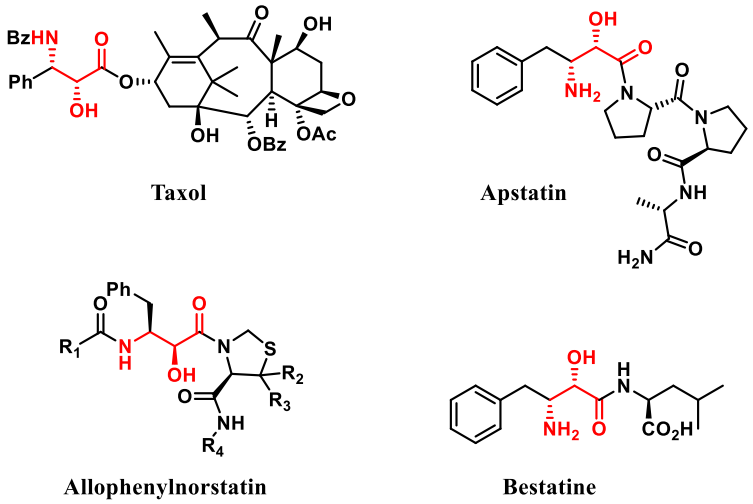

Figure 1.8. Pharmacologic compounds featuring the α-hydroxy-β-amino acid substructure in red.

Oligomers of β-amino acids, also known as β-peptides or homo-β-peptides, can adopt a variety of helical secondary structures[26] that are not observed in natural homo-α-peptides. The nature of these helical secondary structures strongly depends on the substitution patterns of their residues and is determined by the number of atoms involved in the stabilizing hydrogen bonds between residues. In this sense, 14-helix is the most widely studied

helical structure of β-peptides, but 12-, 10-, 8-, and 10/12-helices have been experimentally detected as well (**Figure 1.9**).[27,28]

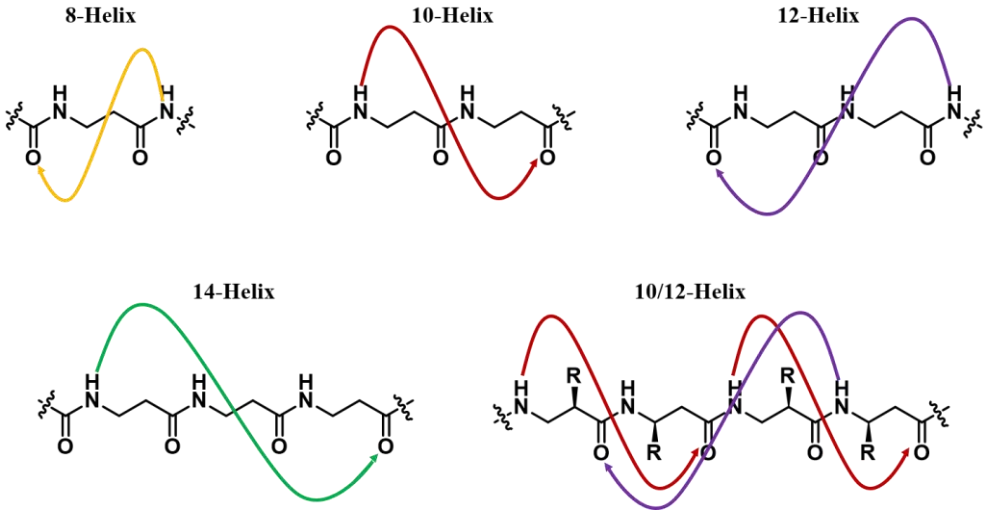

Figure 1.9. Helices types found in homo-β-peptides.

Seebach and co-workers. designed amphiphilic 14-helix β-peptides intended to mimic the amphiphilic α-helix of human apolipoproteins involved in lipid uptake and transport.[29] The absorption of cholesterol by intestinal cells is manifested by α-peptides that form globally amphiphilic α-helices.[30] These new amphiphilic β-peptides were able to mimic this structure and therefore to inhibit the absortion process (**Figure 1.10**).

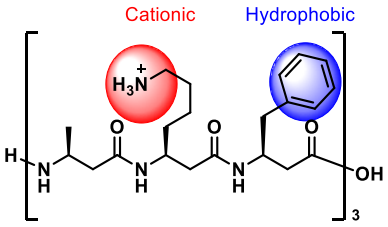

Figure 1.10. Amphiphilic 14-helical (3 residues per turn) cholesterol uptake inhibitor.

1.2 α/β-hybrid peptides

Hybrid α/β-peptides are comprised by α- and β-amino acid residues. The number of conformations observed for α/β-hybrid peptides is huge, depending on the structure and stereochemistry of the β-residue and the sequence of amino acids (**Figure 1.11**).[31,32]

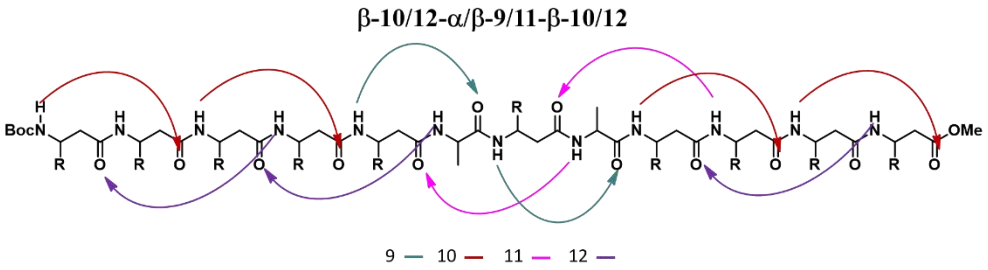

Figure 1.11. Secondary structures of α/β-hybrid peptides.

One of the main advantages of hybrid α/β-peptides is the higher resistance to enzymatic and chemical degradation. In fact, Gellman and co-workers have recently reported that only 20-40% of β-amino acids are needed for this resistance to be observed in peptides, while maintaining their biological activity.[33] Furthermore, Tavenor and co-workers have recently reported that, if an α-amino acid is substituted by a β-amino acid in the sequence of the streptococcal protein GB1, its secondary and tertiary structures are maintained. However, the thermodynamic stability of the hybrids varies depending on the substituent. As shown in **Figure 1.12**, changing an α-Ala or α-Asn to a β^2- or β^3-Ala or Asn, respectively, does not affect the α-helix structure of the peptide.[34]

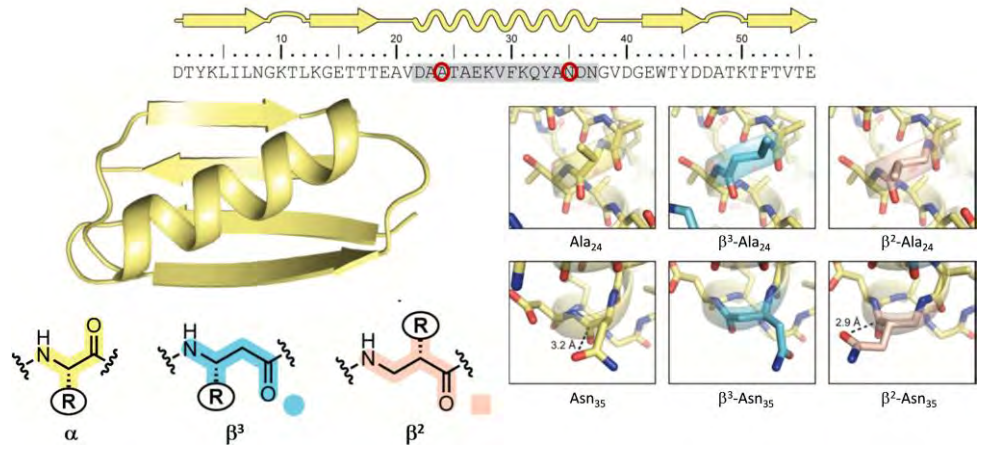

Figure 1.12. Effects in the three-dimensional structure of streptococcal protein GB1 produced by mutating α-amino acids to β^2 or β^3-amino acids.[34]

Kaur and co-workers reported a 10-mer α-peptide[35] which is a potential tumor homing peptide. However, its applicability would be largely hampered by its instability toward proteases. In a more recent study,[36] they synthesized three analogs in which two or three amino acids were replaced by unnatural D-residues or β^3-amino acids, which showed to be proteolytically stable and displayed better affinity profiles for breast cancer cells compared to the natural α-peptide (**Figure 1.13**).

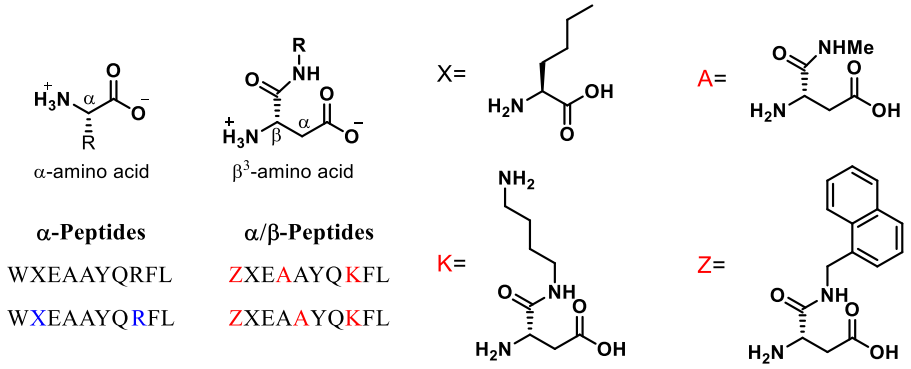

Figure 1.13. Structure of cancer targeting peptides. L-Amino acids are represented in black, D-amino acids in blue, and β-amino acids derived from L-aspartic acid in red.

The use of ribosomes for synthesizing β-amino acids has been studied for decades. In fact, incorporation of multiple β-amino acids into full-length proteins has been achieved, which bids the possibility for studying the structure and function of β-proteins (**Figure 1.14**).[37–44]

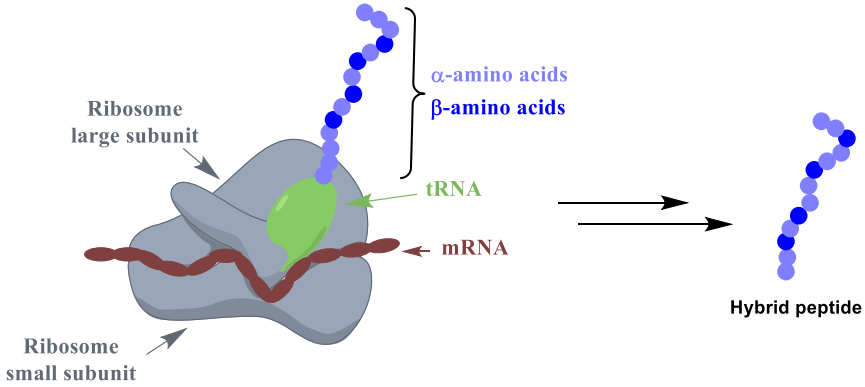

Figure 1.14. General scheme for the *in vivo* synthesis of hybrid α/β-peptides in the ribosome.

1.3 References

(1) Nelson, D.; Cox, M. *Lehninger Principles of Biochemistry*, 6th ed.; 2014.

(2) Voet, D.; Voet, J. G.; Pratt, C. W. *Fundamentals of Biochemistry: Life at the Molecular Level*, 5th ed.; Wiley-VCH Verlag, 2016.

(3) Johnson, L. M.; Gellman, S. H. In *Methods in Enzymology*; Elsevier, 2013; Vol. 523, pp 407–429.

(4) Forsythe, J. G.; Yu, S. S.; Mamajanov, I.; Grover, M. A.; Krishnamurthy, R.; Fernández, F. M.; Hud, N. V. *Angew. Chem. Int. Ed.* **2015**, *54*, 9871–9875.

(5) Newman, D. J.; Cragg, G. M. *Compr. Nat. Prod. II Chem. Biol.* **2010**, 623–646.

(6) Huryn, D. M.; Wipf, P. In *Cancer Drug Design and Discovery*; Elsevier, 2013; pp 91–120.

(7) Avendaño, C.; Menéndez, J. C. *Chapter 10 - Other Approaches to Targeted Therapy*; 2008.

(8) Yurek-George, A.; Cecil, A. R. L.; Mo, A. H. K.; Wen, S.; Rogers, H.; Habens, F.; Maeda, S.; Yoshida, M.; Packham, G.; Ganesan, A. *J. Med. Chem.* **2007**, *50*, 5720–5726.

(9) Haste, N. M.; Perera, V. R.; Maloney, K. N.; Tran, D. N.; Jensen, P.; Fenical, W.; Nizet, V.; Hensler, M. E. *J. Antibiot.* **2010**, *63*, 219–224.

(10) Plaza, A.; Gustchina, E.; Baker, H. L.; Kelly, M.; Bewley, C. A. *J. Nat. Prod.* **2007**, *70*, 1753–1760.

(11) Frączak, O.; Lasota, A.; Kosson, P.; Lešniak, A.; Muchowska, A.; Lipkowski, A. W.; Olma, A. *Peptides* **2015**, *66*, 13–18.

(12) Proulx, C.; Sabatino, D.; Hopewell, R.; Spiegel, J.; García Ramos, Y.; Lubell, W. D. *Future Med. Chem.* **2011**, *3*, 1139–1164.

(13) Weise, N. J.; Parmeggiani, F.; Ahmed, S. T.; Turner, N. J. **2015**.

(14) Cooke, H. A.; Christianson, C. V; Bruner, S. D. *Curr. Opin. Chem. Biol.* **2009**, 13:460-468.

(15) Cooke, H. A.; Bruner, S. D. *Biopolymers* **2010**, *93*, 802–810.

(16) Schwede, T. F.; Retey, J.; Schulz, G. E. *Biochemistry* **1999**, *38*, 5355–5361.

(17) Poppe, L. *Curr. Opin. Chem. Biol.* **2001**, *5*, 512–524.

(18) Wani, M. C.; Taylor, H. L.; Wall, M. E.; Coggon, P.; Mcphail, A. T. *J. Am. Chem. Soc.* **1971**, *93*, 2325–2327.

(19) Kingston, D. G. I. *J. Nat. Prod.* **2000**, *63*, 726–734.

(20) Kingston, D. G. I. *Chem. Commun.* **2001**, 867–880.

(21) Wolfrum, S.; Richardt, G.; Dominiak, P.; Katus, H. A.; Dendorfer, A. *Br. J. Pharmacol.* **2001**, *134*, 370–374.

(22) Talmadge, J.; Black, P.; Pelus, L.; Abe, F. *Biomed & Pharmacother* **1990**, *44*, 85–91.

(23) Pearson, W. H.; Hines, J. V. *J. Org. Chem.* **1989**, *54*, 4235–4237.

(24) Takashiro, E.; Hayakawa, I.; Nitta, T.; Kasuya, A.; Miyamoto, S.; Ozawa, Y.; Yagi, R.; Yamamoto, I.; Shibayama, T.; Nakagawa, A.; Yabe, Y. *Bioorg. Med. Chem.* **1999**, *7*, 2063–2072.

(25) Hayashi, Y.; Kinoshita, Y.; Hidaka, K.; Kiso, A.; Uchibori, H.; Kimura, T.; Kiso, Y. *J. Org. Chem.* **2001**, *66*, 5537–5544.

(26) Cheng, R. P.; Gellman, S. H.; DeGrado, W. F. *Chem. Rev.* **2001**, *101*, 3219–3232.

(27) Martinek, T. A.; Fülöp, F. *Chem. Soc. Rev.* **2012**, *41*, 687–702.

(28) Seebach, D.; Matthews, J. L. *Chem. Commun.* **1997**, *1*, 2015–2022.

(29) Werder, M.; Hauser, H.; Abele, S.; Seebach, D. *Helv. Chim. Acta* **1999**, *82*, 1774–1783.

(30) Boffelli, D.; Compassi, S.; Werder, M.; Weber, F. E.; Phillips, M. C.; Schulthess, G.; Hauser, H. *FEBS Lett.* **1997**, *411*, 7–11.

(31) Horne, W. S.; Gellman, S. H. *Acc. Chem. Res.* **2008**, *41*, 1399–1408.

(32) Pilsl, L. K. A.; Reiser, O. *Amino Acids* **2011**, *41*, 709–718.

(33) Cheloha, R. W.; Sullivan, J. A.; Wang, T.; Sand, J. M.; Sidney, J.; Sette, A.; Cook, M. E.; Suresh, M.; Gellman, S. H. *ACS Chem. Biol.* **2015**, *10*, 844–854.

(34) Tavenor, N. A.; Reinert, Z. E.; Lengyel, G. A.; Griffith, B. D.; Horne, W. S. *Chem. Commun.* **2016**, *52*, 3789–3792.

(35) Ahmed, S.; Mathews, A. S.; Byeon, N.; Lavasanifar, A.; Kaur, K. *Anal. Chem.* **2010**, *82*, 7533–7541.

(36) Soudy, R.; Gill, A.; Sprules, T.; Lavasanifar, A.; Kaur, K. *J. Med. Chem.* **2011**, *54*, 7523–7534.

(37) Fujino, T.; Goto, Y.; Suga, H.; Murakami, H. *J. Am. Chem. Soc.* **2013**, *135*, 1830–1837.

(38) Fujino, T.; Murakami, H. *Chem. Rec.* **2016**, *16*, 365–377.

(39) Fujino, T.; Goto, Y.; Suga, H.; Murakami, H. *J. Am. Chem. Soc.* **2016**, *138*, 1962–1969.

(40) Wang, P. S. P.; Schepartz, A. *Chem. Commun.* **2016**, *52*, 7420–7432.

(41) Melo Czekster, C.; Robertson, W. E.; Walker, A. S.; Söll, D.; Schepartz, A. *J. Am. Chem. Soc.* **2016**, *138*, 5194–5197.

(42) Dedkova, L. M.; Fahmi, N. E.; Paul, R.; Rosario, M.; Zhang, L.; Chen, S.; Feder, G.; Hecht, S. M. *Biochemistry* **2012**, *51*, 401–415.

(43) Maini, R.; Chowdhury, S. R.; Dedkova, L. M.; Roy, B.; Daskalova, S. M.; Paul, R.; Chen, S.; Hecht, S. M. *Biochemistry* **2015**, *54*, 3694–3706.

(44) Maini, R.; Nguyen, D. T.; Chen, S.; Dedkova, L. M.; Chowdhury, S. R.; Alcala-Torano, R.; Hecht, S. M. *Bioorg. Med. Chem.* **2013**, *21*, 1088–1096.

Chapter 2.
Background and goals

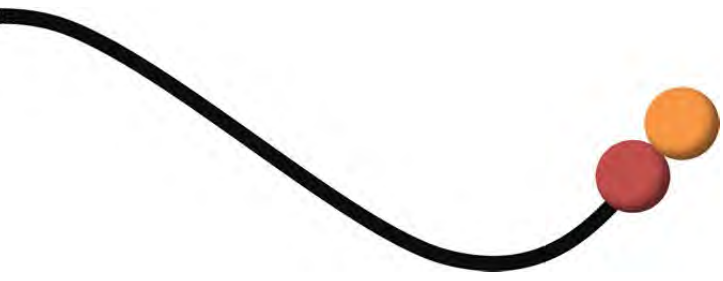

As previously discussed in *chapter 1*, β-amino acids have been gaining importance in the field of biochemistry, particularly those with substituents at geminal positions. There are numerous structures featuring this kind of substitution, namely disubstituted ($\beta^{2,2}$- and $\beta^{3,3}$-), trisubstituted ($\beta^{2,2,3}$- and $\beta^{2,3,3}$-) and tetrasubstituted ($\beta^{2,2,3,3}$-) amino acids (**Figure 2.1**).[1–4]

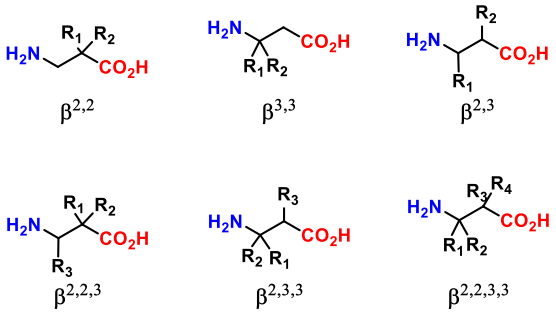

Figure 2.1. Substitution patterns of di-, tri- and tetrasubstituted β-amino acids.

2.1 Synthesis of $\beta^{2,2}$-amino acids

To date, several methods have been described to synthesize these types of β-amino acids with different substitution patterns. However, there are only a few cases reported for synthetizing $\beta^{2,2}$-amino acids derivatives. In the case of achiral $\beta^{2,2}$-amino acids (**Scheme 2.1**),[5] one of the first examples was reported by Kohn and Schmidt in 1907,[6] where they described the treatment of bromopivalic acid with ethanolic NH_3 to afford 3-amino-2,2-dimethylpropanoic acid. Another example is the a dialkylation of methyl cyanoacetate[7,8] followed by a selective reduction of the corresponding cyanoesters[9] to afford achiral $\beta^{2,2}$-amino acids. On the other hand, treatment of silyl ketene acetals with *N*,*N*-bis(trimethylsilyl)-methoxymethylamine is a different strategy described by Okano and co-workers in 1984.[10] As a final

example, a Reformatsky reaction between (benzotriazol)methylamine derivatives and 2-bromoalkanoates can also be used to obtain achiral $\beta^{2,2}$-amino acids.[11]

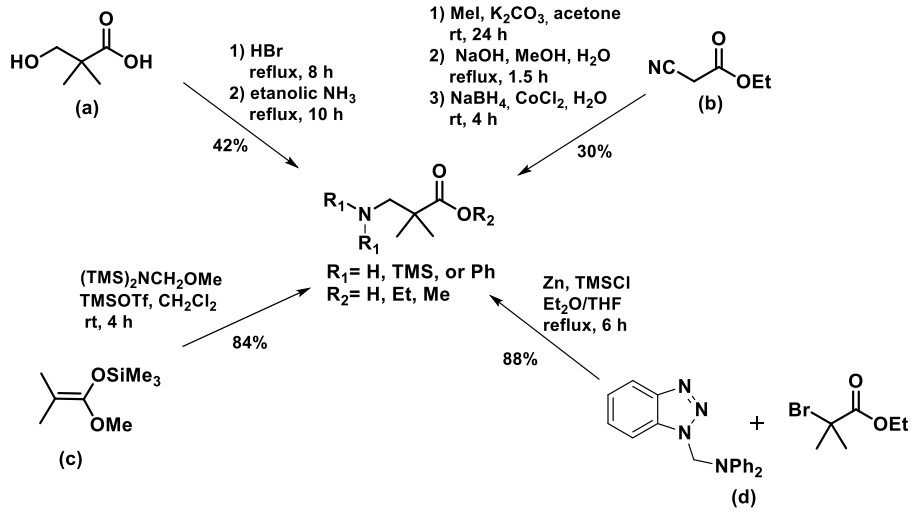

Scheme 2.1. Examples for synthesizing achiral $\beta^{2,2}$-amino acids. a) Treatment of bromopivalic acid with ethanolic NH_3. b) Dialkylation of methyl cyanoacetate and a selective reduction of the corresponding cyanoesters. c) Treatment of silyl ketene acetals with *N,N*-bis(trimethylsilyl)-methoxymethylamine. d) Reformatsky reaction.

For the synthesis of chiral $\beta^{2,2}$-amino acids (**Scheme 2.2**), one of the first examples involved the diastereoselective dialkylation of activated chiral tetrahydropyrimidines and subsequent hydrolysis.[12–15] A similar approach is the diastereoselective dialkylation of chiral cyanoacetates, and subsequent hydrolysis to obtain α,α-dialkylated cyano acetic acids. Hydrogenation of the cyano group leads to the corresponding chiral $\beta^{2,2}$-amino acids.[16] Other examples involve the catalytic asymmetric dialkylation of pyrrolidin-2,3-diones[17] or the catalytic asymmetric allylation of 4-substituted isoxazolin-5-ones.[18] The organocatalytic asymmetric addition of α-substituted β-nitroacrylates has also been proposed.[19] Finally, our research group reported

the diastereoselective Diels-Alder reaction of cyanocinnamates and subsequent reduction to access chiral cyclic $\beta^{2,2}$-amino acids.[20]

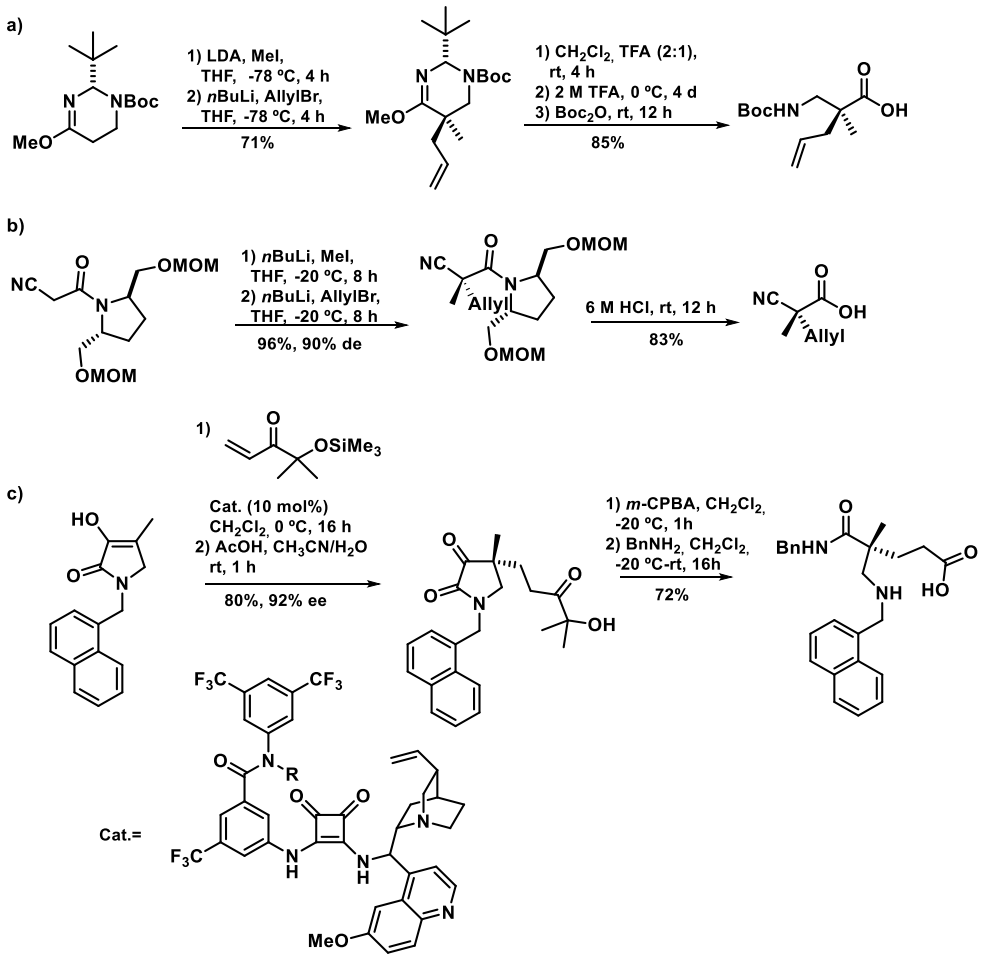

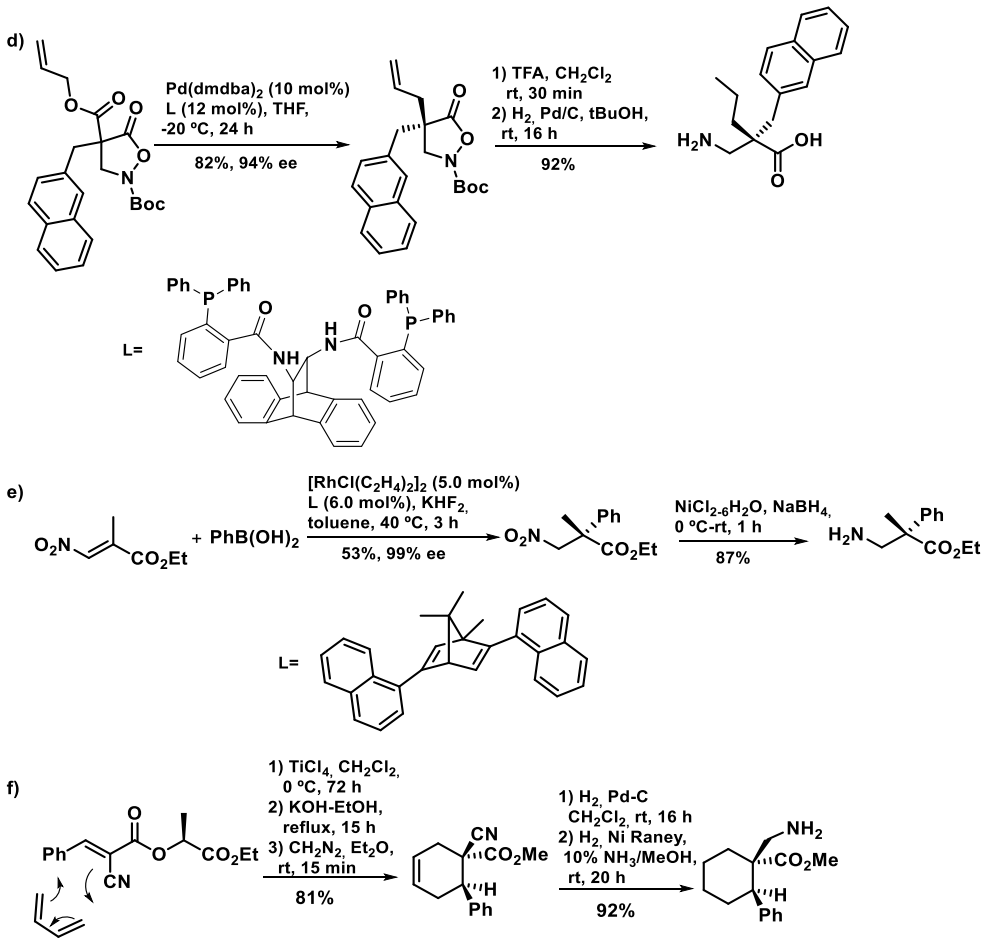

Scheme 2.2. Examples of the synthesis of chiral β[2,2]-amino acids. a) Diastereoselective dialkylation of activated chiral tetrahydropyrimidines. b) Diastereoselective dialkylation of chiral cyanoacetates. c) Catalytic asymmetric dialkylation of pyrrolidin-2,3-diones. d) Catalytic asymmetric allylation of 4-substituted isoxazolin-5-ones. e) Asymmetric addition of α-substituted β-nitroacrylates f) Diastereoselective Diels-Alder reaction of cyanocinnamates.

On the other hand, Gentilucci and co-workers reported the single step cyclization of α-substituted-α-hydroxy-β[2,2]-amino acids in small peptides forming 5-aminomethyl-oxazolidine-2,4-dione (Amo) rings, which favor an unusual β-turn (**Figure 2.2**).[21]

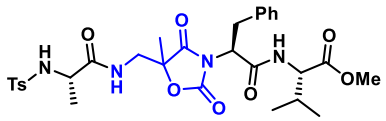

Figure 2.2. Structure of a hybrid α/β^{2,2}-peptide containing the cyclic Amo moiety in blue.

2.2 Cyclic sulfamidates in synthesis

Cyclic sulfamidates have proven to be synthetically versatile electrophiles accessible via readily available from enantiomerically pure amino alcohols. Although 5, 6, 7 and 8-membered cyclic sulfamidates have been described,[22–24] our interest is focused on 5-membered sulfamidates, since they can be precursors of β-amino acids.

These cyclic sulfamidates have become widely used due to the high regio- and stereoselectivity of their corresponding nucleophilic ring-opening reactions. This circumstance has been exploited for the asymmetric synthesis of natural products and biomolecules used in the pharmaceutical industry for the treatment and diagnosis of different diseases.

Some applications of these sulfamidates are the synthesis of (–)-aphanorphine[25] which is an analog of the alkaloid morphine, aspergillomarasmide A[26] which is an inhibitor of metallo-β-lactamases NDM-1 and VIM-2, the enantioselective synthesis of α-benzylated lanthionines[27] (more examples of this reactivity are given below) and the development of new ^{18}F-labelled molecules for brain tumor imaging[28,29] (**Scheme 2.3**).

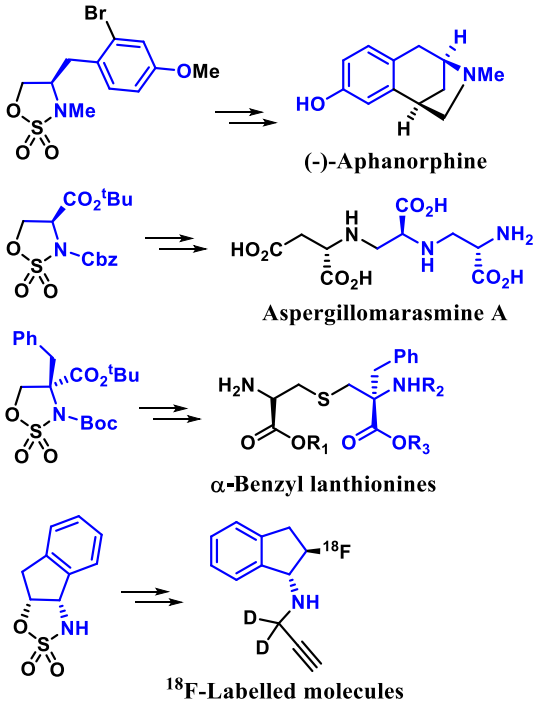

Scheme 2.3. Synthesis of (–)-amphanorphine, aspergillomarasmide A, α-benzylated lanthionine and ^{18}F-labelled molecules obtained from five-membered chiral cyclic sulfamidates.

2.2.1 Synthesis of cyclic sulfamidates

1,2-Cyclic sulfamidates can be efficiently synthesized using several methodologies.[23] One of the most direct synthetic routes involves the treatment of an 1,2-amino alcohol derivative with a reagent that can directly install the –SO_2– moiety. The use of sulfuryl chloride (SO_2Cl_2)[30] is a suitable approach to obtain cyclic 1,2-sulfamidates. However, this methodology has some drawbacks, such as competitive chlorination, formation of aziridines[31] instead of sulfamidates, or polymerization. Hence, the insertion of the –SO_2– moiety is usually carried out in two steps. First, treatment of 1,2-amino alcohols with thionyl chloride ($SOCl_2$)[32] allows forming a cyclic sulfamidite

intermediate in normally high yields.[33] Then, oxidation of cyclic sulfamidites in the presence of a ruthenium catalyst[34,35] normally affords cyclic sulfamidates in excellent yields (**Scheme 2.4**).

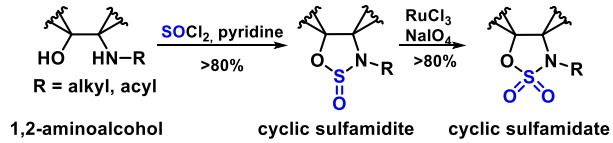

Scheme 2.4. Synthesis of 1,2-cyclic sulfamidates from 1,2-amino alcohols using thionyl chloride and subsequent oxidation**.**

A very potent methodology to obtain five-membered sulfamidates involves treating 1,2-diols with the Burgess reagent ($Et_3N–SO_2–NCO_2Me$) as developed by Nicolaou.[36] The reaction mechanism involves a double sulfonylation of the adjacent hydroxyl groups, followed by an intramolecular nucleophilic substitution (S_Ni). The main limitation of this method is the regioselectivity of the process, determined by a combination of steric and electronic factors (**Scheme 2.5**).

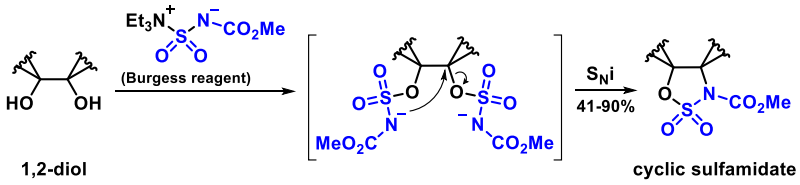

Scheme 2.5. Synthesis of 1,2-cyclic sulfamidates from 1,2-diols using the Burgess reagent**.**

Cyclic sulfamidates can also be obtained from epoxides. One approach to this transformation was developed by Nicolaou,[37] by converting allylic alcohol-derived epoxides to either five- or six-membered sulfamidates by treatment with the Burgess reagent (**Scheme 2.6**). Analogously, Hudlicky and co-

workers.[38] reported the use of simple epoxides to directly obtain cyclic sulfamidates in moderate yields.

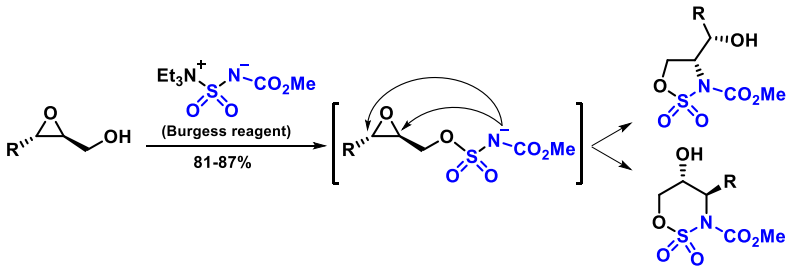

Scheme 2.6. Synthesis of 1,2-cyclic sulfamidates from epoxides**.**

Che and co-workers elaborated on a previous work from Du Bois and coworkers,[39] and demonstrated that intermolecular amidation of saturated C–H bonds was possible *via* ruthenium catalyzed nitrene insertion of sulfonamides. These compounds can be prepared and reacted *in situ*, and these conditions were subsequently applied intramolecularly to the asymmetric synthesis of cyclic sulfamidates (**Scheme 2.7**).[40–43]

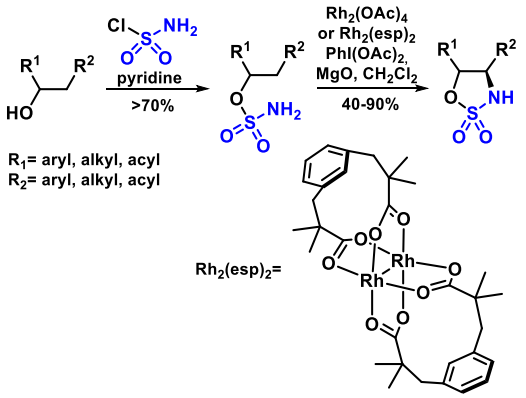

Scheme 2.7. Synthesis of 1,2-cyclic sulfamidates *via* metal-catalyzed nitrene insertion into C–H bonds**.**

Zhou and co-workers reported a method for synthesizing five-membered sulfamidates by asymmetric hydrogenation of an imine precursor.[44] Thus, treatment of alkyl hydroxymethylketones with sulfamoyl chloride (H_2NSO_2Cl), followed by hydrogenation using a chiral Pd-catalyst would afford chiral 1,2-cyclic sulfamidates (**Scheme 2.8**).

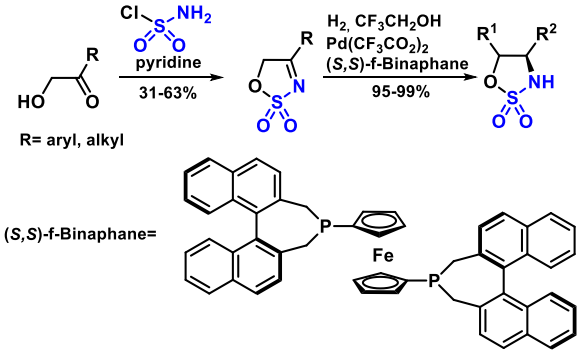

Scheme 2.8. Synthesis of 1,2-cyclic sulfamidates *via* asymmetric hydrogenation of cyclic *N*-sulfinyl imines**.**

2.2.2 Reactivity of cyclic sulfamidates

As previously mentioned, the most studied reactivity of cyclic sulfamidates is their nucleophilic ring-opening reaction. Nucleophilic attack takes place regioselectively and stereospecifically at the oxygen-bearing carbon, since the O–SO_2N fragment is a much better leaving group than the N–SO_3 moiety. This process occurs *via* bimolecular nucleophilic substitution (S_N2) with complete inversion of configuration to deliver a *N*-sulfate intermediate, which may then be hydrolyzed under either protic or Lewis acidic conditions to afford the final product (**Scheme 2.9**).

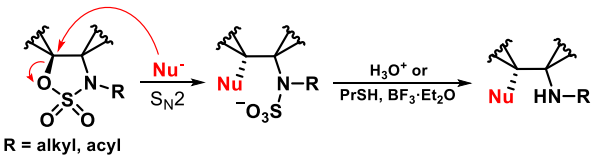

Scheme 2.9. Regio- and stereoselective ring-opening of cyclic sulfamidates and subsequent *N*-sulfate cleavage**.**

Five-membered sulfamidates can be easily obtained from conveniently protected α-hydroxyamino acids (Ser or Thr) by treatment with thionyl chloride followed by Ru-catalyzed oxidation. The nucleophilic ring-opening of these amino acid sulfamidates with a large variety of nucleophiles has produced a plethora of β-substituted-α-amino acids, as demonstrated mainly by the groups of Lubell and others (**Scheme 2.10**).[45]

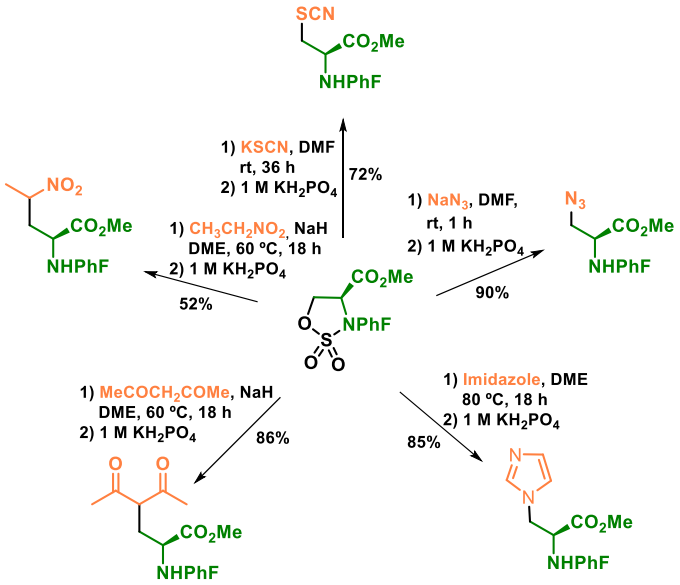

Scheme 2.10. Some examples of ring-opening reactions on L-serine sulfamidate with different nucleophiles.

However, these serine/threonine sulfamidates are known to undergo competitive β-elimination due to the acidic character of their α-hydrogen. This undesired pathway may lead to a mixture of stereoisomers by a subsequent Michael-type addition to the α,β-unsaturated carbonyl intermediates. To overcome this issue, Lubell and co-workers used large protecting groups at either the sulfamide or carbonyl ends to hamper the access of the base thus reducing the appearance of β-elimination products.[45] Of note, this drawback is not observed for sulfamidates derived from β-hydroxyamino acids, such as isoserine,[46] which provide an straightforward entry to enantiopure α-substituted-β-amino acids without competitive reactions (**Scheme 2.11**).

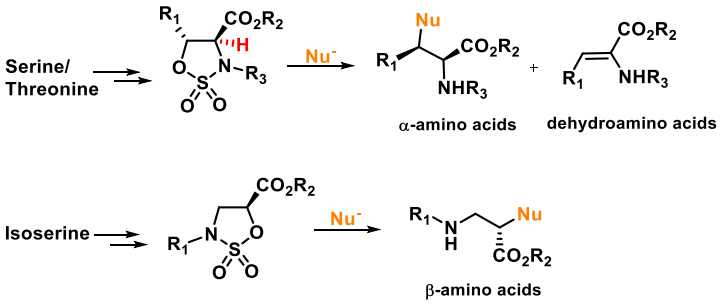

Scheme 2.11. Synthesis of α- or β-amino acids from cyclic sulfamidates. Nu: nucleophile.

Our group has developed a robust methodology to synthetize multiple $\beta^{2,2}$-amino acids from cyclic α-methylisoserine sulfamidates. The ring-opening of these sulfamidates proceeds with total inversion of the configuration at the quaternary carbon (S_N2 mechanism) with sulfur,[47,48] oxygen,[49,50] carbon,[51] fluoride[51] and nitrogen[52–54] nucleophiles. Further acid hydrolysis of the sulfamic acid intermediates afforded the corresponding enantiomerically pure $\beta^{2,2}$-amino acids in good yields (**Scheme 2.12**).

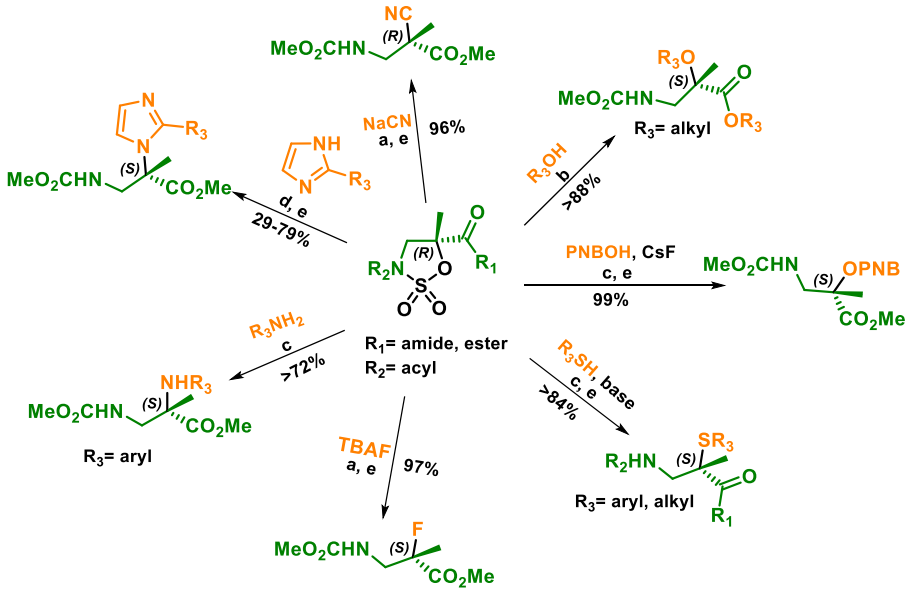

Scheme 2.12. Ring-opening reaction of the α-methylisoserine sulfamidate with oxygen, sulfur, fluoride, nitrogen and carbon nucleophiles. a) DMF, rt, 1-12 h. b) 70-80 ºC, 48 h. c) DMF, 50 ºC, 1-12 h. d) CH_3CN, reflux, 48 h. e) 20% H_2SO_4 / CH_2Cl_2 (1:1), rt, 12 h. PNBOH: *p*-nitrobezoic acid; TBAF: *n*-tetrabutylammonium fluride.

These sulfamidates were also ring-opened with a number of α- and β-1-thiocarbohydrates,[55] including mono- and disaccharides, to obtain a new type of glycoconjugates, namely α/β-1-thioglycosyl-$\beta^{2,2}$-amino acids (**Figure 2.3**).

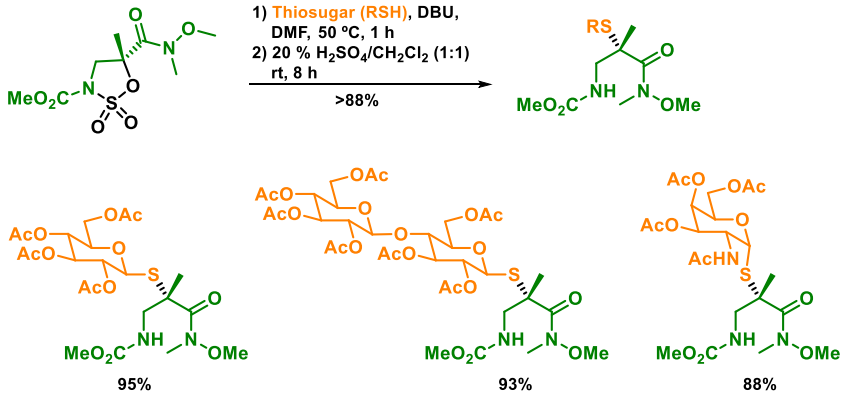

Figure 2.3. Synthesis of α-methylisosysteine glycoconjugates.

Following the same strategy, our group has recently reported the synthesis of dipeptides incorporating the α-methylisoserine sulfamidate, and their corresponding ring-opening reaction with β-1-thioglucose, affording *S*-glycosylated hybrid α/β^{2,2}-dipeptides (**Scheme 2.13**).[56]

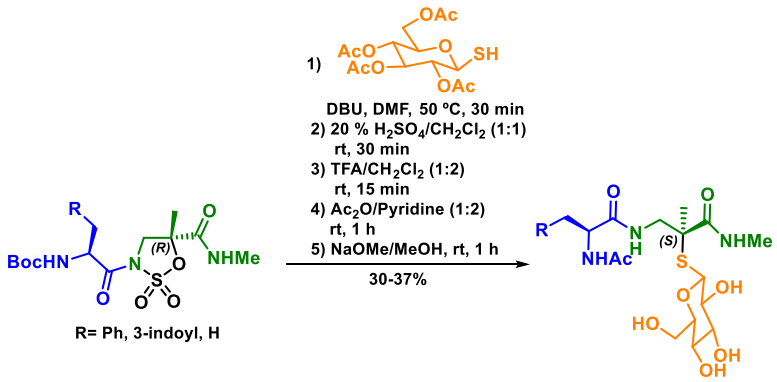

Scheme 2.13. Hybrid α/β^{2,2}-*S*-glyco-dipeptides.

As briefly introduced in the previous section, the ring-opening of cyclic sulfamidates has been used to synthetize enantiomerically pure orthogonally and protected derivatives of the bis-α-amino acids lanthionine and methyllanthionine as an alternative to the ring-opening of lactones[57–59] and aziridines.[60–62] These bis-α-amino acids play a key role in crosslinking polypeptide antibiotics known as lanthibiotics.[63] In this sense, Vederas and Cobb reported the use of the cyclic sulfamidates derived from serine and threonine to obtain orthogonally protected lanthionines or β-methyllanthionines, respectively.[64] Analogously, Zervosen and co-workers synthesized unprotected lanthionines by ring-opening serine sulfamidates in aqueous medium.[65] The versatility of these sulfamidates has allowed to obtain several lanthionine structural analogs.[27,66] Our group synthesized enantiopure

and orthogonally proteced α-methylnorlanthionine, using α-methylisoserine sulfamidate.[48] (**Scheme 2.14**).

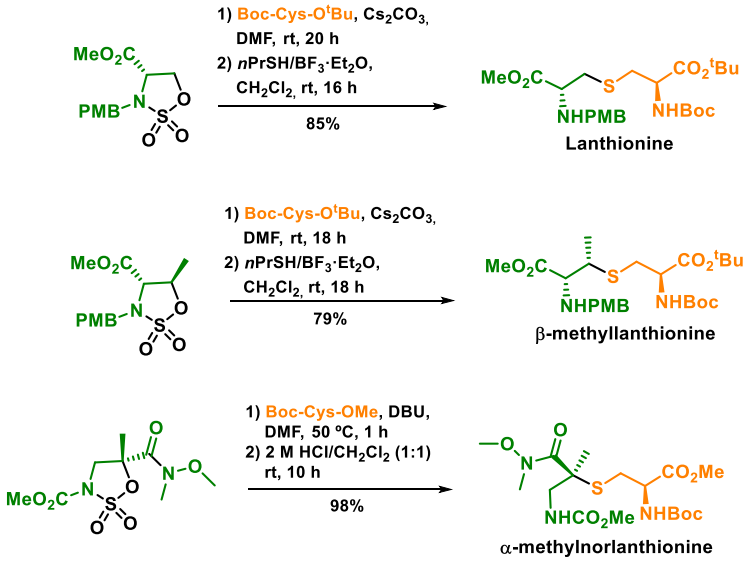

Scheme 2.14. Synthesis of enantiopure and orthogonally protected lanthionine, β-methyllanthionine and α-methylnorlanthionine derivatives from cyclic sulfamidates. PMB: *p*-methoxybenzyl.

2.3 Goals

Bearing this background in mind and as a logical continuation of our research group's work , we envisioned the incorporation of cyclic sulfamidates into biologically relevant peptides, and the subsequent study of their conformational properties and reactivity by combining experimental (NMR, gas-phase IR) and theoretical (Quantum Mechanics, Molecular Dynamics) techniques.

A computational and experimental study on the influence of the sulfamide and carbonyl substituents in the reactivity of α-methylisoserine cyclic sulfamidates is presented in *chapter 3*.

Throughout *chapter 4*, the coupling of several α-amino acids in solution to both sulfamidate termini is described. Then, the subsequent ring-opening reaction with a soft nitrogen nucleophile such as pyridine is evaluated to afford positively charged $\alpha/\beta^{2,2}$-hybrid di- and tri-peptides. The conformational space of those hybrid peptides is studied combining NMR spectroscopy experiments and Molecular Dynamics simulations.

The solid-phase incorporation of α-methylisoserine sulfamidate in longer peptides is addressed in *chapter 5*. Then, different peptides with biological potential as β-amyloid aggregation disrupters are synthesized and evaluated.

Chapter 6 is focused on the solid-phase intermolecular late-stage ring-opening reaction of the sulfamidate with different nucleophiles, with the goal of chemically and fluorescently labeling the corresponding peptides on a solid

support. Additionally, and due to the particular chemistry of these peptides, a new cleavable linker for drug release is developed.

Intra- and intermolecular ring-opening reactions of sulfamidate-containing peptides are described in *chapter 7*, aiming to obtain analogs of cytolysin S ($CylL_S$), a well-known lantipeptide with antimicrobial activity.

Finally, a brief summary of the most relevant results obtained during an international short-term stay at van der Donk's group (University of Illinois at Urbana-Champaign, USA) will be summarized in *chapter 8*.

2.4 References

(1) Minter, A. R.; Fuller, A. A.; Mapp, A. K. *J. Am. Chem. Soc.* **2003**, *125*, 6846–6847.

(2) Fuller, A. A.; Chen, B.; Minter, A. R.; Mapp, A. K. *J. Am. Chem. Soc.* **2005**, *127*, 5376–5383.

(3) Galeazzi, R.; Martelli, G.; Mobbili, G.; Orena, M.; Rinaldi, S. *Org. Lett.* **2004**, *6*, 2571–2574.

(4) Tang, T. P.; Ellman, J. A. *J. Org. Chem.* **2002**, *67*, 7819–7832.

(5) Abele, S.; Seebach, D. *Eur. J. Org. Chem.* **2000**, 1–15.

(6) Kohn, M.; Schmidt, A. *Monatsh. Chem. Verw. Teile Anderer Wiss.* **1907**, *28*, 1055–1062.

(7) Cronin, J. R.; Yuen, G. U.; Pizzarello, S. *Anal. Biochem.* **1982**, *124*, 139–149.

(8) LeBlanc, L. M.; Powers, S. W.; Grossert, J. S.; White, R. L. *Rapid Commun. Mass Spectrom.* **2016**, *30*, 2133–2144.

(9) Testa, E.; Fontanella, L.; Cristiani, G. F.; Mariani, L. *Liebigs Ann. der Chemie* **1961**, *639*, 166–180.

(10) Okano, K.; Morimoto, T.; Sekiya, M. *J. Chem. Soc., Chem. Commun.* **1984**, 883–884.

(11) Katritzky, A. R.; Yannakopoulou, K. *Synthesis* **1989**, 747–751.

(12) Seebach, D.; Boog, A.; Schweizer, W. B. *Eur. J. Org. Chem.* **1999**, 335–360.

(13) Chu, K. S.; Negrete, G. R.; Konopelski, J. P.; Lakner, F. J.; Woo, N. T.; Olmstead, M. M. *J. Am. Chem. Soc.* **1992**, *114*, 1800–1812.

(14) Juaristi, E.; Quintana, D.; Balderas, M.; Garcia-Perez, E. *Tetrahedron: Asymmetry* **1996**, *7*, 2233–2246.

(15) Juaristi, E.; Balderas, M.; Ramírez-Quiros, Y. *Tetrahedron: Asymmetry* **1998**, *9*, 3881–3888.

(16) Hanamoto, T.; Katsuki, T.; Yamaguchi, M. *Tetrahedron Lett.* **1986**, *27*, 2463–2464.

(17) Badiola, E.; Olaizola, I.; Vázquez, A.; Vera, S.; Mielgo, A.; Palomo, C. *Chem. Eur. J.* **2017**, *23*, 8185–8195.

(18) Yu, J. S.; Noda, H.; Shibasaki, M. *Angew. Chem. Int. Ed.* **2018**, *57*, 818–822.

(19) Fang, J. H.; Jian, J. H.; Chang, H. C.; Kuo, T. S.; Lee, W. Z.; Wu, P. Y.; Wu, H. L. *Chem. Eur. J.* **2017**, *23*, 1830–1838.

(20) Avenoza, A.; Cativiela, C.; Paris, M.; Peregrina, J. M. *Tetrahedron: Asymmetry* **1995**, *6*, 1409–1418.

(21) Greco, A.; Tani, S.; De Marco, R.; Gentilucci, L. *Chem. Eur. J.* **2014**, *20*, 13390–13404.

(22) Lorpitthaya, R.; Suryawanshi, S. B.; Wang, S.; Pasunooti, K. K.; Cai, S.; Ma, J.; Liu, X. W. *Angew. Chem. Int. Ed.* **2011**, *50*, 12054–12057.

(23) Bower, J. F.; Rujirawanich, J.; Gallagher, T. *Org. Biomol. Chem.* **2010**, *8*, 1505–1519.

(24) Meléndez, R. E.; Lubell, W. D. *Tetrahedron* **2003**, *59*, 2581–2616.

(25) Bower, J. F.; Szeto, P.; Gallagher, T. *Chem. Commun.* **2005**, 5793–5795.

(26) Albu, S. A.; Koteva, K.; King, A. M.; Al-Karmi, S.; Wright, G. D.; Capretta, A. *Angew. Chem. Int. Ed.* **2016**, *55*, 13259–13262.

(27) Denoël, T.; Zervosen, A.; Lemaire, C.; Joris, B.; Hervé, M.; Blanot, D.; Zaragoza, G.; Luxen, A. *Org. Biomol. Chem.* **2014**, *12*, 9853–9863.

(28) Nag, S.; Lehmann, L.; Kettschau, G.; Toth, M.; Heinrich, T.; Thiele, A.; Varrone, A.; Halldin, C. *Bioorg. Med. Chem.* **2013**, *21*, 6634–6641.

(29) Huang, C.; Yuan, L.; Rich, K. M.; McConathy, J. *Nucl. Med. Biol.* **2013**, *40*, 498–506.

(30) Vanhessche, K. P. M.; Sharpless, K. B. *Chem. Eur. J.* **1997**, *3*, 517–522.

(31) Pilkington, M.; Wallis, J. D. *J. Chem. Soc., Chem. Commun.* **1993**, 1857–1858.

(32) Deyrup, J. A.; Moyer, C. L. *J. Org. Chem.* **1969**, *34*, 175–179.

(33) Gao, Y.; Sharpless, K. B. *J. Am. Chem. Soc.* **1988**, *110*, 7538–7539.

(34) Atfani, M.; Wei, L.; Lubell, W. D. *Org. Lett.* **2001**, *3*, 2965–2968.

(35) Khanjin, N. A.; Hesse, M. *Helv. Chim. Acta* **2003**, *86*, 2028–2057.

(36) Nicolaou, K. C.; Huang, X.; Snyder, S. A.; Bheema Rao, P.; Bella, M.; Reddy, M. V. *Angew. Chem. Int. Ed.* **2002**, *41*, 834–838.

(37) Nicolaou, K. C.; Snyder, S. A.; Longbottom, D. A.; Nalbandian, A. Z.; Huang, X. *Chem. Eur. J.* **2004**, *10*, 5581–5606.

(38) Sullivan, B.; Gilmet, J.; Leisch, H.; Hudlicky, T. *J. Nat. Prod.* **2008**, *71*, 346–350.

(39) Espino, C. G.; Wehn, P. M.; Chow, J.; Du Bois, J. *J. Am. Chem. Soc.* **2001**, *123*, 6935–6936.

(40) Liang, J. L.; Yuan, S. X.; Huang, J. S.; Yu, W. Y.; Che, C. M. *Angew. Chem. Int. Ed.* **2002**, *41*, 3465–3468.

(41) Liang, J. L.; Yuan, S. X.; Huang, J. S.; Che, C. M. *J. Org. Chem.* **2004**, *69*, 3610–3619.

(42) Zhang, J. L.; Huang, J. S.; Che, C. M. *Chem. Eur. J.* **2006**, *12*, 3020–3031.

(43) Lin, X.; Che, C. M.; Phillips, D. L. *J. Org. Chem.* **2008**, *73*, 529–537.

(44) Wang, Y. Q.; Yu, C. Bin; Wang, D. W.; Wang, X. B.; Zhou, Y. G. *Org. Lett.* **2008**, *10*, 2071–2074.

(45) Wei, L.; Lubell, W. D. *Can. J. Chem.* **2001**, *79*, 94–104.

(46) Tovillas, P.; García, I.; Oroz, P.; Mazo, N.; Avenoza, A.; Corzana, F.; Jiménez-Osés, G.; Busto, J. H.; Peregrina, J. M. *J. Org. Chem.* **2018**, *83*, 4973–4980.

(47) Avenoza, A.; Busto, J. H.; Jiménez-Osés, G.; Peregrina, J. M. *J. Org. Chem.* **2006**, *71*, 1692–1695.

(48) Avenoza, A.; Busto, J. H.; Jiménez-Osés, G.; Peregrina, J. M. *Org. Lett.* **2006**, *8*, 2855–2858.

(49) Jiménez-Osés, G.; Avenoza, A.; Busto, J. H.; Peregrina, J. M. *Tetrahedron: Asymmetry* **2008**, *19*, 443–449.

(50) Jiménez-Osés, G.; Avenoza, A.; Busto, J. H.; Rodríguez, F.; Peregrina, J. M. *Chem. Eur. J.* **2009**, *15*, 9810–9823.

(51) Avenoza, A.; Busto, J. H.; Corzana, F.; Jiménez-Osés, G.; Peregrina, J. M. *Chem. Commun.* **2004**, 980–981.

(52) Mata, L.; Avenoza, A.; Busto, J. H.; Peregrina, J. M. *Chem. Eur. J.* **2013**, *19*, 6831–6839.

(53) Mata, L.; Avenoza, A.; Busto, J. H.; Corzana, F.; Peregrina, J. M. *Chem. Eur. J.* **2012**, *18*, 15822–15830.

(54) Mata, L.; Jiménez-Osés, G.; Avenoza, A.; Busto, J. H.; Peregrina, J. M. *J. Org. Chem.* **2011**, *76*, 4034–4042.

(55) Avenoza, A.; Busto, J. H.; Jiménez-Osés, G.; Peregrina, J. M. *Synthesis* **2006**, 641–644.

(56) García-González, I.; Mata, L.; Corzana, F.; Jiménez-Osés, G.; Avenoza, A.; Busto, J. H.; Peregrina, J. M. *Chem. Eur. J.* **2015**, *21*, 1156–1168.

(57) Shao, H.; Lee, C. W.; Zhu, Q.; Gantzel, P.; Goodman, M. *Angew. Chemie Int. Ed.* **1996**, *35*, 90–92.

(58) Li, H.; Jiang, X.; Goodman, M. *J. Pept. Sci.* **2001**, *7*, 82–91.

(59) Arnold, L. D.; May, R. G.; Vederas, J. C. *J. Am. Chem. Soc.* **1988**, *110*, 2237–2241.

(60) Liu, W.; Chan, A. S. H.; Liu, H.; Cochrane, S. A.; Vederas, J. C. *J. Am. Chem. Soc.* **2011**, *133*, 14216–14219.

(61) Knerr, P. J.; Van Der Donk, W. A. *J. Am. Chem. Soc.* **2012**, *134*, 7648–7651.

(62) Mukherjee, S.; Huo, L.; Thibodeaux, G. N.; Van Der Donk, W. A. *Org. Lett.* **2016**, *18*, 6188–6191.

(63) Knerr, P. J.; van der Donk, W. A. *Annu. Rev. Biochem.* **2012**, *81*, 479–505.

(64) Cobb, S. L.; Vederas, J. C. *Org. Biomol. Chem.* **2007**, *5*, 1031–1038.

(65) Denoël, T.; Zervosen, A.; Gerards, T.; Lemaire, C.; Joris, B.; Blanot, D.; Luxen, A. *Bioorg. Med. Chem.* **2014**, *22*, 4621–4628.

(66) Denoël, T.; Zervosen, A.; Lemaire, C.; Plenevaux, A.; Luxen, A. *Tetrahedron* **2014**, *70*, 4526–4533.

Chapter 3. Substituent effects on the reactivity of cyclic α-methylisoserine sulfamidates

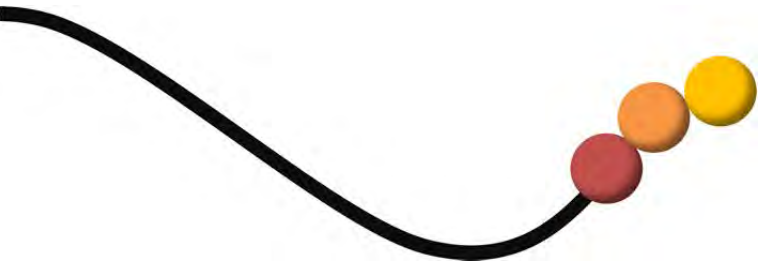

As previously discussed in *chapter 2*, chiral five-membered sulfamidates are prevalent in organic chemistry due to their high versatility and their efficient enantiomeric synthesis.[1–3] Their ring-opening reaction is an efficient pathway to obtain natural products[4–7] and different biomolecules.[8–14] This type of reaction has been previously reported using different families of sulfamidate derivatives,[15–24] which offers a broad variety of synthetic compounds with different characteristics. A survey in the literature revealed that most of the reported ring-opening reactions of five-membered sulfamidates, including metal-catalyzed[25,26] variants, need *N*-protection, since these substrates are more reactive than their unprotected analogues.[27] However, this behavior remains unexplained. There is only one exception, reported by Halcomb and co-workers,[28] in which the ring-opening reaction was achieved using unprotected sulfamidates incorporated in amino acids and peptides derived from L-serine and L-threonine , with β-1-thiocarbohydrates as nucleophiles in aqueous solution (**Figure 3.1**).

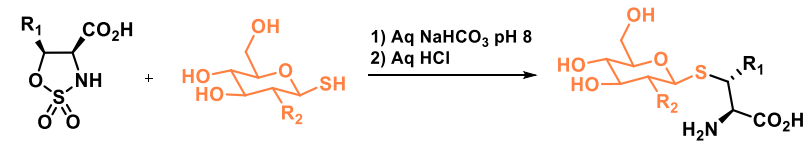

R_1= H or CH_3

R_2= OH or NHAc

Figure 3.1. Ring-opening reaction of unprotected sulfamidates derived from L-serine and L-threonine with β-1-thiocarbohydrates.

Our research group has lately been focused on sulfamidates featuring the α-methylisoserine substructure. In the course of these investigations, we frequently observed that *N*-unprotected substrates never reacted under typical

nucleophilic ring-opening (S_N2) conditions, not even after increasing reaction temperatures or reaction times (**Scheme 3.1**).

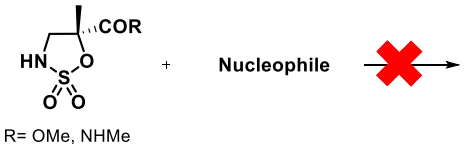

Scheme 3.1. *N*-unprotected sulfamidates derived from α-methylisoserine does not undergo ring-opening reaction with nucleophiles.

Besides the influence of the *N*-terminus, we have also observed quite dramatic changes in the chemoselectivity of the competitive ring-opening (S_N2) and bimolecular elimination (E2) reactions depending on the substituents at the *C*-terminus.[29,30] Intrigued by the special behavior of these sulfamidates, we decided to perform a thorough study of their reactivity, combining quantum mechanics and ring-opening experiments. For this purpose, pyridine was selected as a nucleophile, since it is quite convenient for both theoretical and experimental studies. Pyridine is a slightly basic liquid which can be used as a solvent thus achieving pseudo-first-order conditions, and simply removed under vacuum once the reaction is completed. On the other hand, it is a small, neutral molecule, which reduces computational cost and facilitates geometric optimization (**Scheme 3.2**).

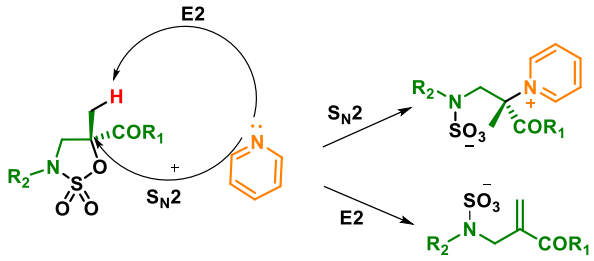

Scheme 3.2. Competitive ring-opening (S_N2) and biomolecular elimination (E2) reactions on quaternary sulfamidates.

3.1 Experimental Assays

The key step to synthesize α-methylisoserine sulfamidates (**Scheme 3.3**) is the Sharpless' asymmetric dihydroxylation were the chirality of the scaffold is established.[31,32] This reaction is carried out on the methacrylic acid Weinreb amide (olefin **B**), previously synthesized from commercially available methacryloyl chloride (olefin **A**), in the presence of a chiral osmium catalyst (AD-mix α), enantioselectively affording diol **C**. This diol is then reacted with the Burgess reagent to give sulfamidate **D**. Finally, different functional group transformations at both termini can be performed to obtain different sulfamidate building blocks (**E**, **F**, **G**, **H**, **I**).[29,33,34]

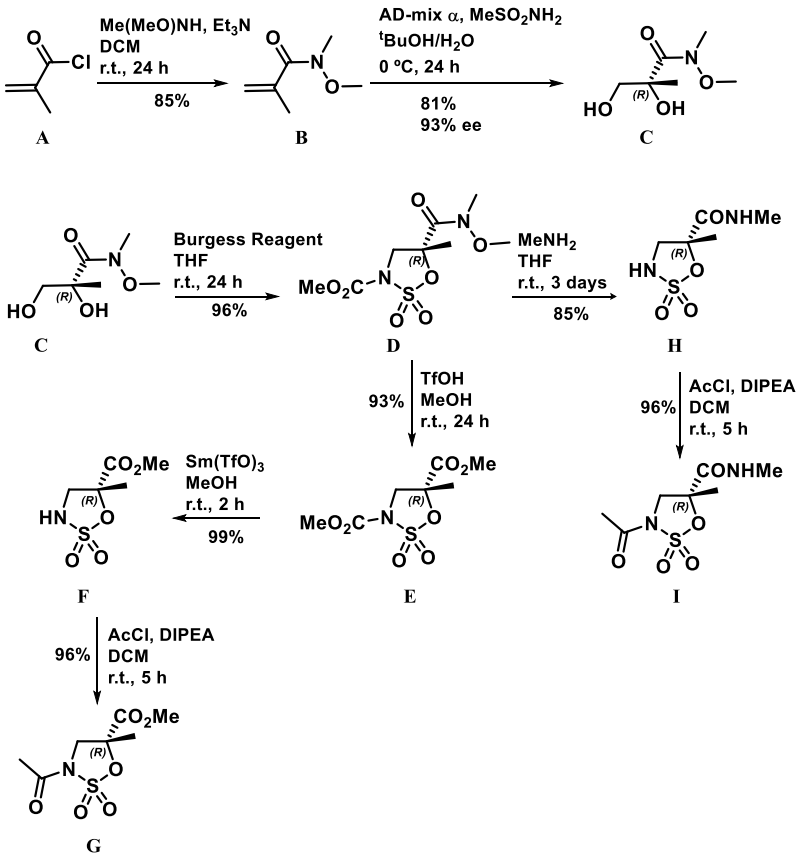

Scheme 3.3. Synthesis of the sulfamidate derivatives **E-I**.

For this study, we considered combinations of unprotected sulfamidate (NH), acetyl (NAc) and methyl carbamate (NCO_2Me) groups at the *N*-terminus, and methyl ester (CO_2Me) and methylamide (CONHMe) groups at the *C*-terminus, corresponding to sulfamidates **E**, **F**, **G**, **H** and **I**. Sulfamidate **I**, which bears *N*-acetyl and methylamide groups, would simulate the behavior of the sulfamidate in a peptide context. Sulfamidates **E-I** were reacted using pyridine as a solvent at the temperatures and reaction times summarized in **Table 3.1**. Once the reaction was finished, as judged by TLC, the solvent was removed under vacuum, and an acidic workup using aqueous 2 M HCl or aqueous 20% H_2SO_4 in DCM (1:1) was performed.

Table 3.1. Ring-opening and elimination reactions of α-methylisoserine sulfamidates **E-I**.

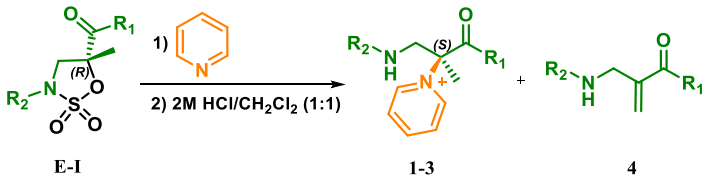

E-I **1-3** **4**

Sulfamidate	R_1	R_2	T (º C)	Time (h)	S_N2[b]	E2[b]
E[a]	OMe	CO_2Me	25	12	**1** (>99%)	n.d.
F	OMe	H	60	24	n.d.	n.d.
G[a]	OMe	COMe	25	12	**2** (>99%)	n.d.
H	NHMe	H	60	24	n.d.	n.d.
I	NHMe	COMe	60	16	**3** (83%)	**4** (17%)

[a]Previosly described by our research group.[33,34] [b]Yields after column chromatography. n.d.: not detected.

As deduced from the experimental data, the presence of carbonyl groups at the *N*-terminus (sulfamidates **E**, **G** and **I**) activates the S_N2 pathway. Additionally, sulfamidate **I**, which bears a methylamide group at the *C*-terminus, activates the E2 pathway. However, unprotected sulfamidate derivatives (**F** and **H**) are unreactive even at high temperatures and after long reaction times. In both cases, starting materials were fully recovered, irrespective of the protecting group at the *C*-terminus. On the other hand, compounds **E** and **G** bearing a methyl ester at the *C*-terminus showed higher reactivity and yielded exclusively the ring-opening products **1** and **2**, respectively, after 12 hours at room temperature. Methylamide sulfamidate **I** needed 60 ºC and 16 hours to achieve high substrate conversions and yielded a mixture of the ring-opening compound **3** (83%) and elimination compound **4** (17%). The terminal alkene α-methylidene-β-alanine was observed as the

unique elimination product, since only the β-hydrogens at the tertiary methyl group can be arranged in an antiperiplanar disposition with respect to the leaving OSO_2N group. This kind of reactivity was reported previously by our research group using basic nucleophiles, such as fluoride or phenoxides (Scheme **3.4**).[29]

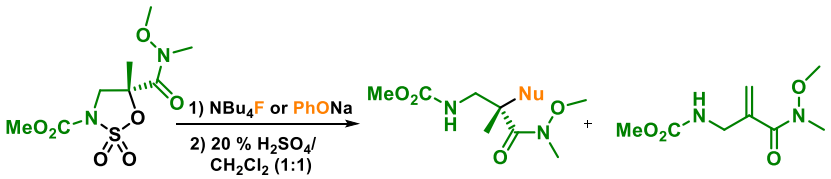

	S_N2	E2
NBu_4F	32%	68%
PhONa	50%	25%

Scheme 3.4. Sulfamidate reactivity previously observed with fluoride or phenoxide nucleophiles.

Pseudo-first-order kinetics for both the ring-opening and elimination reactions of sulfamidate **H** and **I** in pyridine-d_5 were analyzed by ^{1}H NMR spectroscopy (**Figure 3.2**). Sulfamidate **H** remained unchanged, as previously observed. On the other hand, sulfamidate **I** showed a competitive S_N2 (**3'**) and E2 (**4'**) profile, without detecting any intermediate or transient species. The experimental activation barrier for the pseudo-first-order nucleophilic ring opening of sulfamidate **I** at 60 ºC was estimated to be $\Delta G^{\ddagger} = 20.0$ kcal mol^{-1}.

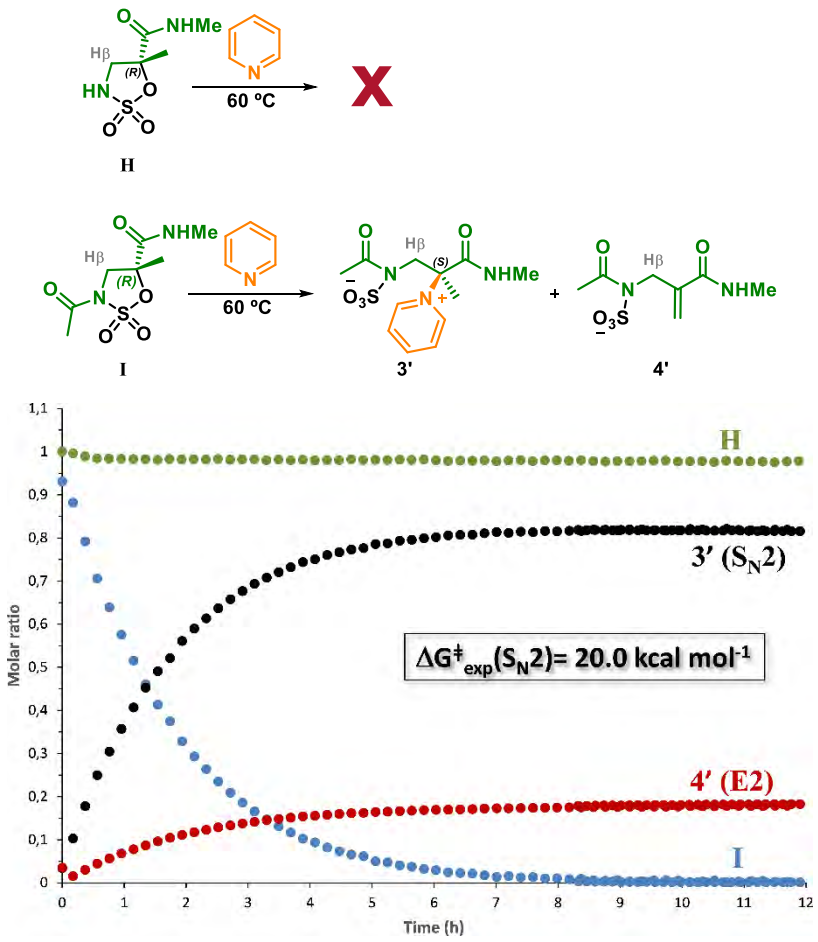

Figure 3.2. Pseudo-first order kinetics for the ring-opening (**SN2**) and elimination (**E2**) reactions of sulfamidate **I** in pyridine-d_5 at 60 ºC. Sulfamidate **H** remained unreacted under the same conditions. The integrations of the peaks corresponding to one of the Hβ of sulfamidates **H**, **I** and compounds **3′** and **4′** were used to determine the molar ratio.

Therefore, we demonstrated that the reactivity at the sulfamidate quaternary carbon (S_N2 or E2) can be completely controlled depending on the substituents at both termini.

3.2 Computational Analysis

Quantum mechanics (QM) performed at the $PCM_{Pyridine}$/M06-2X/6-31+G(d,p) level satisfactorily explained the experimental observations described above (**Figure 3.3**). It should be noted that using equimolecular amounts of pyridine and sulfamidate (second-order conditions) afforded low conversions and yields in the experiments. Conversely, using pyridine as a solvent (pseudo-first-order conditions) allowed complete conversions in reasonable reaction times. Hence, the calculated second-order activation free energies cannot be directly related to the experimental pseudo-first-order activation barriers. However, computed activation enthalpies gave a better representation of the experimental reaction rates due to the neglect of entropy, which is of great importance in biomolecular reactions. Thus, the activation enthalpy calculated for the ring-opening reaction of sulfamidate **I** at 60 ºC was $\Delta H^{\ddagger}$= 22 kcal mol^{-1}, which was in line with the experimentally measured activation barrier at the same temperature, $\Delta G^{\ddagger}_{exp}$= 20 kcal mol^{-1}.

According to the theoretical calculations, ester-substituted sulfamidates **E** and **G** predominantly undergo S_N2-type ring-opening reactions, whilst the elimination pathway is disfavored by at least 5 kcal mol^{-1} (**Figure 3.3**), despite β-hydrogens at the methyl group seem more accessible to the nucleophile/base than the quaternary carbon.

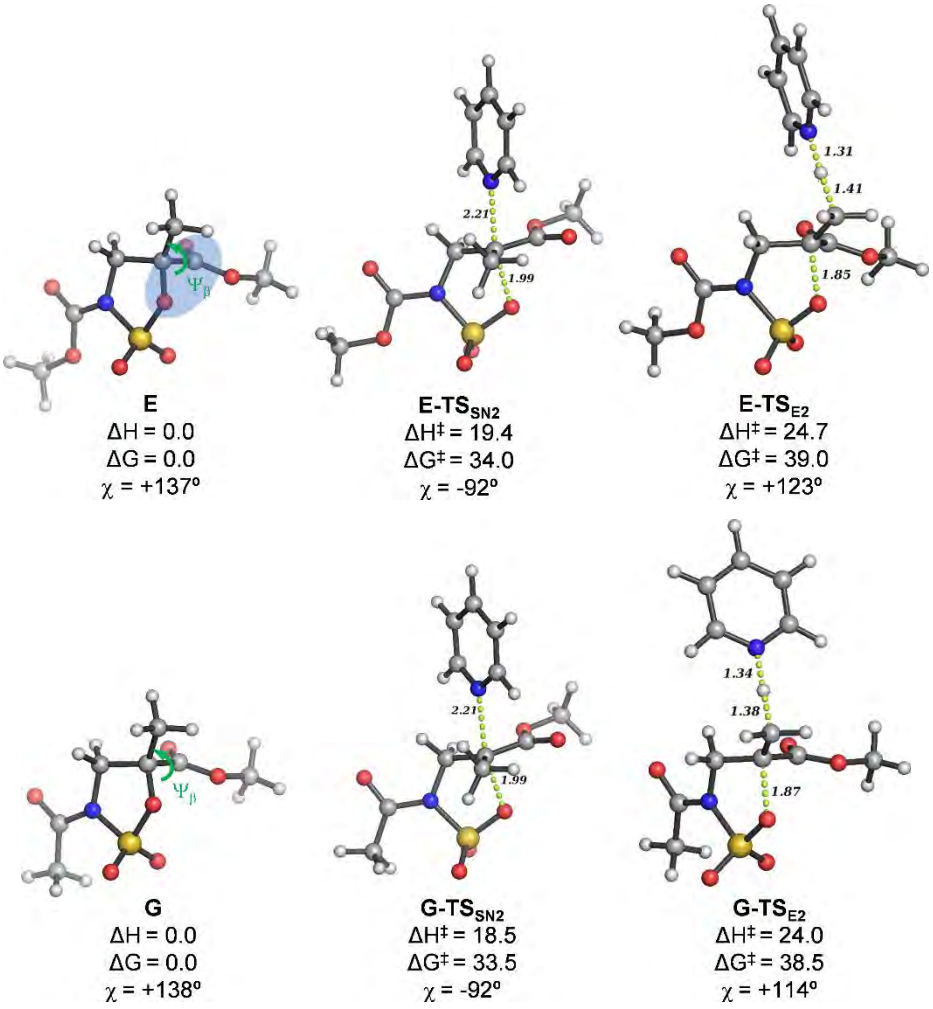

Figure 3.3. Lowest energy structures for the reactant (left) and transition states (TS) for the concerted ring-opening (S_N2, middle) and elimination (E2, right) reactions calculated for sulfamidates **E** (top), and **G** (bottom). Ψ_β = Torsion angle around the ester group in degrees.

On the other hand, amide-substituted sulfamidate **I** is theoretically able to undergo both reaction pathways, substitution and elimination. Activation barriers for both processes were calculated to be almost identical, since the activation energy of the S_N2 pathway increased around 3-4 kcal mol^{-1} and the activation energy for the E2 pathway decreased about 2 kcal mol^{-1} with

respect to those calculated for the ester-substituted sulfamidates **E** and **G** (**Figure 34**).

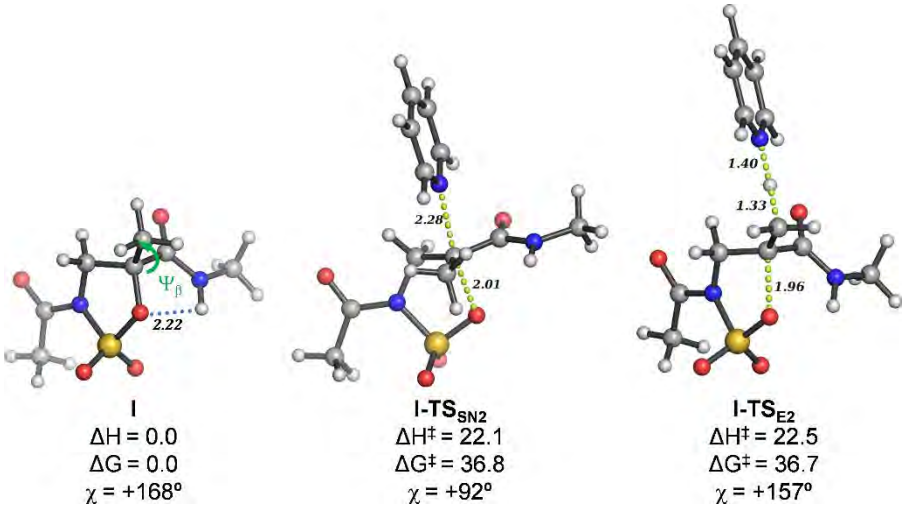

Figure 3.4. Lowest energy structures for the reactant (left) and transition states (TS) for the concerted ring-opening (S_N2, middle) and elimination (E2, right) reactions calculated for sulfamidate **I**. ψ_β = Torsion angle around the amide group in degrees.

The reason for this trend was not easily attributable to electronic or inductive effects, considering that the atomic partial charge at the quaternary carbon in sulfamidate **I** was slightly more positive (q_{NBO}= +0.18 e^-) than sulfamidate **G** (q_{NBO}= +0.16 e^-). The calculated trend was better explained by the higher distortion of the amide moiety with respect to the ester upon planarization of the quaternary carbon at the nucleophilic attack. This planarization of the α-carbon seems to impose an important energy penalty when the geometry of the reactant distorts into that of the S_N2 transition structure (TS) (**Figure 3.5**).

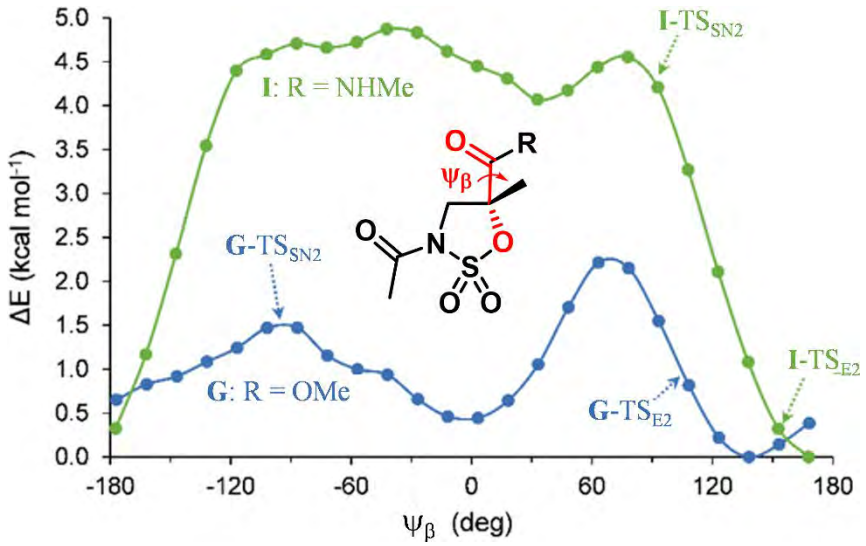

Figure 3.5. Potential energy scan around the torsion angle ψβ in sulfamidates **G** and **I**, calculated with PCM$_{Pyridine}$/M06-2X/6-31+G (d, p).

The calculated torsion profiles around the Cα–CO bonds (ψβ dihedral) for both *N*-acetyl sulfamidates **G** and **I** show that amide-substituted sulfamidate **I** has a higher barrier associated with the rotation of the more polarized amide group, which requires about 4 kcal mol^{-1} to distort into the TS geometry. The origin of this higher rotational barrier is the loss of a hydrogen bond between the amide NH and the sulfamidate endocyclic O atom. On the other hand, it is easier for the ester group of sulfamidate **G** to adopt the TS geometry, with a smaller penalty of 1.5 kcal mol^{-1}. For E2-type reactions, the rotation around the Cα-CO bond is minimal for the corresponding TS of sulfamidate **I**, imposing no energy penalty with respect to the reactant's geometry. This is because the hydrogen bond between the amide N–H and the sulfamidate endocyclic oxigen, which was lost in the S$_N$2 TS for this sulfamidate, is maintained.

In the cases of *N*-unprotected sulfamidates **F** and **H**, the absence of the carbonyl group raises the calculated activation barriers for both reactions (S$_N$2

and E2) by around 3 kcal mol^{-1}, slowing down the reactions about 100 times (**Figure 3.6**).

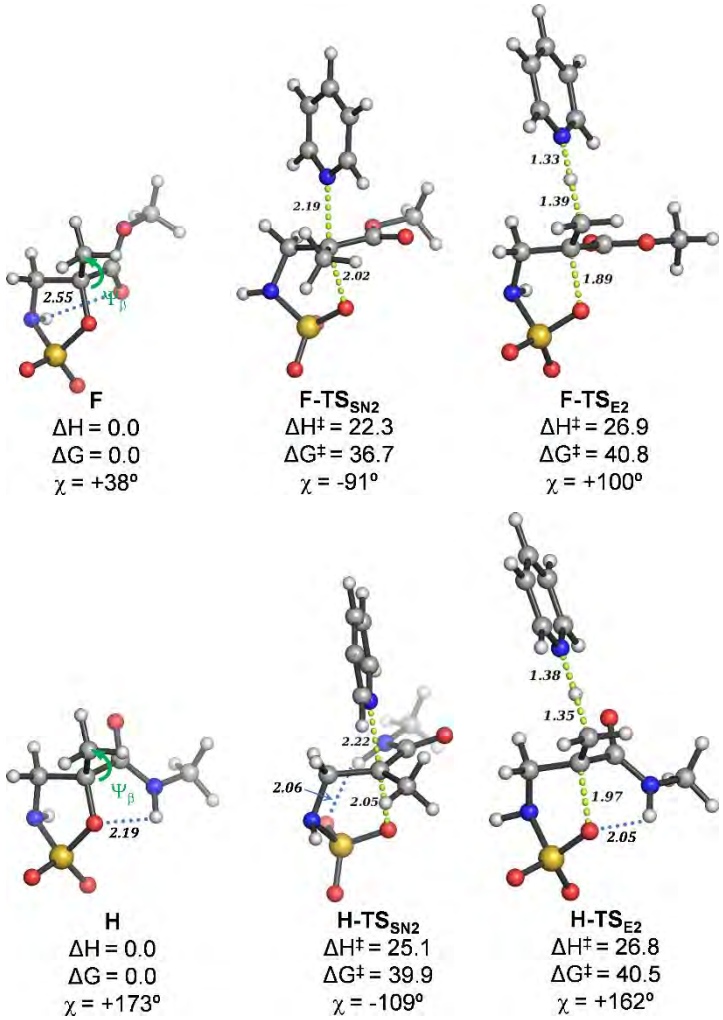

Figure 3.6. Lowest energy structure for the reactants (left) and transition states (TS) for the concerted ring-opening (S_N2, middle) and elimination (E2, right) reactions calculated for sulfamidates **F** (top) and **H** (bottom). ψ_β = Torsion angle around the ester and amide groups in degrees.

This deactivation was calculated to be even stronger if a pyridine molecule is bound to the sulfonamide NH (**H·py**), which increases the activation barrier

for the ring-opening reaction by 4 kcal mol^{-1} with respect to the unsolvated sulfamidate **H**, making the calculated reaction rate 500 times lower. Similarly, if this sulfamidate is totally deprotonated (**H'**) the calculated activation barrier is much higher ($\Delta G^{\ddagger}$ = 54 kcal mol^{-1}), which translates into millions-fold lower reaction rates (**Figure 3.7**).

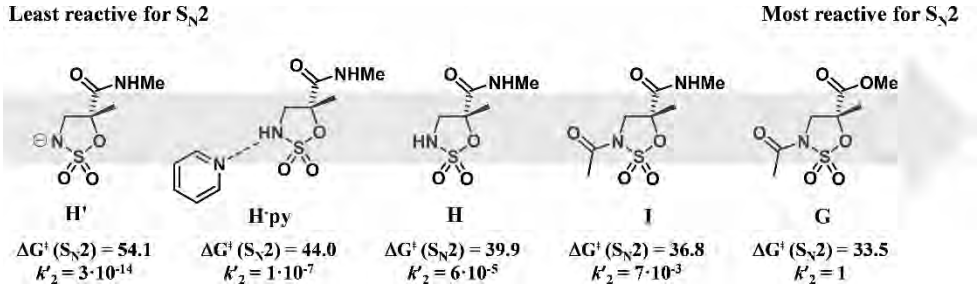

Figure 3.7. Summary of substituent effects on the calculated activation barriers ($\Delta G^{\ddagger}$ in kcal mol^{-1}) for the ring-opening reactions (S_N2) of α-methylisoserine-derived sulfamidates. k'_2 values correspond to the computed relative second-order rate constants.

This theoretical prediction for deprotonated sulfamidate **H'** was studied experimentally. A titration experiment was performed on sulfamidate **H** by monitoring the corresponding ^1H NMR spectrum in $CDCl_3$. In the absence of pyridine, the NH signal appears as a pseudo-triplet due to a weak *J*-coupling to the vicinal CH_2 hydrogens, whose signals appears as two doublets of doublets. Addition of only 0.1 equivalents of pyridine led to a NH signal shape change into a broad singlet and a downfield shift of around 1 ppm. Vicinal CH_2 signals also changed to two doublets. Addition of increasing amounts of pyridine caused a more marked broadening and downfield shift of the NH signal, which finally disappeared (**Figure 3.8**). This experiment strongly suggested that pyridine is somehow interacting with the NH group of the *N*-unprotected sulfamidates, thus decreasing their reactivity.

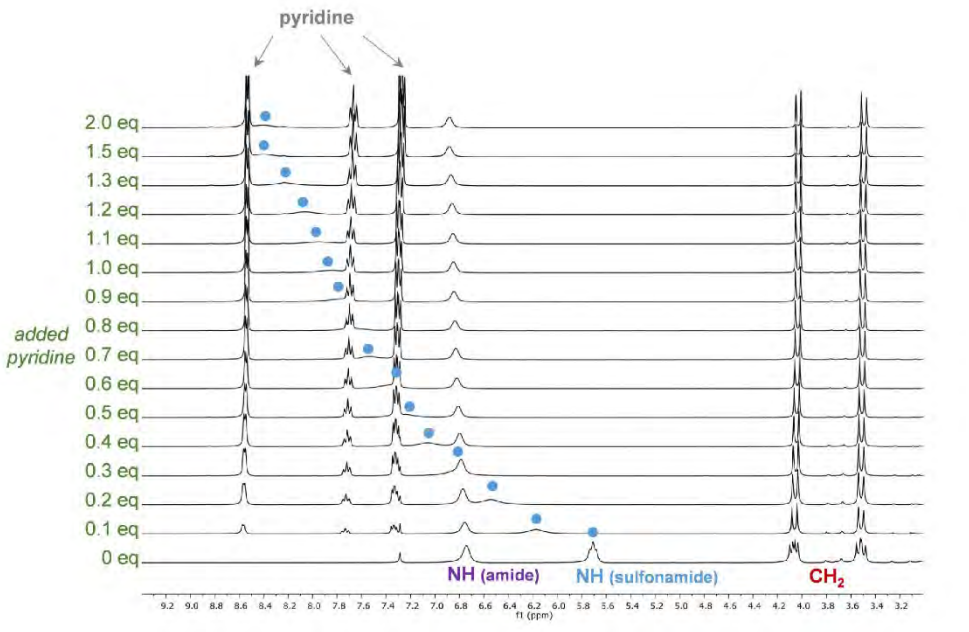

Figure 3.8. Titration of sulfamidate **H** with pyridine monitored by ^{1}H NMR in $CDCl_3$.

The absence of the *N*-carbonyl group avoids delocalization of the partial negative charge generated in the NSO_3 moiety upon Cα–O_{endo} bond cleavage when the sulfamidates are ring-opened. This loss of thermodynamic driving force is revealed by the later character of the S_N2 and E2 transition structures (i.e. shorter $N_{pyridine}\cdots C\alpha$ and $N_{pyridine}\cdots H\beta$ forming bond distances). On the other hand, the accumulation of additional electron density on the same NSO_3 moiety either by partial or full deprotonation of the N–H group strongly disfavors charge transfer from pyridine to the breaking $C\cdots O_{endo}$ bond at the transition state.

3.3 Conclusions

An explanation of the reactivity observed for sulfamidates derived from α-methylisoserine has been provided, combining experiments and theoretical calculations. This study indicates that changing the substituents attached to the *N*- and *C*-terminus of the sulfamidate allows controlling reactivity (S_N2 vs. E2). If the *N*-terminus has a hydrogen atom attached, the reactivity at the quaternary carbon towards either S_N2 or E2 reactions is completely silenced. However, when this position is functionalized with a carbonyl group, the reactions at the quaternary carbon are triggered. On the other hand, the *C*-terminus allows fine tuning the chemoselectivity (S_N2 *vs.* E2). As will be described in the incoming chapters of this thesis, this modulation capability will be very useful for the synthesis of peptides incorporating this scaffold, since further transformations can be performed without undesired ring-opening reactions by using the unprotected sulfamidate as a building block, and the ring-opening pathway can be subsequently activated when needed (**Figure 3.9**).

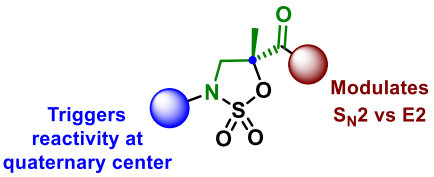

Figure 3.9. Summary of the substituent effects on the reactivity of the α-methylisoserine sulfamidates.

These results have been published in the Journal of Organic Chemistry (*J. Org. Chem.* **2017**, *82*, 13250–13255).

3.4 References

(1) Meléndez, R. E.; Lubell, W. D. *Tetrahedron* **2003**, *59*, 2581–2616.

(2) Spillane, W.; Malaubier, J. B. *Chem. Rev.* **2014**, *114*, 2507–2586.

(3) Saeidian, H.; Abdoli, M.; Mirjafary, Z. *Synthesis* **2015**, *47*, 1057–1075.

(4) Bower, J. F.; Szeto, P.; Gallagher, T. *Chem. Commun.* **2005**, 5793–5795.

(5) Gilmet, J.; Sullivan, B.; Hudlicky, T. *Tetrahedron* **2009**, *65*, 212–220.

(6) Albu, S. A.; Koteva, K.; King, A. M.; Al-Karmi, S.; Wright, G. D.; Capretta, A. *Angew. Chem. Int. Ed.* **2016**, *55*, 13259–13262.

(7) Shiokawa, Z.; Inuki, S.; Fukase, K.; Fujimoto, Y. *Synlett* **2016**, *27*, 616–620.

(8) Ghosh, A.; Sieser, J. E.; Caron, S.; Couturier, M.; Dupont-Gaudet, K.; Girardin, M. *J. Org. Chem.* **2006**, *71*, 1258–1261.

(9) Richter, H. G. F.; Adams, D. R.; Benardeau, A.; Bickerdike, M. J.; Bentley, J. M.; Blench, T. J.; Cliffe, I. A.; Dourish, C.; Hebeisen, P.; Kennett, G. A.; Knight, A. R.; Malcolm, C. S.; Mattei, P.; Misra, A.; Mizrahi, J.; Monck, N. J. T.; Plancher, J. M.; Roever, S.; Roffey, J. R. A.; Taylor, S.; Vickers, S. P. *Bioorganic Med. Chem. Lett.* **2006**, *16*, 1207–1211.

(10) Bower, J. F.; Szeto, P.; Gallagher, T. *Org. Lett.* **2007**, *9*, 3283–3286.

(11) Zeng, Q.; Allen, J. G.; Bourbeau, M. P.; Wang, X.; Yao, G.; Tadesse, S.; Rider, J. T.; Yuan, C. C.; Hong, F. T.; Lee, M. R.; Zhang, S.; Lofgren, J. A.; Freeman, D. J.; Yang, S.; Li, C.; Tominey, E.; Huang, X.; Hoffman, D.; Yamane, H. K.; Fotsch, C.; Dominguez, C.; Hungate, R.; Zhang, X. *Bioorganic Med. Chem. Lett.* **2010**, *20*, 1559–1564.

(12) Richter, H. G. F.; Freichel, C.; Huwyler, J.; Nakagawa, T.; Nettekoven, M.; Plancher, J. M.; Raab, S.; Roche, O.; Schuler, F.; Taylor, S.; Ullmer, C.; Wiegand, R. *Bioorganic Med. Chem. Lett.* **2010**, *20*, 5713–5717.

(13) Andrews, K. M.; Beebe, D. A.; Benbow, J. W.; Boyer, D. A.; Doran, S. D.; Hui, Y.; Liu, S.; McPherson, R. K.; Neagu, C.; Parker, J. C.; Piotrowski, D. W.; Schneider, S. R.; Treadway, J. L.; Vanvolkenberg, M. A.; Zembrowski, W. J. *Bioorganic Med. Chem. Lett.* **2011**, *21*, 1810–1814.

(14) Zhong, Y. L.; Gauthier, D. R.; Shi, Y. J.; McLaughlin, M.; Chung, J. Y. L.; Dagneau, P.; Marcune, B.; Krska, S. W.; Ball, R. G.; Reamer, R. A.; Yasuda, N. *J. Org. Chem.* **2012**, *77*, 3297–3310.

(15) Wei, L.; Lubell, W. D. *Can. J. Chem.* **2001**, *79*, 94–104.

(16) Rashid Baig, N. B.; Chandrakala, R. N.; Sudhir, V. S.; Chandrasekaran, S. *J. Org. Chem.* **2010**, *75*, 2910–2921.

(17) Taylor, C. M.; De Silva, S. T. *J. Org. Chem.* **2011**, *76*, 5703–5708.

(18) Baig, R. B. N.; Varma, R. S. *Chem. Commun.* **2012**, *48*, 5853–5855.

(19) Saha, A.; Baig, R. B. N.; Leazer, J.; Varma, R. S. *Chem. Commun.* **2012**, *48*, 8889–8891.

(20) Malhotra, R.; Dey, T. K.; Dutta, S.; Basu, S.; Hajra, S. *Org. Biomol. Chem.* **2014**, *12*, 6507–6515.

(21) James, T.; MacLellan, P.; Burslem, G. M.; Simpson, I.; Grant, J. A.; Warriner, S.; Sridharan, V.; Nelson, A. *Org. Biomol. Chem.* **2014**, *12*, 2584–2591.

(22) Venkateswarlu, C.; Datta, B.; Chandrasekaran, S. *RSC Adv.* **2014**, *4*, 42952–42956.

(23) Su, H. Y.; Song, Y.; Taylor, M. S. *Org. Biomol. Chem.* **2016**, *14*, 1–8.

(24) Zeng, J. L.; Chachignon, H.; Ma, J. A.; Cahard, D. *Org. Lett.* **2017**, *19*, 1974–1977.

(25) Ursinyova, N.; Bedford, R. B.; Gallagher, T. *Eur. J. Org. Chem.* **2016**, *2016*, 673–677.

(26) James, T.; Simpson, I.; Grant, J. A.; Sridharan, V.; Nelson, A. *Org. Lett.* **2013**, *15*, 6094–6097.

(27) Posakony, J. J.; Grierson, J. R.; Tewson, T. J. *J. Org. Chem.* **2002**, *67*, 5164–5169.

(28) Cohen, S. B.; Halcomb, R. L. *J. Am. Chem. Soc.* **2002**, *124*, 2534–2543.

(29) Avenoza, A.; Busto, J. H.; Corzana, F.; Jiménez-Osés, G.; Peregrina, J. M. *Chem. Commun.* **2004**, 980–981.

(30) Mata, L.; Avenoza, A.; Busto, J. H.; Peregrina, J. M. *Chem. Eur. J.* **2013**, *19*,

6831–6839.

(31) Zaitsev, A. B.; Adolfsson, H. *Synthesis* **2006**, 1725–1756.

(32) Kolb, H. C.; VanNieuwenhze, M. S.; Sharpless, K. B. *Chem. Rev.* **1994**, *94*, 2483–2547.

(33) Mata, L.; Avenoza, A.; Busto, J. H.; Corzana, F.; Peregrina, J. M. *Chem. Eur. J.* **2012**, *18*, 15822–15830.

(34) García-González, I.; Mata, L.; Corzana, F.; Jiménez-Osés, G.; Avenoza, A.; Busto, J. H.; Peregrina, J. M. *Chem. Eur. J.* **2015**, *21*, 1156–1168.

Chapter 4.
Synthesis of mixed positively charged $\alpha/\beta^{2,2}$-peptides

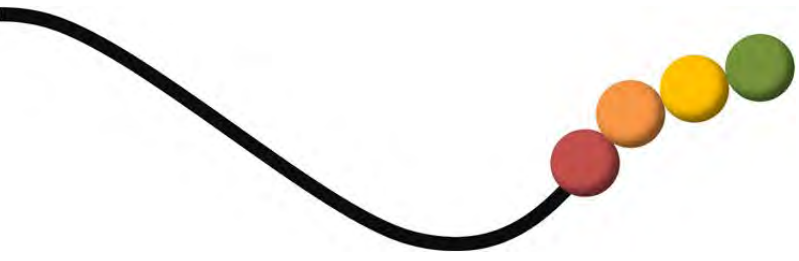

Noncovalent interactions[1–4] have shown to be relevant in diverse areas of chemistry, from materials design to molecular biology. These interactions can be found alone or in combination with others stabilizing the structure of the host-guest complex. One of the most common interactions are hydrogen bonds,[5–7] which are electrostatic attractions between hydrogen atoms and electronegative atoms such as nitrogen, oxygen or fluorine. Hydrophobic interactions between non-polar molecules or residues within polar solvents such as water are also commonly observed. On the other hand, there are salt bridges interactions, consisting of a combination of non-covalent hydrogen bonds and ionic bonds interactions. Finally, X-π interactions (X= CC, CH, NH, OH, SH, cation, anion or halogen), which are interactions between aromatic rings, polarized hydrogens and charged atoms, have also been observed. All of them are already known to provide stability and specificity to the folded structure of proteins among other things. Among these, two major interactions have been attracting a great deal of interest in recent years,[8,9] π-π stacking (non-covalent interactions between aromatic rings, containing π bonds) and cation-π (non-covalent interactions between a cation and a π system), since they are important for controlling the structure and function of macromolecules. Throughout this chapter, we will focus on these type of interactions (**Figure 4.1**).

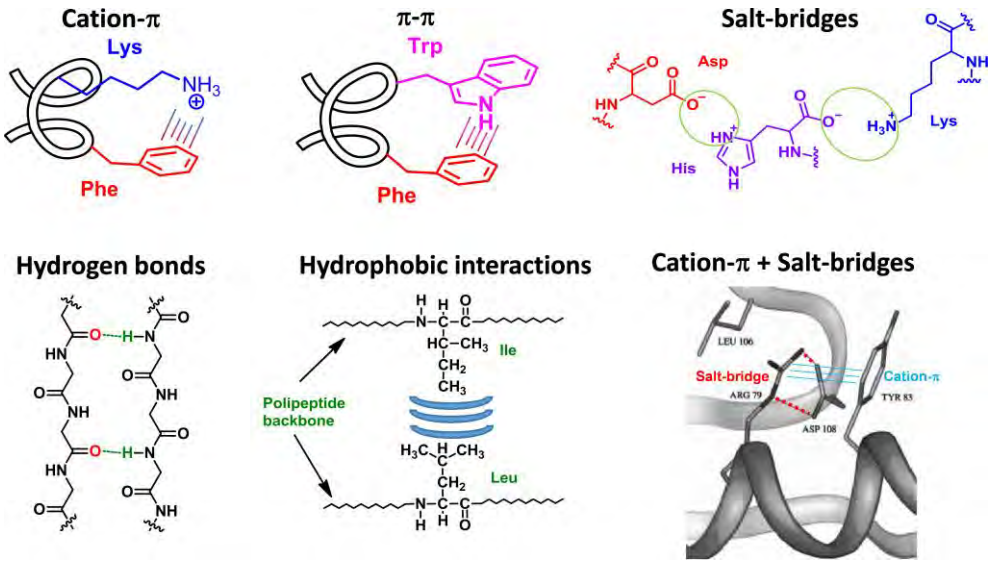

Figure 4.1. Noncovalent interactions.

Noncovalent cation-π interactions take place when a positively charged entity interacts with a neutral π system. This interaction may be even stronger than hydrogen bonds, since the electrostatic attraction between an ion and a neutral molecule is stronger than between two neutral molecules, especially when the neutral molecule is easily polarizable.[10–13]

The first cation-π interaction, was reported by Kebarle and co-workers in 1981. They demonstrated that K^+ ion preferred to bind to benzene rather than to a water molecule.[14] Since this discovery, many research groups have been interested in these interactions, studying them with different ions and π systems.

Cation-π interactions are relevant in different fields, such as host-guest complexes,[15–19] to study molecular recognition between artificial or synthetic receptors and small guest molecules; materials science, to obtain new nanosystems;[20–26] and catalysis and organic synthesis, to study their reaction mechanisms (**Figure 4.2**).[27,28,37–46,29,47,30–36]

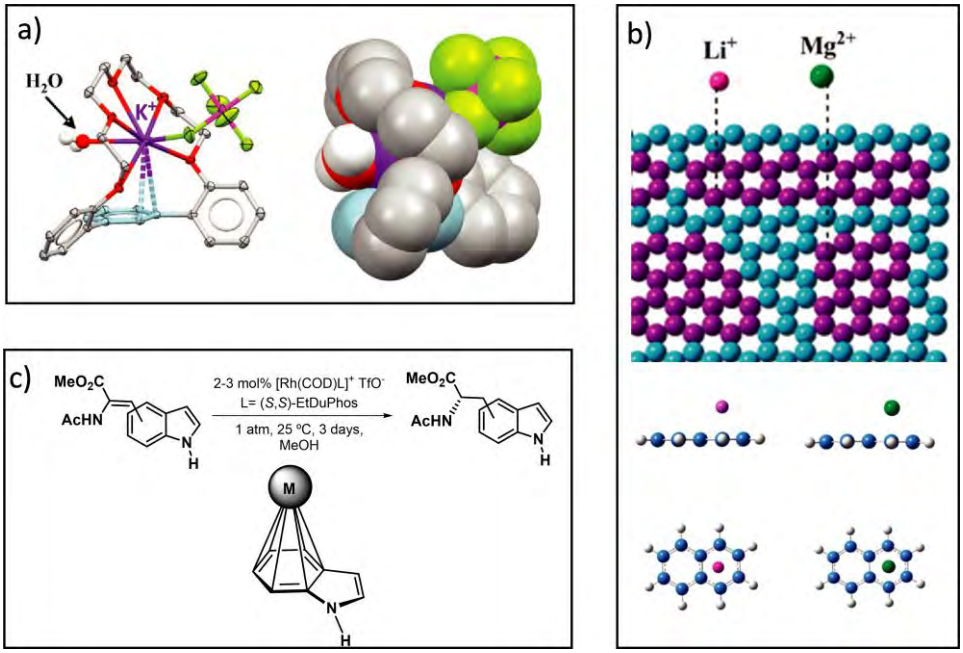

Figure 4.2. Host-Guest chemistry (a),[19] materials science (b)[26] and catalysis (c)[27] examples in which cation-π interaction are relevant.

However, in this chapter we are interested in biological systems, in which Dougherty's group pioneered the study of these systems.[4] In this field, peptides, proteins, enzymes, and antibodies have been studied. In the cases of peptides[48–52] and proteins,[53,54,63–71,55–62] the interactions between side chains are very important because they play an important role in the stabilization of their secondary and tertiary structures. One remarkable example was the geometric analysis of 33 refined protein crystal structures performed by Burley and Petsko. These studies showed that the cation-π interactions between protonated or very polar sidechains (Lys, Arg, Asn, Gln or His) and aromatic rings (Phe, Trp or Tyr) can stabilize the folded structure of proteins.[72]

Kallenbach and co-workers showed that the pair Trp/Arg formed a cation-π interaction on the surface of a peptide, contributing to the stabilization of an

α-helix.[73] In the case of proteins, Gasymov *et al.*, discovered a cation-π interaction, which stabilized the conformation of a loop, in the pair Phe/Lys of tear lipocalin present at the ocular surface.[74]

On the other hand, some research groups have been focused on the possibility of studying the protein functions and enzymatic activities in which cation-π interactions may be relevant, combining X-ray structural elucidation and site-directed mutagenesis.[75,76,85,86,77–84] In this sense, Goldstein and co-workers. determined the crystal structure of the enzyme phosphatidylinositol-specific phospholipase C from *Staphylococcus aureus*, where a cation-π was found to be essential for activity.[87]

These interactions are also crucial for the binding profiles of several antibodies[88–92] to their corresponding antigens or of bioactive drugs to biological receptors (**Figure 4.3**).[83]

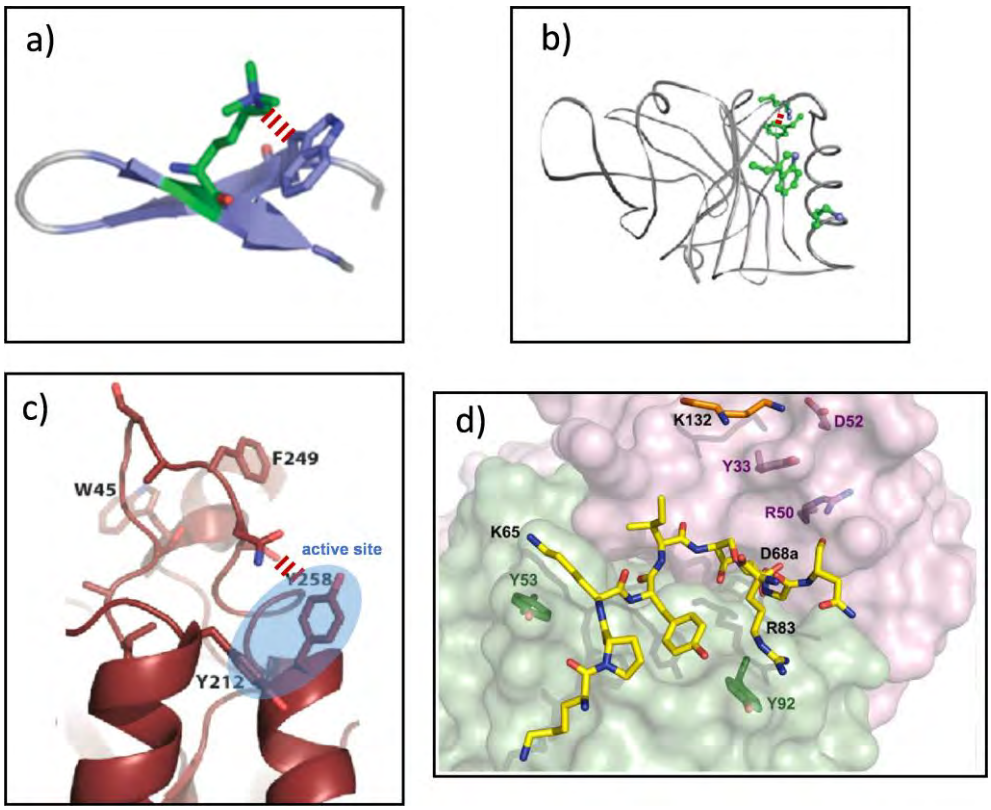

Figure 4.3. Peptides (a),[52] proteins (b),[74] enzymes (c)[87] and antibodies (d)[91] examples showing cation-π interactions.

On the other hand, antimicrobial peptides usually have a net positive charge, which allows preferential binding to the negatively charged outer surface of bacteria.[93,94]

Taking into account the importance of aromatic interactions, such as cation-π and π-π, the main goal of this chapter is to study such attractions in small α/β^{2,2}-peptides. For this purpose, di-, tri-peptides containing cyclic α-methylisoserine sulfamidates will be synthesized. The corresponding ring-opening reaction of the cyclic sulfamidate moiety will be studied using neutral nucleophiles so that the peptide becomes cationic upon ring-opening.

We selected pyridine as the nucleophile, since it is a small neutral molecule and can be used as a solvent, considerably reducing reaction times (**Scheme 4.1**). Finally, the conformational space of some of the resulting positively charged peptides will be evaluated combining NMR experiments (2D-NOESY) and Molecular Dynamics (MD) simulations.

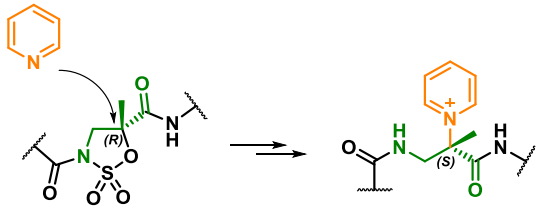

Scheme 4.1. Ring opening reaction of α-methylisoserine cyclic sulfamidate in peptides with pyridine as a nucleophile.

4.1 Peptide synthesis

As an extension of a previous study from our group,[95] a small library of α/β[2,2]-hybrid dipeptides was synthesized by coupling α-amino acids to the *N*-unprotected sulfamidate **H**. Then, we extended the library by coupling α-amino acids at the sulfamidate *C*-terminus. To this aim, we used sulfamidate amino acid **J** obtained quantitatively from sulfamidate **D** after basic hydrolysis (**Scheme 4.2**).

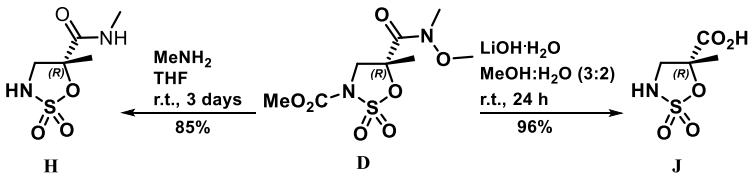

Scheme 4.2. Synthesis of sulfamidate building blocks **H** and **J**.

Coupling α-amino acids at the *N*-terminus of the different starting materials and intermediates was achieved by using TBTU as the coupling agent in dichloromethane at -20 ºC. The use of low temperatures and non-polar solvents was key to avoid the undesired ring-opening of the sulfamidate with nucleophiles present in the coupling cocktail such as benzotriazoles, once the peptide bond is formed.

Coupling α-amino acids at the *C*-terminus of the sulfamidate **J** did not work well under these conditions. Several other coupling reagents were tested, the best yields being achieved using PyBOP and HOAt. After coupling for 18 hours at room temperature, no ring-opening byproducts were observed, and the target compounds were obtained generally in good yields. These results agree with the observations described in *chapter 3*, namely that *N*-terminus unprotected sulfamidates cannot undergo ring-opening reactions.

These dipeptides were elongated at either their *N*- or *C*-terminal positions, following the conditions described above. The resulting di- and tripeptides were capped at their *N*-termini as an acetamide to simulate one last peptide bond, and to promote the sulfamidate ring-opening reaction. All these procedures are summarized in **Scheme 4.3**.

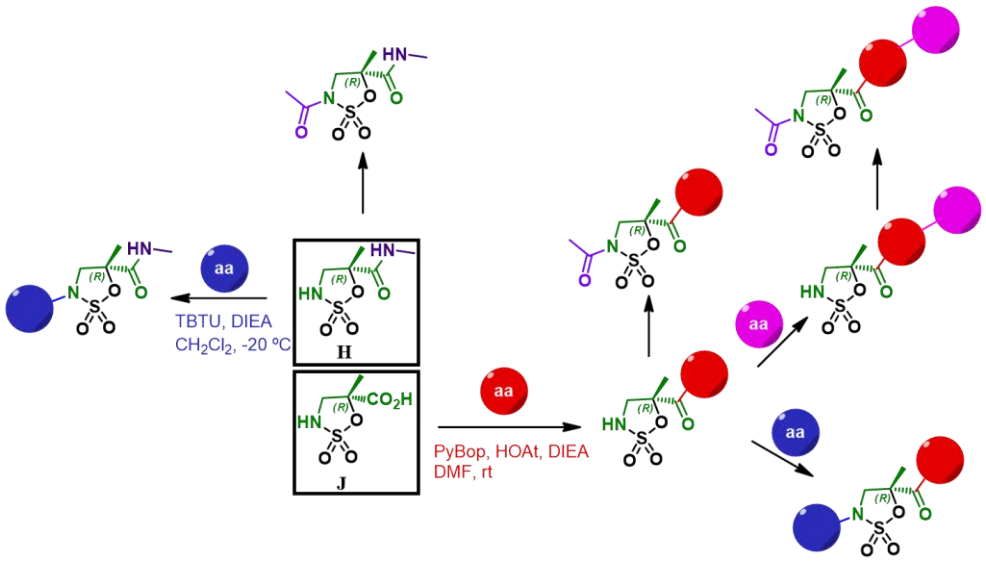

Scheme 4.3. Generation of a small library of hybrid α/β^{2,2}-peptides by coupling α-amino acids at both terminal positions of α-methylisoserine sulfamidates **H** and **J**.

To investigate the occurrence of aromatic interactions, α-amino acids bearing aromatic substructures were selected (Phe, and Trp) as coupling partners (**Scheme 4.4** and **Table 4.1**). In order to couple a following amino acid at the *i+2* position, a deprotection step was necessary (**Table 4.1**, entry 7).

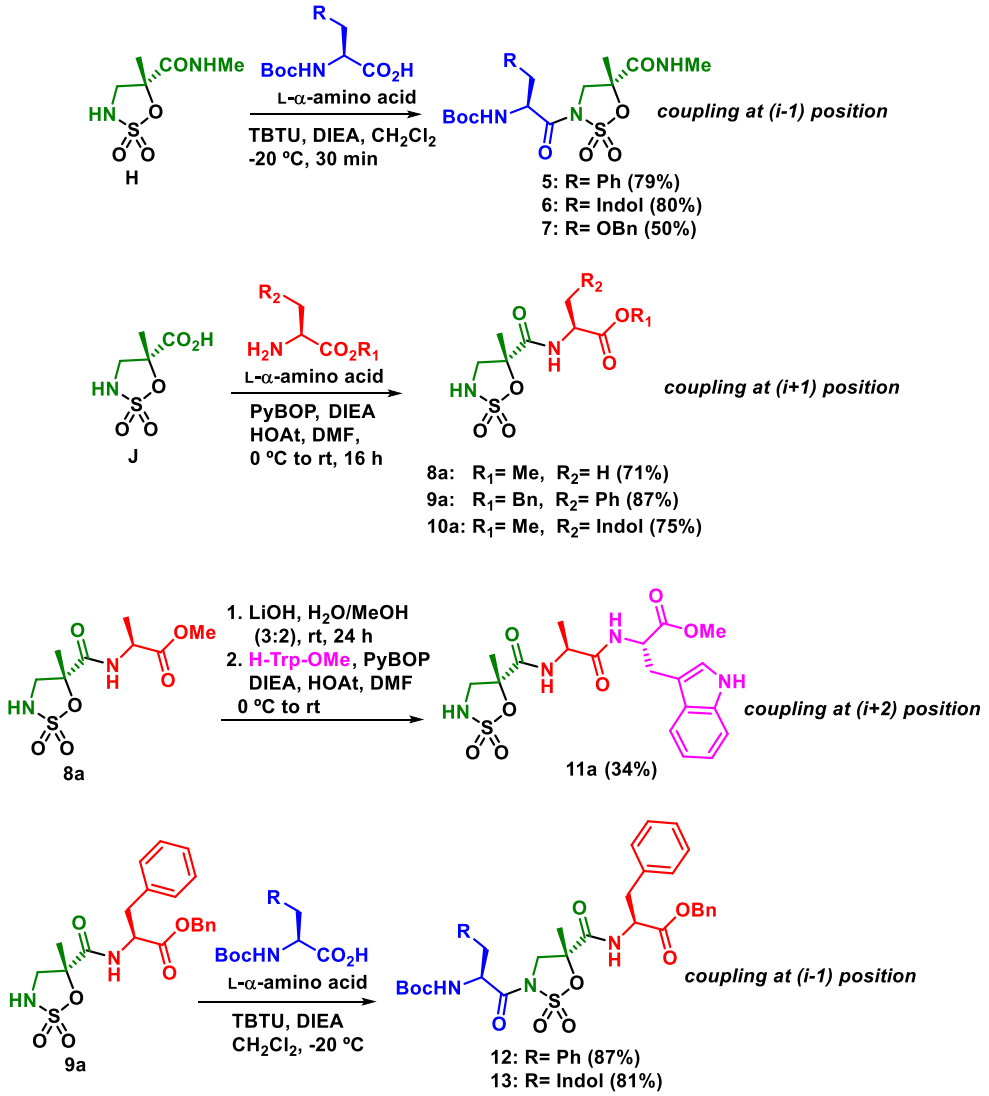

Scheme 4.4. Coupling of different α-amino acid at the *N*- or the *C*-terminus of α-methylisoserine sulfamidates.

Table 4.1. Yields obtained for the di- or tripeptides **5-13**.

Entry	α-amino acid (*i*-1)	Sulfamidate	α-amino acid (*i*+1)	α-amino acid (*i*+2)	Final compound (yield)[a]
1	Boc-Phe-OH	**H**	-	-	**5** (79%)
2	Boc-Trp-OH	**H**	-	-	**6** (80%)
3	Boc-Ser(OBn)-OH	**H**	-	-	**7** (50%)
4	-	**J**	Ala-OMe	-	**8a** (71%)
5	-	**J**	Phe-OBn	-	**9a** (87%)
6	-	**J**	Trp-OMe	-	**10a** (75%)
7	-	**J**	Ala-OMe	Trp-OMe	**11a** (34%)
8	Boc-Phe-OH	**J**	Phe-OBn	-	**12** (87%)
9	Boc-Trp-OH	**J**	Phe-OBn	-	**13** (81%)

[a]Yield after column chromatography.

Then, compounds **8a**, **9a**, **10a** and **11a** were acetylated using pyridine/Ac_2O (2:1) at room temperature for 1 h, affording compounds **8b**, **9b**, **10b** and **11b** with good yields (**Scheme 4.5**).

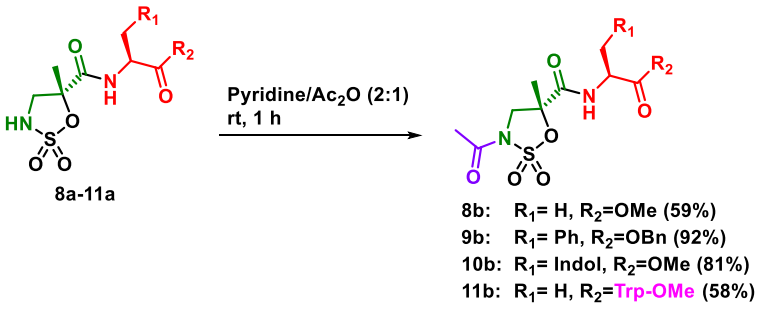

Scheme 4.5. Acetylation of compounds **8a-11a** to obtain peptides **8b-11b**.

Nucleophilic ring-opening reactions were performed on all of the synthetized peptides (**5-7**, **8b-11b**, **12** and **13**) using neat pyridine as nucleophile at 60 ºC for 12 h. Ring-opened Boc-protected peptides were further deprotected by

treatment with TFA/CH_2Cl_2 (1:1) and acetylated using pyridine/Ac_2O (2:1), affording compounds **14-23** in good yields (**Figure 4.4** and **Table 4.2**).

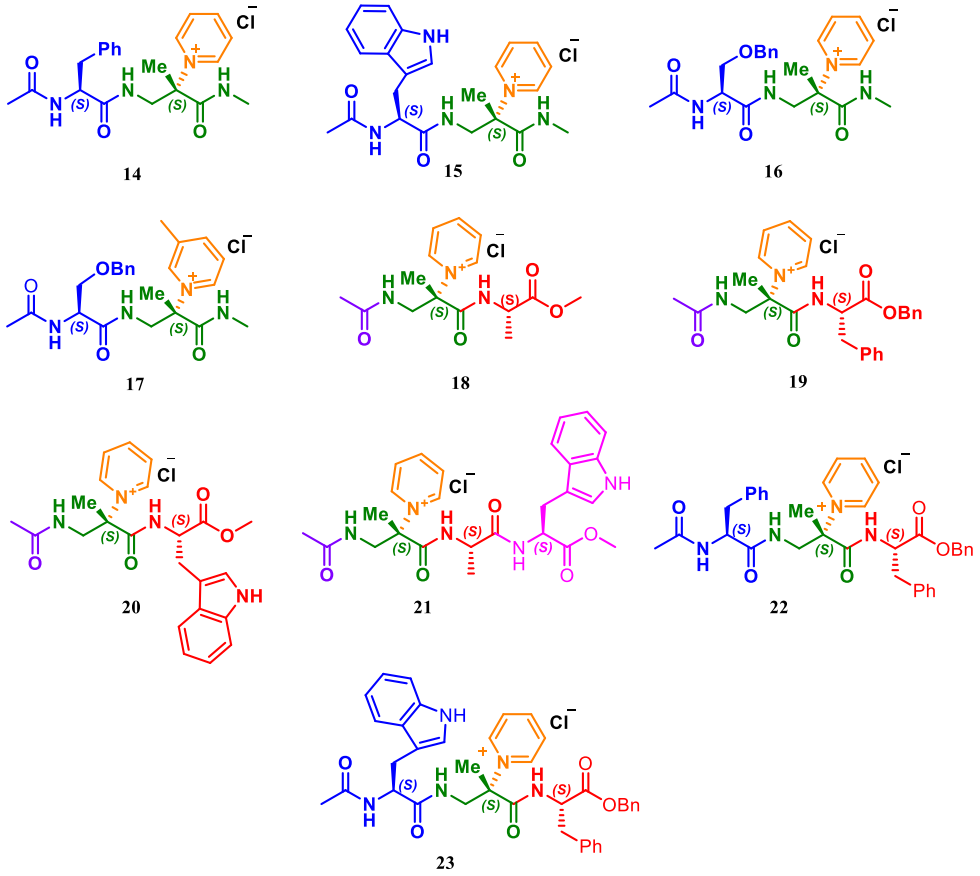

Figure 4.4. Structure of positively charged hybrid peptides **14-23**. In blue is shown the *i*-1 residue, in green, the substructure corresponding to the previous sulfamidate **H** or **J**, in red, the *i*+1 residue, in pink, the *i*+2 residue, in purple, the acetamide group and in orange, the pyridinium side chain.

Table 4.2. Yields obtained for positively charged hybrid peptides **14**-**23**.

Entry	aa-H	Ac-J-aa	Ac-J-aa-aa	aa-J-aa	Final peptide (yield)[a]
1	**5**	-	-	-	**14** (62%)[c]
2	**6**	-	-	-	**15** (51%)[c]
3	**7**	-	-	-	**16** (45%)[c]
4[b]	**7**	-	-	-	**17** (49%)[c]
5	-	**8b**	-	-	**18** (60%)
6	-	**9b**	-	-	**19** (70%)
7	-	**10b**	-	-	**20** (52%)
8	-	-	**11b**	-	**21** (53%)
9	-	-	-	**12**	**22** (30%)[c]
10	-	-	-	**13**	**23** (33%)[c]

[a]Global yields after column chromatography. [b]3-Methyl-pyridinium as a nucleophile was used. [c]Yields obtained after ring-opening, Boc-deprotection and acetylation.

Dipeptides **14-16** (entries 1-3, **Table 4.2**) were obtained in moderate yields after 4 reactions steps. Peptide **7** was ring-opened with 3-methyl-pyridine under the same conditions to give α/β^{2,2}-dipeptide **17** in a similar yield (entry 4, **Table 4.2**). Analogously, α/β^{2,2}-dipeptides (**18-20**) and a α/β^{2,2}-tripeptide (**21**) were also prepared in good yields (entries 5-8 in **Table 4.2**). However, and α/β^{2,2}-tripeptides **22** and **23** (entries 9 and 10) were obtained in low yields after 4 reaction steps. In all the cases, the ring-opening reaction took place with total inversion of configuration at the quaternary center. Small amounts of elimination byproducts (**15′**, **16′**, **18′-23′**) were also observed in some cases as predicted by QM calculations in *chapter 3* (**Figure 4.5**).

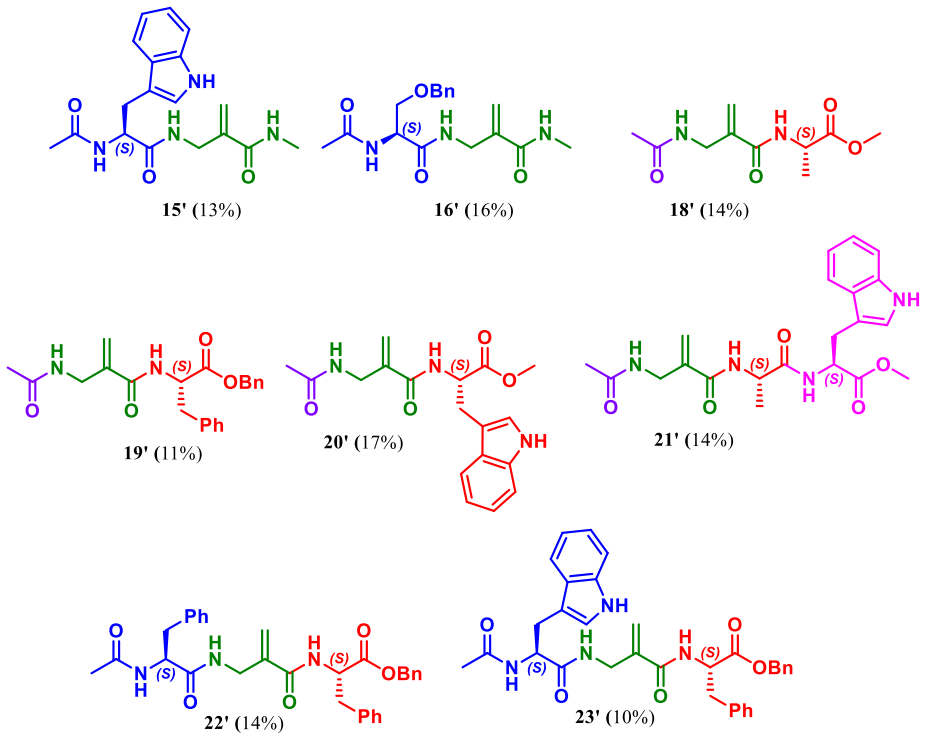

Figure 4.5. α/β-unsaturated peptides obtained as by-products of sulfamidate ring-opening. In blue the *i*-1 residue, in green the part corresponding to the previous sulfamidate **H** or **J**, in red the *i*+1 residue, in pink the *i*+2 residue and in purple the acetamide group.

4.2 Conformational Analysis

The conformational preferences of hybrid peptides **14** and **15** in water were investigated by NOE experiments and MD-tar simulations. The direct interpretation of NOE data in small molecules may lead to the generation of high-energy virtual conformations in terms of a single conformer, since the NOE peaks can correspond to the average of several conformations co-existing in solution. Therefore, and following our reported protocol,[96] the NMR spectroscopic data were combined with time-averaged restrained molecular dynamics (MD-tar) simulations, aiming to obtain a distribution of

low-energy conformers able to quantitatively reproduce the NMR spectroscopic data. This procedure overcomes the limitations inherent to both techniques, namely NMR analysis and unrestricted MD simulations, and provides a robust method to consider molecular flexibility in the interpretation of spectroscopic NMR data.

Experimental distances were deduced from 2D-NOESY cross-peak intensities and were used as restrains in MD-tar simulations using explicit water. The distances obtained from the simulations agreed reasonably well with the experimental ones, confirming that the MD-tar simulations represented in a proper manner the behavior of these peptides in water solution (**Table 4.3**).

Table 4.3. Comparison of the experimental and theoretical distances (in Å) derived from 100 ns MD-tar simulations for compounds **14** (left) and **15** (right).

	Exptl.	MD
NH(J)-Hα(Phe)	2.0	2.4
NH(J)-Hβ$_{ProS}$(J)	2.4	2.7
NH(J)-Hβ$_{ProR}$(J)	2.3	2.6
NH(Phe)-Hα(Phe)	2.4	2.8
NHMe-NH(J)	3.0	3.1
NHMe-Hβ$_{ProR}$(J)	2.4	2.4

	Exptl.	MD
NH(Trp)-H2(Trp)	3.4	3.0
NH(Trp)-Hα (Trp)	2.5	2.8
NH(J)-Hα (Trp)	2.0	2.4
H2(Trp)-Hα(Trp)	3.2	2.9

The most relevant dihedral angles were judged by the Ramachandran plots obtained from the MD simulations. The natural aromatic residues (Phe or Trp) adopt a distribution of extended and folded conformations in both compounds, whereas the β^{2,2}-amino acid is quite rigid, with θ_β and ψ_β values around 180º (**Figures 4.6 and 4.7**).

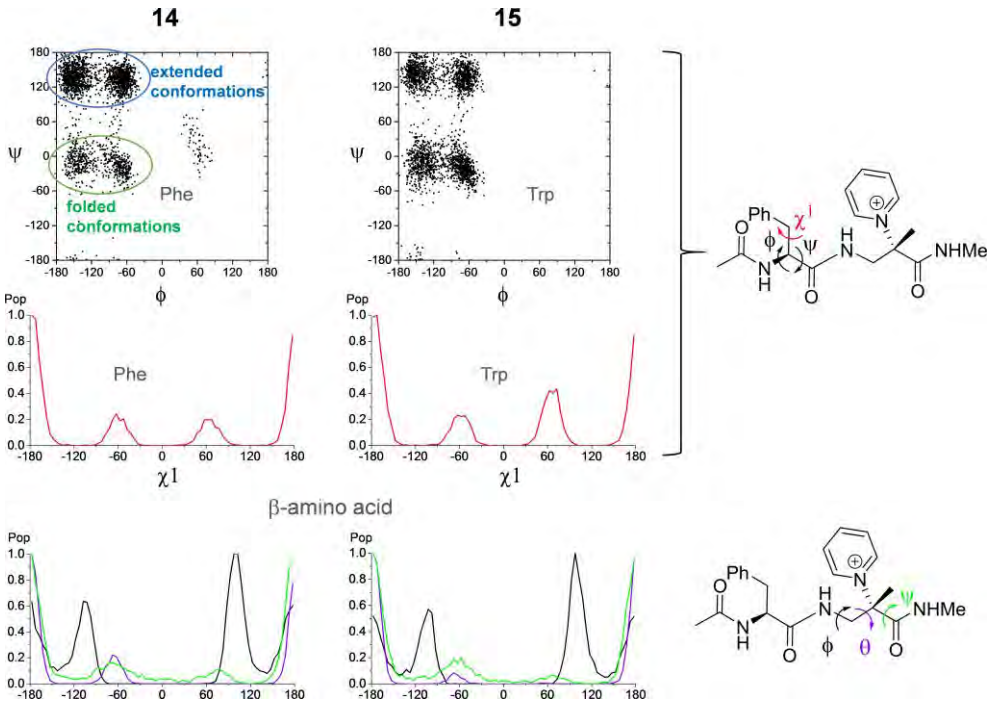

Figure 4.6. Distributions of some relevant torsional angles obtained for peptides **14** and **15** from 100 ns MD-tar simulations in explicit water.

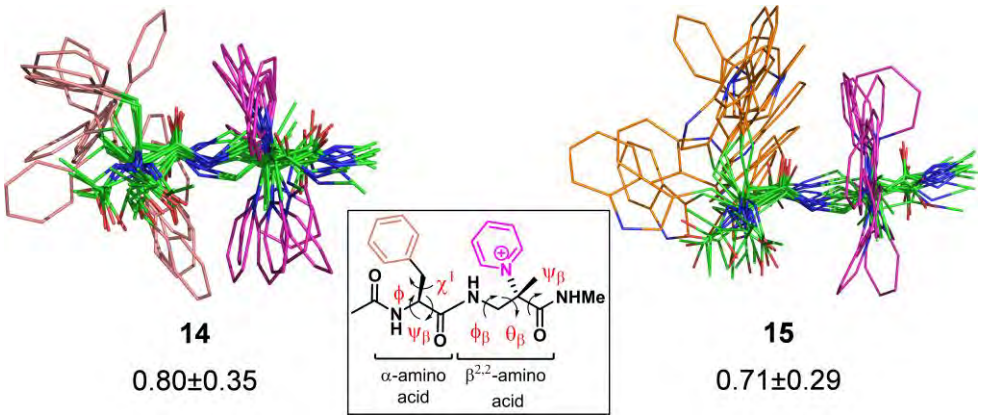

Figure 4.7. Calculated conformational ensembles for peptides **14** and **15** derived from 100 ns MD-tar simulations. Aromatic side chains are shown in pink, and the pyridinium side chain in purple. Root-mean squared deviations (rmsd, average ± standard deviation) are given in Å.

The spatial disposition of the backbone in peptides **14** and **15** allows the appearance of persistent aromatic interactions between the neutral aromatic (phenyl/indolyl) and charged pyridinium moieties. Such interactions are observed around 25% of the total simulation time and their existence is demonstrated the appearance of NOE cross-peaks between inter-residue aromatic protons (**Figure 4.8**).

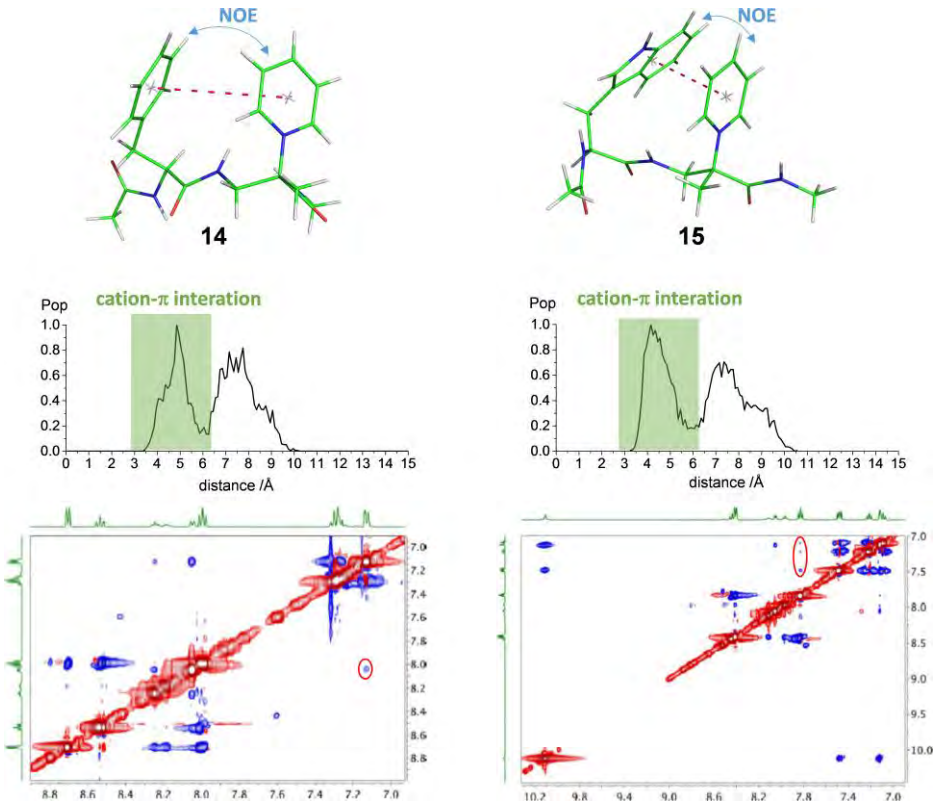

Figure 4.8. Distribution of the distances between the centroids of the aromatic groups in peptides **14** and **15** derived from 100 ns MD-tar simulations in explicit water (top), and the corresponding aromatic hydrogens regions of the 2D-NOESY spectra (bottom).

4.3 Conclusions

A library of α/β^{2,2}-hybrid di- and tri-peptides incorporating an α-methylisoserine sulfamidate has been synthesized. Some of these oligopeptides were activated for sulfamidate ring-opening by capping its *N*-terminal position as a sulfonylacetamide and were able to undergo the ring-opening reaction with total inversion of the configuration at the quaternary carbon using pyridine as a nucleophile. The use of pyridine provided positively charged α/β^{2,2}-hybrid di- and tri-peptides in good yields. MD simulations and 2D-NOESY experiments confirmed that these positively charged peptides engage in noncovalent aromatic interactions between the aromatic ring of the *i*-1 amino acid and the pyridinium moiety. These findings offer new opportunities to access and stabilize novel architectures not previously observed in α- or β-peptides, with potential applications in molecular recognition and drug discovery.

These results have been published in the journal Organic Letters (*Org. Lett.* **2015**, *17*, 5804–5807).

4.4 References

(1) Meyer, E. A.; Castellano, R. K.; Diederich, F. *Interactions with Aromatic Rings in Chemical and Biological Recognition*; 2003; Vol. 42.

(2) Salonen, L. M.; Ellermann, M.; Diederich, F. *Angew. Chem. Int. Ed.* **2011**, *50*, 4808–4842.

(3) Mahadevi, A. S.; Sastry, G. N. *Chem. Rev.* **2013**, *113*, 2100–2138.

(4) Ma, J. C.; Dougherty, D. A. *Chem. Rev.* **1997**, *97*, 1303–1324.

(5) Perrin, C. L.; Nielson, J. B. *Annu. Rev. Phys. Chem.* **1997**, *48*, 511–544.

(6) Joseph, J.; Jemmis, E. D. *J. Am. Chem. Soc.* **2007**, *129*, 4620–4632.

(7) Parthasarathi, R.; Subramanian, V.; Sathyamurthy, N. *J. Phys. Chem. A* **2006**, *110*, 3349–3351.

(8) Hunter, C. A.; Sanders, J. K. M. *J. Am. Chem. Soc.* **1990**, *112*, 5525–5534.

(9) Sinnokrot, M. O.; Valeev, E. F.; Sherrill, C. D. *J. Am. Chem. Soc.* **2002**, *124*, 10887–10893.

(10) Morokuma, K. *Acc. Chem. Res.* **1977**, *10*, 294–300.

(11) Bowen, R. D. *Acc. Chem. Res.* **1991**, *24*, 364–371.

(12) Torrice, M. M.; Bower, K. S.; Lester, H. A.; Dougherty, D. A. *Proc. Natl. Acad. Sci.* **2009**, *106*, 11919–11924.

(13) Kool, E. T.; Waters, M. L. *Nat. Chem. Biol.* **2007**, *3*, 70–73.

(14) Sunner, J.; Nishizawa, K.; Kebarle, P. *J. Phys. Chem.* **1981**, *85*, 1814–1820.

(15) Faraoni, R.; Castellano, R. K.; Gramlich, V.; Diederich, F. *Chem. Commun.* **2004**, 370–371.

(16) Dvornikovs, V.; Smithrud, D. B. *J. Org. Chem.* **2002**, *67*, 2160–2167.

(17) Vysotsky, M. O.; Pop, A.; Broda, F.; Thondorf, I.; Böhmer, V. *Chem. Eur. J.* **2001**, *7*, 4403–4410.

(18) Whiting, A. L.; Hof, F. *Org. Biomol. Chem.* **2012**, *10*, 6885–6892.

(19) Shukla, R.; Lindeman, S. V.; Rathore, R. *Chem. Commun.* **2009**, 5600–5602.

(20) Park, S. J.; Hong, J.-I. *Chem. Commun.* **2001**, 1554–1555.

(21) Kim, S. K.; Sim, W.; Seung, J. *Tetrahedron* **2003**, *44*, 805–809.

(22) Kim, S. K.; Lee, J. K.; Lee, S. H.; Lim, M. S.; Lee, S. W.; Sim, W.; Kim, J. S. *J. Org. Chem.* **2004**, *69*, 2877–2880.

(23) Zyryanov, G. V.; Rudkevich, D. M. *J. Am. Chem. Soc.* **2004**, *126*, 4264–4270.

(24) Sgarlata, V.; Organo, V. G.; Rudkevich, D. M. *Chem. Commun.* **2005**, 5630–5632.

(25) Organo, V. G.; Rudkevich, D. M. *Chem. Commun.* **2007**, 3891–3899.

(26) Umadevi, D.; Sastry, G. N. *J. Phys. Chem. C* **2011**, *115*, 9656–9667.

(27) Carlier, P. R.; Lam, P. C.-H.; Wong, D. M. *J. Org. Chem.* **2002**, *67*, 6256–6259.

(28) Lakshminarasimhan, P.; Sunoj, R. B.; Chandrasekhar, J.; Ramamurthy, V. *J. Am. Chem. Soc.* **2000**, *122*, 4815–4816.

(29) Stratakis, M.; Froudakis, G. *Org. Lett.* **2000**, *2*, 1369–1372.

(30) Stratakis, M.; Nencka, R.; Rabalakos, C.; Adam, W.; Krebs, O. *J. Org. Chem.* **2002**, *67*, 8758–8763.

(31) Stratakis, M.; Kalaitzakis, D.; Stavroulakis, D.; Kosmas, G.; Tsangarakis, C. *Org. Lett.* **2003**, *5*, 3471–3474.

(32) Katz, C. E.; Aubé, J. *J. Am. Chem. Soc.* **2003**, *125*, 13948–13949.

(33) Yao, L.; Aubé, J. *J. Am. Chem. Soc.* **2007**, *129*, 2766–2767.

(34) Gutierrez, O.; Aubé, J.; Tantillo, D. J. *J. Org. Chem.* **2012**, *77*, 640–647.

(35) Katz, C. E.; Ribelin, T.; Withrow, D.; Basseri, Y.; Manukyan, A. K.; Bermudez, A.; Nuera, C. G.; Day, V. W.; Powell, D. R.; Poutsma, J. L.; Aubé, J. *J. Org. Chem.* **2008**, *73*, 3318–3327.

(36) Szostak, M.; Yao, L.; Aube, J. *J. Org. Chem.* **2010**, *75*, 1235–1243.

(37) Yamada, S.; Inoue, M. *Org. Lett.* **2007**, *9*, 1477–1480.

(38) Yamada, S.; Fossey, J. S. *Org. Biomol. Chem.* **2011**, *9*, 7275–7281.

(39) Yamada, S.; Kawamura, C. *Org. Lett.* **2012**, *14*, 1572–1575.

(40) Yamada, S.; Morita, C. *J. Am. Chem. Soc.* **2002**, *124*, 8184–8185.

(41) Acharya, P.; Plashkevych, O.; Morita, C.; Yamada, S.; Chattopadhyaya, J. *J. Org. Chem.* **2003**, *68*, 1529–1538.

(42) Yamada, S.; Misono, T.; Tsuzuki, S. *J. Am. Chem. Soc.* **2004**, *126*, 9862–9872.

(43) Yamada, S.; Uematsu, N.; Yamashita, K. *J. Am. Chem. Soc.* **2007**, *129*, 12100–12101.

(44) Yamada, S.; Misono, T.; Iwai, Y.; Masumizu, A.; Akiyama, Y. *J. Org. Chem.* **2006**, *71*, 6872–6880.

(45) Yamada, S.; Morimoto, Y. *Tetrahedron Lett.* **2006**, *47*, 5557–5560.

(46) Yamada, S. *Org. Biomol. Chem.* **2007**, *5*, 2903–2912.

(47) Yamada, S.; Tokugawa, Y.; Nojiri, Y.; Takamori, E. *Chem. Commun.* **2012**, *48*, 1763–1765.

(48) Burghardt, T. P.; Jurani??, N.; Macura, S.; Ajtai, K. *Biopolymers* **2002**, *63*, 261–272.

(49) Gustiananda, M.; Liggins, J. R.; Cummins, P. L.; Gready, J. E. *Biophys. J.* **2004**, *86*, 2467–2483.

(50) Andersen, N. H.; Olsen, K. A.; Fesinmeyer, R. M.; Tan, X.; Hudson, F. M.; Eidenschink, L. A.; Farazi, S. R. *J. Am. Chem. Soc.* **2006**, *128*, 6101–6110.

(51) Barbaras, D.; Gademann, K. *ChemBioChem* **2008**, *9*, 2398–2401.

(52) Zheng, X.; Wu, C.; Ponder, J. W.; Marshall, G. R. *J. Am. Chem. Soc.* **2012**, *134*, 15970–15978.

(53) Queralt-Rosinach, N.; Mestres, J. *Eur. Biophys. J.* **2010**, *39*, 1471–1475.

(54) Sörme, P.; Arnoux, P.; Kahl-Knutsson, B.; Leffler, H.; Rini, J. M.; Nilsson, U. J. *J. Am. Chem. Soc.* **2005**, *127*, 1737–1743.

(55) Inagaki, Y.; Pham, T. T.; Fujiwara, Y.; Kohno, T.; Osborne, D. A.; Igarashi, Y.; Tigyi, G.; Parrill, A. L. *Biochem. J.* **2005**, *389*, 187–195.

(56) Paddock, M. L.; Weber, K. H.; Chang, C.; Okamura, M. Y. *Biochemistry* **2005**, *44*, 9619–9625.

(57) Wei, Y.; Horng, J. C.; Vendel, A. C.; Raleigh, D. P.; Lumb, K. J. *Biochemistry* **2003**, *42*, 7044–7049.

(58) Klenchin, V. A.; Ringia, E. A. T.; Gerlt, J. A.; Rayment, I. *Biochemistry* **2003**, *42*, 14427–14433.

(59) Parihar, H. S.; Kirschbaum, K. S. *Bioorganic Med. Chem. Lett.* **2002**, *12*, 2743–2747.

(60) Luque, L. E.; Grape, K. P.; Junker, M. *Biochemistry* **2002**, *41*, 13663–13671.

(61) Matthias Ullmann, G.; Hauswald, M.; Jensen, A.; Kostić, N. M.; Knapp, E. W. *Biochemistry* **1997**, *36*, 16187–16196.

(62) Scrutton, N. S.; Raine, A. R. C. *Biochem. J.* **1996**, *319*, 1–8.

(63) Chen, C. C.; Hsu, W.; Kao, T. C.; Horng, J. C. *Biochemistry* **2011**, *50*, 2381–2383.

(64) Kenoth, R.; Kamlekar, R. K.; Simanshu, D. K.; Gao, Y.; Malinina, L.; Prendergast, F. G.; Molotkovsky, J. G.; Patel, D. J.; Venyaminov, S. Y.; Brown, R. E. *Biochemistry* **2011**, *50*, 5163–5171.

(65) Pan, Y.; Zhang, K.; Qi, J.; Yue, J.; Springer, T. A.; Chen, J. *Proc. Natl. Acad. Sci.* **2010**, *107*, 21388–21393.

(66) Jehle, S.; Rajagopal, P.; Bardiaux, B.; Markovic, S.; Stout, J. R.; Higman, V. A.; Klevit, R. E.; Rossum, B. Van; Oschkinat, H. *Nat. Struct. Mol. Biol.* **2010**, *17*, 1037–1042.

(67) Vivoli, M.; Angelucci, F.; Ilari, A.; Morea, V.; Angelaccio, S.; Di Salvo, M. L.; Contestabile, R. *Biochemistry* **2009**, *48*, 12034–12046.

(68) Hoette, T. M.; Abergel, R. J.; Xu, J.; Strong, R. K.; Raymond, K. N. *J. Am. Chem. Soc.* **2008**, *130*, 17584–17592.

(69) Wickstrom, L.; Bi, Y.; Hornak, V.; Raleigh, D. P.; Simmerling, C. *Biochemistry* **2007**, *46*, 3624–3634.

(70) Prajapati, R. S.; Sirajuddin, M.; Durani, V.; Sreeramulu, S.; Varadarajan, R. *Biochemistry* **2006**, *45*, 15000–15010.

(71) Raines, D. E. *J. Pharmacol. Exp. Ther.* **2004**, *311*, 14–21.

(72) Burley, S. K.; Petsko, G. A. *FEBS Lett.* **1986**, *203*, 139–143.

(73) Shi, Z.; Olson, C. A.; Kallenbach, N. R. *J. Am. Chem. Soc.* **2002**, *124*, 3284–3291.

(74) Gasymov, O. K.; Abduragimov, A. R.; Glasgow, B. J. *Biochemistry* **2012**, *51*, 2991–3002.

(75) Wouters, J. *Protein Sci.* **1998**, *7*, 2472–2475.

(76) Zabell, A. P. R.; Schroff, A. D.; Bain, B. E.; Van Etten, R. L.; Wiest, O.; Stauffacher, C. V. *J. Biol. Chem.* **2006**, *281*, 6520–6527.

(77) Parrill, A. L.; Wanjala, I. W.; Pham, T.; Baker, D. L. *BMC Biochem.* **2011**, *12:65*.

(78) Collard, F.; Fagan, R. L.; Zhang, J.; Nemet, I.; Palfey, B. A.; Monnier, V. M. *Biochemistry* **2011**, *50*, 7977–7986.

(79) Faraldos, J. A.; Antonczak, A. K.; González, V.; Fullerton, R.; Tippmann, E. M.; Allemann, R. K. *J. Am. Chem. Soc.* **2011**, *133*, 13906–13909.

(80) Bale, S.; Brooks, W.; Hanes, J. W.; Mahesan, A. M.; Guida, W. C.; Ealick, S. E. *Biochemistry* **2009**, *48*, 6423–6430.

(81) Zhang, M.; Cho, E. J.; Burstein, G.; Siegel, D.; Zhang, Y. *ACS Chem. Biol.* **2011**, *6*, 511–519.

(82) Singh, S.; Ashish; Dikshit, K. L. *FEBS Lett.* **2012**, *586*, 653–658.

(83) Janardhan, S.; Srivani, P.; Sastry, G. N. *Curr. Med. Chem.* **2006**, *13*, 1169–1186.

(84) Bindu, P. H.; Sastry, G. M.; Murty, U. S.; Sastry, G. N. *Biochem. Biophys. Res. Commun.* **2004**, *319*, 312–320.

(85) Hima Bindu, P.; Madhavi Sastry, G.; Narahari Sastry, G. *Biochem. Biophys. Res. Commun.* **2004**, *320*, 461–467.

(86) Chourasia, M.; Sastry, G. M.; Sastry, G. N. *Biochem. Biophys. Res. Commun.* **2005**, *336*, 961–966.

(87) Goldstein, R.; Cheng, J.; Stec, B.; Roberts, M. F. *Biochemistry* **2012**, *51*, 2579–2587.

(88) Gruber, K.; Zhou, B.; Houk, K. N.; Lerner, R. A.; Shevlin, C. G.; Wilson, I. A. *Biochemistry* **1999**, *38*, 7062–7074.

(89) Tayubi, I. a.; Sethumadhavan, R. *Biochemistry* **2010**, *75*, 912–918.

(90) Paschall, C. M.; Hasserodt, J.; Jones, T.; Lerner, R. A.; Janda, K. D.; Christianson, D. W. *Angew. Chem. Int. Ed.* **1999**, *38*, 1743–1747.

(91) Glesner, J.; Wünschmann, S.; Li, M.; Gustchina, A.; Wlodawer, A.; Himly,

M.; Chapman, M. D.; Pomés, A. *PLoS One* **2011**, *6*, 1–11.

(92) Lin, C.; Chinnappan, R.; Acharya, K.; Pellequer, J. L.; Jankowiak, R. *Biophys. Chem.* **2011**, *154*, 35–40.

(93) Paulsen, M. H.; Karlsen, E. A.; Ausbacher, D.; Anderssen, T.; Bayer, A.; Ochtrop, P.; Hedberg, C.; Haug, T.; Ericson Sollid, J. U.; Strøm, M. B. *J. Pept. Sci.* **2018**, *24*, e3117.

(94) Shai, Y. *Membr. Act. Antimicrob. Pept.* **2002**, *66*, 236–248.

(95) García-González, I.; Mata, L.; Corzana, F.; Jiménez-Osés, G.; Avenoza, A.; Busto, J. H.; Peregrina, J. M. *Chem. Eur. J.* **2015**, *21*, 1156–1168.

(96) Corzana, F.; Busto, J. H.; Engelsen, S. B.; Jiménez-Barbero, J.; Asensio, J. L.; Peregrina, J. M.; Avenoza, A. *Chem. Eur. J.* **2006**, *12*, 7864–7871.

Chapter 5.
Inhibition of amyloid fibrillation with sulfamidate-modified BSBP

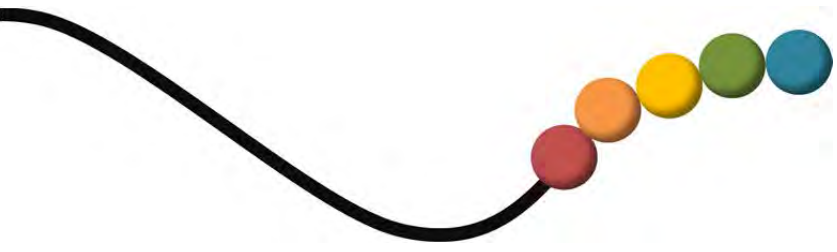

Alzheimer's disease (AD) is one of the main causes of dementia and a leading cause of death in the world.[1] It was firstly described by the German psychiatrist Alois Alzheimer in 1906, when he psychoanalyzed a patient, who had several strange symptoms and short-term memory losses.[2] When the patient died, Alzheimer examined the brain in collaboration with two Italians doctors and detected amyloid plaques and neurofibrillary tangles. These brain anomalies would become identifiers of what later became known as Alzheimer's disease. AD is a progressive and devastating neurodegenerative disorder characterized by memory loss and a variety of cognitive disabilities,[3,4] such as problems with language or disorientation (**Figure 5.1**).

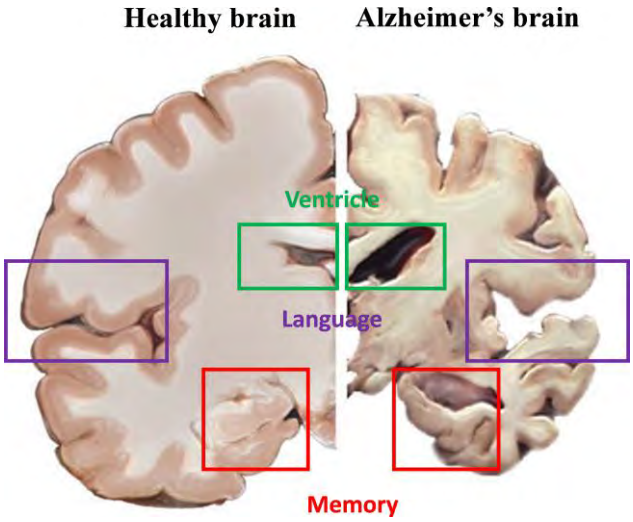

Figure 5.1. Brain cross-sections (left: healthy brain, right: Alzheimer's disease-affected brain).

To date, this disease has no cure or effective treatment. Only certain drugs have been developed to mitigate the symptoms. These symptoms usually appear in people between 60 and 70 years old. Many experts believe that this disease is an inevitable consequence of aging and every elder person will

show some of the symptoms from 90 years old on. However, other risk factors such as depression, hypertension or head injuries may accelerate the process (**Figure 5.2**).

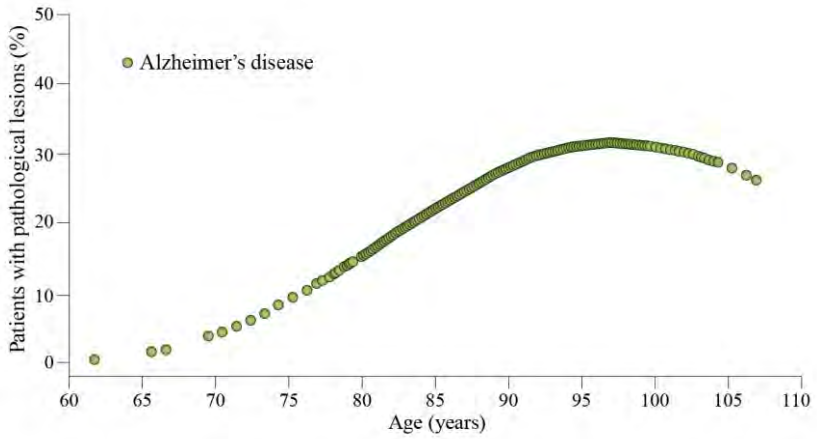

Figure 5.2. Alzheimer disease of different patients vs age.[5,6]

Nowadays, the research lines to find a cure for this disease are focused on two possible mechanisms. One of them is based on the so-called *Tau* proteins and, the other, on the so-called *β-amyloid* protein.

Tau proteins

Healthy neurons are composed of a cytoskeleton formed by microtubules. These act as rails that guide nutrients and other biomolecules from the neuronal body to the ends of the axons, and *vice versa*. *Tau proteins* are responsible for stabilizing these microtubules. However, when this protein is hyperphosphorylated, due to eventual chemical changes within the cell, they form aggregates, creating neurofibrillary tangles, and disintegrating the transport system of the neuron. As a consequence, neurons begin to die and the disease shows the first symptoms (**Figure 5.3**).[7]

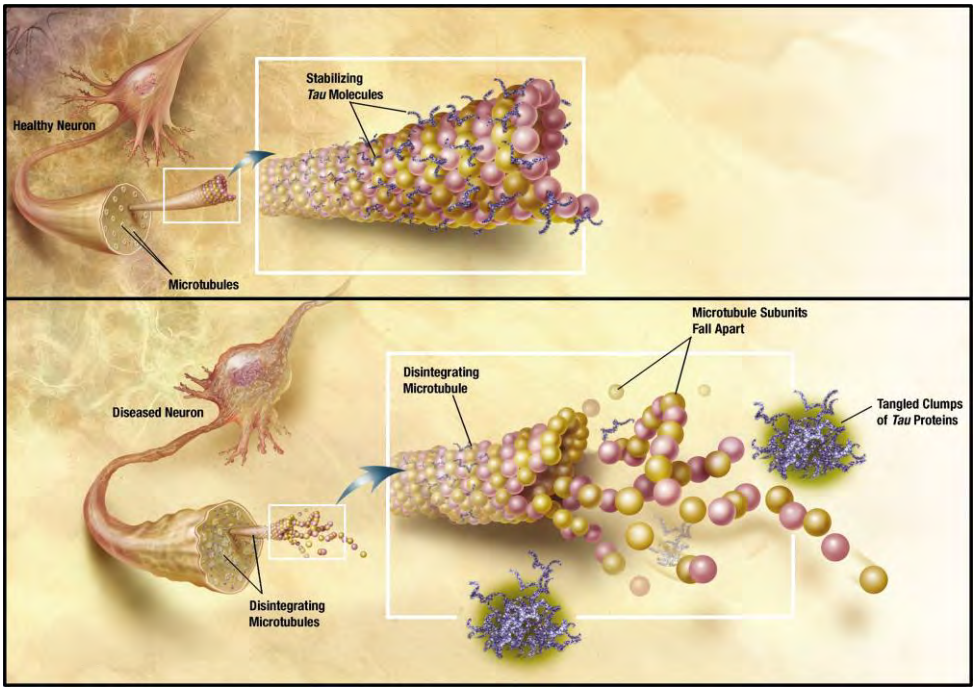

Figure 5.3. Tau protein neurodegeneration mechanism (reproduced from https://www.nia.nih.gov/health/what-happens-brain-alzheimers-disease)

β-amyloid

On the other hand, the amyloid precursor protein (APP) located in the cell wall of the neurons is crucial for their growth, survival and regeneration. Eventually, this protein undergoes proteolysis by the γ- and β- secretases generating, among other products, the so-called *β-amyloid protein* (βA), a peptide formed by 36 to 42 amino acids (amino acid sequence in humans: DAEFRHDSGYEVHHQKLVFFAEDVGSNKGAIIGLMVGGVVIA)
whose biological functions include protection against oxidative stress and antimicrobial activity. Mutations in the gene coding for APP induce an increase in the production of β-amyloid, causing aggregation into oligomers, then fibrils and, if production rises high enough, plaques which eventually cause cell death (**Figure 5.4**).[8]

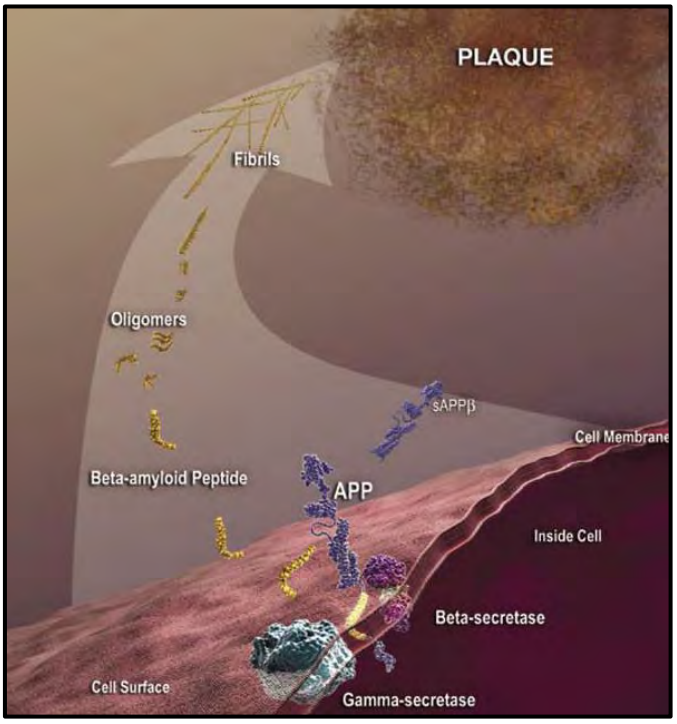

Figure 5.4. β-amyloid neurodegeneration mechanism (reproduced from https://commons.wikimedia.org/wiki/File:Alzheimers_disease-Beta-amyloid_plaque_formation.png)

There are many research groups focused on the study of this last mechanism and the development of new strategies to avoid β-amyloid accumulation. Some of this strategies consist of interfering on the formation and deposition of fibrils:[9–11]

- Screening of chemical compounds libraries and the search for endogenous cellular factors capable of binding to βA.
- Passive and active immunization.
- Design of small organic ligands able to specifically bind to βA.
- Inhibition of the β- or γ-secretase enzymatic activity.
- Activation of βA degradation pathways.

- Inhibition of other effects of the disease, such as inflammation and oxidative stress, that may be directly associated with the formation of fibrils.

The identification of compounds able to stabilize the βA α-helix native structure or to destabilize the non-native β-sheet structure that proceeds fibril aggregation is one of the most recent research therapeutic lines for the treatment of amyloidogenic pathological conditions.[9,10,12,13]

One of the most promising strategies was developed by Soto and co-workers and is based on using small peptides able to bind to native β-amyloid monomer without participating on the β-sheet structure. Thus, the bonds between oligomers are destabilized, preventing the formation of plaques and ultimately neuron death. These peptides called β-sheet breaker peptides (BSBP) incorporate a single mutation -valine into proline- in the β-amyloid hydrophobic core (LVFF) responsible for fibril formation (**Figure 5.5**).[14,15]

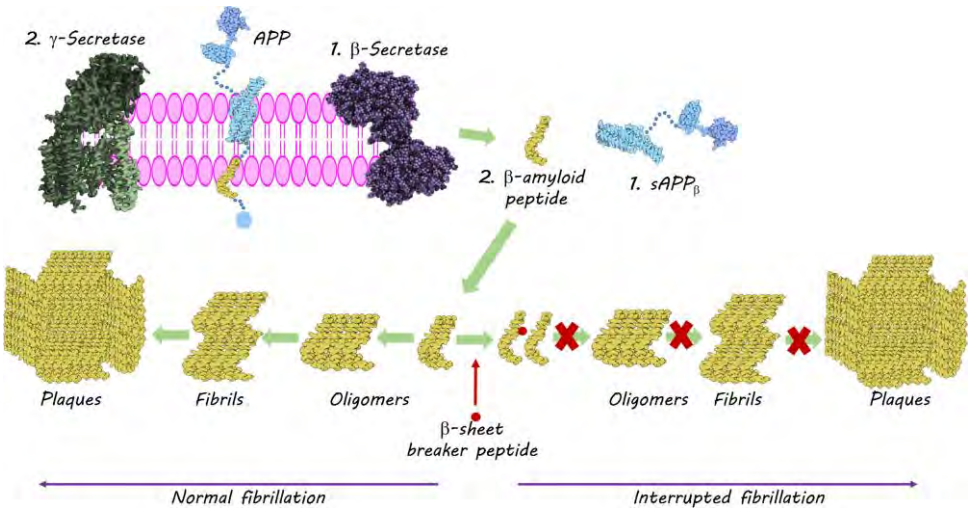

Figure 5.5. β-sheet breaker peptides mechanism.

Based on the same strategy, other research groups have developed different candidates by modifying Soto's small peptide. Some of these modifications include: *N*-methylation of one of the two phenylalanines,[16,17] thus impeding the formation of the hydrogen bond through the corresponding amide group; incorporation of two α,β-unsaturated phenylalanines (α,β-dehydrophenylalanines),[18] thus rigidifying and changing the motif's three-dimensional structure; substitution of the unnatural proline (natively a valine) by aspartic acid,[19] which generates a breaker element *in situ* resulting in a kink into the peptide backbone; fluorination of hydrophobic amino acids (valine, phenylalanine or proline),[20] thus changing the polarization of the C–H geminal bonds. Finally, retro-inverse analogues of the motif generated by substituting the L-amino acids for D-counterparts and reversing the sequence, have been also used (**Figure 5.6**).[21,22]

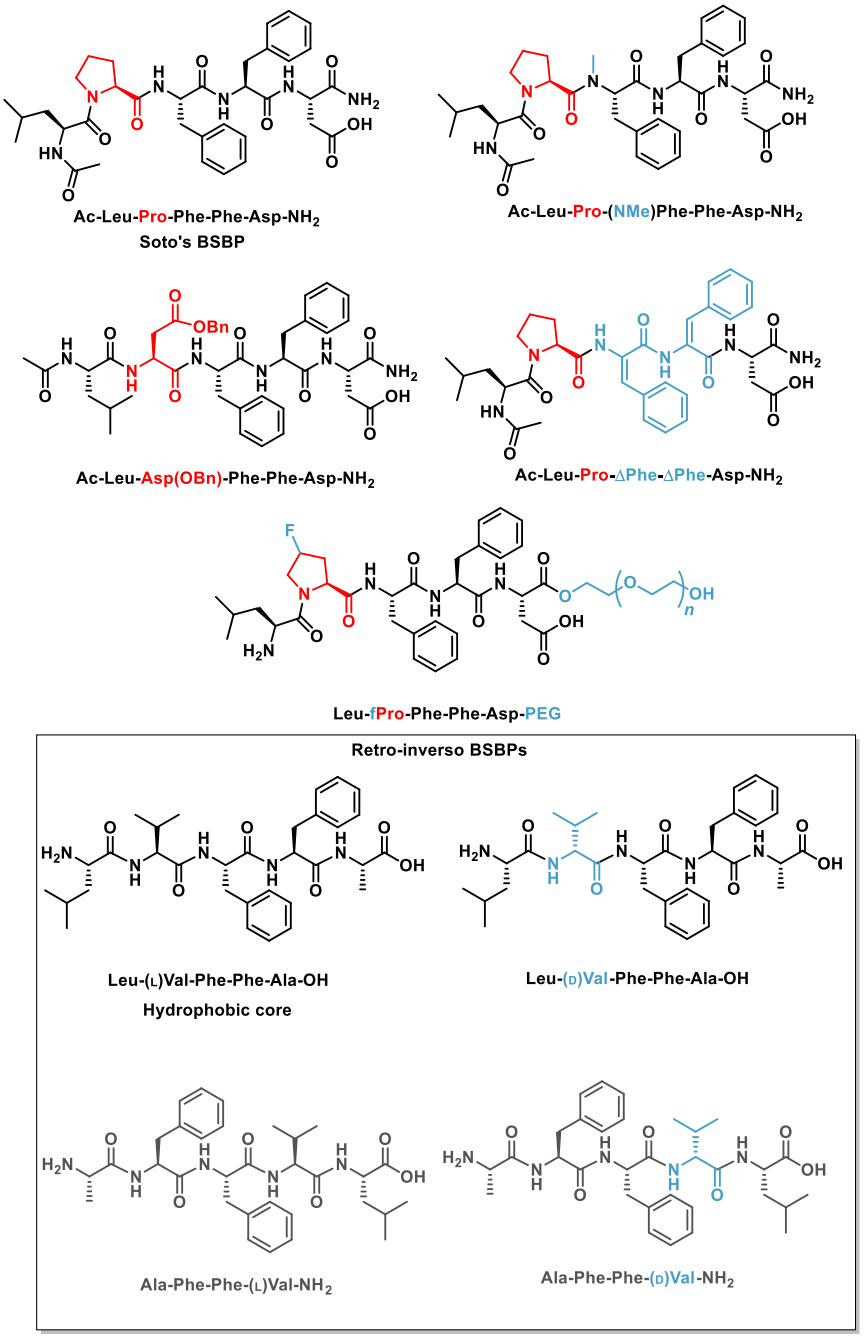

Figure 5.6. β-sheet breaker peptides incorporating natural α-amino acids.

In order to increase the resistance to proteolysis of these natural candidates, non-proteinogenic amino acids, such as *o*-aminobenzoic acid,[23] azetidin-2-carboxylic acid, 3-phenyl derivatives, β-homoproline or β-sulfonylproline have also been proposed. *N*-terminal sulfonamide derivatives have also been investigated since they could form atypical hydrogen bonds, due to the presence of two oxygen atoms bound to sulfur (**Figure 5.7**).[24–26]

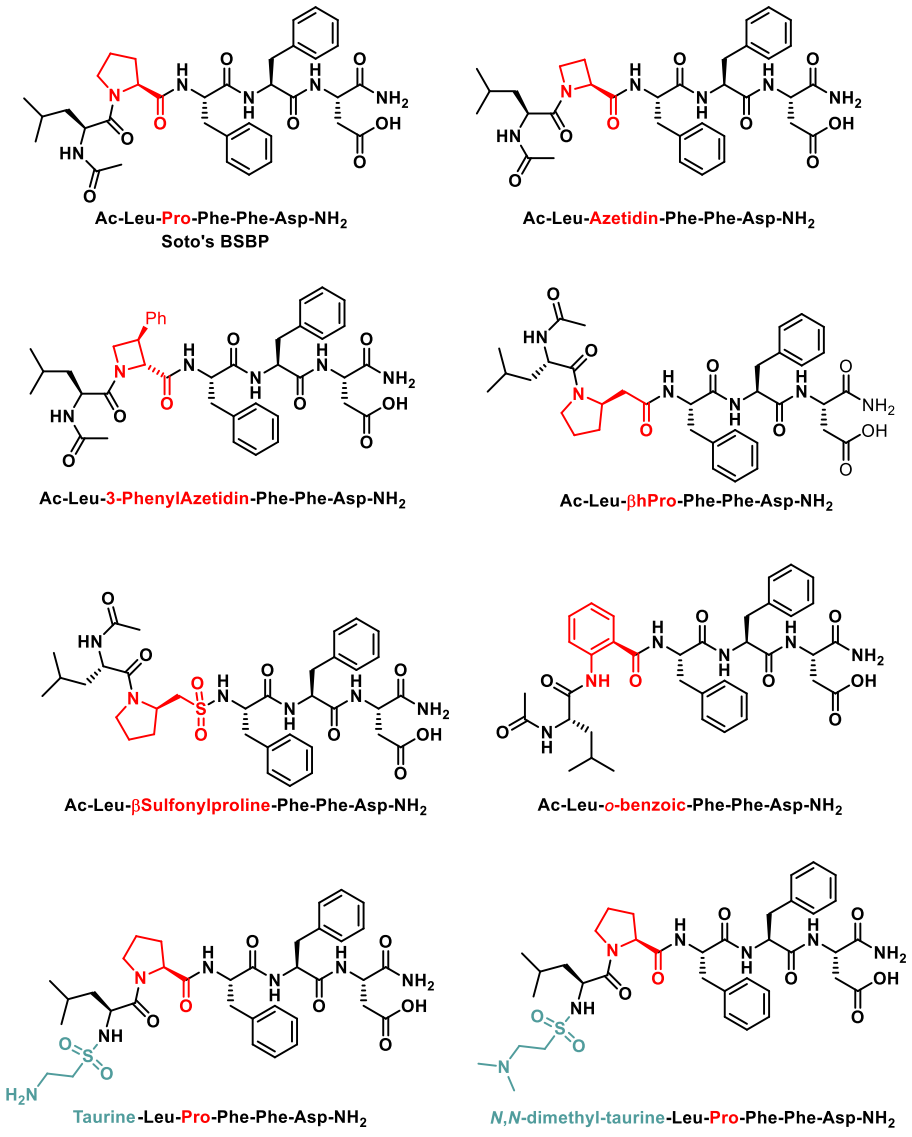

Figure 5.7. β-sheet breaker peptides incorporating unnatural amino acid residues.

Taking into account all of these ideas, we aimed to synthesize new BSBPs based on the β-amyloid hydrophobic fragment LVFF. The valine residue will be replaced by a $\beta^{2,2}$-amino acid, namely α-methylisoserine sulfamidate, which can be regarded as a proline mimic. We hypothesized that the endo- and exocyclic oxygen atoms present in the sulfamidate scaffold, in addition to its cyclic structure, would create new patterns of interactions, giving rise to a novel type of folded structures and, ultimately, inhibiting the aggregation of the β-amyloid. (**Figure 5.8**).

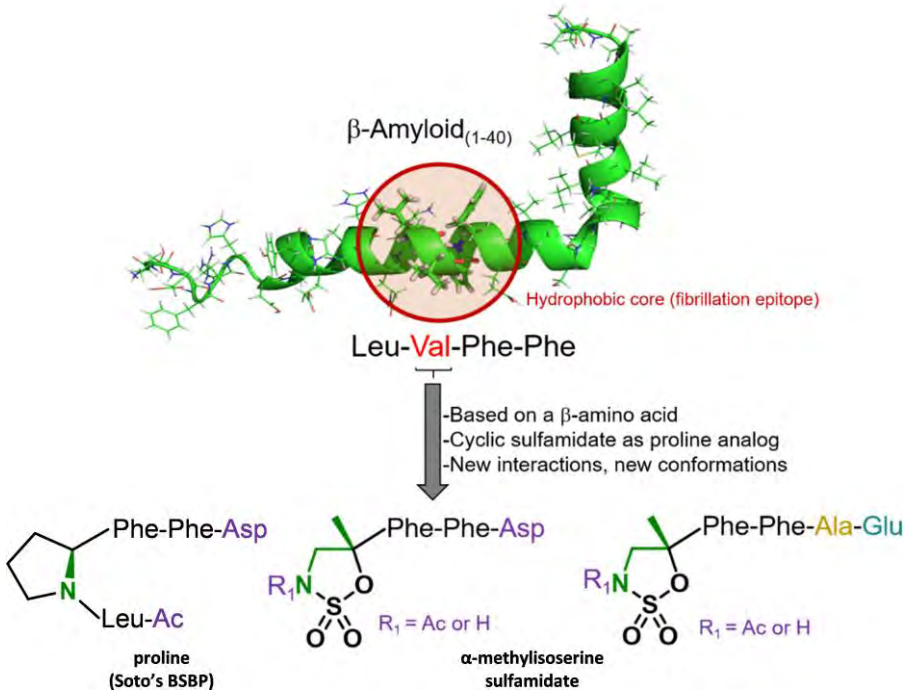

Figure 5.8. Figure of our β-sheet breaker peptides based on Soto's motif (Ac-Leu-Pro-Phe-Phe-Asp).

5.1 Synthesis of new BSBPs

To confirm this hypothesis, we designed and synthesized peptides based on Soto's motif by Solid-Phase Peptide Synthesis (SPPS), incorporating our α-methylisoserine sulfamidate. Keeping in mind our experience and challenges in the synthesis of small peptides incorporating sulfamidates in homogeneous phase,[27] for this work, the coupling of this scaffold in longer peptides was developed and optimized using the more convenient microwave-assisted SPPS (MW-SPPS). The main advantages of incorporating amino acids using a solid support are the higher purity of the final peptide and the possibility of synthesizing longer peptides, in comparison to homogeneous phase synthesis.

Solid Phase Peptide Synthesis

The concept of solid phase synthesis was developed in 1963 by Merrifield.[28] In modern SPPS, the instrument is equipped with a channel system to automatically perform pumping, mixing, and removal of solutions. The automated peptide synthesizer contains bottles for all chemicals (amino acids, solvents, activator and base) and ensures adequate delivery and disposal of the solutions.

SPPS needs an insoluble solid support, called resin, which contains a linker capable to liberate the peptide in the last step. In this type of synthesis, the carboxylic acid of the first amino acid is coupled to the resin. Resins consist of polymer particles that bind to the *C*-terminus of the growing peptide and protect it from potential side-reactions during the process.

In order to get better results and increase the reaction yield, the *N*-terminal group and reactive side-chain moieties of amino acids must be blocked. *N*-terminal protecting groups must be removed specifically after each successful coupling step, while the side-chain protecting groups and the resin linkage

keep protected against unwanted side-reactions. Additionally, the carboxyl groups of the sequentially added amino acids must be activated by coupling agents to increase their electrophilicity towards the formation of the new peptide bond. After loading of the resin, the *N*-terminal protecting group of the first amino acid is removed and the next activated amino acid can be coupled. These alternating steps of terminal *N*-deprotection, activation and coupling are repeated until the desired peptide is obtained. As the next step, it is desirable to simultaneously remove the side-chain protecting groups and liberate the peptide from the resin. This process is called *"cleavage"*, and in our case, it will be performed under acidic conditions (**Scheme 5.1**).

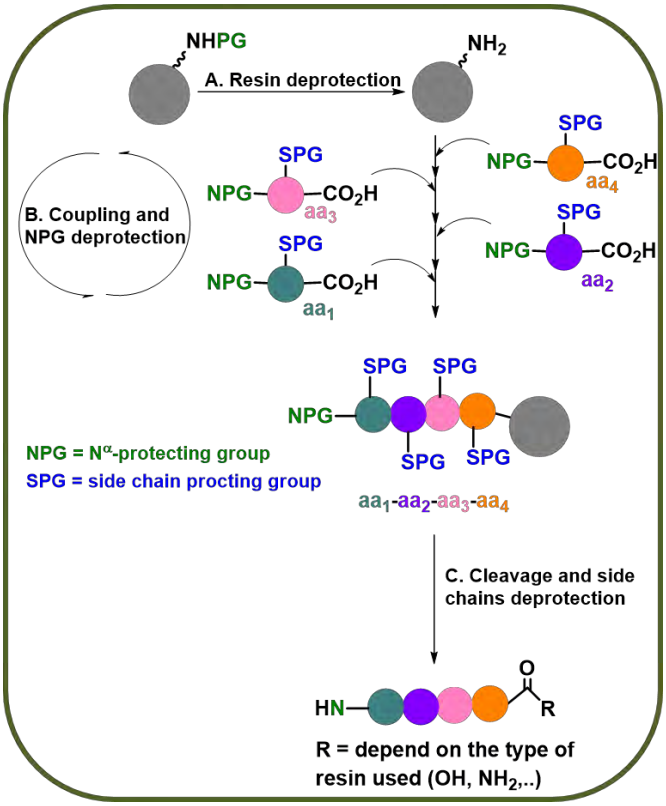

Scheme 5.1. Scheme of a general SPPS route.

The crude product can be easily separated from the resin by filtration and purified by standard chromatographic methods such as HPLC. The correct peptide signal can be identified by mass spectrometry (MS) with soft ionization techniques such as ESI or MALDI-TOF.

Coupling α-methylisoserine sulfamidate (J) to H-**[peptide]-*resin***

The sequence Phe-Phe-Asp was selected as a benchmark for optimizing the coupling step to obtain peptide **24** [**J**-Phe-Phe-Asp-NH_2]. Different temperatures, times and coupling reagents were tested. The influence of microwave assistance was also assayed using a CEM Liberty-Blue instrument (**Table 5.1**). When coupling was attempted manually without microwave assistance, no coupling product was detected after 18 h at room temperature and only starting material (Phe-Phe-Asp-NH_2) was recovered after final cleavage (**Table 5.1**, entries 1-5). Instead, microwave assistance was needed for the coupling reaction to work successfully in just a few minutes (**Table 5.1**, entries 6-8), the best conditions being summarized in entry 8 of **Table 5.1**. Of note, there was no need to protect the *N*-terminus of sulfamidate **J** due to its unreactive sulfonamide character, which additionally precludes ring-opening during the peptide coupling step.[29]

Table 5.1. Optimization of sulfamidate **J** peptide coupling through its *C*-terminus.

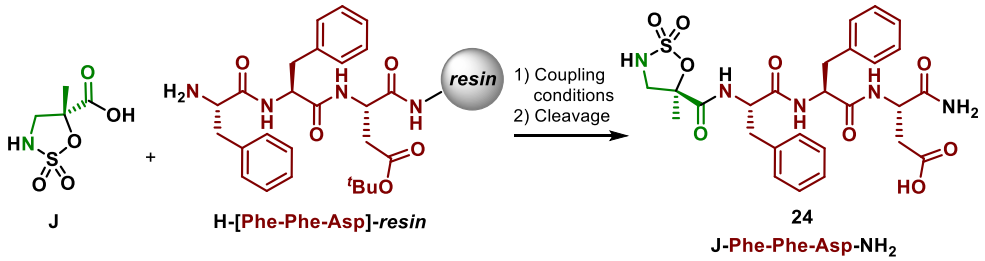

Entry	Mode	Coupling reagents	Base	Solvent	Time	Temperature (ºC)	Conversion (%)[a]
1		PyBOP/HOAt	DIPEA	DMF	18 h	25	0
2		HBTU	DIPEA	DMF	18 h	25	0
3	Manual	HOAt/DIC	-----	DMF	18 h	25	0
4		HOBt/DIC	-----	THF	18 h	25	0
5		HOBt/DIC	-----	CH_3CN	18 h	25	0
6		HBTU/HOBt	DIPEA	DMF	20 min	75	62
7	Microwave-assisted, automatic	HBTU/HOBt	DIPEA	DMF	10 min	90	64
8		Oxyma/DIC	-----	DMF	20 min	75	87
9		Oxyma/DIC	-----	DMF	10 min	90	80

[a]Estimated by HPLC in the crude mixture.

Coupling amino acids at the *N*-terminus of H-**J**-[peptide]-*resin*

Once the coupling of the sulfamidate **J** to the growing peptide was optimized, the coupling of another amino acid at the *N*-terminus of the sulfamidate was attempted. In this sense, the sequence Ac-Leu-**J**-Phe-Phe-Asp-NH_2 was selected for solid-phase coupling optimization (**Scheme 5.2**). Initially, Oxyma Pure® and DIC were used as coupling reagents in DMF using microwave assistance (75 ºC) for 20 min since it showed the best conversion ratios for coupling sulfamidate **J** to resin-supported peptide **24** (**Table 5.1**, entry **8**). However, the desired peptide was not obtained after Fmoc removal from terminal Leu, subsequent *N*-acetylation and final cleavage reactions. Instead, ring-opening of the sulfamidate moiety and incorporation of unexpected functional groups into the peptide structure was detected by MS.

This was also observed when using HBTU and HOBt as coupling agents and DIPEA as a base (**Scheme 5.2**). These results indicate that the coupling reagent is not innocent in this unusual coupling, since using nucleophilic coupling reagents, such as oximes or *N*-hydroxybenzotriazoles leads led to undesired ring-opening reactions at the cyclic sulfamidate affording peptides **25** and **26**, respectively. Such undesired ring-opening side-reactions during peptide coupling with *N*-carbonyl-derived sulfamidates –in contrast to the *N*-unprotected analogues– were previously described by our research group.[27]

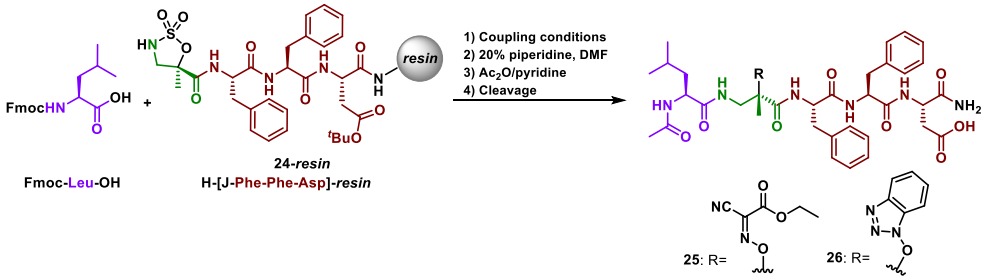

Scheme 5.2. Undesired ring-opening reactions of cyclic sulfamidate by oximes and benzotriazoles present in the coupling reagents.

In order to minimize the occurrence of side-reactions and determine the conversion ratios of the coupling reaction, different coupling conditions were assayed and the cleavage reaction was performed right after the coupling reaction to obtain Fmoc protected peptide **27** [Fmoc-Leu-**J**-Phe-Phe-Asp-NH_2] from resin-supported peptide **24**. The ring-opening reaction by *N*-hydroxybenzotriazole using TBTU was effectively minimized performing the coupling process at low temperatures (**Table 5.2**, entry 1). However, this methodology could be automated due to technical limitations. Alternatively, non-nucleophilic DIC and DIPEA as the coupling reagent and base, respectively, were tested at different temperatures and reaction times for the

microwave-assisted automated coupling (**Table 5.2** entries 2-6). These improved conditions solved the aforementioned problem and led to high coupling conversions. The protocol described in entry 6 was selected for subsequent automated syntheses.

Table 5.2. Optimization of amino acid coupling at sulfamidate **J** *N*-terminus.

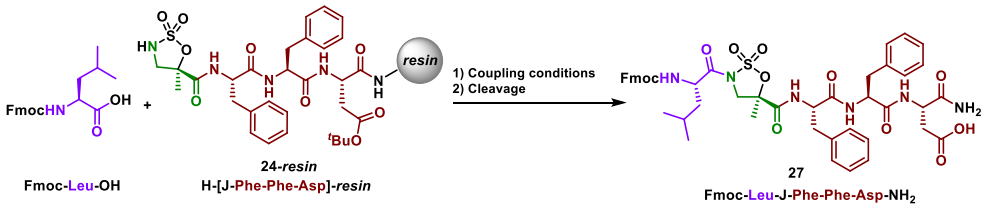

Entry	Mode	Coupling agents	Base	Solvent	Time	Temperature (ºC)	Conversion (%)[a]
1	Manual	TBTU	DIPEA	DCM	30 min	-20	88
2		DIC	DIPEA	DMF	15 min	25	69
3	Microwave-	DIC	DIPEA	DMF	2 min	90	70
4	assisted,	DIC	DIPEA	DMF	15 min	90	76
5	automatic	DIC	DIPEA	DMF	25 min	75	87
6		DIC	DIPEA	DMF	20 min	75	90

[a]Estimated by HPLC in the crude mixture.

However, although several Fmoc-protected amino acids such as leucine and alanine could be coupled at the *N*-terminus of resin-supported peptide **24** containing sulfamidate **J** under the aforementioned optimized conditions, the selective cleavage of the *N*-terminal Fmoc group necessary to elongate the peptide chain and/or acetylate this position could not be achieved under any of the multiple tested conditions including different solvents (DMF, acetonitrile, chloroform), bases (piperidine, morpholine, DBU, DIPEA), concentrations and reaction times. Instead, peptide **24** was fully recovered in all cases after cleavage from the resin, thus revealing the high instability of the amino acid-sulfamidate amide bond. As an alternative approach to obtain the target sequence, *N*-acetyl-leucine was directly coupled to the sulfamidate

N-terminus of resin-supported peptide **24** using DIC/DIPEA at room temperature for 16 h (**Scheme 5.3**). In this case, microwave assistance was not used to avoid side-reactions. Although this strategy did allow obtaining peptide **28 [**Ac-Leu-**J**-Phe-Phe-Asp-NH_2] in a moderate global yield (43%), two epimers in a 1:3 ratio at the terminal leucine were detected. Although such diastereomers could be separated by HPLC, their absolute configuration could not be determined. This racemization process is frequently observed when coupling *N*-acetylated amino acids using carboxylate group activators via oxazol-5(4*H*)-one formation.[30] Additionally, when peptide **28** was dissolved in aqueous PBS buffer (pH 7.5), its *N*-terminal leucine residue was again cleaved to give peptide **24** according to the NMR, MS and HPLC data.

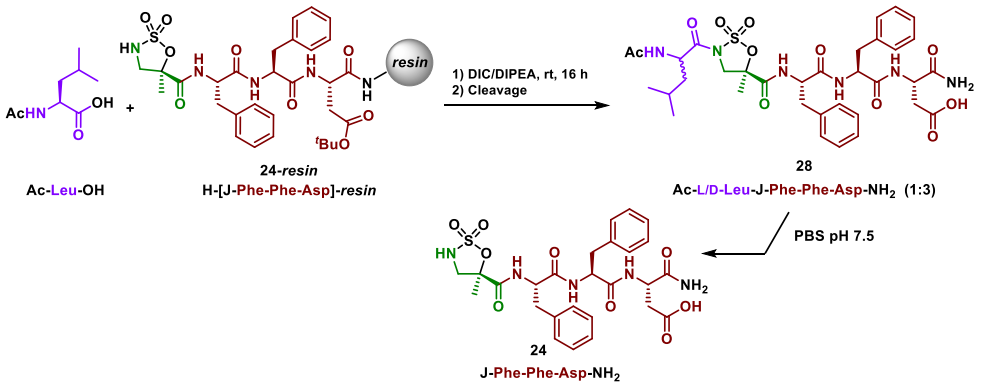

Scheme 5.3. Non-stereoselective coupling of *N*-acetyl amino acids to sulfamidate peptides and subsequent *N*-terminal residue cleavage in aqueous buffer.

Therefore, and although this compound would be directly comparable to Soto's motif (Ac-Leu-Pro-Phe-Phe-Asp), it was finally discarded for further studies due to the lack of complete stereochemical assessment and, more importantly, its instability in solution.

Synthesis of BSBPs candidates

For the synthesis of BSBPs candidates and subsequent amyloid protein aggregation studies, a small peptide library comprising the minimal sequences Xxx-Phe-Phe-Yyy (Xxx = Pro or sulfamidate **J**; Yyy = Asp or Ala-Glu) was built. The potential structural-biological consequences of acetylating the sulfamidate *N*-terminus, as well as extending the motif's length and changing the nature of the negatively charged residue (Asp in Soto's original design *vs*. Ala-Glu in native β-amyloid) was evaluated by synthesizing the following peptides: **29**: [Ac-Leu-Pro-Phe-Phe-Asp-NH_2] (Soto's original BSBP; reference), **30**: [Ac-Pro-Phe-Phe-Asp-NH_2] (shorter version of Soto's BSBP), **31**: [Ac-**J**-Phe-Phe-Asp-NH_2], **24**: [**J**-Pro-Phe-Phe-Asp-NH_2] (described above), **32**: [Ac-Pro-Phe-Phe-Ala-Glu-NH_2] (longer version of Soto's BSBP), **33**: [Ac-**J**-Phe-Phe-Ala-Glu-NH_2], **34**: [**J**-Phe-Phe-Ala-Glu-NH_2].

MW-SPPS standard optimized conditions were used for the construction of the natural and pre-sulfamidate sequences, using Oxyma Pure®/DIC as coupling reagents and 20% piperidine in DMF for Fmoc deprotection. α-Methylisoserine sulfamidate (**J**) and the subsequent amino acid (Fmoc-Leu-OH) were coupled to H-[peptide]-*resin* using the optimized methodologies described above (**Table 5.1**, entry 8 and **Table 5.2**, entry 6), and acetic anhydride/pyridine (1:2) were used for the final *N*-terminal acetylation reaction where necessary. After treatment with TFA/H_2O/TIS (95:2.5:2.5) for simultaneous deprotection of the peptide side chains and peptide cleavage from the resin, followed by purification by HPLC and lyophilization, peptides **24** and **29-34** were used in the subsequent structural and biological studies.

5.2 Conformational studies

Structural studies in aqueous solution by circular dichroism

The conformational preferences of these peptides in aqueous solution were first studied by circular dichroism (CD). CD is a spectroscopic absorption technique, which provides information about the structure of biological macromolecules in solution, allowing the detection of the most frequent secondary structures, such as β-sheets, α-helices, turns or random coils in proteins.

The corresponding CD spectra for either natural or unnatural peptides comprising the Phe-Phe-Ala-Glu sequence, showed a slightly better-defined structure than the peptides incorporating the shorter Phe-Phe-Asp sequence. Notably, the characteristic β-sheet profile was not observed for any of them. Instead, a polyproline-II helix-like conformation seems to be preferred for these peptides. Not showing a β-sheet-like structure themselves is a pre-requisite for the candidate peptides to behave as potential anti-amyloidogenic BSBPs (**Figure 5.9**).

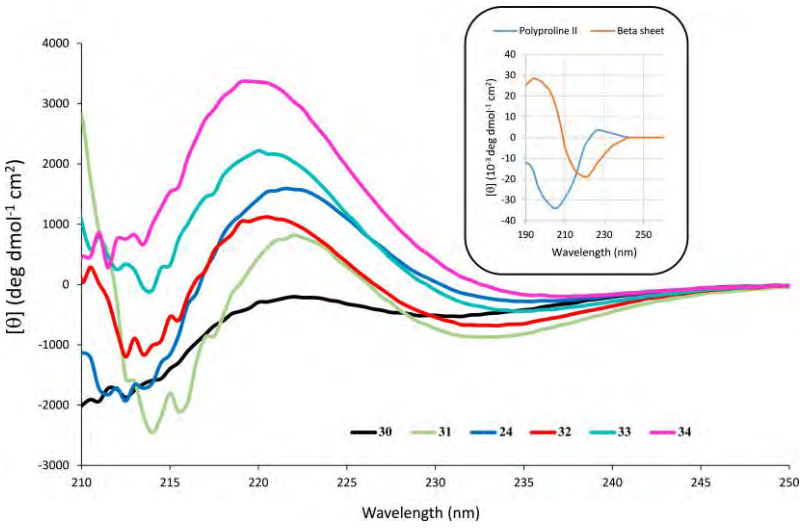

Figure 5.9. Circular dichroism spectra of synthetized BSBP candidates **24**, **30** and **31**-**34**.

Structural studies in aqueous solution by NMR and Molecular Dynamics simulations

NMR experiments and Molecular Dynamics simulations with time-averaged restraints (MD-tar) were combined to obtain a more detailed representation of the secondary structure of peptides **24**, **31**, **33** and **34**. Unfortunately, the same type of analysis could not be repeated with reference peptides incorporating a Val (as in the natural β-amyloid hydrophobic core) or a Pro (as in Soto's BSBP) residues in place of our sulfamidate, due to their very poor solubility in the used aqueous medium at the concentration required for the 400 MHz ^{1}H NMR experiments (around 20 mM). 2D-NOESY experiments were registered for each peptide dissolved in a 9:1 mixture of phosphate buffered saline (PBS, pH=5.7) in H_2O/D_2O at 298 K. Experimental distances were deduced from 2D-NOESY cross-peak intensities and were used as geometrical restrains in the MD-tar simulations using explicit water. The average distances obtained from the simulations were consistent with the experimental ones, confirming that such calculations are able to correctly capture the structural behavior of these peptides in water solution (**Figure 5.10**). Of note, the experimentally measured $^{3}J_{NH–H\alpha}$ coupling constants (6.1–8.3 Hz) suggest that these peptides are quite flexible without adopting a clearly defined, predominant conformation in solution.[31,32]

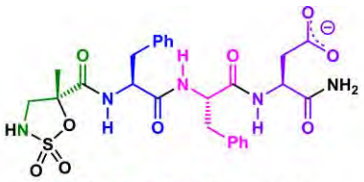

J-Phe-Phe-Asp-NH$_2$ (24)

position: *i (i+1) (i+2) (i+3)*

Distance	Exp.	MD-tar
NH*Phe2*-Hα*Phe2*	2.7	2.9
NH*Phe2*-Me***J***	3.3	3.4
NH*Phe3*-Hα*Phe3*	2.5	2.8
NH*Phe3*-Hα*Phe2*	2.3	2.3
NH*Asp4*-Hα*Phe3*	2.1	2.3
NH*Asp4*-Hα*Asp4*	2.7	2.8

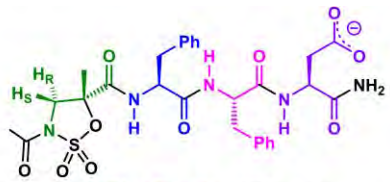

Ac-J-Phe-Phe-Asp-NH$_2$ (31)

position: *(i-1) i (i+1) (i+2) (i+3)*

Distance	Exp.	MD-tar
NH*Phe2*-Hα*Phe2*	2.7	2.9
NH*Phe2*-Me***J***	3.0	3.2
NH*Phe3*-Hα*Phe3*	2.3	2.6
NH*Phe3*-Hα*Phe2*	2.1	2.3
Ac-H*proR*_***J***	2.6	2.9
Ac-H*proS*_***J***	3.1	2.9

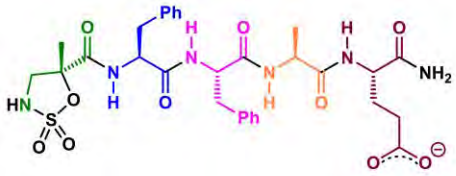

J-Phe-Phe-Ala-Glu-NH$_2$ (34)

position: *i (i+1) (i+2) (i+3) (i+4)*

Distance	Exp.	MD-tar
NH*Phe2*-Hα*Phe2*	2.5	2.8
NH*Phe2*-Me***J***	3.1	3.3
NH*Phe3*-Hα*Phe3*	2.6	2.9
NH*Phe3*-Hα*Phe2*	2.3	2.4
NH*Ala4*-Hα*Phe3*	2.0	2.2
NH*Ala4*-Hα*Ala4*	2.6	2.8

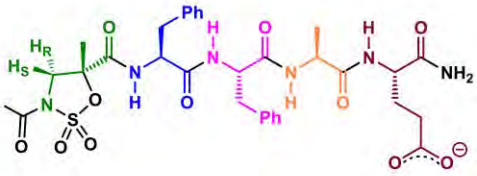

Ac-J-Phe-Phe-Ala-Glu-NH$_2$ (33)

position: *(i-1) i (i+1) (i+2) (i+3) (i+4)*

Distance	Exp.	MD-tar
NH*Phe2*-Hα*Phe2*	2.8	2.9
NH*Phe2*-Me***J***	3.1	3.3
NH*Phe3*-Hα*Phe3*	2.5	2.8
NH*Phe3*-Hα*Phe2*	2.2	2.3
NH*Ala4*-Hα*Phe3*	2.0	2.3
Ac-H*proR*_***J***	2.7	2.9
Ac-H*proS*_***J***	3.1	2.9

Figure 5.10. Comparison between experimental and MD-tar-derived H–H distances obtained from 500 ns simulations in explicit water for peptides **24**, **31**, **33** and **34**. Experimental distances were semi-quantitatively determined by integrating the volume of the corresponding NOESY cross-peaks. All distances are given in Å.

The preferred conformations for the most relevant backbone dihedral angles (ψ_β, for sulfamidate $\beta^{2,2}$-amino acid, see **Figure 5.11**; ϕ_α, ψ_α, for α-amino acids, see **Figure 5.12**) of peptides **24**, **31**, **33** and **34** were evaluated and

represented as Ramachandran-type plots in which conformer populations have been translated into their relative energies (ΔE) through Boltzmann distributions at 298 K. In the case of the sulfamidate $\beta^{2,2}$-amino acid moiety, the canonical Ramachandran plot (ϕ_α, ψ_α) cannot be used.

The strong conformational restrictions imposed by the tertiary α-methyl group of our (*R*)-α-methylisoserine sulfamidate, lock the ψ_β dihedral angle between –120º and –150º and, as result, a conserved interaction between the amide N–H of the (*i* + 1) residue (Phe) and the endocyclic oxygen (O_{endo}) of the sulfamidate is formed (averaged distance in all peptides ~2.4 Å)[29] (see **Figure 5.11** panels **b** and **c** for peptide **24** as an example). Variable-temperature ^{1}H NMR experiments suggested that such interaction might not be a canonical hydrogen bond, in agreement with its geometrical features derived from the MD simulations. The terminal *N*-acetylsulfonamide in peptides **31** and **33** is locked into a *cis* amide bond disposition as confirmed by medium NOE (Ac–H_{proR} and Ac–H_{proS}) (see Supplementary Information II: Tables & Figures, *chapter 5*, **Figures S2** and **S3**), which differs from the normal *trans* preference in α-proline, and resembles the behavior observed for β-proline.[33,34]

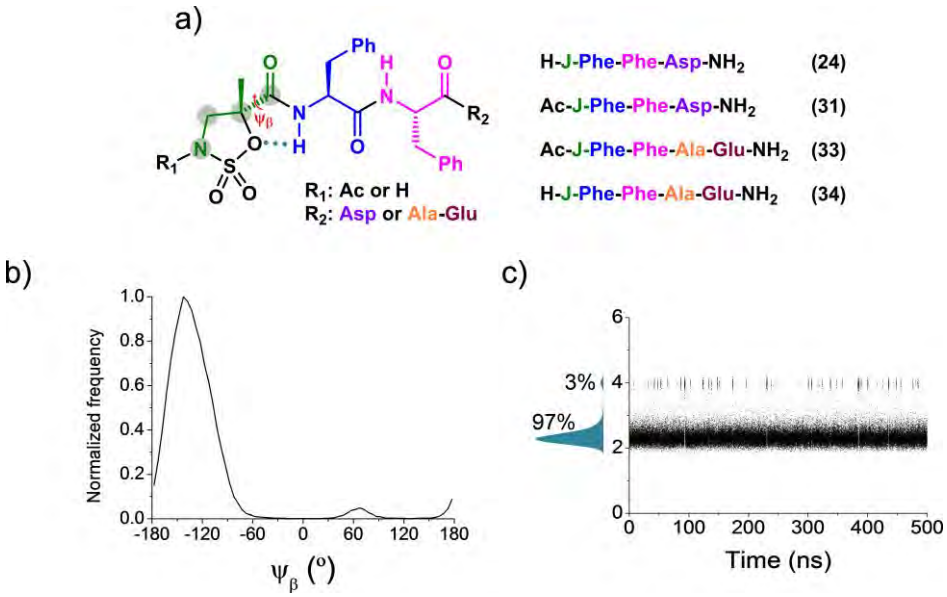

Figure 5.11. a) Chemical structure for peptides **24, 31, 33** and **34** highlighting the dihedral angle ψ_β . b) Relative population of the ψ_β angle obtained from the 500 ns MD-tar simulation in explicit water for peptide **24**. c) NH*Phe2*–Oendo***J*** distance distribution derived from the 500 ns MD-tar simulation in explicit water for peptide **24**. Distances are given in angstrom (Å). Similar distributions were observed for peptides **31**, **33** and **34** (see Supplementary Information II: Tables & Figures, *chapter 5*, **Figure S1**).

The conformational bias impossed by the cyclic sulfamidate is transferred to the adjacent amino acids. Particularly, the (*i* + 1) Phe residue predominantly displays in all the studied peptides a folded polyproline-II helix conformation (PPII, $\varphi_\alpha \sim -60°$, $\psi_\alpha \sim +150°$), with minor populations of extended β-sheet conformations (β, $\varphi_\alpha \sim -150°$, $\psi_\alpha \sim +150°$) as shown in **Figures 5.12** to **5.15**. These conformational preferences resemble those described for residues adjacent to cyclic amino acids such as residues preceding a proline.[35]

In both the *N*-unprotected (**24**) and *N*-protected (**31**) shorter peptides (**Figures 5.12** and **5.13**, respectively), the (*i* + 2) Phe residues exhibit increasingly more folded conformations with significant population of the left-handed α-helix conformation in peptide **31** (α_L, $\varphi_\alpha \sim +60°$, $\psi_\alpha \sim +45°$) and a minor presence

of the right-handed α-helix (α_R, $\varphi_\alpha \sim -60°$, $\psi_\alpha \sim -45°$). . The predominance of such folded arrangements is even more evident for the *C*-terminal (*i* + 3) Asp residue.

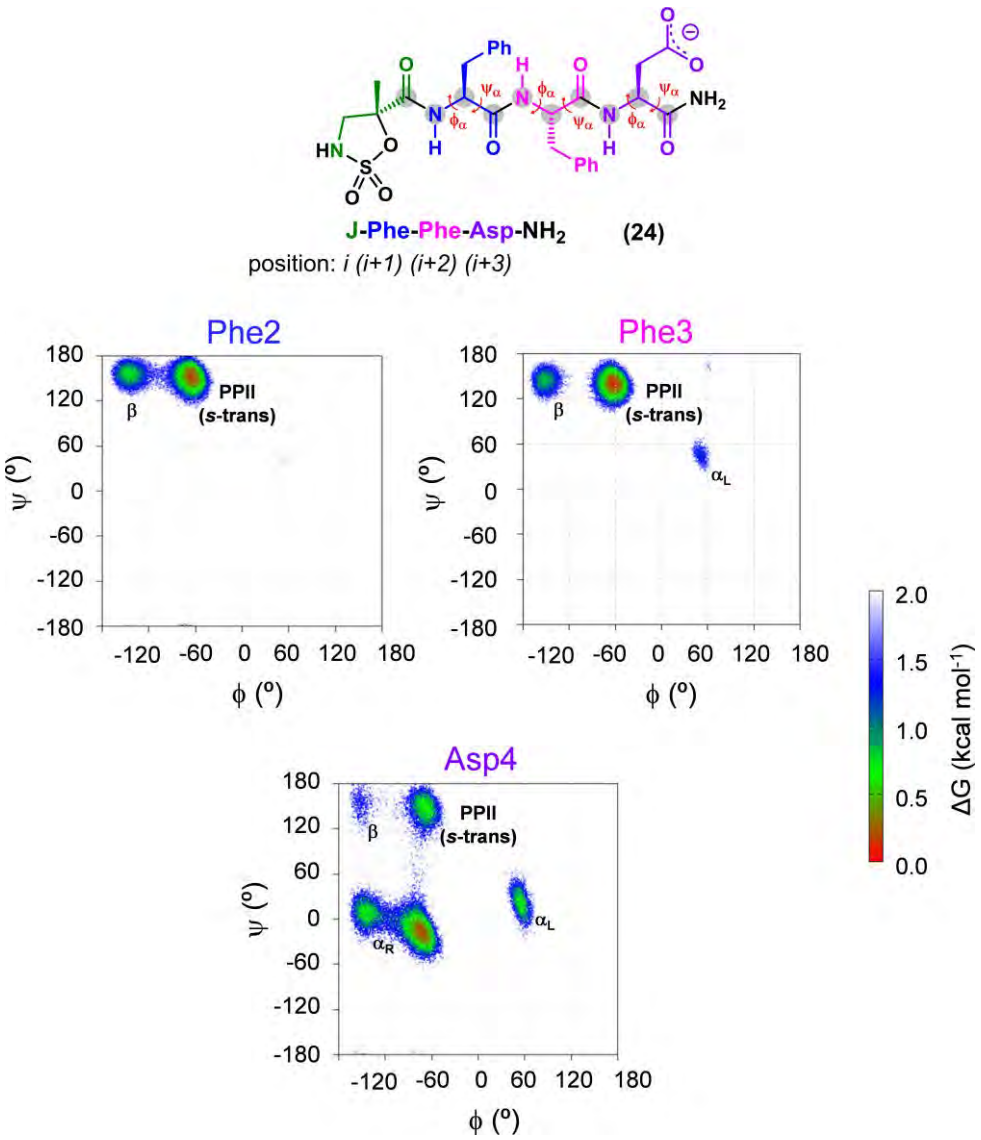

Figure 5.12. Per-residue Ramachandran plots derived from 500 ns MD-tar simulations for the backbone dihedral angles of peptide **24**. Explored conformations are shown as colored regions ranging from highly populated (*i.e.* stable, $\Delta E \leq 0.0$-1.0 kcal mol^{-1}, red-green dots) to poorly populated (*i.e.* unstable, $\Delta E \geq 1.0$-2.0 kcal mol^{-1}, blue-white dots) structures.

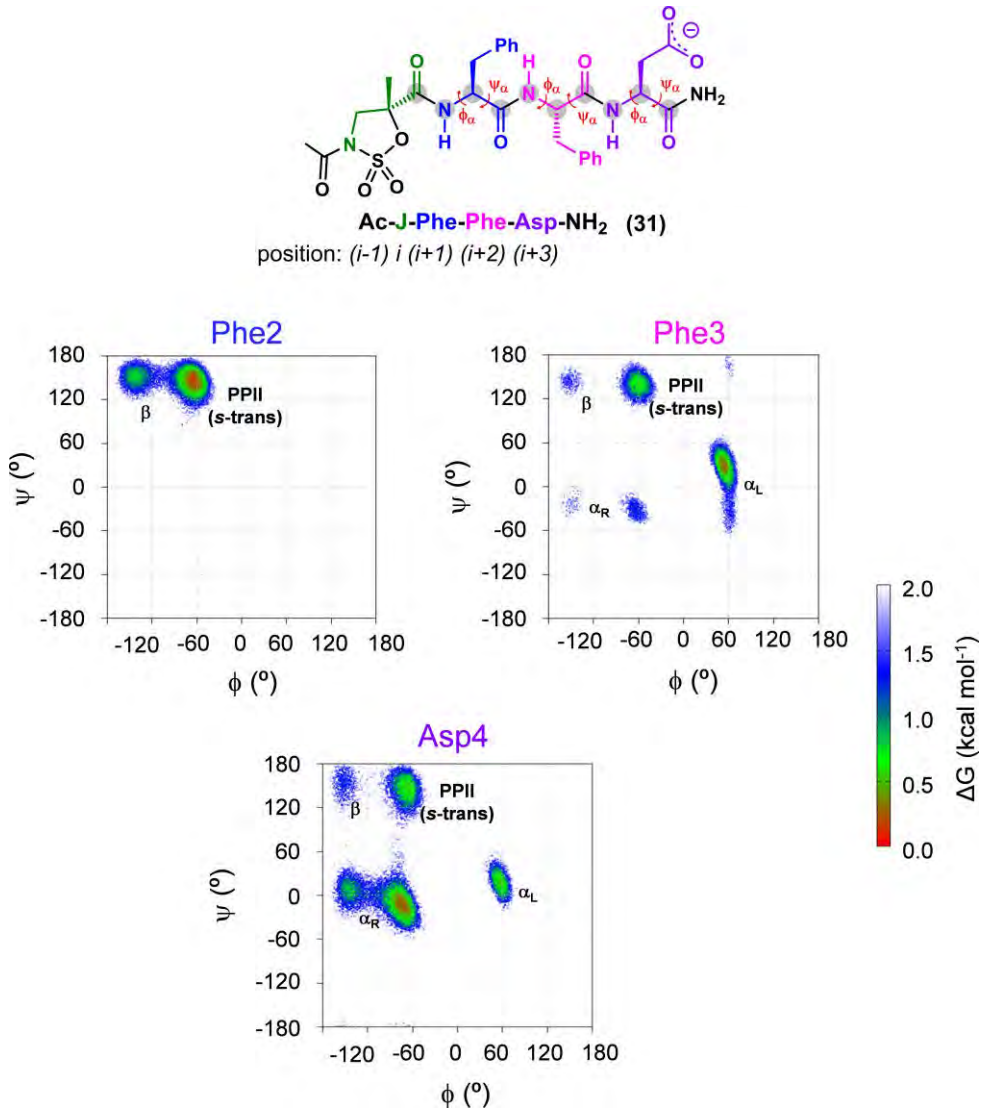

Figure 5.13. Per-residue Ramachandran plots derived from 500 ns MD-tar simulations for the backbone dihedral angles of peptide **31**. Explored conformations are shown as colored regions ranging from highly populated (*i.e.* stable, $\Delta E \leq 0.0$-1.0 kcal mol^{-1}, red-green dots) to poorly populated (*i.e.* unstable, $\Delta E \geq 1.0$-2.0 kcal mol^{-1}, blue-white dots) structures.

Longer peptides **33** and **34** (**Figures 5.14** and **5.15**, respectively) showed conformational preferences similar to those found for shorter peptides **24** and **31**. The (*i* + 1) and (*i* + 2) Phe residues display a predominantly folded

polyproline-II helix conformation (PPII, $\varphi_\alpha \sim -60^\circ$, $\psi_\alpha \sim +150^\circ$), with a minor presence of extended β-sheet conformations (β, $\varphi_\alpha \sim -150^\circ$, $\psi_\alpha \sim +150^\circ$). No α-helix conformations are observed for the (*i* + 2) Phe residues in these cases. Although (*i* + 3) Ala residues are able to adopt α-helix conformations (α_R, $\varphi_\alpha \sim -60^\circ$, $\psi_\alpha \sim -45^\circ$, and α_L, $\varphi_\alpha \sim +60^\circ$, $\psi_\alpha \sim +45^\circ$), they exhibit a preference for polyproline II as well (PPII, $\varphi_\alpha \sim -60^\circ$, $\psi_\alpha \sim +150^\circ$). However, α-helix conformations are preferred by the *C*-terminal (*i* + 4) Glu residues, reflecting the lack of conformational bias exerted by the sulfamidate residue at remote positions of the peptide chains (i.e. the propensity to adopt PPII-type conformations decreases as the distance to the *N*-terminal sulfamidate increases).

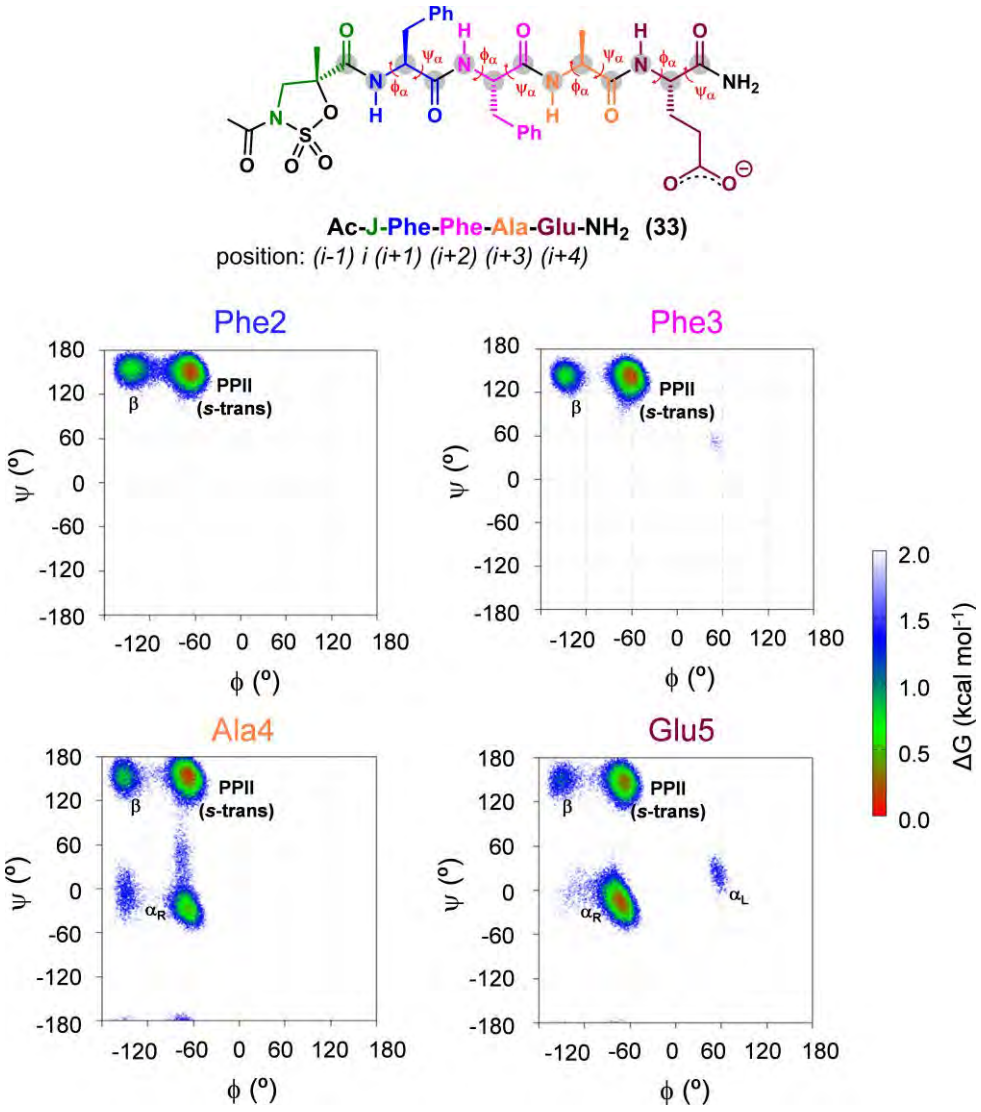

Figure 5.14. Per-residue Ramachandran plots derived from 500 ns MD-tar simulations for the backbone dihedral angles of peptide **33**. Explored conformations are shown as colored regions ranging from highly populated (*i.e.* stable, $\Delta E \leq 0.0$-1.0 kcal mol^{-1}, red-green dots) to poorly populated (*i.e.* unstable, $\Delta E \geq 1.0$-2.0 kcal mol^{-1}, blue-white dots) structures.

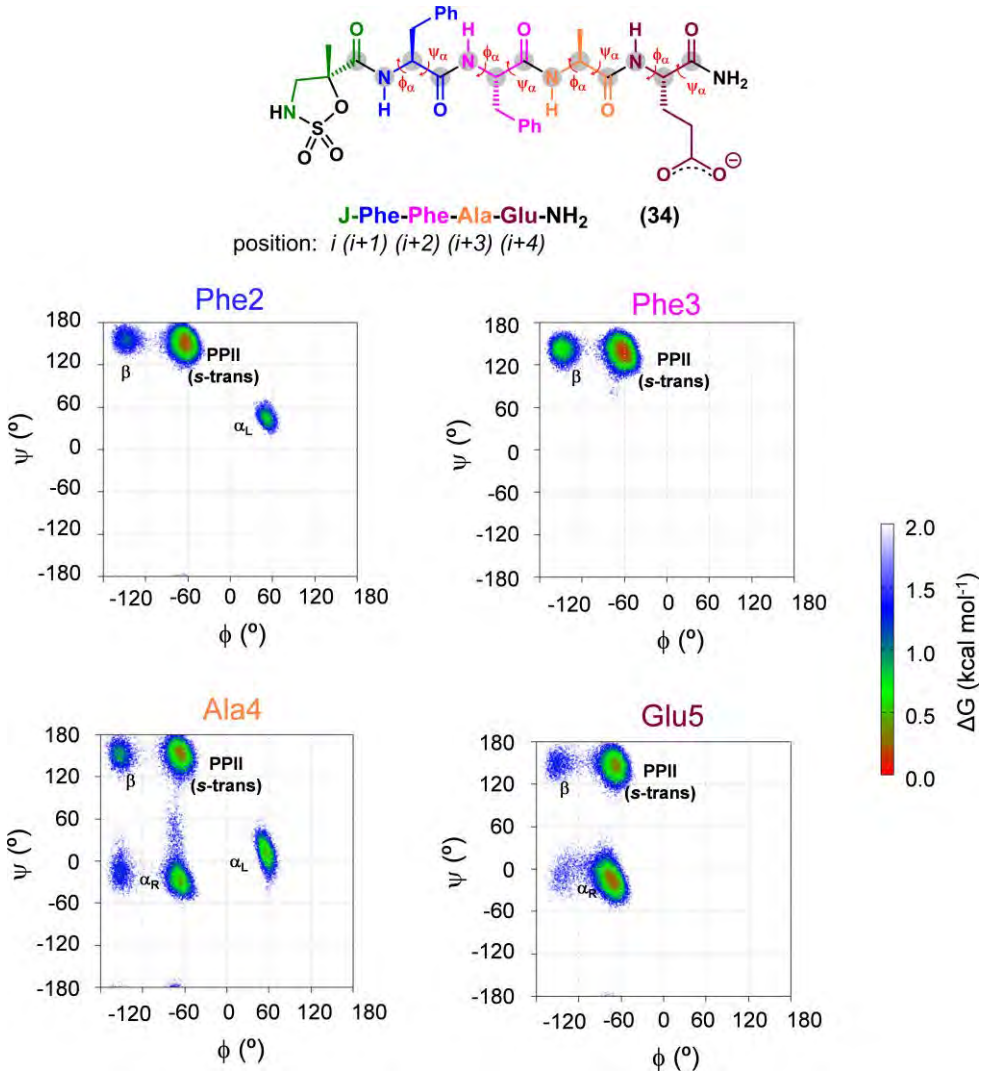

Figure 5.15. Per-residue Ramachandran plots derived from 500 ns MD-tar simulations for the backbone dihedral angles of peptide **34**. Explored conformations are shown as colored regions ranging from highly populated (*i.e.* stable, $\Delta E \leq 0.0$-1.0 kcal mol^{-1}, red-green dots) to poorly populated (*i.e.* unstable, $\Delta E \geq 1.0$-2.0 kcal mol^{-1}, blue-white dots) structures.

MD-tar simulations showed that the four peptides have a large propensity to adopt various folded conformations, in good agreement with the circular dichroism (CD) experiments, which showed a preponderance of folded PPII-like conformations in water solution (**Figure 5.9**). These conformational

preferences preclude the formation of β-sheet structures such as those occurring at the LVFF hydrophobic core of the β-amyloid protein, which subsequently lead to oligomerization and fibrillation. Not only the cyclic nature of the α-methylisoserine sulfamidate itself, which replaces the Val residue in the natural β-amyloid and the Pro residue in Soto's anti-amyloidogenic BSBP, but the very strong conformational bias imposed by this $\beta^{2,2}$-amino acid to the adjacent (i + 1) residue transmitted through the ψ_β dihedral to the rest of the peptide chain are responsible for this special structural behavior. The novel turn observed in our BSBP candidates is likely stabilized by a electrostatic interaction between the amide N–H of the (i + 1) residue (Phe) and the endocyclic oxygen (O_{endo}) of the sulfamidate appearing as a result of the highly conserved ψ_β values.

Structural studies in the gas phase by infrared double resonance ion-dip (IRID) spectroscopy

In an attempt to elucidate the intrinsic conformational preferences of our anti-amyloidogenic candidates in a desolvated environment more closely resembling the hydrophobic surrounding of a β-amyloid fibrils or aggregates, we studied the structural properties of the minimal motif **J**-Phe-Phe-NH_2 in the gas phase. For this purpose, we synthesized this peptide through SPPS and studied its structural features in the gas phase using spectroscopic techniques based on infrared double resonance ion-dip (IRID), in collaboration with the group of Dr. Emilio Cocinero at the Biofisika Institute (CSIC – UPV/EHU).[36–38]

The well-stablished protocol for IRID-based structural determination consists on deconvoluting the information encoded in the gas phase experiment through a careful examination of the whole conformational space of the analyzed compound with quantum mechanics and the subsequent calculation

of the vibrational frequencies for each low-energy conformer. Then, an averaged theoretical spectrum is predicted by weighting the intensities of each individual vibration with the calculated population for each conformer. Finally, this theoretical spectrum is compared with the experimental IRID one, and if a good agreement is obtained, the nature of the experimental absorption bands and ultimately the tridimensional structure of the molecule at the atomic level (i.e. the low-energy conformational ensemble) can be accurately assessed.

This technique requires the presence of aromatic moieties in the molecule for conformational monitoring and selection through UV-Vis absorption spectroscopy. Since the sulfamidate-based BSBP consensus sequence **J**-Phe-Phe-NH_2 already has two aromatic phenylalanines as constituent residues, and is a sufficiently small molecule, thus being computationally tractable, it was considered an appropriate substrate for this kind of analysis.

The gas phase IRID spectrum of this peptide corresponding to the N–H stretching vibrations, which provide fingerprint information about the characteristic hydrogen bond network pattern, and thus folding, of the low-energy conformation(s) of the molecule shows an intense absorption band at around 3150 cm^{-1}, three overlapping bands in the 3350-3450 cm^{-1} region and one distinct band at around 3500 cm^{-1} (**Figure 5.17a**). The presence of well-resolved and separated bands suggests that only a few conformations engaged in a distinctive hydrogen bond network are dominant in the gas phase.

The whole conformational space of peptide **J**-Phe-Phe-NH_2 was analyzed quantum mechanically by fully optimizing 1152 starting structures with M06-2X/6-31+G(d,p) in the gas phase (**Figure 5.16**).

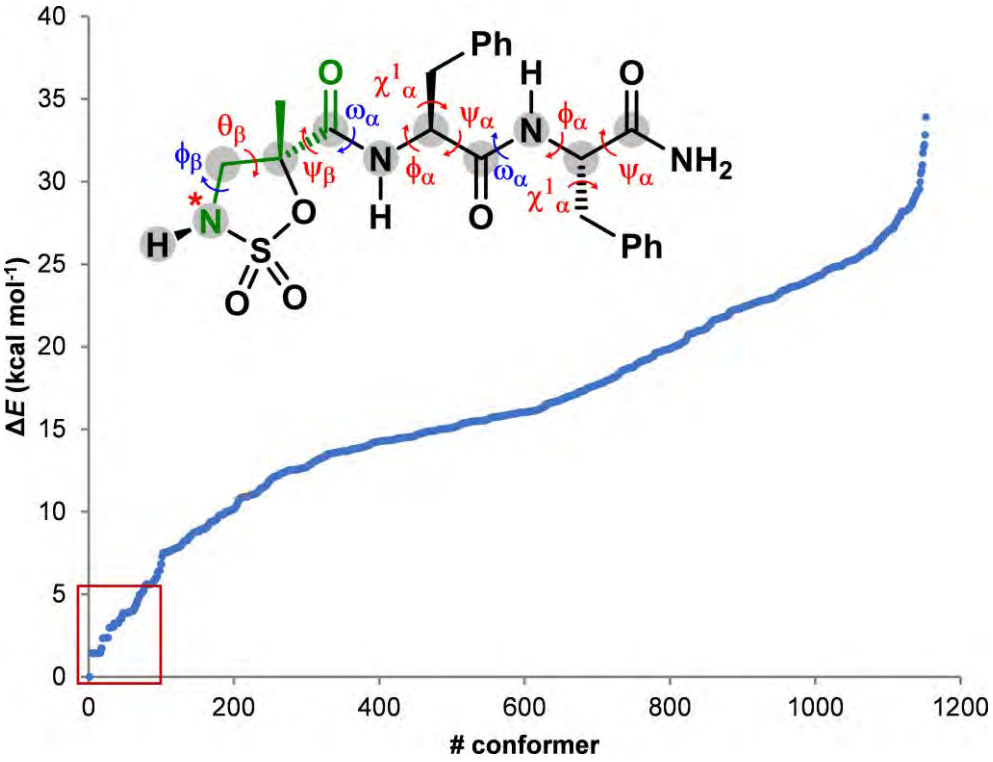

Figure 5.16. Quantum mechanical exploration of the conformational space of peptide H-**J**-Phe-Phe-NH_2 in the gas phase with M06-2X/6-31+G(d,p). The systematically analyzed dihedral angles are shown in red and those maintained in the initial conformation are shown in blue. The backbone atoms used to define dihedral angles are highlighted with grey circles. The plot shows the relative energy (ΔE) of the different conformations after full geometry optimization, ordered from lower to higher energies. The red square shows the fraction of low-energy conformations selected for further geometry optimization at higher theory levels.

Then, the 20 lowest-energy conformers with a relative energy (ΔE) within the 0-5 kcal mol^{-1} range accounting for ~98% of the structural population as calculated through a Boltzmann distribution at 298 K, were re-optimized at B3LYP-GD3BJ/6-311++G(2d,p). Vibration frequencies were calculated at the same theory level using the harmonic oscillator approximation and using pre-defined scaling factors.[39] The superior capability of this dispersion-corrected functional to correctly distinguish the most stable conformation of

medium-sized flexible molecules in which both polar and van der Waals interactions are important, particularly in the context of gas phase spectroscopy, has been recently reported.[36]

Conformation **I** is the lowest-energy one and its calculated infrared frequencies match almost perfectly those measured experimentally, indicating that such conformer is very likely the most populated one in the gas phase, contributing predominantly to the experimental IRID spectrum (**Figure 5.17**). The five lowest-energy conformations **I-V** account for ~95% of the whole conformational population and are all very similar both structurally (i.e. all are folded) and spectroscopically (**Figure 5.17c and 5.17d**), conformation **II** being the most different due to the absence of an intramolecular hydrogen bond between sulfamidate N–H and peptide backbone C=O groups. These residual conformations are likely responsible for the band broadening observed in the experimental IRID spectrum.

Conformation **I** shows a completely folded secondary structure as a result of an intricate hydrogen bond network involving the α-methylisoserine sulfamidate N–H, S=O_{exo} and S–O_{endo} atoms. As previously reported[29] and observed also in the MD simulations described above, the tertiary α-methyl group of our (*R*)-α-methylisoserine sulfamidate plays a decisive role to lock the sulfamidate amide bond in a very stable and unusual arrangement (ψ_β = –137º). As a result of this conformational lock, the Phe residue attached to the sulfamidate (*i* + 1 position) is stabilized in an α-helix conformation (φ_α ~ –62º, ψ_α ~ –34º) through the direct N–H to S–O_{endo} intereaction persistently observed in solution for all peptides (see previous section), and the consecutive terminal Phe (*i* + 2 position) folds into an inverse γ-turn conformation through hydrogen bonds between its C=O and N–H groups with sulfamidate N–H and S=O_{exo} groups, respectively. The non-extended

orientation of the two Phe side chains (g^-, $\chi^1{}_\alpha = +50°$ for Phe1; g^+, $\chi^1{}_\alpha = -62°$ for Phe2) create a hydrophobic patch through aromatic C–H/π interactions between the two nearly perpendicular phenyl rings which encapsulate one the two sulfamidate S=O_{exo} groups.

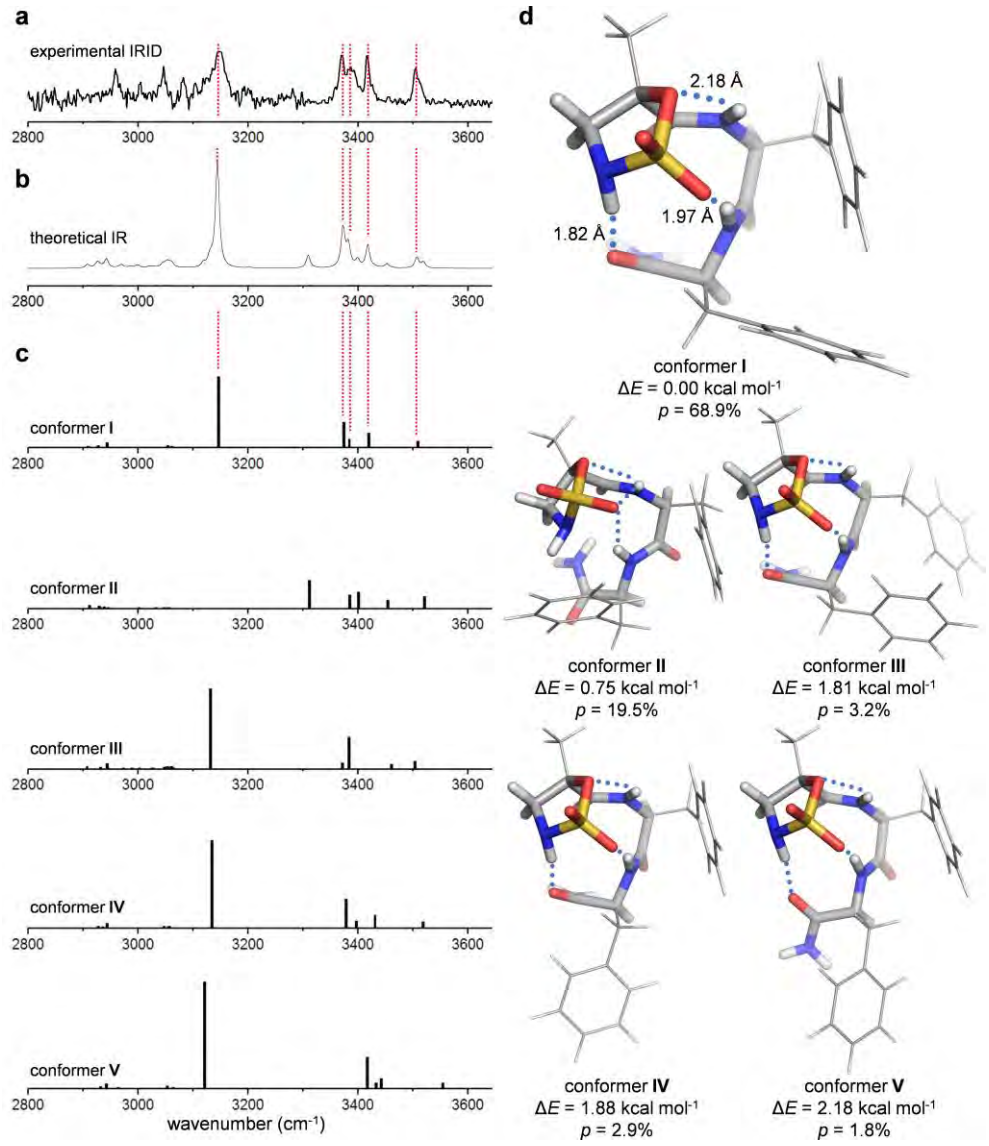

Figure 5.17. Experimental IRID (a) and conformationally-averaged theoretical IR (b) spectra (N–H vibrations region) of peptide **J**-Phe-Phe-NH_2 in the gas phase. c) Calculated N–H vibrations for lowest-energy conformations **I-V**. The high correspondence between calculated and observed bands is highlighted with red dotted lines. d) Three-dimensional structures, relative energies (ΔE) and populations at 298 K (p) calculated for conformations **I-V** with B3LYP-GD3BJ/6-311++G(2d,p). Non-polar hydrogens are omitted for clarity Hydrogen bonds are highlighted with blue dotted lines and distances are shown in angstrom (Å).

The nature of the observed IRID absorption bands was assessed through the calculated vibrations for the largely predominant, minimum-energy conformation **I**. The intense band at ~3150 cm^{-1} corresponds to the sulfamidate N–H and it is the most characteristic absorption of peptide **J**-Phe-Phe-NH_2, separated from other amide vibrations in the molecule. Most notably, the sulfamidate N–H···C=O hydrogen bond lowers the frequency of this vibration by ~165 cm^{-1} with respect to that calculated in conformation **II** in which this hydrogen bond is absent. The three overlapping bands in the 3350-3450 cm^{-1} region correspond to N–H vibrations of the second Phe amide bond, terminal amide and first Phe amide bond, respectively. Finally, the band at ~3500 cm^{-1} corresponds to an additional vibration of the terminal amide.

This observation confirms our initial hypothesis that this densely functionalized five-membered cyclic amino acid confers strong bias towards novel non-extended conformations to small peptides in which it is incorporated, with high potential for disrupting extended β-sheet structures such as those present in amyloid fibrils.

5.3 Biological studies

Thioflavin-T (ThT) fluorescence assay

To study the ability of sulfamidatecontaining peptides to behave as BSBPs, it is crucial to study the aggregation of the β-amyloid peptide in the presence of these candidates. One of the most used strategies in this regard is the monitorization of the fluorescence intensity of thioflavin T (ThT).[40]

Thioflavin T is a benzothiazole salt, which is used as a dye to visualize and quantify the presence of protein aggregates such those occurring in β-amyloid. It was firstly used as a fluorescent marker of amyloid in 1959. Vassar and Culling groups observed a dramatic increase in fluorescence

brightness when ThT selectively localized to amyloid deposits.[41] A few decades later, Naiki and LeVine groups demonstrated that ThT displays a dramatic large shift of the excitation maximum from 385 nm to 450 nm and the emission maximum from 445 nm to 482 nm when bound to the fibrils. Additionally, the increase observed for the fluorescence intensity upon fibril binding, makes it a rarely sensitive and effective marker, which allows monitoring fibril aggregation in real time and in solution.[42–44]

Wu *et al*. studied the mechanism of amyloid-dye interactions, demonstrating that ThT binds parallelly to the long axis of the fibril surface in grooves formed by side-chain ladders. Furthermore, ThT prefers to interact with channels formed by aromatic residues, such as the Val-Phe motif (**Figure 5.18**). [45–47]

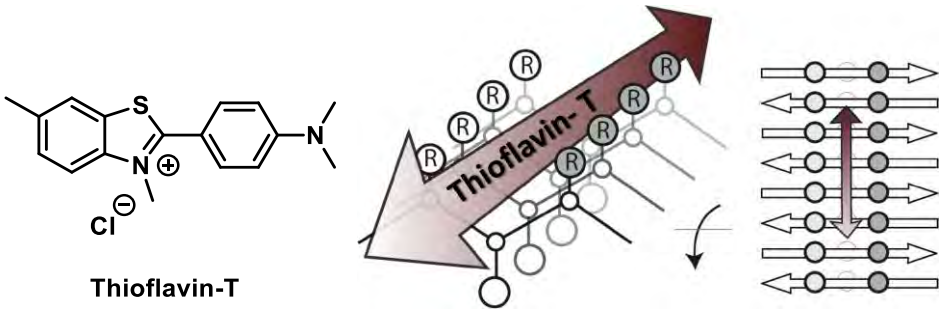

Figure 5.18. ThT structure (left) and structural rationale for fibril-ThT interactions (right).[45–47]

ThT assays of βA aggregation typically display a sigmoidal curve divided in three phases: lag phase (lack of mature fibrils), growth phase (rapid increase of fibrils concentration) and equilibrium phase (predominance of mature fibrils) (**Figure 5.19**).

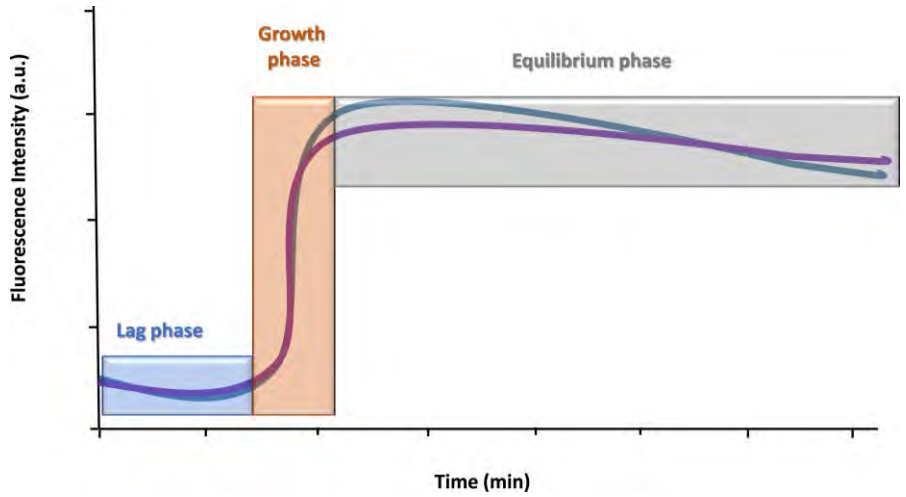

Figure 5.19. Typical graph of βA aggregation monitored by ThT fluorescence assays.

The kinetics of amyloid agglomeration in the presence of our sulfamidate-based BSBP candidates were monitored by time-dependent ThT fluorescence assays. Positive control peptide **29** (Soto's Pro-based BSBP) and peptides **24**, **30**, **31**, **32**, **33** and **34** were each co-incubated with $\beta_{(1-40)}$-amyloid in an aqueous phosphate buffered saline (PBS, pH 7.4) at 37 °C for 24 hours with continuous shaking (200 rpm) using a 96-well black plate. In order to investigate the dose dependence, 2-, 5- and 10-fold molar excess of the BSBPs were used for each experiment. ThT was added and the fluorescence intensity (442 nm for excitation and 482 nm for emission) was recorded with 10 minutes reading intervals and 5 seconds shaking before each reading. All the samples were measured three times and the average value was used.

The kinetic aggregation assay of $\beta A_{(1-40)}$ alone showed a steadily increase in the fluorescence intensity (brown line in **Figure 5.20**), which is a characteristic property of the fibrillar nature of the peptide and correlates to the amount of fibrils present.[48] The other colored curves in **Figure 5.20** correspond to the β-amyloid co-incubated with the BSBP candidates at

different concentrations, exhibiting a similar profile than untreated $\beta A_{(1\text{-}40)}$. Some of the experiments showed a decrease in the fluorescence intensity between the growth phase and the equilibrium phase, indicating that those peptides may act as inhibitors of amyloid aggregation. In general, candidates **32**, **33** and **34** showed better inhibition properties than peptides **24**, **30** and **31**.

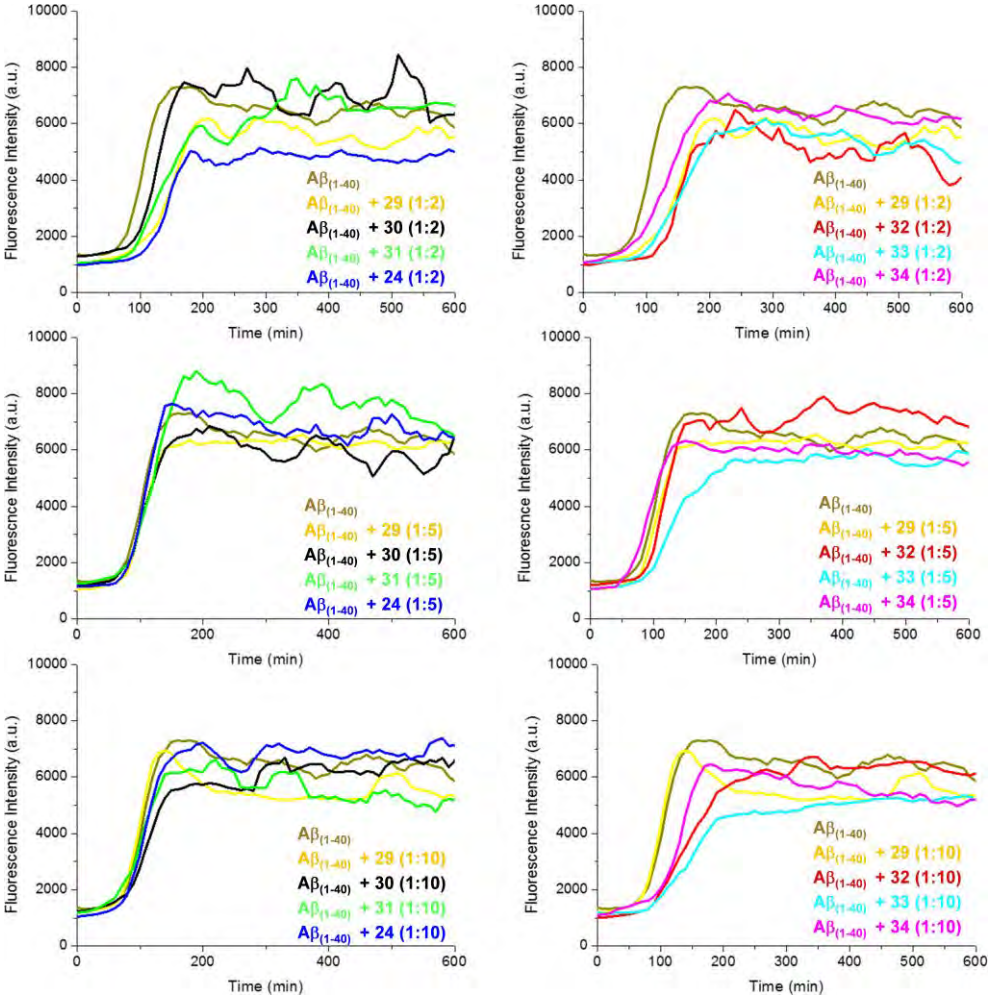

Figure 5.20. ThT fluorescence assays (fluorescence intensity *vs*. time for the monitoring of amyloid (15 μM) fibrillation in the presence of peptides **24**, **30** and **31** (left) and in peptides **32**, **33** and **34** (right). Peptide **29** is used as a positive control. The molar ratios between the amyloid and BSBP candidate are shown in parentheses).

In order to quantify the fibrillation of β-amyloid in the presence of the BSBP candidates, the maximum value of each curve between the growth phase and the equilibrium phase was taken, using as a reference the one obtained for the isolated amyloid, to which an arbitrary value of 1 was assigned (**Figures 5.21** and **5.22**).

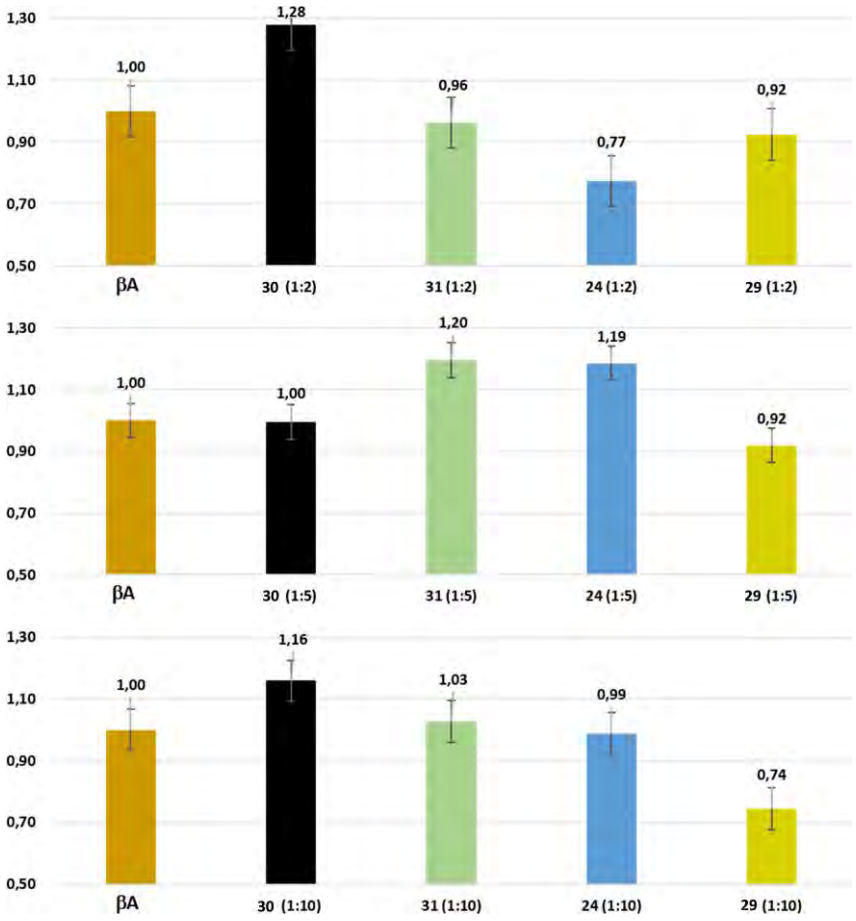

Figure 5.21. Relative maximum fluorescence intensities obtained from the ThT fluorescence assays for the amyloid alone (**orange**) and co-incubated with peptides **24** (**blue**), **30** (**black**), **31** (**green**), and Soto's BSBP **29** (**yellow**). The molar ratios between the amyloid and BSBP candidate are shown in parentheses).

Figure 5.22. Relative maximum fluorescence intensities obtained from ThT fluorescence assays for the amyloid alone (**orange**) and co-incubated with peptides **32** (**red**), **33** (**turquoise**) and **34** (**pink**) and Soto's BSBP **29** (**yellow**). The molar ratios between the amyloid and BSBP candidate are shown in parentheses).

In the case of using 2 equivalents of BSBPs with respect to the β-amyloid, it is generally observed that longer peptides (**Figure 5.22**) inhibit fibrillation better than shorter ones (**Figure 5.21**) and show superior properties than the one reported by Soto. When using 5 equivalents, longer peptides **33** and **34** display the best inhibition properties. Finally, with 10 equivalents all the longer peptides inhibit fibrillation.

In view of these results, it can be concluded that compound **33**, which incorporates the acetylated sulfamidate in the longer sequence (Ac-**J**-Phe-Phe-Ala-Glu), shows the best inhibition properties at all the studied concentrations, being even better than the one reported by Soto.

Circular dichroism for βA (1-40) co-incubated with BSBPs

Another way to qualitatively study amyloid fibrillation is by analyzing its circular dichroism (CD) spectrum.[40] The conformation of the amyloid after incubation in the absence and presence of the breaker peptides was analyzed through CD.

The spectra obtained for freshly prepared, untreated amyloid at zero time (gray) and after 24 h of incubation at 37 °C (gold) are shown in **Figure 5.23**. As can be seen, at time zero when the amyloid is not aggregated, the spectrum shows a pattern typical of random coil structures with a pronounced minimum around 200 nm. However, after incubation, the spectrum shows a pattern typical of β-sheet arrangemets, with a soft minimum around 220 nm. These control experiments clearly indicate that β-amyloid fully aggregates during the experiment time.

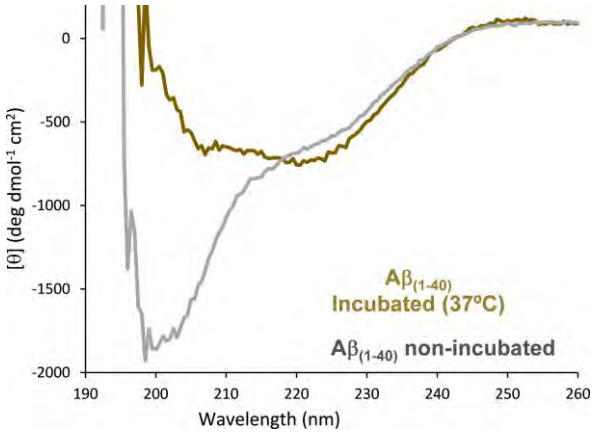

Figure 5.23. Circular dichroism spectra of β-amyloid (15 μM) for freshly prepared (in grey) and after 24 h incubation at 37 ºC.

Analogous CD analyses were performed after incubating the amyloid in the presence of 2 equivalents of the BSBPs at 37 °C for 24 hours. Limited amounts of the inhibitors were used to avoid interference with the measurements. The CD spectra of βA in the presence of BSBPs (**24**, **32**, **33** and **34**) significantly differ from that of the untreated amyloid sample (**Figure 5.24**), suggesting the inhibition of β-fibrils formation and preservation of the protein disordered. These results are consistent with the ThT fluorescence experiments.

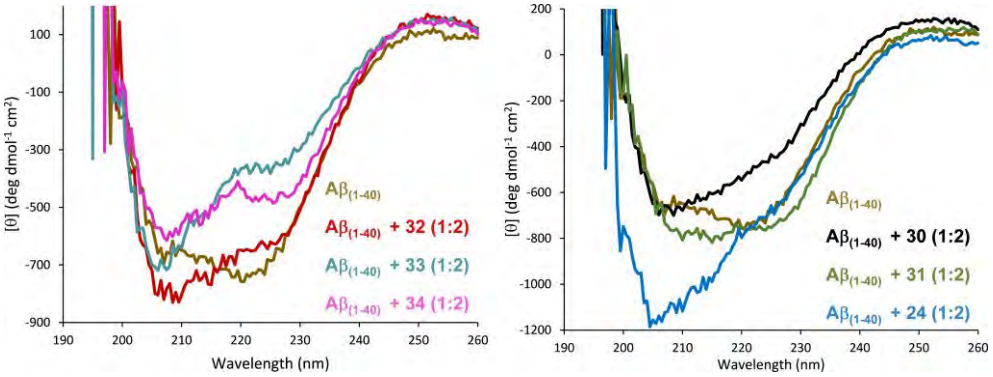

Figure 5.24. Circular dichroism β-amyloid (15 μM) at 37 ºC for 24 h with peptides **32**, **33** and **34** (1:2) (left) and circular dichroism β-amyloid (15 μM) at 37 ºC for 24 h with peptides **24**, **30** and **31** (right).

After incubating the samples at 37 ºC for a prolonged period (7 days) the same trend is maintained. These observations demonstrate that our sulfamidate-based peptides persistently inhibit the amyloid aggregation, likely targeting and stabilizing its monomer helical structure. (**Figure 5.25**).

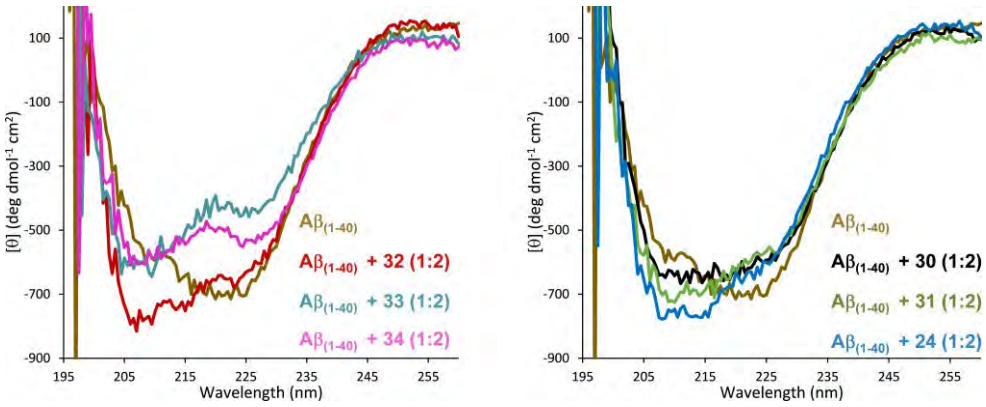

Figure 5.25. Circular dichroism spectra of β-amyloid (15 μM) after incubation at 37 ºC for 7 days in the presence of peptides **32**, **33** and **34** (1:2 βA:BSSP ratio) (left) and peptides **24**, **30** and **31** (1:2 βA:BSSP ratio) (right).

5.4 Conclusions

A new class of conformationally restricted BSBPs based on the hydrophobic core of β-amyloid has been developed. These BSBPs incorporate a five membered cyclic sulfamidate derived from α-methylisoserine, which confers a conformational rigidity to the adjacent residues. The resulting peptides adopt mostly folded conformations, as determined by CD, NMR, MD-tar and IRID experiments. We have proven that peptides incorporating this sulfamidate are able to modestly inhibit β-sheet agglomeration of the β-amyloid protein *in vitro*, which prevents amyloid fibril formation. Peptide **33** has shown to be the best BSBP candidate as judged by ThT fluorescence and CD experiments, even after one-week amyloid incubation. This new family of rationally designed BSBPs may be promising for the development of new drugs for the treatment of Alzheimer's and other neurodegenerative diseases by targeting the native folded structure of the β-amyloid monomer in solution. The capability of these candidates to disrupt the amyloid fibril agglomeration will be evaluated in cells.

5.5 References

(1) Stelzma, R. A.; Schnitzlein, H. N.; Murllagh, F. R. *Clin. Anat.* **1995**, *8*, 429–431.

(2) Maurer, U.; Maurer, K. *Alzheimer: The Life of a Physician and the Career of a Disease.*; Columbia University Press: New York, 2003.

(3) Chiti, F.; Dobson, C. M. *Annu. Rev. Biochem.* **2006**, *75*, 333–366.

(4) Scherzinger, E.; Sittler, A.; Schweiger, K.; Heiser, V.; Lurz, R.; Hasenbank, R.; Bates, G. P.; Lehrach, H.; Wanker, E. E. *Proc. Natl. Acad. Sci.* **1999**, *96*, 4604–4609.

(5) Nelson, P. T.; Schmitt, F. A.; Lin, Y.; Abner, E. L.; Jicha, G. A.; Patel, E.; Thomason, P. C.; Neltner, J. H.; Smith, C. D.; Santacruz, K. S.; Sonnen, J. A.; Poon, L. W.; Gearing, M.; Green, R. C.; Woodard, J. L.; Van Eldik, L. J.; Kryscio, R. J. *Brain* **2011**, *134*, 1506–1518.

(6) Masters, C. L.; Bateman, R.; Blennow, K.; Rowe, C. C.; Sperling, R. A.; Cummings, J. L. *Nat. Rev. Dis. Prim.* **2015**, *1*, 1–18.

(7) Nelson, P. T.; Alafuzoff, I.; Bigio, E. H.; Bouras, C.; Braak, H.; Cairns, N. J.; Castellani, R. J.; Crain, B. J.; Davies, P.; Tredici, K. Del; Duyckaerts, C.; Frosch, M. P.; Haroutunian, V.; Hof, P. R.; Hulette, C. M.; Hyman, B. T.; Iwatsubo, T.; Jellinger, K. A.; Jicha, G. A.; Kövari, E.; Kukull, W. A.; Leverenz, J. B.; Love, S.; Mackenzie, I. R.; Mann, D. M.; Masliah, E.; McKee, A. C.; Montine, T. J.; Morris, J. C.; Schneider, J. A.; Sonnen, J. A.; Thal, D. R.; Trojanowski, J. Q.; Troncoso, J. C.; Wisniewski, T.; Woltjer, R. L.; Beach, T. G. *J. Neuropathol. Exp. Neurol.* **2012**, *71*, 362–381.

(8) Minati, L.; Edginton, T.; Grazia Bruzzone, M.; Giaccone, G. *Am. J. Alzheimers. Dis. Other Demen.* **2009**, *24*, 95–121.

(9) Estrada, L. D.; Lasagna, C.; Soto, C. In *Pharmacological Mechanisms in Alzheimer's Therapeutics*; Springer, 2007; p 238.

(10) Citron, M. *Nat. Rev. Drug Discov.* **2010**, *9*, 387–398.

(11) Francioso, A.; Punzi, P.; Boffi, A.; Lori, C.; Martire, S.; Giordano, C.;

D'Erme, M.; Mosca, L. *Bioorg. Med. Chem.* **2015**, *23*, 1671–1683.

(12) Amijee, H.; Madine, J.; Middleton, D. A.; Doig, A. J. *Biochem. Soc. Trans.* **2009**, *37*, 692–696.

(13) Nerelius, C.; Sandegren, A.; Sargsyan, H.; Raunak, R.; Leijonmarck, H.; Chatterjee, U.; Fisahn, A.; Imarisio, S.; Lomas, D. A.; Crowther, D. C.; Strömberg, R.; Johansson, J. *Proc. Natl. Acad. Sci.* **2009**, *106*, 9191–9196.

(14) Soto, C.; Sigurdsson, E. M.; Morelli, L.; Kumar, R. A.; Castaño, E. M.; Frangione, B. *Nat. Med.* **1998**, *4*, 822–826.

(15) Adessi, C.; Soto, C. *Drug Dev. Res.* **2002**, *56*, 184–193.

(16) Adessi, C.; Frossard, M. J.; Boissard, C.; Fraga, S.; Bieler, S.; Ruckle, T.; Vilbois, F.; Robinson, S. M.; Mutter, M.; Banks, W. A.; Soto, C. *J. Biol. Chem.* **2003**, *278*, 13905–13911.

(17) Cruz, M.; Tusell, J. M.; Grillo-Bosch, D.; Albericio, F.; Serratosa, J.; Rabanal, F.; Giralt, E. *J. Pept. Res.* **2004**, *63*, 324–328.

(18) Giordano, C.; Punzi, P.; Lori, C.; Chiaraluce, R.; Consalvi, V. *ChemPlusChem* **2014**, *79*, 1036–1043.

(19) Nadimpally, K. C.; Paul, A.; Mandal, B. *ACS Chem. Neurosci.* **2014**, *5*, 400–408.

(20) Loureiro, J. A.; Crespo, R.; Börner, H.; Martins, P. M.; Rocha, F. A.; Coelho, M.; Carmo Pereira, M.; Rocha, S. *J. Mater. Chem. B* **2014**, *2*, 2259–2264.

(21) Chorev, M.; Goodman, M. *Trends Biotechnol.* **1995**, *13*, 438–445.

(22) Fletcher, M. D.; Campbell, M. M. *Chem. Rev.* **1998**, *98*, 763–796.

(23) Paul, A.; Nadimpally, K. C.; Mondal, T.; Thalluri, K.; Mandal, B. *Chem. Commun.* **2015**, *51*, 2245–2248.

(24) Giordano, C.; Masi, A.; Pizzini, A.; Sansone, A.; Consalvi, V.; Chiaraluce, R.; Lucente, G. *Eur. J. Med. Chem.* **2009**, *44*, 179–189.

(25) Giordano, C.; Sansone, A.; Masi, A.; Masci, A.; Mosca, L.; Chiaraluce, R.; Pasquo, A.; Consalvi, V. *Chem. Biol. Drug Des.* **2012**, *79*, 30–37.

(26) Minicozzi, V.; Chiaraluce, R.; Consalvi, V.; Giordano, C.; Narcisi, C.; Punzi, P.; Rossi, G. C.; Morante, S. *J. Biol. Chem.* **2014**, *289*, 11242–11252.

(27) Mazo, N.; García-González, I.; Navo, C. D.; Corzana, F.; Jiménez-Osés, G.; Avenoza, A.; Busto, J. H.; Peregrina, J. M. *Org. Lett.* **2015**, *17*, 5804–5807.

(28) Merrifield, R. B. *J. Am. Chem. Soc.* **1963**, *85*, 2149–2154.

(29) Navo, C. D.; Mazo, N.; Avenoza, A.; Busto, J. H.; Peregrina, J. M.; Jiménez-Osés, G. *J. Org. Chem.* **2017**, *82*, 13250–13255.

(30) Yang, Y. *Side Reactions in Peptide Synthesis*, 1st ed.; Elsevier, 2015; Vol. 13.

(31) Parrot, I.; Huang, P. C.; Khosla, C. *J. Biol. Chem.* **2002**, *277*, 45572–45578.

(32) Wuethrich, K. *NMR of Proteins and Nucleic Acids*; Wiley, 1986.

(33) Sandvoss, L. M.; Carlson, H. A. *J. Am. Chem. Soc.* **2003**, *125*, 15855–15862.

(34) Mantsyzov, A. B.; Savelyev, O. Y.; Ivantcova, P. M.; Bräse, S.; Kudryavtsev, K. V.; Polshakov, V. I. *Front. Chem.* **2018**, *6:91*.

(35) Ho, B. K.; Brasseur, R. *BMC Struct. Biol.* **2005**, 5:14.

(36) Uriarte, I.; Insausti, A.; Cocinero, E. J.; Jabri, A.; Kleiner, I.; Mouhib, H.; Alkorta, I. *J. Phys. Chem. Lett.* **2018**, *9*, 5906–5914.

(37) Bermejo, I. A.; Usabiaga, I.; Compañón, I.; Castro-López, J.; Insausti, A.; Fernández, J. A.; Avenoza, A.; Busto, J. H.; Jiménez-Barbero, J.; Asensio, J. L.; Peregrina, J. M.; Jiménez-Osés, G.; Hurtado-Guerrero, R.; Cocinero, E. J.; Corzana, F. *J. Am. Chem. Soc.* **2018**, *140*, 9952–9960.

(38) Carini, M.; Ruiz, M. P.; Usabiaga, I.; Fernández, J. A.; Cocinero, E. J.; Melle-Franco, M.; Diez-Perez, I.; Mateo-Alonso, A. *Nat. Commun.* **2017**, 8:15195.

(39) NIST Computational Chemistry Comparison and Benchmark Database NIST Standard Reference Database Number 101 Release 19, April 2018, Editor: Russell D. Johnson III DOI:10.18434/T47C7Z.

(40) Song, Y.; Moore, E. G.; Guo, Y.; Moore, J. S. *J. Am. Chem. Soc.* **2017**, *139*, 4298–4301.

(41) Vassar, P. S.; Culling, C. F. *Arch. Pathol.* **1959**, *68:487-98*.

(42) Naiki, H.; Higuchi, K.; Hosokawa, M.; Takeda, T. *Anal. Biochem.* **1989**, *177*, 244–249.

(43) LeVine, H. *Protein Sci.* **1993**, *2*, 404–410.

(44) LeVine, H. *Amyloid* **1995**, *2:1*, 1–6.

(45) Biancalana, M.; Makabe, K.; Koide, A.; Koide, S. *J. Mol. Biol.* **2009**, *385*, 1052–1063.

(46) Wu, C.; Wang, Z.; Lei, H.; Duan, Y.; Bowers, M. T.; Shea, J. E. *J. Mol. Biol.* **2008**, *384*, 718–729.

(47) Wu, C.; Wang, Z.; Lei, H.; Zhang, W.; Duan, Y. *J. Am. Chem. Soc.* **2007**, *129*, 1225–1232.

(48) Pinotsi, D.; Buell, A. K.; Dobson, C. M.; Kaminski Schierle, G. S.; Kaminski, C. F. *ChemBioChem* **2013**, *14*, 846–850.

Chapter 6.
Synthesis of chemically active α/β-peptides

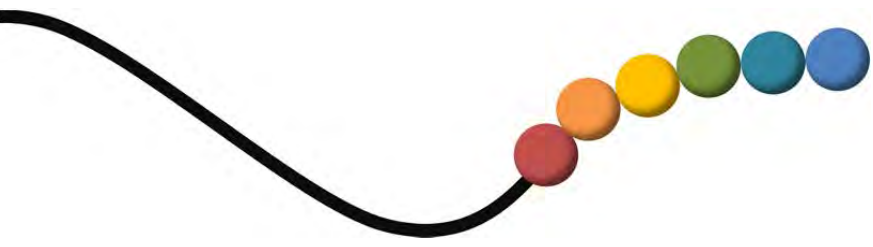

Mucins are a family of high molecular weight glycosylated proteins present in mucus, which play a key role in several biological processes.[1–3] To date, 21 different mucins have been discovered, all of them having a variable number of tandem sequences rich in proline, serine and threonine residues. The MUC1 is one of the most studied mucins and is constituted by 20 to 125 tandem-type repeats of a core sequence of 20 amino acids: HGVTSAPDTRPAPGSTAPPA.[4–7] This sequence has three important regions, GVTSA, where the GalNAc transferases enzymes[8] start the glycosylation process, PDTRP, recognized by anti-MUC1 antibodies[9] and related to several types of cancer and GSTAP, recognized by anti-Tn antigen antibodies[10] (**Figure 6.1**).

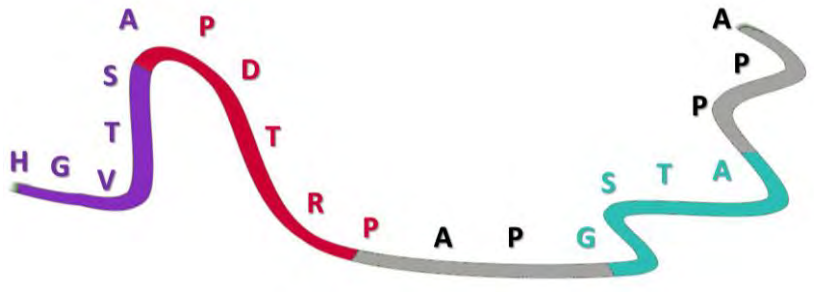

Figure 6.1. Sequence of MUC1 showing the three recognition regions in different colors.

The main goal of this chapter is the synthesis of analogs of the MUC1 protein epitope recognized by anti-MUC1 antibodies, incorporating our α-methylisoserine cyclic sulfamidate as a mimic of the initial serine residue (SAPDTRP). In order to modulate the conformations or introduce active compounds, the reactivity of the cyclic sulfamidate in a peptidic context will be studied by assaying several ring-opening reactions both in solution and on a solid support. Finally, we will investigate the ability of this sulfamidate to

release cargos attached to the *N*-terminal position of the peptides in a controlled manner.

6.1 Sulfamidate ring-opening reactions in solid phase

Performing chemical reactions on a solid support has considerable advantages with respect to solution chemistry. Reaction mixtures are commonly cleaner, lower purification steps are needed, and, in a peptide context, it allows the controlled elongation of the peptide chain. However, reaction monitoring under heterogeneous conditions may be difficult. Several types of reactions[11] using a solid support, in addition to prototypical amide bond formation, have been already described, such as cross-coupling (Heck, Stille, Suzuki),[12–17] cycloadditions (Diels-Alder, 1,3-dipolar),[18–20] enzymatic couplings,[21–23] Michael additions,[24] or nucleophilic substitution (*N*-, *O*-, *C*-, *S*-alkylations, glycosylation).[14,25–32] As an example, Boguslavsky's[33] or Albericio's[34] groups have recently reported 1,3-dipolar reactions between azides and alkynyl derivatives on a solid support catalyzed by copper(I) salts (**Scheme 6.1**).

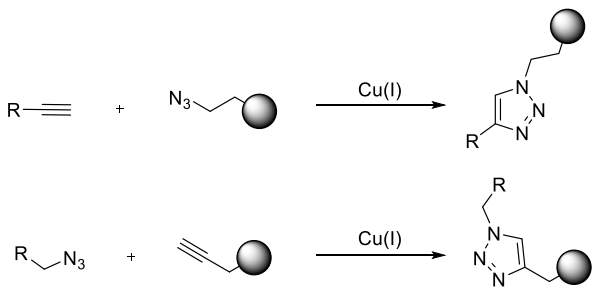

Scheme 6.1. Copper-catalyzed azide-alkyne cycloadditions using a solid support.

However, to date, only a few cases of heterogeneous reactions using cyclic sulfamidates have been reported. Halcomb introduced the sulfamidates

derived from L-serine and L-threonine in peptides and carried out a ring-opening reaction in resin, using β-1-thioglucose as a nucleophile to obtain thioglycopeptides.[35]

In contrast, Lubell performed sulfamidate ring-opening reactions using a peptide bound to the resin to obtain lactams (**Scheme 6.2**).[36–38]

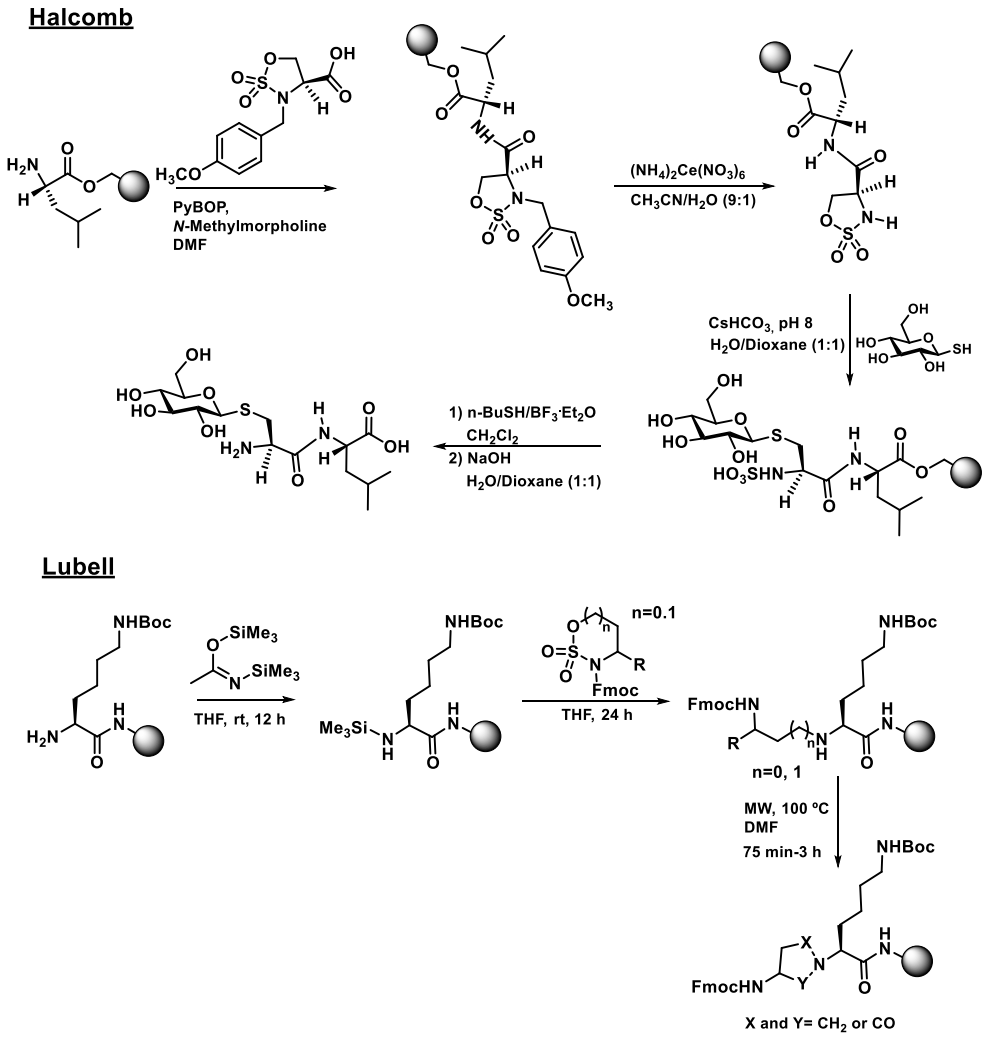

Scheme 6.2. Examples of ring-opening reactions of sulfamidates in solid phase.

Following the strategies developed by our group for the ring-opening of cyclic sulfamidates with different nucleophiles in homogenous phase, either alone or incorporated in small peptides,[39–44] we decided to expand this reactivity to longer peptides using a solid support. For this purpose, a slightly longer version of the well-known epitope of the MUC1 protein including the preceding serine (SAPDTRP) was selected. The initial serine of this sequence was substituted by our α-methylisoserine sulfamidate with the double goal of testing its ring-opening reaction at the quaternary carbon in a solid support and within a true peptide context but, more importantly, to probe the possibility of late-stage synthesis of chemically labelled and active hybrid $\alpha/\beta^{2,2}$-peptides using the MUC1 antibody recognition epitope as a biologically relevant proof of concept. The azide anion, 7-mercapto-4-methylcoumarin and protected β-1-thioglucose were selected as nucleophiles in order to chemically tag, fluorescently label and glycosylate the corresponding peptides as examples of site-selective peptide modification.

We first synthesized by SPPS and purified the precursor peptides **35** (Ac-**J**-APDTRP-NH_2, 78% global yield) and peptide **36** (**J**-APDTRP-NH_2, 86% global yield) using the optimized sulfamidate coupling protocol described in the previous chapter.

The azide group (N_3) has lately been attracting a great deal of interest in bioorthogonal chemistry and protein labelling[45] using copper-catalyzed and strain-promoted 1,3-dipolar cycloadditions. This kind of reactions is extensively utilized and studied in bioconjugation. For example, Ting and co-workers labelled specific cell surface proteins using an azide-tagged protein and a very reactive strained cyclooctyne-fluorophore in the absence of cytotoxic metal catalysts (**Scheme 6.3**).[46]

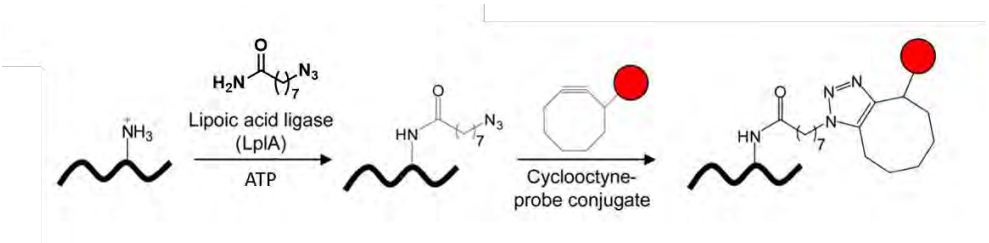

Scheme 6.3. Copper-free strain-promoted azide-alkyne cycloaddition in peptide bioconjugation.[46]

The ring-opening reaction of peptide **35** using the azide anion as a nucleophile was evaluated, both in homogeneous and in solid phases with comparative purposes. In homogeneous phase (after cleaving the sulfamidate peptide from the resin), we used 20 equivalents of NaN_3 in H_2O. The reaction was monitored by HPLC (**Figure 6.2**), observing the fast consumption of the starting material and the appearance of two new signals after 2 h, corresponding to the *N*-deacetylated peptide **36** and the targeted peptide **37′**.

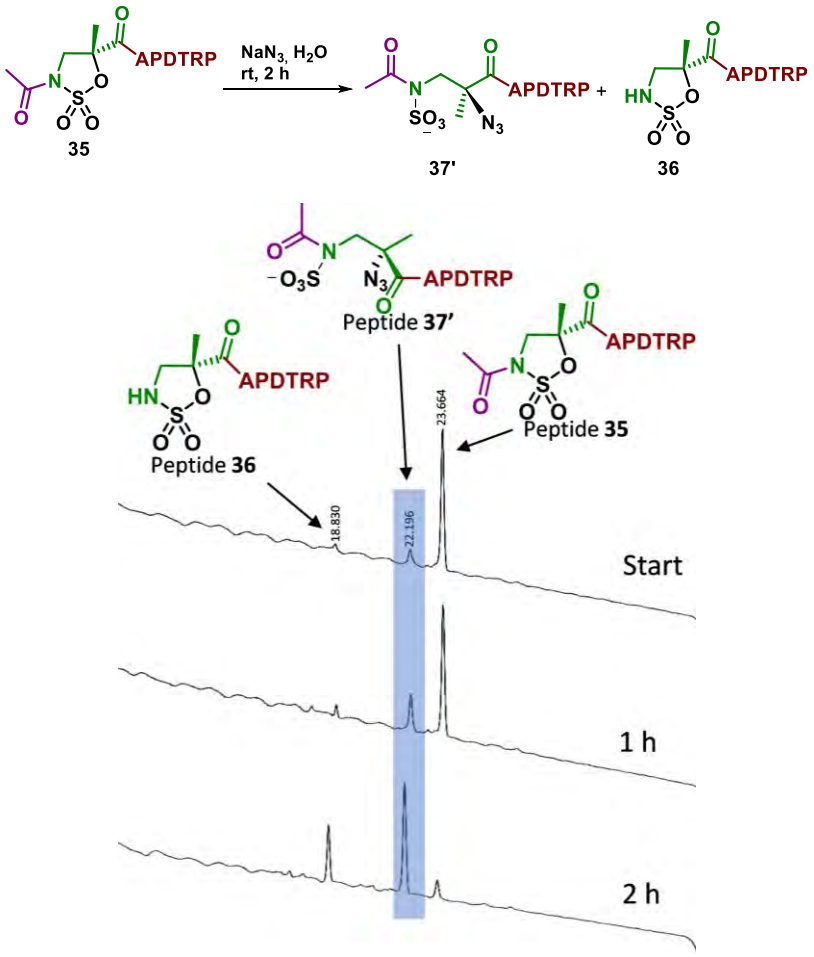

Figure 6.2. Ring-opening of sulfamidate-containing peptide **35** with azide anion in homogeneous phase monitored by HPLC. HPLC analyses were performed using linear gradient of 1 % to 31% B solvent in 37 min. Solvent A: H_2O containing 0.1% TFA (v/v); solvent B: acetonitrile.

We then attempted the ring-opening reaction in solid phase, using 20 equivalents of NaN_3 in DMF at room temperature for 3 hours. After cleaving the peptide from the resin using TFA/TIS/H_2O (95:2.5:2.5), the SO_3^- group was concomitantly removed. Of note, *N*-deacetylation of the sulfamidate was

not observed and the desired azide-labelled peptide **37** was obtained in a 31% global yield after HPLC purification.

From these results, we can conclude that the heterogeneous ring-opening reaction of sulfamidate is highly convenient compared to its homogeneous version, since it minimizes undesired side reactions with the nucleophile or the unprotected peptide side chains and allows much easier pre-purification prior to semi-preparative HPLC (i.e. removal of salts and high-boiling point solvents by simple filtration). Notably, the ring-opening products are diastereomerically pure, which strongly suggests that the S_N2-type mechanism with complete inversion of configuration at the quaternary carbon demonstrated early on for small-molecule tertiary sulfamidates also operates in a peptide context.[42,47]

Then, we studied the reactivity of this azide-labelled peptide towards 1,3-dipolar cycloaddition reaction. Hence, peptide **37** (1 equiv.) and the racemic cyclooctyne strained bicyclo[6.1.0]non-4-yn-9-ylmethanol (2 equiv.) were dissolved in a H_2O/CH_3CN (1:3) mixture and allowed to react at 25 ºC, the reaction being monitored by HPLC. As shown in **Figure 6.3**, nearly all peptide **37** was consumed after 30 min, and two new diastereomeric products, **38** and **38′**, were cleanly generated in a 1:1 ratio. After 2 hours, the starting material reacted completely. The reaction mixture was then lyophilized and purified by HPLC obtaining the diastereomers **38** and **38′** in a combined 77% yield.

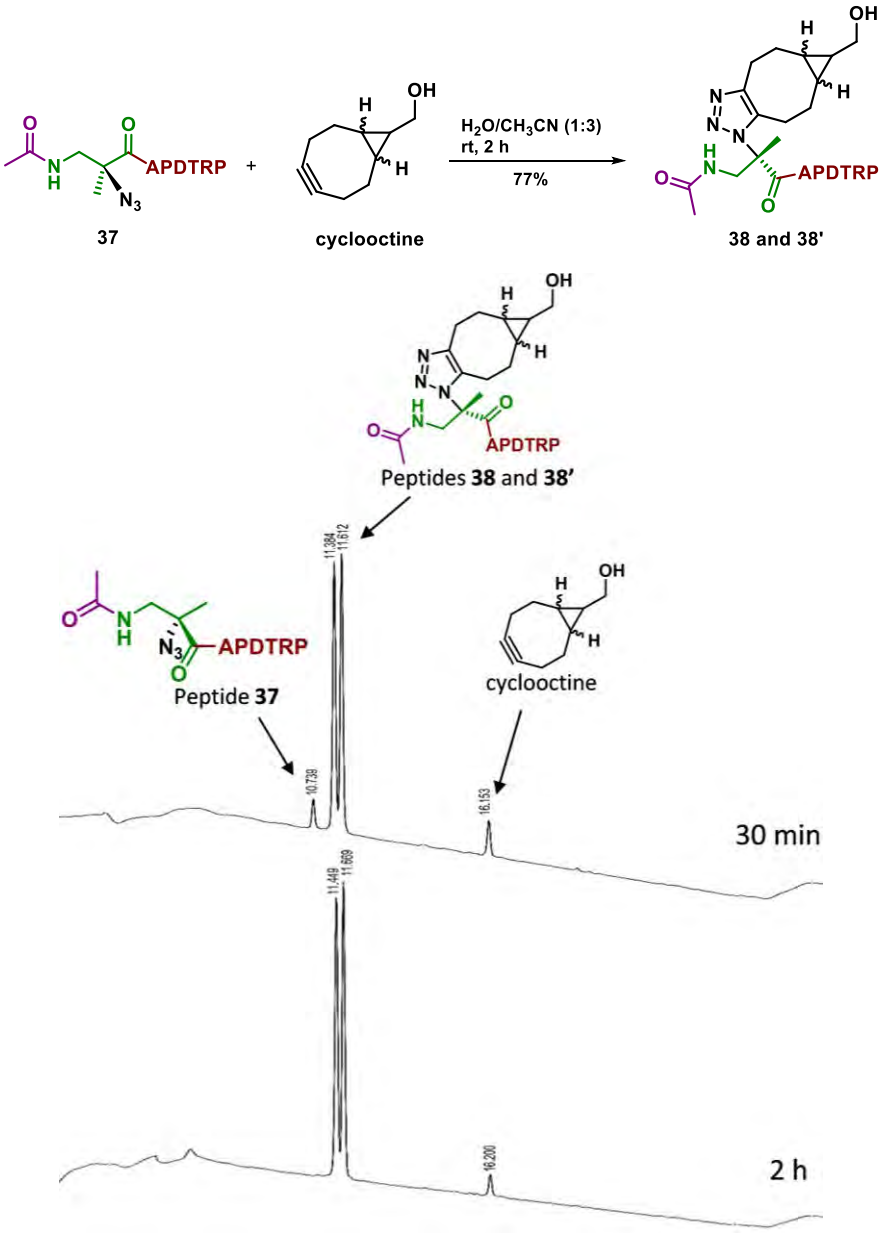

Figure 6.3. Strain-promoted 1,3-dipolar reaction of peptide **37** with a cyclooctyne tag monitored by HPLC. HPLC analyses were performed using a linear gradient of 5% to 65% B in 27 min. Solvent A: H_2O containing 0.1% TFA (v/v); solvent B: acetonitrile.

On the other hand, fluorescent molecules are very important in pharmacology and biochemistry, since they can be used as detection labels for direct visualization of proteins or cells.[48] Hence, we selected 7-mercapto-4-methylcoumarin (Coum) as a nucleophile, which would confer luminescent properties to the peptide, after the ring-opening reaction considering the results just described for the azide anion. The reaction was performed on solid support only, using 10 equivalents of Coum and 9 equivalents of DIPEA as base in DMF at 25 ºC for 1.5 hours. After cleavage from the resin and HPLC purification, a unique compound **39** corresponding to the labelled peptide was obtained in a moderate yield (45%) (**Scheme 6.4**). The fluorescence spectra of peptide **39** were acquired, obtaining an excitation maximum (λ_{exc}) at 331 nm and an emission maximum (λ_{em}) at 399 nm in DMSO, which are slightly blue-shifted with respect to those of Coum (**Figure 6.4**).

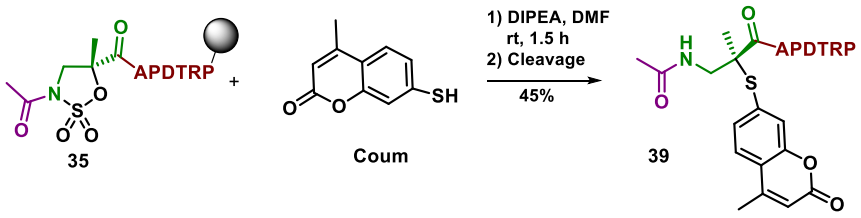

Scheme 6.4. Ring-opening reaction on-resin of peptide **35** with Coum to obtain peptide **39**.

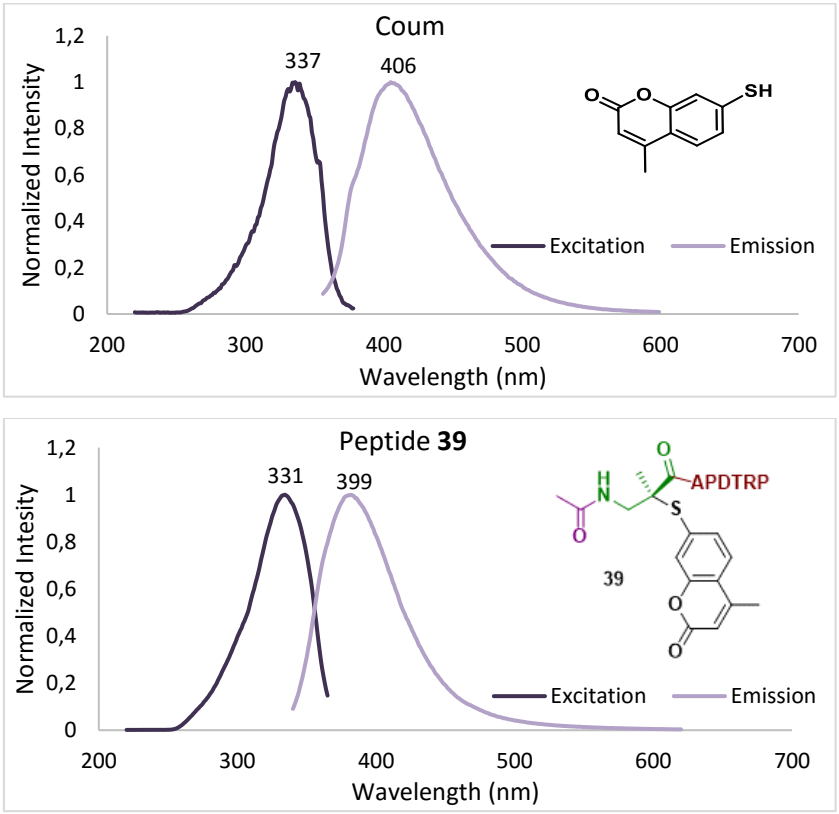

Figure 6.4. Excitation and emission spectra for Coum (top) and peptide **39** (bottom) in DMSO.

Finally, glycosylation is one of the most prevalent post-translational modifications (PTM) of peptides and proteins, with a defining impact on its structure and function.[49] This PTM is present in biologically active peptides such as antimicrobial sublancin.[50] Glycosylamino acids and glycopeptides

can be prepared by different methodologies. The most common one involves the use of carbohydrates as electrophiles and amino acids as nucleophiles, as in the Koenigs-Knorr[51] or Schmidt[52,53] reactions. On the other hand, our group has worked on a different methodology, using carbohydrates as nucleophiles and amino acids – in our case activated as cyclic sulfamidates– as electrophiles.[54]

Here, we used this methodology to perform a glycosylation reaction using a protected β-1-thioglucose as a sulfur nucleophile. Tetra-*O*-acetyl-β-1-thioglucose (10 equiv.) and DIPEA (9 equiv.) were reacted with resin-supported peptide **35** for 1.5 h. After deprotection of the carbohydrate acetyl groups using 70% hydrazine in methanol, cleavage from the resin and HPLC purification, a unique glycosylated peptide **40** was obtained in a moderate global yield (16%) (**Scheme 6.5**). Notably, the acetyl group at the peptide *N*-terminus was removed during the process instead of the SO_3^- moiety, which is normally cleaved upon acidic treatment. This finding confirms the high reactivity of carbonyl groups attached to *N*-sulfamic moieties such as those in either cyclic or ring-opened sulfamidates towards certain nucleophiles or bases such as hydrazine, as described before for the treatment of peptide **35** with sodium azide where significant *N*-deacetylation was observed.

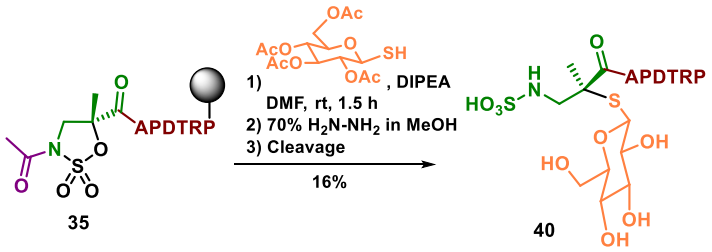

Scheme 6.5. On-resin thioglycosylation of sulfamidate peptide **35**.

6.2 Drug release using sulfamidate as cleavable linker

The ability to cleave chemical bonds between two entities in a controlled manner can be an effective tool to regulate the release of chemical functionalities. This feature has been used in organic synthesis[55] and, more recently, in chemical biology[56] including proteomics,[57,58] imaging,[59,60] DNA sequencing[61,62] and drug development.[63–65] These linkers must be resistant to the synthesis and purification processes, as well as compatible with biological molecules and environments, but are also required to be labile under certain conditions. In the case of drug delivery, prodrugs generally consist of two elements: the active agent (inactive drug) and a "carrier" bound through a cleavable linker, usually triggered by enzymatic hydrolysis or chemical conditions specific to the diseased tissue (**Figure 6.5**).

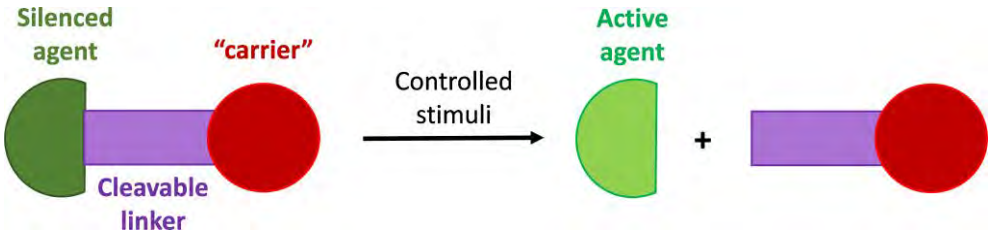

Figure 6.5. Schematic representation of controlled prodrug release.

In cancer treatment, using peptides or proteins as carriers is one of the most common strategies for drug delivery.[66] These peptides need to have high, selective affinity to target receptor over-expressed on cancer cells, and to trigger internalization process. On the other hand, the cleavable linker need to be stable out of the cell and released very fast intracellularly.

The goal in this section is to develop a new cleavable linker, based on the sulfamidate derived from α-methylisoserine.

As described through many examples throughout this thesis, we have observed that some functional groups, especially carbonyl groups (i.e. carbamates and amides) attached to the nitrogen of α-methylisoserine sulfamidate are quickly released under certain conditions. As observed in *chapter 5*, *i*-1 amino acid attached to the sulfamidate was cleaved during the Fmoc deprotection step, using 20% piperidine (a strong nucleophile and base) in DMF. In this same chapter, we described *N*-deacetylation of cyclic sulfamidates with azide anion and hydrazine. A similar behavior has been observed in linear sulfonamides, which have been used as linkers for SPPS of thioester peptides (**Scheme 6.6**).[67,68]

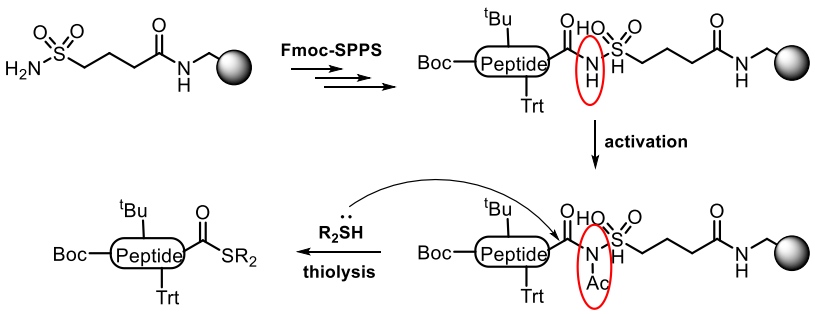

Scheme 6.6. Fmoc-based peptide thioester synthesis on the sulfonamide 'safety-catch' resin.

Inspired by this concept, we decided to deeply study this particular behavior of our sulfamidate attached to oligopeptides. Therefore, we decided to turn this apparent drawback into an advantage, envisioning this cyclic sulfamidate as a chemically labile carrier of biologically relevant molecules (**Figure 6.6**).

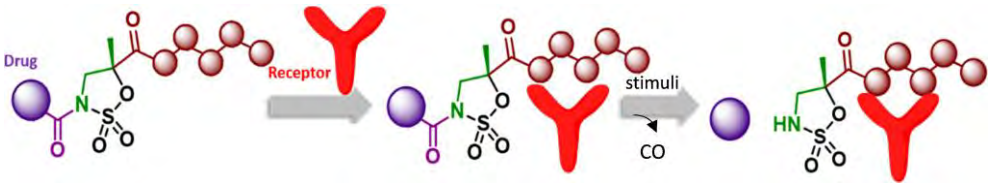

Figure 6.6. Sulfamidate as a labile cargo carrier.

First, we synthesized peptide Fmoc-A-**J**-APDTRP-NH_2 (**41**), following the conditions described in *chapter 5*. We observed that treatment with 20% piperidine in DMF (typical Fmoc-deprotection conditions) instantaneously cleaved the sulfonamide peptide bond, affording uniquely peptide **36**, **J**-APDTRP-NH_2. In fact, after treatment with much less aggressive Fmoc-deprotection reagents such as 2% DBU, 50% morpholine, or 20% DIPEA + 1.6% DBU in DMF, we observed again the fast clean cleavage of the Fmoc-Ala residue, obtaining always peptide **36** (**Figure 6.7**). These results demonstrate that even poorly nucleophilic bases trigger sulfamidate *N*-defunctionalization, suggesting that a base-promoted mechanism might operate in this transformation.

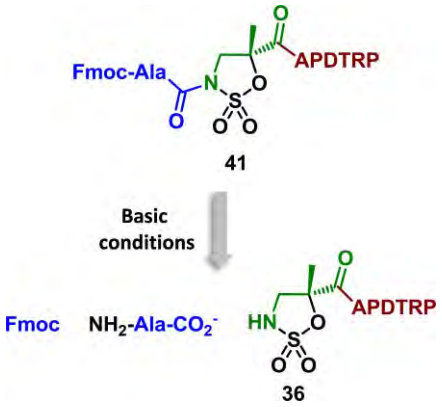

Figure 6.7. Reactivity of peptide **41** under different Fmoc deprotection conditions.

Therefore, combining both strategies (APDTRP sequence recognition and sulfamidate cleavage), we have designed a molecule that would recognize anti-MUC1 tumor antibodies specifically, and would release the cargo molecule attached to the sulfamidate due to pH variations across different cells, organelles or media.

The molecules that we used for this study as a proof-of-concept were biotin, which is a water-soluble vitamin involved in several metabolic processes as an enzyme cofactor,[69] and chlorambucil, which is a well-known chemotherapy drug frequently used for the treatment of some types of cancer, such as ovarian carcinoma and lymphomas.[70] Both molecules were on-resin coupled to sulfamidate-containing peptide **36** through their carboxylic group using TBTU/DIPEA at -20 ºC for 45 min in DMF. As described in *chapter 5*, performing the coupling at low temperature is essential to avoid cleavage of the newly formed sulfonamide bond and/or the ring-opening reaction with nucleophiles in the mixture. After peptide cleavage and purification by HPLC, peptides **42** and **43** were obtained in 62% and 33% yields, respectively (**Scheme 6.7**).

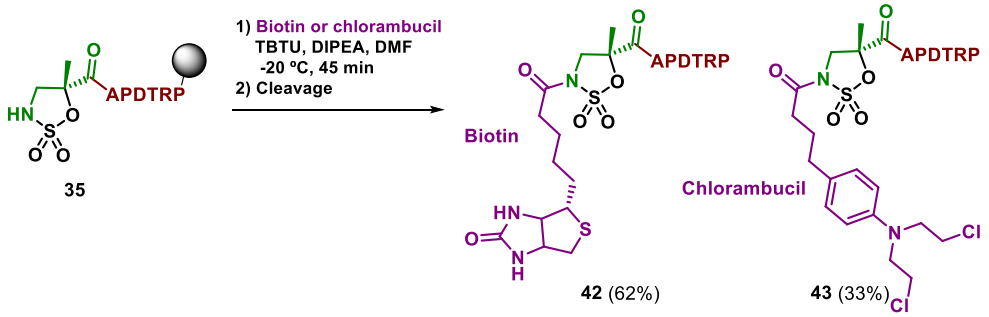

Scheme 6.7. SPPS synthesis of sulfamidate peptides **42** and **43** labelled at their *N* termini.

A kinetic study of pH-dependent chlorambucil release from peptide **43** was performed in different media. Peptide **43** was dissolved in PBS buffer (pH 7.4) simulating the physiological medium of a healthy cell environment, and another sample was dissolved in slightly acidic water (pH 6.3), simulating cancer cells media, which usually have an average pH around 6. Aliquots were taken periodically and then monitored by HPLC, observing a typical exponential decay. Notably, acidic medium accelerates the cleavage of chlorambucil by nearly 4-fold ($k_{6.3}$ = 0.23 h^{-1}; $k_{7.4}$ = 0.06 h^{-1}). This implies that the cytotoxic drug would remain attached to the sulfamidate peptide for longer times in healthy cells and it would be released faster in cancer cells. The very different lipophilicity of the peptide-attached and free chlorambucil (bearing a carboxylic acid), combined with the different ability of healthy and cancer cells to recognize and internalize the APDTRP sequence, might act synergistically to confer selective chemotherapy properties to peptides, such as **43**. These results suggest that this sulfamidate has a potential application for pH-dependent drug release (**Figure 6.8**). We plan to further extend this study by performing cytotoxicity assays with different known tumor-targeting peptide sequences in cancer cells in the near future.

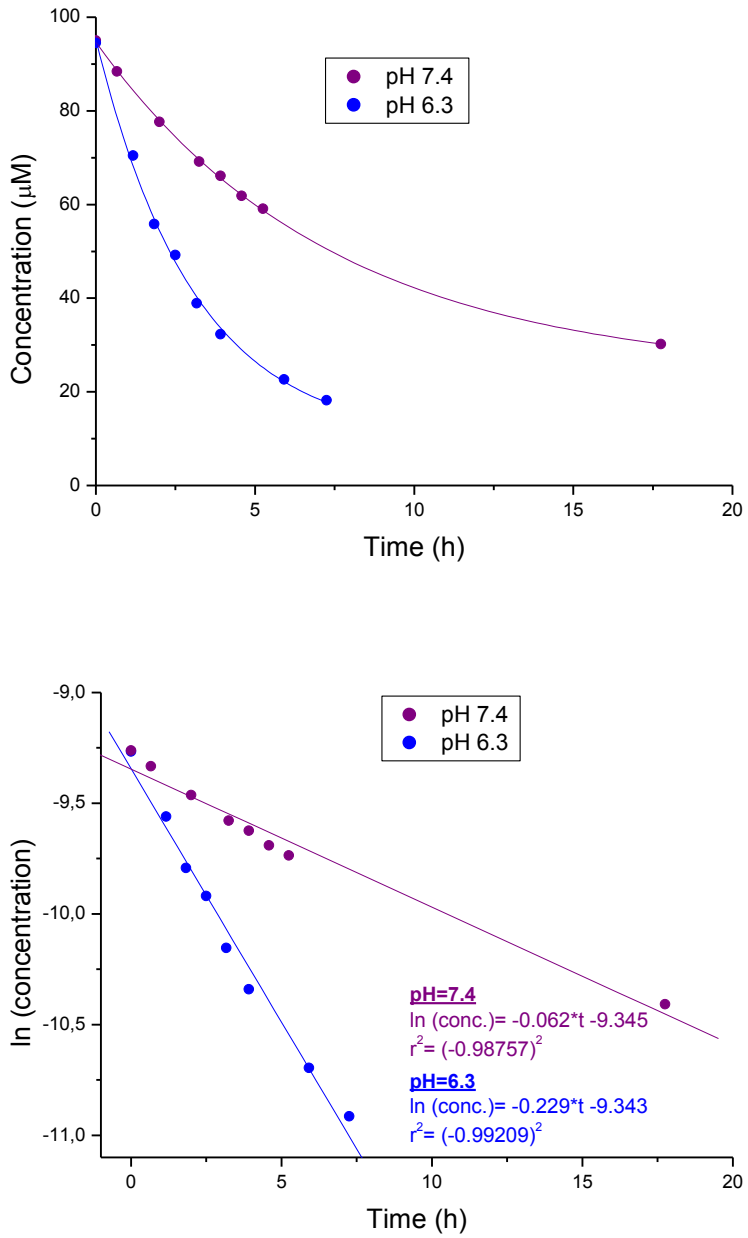

Figure 6.8. a) Graph representation of peptide **43** concentration *vs.* time measured at two different pH values. b) Graph representation of peptide **43** logarithm concentration vs time measured at two different pH values, which probes the first or pseudo-first order of the cargo release process.

6.3 Conclusions

We first demonstrated that the cyclic α-methylisoserine sulfamidate can be ring-opened on-resin as well as in homogeneous phase with various nucleophiles when incorporated in peptides, but with the advantage that the reaction is cleaner and less purification steps are needed under hetereogenous conditions. This methodology allows readily obtaining longer mixed α,$\beta^{2,2}$-peptides with different properties depending on the nucleophile selected. However, the high lability of the peptide bonds involving sulfamidate nitrogen precludes peptide chain elongation at the *N*-terminus..

Then, a new pH-dependent cleavable linker for controlled cargo release was developed, taking advantage of the lability of the peptide bonds at the *N*-terminus of the α-methylisoserine sulfamidate.

6.4 References

(1) Dwek, R. A. *Chem. Rev.* **1996**, *96*, 683–720.

(2) Sears, P.; Wong, C. H. *Cell. Mol. Life Sci.* **1998**, *54*, 223–252.

(3) Gaidzik, N.; Westerlind, U.; Kunz, H. *Chem. Soc. Rev.* **2013**, *42*, 4421–4442.

(4) Taylor-Papadimitriou, J.; Burchell, J.; Miles, D. W.; Dalziel, M. *Biochim. Biophys. Acta - Mol. Basis Dis.* **1999**, *1455*, 301–313.

(5) Taylor-Papadimitriou, J.; Burchell, J. .; Plunkett, T.; Graham, R.; Correa, I.; Miles, D.; Smith, M. *J Mammary Gland Biol Neoplasia* **2002**, *7*, 209–221.

(6) Parry, A. L.; Clemson, N. A.; Ellis, J.; Bernhard, S. S. R.; Davis, B. G.; Cameron, N. R. *J. Am. Chem. Soc.* **2013**, *135*, 9362–9365.

(7) Martínez-Sáez, N.; Peregrina, J. M.; Corzana, F. *Chem. Soc. Rev.* **2017**, *46*, 7154–7175.

(8) Dziadek, S.; Griesinger, C.; Kunz, H.; Reinscheid, U. M. *Chem. Eur. J.* **2006**, *12*, 4981–4993.

(9) Takeuchi, H.; Kato, K.; Denda-Nagai, K.; Hanisch, F. G.; Clausen, H.; Irimura, T. *J. Immunol. Methods* **2002**, *270*, 199–209.

(10) Huang, Z. H.; Shi, L.; Ma, J. W.; Sun, Z. Y.; Cai, H.; Chen, Y. X.; Zhao, Y. F.; Li, Y. M. *J. Am. Chem. Soc.* **2012**, *134*, 8730–8733.

(11) Hermkens, P. H. H.; Ottenheijm, H. C. J.; Rees, D. *Tetrahedron* **1996**, *52*, 4527–4554.

(12) Young, J. K.; Nelson, J. C.; Moore, J. S. *J. Am. Chem. Soc.* **1994**, *116*, 10841–10842.

(13) Hiroshige, M.; Hauske, J. R.; Zhou, P. **1995**, *36*, 4567–4570.

(14) Goff, D. A.; Zuckermann, R. N. *J. Org. Chem.* **1995**, *60*, 5744–5745.

(15) Forman, F. W.; Sucholeiki, I. *J. Org. Chem.* **1995**, *60*, 523–528.

(16) Plunkett, M. J.; Ellman, J. A. *J. Am. Chem. Soc.* **1995**, *117*, 3306–3307.

(17) Plunkett, M. J.; Ellman, J. A. *J. Org. Chem.* **1995**, *60*, 6006–6007.

(18) Ritter, H.; Sperber, R. *Macromolecules* **1994**, *27*, 5919–5920.

(19) Beebe, X.; Chiappari, C. L.; Olmstead, M. M.; Kurth, M. J.; Schore, N. E. *J.*

Org. Chem. **1995**, *60*, 4204–4212.

(20) Murphy, M. M.; Schullek, J. R.; Gordon, E. M.; Gallop, M. A. *J. Am. Chem. Soc.* **1995**, *117*, 7029–7030.

(21) Schuster, M.; Wang, P.; Wong, C. H.; Paulson, J. C. *J. Am. Chem. Soc.* **1994**, *116*, 1135–1136.

(22) Halcomb, R. L.; Huang, H.; Wong, C.-H. *J. Am. Chem. Soc.* **1994**, *116*, 11315–11322.

(23) Meldal, M.; Auzanneau, F. I.; Hindsgaul, O.; Palcic, M. M. *J. Chem. Soc., Chem. Commun.* **1994**, 1849–1850.

(24) Chen, C.; Ahlberg Randall, L. A.; Miller, R. B.; Jonesl, A. D.; Kurth, M. J. *J. Am. Chem. Soc.* **1994**, *116*, 2661–2662.

(25) Kick, E. K.; Ellman, J. A. *J. Med. Chem.* **1995**, *38*, 1427–1430.

(26) Boojamra, C. G.; Burow, K. M.; Ellman, J. A. *J. Org. Chem.* **1995**, *60*, 5742–5743.

(27) Goff, D. A.; Zuckermann, R. N. *J. Org. Chem.* **1995**, *60*, 5748–5749.

(28) Dankwardt, S. M.; Newman, S. R.; Krstenansky, J. L.; Alto, P. *Tetrahedron Lett.* **1995**, *36*, 4923–4926.

(29) Zuckermann, R. N.; Martin, E. J.; Spellmeyer, D. C.; Stauber, G. B.; Shoemaker, K. R.; Kerr, J. M.; Figliozzi, G. M.; Goff, D. A.; Siani, M. A.; Simon, R. J.; Banville, S. C.; Brown, E. G.; Wang, L.; Richter, L. S.; Moos, W. H. *J. Med. Chem.* **1994**, *37*, 2678–2685.

(30) Zuckermann, R. N.; Kerr, J. M.; Moosf, W. H.; Kent, S. B. H. *J. Am. Chem. Soc.* **1992**, *114*, 10646–10647.

(31) Virgilio, A. A.; Ellman, J. A. *J. Am. Chem. Soc.* **1994**, *116*, 11580–11581.

(32) Douglas, S. P.; Whitfield, D. M.; Krepinsky, J. J. *J. Am. Chem. Soc.* **1995**, *117*, 2116–2117.

(33) Oyelere, A. K.; Chen, P. C.; Yao, L. P.; Boguslavsky, N. *J. Org. Chem.* **2006**, *71*, 9791–9796.

(34) Castro, V.; Rodríguez, H.; Albericio, F. *ACS Comb. Sci.* **2016**, *18*, 1–14.

(35) Cohen, S. B.; Halcomb, R. L. *J. Am. Chem. Soc.* **2002**, *124*, 2534–2543.

(36) Boutard, N.; Turcotte, S.; Beauregard, K.; Quiniou, C.; Chemtob, S.; Lubell, W. D. *J. Pept. Sci.* **2011**, *17*, 288–296.

(37) Boutard, N.; Jamieson, A. G.; Ong, H.; Lubell, W. D. *Chem. Biol. Drug Des.* **2010**, *75*, 40–50.

(38) Jamieson, A. G.; Boutard, N.; Beauregard, K.; Bodas, M. S.; Ong, H.; Quiniou, C.; Chemtob, S.; Lubell, W. D. *J. Am. Chem. Soc.* **2009**, *131*, 7917–7927.

(39) Mata, L.; Avenoza, A.; Busto, J. H.; Corzana, F.; Peregrina, J. M. *Chem. Eur. J.* **2012**, *18*, 15822–15830.

(40) Mata, L.; Jiménez-Osés, G.; Avenoza, A.; Busto, J. H.; Peregrina, J. M. *J. Org. Chem.* **2011**, *76*, 4034–4042.

(41) Avenoza, A.; Busto, J. H.; Jiménez-Osés, G.; Peregrina, J. M. *Synthesis* **2006**, 641–644.

(42) Avenoza, A.; Busto, J. H.; Corzana, F.; Jiménez-Osés, G.; Peregrina, J. M. *Chem. Commun.* **2004**, 980–981.

(43) Jiménez-Osés, G.; Avenoza, A.; Busto, J. H.; Peregrina, J. M. *Tetrahedron: Asymmetry* **2008**, *19*, 443–449.

(44) Mata, L.; Avenoza, A.; Busto, J. H.; Peregrina, J. M. *Chem. Eur. J.* **2013**, *19*, 6831–6839.

(45) Breidenbach, M. A.; Gallagher, J. E. G.; King, D. S.; Smart, B. P.; Wu, P.; Bertozzi, C. R. *Proc. Natl. Acad. Sci.* **2010**, *107*, 3988–3993.

(46) Fernández-Suárez, M.; Baruah, H.; Martínez-hernández, L.; Xie, K. T.; Baskin, J. M.; Bertozzi, C. R.; Ting, A. Y. *Nat. Biotechnol.* **2009**, *25*, 1483–1487.

(47) Navo, C. D.; Mazo, N.; Avenoza, A.; Busto, J. H.; Peregrina, J. M.; Jiménez-Osés, G. *J. Org. Chem.* **2017**, *82*, 13250–13255.

(48) Listunov, D.; Mazères, S.; Volovenko, Y.; Joly, E.; Génisson, Y.; Maraval, V.; Chauvin, R. *Bioorganic Med. Chem. Lett.* **2015**, *25*, 4652–4656.

(49) Hans-Joachim, G. *The Sugar Code Fundamentals of Glycosciences*; Wiley-Blackwell: Weinheim, 2009.

(50) Oman, T. J.; Boettcher, J. M.; Wang, H.; Okalibe, X. N.; van der Donk, W. A. *Nat. Chem. Biol.* **2011**, *7*, 78–80.

(51) Martínez-Sáez, N.; Supekar, N. T.; Wolfert, M. A.; Bermejo, I. A.; Hurtado-Guerrero, R.; Asensio, J. L.; Jiménez-Barbero, J.; Busto, J. H.; Avenoza, A.; Boons, G.-J.; Peregrina, J. M.; Corzana, F. *Chem. Sci.* **2016**, *7*, 2294–2301.

(52) Corzana, F.; Busto, J. H.; Marcelo, F.; García de Luis, M.; Asensio, J. L.; Martín-Santamaría, S.; Sáenz, Y.; Torres, C.; Jiménez-Barbero, J.; Avenoza, A.; Peregrina, J. M. *Chem. Commun.* **2011**, *47*, 5319–5321.

(53) Corzana, F.; Busto, J. H.; De Luis, M. G.; Fernández-Tejada, A.; Rodríguez, F.; Jiménez-Barbero, J.; Avenoza, A.; Peregrina, J. M. *Eur. J. Org. Chem.* **2010**, 3525–3542.

(54) Tovillas, P.; García, I.; Oroz, P.; Mazo, N.; Avenoza, A.; Corzana, F.; Jiménez-Osés, G.; Busto, J. H.; Peregrina, J. M. *J. Org. Chem.* **2018**, *83*, 4973–4980.

(55) Gil, C.; Bräse, S. *Curr. Opin. Chem. Biol.* **2004**, *8*, 230–237.

(56) Scott, P. J. H.; Steel, P. G. *Eur. J. Org. Chem.* **2006**, 2251–2268.

(57) Rudolf, G. C.; Heydenreuter, W.; Sieber, S. A. *Curr. Opin. Chem. Biol.* **2013**, *17*, 110–117.

(58) Leitner, A.; Walzthoeni, T.; Kahraman, A.; Herzog, F.; Rinner, O.; Beck, M.; Aebersold, R. *Mol. Cell. Proteomics* **2010**, *9*, 1634–1649.

(59) Olson, E. S.; Jiang, T.; Aguilera, T. A.; Nguyen, Q. T.; Ellies, L. G.; Scadeng, M.; Tsien, R. Y. *Proc. Natl. Acad. Sci.* **2010**, *107*, 4311–4316.

(60) Tian, R.; Li, M.; Wang, J.; Yu, M.; Kong, X.; Feng, Y.; Chen, Z.; Li, Y.; Huang, W.; Wu, W.; Hong, Z. *Org. Biomol. Chem.* **2014**, *12*, 5365–5374.

(61) Metzker, M. L. *Nat. Rev. Genet.* **2010**, *11*, 31–46.

(62) Gao, L.; Lu, Z. *Biochem. Biophys. Res. Commun.* **2009**, *387*, 421–424.

(63) Testa, B. *Curr. Opin. Chem. Biol.* **2009**, *13*, 338–344.

(64) Nori, A.; Kopeček, J. *Adv. Drug Deliv. Rev.* **2005**, *57*, 609–636.

(65) Mahato, R.; Tai, W.; Cheng, K. *Adv. Drug Deliv. Rev.* **2011**, *63*, 659–670.

(66) Vrettos, E. I.; Mező, G.; Tzakos, A. G. *Beilstein J. Org. Chem.* **2018**, *14*,

930–954.

(67) Shin, Y.; Winans, K. A.; Backes, B. J.; Kent, S. B. H.; Ellman, J. A.; Bertozzi, C. R. *J. Am. Chem. Soc.* **1999**, *121*, 11684–11689.

(68) Thomas, F. *J. Pept. Sci.* **2013**, *19*, 141–147.

(69) Cowell, J.; Buck, M.; Essa, A. H.; Clarke, R.; Vollmer, W.; Vollmer, D.; Hilkens, C. M.; Isaacs, J. D.; Hall, M. J.; Gray, J. *ChemBioChem* **2017**, *18*, 1688–1691.

(70) Miksa, B.; Sierant, M.; Skorupska, E.; Michalski, A.; Kazmierski, S.; Steinke, U.; Rozanski, A.; Uznanski, P. *Colloids Surfaces B Biointerfaces* **2017**, *159*, 820–828.

Chapter 7. Chemical synthesis of a cytolysin analog

Lanthipeptides[1–3] are broad spectrum antimicrobial ribosomally synthesized and post-translationally modified peptides containing sulfur cross-linked lanthionine (Lan) and/or methyllanthionine (MeLan). These residues are formed by a Michael-type addition reaction of a cysteine (Cys) to a dehydroalanine (Dha) or dehydrobutyrine (Dhb), respectively, previously formed by dehydration of Ser or Thr residues (**Figure 7.1**).[4]

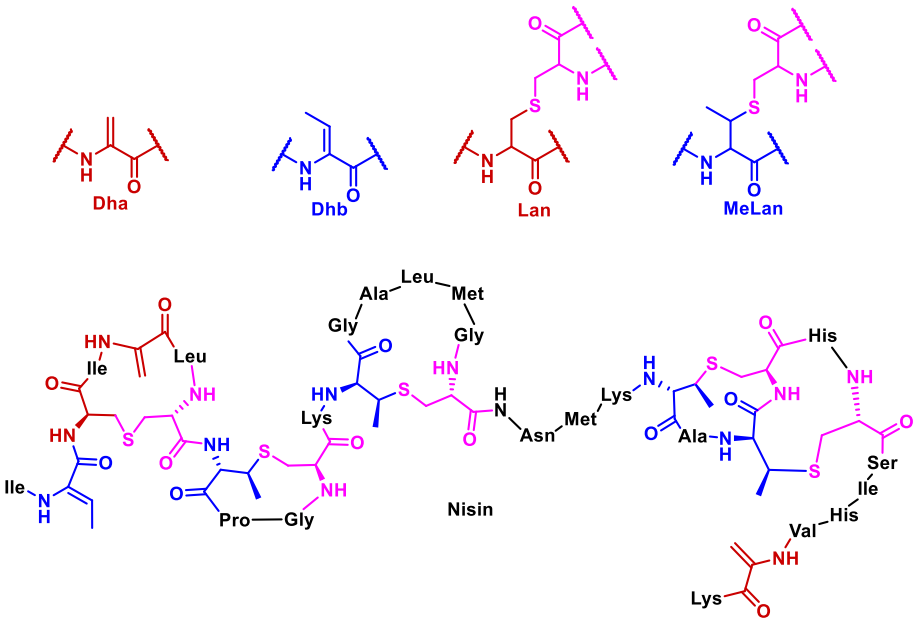

Figure 7.1. Structures of dehydroalanine (Dha), dehydrobutyrine (Dhb), lanthionine (Lan) and methyllanthionine (MeLan) and nisin.

The number of lanthipeptides described has increased in the last decades, from 26 in 1997 to more than 100 characterized peptides in 2015 (**Figure 7.2**).[5] This emphasizes the great deal of interest that lanthipeptides are attracting.

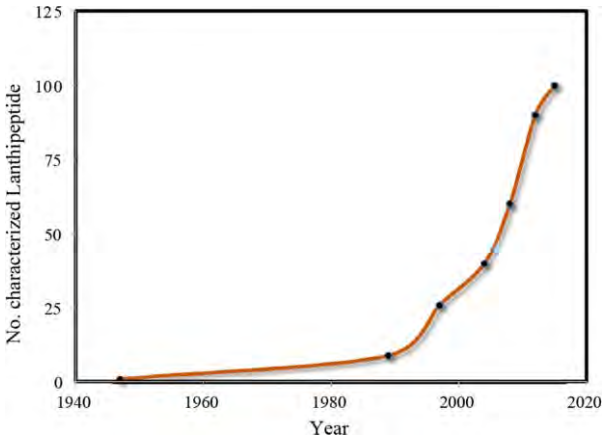

Figure 7.2. Characterized lanthipeptides over the years.[5]

One of the most common methodologies to obtain and study lanthipeptides is protein production using bacterial systems (*E.coli*).[6–9] This technique is quite useful since it allows quickly obtaining relatively high amounts of product and, combined with directed mutagenesis, provides access to large libraries of analogs and derivatives. However, this technique has some drawbacks. First, the DNA sequence of every enzyme participating in the biosynthesis of a certain lanthipeptide has to be known. Even if the gene sequence is known, its correct expression might be problematic, since different factors such as solubility in the expression media, appropriate folding or ligand binding play crucial rules. Moreover, if a specific step of the biosynthesis is to be studied separately, this may not be the most appropriate approach. In this sense, SPPS is an alternative to chemically synthesize lanthipeptides which has had an enormous impact over the last decades.[10] The first total synthesis of a lanthipeptide (nisin), was developed by Shiba and co-workers,[11] although in a very low global yield (0.003%). Most recent examples involving SPPS have achieved higher global yields (0.01-2.5%) and include the synthesis of lactocin S,[12–14] lacticin 3147,[15–18] analogs of epilancin 15X,[19] lacticin 481 and its analogs,[20] or cytolysin S ($CylL_S$) analogs[21] (**Table 7.1**).

Table 7.1. Some examples of chemically synthesized lanthipeptides, analogs and mimics.[5]

Lanthipeptides, analogs or mimics	Global yield (%)	number of steps	Average yield per step (%)
Nisin[11]	0.003	ND	70
Lactosin S[14]	10	71	97
Lacticin 3147[18]	1.0-1.4	>50	>95
Lacticin 481[20]	1.3	52	92
Epilacin 15X[19]	1.6	59	93
DAP-substituted ring A of lactocin S[13]	2.5	>71	93
Norleucine substituted lactocin S[12]	0.8	>70	ND
Nle, DAP-substituted lactocin S[12]	1.8	>70	ND
N-terminal oxazole lactocin S[12]	0.3	>70	ND
Alkene substituted lacticin 3147 Ltnβ[17]	0.5	53	76
Oxygen-substituted lacticin 3147[16]	0.3	53	90
Bis(desmethyl)lacticin 3147[15]	1.3	>50	84
LL-diastereomers of lacticin 481[20]	1.3	>53	92
N-truncated variant of Epilancin 15X[19]	1.9	45	92
Cytolysin S[21]	0.01	45	83

ND= not determined

Cytolysin[22,23] is produced by *Enterococcus faecalis* and is a two-component lanthibiotic formed by the post-translationally modified peptides cytolysin L ($CylL_L$) and cytolysin S ($CylL_S$). It is toxic to Gram-positive bacteria[24,25] and is the only lanthibiotic that shows hemolytic activity against eukaryotic cells.[26] Van der Donk's group recently described the SPPS synthesis of two structural analogs of $CylL_S$ **(Figure 7.3)** in which Dhb2 is mutated to Dha (Dhb2Dha) and the absolute configuration of one methyllanthionine lanthiresidue was changed from DL-MeLan to LL-MeLan[21] (see **Table 7.1**).

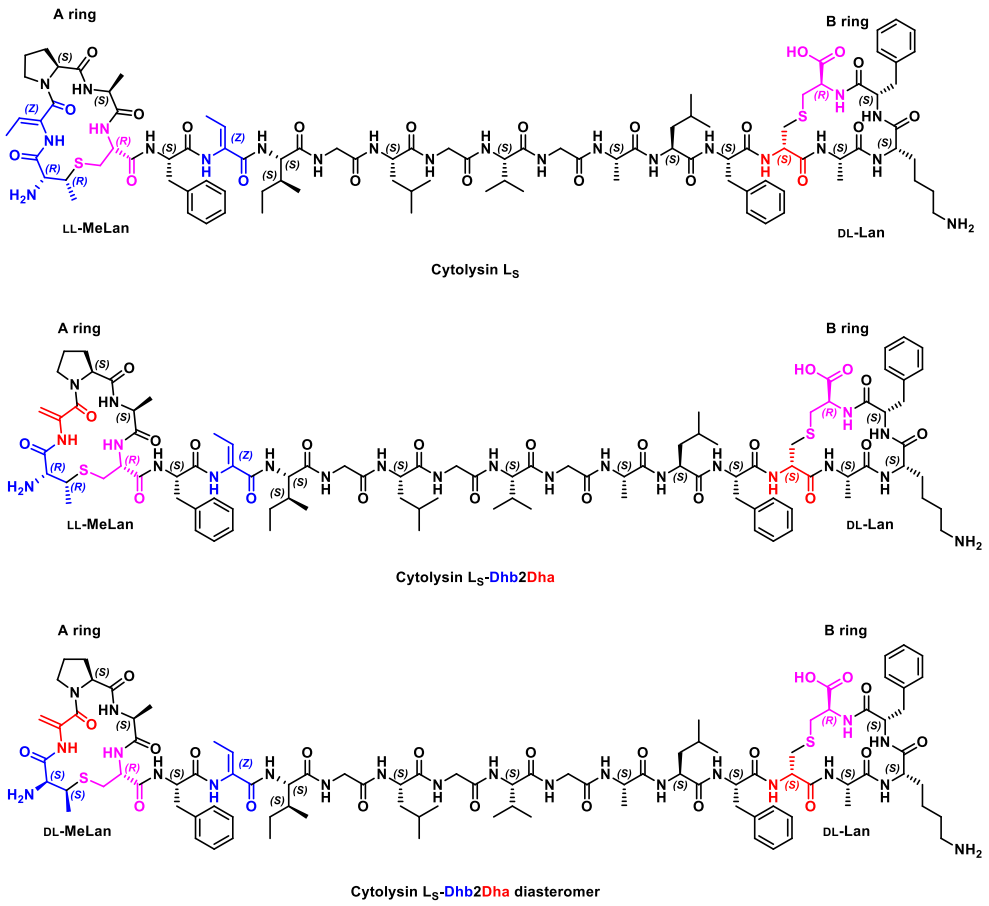

Figure 7.3. Structures of natural CylL$_S$ (top) and two CylL$_S$ analogs: CylL$_S$- Dhb2Dha, LL A ring, DL B ring (middle), and CylL$_S$- Dhb2Dha, DL A ring, DL B ring (bottom).

Bearing this background in mind, the main goal of this chapter is the stereocontrolled SPPS synthesis of a CylL$_S$ analog. Structural modifications will be introduced in ring A by substituting the native 2-aminobutyric acid (Abu) by the $\beta^{2,2}$-amino acid α-methyl-β-alanine (αMeβAla). The key step of this protocol will be the chemo-, regio- and stereoselective intramolecular nucleophilic ring-opening reaction of our α-methylisoserine sulfamidate by a conveniently deprotected cysteine leading to norlanthionine mimics. This post-synthetic maturation step will overcome the important limitation of non-

stereoselective sulfa-Michael additions to dehydroamino acids in native sequences under non-enzymatic conditions (**Figure 7.4**).

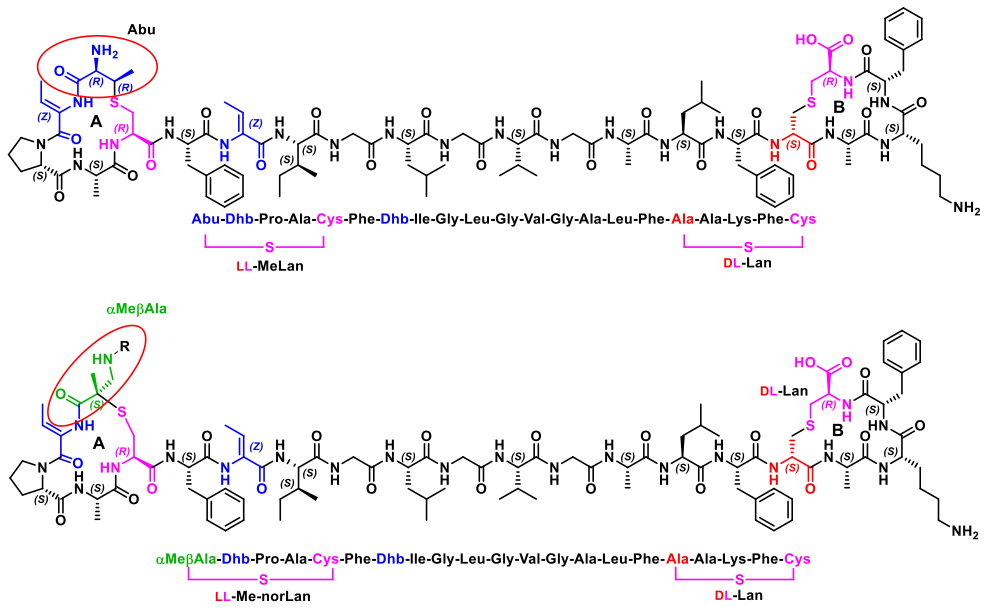

Figure 7.4. Structures of native CylL$_S$ (top) and our modified CylL$_S$ analog (bottom).

7.1 Intramolecular ring-opening reactions

Before proceeding with the SPPS of the full-length CylL$_S$ analog, the ability of our α-methylisoserine sulfamidate to undergo chemoselective intramolecular ring-opening with a cysteine thiol in the presence of other nucleophilic sidechains was tested. Hence, peptide **44** (FmocA-**J**-AHNCG-NH_2) and its *N*-deacylated variant **45**, both bearing highly polar residues such as histidine and asparagine and a nucleophilic target cysteine, were synthesized following the methodology described in *chapter 5*. In order to monitor the reaction by NMR, which allows obtaining more detailed structural information of the process than HPLC, peptide **44** was dissolved in

570 µL of a mixture of CD_3CN/D_2O (96:4) and Et_3N (1.6 equiv.) was added as a base to activate Cys. Immediately, the solution became cloudy and after a few seconds it became transparent again. At this time, the ^1H NMR spectrum of the crude mixture showed a unique product, whose signal pattern was quite different from that of the starting material and closely resembling the spectrum of *N*-deacylated **45**, although clearly preserving the Fmoc-Ala fragment (**Figure 7.5**). The signals corresponding to the tertiary methyl and CH_2 groups of the sulfamidate shifted to slightly lower ppm values, while maintaining their usual *J*-coupling pattern, suggesting that sulfamidate did not undergo ring-opening and that no amino acid was present at the *N*-terminus.

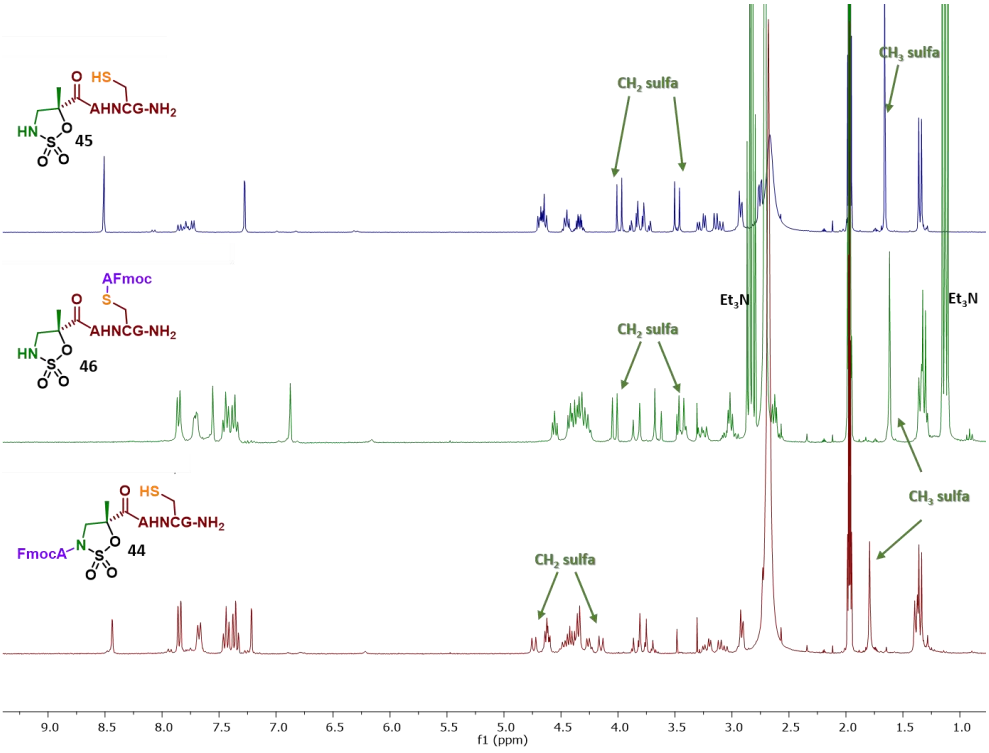

Figure 7.5. ^1H NMR spectra for peptide **44** (bottom) and after treatment with Et_3N (middle). *N*-deacylated peptide **45** (top) is shown as a reference.

HPLC analysis of the mixture also showed a unique signal at a retention time similar to that of the starting peptide (**Figure 7.6**). The new peptide showed the same mass (M= 956.30 amu) than the starting material (peptide **44**) confirming that both compounds contain the same residues. These results suggest that the FmocAla residue had been transferred from the nitrogen atom of the sulfamidate to the sulfur atom of the cysteine via intramolecular (*N*→*S*)-transacylation (i.e. acyl shift or migration) to give peptide **46**, instead of the cysteine undergoing sulfamidate ring-opening. This result demonstrates again the highly activated character of the carbonyl groups attached to that position, as seen on previous chapters.

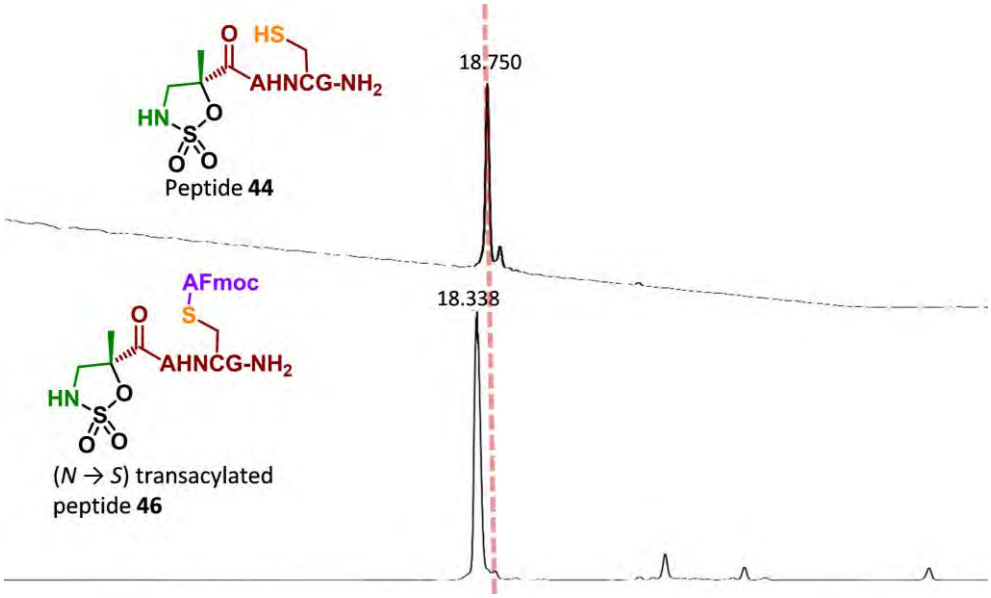

Figure 7.6. HPLC analysis of the reaction of peptide **44** before (top) and after treatment with Et_3N yielding peptide **46** (bottom). HPLC analyses were performed using a linear gradient of 1% to 71% of solvent B in 35 min. Solvent A: H_2O containing 0.1% TFA (v/v); solvent B: acetonitrile.

This type of reactivity is also observed in class II intein-like peptides, where a (*N*→*S*)-acyl shift followed by a trans(thio)esterification takes place before Asn-mediated protein splicing to cleave the intein and extein fragments (all reactions are catalyzed by enzymes in this case) (**Scheme 7.1**).[27]

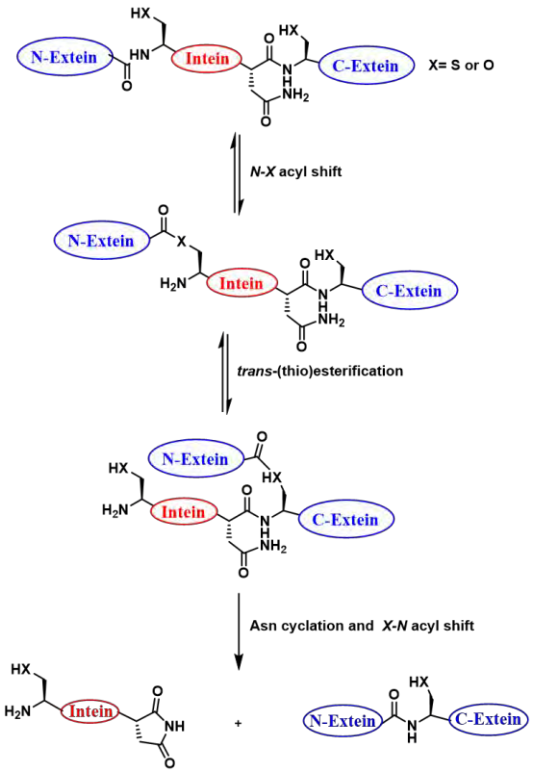

Scheme 7.1. (*N*→*X*) acyl shift involved in the mechanism of protein splicing in inteins. Usually X is the thiol group (SH) of a nucleophilic cysteine.

To test the influence that the distance between the sulfamidate and the nucleophilic cysteine could have on the chemoselectivity of the process (transacylation *vs.* ring opening), different analogous sequences with the cysteine placed at different positions of same-length and shorter motifs were analyzed. Hence, peptides **47** (FmocA-**J**-AHCNG-NH_2), **48** (FmocA-**J**-

AHNGC-NH_2) and **49** (FmocA-**J**-HNCG-NH_2) were synthesized, using the methodology described in *chapter 5*. They were separately dissolved in a mixture of CD_3CN/D_2O (96:4) and Et_3N (1.6 equiv.) was then added to each sample. The same variations were observed in the ^1H NMR spectra of all mixtures (**Figure 7.7**), suggesting that instantaneous and complete transacylation takes place regardless the position of the nucleophile.

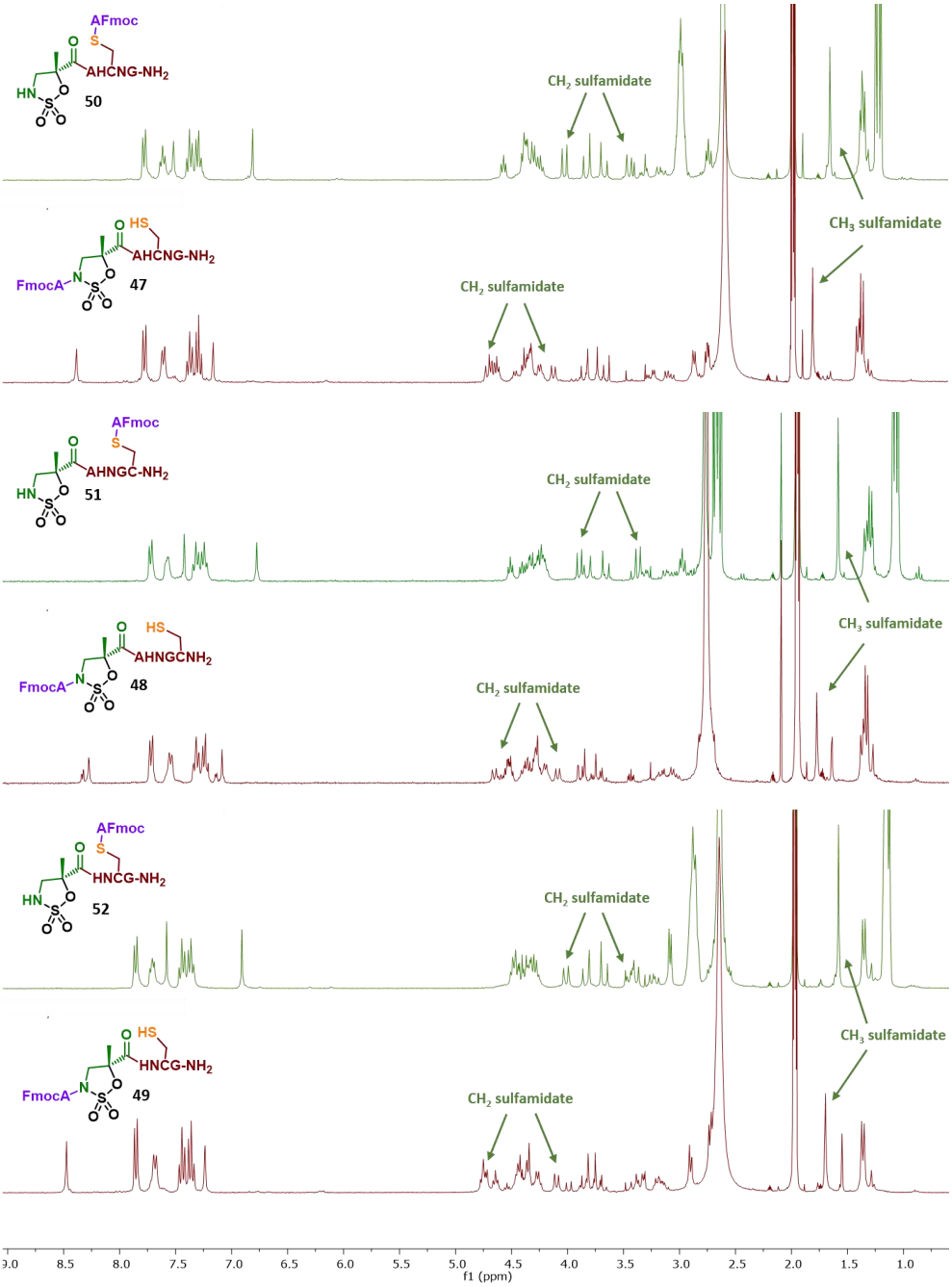

Figure 7.7. ^{1}H NMR spectra showing the (*N*→*S*) transacylation reactions of peptides **47-49** to give **50-52**.

Other nucleophilic amino acids were also evaluated by changing the Cys residue to Ser (peptide **53**), Thr (peptide **54**) or Lys (peptide **55**) in the original sequence. Under the same conditions (i.e. addition of 1.6 equiv. of Et_3N in CD_3CN/D_2O (96:4)), the transacylation reaction took place in the Lys-containing peptide (**55**) also in a few seconds as in the case of Cys. However, for the peptides containing Ser (**53**) and Thr (**54**), the reaction was not completed after 3 hours, due to the much lower nucleophilicity of the hydroxyl group compared to the thiol group of Cys or the amino group of Lys (**Figure 7.8**).

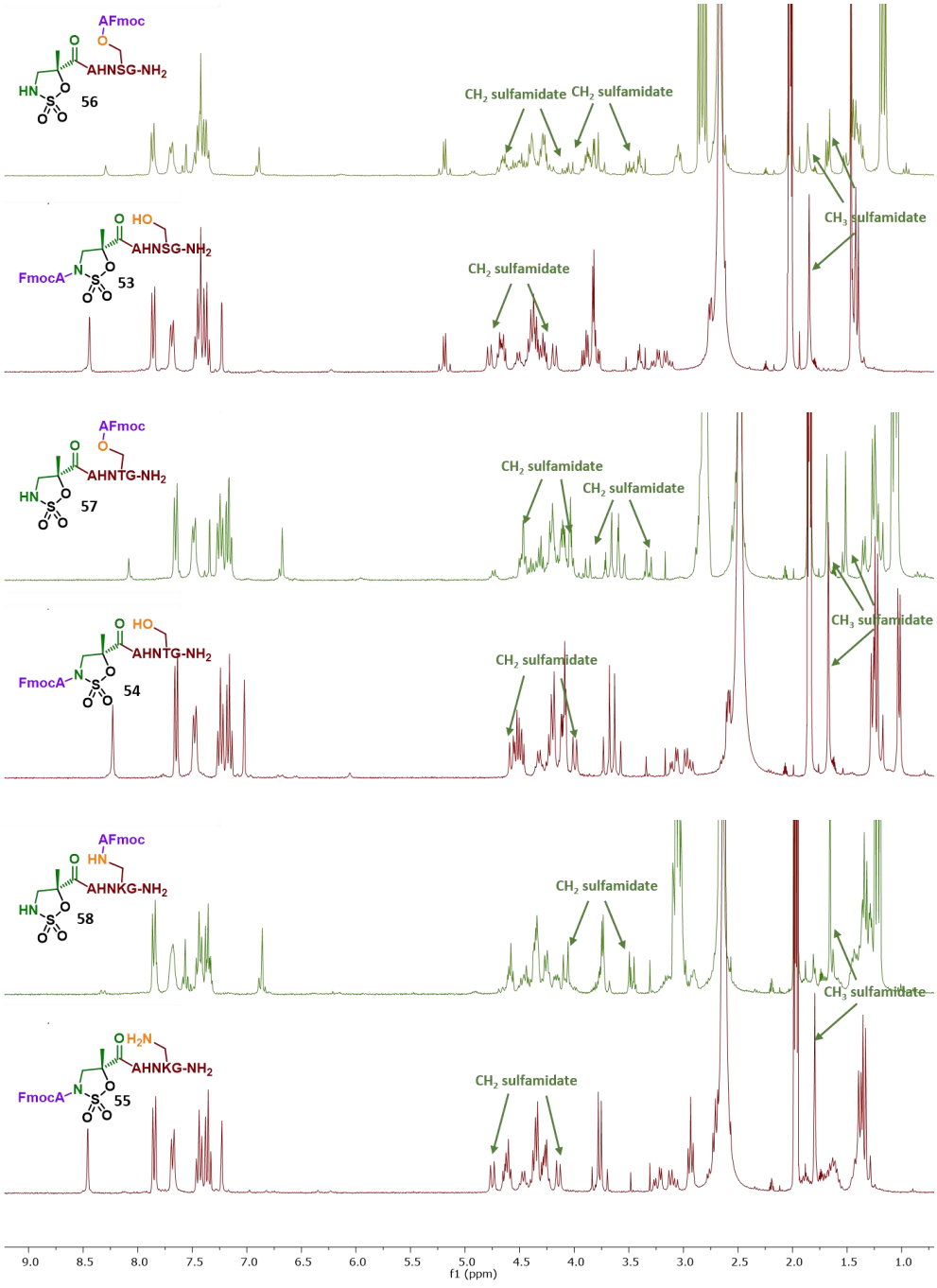

Figure 7.8. ^{1}H NMR spectra showing the (*N*→*O*) and (*N*→*N*) transacylation reactions of peptides **53-55** to give **56-58**.

Treatment with a large excess of *N*-ethylmaleimide (NEM) was performed on *S*-free and *S*-acylated peptides to test whether the thiol group of the cysteine was unprotected or not, as a confirmation of the occurrence of the transacylation reaction. Peptide **45** and transacylated peptide **46** were reacted with 15 equiv. of NEM in PBS buffer (50 mM, pH 7.4). After reacting for 2 hours at room temperature, the reaction mixtures were ziptiped and analyzed by ESI-MS (**Figure 7.9**). Cysteine of peptide **45** showed to be completely blocked by NEM. We also observed a small signal corresponding to the addition of a second NEM molecule, which may have reacted with either the NH of the sulfamidate or the histidine sidechain via *N*-Michael addition reaction. On the contrary, the main signal observed for transacylated peptide **46** after the NEM assay corresponded to the starting material, confirming that its cysteine was already acylated. Similar to what described for peptide **45**, a small signal corresponding to the addition of one molecule (likely to His sidechain or sulfamidate NH) was also detected.

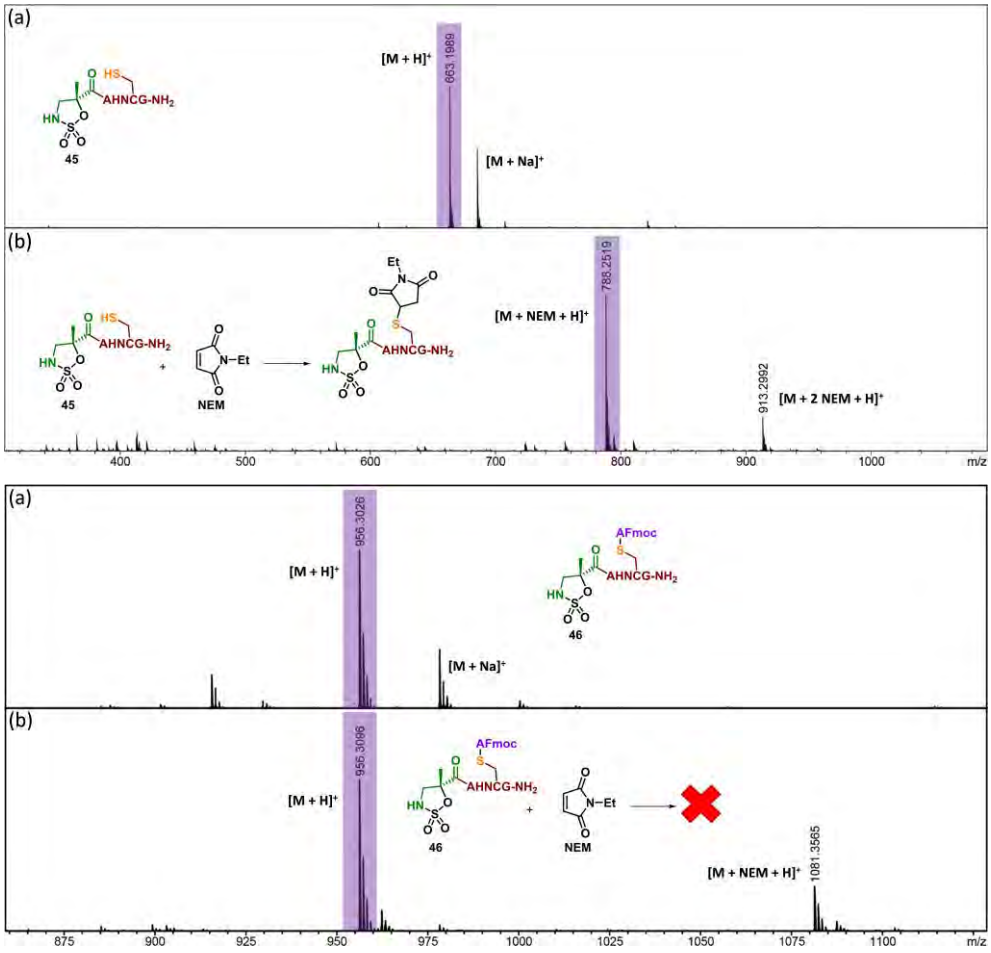

Figure 7.9. ESI-MS spectra of peptides **45** (top) and **46** (bottom) before (spectrum (a)) and after (spectrum (b)) treatment with *N*-ethylmaleimide (NEM).

The discovery of this (*N*→*X; X* = *S*, *N*, *O*)-transacylation reaction, which is unprecedented and arises from the now well-known high reactivity of carbonyl substituents at the *N*-terminus of our α-methylisoserine sulfamidate, offer potentially interesting possibilities for fast and efficient peptide sidechain modification. However, it completely precludes the desired intramolecular ring-opening reaction necessary to achieve the last-stage thioether formation leading to lanthipeptides such as the target $CylL_S$ analog.

In an attempt to avoid undesired inter- or intramolecular cleavage of *N*-carbonyl groups attached to the sulfamidate, while maintaining the necessary *N*-activation of the sulfamidate described in *chapter 3*, we explored the unreported substitution of *N*-carbonyl by *N*-sulfonyl functionalization. To this end, we selected the dansyl group (Dns), which, in addition to providing sulfamidate activation, would confer luminescence properties to the peptides. To the best of our knowledge, this type of sulfamidate functionalization has never been explored before. Following the optimized conditions described for sulfamidate *N*-acylation, but using dansyl chloride, peptide **59** (Dns-**J**-AHNCG-NH_2) was obtained in a good yield (42%) after HPLC purification (**Scheme 7.2**).

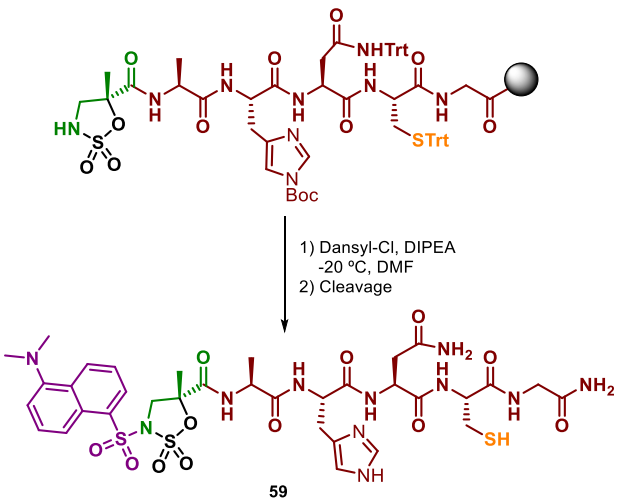

Scheme 7.2. Synthesis and structure of peptide **59**.

Then, peptide **59** was dissolved in CD_3CN/D_2O (96:4) in a quartz NMR tube and Et_3N (1.6 equiv.) was added. The reaction mixture became cloudy immediately after adding the base and the NMR signal profile changed. The signals corresponding to the H_α of Asn and H_α of Cys shifted upfield and the

CH_2 of Asn changed its *J*-coupling pattern and shifted downfield. More importantly, the CH_2 of sulfamidate shifted downfield and the H–H coupling constant increased from 10.3 to 15.5 Hz, strongly suggesting that a ring-opening reaction had took place (**Figure 7.10**).

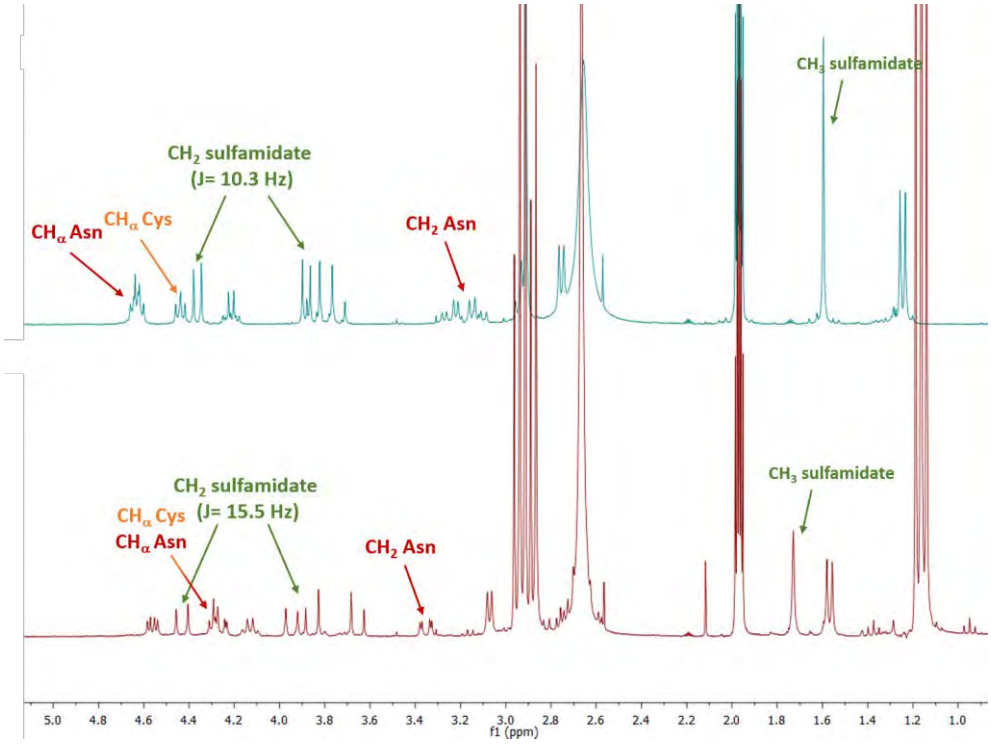

Figure 7.10. NMR spectra of peptide **59** before (top) and after (bottom) treatment with Et_3N.

HPLC analysis of the reaction was also carried out, revealing the fast and clean generation of a unique new compound with a lower retention time (**Figure 7.11**). This change in retention time, not observed when the (*N*→*S*) transacylation took place in the same peptide (**Figure 7.6**), suggests that the new peptide **60** is more polar than starting peptide **59**, again suggesting the occurrence of the desired intramolecular ring-open reaction, since a negative charge corresponding to the sulfamic group (*N*-SO_3^-), would have been

generated. Much to our delight, ESI-MS analysis confirmed that the pursued cyclization had indeed took place, given that the mass of peptide **60** coincided with the predicted one (M= 894.234 amu). Peptide **60** was obtained in excellent yield (84%) after HPLC purification.

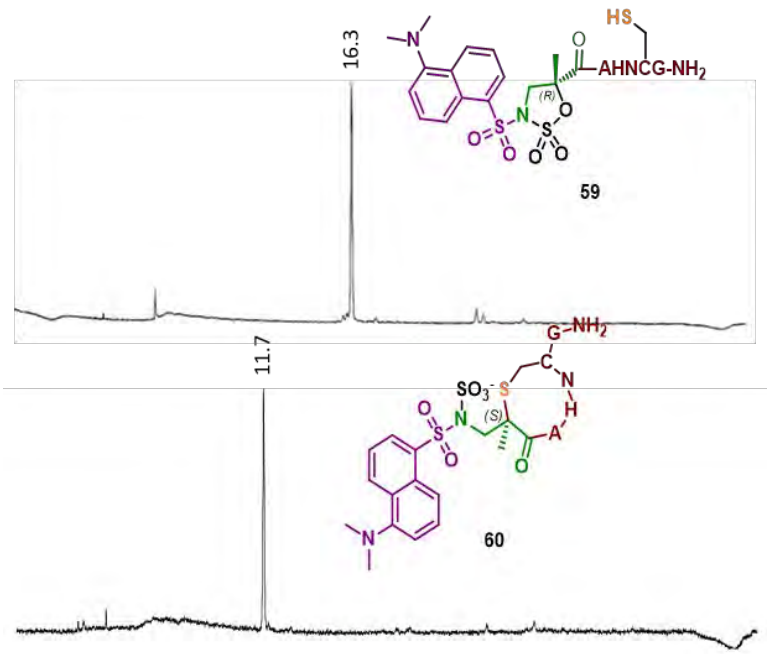

Figure 7.11. HPLC analysis of the reaction of peptide **59** before (top) and after treatment with Et_3N yielding peptide **60** (bottom). HPLC analyses were performed using a linear gradient of 1% to 71% of solvent B in 35 min. Solvent A: H_2O containing 0.1% TFA (v/v); solvent B: acetonitrile.

Strikingly, a dramatic increase of fluorescence was observed in peptide **59** upon cyclization to peptide **60** (**Figure 7.12**). Apparently, the fluorescence of the dansyl group in sulfamidate peptide **59** is quenched, and fluorescence is recovered upon sulfamidate ring-opening. This unexpected finding allows

direct visualization of the reaction progress, and offers the potential to using this type of α-methylisoserine peptides as pH sensors in cells.

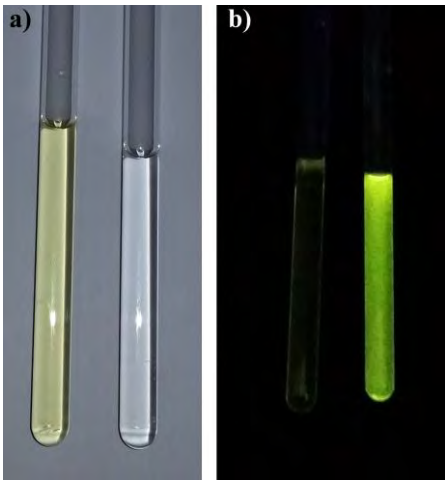

Figure 7.12. a) Luminescence under white light of peptide **59** (left) and peptide **60** (right) in CD_3CN/D_2O. b) Luminescence under UV-light (366 nm) of peptide **59** (left) and peptide **60** (right) in CD_3CN/D_2O.

7.2 Synthesis of a CylL$_S$ ring A analog

After discovering that *N*-sulfonyl substituents are able to trigger the desired sulfamidate intramolecular ring-opening reaction, we evaluated the feasibility of performing this key reaction on a more complex amino acid sequence and leading to a modified version of CylL$_S$ ring A incorporating a $\beta^{2,2}$-amino acid. To this aim, a variation of van der Donk's synthetic route towards CylL$_S$ using a sulfonyl-protecting group such as 4-nitrobenzyl sulfamate (*N–Ns*), was then attempted (**Figure 7.13**).

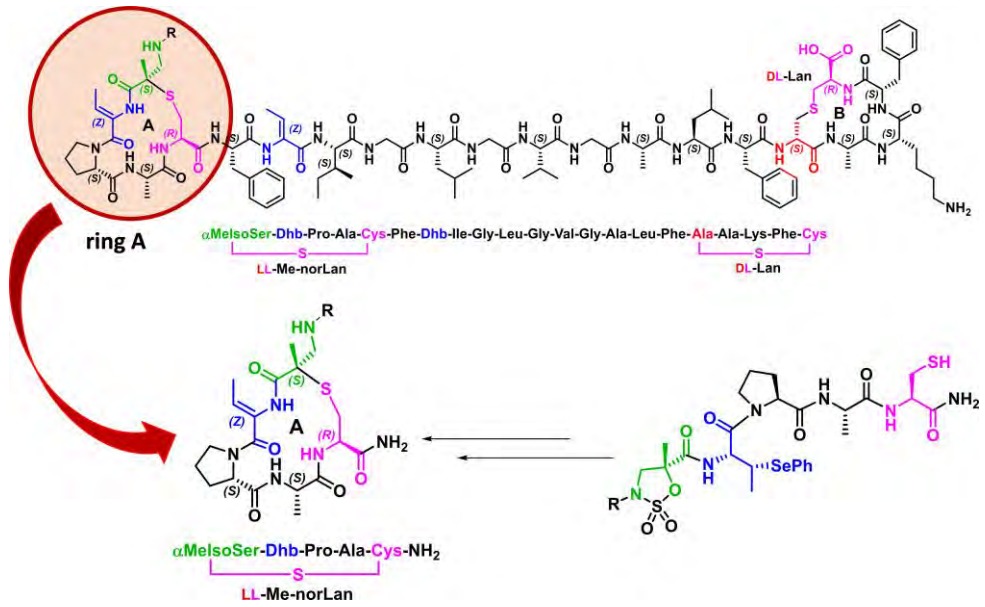

Figure 7.13. Strategy for the synthesis of a CylL$_S$ analog incorporating a $\beta^{2,2}$-amino acid in ring A (R = sulfonyl).

Before attempting the sulfamidate ring-opening, the electrophilic dehydrobutyrine (Dhb) residue present in the sequence needed to be masked to allow sequence elongation and to avoid potential competition with the sulfamidate through the *S*-Michael addition of cysteine. To this end and inspired by van der Donk's work,[28–30] we selected *Se*-phenyl-β-methylselenocysteine as a synthetic equivalent, which can be easily converted to Dhb by oxidative elimination. Non-commercially available building block **63** was obtained from L-threonine after five steps in 16% global yield (**Scheme 7.3**). First, threonine was orthogonally protected to obtain Fmoc-Thr-OMe. Tosylation of the alcohol group afforded compound **61** (67% yield), which was reacted with phenylselenide to obtain compound **62** in good yield (70 %). Finally, a selective hydrolysis of the methyl ester in the presence of the Fmoc group was carried out to obtain selenocysteine derivative **63** in good yield (83%).

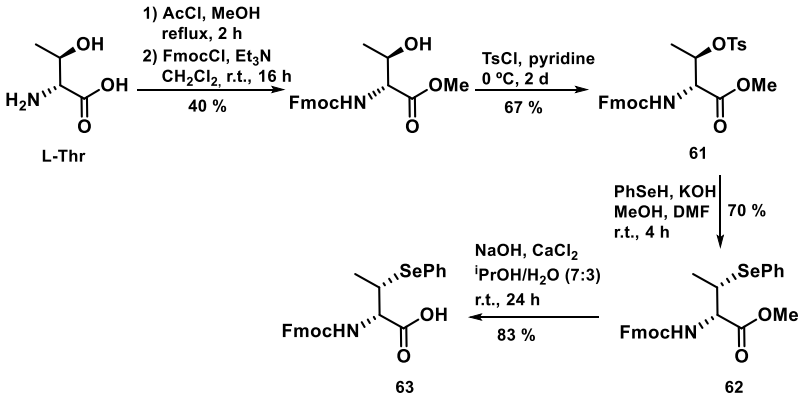

Scheme 7.3. Synthesis of building block **63**.

Linear peptide **64** was then synthesized using Rink Amide MBHA resin, HATU as a coupling reagent and DIPEA as a base for natural amino acids. Building block **63** was coupled following the conditions described by van der Donk´s group,[28,30] using HOAT and DIC as coupling reagents at room temperature for two hours. Once building block **63** was coupled, the Fmoc group was removed using optimized deprotection conditions (20% piperidine in DMF, 3 x 1 min). This careful Fmoc deprotection was done to prevent epimerization of selenocysteine. Then, sulfamidate **J** was coupled using the conditions described on *chapter 5*, and its *N*-terminus was protected with the nosyl (4-nitrobenzenesulfonyl, Ns) group, using a double coupling strategy with NsCl (6 equiv.) and DIPEA (6 equiv.) in DMF at -20 ºC for 45 min. Finally, the peptide was cleaved from the resin with TFA:TIS:H_2O:DODT (94:1:2.5:2.5) at room temperature for 1 hour, affording peptide **64** in a moderate global yield (18%) (**Scheme 7.4**).

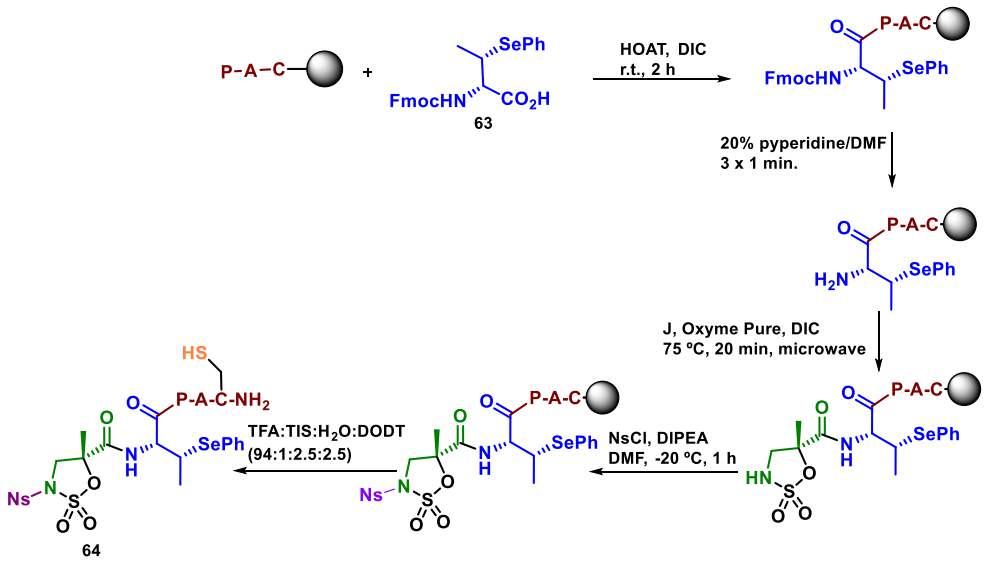

Scheme 7.4. SPPS synthesis of peptide **64**.

The ring-opening of the nosyl-activated sulfamidate with unprotected thiol of cysteine was performed using the conditions described in the previous section (1.6 equiv. of Et_3N in CD_3CN/D_2O (96:4)). The reaction progress was monitored by ^1H NMR, confirming that the reaction was completed after 30 minutes, and affording peptide **65** as a unique diastereomerically pure compound. This was also confirmed by ESI-MS and HPLC analysis of the reaction mixture, showing that the retention time of the initial signal decreased around 8 minutes, corresponding to the formation of a more polar compound. The reaction mixture was then purified through a solid-phase extraction (SPE) C18-cartridge and cyclic peptide **65** was dissolved in a 2 M HCl/CH_3CN (1:1) mixture to remove the SO_3^- moiety. After stirring for 30 minutes at room temperature, the reaction mixture was lyophilized, cleanly obtaining cyclic peptide **66**, as confirmed by ESI-MS and HPLC. Finally, oxidative elimination of *Se*-phenylselenocysteine with $NaIO_4$ to form the Dhb

residue quantitatively yielded peptide **67** after flash purification through a SPE C18-cartridge (**Scheme 7.5** and **Figure 7.14**).

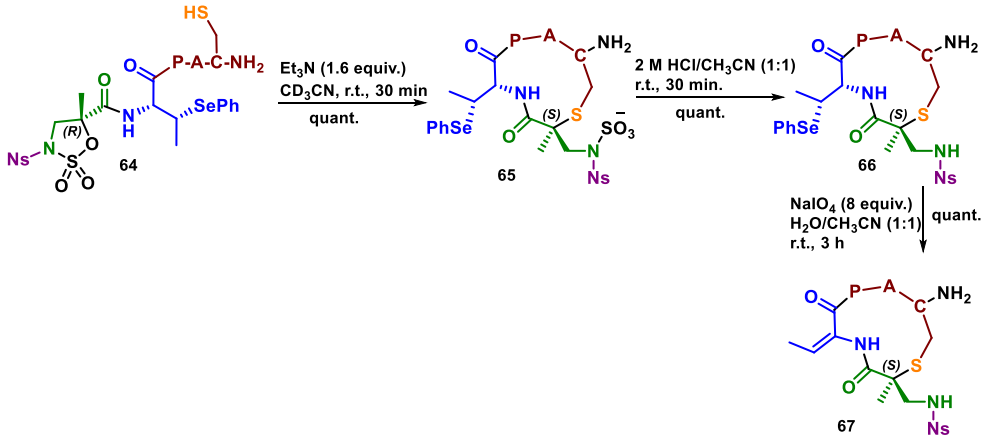

Scheme 7.5. Synthesis of modified CylL$_S$ ring A. **67**.

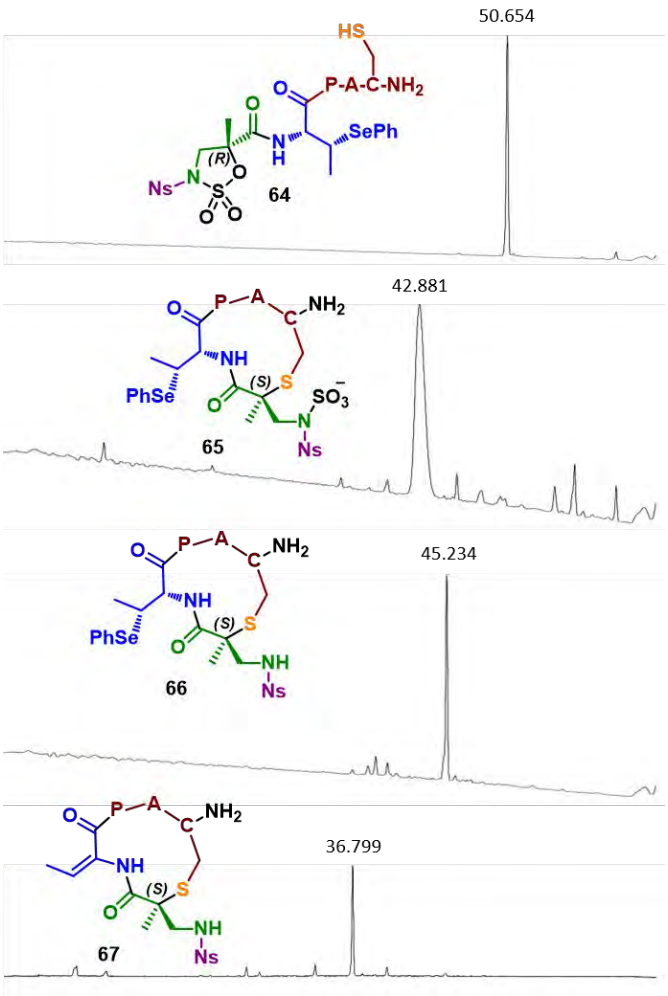

Figure 7.14. HPLC analysis of the mixtures of the reactions sequence starting from peptide **64** throughout **67.** HPLC analyses were performed using linear gradient of 1% to 65% of solvent B in 64 min. Solvent A: H_2O containing 0.1% TFA (v/v); solvent B: acetonitrile.

As can be inferred from the HPLC chromatograms, intermediate peptides **65** and **66**, as well as final peptide **67** were obtained with high purity indicating the absence of secondary reactions. Unfortunately, all attempts to remove the nosyl group with different thiols and bases were unsuccessful, so we decided

to maintain the sulfonyl-type tag at the *N*-terminus of the final peptides prepared through this methodology. Particularly, and in view of the preliminary results described in the previous sections, the dansyl group will be used as both a sulfamidate ring-opening promoter and a fluorescent label installed at the synthetic lanthipeptide analogues to visualize their cellular localization.[31]

7.3 Synthesis of a fluorescent full-length CylL$_S$ analog

The successful synthesis of cyclic peptide **67** encouraged us to attempt the synthesis of the full-length CylL$_S$ analog. To this aim, the orthogonally protected DL-Lan building block **69** was synthesized following the methodology described by van der Donk's group.[19,21,32] The key step of this protocol is the nucleophilic substitution reaction between the bromoalanine derivative **68** and the *in situ* formed Fmoc-Cys-O^{t}Bu derivative under phase-transfer catalysis conditions (**Scheme 7.6**).

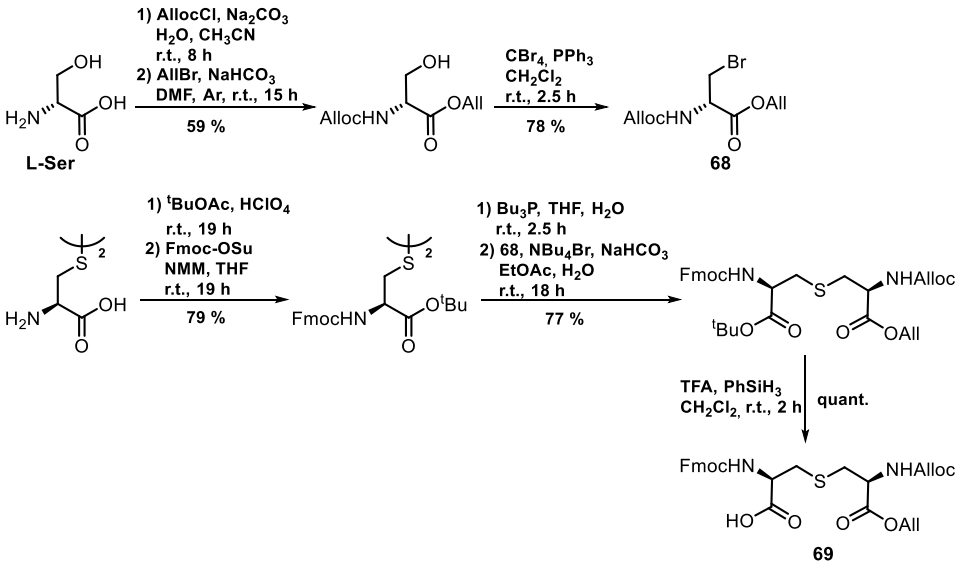

Scheme 7.6. Synthesis of building block **69**.

Once building blocks **63** and **69** were obtained, the $CylL_S$ analog was synthesized at the 0.05 mmol scale by SPPS, using the HMPB ChemMatrix resin in order to obtain the *C*-terminus as a carboxylic acid. The first lanthionine bis-amino acid building block **69** was coupled using DIC and DMAP as coupling reagents. The next residues (Phe, Lys, and Ala) were coupled using HATU as a coupling reagent and DIPEA as a base. Deprotection of allyl ester and allyl carbamate groups was achieved using palladium tetrakis-(triphenylphosphine) and morpholine in DMF, and the macrolactamization reaction to form $CylL_S$ cycle B was performed using PyAOP, HOAt and collidine, following the conditions described by van der Donk´s group.[21] The next amino acids (IGLGVGALF) were automatically coupled using Oxyma-Pure® and DIC as coupling reagents under microwave radiation. Building-block **63** was then manually coupled following the aforementioned conditions for peptide **64**. In order to avoid racemization of selenium- containing residues, Fmoc group was removed using 20% piperidine in DMF (3 x 1 min). This deprotection protocol was used for all the remaining amino acids in the sequence. Next, Phe, Cys, Ala and Pro were manually coupled using HATU and DIPEA as a coupling reagent and a base, respectively. Then, another masked Dhb selenocysteine building block **63** was coupled, and sulfamidate **J** was finally coupled using the conditions described in *chapter 5*. The sulfamidate *N*-terminus was fluorescently tagged with a dansyl group, using dansyl chloride (6 equiv.) and DIPEA (6 equiv.) in DMF at -20 ºC for 45 min. Finally, peptide cleavage and protecting groups removal was performed using TFA:TIS:H_2O:DODT (94:1:2.5:2.5) at room temperature for 1 hour, affording peptide **70** as confirmed by MALDI-TOF analysis. Despite the low signal-noise ratio in the HPLC chromatogram, we determined that peptide elutes at 20.2min (**Figure 7.15**).

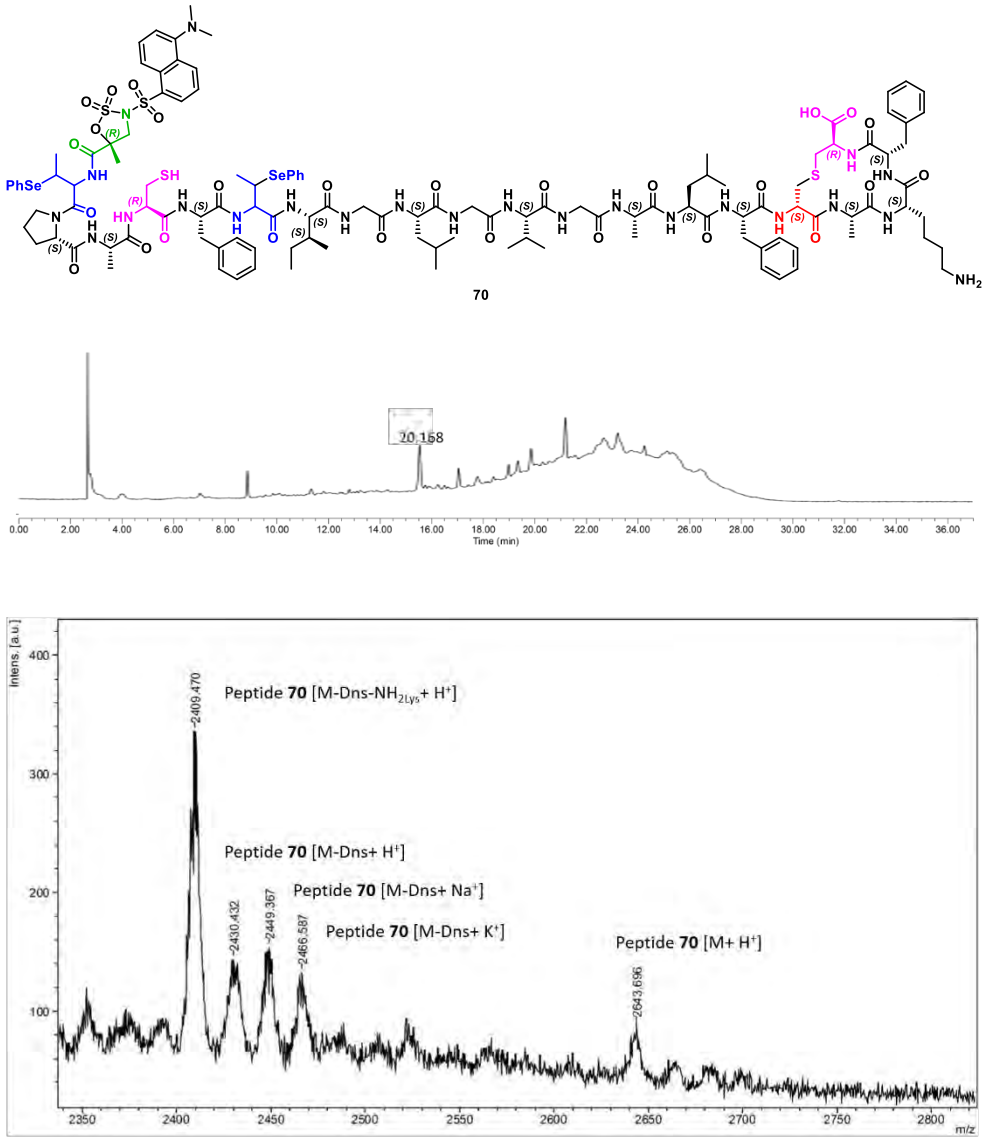

Figure 7.15. Structure of peptide **70** (top). HPLC chromatogram for peptide **70** (middle), obtained using a linear gradient of 5% to 95% of solvent B in 37 min. Solvent A: H_2O containing 0.1% TFA (v/v); solvent B: acetonitrile. MALDI-TOF spectrum of an HPLC-purified sample of peptide **70** (bottom).

To perform the post-synthetic sulfamidate ring-opening cyclization leading to our modified version of $CylL_S$ cycle A, unpurified peptide **70** was dissolved in DMSO and 3.2 equiv. of Et_3N were added. Peptide **71** was obtained quantitatively after 30 min, as judged by MALDI-TOF analysis of the reaction mixture and the appearance of a new signal in the HPLC chromatogram (t= 29.154 min) (**Figure 7.16**).

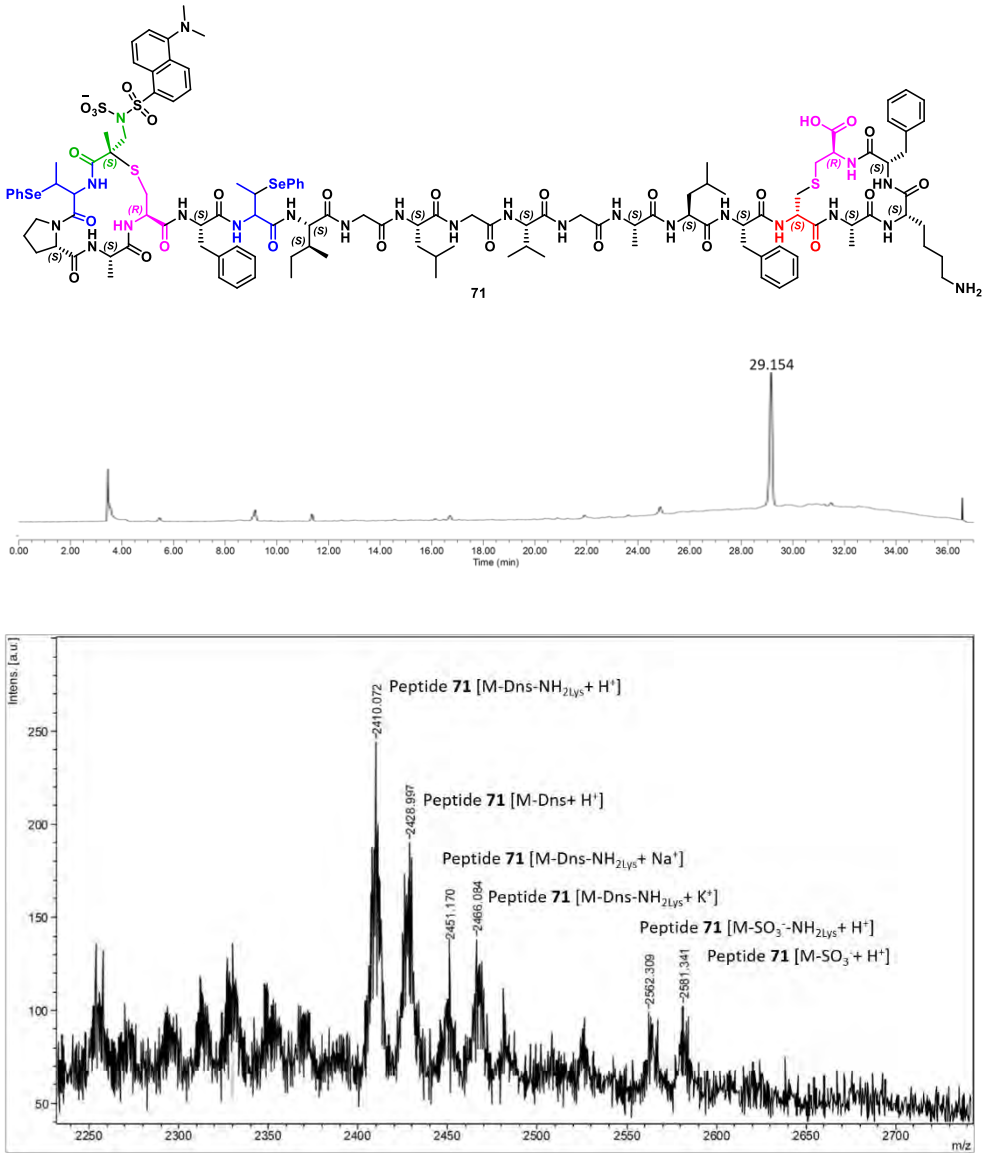

Figure 7.16. Structure of peptide **71** (top). HPLC chromatogram of peptide **71** (middle), performed using a linear gradient of 5% to 95% of solvent B in 37 min. Solvent A: H_2O containing 0.1% TFA (v/v); solvent B: acetonitrile. MALDI-TOF (bottom).

Finally, a mild oxidation of unpurified peptide **71** using DMSO and concentrated HCl (final HCl concentration: 0.6 M) at room temperature for 3 hours was performed to simultaneously unmask the Dhb residues and remove the sulfamic moiety (SO_3^-), cleanly obtaining the target $CylL_S$ analog **72** (**Figure 7.17**). Thus, we serendipitously discovered that DMSO in acidic conditions is able to readily oxidize *Se*-phenylselenocysteine, without using $NaIO_4$, which shortens the reactions sequence and increases the global yield.

As judged by HPLC analysis (retention time t = 31.433 min), a unique peptide was quantitatively obtained after the two steps, namely cyclization and oxidation.

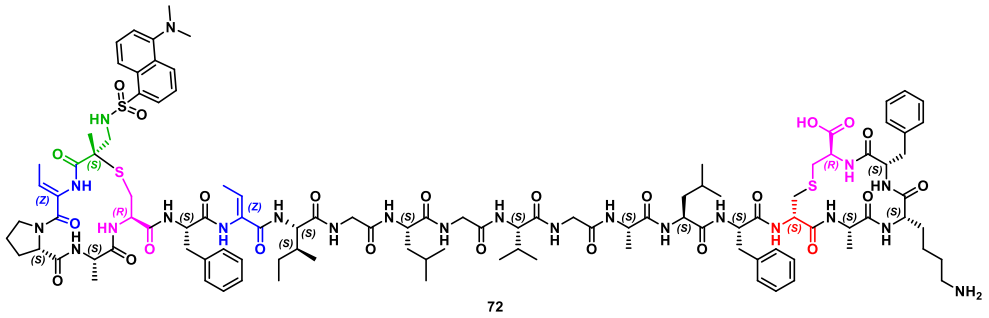

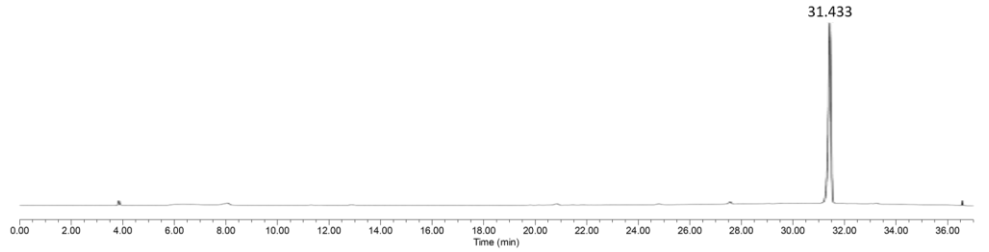

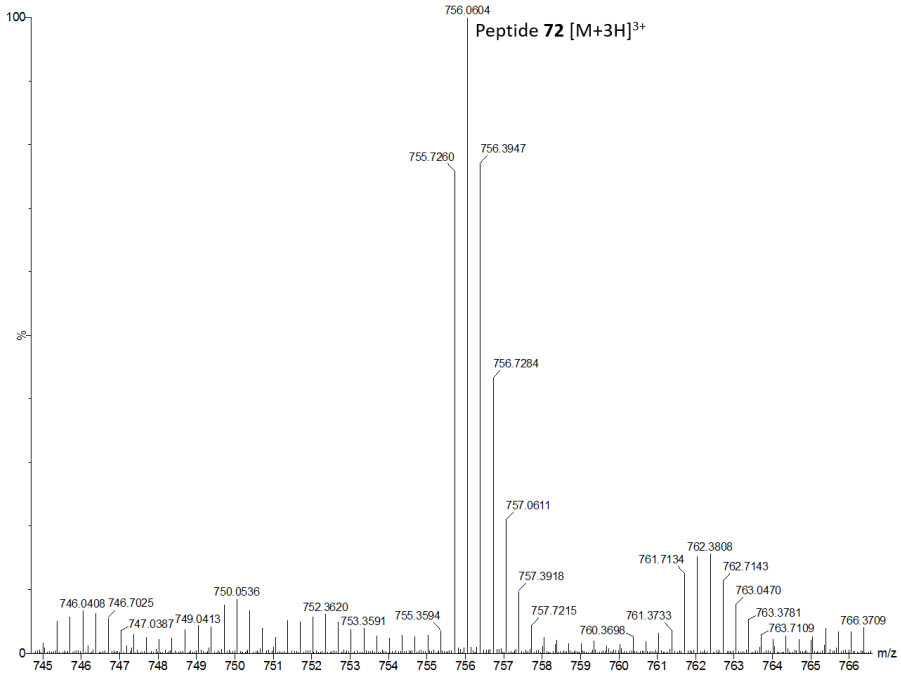

Figure 7.17. Structure of peptide **72** (top). HPLC chromatogram of peptide **72** (middle), performed using a linear gradient of 5% to 95% of solvent B in 37 min. Solvent A: H_2O containing 0.1% TFA (v/v); solvent B: acetonitrile. MALDI-TOF (bottom).

In view of the good results obtained for this CylL$_S$ analog, three additional analogs will be synthesized in the near future following this methodology. One of them will have the opposite configuration at the αMeβAla residue, so that the *S* enantiomer of the α-methylisoserine sulfamidate will be used. The other two analogs will respectively incorporate both enantiomers of α-methylalanine (αMeαAla), by coupling and ring-opening the corresponding sulfamidates derived from α-methylserine (MeSer). The corresponding hemolytic and antimicrobial assays of all CylL$_S$ analogs will be carried out in collaboration with van der Donk's group.

7.4 Conclusions

In this chapter, we have studied the intramolecular ring-opening reaction of α-methylisoserine sulfamidate incorporated into oligopeptides. We observed that if the *N*-terminus is functionalized with carbonyl groups, a transacylation reaction is favored instead of the ring-opening reaction. However, if the *N*-terminus is protected with sulphonyl groups, such as dansyl or nosyl groups, the intramolecular ring-opening reaction is favored. Through this strategy, we were able to synthesize a full-length fluorescent analog of CylL$_S$, which incorporates an α-methyl-β-alanine (αMeβAla) $\beta^{2,2}$-amino acid.

7.5 References

(1) Repka, L. M.; Chekan, J. R.; Nair, S. K.; van der Donk, W. A. *Chem. Rev.* **2017**, *117*, 5457–5520.

(2) Knerr, P. J.; van der Donk, W. A. *Annu. Rev. Biochem.* **2012**, *81*, 479–505.

(3) Arnison, P. G.; Bibb, M. J.; Bierbaum, G.; Bowers, A. A.; Bugni, T. S.; Bulaj, G.; Camarero, J. A.; Campopiano, D. J.; Challis, G. L.; Clardy, J.; Cotter, P. D.; Craik, D. J.; Dawson, M.; Dittmann, E.; Donadio, S.; Dorrestein, P. C.; Entian, K.-D.; Fischbach, M. A.; Garavelli, J. S.; Göransson, U.; Gruber, C. W.; Haft, D. H.; Hemscheidt, T. K.; Hertweck, C.; Hill, C.; Horswill, A. R.; Jaspars, M.; Kelly, W. L.; Klinman, J. P.; Kuipers, O. P.; Link, A. J.; Liu, W.; Marahiel, M. A.; Mitchell, D. A.; Moll, G. N.; Moore, B. S.; Müller, R.; Nair, S. K.; Nes, I. F.; Norris, G. E.; Olivera, B. M.; Onaka, H.; Patchett, M. L.; Piel, J.; Reaney, M. J. T.; Rebuffat, S.; Ross, R. P.; Sahl, H.-G.; Schmidt, E. W.; Selsted, M. E.; Severinov, K.; Shen, B.; Sivonen, K.; Smith, L.; Stein, T.; Süssmuth, R. D.; Tagg, J. R.; Tang, G.-L.; Truman, A. W.; Vederas, J. C.; Walsh, C. T.; Walton, J. D.; Wenzel, S. C.; Willey, J. M.; van der Donk, W. A. *Nat. Prod. Rep.* **2013**, *30*, 108–160.

(4) Chatterjee, C.; Paul, M.; Xie, L.; van der Donk, W. A. *Chem. Rev.* **2005**, *105*, 633–683.

(5) Ongey, E. L.; Neubauer, P. *Microb. Cell Fact.* **2016**, *15:97*.

(6) Rosano, G. L.; Ceccarelli, E. A. *Front. Microbiol.* **2014**, *5:172*.

(7) van der Donk, W. A.; Nair, S. K. *Curr. Opin. Struct. Biol.* **2014**, *29:58-60*.

(8) Velásquez, J. E.; van der Donk, W. A. *Curr. Opin. Chem. Biol.* **2011**, *15:11-21*.

(9) Yu, Y.; Mukherjee, S.; van der Donk, W. A. *J. Am. Chem. Soc.* **2015**, *137*, 5140–5148.

(10) Tabor, A. B. *Org. Biomol. Chem.* **2011**, *9*, 7606–7628.

(11) Fukase, K.; Kitazawa, M.; Sanu, A.; Fujita, H.; Horimoto, S.; Wakamita, T.; Shiba, T. *Tetrahedron Lett.* **1988**, *29*, 795–798.

(12) McKinnie, S. M. K.; Ross, A. C.; Little, M. J.; Vederas, J. C. *Med. Chem. Comm.* **2012**, *3*, 971–975.

(13) Ross, A. C.; McKinnie, S. M. K.; Vederas, J. C. *J. Am. Chem. Soc.* **2012**, *134*, 2008–2011.

(14) Ross, A. C.; Liu, H.; Pattabiraman, V. R.; Vederas, J. C. *J. Am. Chem. Soc.* **2010**, *132*, 462–463.

(15) Pattabiraman, V. R.; McKinnie, S. M. K.; Vederas, J. C. *Angew. Chem. Int. Ed.* **2008**, *47*, 9472–9475.

(16) Liu, H.; Pattabiraman, V. R.; Vederas, J. C. *Org. Lett.* **2009**, *11*, 5574–5577.

(17) Pattabiraman, V. R.; Stymiest, J. L.; Derksen, D. J.; Martin, N. I.; Vederas, J. C. *Org. Lett.* **2007**, *9*, 699–702.

(18) Liu, W.; Chan, A. S. H.; Liu, H.; Cochrane, S. A.; Vederas, J. C. *J. Am. Chem. Soc.* **2011**, *133*, 14216–14219.

(19) Knerr, P. J.; van der Donk, W. A. *J. Am. Chem. Soc.* **2012**, *134*, 7648–7651.

(20) Knerr, P. J.; van der Donk, W. A. *J. Am. Chem. Soc.* **2013**, *135*, 7094–7097.

(21) Mukherjee, S.; Huo, L.; Thibodeaux, G. N.; van der Donk, W. A. *Org. Lett.* **2016**, *18*, 6188–6191.

(22) Tang, W.; van der Donk, W. A. *Nat. Chem. Biol.* **2013**, *9*, 157–159.

(23) Dong, S. H.; Tang, W.; Lukk, T.; Yu, Y.; Nair, S. K.; van der donk, W. A. *Elife* **2015**, *4:e07607*.

(24) Gilmore, M. S.; Segarra, R. A.; Booth, M. C.; Bogie, C. P.; Hall, L. R.; Clewell, D. B. *J. Bacteriol.* **1994**, *176*, 7335–7344.

(25) Lawton, E. M.; Ross, R. P.; Hill, C.; Cotter, P. D. *Mini-Reviews Med. Chem.* **2007**, *7*, 1236–1247.

(26) Bierbaum, G.; Sahl, H.-G. *Curr. Pharm. Biotechnol.* **2009**, *10*, 2–18.

(27) Volkmann, G.; Mootz, H. D. *Cell. Mol. Life Sci.* **2013**, *70*, 1185–1206.

(28) Zhou, H.; van der Donk, W. A. *Org. Lett.* **2002**, *4*, 1335–1338.

(29) Okeley, N. M.; Zhu, Y.; van der Donk, W. A. *Org. Lett.* **2000**, *2*, 3603–3606.

(30) Levengood, M. R.; van der Donk, W. A. *Nat. Protoc.* **2007**, *1*, 3001–3010.

(31) Bindman, N. A.; van der Donk, W. A. *J. Am. Chem. Soc.* **2013**, *135*, 10362–

10371.

(32) Knerr, P. J.; Tzekou, A.; Ricklin, D.; Qu, H.; Chen, H.; van der Donk, W. A.; Lambris, J. D. *ACS Chem. Biol.* **2011**, *6*, 753–760.

Chapter 8.
Short-stay at the University of Illinois, USA

8.1 LahT150

Lanthipeptides are peptides synthesized and post-translationally modified by bacteria that have sulfur-cross-linked lanthionine and/or methyllanthionine and that are being widely studied due to their antimicrobial properties.[1–3] These peptides are expressed as inactive precursor peptides comprising a *leader* peptide and *core* peptide. The *leader* peptide is selectively recognized by several enzymes that then carry out the corresponding post-translational modifications on the *core* peptide. Then, the *leader* peptide is recognized by a protease, which cleaves both fragments, releasing the modified biologically active *core* peptide (**Figure 8.1**).

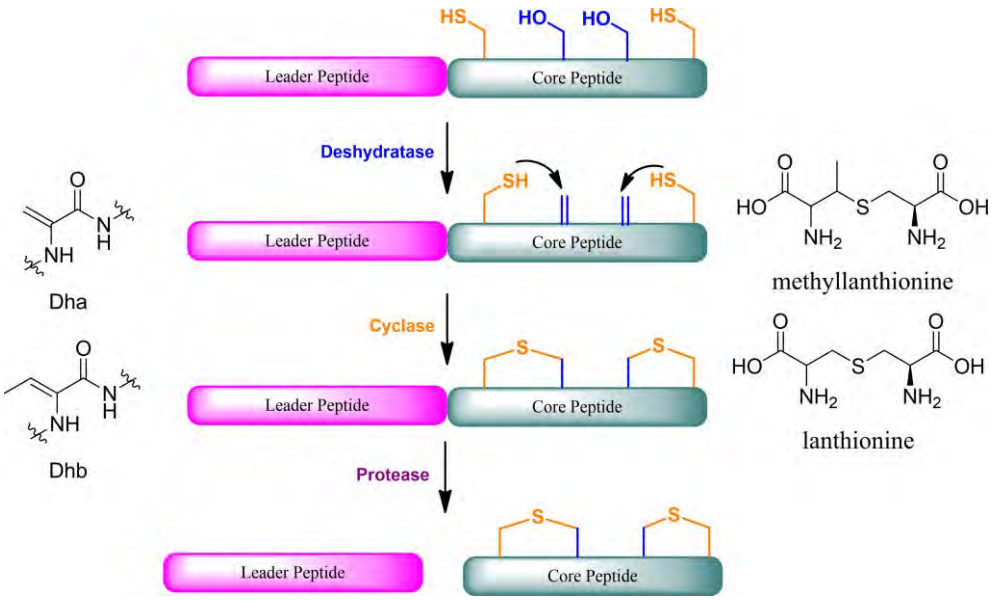

Figure 8.1. Biosynthesis of **lanthipeptides**.

LahT150 is a protease discovered by van der Donk's group, which stands out for its promiscuity, that is, for its ability to perform proteolysis in different types of **lanthipeptides**. It has been recently discovered that only a few amino

acids of the *leader* peptide are needed for recognition by LahT150, namely the sequence NLSDDELEGVAGG, which is common in many **lanthipeptides** recognized by LahT150. However, the three-dimensional structure of LahT150 and particularly its active site remain unknown. Since previous attempts to crystallize the enzyme in complex with the substrate were not satisfactory, we proposed as main goals for the short-stay at van der Donk's lab (University of Illinois at Urbana-Champaign, USA) an alternative method, namely synthesizing analogs of the *leader* peptide able to bind covalently to it and inhibit its activity. In this way, we would be able to obtain information about the enzyme structure, and the interaction mode with the **lanthipeptide** (**Figure 8.2**).

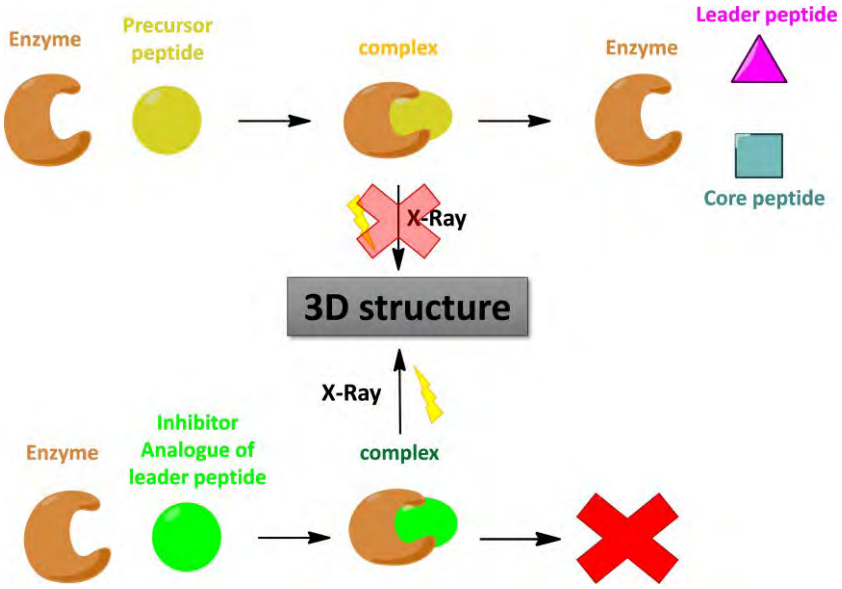

Figure 8.2. Enzymatic proteolysis of precursor peptides to cleave *leader* and *core* peptides and inhibition reaction proposed for obtaining an X-ray structure.

It is known that Laht150 is a Cys-based protease. Aldehydes and Michael acceptors were hence selected as inhibitors, since they form covalent bonds with cysteine.[4,5] These inhibitors are glycine derivatives, located at the *C*-terminus of the leader peptide. Once the inhibitor warheads were synthesized, they were coupled at the *C*-terminus of the recognized peptide (NLSDDELEGVAG), previously synthesized by solid phase peptide synthesis and purified by HPLC (**Figure 8.3**).

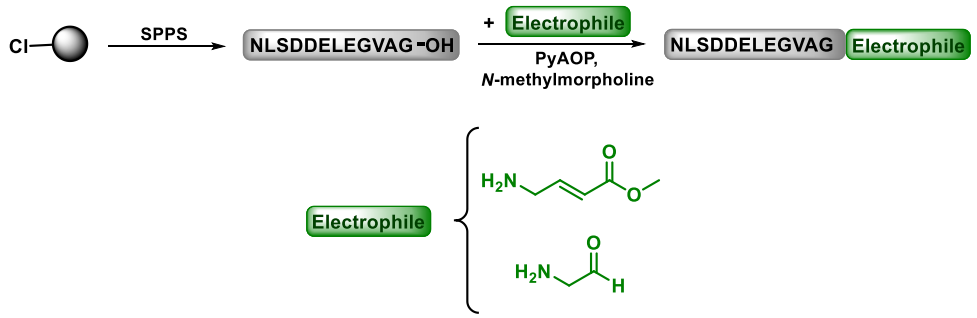

Figure 8.3. Synthesis of LahT150 inhibitors.

The enzymatic reaction with LahT150 was then optimized by evaluating different concentrations of the protein and the substrate. MALDI analysis confirmed that the inhibitors bound to the enzyme. To verify that the inhibitors bound in a specific manner to the active site, a competition study a known **lanthipeptide** was carried out with. The results obtained were similar to those observed when the cysteine of the active site was suppressed by directed mutagenesis, thus confirming the correct union of the inhibitors. The structure of the inhibitor-bound complex was then able to be solved by X-ray diffraction analysis, confirming the identity of the catalytic triad (Cys-His-Asp) (**Figure 8.4**).

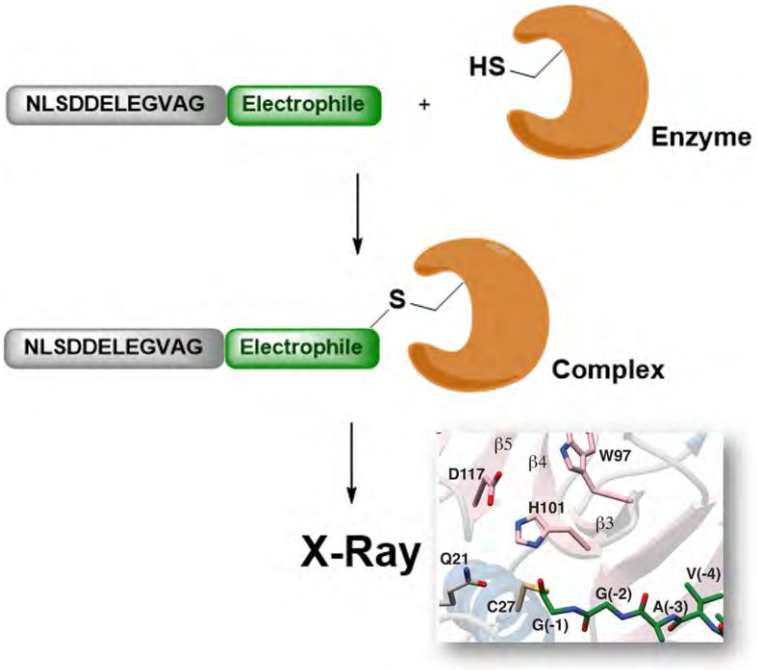

Figure 8.4. Inhibition of LahT150 for obtaining an X-ray structure. In the X-ray image, the inhibitor peptide and LahT150 are shown in green and pink, respectively.

These results have been published in the journal eLife (*eLife* **2019**, 8:e42305).

8.2 References

(1) Repka, L. M.; Chekan, J. R.; Nair, S. K.; van der Donk, W. A. *Chem. Rev.* **2017**, *117*, 5457–5520.

(2) Knerr, P. J.; van der Donk, W. A. *Annu. Rev. Biochem.* **2012**, *81*, 479–505.

(3) Arnison, P. G.; Bibb, M. J.; Bierbaum, G.; Bowers, A. A.; Bugni, T. S.; Bulaj, G.; Camarero, J. A.; Campopiano, D. J.; Challis, G. L.; Clardy, J.; Cotter, P. D.; Craik, D. J.; Dawson, M.; Dittmann, E.; Donadio, S.; Dorrestein, P. C.; Entian, K.-D.; Fischbach, M. A.; Garavelli, J. S.; Göransson, U.; Gruber, C. W.; Haft, D. H.; Hemscheidt, T. K.; Hertweck, C.; Hill, C.; Horswill, A. R.; Jaspars, M.; Kelly, W. L.; Klinman, J. P.; Kuipers, O. P.; Link, A. J.; Liu, W.; Marahiel, M. A.; Mitchell, D. A.; Moll, G. N.; Moore, B. S.; Müller, R.; Nair, S. K.; Nes, I. F.; Norris, G. E.; Olivera, B. M.; Onaka, H.; Patchett, M. L.; Piel, J.; Reaney, M. J. T.; Rebuffat, S.; Ross, R. P.; Sahl, H.-G.; Schmidt, E. W.; Selsted, M. E.; Severinov, K.; Shen, B.; Sivonen, K.; Smith, L.; Stein, T.; Süssmuth, R. D.; Tagg, J. R.; Tang, G.-L.; Truman, A. W.; Vederas, J. C.; Walsh, C. T.; Walton, J. D.; Wenzel, S. C.; Willey, J. M.; van der Donk, W. A. *Nat. Prod. Rep.* **2013**, *30*, 108–160.

(4) Westerik, J. O.; Wolfenden, R. *J. Biol. Chem.* **1972**, *247*, 8195–8197.

(5) Thompson, R. C. *Biochemistry* **1973**, *12*, 47–51.

Chapter 9.
Conclusions/ Conclusiones

9.1 Conclusions

Throughout this Doctoral Thesis several experimental and theoretical results have been presented, allowing to establish these conclusions:

1. Combining experiments and computations, we have been able to control the reactivity of cyclic sulfamidates featuring the α-methylisoserine substructure, which depends on the substituents attached to their *N*- or *C*-termini. If the *N*-terminus is unprotected (NH), S_N2 or E2 reactions are deactivated due to total or partial deprotanation of the sulfamidate NH and the accumulation of negative charge at the transition state. However, when the NH moiety is protected with carbonyl groups (amide or carbamate), the quaternary carbon is activated to undergo either S_N2 or E2 reactions. On the other hand, the substituents at *C*-terminus allow fine tuning the chemoselectivity, favoring the S_N2 ring-opening when an ester is attached, and enabling E2 in the case of amides.

2. We were able to couple α-amino acids at both termini of the sulfamidate in solution, obtaining a small library of $\alpha/\beta^{2,2}$-hybrid di- and tri-peptides. Some of these peptides were activated by capping the *N*-terminal position of the sulfamidate as an acetamide. The ring-opening reaction with a soft nucleophile (pyridine) was carried out, affording positively charged $\alpha/\beta^{2,2}$-hybrid di- and tri-peptides. MD simulations and 2D-NOESY experiments confirmed that these positively charged peptides show noncovalent aromatic interactions

between the aromatic rings of the α-amino acids coupled to the sulfamidate and the quaternary pyridinium moiety.

3. We were able to incorporate the sulfamidate, *via* solid phase peptide synthesis, in longer peptides of biological interest. Once the coupling conditions were optimized, we developed a new class of conformationally restricted β-sheet breaker peptides based on the hydrophobic core of β-amyloid protein (βA), incorporating the α-methylisoserine sulfamidate. These peptides have shown to act as inhibitors of βA aggregation as confirmed by thioflavin-T (ThT) fluorescence assays and circular dichroism (CD). This new family of BSBPs may be promising for the development of new drugs for the treatment of Alzheimer's and other neurodegenerative diseases.

4. We demonstrated that our cyclic sulfamidates can undergo ring-opening reactions on resin as well as in homogeneous phase, with the advantage that the reaction on solid support is cleaner and purification is much easier. In this sense, we were able to obtain chemically fluorescently, labelled and glycosylated $\alpha/\beta^{2,2}$-peptides, in some cases ready for subsequent click chemistry functionalization.

5. We designed a new cleavable linker, taking advantage of the reactivity of the α-methylisoserine sulfamidate at the *N*-terminus to dissociate carbonyl groups attached to it. We demonstrated that pH and the presence of nucleophiles in the medium enhance this reactivity, which can be used for controlled cargo release.

6. We studied the intramolecular ring-opening reaction of the α-methylisoserine sulfamidate, finding that carbonyl groups attached to its *N*-terminus favor *N*→*S* transacetylation instead of ring-opening reactions. However, sulfonyl groups, such as dansyl or nosyl, activate the intramolecular nucleophilic ring-opening reaction. This methodology was used to synthesize a new fluorescently labeled analog of lanthipeptide $CylL_S$, in which its cycle A incorporates the $\beta^{2,2}$-amino acid α-methyl-β-alanine (αMeAla).

7. During an international short-term research stay at Wilfred van de Donk's group (University of Illinois at Urbana Champaign, USA), we designed and synthesized protease inhibitors to covalently bind to protease LahT150. These inhibitors are based on a short sequence of the so-called leader peptide modified with an aldehyde or a Michael acceptor at the *C*-terminus. The structure of the enzyme-inhibitor complex was solved through X-ray diffraction analysis, providing information about the active site structure and peptide substrate recognition.

9.2 Conclusiones

A lo largo de esta Tesis Doctoral se han presentado varios resultados experimentales y teóricos, que permiten establecer estas conclusiones:

1. Se ha estudiado la reactividad de sulfamidatos que presentan α-metilisoserina en su estructura combinando técnicas experimentales y cálculos computacionales. Se determinó que se puede controlar dicha reactividad dependiendo de los sustituyentes que tenga el sulfamidato

en la posición *N*- o *C*- terminal. Si la posición *N*-terminal del sulfamidato no se encuentra protegida, las reacciones de tipo S_N2 y E2 no tienen lugar. Sin embargo, cuando este se encuentra protegido con grupos carbonilo (carbamato o amida), se activa la reactividad en el carbono cuaternario y el grupo metilo terciario. Por otro lado, dependiendo del grupo que ocupe la posición *C*-terminal (ester o amida) se puede controlar la quimioselectividad de la reacción (S_N2 vs E2).

2. Se han conseguido acoplar α-aminoácidos en los extremos carboxilo y sulfonamida del sulfamidato en fase homogénea, obteniendo así una pequeña librería de α/$\beta^{2,2}$-di- y tri-péptidos hibridos. Algunos de ellos fueron activados protegiendo la posición *N*-terminal del sulfamidato en forma de acetamida y se llevaron a cabo reacciones de apertura con un nucleófilo débil empleado como disolvente (piridina), obteniendose α/$\beta^{2,2}$-di- y tri-péptidos hibridos cargados positivamente. Los experimentos de 2D-NOESY y simulaciones de dinámica molecular, confirmaron que estos péptidos cargados positivamente muestran interacciones aromáticas no covalentes entre el anillo aromático de los α-aminoácidos acoplados al sulfamidato y el grupo piridinio cuaternario.

3. Se ha conseguido incorporar el sulfamidato en fase sólida para sintetizar péptidos de mayor tamaño y de interés biológico. En primer lugar se exploraran diferentes estrategias para incorporar el sulfamidato como *building block* en fase sólida y se diseñaron una nueva clase de rompedores de láminas beta (BSBP, en inglés)

conformacionalmente restringidos basados en el *core* hidrofóbico de la proteína β-amiloide (βA), incorporando el sulfamidato de α-metilisoserina. Los péptidos que incorporan el sulfamidato son capaces de inhibir la agregación del βA, tal y como se confirmó mediante análisis de fluorescencia de tioflavina-T y dicroísmo circular. Esta nueva familia de BSBPs pueden ser prometedores para el desarrollo de nuevos medicamentos para el tratamiento de enfermedades neurogenerativas como el síndrome de Alzheimer.

4. Se han conseguido llevar a cabo reacciones de apertura en fase sólida sobre péptidos que contienen nuestro sulfamidato, presentando la ventaja de que la reacción es más eficiente y genera menos subproductos, simplificando el proceso de purificación. De esta manera, se han obtenido α,$\beta^{2,2}$-péptidos etiquetados químicamente, pre-funcionalizados para llevar a cabo química *click* y glicosilados con buenos rendimientos.

5. Hemos diseñado un nuevo *linker* lábil, aprovechando la capacidad que posee el sulfamidato de α-metilisoserina para liberar los sustituyentes de tipo carbonilo unidos a su posición *N*-terminal. Se ha demostrado que la presencia de determinados nucleófilos en el medio o el pH del mismo afectan de manera significativa a esa reactividad, pudiendo ser usada esta estrategia para la liberación de fármacos y moléculas de interés biológico de forma controlada.

6. Se han estudiado reacciones de apertura intramolecular de péptidos que contienen el sulfamidato de α-metilisoserina, observando que

grupos carbonilo unidos a su extremo *N*-terminal favorecen reacciones de *N*→*S* transacilación en lugar de apertura. Sin embargo, la presencia de grupos sulfonilo, como dansilo o nosilo en la misma posición, activa la reacción de apertura nucleófila intramolecular. Esta metodología fue usada para la síntesis de un nuevo análogo fluorescente del lantipéptido citolisina, CylL$_S$, en el cual su anillo A incorpora el $\beta^{2,2}$-aminoácido, α-metil-β-alanina (αMeβAla).

7. Durante mi estancia breve de investigación en el grupo del profesor Wilfred van der Donk (Universidad de Illinois en Urbana-Champaign, EEUU), se diseñaron y sintetizaron inhibidores de proteasas, basados en una breve secuencia de consenso reconocida por la enzima para liberar los denominados *leader peptides*, antes de la excreción de lantipéptidos antimicrobianos al espacio extracelular. Estos péptidos se funcionalizaron con aldehídos y aceptores de Michael en su extremo *C*-terminal con el propósito de unirlos covalentemente a la enzima LahT150. La estructura del complejo enzima-inhibidor se resolvió cristalográficamente, proporcionando información sobre el sitio activo y el modo de unión y reconocimiento del sustrato peptídico.

9.3 Scientific publications derived from this Thesis

- *Synthesis of Mixed α/β^{2,2}-Peptides by Site-Selective Ring-Opening of Cyclic Quaternary Sulfamidates.*
  Mazo, N.; García-González, I.; Navo, C. D.; Corzana, F.; Jiménez-Osés, G.; Avenoza, A.; Busto, J. H.; Peregrina, J. M.; *Org. Lett.* **2015**, *17*, 5804 –5807

- *Substituent Effects on the Reactivity of Cyclic Tertiary Sulfamidate.*
  Navo, C. D.; Mazo, N.; Avenoza, A.; Busto, J. H.; Peregrina, J. M.; Jiménez-Osés, G.; *J. Org. Chem.* **2017**, *82*, 13250 –13255

- *Insights into AMS/PCAT transporters from biochemical and structural characterization of a double Glycine motif protease.*
  Bobeica, S. C.; Dong, S.; Huo, L.; Mazo, N.; McLaughlin, M. I. H.; Jiménez-Osés, G.; Nair, S. K.; van der Donk, W. A.; *eLife* **2019**, 8:e42305

9.4 Collaborative scientific publications

- *Tn Antigen Mimics by Ring-Opening of Chiral Cyclic Sulfamidates with Carbohydrate C1-S and C1-O-Nucleophiles.*
  Tovillas, P.; García-González, I.; Oroz, P.; Mazo, N.; Avenoza, A.; Corzana, F.; Jiménez-Osés, G.; Busto, J. H.; Peregrina, J. M.; *J. Org. Chem.* **2018**, *83*, 4973 –4980

- *Elusive Dehydroalanine Derivatives with Enhanced Reactivity.*
  Aydillo, C.; Mazo, N.; Navo, C. D.; Jiménez-Osés, G.; *ChemBioChem* 10.1002/cbic.201800758

9.5 Participation in scientific meetings

- **Oral communication:** *Inhibición de la fibrilación de beta-amiloide mediante péptidos híbridos*. N. Mazo and G. Jiménez-Osés. *IX Jornada de Química CISQ*. Logroño (Spain). June 15 of 2018.

- **Flash Communication:** *Synthesis of Mixed α/β^{2,2}-Peptides by Site-Selective Ring-Opening of Cyclic Quaternary Sulfamidates*. N. Mazo, A. Avenoza, J. H. Busto, J. M. Peregrina, G. Jiménez-Osés. *III Biennial Meeting of the Chemical Biology Group, XII Carbohydrate symposium*. Madrid (Spain). March 14-16 of 2016.

- **Poster and Award of Chemical Biology Group-RSEQ for the best poster presentation:** *Inhibition of amyloid fibrillation with sulfamidate-modified beta-sheet breaker peptides*. N. Mazo and G. Jiménez-Osés. 16th Iberian Peptide Meeting/ 4th Chemical Biology Group Meeting (4GEQB). Barcelona (Spain). February 05-07 of 2018.

- **Poster:** *Mixed peptides incorporating β^{2,2}-amino acids.* N. Mazo, I. García-González, F. Corzana, A. Avenoza, J.H. Busto, J.M. Peregrina. *II Meeting of the RSEQ Chemical Biology Group*. Bilbao (Spain). February 04-06 of 2014.

- **Poster:** *S-Glycosylated mixed α,β-peptides stabilized by CH/π interactions.* N. Mazo, I. García-González, F. Rodríguez, F. Corzana, A. Avenoza, J.H. Busto, J.M. Peregrina. *XI Carbohydrate symposium*. Logroño (Spain). May 28-30 of 2014.

- **Poster:** *Conformational Preferences of Hybrid α/β-Peptide Modulated by Cation-π Interactions*. N. Mazo, I. García-González, F. Corzana, A. Avenoza, J.H. Busto, J.M. Peregrina. *XI Young Research Symposium*. Bilbao (Spain). November 04-07 of 2014.

- **Poster:** *Synthesis of α/β-peptides by nucleophilic opening of cyclic sulfamidates incorporated into α-peptides.* N. Mazo, I. García-González, G. Jiménez-Osés, A. Avenoza, J.H. Busto, F. Corzana, J.M. Peregrina. *XXXV Bienal Meeting of the RSEQ*. A Coruña (Spain). July 19-23 of 2015.

- **Poster:** *Synthesis of α/β-peptides by nucleophilic opening of cyclic sulfamidates incorporated into α-peptides.* N. Mazo, I. García-González, G. Jiménez-Osés, A. Avenoza, J.H. Busto, F. Corzana, J.M. Peregrina. *11th International Meeting of the Portuguese Carbohydrate Chemistry Group.* Viseu (Portugal). September 06-10 of 2015.

- **Poster:** *Incorporation of a cyclic sulfamidate in peptides using solid-phase peptide synthesis.* N. Mazo, A. Avenoza, J. H. Busto, J. M. Peregrina, G. Jiménez-Osés. *XIII Young Research Symposium.* Logroño (Spain). November 08-11 of 2016.

- **Poster:** *Solid-phase ring-opening reactions on cyclic a-methylisoserine.* N. Mazo, A. Avenoza, J. H. Busto, J. M. Peregrina, G. Jiménez-Osés. *XXXVI Biennial Meeting of the RSEQ.* Sitges (Spain). June 25-29 of 2017.

9.6 Organizer in scientific meetings

- *XI Carbohydrate symposium*. Logroño (Spain). May 28-30 of 2014.

- *One-day Symposium on Computational Chemical Biology honoring Ken Houk*. La Rioja (Spain). April 22 of 2016.

- *XIII Young Research Symposium.* Logroño (Spain). November 08-11 of 2016.

Chapter 10.
Experimental section

10.1 Reagents and general procedures

Commercially available reagents were used without further purification. All the solvents were purified using standard procedures. Thin-layer chromatography (TLC) was performed on silicagel plates (Polychrom SI F_{254}), using UV-light, phosphomolybdic acid, potassium permanganate or ninhydrin as stains. Column chromatography was performed using silica gel (0.04-0.06 mm, 230-240 mesh). Melting points were determined on a Buchi B-545. Mass spectrometry analyses were performed on a HP 5989B, using electron impact ionization (EI). Electrospray-mass spectrometry (ESI-MS) were performed on the same equipment with HP 59987A interface and were registered in positive ion mode. A Bruker Microtof-Q spectrometer was also used. Sodium formate was used as external reference for high-resolution mass spectroscopy (HRMS). Optical rotation angles were measured on a Perkin-Elmer 341 polarimeter, using a sodium lamp (λ = 589 nm) at 25 ºC in 1.0 dm long cells (0.35 or 1.0 mL).

10.2 Quantum mechanical calculations

QM calculations were performed at Memento cluster (BiFi, University of Zaragoza) and Beronia cluster (University of La Rioja). Full geometry optimizations were carried out with Gaussian 09[1] using the M06-2X hybrid functional[2] and 6-31+G (d,p) basis set with ultrafine integration grids. Bulk solvent effects in pyridine were considered implicitly through the IEF-PCM polarizable continuum model.[3] The possibility of different conformations was considered for all structures. All stationary points were characterized by a frequency analysis performed at the same level used in the geometry optimizations from which thermal corrections were obtained at the reaction

temperature (333.15 K). The quasiharmonic approximation reported by Truhlar and co-workers was used to replace the harmonic oscillator approximation for the calculation of the vibrational contribution to enthalpy and entropy.[4] Scaled frequencies were not considered. Mass-weighted intrinsic reaction coordinate calculations were carried out by using the Gonzalez and Schlegel scheme[5,6] to ensure that the transition structures indeed connected the appropriate reactants and products. Gibbs free energies (ΔG) of the lowest energy conformers were used for the discussion on the relative stabilities of the considered structures, unless otherwise stated. Electronic energies, entropies, enthalpies, Gibbs free energies, and lowest frequencies of the calculated structures are available in *Chapter 11: Supplementary Information*.

10.3 Unrestrained Molecular Dynamics simulations

Molecular dynamics simulations were carried out at the Finis-Terrae cluster of the *Centro de Supercomputación de Galicia* (CESGA) and at an in-house GPU cluster. Parameters for the $\beta^{2,2}$-amino acid residues were generated with the antechamber module of Amber12 using the general Amber force field (GAFF) for the rest of the molecule, with partial charges set to fit the electrostatic potential generated with HF/6-31G(d) by RESP[7] The charges were calculated according to the Merz-Singh-Kollman scheme using Gaussian 09[1] Each peptide was immersed in a water box with a 10 Å buffer of TIP3P[8] water molecules. The systems were neutralized by adding explicit counter ions (Cl^-). All subsequent simulations were performed using the *ff03.r1* force field.[9] A two-stage geometry optimization approach was performed. The first stage minimizes only the positions of solvent molecules and ions, and the second stage is an unrestrained minimization of all the atoms

in the simulation cell. The systems were then heated by incrementing the temperature from 0 to 300 K under a constant pressure of 1 atm and periodic boundary conditions. Harmonic restraints of 30 kcal/mol were applied to the solute, and the Andersen temperature coupling scheme[10] was used to control and equalize the temperature. The time step was kept at 1 fs during the heating stages, allowing potential inhomogeneities to self-adjust. Water molecules were treated with the SHAKE algorithm such that the angle between the hydrogen atoms is kept fixed. Long-range electrostatic effects were modeled using the particle-mesh-Ewald method.[11] An 8 Å cutoff was applied to Lennard-Jones and electrostatic interactions. Each system was equilibrated for 2 ns with a 2 fs timestep at a constant volume and temperature of 300 K. Production trajectories were then run for additional 100 ns under the same simulation conditions.

10.4 Molecular Dynamics simulations with time-averaged restraints (MD-tar)

MD-tar simulations were performed with the *pmemd.cuda* module of AMBER 12 (*parm99* force field), which was implemented with GAFF parameters. Distances derived from the NOE interactions were included as time-averaged distance restraints. A $\langle r^{-6} \rangle^{1/6}$ average was used for the distances. Final trajectories were run using an exponential decay constant of 8000 ps with a dielectric constant $\varepsilon = 80$ or in explicit TIP3P water molecules.

10.5 Coupling of α-methylisoserine sulfamidate to peptides by solid phase peptide synthesis (SPPS)

Solid phase peptide synthesis was performed on a Liberty Microwave (CEM Corporation, Mathews, NC). Rink amide MBHA (1.0 equiv.) was used as

resin, DIC and Oxyma pure as coupling agents, a 20% (v/v) solution of piperidine in DMF for Fmoc deprotection and a 1:2 mixture of Ac_2O/Pyridine for the final acetylation. Natural Fmoc-protected amino acids (5 equiv.) were coupled using the standard protocol.

Sulfamidate building block **J** (5.0 equiv.) was coupled using Oxyma (1.10 equiv.), DIC (20.0 equiv.) in DMF (2 mL) assisted by microwaves at 75 ºC for 20 min. The following (i+1) amino acid (5.0 equiv.) was coupled using DIC (20.0 equiv.), DIPEA (1.1 equiv.) in DMF (2 mL) under microwaves at 75 ºC for 20 min. Biotin and chlorambucil (5.0 equiv.), were manually coupled using TBTU (4.95 equiv.) and DIPEA (20 equiv.) in DMF (2 mL) at -20 ºC for 45 min. Dansyl chloride and nosyl chloride (6.0 equiv.) were manually coupled with DIPEA (6 equiv.) in DMF (2 mL) at -20 ºC for 45 min.

Final cleavage from the resin and removal of the protecting groups were performed using cocktail **A:** TFA (1900 μL), TIS (50 μL) and H_2O (50 μL) or cocktail **B**: TFA (1880 μL), TIS (20 μL), H_2O (50 μL) and DODT (50 μL). The cocktail **B** was used only for peptides containing a thiol, whereas cocktail **A** was used for the rest of the peptides. The mixture was stirred for 1 h. At this point, cold Et_2O was added producing a precipitate that isolated by centrifugation and decantation of the supernatant. The final crude was purified by reverse phase semi-preparative HPLC.

10.6 Thioflavin T (ThT) Fluorescence assays

ThT Fluorescence assays were conducted in 96-well black plate at 37 ºC with continuous shaking (200 rpm) in a TECAN SPARK 10M instrument. ThT fluorescence was recorded with 10 minutes reading intervals and 5 seconds shaking before the read (442 nm excitation, 482 nm emission). At least three

independent experiments were carried out for each ThT assay. Each well contained 20 mM PBS buffer solution (pH 7.4), 20 μM ThT and 15 μM βA (1-40) with and without BSBPs (30 μM 1:2, 75 μM 1:5, 150 μM for a 1:10 βA:BSSP ratio) in a total volume of 200 μL.

Preparation of buffered ThT stock solution. Commercially available ThT was purchased from Sigma Aldrich and a stock solution of concentration 1 mM in PBS (50 mM, pH 7.4) was freshly prepared and stored at 4 ºC with a dark cover to prevent degradation from light.

10.7 Circular Dichroism (CD) assays

BSBP candidates:

Purified solid peptide samples were dissolved in PBS (50 mM, pH 7.4) to obtain a 500 μM stock solution. 600 μL of the sample were taken in a cuvette (1 mm pathlength). Spectra were recorded from 190 nm to 260 nm on an Applied Photophysics Chirascan instrument. Measured ellipticity for a *N*-mer peptide (mDeg) was converted to mean residue molar ellipticity (θ) using the equation [1]:

$$\theta(\mathrm{deg}\, cm^2\, dmol^{-1}) = \frac{Ellipticity(mDeg) \cdot 10^6}{Pathlength(mm) \cdot [Protein](\mu M) \cdot N}$$

Equation 1. Equation to calculate the ellipticity (θ)

BSBPs co-incubated with βA (1-40):

βA (1-40) (15 μM) was separately co-incubated with the BSBPs at different molar ratios (30 μM, 75 μM and 150 μM) at 37 ºC for 24 hours and 7 days in PBS (20 mM, pH 7.4). 600 μL of the sample was taken in a cuvette (1 mm pathlength). Spectra were recorded from 190 nm to 260 nm on an Applied

Photophysics Chirascan instrument. Measured ellipticity (mDeg) for a *N*-mer peptide was converted to mean residue molar ellipticity (θ) using equation [1]

10.8 Experimental setup for registering the IRID spectra in the gas phase

The analyzed peptide provided two chromophore groups (phenylalanines) required for detection through mass-selected ultraviolet (UV) photoionization. The peptide was mixed with carbon nanotubes (Multi-Walled Carbon Nanotubes, purity >90%, 10-30 mm diameter, Sun NanoTech Co Ltd) and were deposited in a cylindrical sample holder (4.5 mm diameter, 15 mm long) by pressing the cylinder against the desired mixture. The sample was vaporized by laser desorption (1064 nm, Quantel Ultra) into an expansion supersonic jet of argon before passing through a 4 mm skimmer to create a collimated molecular beam which then intersected tunable UV and IR laser beams in the extraction region of a linear time-of-flight (TOF) mass spectrometer (Jordan Inc.). One color mass-selected photoionization spectra, recorded using a frequency-doubled pulsed Nd:YAG-pumped dye laser operating at 10 Hz, were followed by conformer-specific spectroscopy in the IR using IR-UV ion dip (IRID) double resonance spectroscopy. The tunable IR radiation was provided by an OPO/OPA laser system (LaserVision). The delay between the pump and the probe laser pulses was ~150 ns in the IRID double resonance experiments (see figures below).

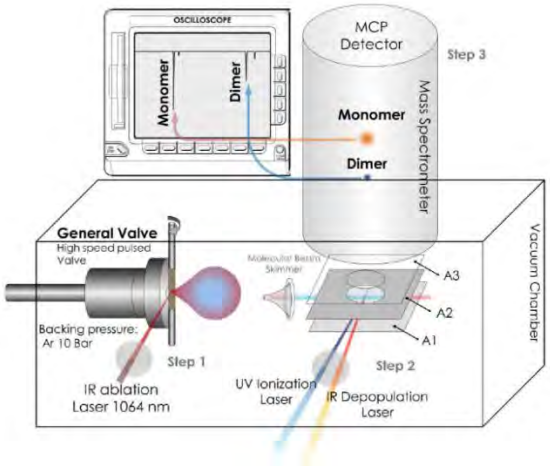

Figure 10.1. Experimental setup for registering the IR-UV spectra in the gas phase. Ar was used as carrier gas to create the expansion at typical pressures of 10 bar. The valve was equipped with a nozzle of 0.5 mm diameter. The diameter of the skimmer was 4 mm. Voltages applied to send the ions to the detector were A1: 4000V; A2: 3700V; A3: grounded.

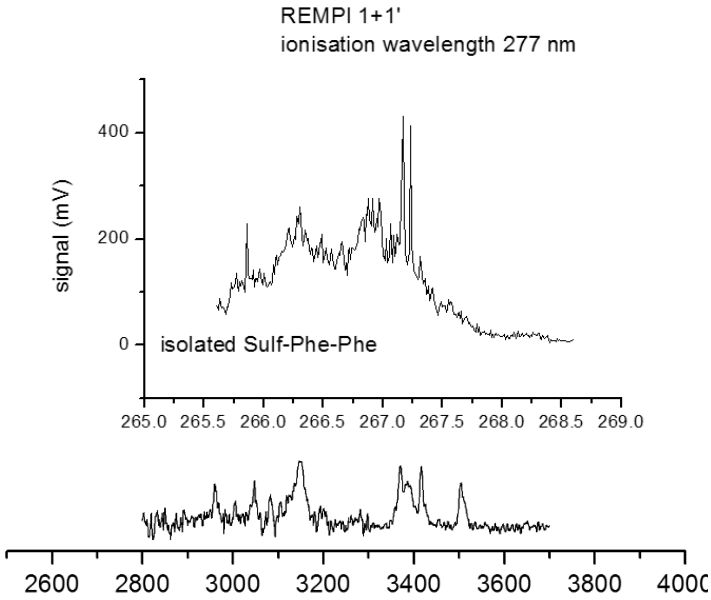

Figure 10.2. Experimental data registered for J-Phe-Phe-NH_2 peptide in the gas phase. In the upper part, the Resonance-Enhanced MultiPhoton Ionization (REMPI) spectroscopy at several resolutions is presented and the selected ionization frequencies used to obtain the IR-UV spectra is highlighted. At the bottom, the IR-UV ion-dip (IRID) spectrum is shown.

10.9 Optimization of the theoretical method to elucidate the structures from IRID experiments

The whole conformational space of peptide **J**-Phe-Phe-NH_2 was analyzed quantum mechanically by fully optimizing 1152 starting structures with M06-2X/6-31+G(d,p) in the gas phase. The degrees of freedom considered for the structural sampling included four backbone and three sidechain plausible conformations for each of the two Phe residues: right-handed α-helix (α_R, φ_α ~ –45º, ψ_α ~ –45º), β-sheet (β, φ_α ~ –150º, ψ_α ~ +150º), polyproline-II helix (PPII, φ_α ~ –75º, ψ_α ~ +150º), inverse γ-turn (γ, φ_α ~ –80º, ψ_α ~ +70º), *trans* (*t*, χ^1_α ~ 180º), *gauche*$^+$ (g^+, χ^1_α ~ –60º) and gauche$^-$ (g^-, χ^1_α ~ +60º); two rotamers around the sulfamidate amide bond (ψ_β ~ +60º, –110º);[12] two twist (*T*, θ_β ~ +80º) and envelope conformers of the sulfamidate five-membered ring (*E*, θ_β ~ +[130–145º]); and two configurations of the sulfonamide nitrogen atom accessible through fast pyramidal inversion (*R*, φ_β ~ +[70–160º]; *S*, φ_β ~ –[70–160º]). For all amide bonds (NH–CO) the most stable *trans* conformation (ω_α ~180º) was only considered. Then, the 20 lowest-energy conformers with a relative energy (ΔE) in the 0-5 kcal mol^{-1} range accounting for ~98% of the structural population as calculated through a Boltzmann distribution at 298 K, were re-optimized at higher levels of theory using different density functionals with and without empiric dispersion (i.e. van der Waals) corrections such as M06-2X, ωB97X-D, B3LYP-GD3BJ, B3PW91-GD3BJ and the bigger basis set 6-311++G(2d,p). Vibration frequencies were calculated at the same theory levels using the harmonic oscillator approximation and using pre-defined scaling factors.[13]

Since the frequencies and intensities of infrared vibrations calculated with different density functionals are normally quite similar, the most decisive factor determining the accuracy of the theoretical spectrum, and thus its

coincidence with the experimental one, is the relative energy, which translates into population at a given temperature, of the low-energy conformers. A consistent trend was observed in our case within all the tested methods, the same two conformations being dominant in all cases and amounting 80-95% of the conformational population. The relative stability of these conformers varies from one method to another and is in the range of ±0.2-1.5 depending on the method and type of energy examined (electronic energy, E; zero-point corrected electronic energy, E_{ZPE}; enthalpy at 298 K, H_{298}; free energy and 298 K, G_{298}). B3LYP-GD3BJ/6-311++G(2d,p), for which conformation **I** is the lowest-energy one, was selected as the most appropriate method for deriving the theoretical IR spectrum.

10.10 Methodology for *N*-ethylmaleimide (NEM) assay

Maleimides react with sulfhydryls at pH 6.5-7.5 to form stable thioether bonds. Peptides to be blocked in were dissolved in PBS buffer, pH 7.4 (7 mg/mL). A 12.5 mg/mL stock solution of *N*-ethylmaleimde (NEM) was prepared in ultrapure water, and a minimum of a 15 equiv. of NEM (56 μL) per sulfhydry groups to be blocked were added, and the reaction stirred for 2 h at room temperature. The reaction progression was analyzed by ESI-MS.

10.11 NMR experiments

^{1}H (^{13}C) NMR experiments were performed at 300 (75), 400 (100) and 500 (125) MHz. ^{19}F NMR experiments were performed at 376 MHz. 2D COSY and HSQC experiments were carried out to assist on signal assignment. NOESY experiments were recorded at 298 K and pH = 6.0-6.5 in H_2O/D_2O (9:1) using phase-sensitive ge-2D NOESY with WATERGATE for H_2O/D_2O (9:1). NOEs intensities were normalized with respect to the diagonal peak at zero mixing time. Distances with structural information were semi-quantitatively determined by integrating the volume of the corresponding cross-peaks. Chemical shifts are given in ppm (δ) and coupling constants (J) in hertz (Hz). Chloroform, with TMS as internal reference, methanol and water were used as deuterated solvents. The results of these experiments were processed with MestReNova software.

10.12 Luminescence assays

Luminescence spectra were recorder at room temperature with a Jobin-Yvon Horiba Fluorolog 3-22 Tau-3 spectrofluorometer. Data was analyzed with the Origen 6.1 program.

10.13 Synthesis

Methyl (*S*)-3-((methoxycarbonyl)amino)-2-methyl-2-(1l4-pyridin-1-yl) propanoate, chloride salt [1]

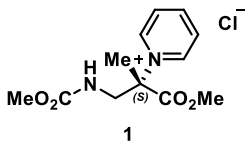

1

Compound **1'** (50 mg, 0.15 mmol) was dissolved in a 1:1 mixture of 2 M HCl/DCM. After stirring for 30 minutes at room temperature, the layers were separated, and the aqueous phase was lyophilized, affording compound **1** quantitatively (43 mg, 0.15 mmol). $[\alpha]_D^{20}$ = -8.5 (*c* 1.00 in H_2O). HRMS (ESI) m/z = 253.1183, calculated for $C_{12}H_{17}N_2O_4$ (M^+) = 253.1183. ^{1}H NMR (400 MHz, D_2O) δ (ppm): 2.03 (s, 3H, C*H*$_3$), 3.37 (s, 3H, NHCO$_2$C*H*$_3$), 3.75-3.90 (m, 4H, CO$_2$C*H*$_3$, NHC*H*$_2$C), 4.06 (d, 1H, *J* = 15.3 Hz, NHC*H*$_2$C), 7.98-8.07 (m, 2H , Py$_{meta}$), 8.50-8.60 (m, 1H, Py$_{para}$), 8.87-8.97 (m, 2H, Py$_{orto}$). ^{13}C NMR (100 MHz, D_2O) δ (ppm): 20.2 (*C*H$_3$), 47.4 (NH*C*H$_2$C), 52.7 (NHCO$_2$*C*H$_3$), 54.6 (CO$_2$*C*H$_3$), 76.7 (NHCH$_2$*C*), 127.8 (Py$_{meta}$), 143.5 (Py$_{orto}$), 147.3 (Py$_{meta}$), 159.0 (NH*C*O$_2$CH$_3$), 170.1 (*C*O$_2$CH$_3$).

(*S*)-3-Acetamido-*N*,2-dimethyl-2-(1l4-pyridin-1-yl)propanamide, chloride salt [3] and 2-(acetamidomethyl)-*N*-methylacrylamide [4]

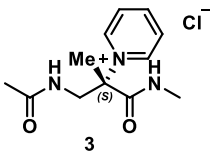

3

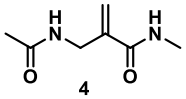

4

Compound **I** (40 mg, 0.20 mmol) was dissolved in pyridine (2 mL) and stirred at 60 ºC for 12 hours. After concentration, the resulting crude was dissolved in a mixture of DCM and 2 M HCl aqueous solution (1:1, 2 mL) and allowed to react for 30 minutes at room temperature. Finally, water was added and washed with $CHCl_3$/^{i}PrOH (3:1), concentration of the aqueous

phase and purification by HPLC in reversed-phase afforded compound **3** (40 mg, 83%) and compound **4** (4 mg, 17 %) both as viscous colorless oils.

Semi-preparative HPLC gradient (t_R **3** = 18.05, t_R **4** = 19.18)

Time (min)	Flow (mL/min)	H_2O + 0.1% TFA (%)	Acetonitrile (%)
0	10	100	0
5	10	100	0
25	10	70	30
30	10	100	0

$[a]_D^{20}$= -9.5 (*c* 1.00 en H_2O). HRMS (ESI) m/z = 236.1397, calculated for $C_{12}H_{18}N_3O_2^+$ (M^+) = 236.1394. ^{1}H NMR (400 MHz, D_2O) δ (ppm): 1.75 (s, 3H, C*H*$_3$), 1.99 (s, 3H, Ac), 2.73 (s, 3H, CONHC*H*$_3$), 3.78 (d, 1H, *J* = 14.8 Hz, NHC*H*$_2$C), 4.09 (d, 1H, *J* = 14.6 Hz, NHC*H*$_2$C), 7.97-8.07 (m, 2H, Py_{meta}), 8.50-8.62 (m, 1H, Py_{para}), 8.85-8.94 (m, 2H, Py_{orto}). ^{13}C NMR (100 MHz, D_2O) δ (ppm): 20.9 (Ac), 21.3 (*C*H$_3$), 26.5 (CONHC*H*$_3$), 45.7 (NH*C*H$_2$C), 76.8 (NHCH$_2$*C*), 128.0 (Py_{meta}), 143.5 (Py_{orto}), 147.3 (Py_{meta}), 170.1, 174.8 (CO). HRMS (ESI) m/z = 179.0798, calculated for $C_7H_{12}N_2O_2Na^+$ (MNa^+) = 179.0791. ^{1}H NMR (400 MHz, D_2O) δ (ppm): 2.01 (s, 3H, Ac), 2.78 (s, 3H, CONHC*H*$_3$), 4.00 (s, 2H, NHC*H*$_2$C), 5.51 (s, 1H, CCH$_2$), 5.76 (s, 1H, CCH$_2$). ^{13}C NMR (100 MHz, D_2O) δ (ppm): 24.2 (Ac), 28.3 (CONH*C*H$_3$), 42.8 (NH*C*H$_2$C), 122.8 (C*C*H$_2$), 142.1 (*C*CH$_2$), 173.0, 176.7 (CO).

***Tert*-butyl ((*S*)-1-((*R*)-5-methyl-5-(methylcarbamoyl)-2,2-dioxido-1,2,3-oxathiazolidin-3-yl)-1-oxo-3-phenylpropan-2-yl)carbamate [5]**

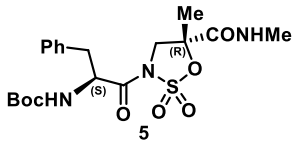

N-Boc-L-phenylalanine (341 mg, 1.29 mmol) was dissolved in dry CH_2Cl_2 (24 mL) in a schlenk under argon atmosphere at room temperature. Then, DIEA (0.81 mL, 4.29 mmol) and TBTU (413 mg, 1.29 mmol) were added and allowed to react for 5 minutes. The temperature was lowered to -20 °C, sulfamidate **H** (208 mg, 1.07 mmol) was added and stirred for 30 minutes. After washed with brine, 0.1 M HCl aqueous solution and a 5% aqueous solution of $NaHCO_3$, the organic phase was dried with anhydrous Na_2SO_4, filtered and concentrated. Purification by column chromatography on silica gel (AcOEt/Hexane, 8:2) affording compound **5** (299 mg, 0.678 mmol, 63%) as a white solid. $[\alpha]_D^{20}$ = -0.43 (*c* 1.00 in $CHCl_3$). Mp= 80-93 ºC. HRMS (ESI) *m/z* = 464.1473, calculated for $C_{19}H_{27}N_3O_7SNa^+$ (MNa^+) = 464.1467. ^{1}H NMR (400 MHz, $CDCl_3$) δ (ppm): 1.39 (s, 9 H, C(C*H*$_3$)$_3$), 1.66 (s, 3H, C*H*$_3$), 2.85-3.03 (m, 4H, CONHC*H*$_3$, C*H*$_2$ of Phe), 3.18 (dd, 1H, *J* = 13.6, 6.1 Hz, C*H*$_2$ of Phe), 3.67 (br s, 1H, C*H*$_2$ of Sulfamidate), 4.53(d, 1H, *J* = 10.7 Hz, C*H*$_2$ of Sulfamidate), 4.80 (br s, 1H, C*H* of Phe), 5.10 (br s, 1H, N*H*Boc), 6.52 (br s, 1H, N*H*Me), 7.17-7.37 (m, 5H, Arom). ^{13}C NMR (100 MHz, $CDCl_3$) δ (ppm): 23.8 (*C*H$_3$), 26.7 (CONH*C*H$_3$), 28.3 (C(*C*H$_3$)$_3$), 38.8 (*C*H$_2$ of Phe), 52.8 (*C*H$_2$ of Sulfamidate), 54.9 (*C*H of Phe), 80.6 (*C*(CH$_3$)$_3$), 86.3 (*C*CH$_3$), 127.4, 128.9, 129.5, 135.3 (Arom), 154.8, 168.6, 169.6(*C*O).

Tert-butyl ((_S_)-3-(1_H_-indol-3-yl)-1-((_R_)-5-methyl-5-(methylcarbamoyl)-2,2-dioxido-1,2,3-oxathiazolidin-3-yl)-1-oxopropan-2-yl)carbamate [6]

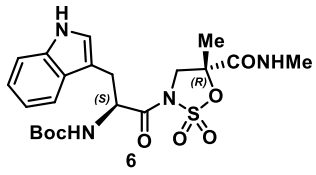

6

_N_-Boc-L-tryptophan (76 mg, 0.31 mmol) was dissolved in dry CH_2Cl_2 (20 mL) in a schlenk under argon atmosphere at room temperature. Then, DIEA (0.23 mL, 1.24 mmol) and TBTU (99 mg, 0.31 mmol) were added and allowed to react for 5 minutes. The temperature was lowered to -20°C, sulfamidate **H** (60 mg, 0.31 mmol) was added and stirred for 30 minutes. After washed with brine, 0.1 M HCl aqueous solution and a 5% aqueous solution of $NaHCO_3$, the organic phase was dried with anhydrous Na_2SO_4, filtered and concentrated. Purification by column chromatography on silica gel (AcOEt/Hexane, 8:2) affording compound **6** (104 mg, 70%) as a white solid. $[\alpha]_D^{20}$ = +10.7 (_c_ 1.00 in $CHCl_3$). Mp= 83-87 ºC. HRMS (ESI) _m/z_ = 503.1570, calculated for $C_{21}H_{28}N_4O_7SNa^+$ (MNa^+) = 503.1571. ^{1}H NMR (400 MHz, $CDCl_3$) δ (ppm): 1.38-1.48 (m, 12H, $C(CH_3)_3$, CH_3), 2.87 (s, 3H, $CONHCH_3$), 3.27-3.33 (m, 2H, CH_2 of Trp), 3.59 (s, 1H, CH_2 of Sulfamidate), 4.43 (s, 1H, CH_2 of Sulfamidate), 4.88 (s, 1H, C_H_ of Trp), 5.16 (s, 1H, N_H_CH), 6.44 (s, 1H, CON_H_CH_3), 7.07 (s, 1H, C_H_C), 7.12-7.64 (m, 4H, Arom), 8.21 (s, 1H, N_H_arom). ^{13}C NMR (100 MHz, $CDCl_3$) δ(ppm): 23.4 (CH_3), 26.7 ($CONHCH_3$), 28.4 ($C(CH_3)_3$), 28.7 (CH_2 of Trp), 53.0 (CH_2 of Sulfamidate), 54.1 (_C_H of Trp), 80.6 ($C(CH_3)_3$), 85.9 (NCH_2C), 109.1 (CH_C_), 123.7 (_C_HC), 115.5, 118.6, 120.3, 122.7, 127.4, 136.3 (Arom), 155.1 (_C_O del Boc), 168.6 ($CONCH_2$), 170.3 (_C_ONH).

***Tert*-butyl ((*S*)-3-(benzyloxy)-1-((*R*)-5-methyl-5-(methylcarbamoyl)-2,2-dioxido-1,2,3-oxathiazolidin-3-yl)-1-oxopropan-2-yl)carbamate [7]**

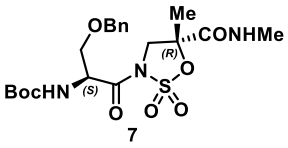

7

N-Boc-*O*-benzyl-L-serine (76 mg, 0.26 mmol) was dissolved in dry CH_2Cl_2 (20 mL) in a schlenk under argon atmosphere at room temperature. Then, DIEA (0.20 mL, 1.03 mmol) and TBTU (83 mg, 0.26 mmol) were added and allowed to react for 5 minutes. The temperature was lowered to -20°C, sulfamidate **H** (50 mg, 0.26 mmol) was added and stirred for 30 minutes. After washed with brine, 0.1 M HCl aqueous solution and a 5% aqueous solution of $NaHCO_3$, the organic phase was dried with anhydrous Na_2SO_4, filtered and concentrated. Purification by column chromatography on silica gel (AcOEt/Hexane, 8:2) affording compound **7** (61 mg, 50%) as a white solid. $[\alpha]_D^{20}$ = - 13.9 (*c* 1.00 in $CHCl_3$). Mp= 52-56 ºC. HRMS (ESI) *m/z* = 494.1582, calculated for $C_{20}H_{29}N_3O_8SNa^+(MNa^+)$= 494.1568. ^{1}H NMR (400 MHz, $CDCl_3$) δ (ppm): 1.44 (s, 9H, C(C*H*$_3$)$_3$), 1.68 (s, 3H, C*H*$_3$), 2.87 (s, 3H, CONHC*H*$_3$), 3.70 (dd, 1H, *J* = 9.5 Hz, *J* = 6.0 Hz, C*H*$_2$ of Ser), 3.78-3.85 (m, 1H, C*H*$_2$ of Ser), 4.16 (d, 1H, *J* = 10.7 Hz, C*H*$_2$ of Sulfamidate), 4.48 (d, 1H, *J* = 10.7 Hz, C*H*$_2$ of Sulfamidate), 4.52 (s, 2H, OC*H*$_2$Ph), 4.85 (s, 1H, C*H* of Ser), 5.37 (s, 1H, N*H*C(CH$_3$)$_3$), 6.44 (s, 1H, CON*H*Me), 7.22-7.40 (m, 5H, Arom). ^{13}C NMR (100 MHz, $CDCl_3$) δ (ppm): 23.7 (*C*H$_3$), 26.6 (CONH*C*H$_3$), 28.3 (C(*C*H$_3$)$_3$), 52.8 (*C*H$_2$ of Sulfamidate), 53.4 (*C*H of Ser), 69.7 (*C*H$_2$ of Ser), 73.5 (O*C*H$_2$Ph), 80.6 (*C*(CH$_3$)$_3$), 86.3 (NCH$_2$*C*), 127.9, 128.1, 128.6, 137.1 (Arom), 154.9 (*C*O del Boc), 168.5 (*C*ONCH$_2$), 168.4 (*C*ONH).

Methyl ((*R*)-5-methyl-2,2-dioxido-1,2,3-oxathiazolidine-5-carbonyl)-L-alaninate [8a]

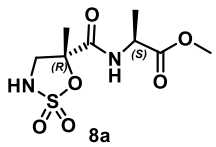

8a

In a schlenk under argon atmosphere, to a solution of L-Ala-OMe hydrochloride (104 mg, 0.745 mmol) in DMF (1.2 mL), sulfamidate **J** (135 mg, 0.745 mmol), DIEA (270 µL, 1.550 mmol), PyBOP (388 mg, 0.745 mmol) and a 0.6 M solution of HOAt in DMF (1.3 ml, 0.780 mmol), were added at 0 °C. The reaction mixture was allowed to warm to room temperature, and stirred for 17 h. The reaction mixture was then cooled to 0 °C and quenched with saturated aqueous $NaHCO_3$, extracted with CH_2Cl_2, washed with brine, and dried over Na_2SO_4. The solution was concentrated and the residue was purified by column chromatography (EtOAc/Hex, 1:1) to give sulfamidate **8a** (141 mg, 71%) as colorless oil. $[a]_D^{20}$= -19.7 (*c* 1.0 in $CHCl_3$). HRMS (ESI) m/z = 267.1121, calculated for $C_8H_{14}N_2O_6SH^+$ (MH^+) = 267.0651. ^{1}H NMR (400 MHz, $CDCl_3$) δ (ppm): 1.49 (d, 3H, *J* = 7.4 Hz, C*H*$_3$ of Ala), 1.73 (s, 3H, C*H*$_3$), 3.50 (dd, 1H, *J* = 12.9 Hz, *J* = 11.1 Hz, C*H*$_2$ of Sulfamidate), 3.77 (s, 3H, CO_2CH_3), 3.99 (dd, 1H, *J* = 12.9 Hz, *J* = 6.9 Hz, C*H*$_2$ of Sulfamidate), 4.45-4.63 (m, 1H, C*H* of Ala), 5.71 (dd, 1H, *J* = 10.8 Hz, *J* = 7.0 Hz, CH_2NH), 6.98 (d, 1H, *J* = 7.3 Hz, N*H*CH). ^{13}C NMR (100 MHz, $CDCl_3$) δ (ppm): 17.1 (CH_3 of Ala), 22.0 (CH_3), 49.0 (*C*H of Ala), 53.1 (CO_2CH_3), 53.5 (CH_2 of Sulfamidate), 91.2 (CCH_3), 170.9, 173.4 (CO).

Benzyl ((*R*)-5-methyl-2,2-dioxido-1,2,3-oxathiazolidine-5-carbonyl)-L-phenylalaninate [9a]

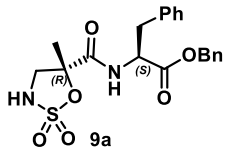

In a schlenk under argon atmosphere, to a solution of L-Phe-OBn hydrochloride (974 mg, 3.593 mmol) in DMF (4.0 mL), sulfamidate **J** (650 mg, 3.593 mmol), DIEA (1.22 mL, 7.007 mmol), PyBOP (1.891 g, 3.593 mmol) and a 0.6 M solution of HOAt in DMF (6.0 ml, 3.6 mmol), were added at 0 °C. The reaction mixture was allowed to warm to room temperature, and stirred for 17 h. The reaction mixture was then cooled to 0 °C, and quenched with saturated aqueous $NaHCO_3$, extracted with CH_2Cl_2, washed with brine, and dried over Na_2SO_4. The solution was concentrated and the residue was purified by column chromatography (EtOAc/Hex, 6.5:3.5) to give sulfamidate **9a** (1.307 g, 87%) as colorless oil. $[a]_D^{20}$= -27.6 (*c* 1.0 in $CHCl_3$). HRMS (ESI) m/z = 419.1307, calculated for $C_{20}H_{22}N_2O_6SH^+$ (MH^+) = 419.1277. ^{1}H NMR (400 MHz, $CDCl_3$) δ (ppm): 1.51 (s, 3H, C*H*$_3$), 3.00 (dd, 1H, *J* = 14.1 Hz, *J* = 7.9 Hz, C*H*$_2$ of Phe), 3.16 (dd, 1H, *J* = 14.2 Hz, *J* = 5.3 Hz, C*H*$_2$ of Phe), 3.20-3.30 (m, 1H, C*H*$_2$ of Sulfamidate), 3.70-3.80 (m, 1H, C*H*$_2$ of Sulfamidate), 4.70-7.75 (m, 1H, C*H* of Phe), 5.00-5.19 (m, 3H, N*H*CH_2, C*H*$_2$Ph), 6.86 (d, 1H, *J* = 7.5 Hz, N*H*CH), 7.01 (d, 2H, *J* = 7.4 Hz, Arom), 7.16-7.34 (m, 8H, Arom). ^{13}C NMR (100 MHz, $CDCl_3$) δ (ppm): 22.1 (*C*H_3C), 37.0 (CH_2 of Phe), 53.3 (*C*H_2 of Sulfamidate), 54.0 (CH of Phe), 68.1 (*C*H_2Ph), 90.9 (*C*CH_3), 127.6, 128.7, 128.8, 128.9, 129.0, 129.1, 129.1, 129.7, 134.8, 135.1 (Arom), 170.7, 171.3 (CO).

Methyl ((*R*)-5-methyl-2,2-dioxido-1,2,3-oxathiazolidine-5-carbonyl)-L-tryptophanate [10a]

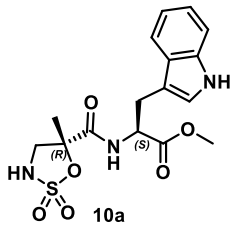

In a schlenk under argon atmosphere, to a solution of L-Trp-OMe hydrochloride (95 mg, 0.374mmol) in DMF (1.2 mL), sulfamidate **J** (67 mg, 0.374 mmol), DIEA (135 µL, 7.750 mmol), PyBOP (197 mg, 0.347 mmol) and a 0.6 M solution of HOAt in DMF (0.65 ml, 0.390 mmol), were added at 0 °C. The reaction mixture was allowed to warm to room temperature, and stirred for 17 h. The reaction mixture was then cooled to 0 °C and quenched with saturated aqueous $NaHCO_3$, extracted with CH_2Cl_2, washed with brine, and dried over Na_2SO_4. The solution was concentrated and the residue was purified by column chromatography (EtOAc/Hex, 7:3) to give sulfamidate **10a** (106 mg, 75%) as yellow oil. $[a]_D^{20}$= -17.8 (*c* 1.0 in $CHCl_3$). HRMS (ESI) m/z = 382.1101, calculated for $C_{16}H_{19}N_3O_6SH^+$ (MH^+) = 382.1073. ^{1}H NMR (400 MHz, $CDCl_3$) δ (ppm): 1.54 (s, 3H, C*H*$_3$), 3.35 (m, 3H, CH_2 of Trp, C*H*$_2$ of Sulfamidate), 3.72 (s, 3H, CO_2CH_3), 3.86 (dd, 1H, *J* = 12.9 Hz, *J* = 6.8 Hz, C*H*$_2$ of Sulfamidate), 4.79 (m, 1H,C*H* of Trp), 5.56 (dd, 1H, *J* = 10.4 Hz, *J* = 7.1 Hz, CH_2NH), 7.03 (d, 1H, *J* = 1.7 Hz, $CH_{vinylic}$), 7.05-7.23 (m, 2H, N*H*CH, Arom), 7.19 (t, 1H, *J* = 7.5 Hz, Arom), 7.34 (d, 1H, *J* = 8.1 Hz, Arom), 7.53 (d, 1H, *J* = 7.9 Hz, Arom), 8.35 (br s, 1H, N*H*$CH_{vinylic}$). ^{13}C NMR (100 MHz, $CDCl_3$) δ (ppm): 21.9 (*C*H_3), 26.8 (CH_2 of Trp), 53.0 (CO_2CH_3), 53.2 (*C*H_2 of Sulfamidate), 53.5 (CH of Trp), 91.0 (*C*CH_3), 109.1, 111.6, 118.3, 119.9, 122.6, 123.1, 127.2, 136.4 (Arom) 170.8, 172.4 (CO).

Methyl ((*R*)-5-methyl-2,2-dioxido-1,2,3-oxathiazolidine-5-carbonyl)-L-alanyl-L-tryptophanate [11a]

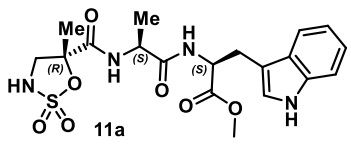

11a

Sulfamidate **8a** (44 mg, 0.165 mmol) and $LiOH{\cdot}H_2O$ (70 mg, 1.66 mmol) were suspended in a mixture of MeOH/H_2O (3:2, 15 mL) and the mixture was stirred at room temperature for 24 h. After that, the generated suspension was concentrated, and after evaporation of MeOH, acidified with a 20% H_2SO_4 aqueous solution. The extraction of the aqueous layer with CH_2Cl_2, and $CHCl_3$:^{i}PrOH (3:1) gives, after drying over Na_2SO_4 and concentrating under vacuum, a white solid which was used without further purification. In a schlenk under argon atmosphere to a solution of L-Trp-OMe hydrochloride (42 mg, 0.165mmol) in DMF (1.2 mL), the above carboxylic acid (42 mg, 0.165 mmol), DIEA (60 µL, 3.444 mmol), PyBOP (87 mg, 0.165 mmol) and a 0.6 M solution of HOAt in DMF (0.31 ml, 0.185 mmol), were added at 0 °C. The reaction mixture was allowed to warm to room temperature, and stirred for 17 h. The reaction mixture was then cooled to 0 °C, and quenched with saturated aqueous $NaHCO_3$, extracted with CH_2Cl_2, washed with brine, and dried over Na_2SO_4. The solution was concentrated and the residue was purified by column chromatography (EtOAc/Hex, 9:1) to give **11a** (31 mg, 59%) as a yellow oil. $[a]_D^{20}$= -4.8 (*c*1.0 in $CHCl_3$). HRMS (ESI) m/z = 453.1438 calculated for $C_{19}H_{24}N_4O_6SH^+$ (MH^+) = 453.1444.

^{1}H NMR (400 MHz, $CDCl_3$) δ (ppm): 1.20 (d, 3H, *J* = 7.3 Hz, C*H*$_3$ of Ala), 1.69 (s, 3H, C*H*$_3$), 3.21 (dd, 1H, *J* = 14.8 Hz, *J*= 7.3 Hz, C*H*$_2$ of Trp), 3.32 (dd, 1H, *J* = 14.9 Hz, *J* = 5.1 Hz, C*H*$_2$ of Trp), 3.42 (dd, 1H, *J* = 12.5 Hz, *J* = 10.4 Hz, C*H*$_2$ of Sulfamidate), 3.72 (s, 3H, OC*H*$_3$), 4.08 (dd, 1H, *J* = 12.7 Hz, *J* = 6.3 Hz, C*H*$_2$ of Sulfamidate), 4.31 (t, 1H, *J* = 7.3 Hz, C*H* of Ala),

4.95-5.02 (m, 1H, C*H* of Trp), 6.61-6.71 (m, 2H, CH_2NH, NH of Trp), 6.78 (d, 1H, *J* = 7.1 Hz, , NH of Ala), 7.06 (d, 1H, *J* = 2.0 Hz, $CH_{vinylic}$), 7.10-7.15 (m, 2H, Arom), 7.18 (t, 1H, *J* = 7.1 Hz, Arom), 7.35 (d, 1H, *J* = 8.0 Hz, Arom), 7.56 (d, 1H, *J* = 7.8 Hz, Arom), 8.18 (br s, 1H, $NHCH_{vinylic}$).
^{13}C NMR (100 MHz, $CDCl_3$) δ (ppm): 17.4 (CH_3 of Ala), 22.0 (CH_3), 27.9 (CH_2 of Trp), 50.7 (*C*H of Ala), 52.7 (*C*H of Trp), 53.0 (OCH_3), 53.5 (CH_2 of Sulfamidate), 91.8 (NCH_2C), 110.0, 111.4, 118.6, 119.8, 122.4, 123.1, 127.8, 136.2 (Arom) 170.5, 171.6, 173.7 (CO).

Methyl-((*R*)-3-acetyl-5-methyl-2,2-dioxido-1,2,3-oxathiazolidine-5-carbonyl)-L-alaninate [8b]

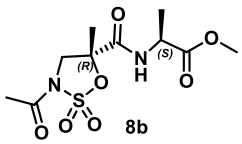

Compound **8a** (30 mg, 0.11 mmol) was added into a schlenk under argon atmosphere and dissolved in pyridine (2 mL). Then, acetic anhydride (1 mL) was added and allowed to react for 1.5 h at room temperature. After concentration and purification by column chromatography on silica gel (AcOEt/Hexane, 4:6), compound **8b** (20 mg, 59%) was obtained as a viscous yellow oil.
$[a]_D^{20}$= -37.5º (*c* 1.0 in $CHCl_3$). HRMS (ESI) m/z =309.0748, calculated for $C_{10}H_{16}N_2O_7SH^+$ (MH^+) = 309.0751. ^{1}H NMR (400 MHz, $CDCl_3$) δ (ppm): 1.47 (d, 3H, *J* = 7.2 Hz, C*H*$_3$ of Ala), 1.83 (s, 3H, C*H*$_3$), 2.44 (s, 3H, Ac), 3.77 (s, 3H, OC*H*$_3$), 3.99 (d, 1H, *J* = 11.3 Hz, C*H*$_2$ of Sulfamidate), 4.52 (d, 1H, *J* = 11.3 Hz, C*H*$_2$ of Sulfamidate), 4.54-4.58 (m, 1H, C*H* of Ala), 6.98-7.09 (m, 1H, N*H*). ^{13}C NMR (100 MHz, $CDCl_3$) δ (ppm): 17.9 (CH_3 of Ala), 22.2 (Ac), 23.6 (CH_3), 48.6 (*C*H of Ala), 52.6 (CH_2 of Sulfamidate), 52.8 (OCH_3), 86.1 (NCH_2C), 166.1, 167.8, 172.1 (CO).

Benzyl-((*R*)-3-acetyl-5-methyl-2,2-dioxido-1,2,3-oxathiazolidine-5-carbonyl)-L-phenylalaninate [9b]

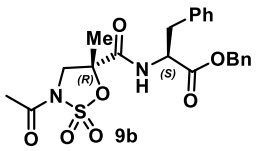

Compound **9a** (67 mg, 0.14 mmol) was added into a schlenk under argon atmosphere and dissolved in pyridine (2.8 mL). Then, acetic anhydride (1.4 mL) was added and allowed to react for 1.5 h at room temperature. After concentration and purification by column chromatography on silica gel (AcOEt/Hexane, 4:6), compound **9b** (68 mg, 92%) was obtained as a viscous colorless oil. $[a]_D^{20}$= -33.8 (*c* 1.0 en $CHCl_3$). HRMS (ESI) m/z = 483.1198, calculated for $C_{22}H_{24}N_2O_7SNa^+$ (MNa^+) = 483.1196. ^{1}H NMR (400 MHz, $CDCl_3$) δ (ppm): 1.66 (s, 3H, C*H*$_3$), 2.39 (s, 3H, Ac), 2.99-3.15 (m, 1H, C*H*$_2$ of Phe), 3.19-3.35 (m, 1H, C*H*$_2$ of Phe), 3.92 (d, 1H, *J* = 11.3 Hz, C*H*$_2$ of Sulfamidate), 4.45 (d, 1H, *J* = 11.3 Hz, C*H*$_2$ of Sulfamidate), 4.83-4.90 (m, 1H, C*H* of Phe), 5.13-5.26 (m, 2H, OC*H*$_2$Ph), 6.90 (d, 1H, *J* = 7.8 Hz, N*H*CH), 6.95-7.45 (m, 10H, Arom). ^{13}C NMR (100 MHz, $CDCl_3$) δ (ppm): 22.1 (Ac), 23.6 (*C*H_3),37.5 (*C*H_2 of Phe), 52.4 (*C*H_2 of Sulfamidate), 53.5 (*C*H of Phe), 67.7 (O*C*H_2Ph), 86.0 (NCH_2*C*), 127.4, 128.7, 129.2, 134.9, 135.1 (Arom), 166.1, 167.7, 170.1 (CO).

Methyl-((*R*)-3-acetyl-5-methyl-2,2-dioxido-1,2,3-oxathiazolidine-5-carbonyl)-L-tryptophanate [10b]

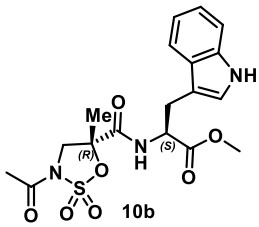

Compound **10a** (34 mg, 0.08 mmol) was added into a schlenk under argon atmosphere and dissolved in pyridine (1.6 mL). Then, acetic anhydride (0.8 mL) was added and allowed to react for 1.5 h at room temperature. After concentration and purification by column chromatography

on silica gel (AcOEt/Hexane, 7:3), compound **10b** (30 mg, 81%) was obtained as a viscous yellow oil. $[a]_D^{20}$= -18.1º (*c* 1.0 in $CHCl_3$). HRMS (ESI) m/z =424.1185, calculated for $C_{18}H_{21}N_3O_7SH^+$ (MH^+) = 424.1173. ^{1}H NMR (400 MHz, $CDCl_3$) δ (ppm): 1.62 (s, 3H, C*H*$_3$), 2.39 (s, 3H, Ac), 3.30-3.46 (m, 2H, C*H*$_2$ of Trp), 3.74 (s, 3H, OC*H*$_3$), 3.92 (d, 1H, *J* = 11.3 Hz, C*H*$_2$ of Sulfamidate), 4.47 (d, 1H, *J* = 11.3 Hz, C*H*$_2$ of Sulfamidate), 4.84-4.90 (m, 1H, C*H* of Trp), 6.98 (d, 1H, *J* = 7.6 Hz, N*H*CH), 7.00-7.56 (m, 5H, Arom), 8.21 (s, 1H, N*H* of Trp). ^{13}C NMR (100 MHz, $CDCl_3$) δ (ppm): 22.2 (Ac), 23.4 (*C*H$_3$), 27.4 (*C*H$_2$ of Trp), 52.7 (*C*H$_2$ of Sulfamidate), 52.8 (O*C*H$_3$), 53.5 (*C*H of Trp), 86.2 (NCH$_2$*C*), 109.6, 111.5, 118.5, 119.9, 122.6, 122.9, 127.5, 136.3 (Arom), 166.2, 167.9, 171.2 (CO).

Methyl-((*R*)-3-acetyl-5-methyl-2,2-dioxido-1,2,3-oxathiazolidine-5-carbonyl)-L-alanyl-L-tryptophanate [11b]

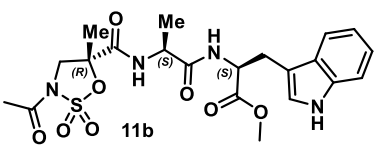

11a (55 mg, 0.12 mmol) was added into a schlenk under argon atmosphere and dissolved in pyridine (2 mL). Then, acetic anhydride (1 mL) was added and allowed to react for 1.5 h at room temperature. After concentration and purification by column chromatography on silica gel (AcOEt/Hexane, 9:1), compound **11b** (34 mg, 58%) was obtained as a viscous yellow oil. $[a]_D^{20}$= -4.1 (*c* 1.0 in $CHCl_3$). HRMS (ESI) m/z = 495.1549, calculated for $C_{21}H_{26}N_4O_8SH^+$ (MH^+) = 495.1544. ^{1}H NMR (400 MHz, $CDCl_3$) δ (ppm): 1.27 (d, 3H, *J*= 7.0 Hz, C*H*$_3$ of Ala), 1.69 (s, 3H, C*H*$_3$), 2.19 (s, 3H, Ac), 3.15-3.29 (m, 2H, C*H*$_2$ of Trp),3.61 (s, 3H, OC*H*$_3$), 3.79 (d, 1H, *J* = 11.1 Hz, C*H*$_2$ of Sulfamidate), 4.23 (d, 1H, *J* = 11.1 Hz, C*H*$_2$ of Sulfamidate), 4.42 (t, 1H, *J* = 7.2 Hz, C*H* of Ala), 4.87 (dd, 1H, *J* = 9.5 Hz,

J = 4.1 Hz, C*H* of Trp), 6.64 (d, 1H, *J* = 8.1 Hz, N*H* of Trp), 6.87 (m, 2H, N*H* de la Ala and C$H_{vinylic}$ of Trp), 6.97-7.45 (m, 4H, Arom of Trp), 8.31(s, 1H, N*H* of Arom Trp). ^{13}C NMR (100 MHz, $CDCl_3$) δ (ppm): 18.2 (*C*H_3 of Ala), 22.2 (Ac), 23.7 (*C*H_3), 27.5 (*C*H_2 of Trp), 49.6 (*C*H of Ala), 52.6 (O*C*H_3), 52.7 (*C*H_2 of Sulfamidate), 53.0 (*C*H of Trp), 85.9 (NCH_2*C*), 123.1 ($C_{vinylic}$ of Trp), 109.8, 111.6, 118.4, 119.7, 122.3, 127.7, 136.2 (Arom), 166.4, 167.9, 170.8, 172.0 (CO).

Benzyl-((*R*)-3-((*tert*-butoxycarbonyl)-L-phenylalanyl)-5-methyl-2,2-dioxido-1,2,3-oxathiazolidine-5-carbonyl)-L-phenylalaninate [12]

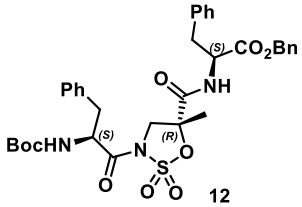

12

To a solution of N-Boc-L-Phe-OH (134 mg, 0.50 mmol) in CH_2Cl_2 (10 mL) was added DIEA (0.35 ml, 2.00 mmol) and TBTU (159 mg, 0.50 mmol). The reaction mixture was stirred at room temperature for 5 min. Then, the mixture was cooled at -20˚C and compound **9b** (209 mg, 0.50 mmol) was added and stirred at -20 ˚C. After 30 minutes the resulting mixture was warmed to room temperature and washed with brine (15 mL). Then, the aqueous layer was extracted with CH_2Cl_2 (2 x 10 mL). The organic phases were combined and washed with 0.1N HCl (15 mL) and $NaHCO_3$ 5 % (15 mL) and dried over anhydrous Na_2SO_4. After evaporation of the solvent, the residue was purified by a silica gel column chromatography (hexane/EtOAc, 4:6) to give compound **12** (290 mg, 87%) as a colorless oil. $[a]_D^{20}$= -20.3 (*c*1.0 in $CHCl_3$). HRMS (ESI) m/z = 666.2522, calculated for $C_{34}H_{39}N_3O_9SH^+$ (MH^+) = 666.2485. ^{1}H NMR (400 MHz, $CDCl_3$) δ (ppm): 1.30 (s, 9H, $C(CH_3)_3$), 1.46 (s, 3H, C*H*$_3$), 2.83 (dd, 1H, *J* = 12.4 Hz, *J* = 7.6 Hz, C*H*$_2$ of Phe), 2.99 (dd, 1H, *J* = 14.0 Hz, *J* = 6.9 Hz, C*H*$_2$ of Phe), 3.03-

3.20 (m, 2H, CH_2 of Phe), 3.63 (br s, 1H, CH_2 of Sulfamidate), 4.43 (d, 1H, J = 10.8 Hz , CH_2 of Sulfamidate), 4.65-4.83 (m, 2H, CH of Phe, CH of Phe), 4.95 (d, 1H, J = 5.6 Hz, N*H*Boc), 5.07 (dd, 2H, J = 32.5, J = 12.1 Hz, OCH_2Ph), 6.83 (d, 1H, J = 7.6, N*H*CH), 6.92 (br s, 2H, Arom), 7.07-7.32 (m, 13H, Arom). ^{13}C NMR (100 MHz, $CDCl_3$) δ (ppm): 23.5 (*C*H_3), 28.3 (*C*$(CH_3)_3$), 37.6 (*C*H_2 of Phe), 37.9 (*C*H_2 of Phe), 52.5 (CH_2 of Sulfamidate), 53.5 (*C*H of Phe), 54.9 (*C*H of Phe), 67.8 (O*C*H_2Ph), 80.5 (*C*$(CH_3)_3$), 86.0 (*C*CH_3), 127.4, 127.5, 128.8, 128.9, 129.0, 129.3, 129.5, 129.6, 134.3, 135.1, 135.6 (Arom), 154.8, 167.9, 169.3, 170.2 (CO).

Benzyl-((*R*)-3-((*tert*-butoxycarbonyl)-L-tryptophyl)-5-methyl-2,2-dioxido-1,2,3-oxathiazolidine-5-carbonyl)-L-phenylalaninate [13]

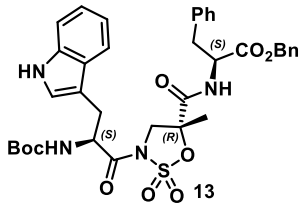

To a solution of N-Boc-L-Trp-OH (76 mg, 0.31 mmol) in CH_2Cl_2 (10 mL) was added DIEA (0.23 mL, 1.24 mmol) and TBTU (99 mg, 0.31 mmol). The reaction mixture was stirred at room temperature for 5 min. Then, the mixture was cooled at -20˚C and compound **9b** (130 mg, 0.31 mmol) was added and stirred at -20 ˚C. After 30 minutes the resulting mixture was warmed to room temperature and washed with brine (15ml). Then, the aqueous layer was extracted with CH_2Cl_2 (2 x 10 ml).The organic phases were combined and washed with 0.1N HCl (15 ml) and $NaHCO_3$ 5 % (15 ml) and dried over anhydrous Na_2SO_4. After evaporation of the solvent, the residue was purified by a silica gel column chromatography (hexane/EtOAc, 6:4) to give compound **13** (177 mg, 81%) as a colorless oil. $[a]_D^{20}$= -10.3 (c1.0 in $CHCl_3$). HRMS (ESI) m/z = 727.2189, calculated for $C_{36}H_{40}N_4O_9SNa^+$ (MNa^+) = 727.2414. ^{1}H NMR (400 MHz, $CDCl_3$) δ (ppm):

1.26 (s, 3H, C*H*$_3$), 1.39 (s, 9H, C(CH$_3$)$_3$), 3.04 (dd, 1H, *J* = 13.8 Hz, *J* = 6.9 Hz, C*H*$_2$ of Phe), 3.16-3.39 (m, 3H, C*H*$_2$ of Phe, C*H*$_2$ of Phe), 3.59 (br s, 1H, C*H*$_2$ of Sulfamidate), 4.39 (d, 1H, *J* = 9.3 Hz , C*H*$_2$ of Sulfamidate), 4.75-4.93 (m, 2H, C*H* of Phe, C*H* of Trp), 5.04-5.19 (m, 3H, CH$_2$ of Bn, N*H*Boc), 6.88 (d, 1H, *J* = 5.6, N*H*CH), 6.94-7.03 (m, 3H, CH$_{vin}$, Arom), 7.09-7.39 (m, 11H, Arom), 7.60 (d, 1H, *J* = 7.4, Arom), 8.23 (s, 1H, , N*H*CH$_{vin}$). ^{13}C NMR (100 MHz, CDCl$_3$) δ (ppm): 23.3 (*C*H$_3$), 28.4 (*C*(CH$_3$)$_3$), 28.4 (*C*H$_2$ of Trp), 37.6 (*C*H$_2$ of Phe), 52.5 (*C*H$_2$ of Sulfamidate), 53.6 (*C*H of Phe), 54.1 (*C*H$_2$ of Trp), 67.8 (O*C*H$_2$Ph), 80.5 (*C*(CH$_3$)$_3$), 85.6 (*C*CH$_3$), 109.2, 111.4, 118.7, 120.1, 122.5, 123.8, 127.5, 127.6, 128.8, 128.9, 129.0, 129.1, 129.3, 134.9, 135.2, 136.3 (Arom), 155.0, 167.9, 169.9, 170.2 (CO).

1-((*S*)-3-((*S*)-2-Acetamido-3-phenylpropanamido)-2-methyl-1-(methyl-amino)-1-oxopropan-2-yl)pyridin-1-ium chloride [14]

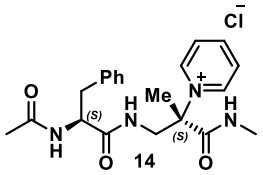

Compound **5** (40 mg, 0.09 mmol) was dissolved in pyridine (2 mL) and stirred at 60 ºC for 12 hours. After concentration, the resulting crude was dissolved in a mixture of CH$_2$Cl$_2$ and 2 M HCl aqueous solution (1:1, 2.5 mL) and allowed to react for 30 minutes at room temperature. After concentration, the crude was dissolved in a mixture of TFA and CH$_2$Cl$_2$ (1:2, 3 mL) and stirred for 30 minutes at room temperature. After concentration, the crude was dissolved in pyridine (2 mL) and acetic anhydride (1 mL). After stirring for 1 h at room temperature, the crude was extracted with CHCl$_3$/^{i}PrOH (3:1) and water and the aqueous phase was concentrated and purified with a reverse phase cartridge Sep-pack C$_{18}$ to obtain compound **14** (23 mg, 62%) as a viscous colorless oil. $[\alpha]_D^{20}$ = -2.4 (*c* 1.00 in H$_2$O).

HRMS (ESI) *m/z* = 383.2087, calculated for C$_{21}$H$_{27}$N$_4$O$_3^+$ (M$^+$) = 383.2078.

^{1}H NMR (400 MHz, D_2O) δ (ppm): 1.92 (s, 3H, C*H*$_3$), 1.95 (s, 3H, Ac), 2.80 (s, 3H, CONHC*H*$_3$), 2.87-2.92 (m, 2H, C*H*$_2$ of Phe), 3.81 (d, 1H, *J* = 14.9 Hz, NHC*H*$_2$C), 4.12 (d, 1H, *J* = 14.9 Hz, NHC*H*$_2$C), 4.35 (t, 1H, *J* = 7.9 Hz, C*H* of Phe), 7.18-7.47 (m, 5H, Arom of Ph), 8.03-8.87 (m, 5H, Arom of Py).
^{13}C NMR (100 MHz, D_2O) δ (ppm): 20.5 (Ac), 21.4 (*C*H$_3$), 26.5 (CONH*C*H$_3$), 36.6 (*C*H$_2$ of Phe), 45.8 (NH*C*H$_2$C), 55.3 (*C*H of Phe), 76.5 (NHCH$_2$*C*), 127.3, 128.8, 129.0, 136.1 (Arom of Ph), 128.0, 143.4, 147.2 (Arom of Py), 169.9 (NH*C*OCH$_3$), 173.8 (NH*C*OCH), 174.3 (*C*ONHCH$_3$).

1-((*S*)-3-((*S*)-2-Acetamido-3-(1*H*-indol-3-yl)propanamido)-2-methyl-1-(methylamino)-1-oxopropan-2-yl)pyridin-1-ium chloride [15] and (*S*)-2-((2-acetamido-3-(1*H*-indol-3-yl)propanamido)methyl)-*N*-methylacrylamide [15′]

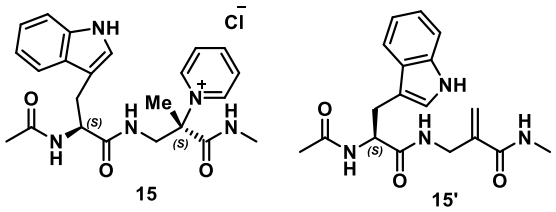

Compound **6** (76 mg, 0.16 mmol) was dissolved in pyridine (3 mL) and stirred at 60 ºC for 12 hours. After concentration, the resulting crude was dissolved in a mixture of CH_2Cl_2 and 2 M HCl aqueous solution (1:1, 3.8 mL) and allowed to react for 30 minutes at room temperature. After concentration, the crude was dissolved in a mixture of TFA and CH_2Cl_2 (1:2, 4.5 mL) and stirred for 30 minutes at room temperature. After concentration, the crude was dissolved in pyridine (3 mL) and acetic anhydride (1.5 mL). After stirring for 1 h at room temperature, the crude was extracted with $CHCl_3$/^{i}PrOH (3:1) and water and the aqueous phase was concentrated and purified with a reverse

phase cartridge Sep-pack C_{18} to obtain compound **15** (34 mg, 51%) as a viscous yellow oil. The elimination product was found in the organic phase. Concentration and purification by column chromatography on silica gel (CH_2Cl_2/MeOH, 9:1) affording compound **15′** (7 mg, 13%) as a viscous yellow oil. Compound **15**: $[\alpha]_D^{20}$ = +8.3 (*c* 1.00 in H_2O). HRMS (ESI) *m/z* = 422.2189, calculated for $C_{23}H_{28}N_5O_3^+$ (M^+) = 422.2187. ^{1}H NMR (400 MHz, D_2O) δ (ppm): 1.73 (s, 3H, C*H*$_3$), 1.96 (s, 3H, Ac), 2.77 (s, 3H, CONHC*H*$_3$), 3.09-3.13 (m, 2H, C*H*$_2$ of Trp), 3.90 (d, 1H, *J* = 14.9 Hz, NHC*H*$_2$C), 3.84 (d, 1H, *J* = 14.9 Hz, NHC*H*$_2$C), 4.43 (t, 1H, *J* = 7.8 Hz, C*H* of Trp), 7.16-7.61 (m, 4H, Arom of Trp), 7.22 (s, 1H, C*H*C) 7.87-8.59 (m, 5H, Arom of Py).
^{13}C NMR (100 MHz, D_2O) δ (ppm): 22.4 (*C*H$_3$), 24.0 (Ac), 29.1 (CONH*C*H$_3$), 29.3 (*C*H$_2$ of Trp), 48.0 (NH*C*H$_2$C), 57.2 (*C*H of Trp), 78.8 (NHCH$_2$*C*), 111.1 (CH$_2$*C*), 115.5, 120.6, 122.0, 124.6, 129.0, 138.4 (Arom of Trp), 127.0 (*C*HC), 130.3, 145.3, 149.4 (Arom of Py), 172.3 (NH*C*OCH$_3$), 176.2 (NH*C*OCH), 177.1 (*C*ONHCH$_3$).

Compound **15′**: $[\alpha]_D^{20}$ = +2.2 (*c* 0.83 in H_2O). HRMS (ESI) *m/z* = 365.1580, calculated for $C_{18}H_{22}N_4O_3Na^+$ (NaM^+) = 365.1584. ^{1}H NMR (400 MHz, D_2O) δ (ppm): 1.90 (s, 3H, Ac), 2.63 (s, 3H, CONHC*H*$_3$), 3.10-3.15 (m, 2H, C*H*$_2$ of Trp), 3.64-3.84 (m, 2H, NHC*H*$_2$C), 4.49 (t, 1H, *J* = 7.5 Hz, C*H* of Trp), 5.09 (s, 1H, CC*H*$_2$), 5.52 (s, 1H, CC*H*$_2$), 7.02-7.61 (m, 5H, Arom).
^{13}C NMR (100 MHz, D_2O) δ (ppm): 24.0 (Ac), 28.3 (CONH*C*H$_3$), 29.4 (*C*H$_2$ of Trp), 42.5 (NH*C*H$_2$C), 57.4 (*C*H of Trp), 111.3 (CH$_2$*C*), 114.3, 120.8, 121.7, 124.3, 126.8, 138.6 (Arom), 129.2 (*C*HC), 123.2 (C*C*H$_2$), 141.4 (*C*CH$_2$), 172.6 (NH*C*OCH$_3$), 176.2 (NH*C*OCH), 176.5 (*C*ONHCH$_3$).

1-((*S*)-3-((*S*)-2-Acetamido-3-(benzyloxy)propanamido)-2-methyl-1-(methylamino)-1-oxopropan-2-yl)pyridin-1-ium chloride [16] and (*S*)-2-((2-acetamido-3-(benzyloxy)propanamido)methyl)-*N*-methylacrylamide [16′]

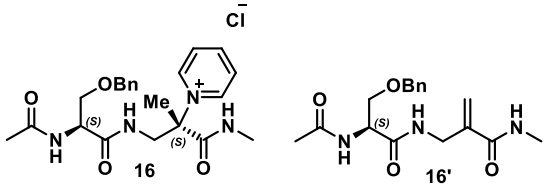

Compound **7** (60 mg, 0.11 mmol) was dissolved in pyridine (2 mL) and stirred at 60 ºC for 12 hours. After concentration, the resulting crude was dissolved in a mixture of CH_2Cl_2 and 2 M HCl aqueous solution (1:1, 2.5 mL) and allowed to react for 30 minutes at room temperature. After concentration, the crude was dissolved in a mixture of TFA and CH_2Cl_2 (1:2, 3 mL) and stirred for 30 minutes at room temperature. After concentration, the crude was dissolved in pyridine (2 mL) and acetic anhydride (1 mL). After reacting for 1 h at room temperature, extracting with $CHCl_3$/^{i}PrOH (3:1) and water, concentrating the aqueous phase and purifying with a reverse phase cartridge Sep-pack C_{18}, compound **16** (21 mg, 45%) was obtained as a viscous colorless oil. The elimination product was found in the organic phase. Concentration and purification by column chromatography on silica gel (CH_2Cl_2/MeOH, 9:1) affording compound **16′** (6 mg, 16%) as a viscous colorless oil.

Compound **16**:$[\alpha]_D^{20}$ = -8.3 (*c* 1.00 in H_2O). HRMS (ESI) *m/z* = 413.2191, calculated for $C_{22}H_{29}N_4O_4^+$ (M^+) = 413.2183. ^{1}H NMR (400 MHz, D_2O) δ (ppm): 2.00 (s, 6H, C*H*$_3$, Ac), 2.81 (s, 3H, CONHC*H*$_3$), 3.62-3.68 (m, 2H, C*H*$_2$ of Ser), 3.91 (d, 1H, *J* = 14.9 Hz, NHC*H*$_2$C), 4.16 (d, 1H, *J* = 14.9 Hz, NHC*H*$_2$C), 4.29 (t, 1H, *J* = 5.1 Hz, C*H* of Ser), 4.53 (d, 1H, *J* = 11.7 Hz,

OC*H*$_2$Ph), 4.58 (d, 1H, *J* = 11.7 Hz, OC*H*$_2$Ph),7.36-7.53 (m, 5H, Arom of Ph), 7.93-8.89 (m, 5H, Arom of Py). ^{13}C NMR (100 MHz, D_2O) δ (ppm): 23.2 (*C*H$_3$), 23.8 (Ac), 28.8 (CONH*C*H$_3$), 48.2 (NH*C*H$_2$C), 56.3 (*C*H of Ser), 70.7 (*C*H$_2$ of Ser), 75.4 (O*C*H$_2$Ph), 79.0 (NHCH$_2$*C*), 130.4, 130.6, 131.2, 139.4 (Arom of Ph), 130.3, 145.7, 149.5 (Arom of Py), 172.3, 175.1, 176.6 (NH*C*OCH$_3$, NH*C*OCH, *C*ONHCH$_3$). Compound **16'**: $[\alpha]_D^{20}$ = -5.4 (*c* 1.00 in H_2O). HRMS (ESI) *m/z* = 334.1765, calculated for $C_{17}H_{24}N_3O_4^+$ $(M+H)^+$ = 334.1761. ^{1}H NMR (400 MHz, D_2O) δ (ppm): 2.05 (s, 3H, Ac), 2.76 (s, 3H, CONHC*H*$_3$), 3.75-3.88 (m, 2H, C*H*$_2$ of Ser), 4.03 (s, 2H, NHC*H*$_2$C), 4.49 (t, 1H, *J* = 4.9 Hz, C*H* of Ser), 4.57 (d, 1H, *J* = 11.8 Hz, OC*H*$_2$Ph), 4.61 (d, 1H, *J* = 11.8 Hz, OC*H*$_2$Ph), 5.49 (s, 1H, C*H*$_2$C), 5.73 (s, 1H, C*H*$_2$C), 7.34-7.52 (m, 5H, Arom). ^{13}C NMR (100 MHz, D_2O) δ (ppm): 21.7 (Ac), 25.9 (CONH*C*H$_3$), 40.3 (NH*C*H$_2$C), 54.1 (*C*H of Ser), 68.7 (*C*H$_2$ of Ser), 73.0 (O*C*H$_2$Ph), 120.4 (C*C*H$_2$), 128.3, 128.3, 128.7, 137.0 (Arom), 139.3 (*C*CH$_2$), 170.4, 171.8, 174.4 (NH*C*OCH$_3$, NH*C*OCH, *C*ONHCH$_3$).

1-((*S*)-3-((*S*)-2-Acetamido-3-(benzyloxy)propanamido)-2-methyl-1-(methylamino)-1-oxopropan-2-yl)-3-methylpyridin-1-ium chloride [17]

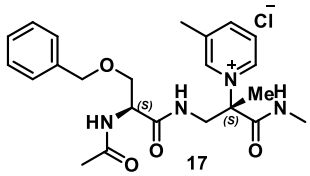

17

Compound **7** (60 mg, 0.13 mmol) was dissolved in 3-methylpyridine (2 mL) and stirred at 60 ºC for 12 hours under argon atmosphere. After concentration, the resulting crude was dissolved in a mixture of CH_2Cl_2 and 2 M HCl aqueous solution (1:1, 2.5 mL) and allowed to react for 30 minutes at room temperature. After concentration, the crude was dissolved in a mixture of TFA and CH_2Cl_2 (1:2, 3 mL) and stirred for 30 minutes at room temperature. After concentration, the crude was dissolved in

pyridine (2 mL) and acetic anhydride (1 mL). After reacting for 1 h at room temperature, extracting with $CHCl_3$/^{i}PrOH (3:1) and water, concentrating the aqueous phase and purifying with a reverse phase cartridge Sep-pack C_{18}, compound **17** (27 mg, 49%) was obtained as a viscous yellow oil. $[\alpha]_D^{20}$ =-56.9 (*c* 1.0 in H_2O). HRMS (ESI) m/z = 427.2342, calculated for $C_{23}H_{31}N_4O_4^+$ (M^+) = 427.2340. ^{1}H NMR (400 MHz, D_2O) δ (ppm): 1.93-2.04 (m, 6H, C*H*$_3$, *Ac*), 2.54 (s, 3H, C*H*$_3$-py), 2.80 (s, 3H, CONHC*H*$_3$), 3.61-3.69 (m, 2H, C*H*$_2$ of Ser), 3.90 (d, 1H, *J* = 14.9 Hz, NHC*H*$_2$C), 4.14 (d, 1H, *J* = 14.9 Hz, NHC*H*$_2$C), 4.28 (t, 1H, *J* = 5.1 Hz, C*H* of Ser), 4.50-4.59 (m, 2H, OC*H*$_2$Ph), 7.35-7.50 (m, 5H, Arom of Bn), 7.87 (t, 1H, *J* = 7.1 Hz, *H* py in meta), 8.40 (d, 1H, *J* = 8.1 Hz, *H* py in para), 8.57 (d, 1H, *J* = 6.5 Hz, *H* py in orto), 8.72 (s, 1H, *H* py in orto). ^{13}C NMR (100 MHz, D_2O) δ (ppm): 17.8 (*C*H$_3$-py), 20.9, 21.6 (*C*H$_3$, Ac), 26.5 (CONH*C*H$_3$), 45.9 (NH*C*H$_2$C), 54.0 (*C*H of Ser), 68.4 (*C*H$_2$ of Ser),73.0 (O*C*H$_2$Ph), 76.0 (NHCH$_2$*C*), 127.2 ($C_{\text{H py in meta}}$), 128.3, 128.4, 128.5, 128.8, 137.0 ($C_{Arom\ of\ \text{Bn}}$), 140.4 ($C_{\text{H py in orto}}$), 142.8 ($C_{\text{H py in orto}}$), 147.7 ($C_{\text{H py in para}}$), 170.1 (*C*ONHMe), 172.0 (*C*ONHCH$_2$C), 174.2 (NH*C*OCH$_3$).

1-((*S*)-3-Acetamido-1-(((*S*)-1-methoxy-1-oxopropan-2-yl)amino)-2-methyl-1-oxopropan-2-yl)pyridin-1-ium chloride [18] and methyl (2-(acetamidomethyl)acryloyl)-L-alaninate [18']

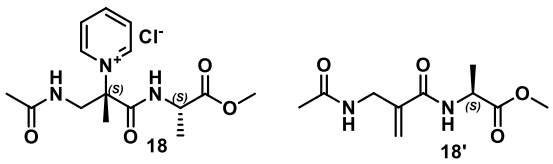

Compound **8b** (20 mg, 0.11 mmol) was dissolved in pyridine (1 mL) in a schlenk under argon atmosphere and allowed to react for 12 hours at 60 ºC.

After concentration, the resulting crude was dissolved in a mixture of CH_2Cl_2 and 2 M HCl aqueous solution (1:1, 1.4 mL) and stirred for 30 minutes at room temperature. Extraction with $CHCl_3$/^{i}PrOH (3:1) and water, concentration of the aqueous phase and purification with a reverse phase cartridge Sep-pack C_{18} affording compound **18** (14 mg, 60%) as a viscous colorless oil. The elimination product was found in the organic phase. Concentration and purification by column chromatography on silica gel (CH_2Cl_2/MeOH, 95:5) affording compound **18'** (2 mg, 14%) as a viscous colorless oil. Compound **18**: $[a]_D^{20}$= -29.6 (*c* 1.0 in H_2O). HRMS (ESI) m/z = 308.1610, calculated for $C_{15}H_{22}N_3O_4^+$ (M^+) = 308.1605. ^{1}H NMR (400 MHz, D_2O) δ (ppm): 1.40 (d, 3H, *J* = 7.4 Hz, C*H*$_3$ of Ala), 1.85 (s, 3H, C*H*$_3$), 2.13 (s, 3H, Ac),3.79 (s, 3H, OC*H*$_3$), 3.85 (d, 1H, *J* = 14.9 Hz, NHC*H*$_2$C), 4.17 (d, 1H, *J* = 14.9 Hz, NHC*H*$_2$C), 4.53 (q, 1H, *J* = 7.3 Hz, C*H* of Ala), 8.11-9.04 (m, 5H, Arom). ^{13}C NMR (100 MHz, D_2O) δ (ppm): 15.2 (*C*H$_3$ of Ala), 20.8 (Ac), 21.3 (*C*H$_3$), 45.8 (NH*C*H$_2$C), 49.5 (*C*H of Ala), 53.1 (O*C*H$_3$), 76.6 (NHCH$_2$*C*), 128.1, 143.5, 147.5 (Arom), 169.7, 174.4, 174.9 (*C*O). Compound **18'**: $[a]_D^{20}$= -7.0 (*c* 0.5 in $CHCl_3$). HRMS (ESI) m/z = 229.1186, calculated for $C_{10}H_{17}N_2O_4^+$ (H^+) = 229.1183. ^{1}H NMR (400 MHz, $CDCl_3$) δ (ppm): 1.45 (d, 3H, *J* = 7.2 Hz, C*H*$_3$ of Ala), 2.01 (s, 3H, Ac),3.76 (s, 3H, OC*H*$_3$), 4.04-4.23 (m, 2H, NHC*H*$_2$C), 4.53 (t, 1H, *J* = 7.2 Hz, C*H* Ala), 5.60 (s, 1H, CC*H*$_2$), 5.97 (s, 1H, CC*H*$_2$), 6.06 (s, 1H, AcN*H*), 7.10 (s, 1H, N*H* of Ala). ^{13}C NMR (100 MHz, $CDCl_3$) δ (ppm): 17.9 (*C*H$_3$ of Ala), 23.2 (Ac), 41.2 (NH*C*H$_2$C), 48.4 (*C*H of Ala), 52.5 (O*C*H$_3$), 77.2 (NHCH$_2$*C*), 123.2 (C*C*H$_2$), 140.1 (*C*CH$_2$), 166.1, 170.6, 173.3 (*C*O).

1-((*S*)-3-Acetamido-1-(((*S*)-1-(benzyloxy)-1-oxo-3-phenylpropan-2-yl)amino)-2-methyl-1-oxopropan-2-yl)pyridin-1-ium chloride [19] and benzyl (2-(acetamidomethyl)acryloyl)-L-phenylalaninate [19′]

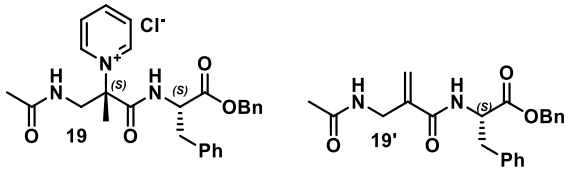

Compound **9b** (32 mg, 0.069 mmol) was dissolved in pyridine (1.2 mL) in a schlenk under argon atmosphere and allowed to react for 12 hours at 60 ºC. After concentration, the resulting crude was dissolved in a mixture of CH_2Cl_2 and 2 M HCl aqueous solution (1:1, 1.4 mL) and stirred for 30 minutes at room temperature. Extraction with $CHCl_3$/^{i}PrOH (3:1) and water, concentration of the aqueous phase and purification with a reverse phase cartridge Sep-pack C_{18} affording compound **19** (23 mg, 70%) as a viscous colorless oil. The elimination product was found in the organic phase. Concentration and purification by column chromatography on silica gel (CH_2Cl_2/MeOH, 95:5) affording compound **19′** (3 mg, 11%) as a viscous colorless oil. Compound **19**: $[a]_D^{20}$= -37.7 (*c* 1.0 in H_2O). HRMS (ESI) m/z = 460.2236, calculated for $C_{27}H_{30}N_3O_4^+$ (M^+) = 460.2231. ^{1}H NMR (400 MHz, D_2O) δ (ppm): 1.76 (s, 3H, C*H*$_3$), 1.86 (s, 3H, Ac), 2.87-2.98 (m, 1H, C*H*$_2$ of Phe), 3.35-3.44 (m, 1H, C*H*$_2$ of Phe), 3.66 (d, 1H, *J* = 15.0 Hz, NHC*H*$_2$C), 3.95 (d, 1H, *J* = 15.0 Hz, NHC*H*$_2$C), 4.95 (dd, 1H, *J* = 11.3 Hz, *J* = 5.2 Hz, C*H* of Phe), 5.27 (s, 2H, OC*H*$_2$Ph), 7.17-8.58 (m, 15H, Arom). ^{13}C NMR (100 MHz, D_2O) δ (ppm): 20.3 (Ac), 21.2 (*C*H$_3$), 35.4 (*C*H$_2$ of Phe), 45.8 (NH*C*H$_2$C), 54.2 (*C*H of Phe), 68.1 (O*C*H$_2$Ph), 76.4 (NHCH$_2$*C*), 127.4, 127.8, 128.0, 128.7, 128.8, 128.9, 129.0, 129.2, 135.1, 136.5, 142.9, 147.3 (Arom), 169.6, 172.0, 174.7 (*C*O). Compound **19′**: $[a]_D^{20}$= +9.8 (*c* 0.75 in $CHCl_3$).

HRMS (ESI) m/z = 381.1809, calculated for $C_{22}H_{25}N_2O_4^+$ (H^+) = 381.1810. ^{1}H NMR (400 MHz, $CDCl_3$) δ (ppm): 1.96 (s, 3H, Ac),3.07-3.30 (m, 2H, C*H*$_2$ of Phe), 4.00-4.24 (m, 2H, NHC*H*$_2$C), 4.88-4.97 (m, 1H, C*H* of Phe), 5.13-5.26 (m, 2H, OC*H*$_2$Ph),5.59 (s, 1H, CC*H*$_2$), 5.83 (s, 1H, CC*H*$_2$), 6.01-6.09 (m, 1H, N*H*CH$_2$), 6.92 (d, 1H, *J*= 7.6 Hz, N*H*CH), 7.09-7.45 (m, 10H, Arom). ^{13}C NMR (100 MHz, $CDCl_3$) δ (ppm): 23.2 (Ac), 37.6 (*C*H$_2$ of Phe), 41.2 (NH*C*H$_2$C), 53.7 (*C*H of Phe), 67.3 (O*C*H$_2$Ph), 122.7 (C*C*H$_2$), 127.1, 128.6, 128.7, 129.2, 135.2, 135.9 (Arom), 140.2 (*C*CH$_2$), 166.5, 170.5, 171.3 (*C*O).

1-((*S*)-1-(((*S*)-3-(1*H*-Indol-3-yl)-1-methoxy-1-oxopropan-2-yl)amino)-3-acetamido-2-methyl-1-oxopropan-2-yl)pyridin-1-ium chloride [20] and methyl (2-(acetamidomethyl)acryloyl)-L-tryptophanate [20′]

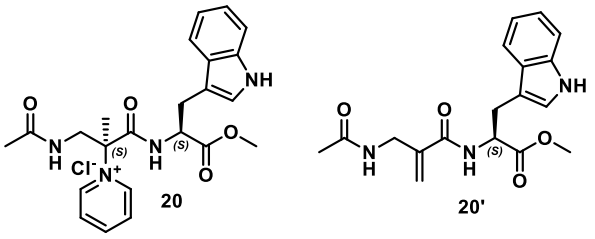

Compound **10a** (30 mg, 0.071 mmol) was dissolved in pyridine (1 mL) in a schlenk under argon atmosphere and allowed to react for 12 hours at 60 ºC. After concentration, the resulting crude was dissolved in a mixture of CH_2Cl_2 and 2 M HCl aqueous solution (1:1, 1.4 mL) and stirred for 30 minutes at room temperature. Extraction with $CHCl_3$/^{i}PrOH (3:1) and water, concentration of the aqueous phase and purification with a reverse phase cartridge Sep-pack C_{18} affording compound **20** (16 mg, 52%) as a viscous yellow oil. The elimination product was found in the organic phase. Concentration and purification by column chromatography on silica gel (CH_2Cl_2/MeOH, 95:5) affording compound **20′** (4 mg, 17%) as a viscous

yellow oil. Compound **20**: $[a]_D^{20}$= -70.2 (*c* 1.0 in H_2O). HRMS (ESI) m/z = 423.2031, calculated for $C_{23}H_{27}N_4O_4^+$ (M^+) = 423.2027. ^{1}H NMR (400 MHz, D_2O) δ (ppm): 1.72 (s, 3H, C*H*$_3$), 1.96 (s, 3H, Ac), 2.99-3.16 (m, 1H, C*H*$_2$ of Trp), 3.40-3.55 (m, 1H, C*H*$_2$ of Trp), 3.63 (d, 1H, *J* = 14.8 Hz, NHC*H*$_2$C), 3.84 (s, 1H, OC*H*$_3$), 3.89 (d, 1H, *J* = 14.8 Hz, NHC*H*$_2$C), 5.13 (dd, 1H, *J* = 11.6 Hz, *J* = 4.8 Hz, C*H* of Trp), 7.08-8.50 (m, 10H, Arom). ^{13}C NMR (100 MHz, D_2O) δ (ppm): 20.1 (Ac), 21.1 (*C*H$_3$), 25.9 (*C*H$_2$ of Trp), 45.8 (NH*C*H$_2$C), 53.2 (O*C*H$_3$, *C*H of Trp), 76.3 (NHCH$_2$*C*), 109.2, 112.1, 118.4, 119.6, 122.2, 124.3, 126.5, 127.6, 136.1, 142.5, 147.1 (Arom), 169.5, 173.2, 174.6 (*C*O). Compound **20'**: $[a]_D^{20}$= -+9.1 (*c* 1.0 in $CHCl_3$). HRMS (ESI) m/z = 366.1419, calculated for $C_{18}H_{21}N_3O_4Na^+$ (Na^+) = 366.1424. ^{1}H NMR (400 MHz $CDCl_3$) δ (ppm): 1.94 (s, 3H, Ac), 3.28-3.48 (m, 2H, C*H*$_2$ of Trp), 3.63 (d, 1H, *J* = 14.8 Hz, NHC*H*$_2$C), 3.76 (s, 3H, OC*H*$_3$), 4.01-4.17 (m, 2H, NHC*H*$_2$C), 4.91-5.00 (m, 1H, C*H* of Trp), 5.57 (s, 1H, CC*H*$_2$), 5.74 (s, 1H, CC*H*$_2$), 6.03-6.15 (m, 1H, CON*H*CH$_2$), 6.84 (d, 1H, *J* = 7.5 Hz, N*H* of Trp), 7.05 -7.62 (m, 5H, Arom), 8.20 (s, 1H, N*H* of aromatic ring of Trp). ^{13}C NMR (100 MHz, $CDCl_3$) δ (ppm): 23.2 (Ac), 27.4 (*C*H$_2$ of Trp), 41.2 (*C*H$_2$ NHC*H*$_2$C), 52.4 (O*C*H$_3$), 53.3 (*C*H of Trp), 77.2 (NHCH$_2$*C*), 122.4 (C*C*H$_2$), 110.2, 111.3, 118.6, 119.8, 122.8, 127.6, 136.2 (Arom), 140.1 (*C*CH$_2$), 166.6, 170.3, 172.2 (*C*O).

1-((4*S*,7*S*,10*S*)-4-((1*H*-Indol-3-yl)methyl)-7,10-dimethyl-3,6,9,13-tetraoxo-2-oxa-5,8,12-triazatetradecan-10-yl)pyridin-1-ium chloride [21] and methyl (2-(acetamidomethyl)acryloyl)-L-alanyl-L-tryptophanate [21']

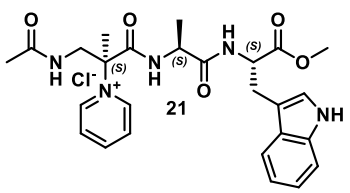

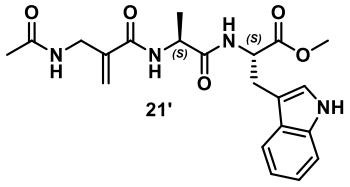

Compound **11b** (27 mg, 0.055 mmol) was dissolved in pyridine (1 mL) in a schlenk under argon atmosphere and allowed to react for 12 hours at 60 ºC. After concentration, the resulting crude was dissolved in a mixture of CH_2Cl_2 and 2 M HCl aqueous solution (1:1, 1.4 mL) and stirred for 30 minutes at room temperature. Extraction with $CHCl_3$/^{i}PrOH (3:1) and water, concentration of the aqueous phase and purification by HPLC in reversed-phase affording the compound **21** (16 mg, 53%) as a viscous yellow oil. The elimination product was found in the organic phase. Concentration and purification by column chromatography on silica gel (CH_2Cl_2/MeOH, 95:5) affording compound **21'** (3 mg, 14%) as a viscous yellow oil.

Semi-preparative HPLC gradient (t_R **21**= 20.33)

Time (min)	Flow (mL/min)	H_2O + 0.1% TFA (%)	Acetonitrile (%)
0	10	85	15
20	10	65	35
25	10	30	70
35	10	85	15

Compound **21**: $[a]_D^{20}$= -14.2 (c 1.0 in H_2O). HRMS (ESI) m/z = 494.2399, calculated for $C_{26}H_{32}N_5O_5^+$ (M^+) = 494.2398. ^{1}H NMR (400 MHz, D_2O) δ

(ppm): 1.29 (d, 3H, *J* = 7.3 Hz, C*H*$_3$ of Ala), 1.82 (s, 3H, C*H*$_3$), 1.88 (s, 3H, Ac), 3.29-3.46 (m, 2H, C*H*$_2$ of Trp), 3.62-3.77 (m, 4H, NHC*H*$_2$C, OC*H*$_3$), 3.96 (d, 1H, *J* = 14.8 Hz, NHC*H*$_2$C), 4.35 (q, 1H, *J* = 7.2 Hz, C*H* of Ala), 4.82 (dd, 1H, *J* = 7.6 Hz, *J* = 5.9 Hz, C*H* of Trp), 7.10 -8.86 (m, 10H, Arom). ^{13}C NMR (100 MHz, D_2O) δ (ppm): 18.1(*C*H$_3$ of Ala), 22.9 (Ac), 23.7 (*C*H$_3$), 29.0 (*C*H$_2$ of Trp), 48.1 (NH*C*H$_2$C), 52.9 (*C*H of Ala), 55.3 (O*C*H$_3$), 55.9 (*C*H of Trp), 78.9 (NHCH$_2$*C*), 111.1, 114.3, 120.7, 121.9, 124.4, 127.0, 129.2, 130.4, 138.5, 145.7, 149.8 (Arom), 171.7, 176.2, 176.6, 177.2 (*C*O). Compound **21'**: $[\alpha]_D^{20}$= +3.5 (*c* 0.75 in $CHCl_3$). HRMS (ESI) m/z = 437.1793, calculated for $C_{21}H_{26}N_4O_5Na^+$ (Na^+) = 437.1795. ^{1}H NMR (400 MHz, $CDCl_3$) δ (ppm): 1.35 (d, 3H, *J*= 7.1 Hz, C*H*$_3$ of Ala), 1.92 (s, 3H, Ac), 3.25 (dd, 1H, *J* = 14.9 Hz, *J*= 5.9 Hz, C*H*$_2$ of Trp), 3.38 (dd, 1H, *J* = 14.8 Hz, *J* = 5.1 Hz C*H*$_2$ of Trp), 3.71 (s, 3H, OC*H*$_3$), 4.00-4.06 (m, 2H, NHC*H*$_2$C), 4.43-4.54 (m, 1H, C*H* of Ala), 4.82-4.91 (m, 1H, C*H* of Trp), 5.47 (s, 1H, CC*H*$_2$), 5.70 (s, 1H, CC*H*$_2$), 5.96-6.06 (m, 1H, CON*H*CH$_2$), 6.65 (d, 1H, *J* = 7.5 Hz, N*H* of Trp), 6.75 (d, 1H, *J* = 7.5 Hz, N*H* of Ala), 6.96-7.59 (m, 5H, Trp), 8.60 (s, 1H, N*H* of aromatic ring of Trp). ^{13}C NMR (100 MHz, $CDCl_3$) δ (ppm): 17.2 (*C*H$_3$ of Ala), 23.1 (Ac), 27.4 (*C*H$_2$ of Trp), 41.1 (NH*C*H$_2$C), 49.0 (*C*H of Ala), 52.5 (O*C*H$_3$), 52.8 (*C*H of Trp), 77.2 (NHCH$_2$*C*), 122.1 (C*C*H$_2$), 109.6, 111.4, 118.6, 119.5, 121.9, 123.3, 127.5, 136.2 (Arom), 139.9 (*C*CH$_2$), 166.4, 170.8, 171.5, 172.2 (*C*O).

1-((4*S*,7*S*,11*S*)-4,11-Dibenzyl-7-methyl-3,6,10,13-tetraoxo-1-phenyl-2-oxa-5,9,12-triazatetradecan-7-yl)pyridin-1-ium chloride [22] and benzyl (2-(((*S*)-2-acetamido-3-phenylpropanamido)methyl)acryloyl)-L-phenylalaninate [22']

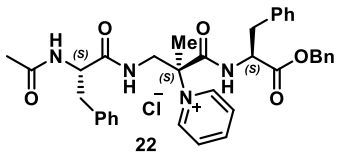

22

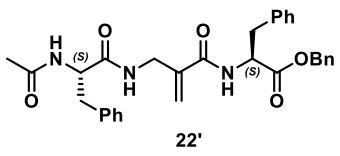

22'

Compound **12** (27 mg, 0.041 mmol) was dissolved in pyridine (1 mL) and stirred at 60 ºC for 12 hours. After concentration, the resulting crude was dissolved in a mixture of CH_2Cl_2 and 2 M HCl aqueous solution (1:1, 1.4 mL) and allowed to react for 30 minutes at room temperature. After concentration, the crude was dissolved in a mixture of TFA and CH_2Cl_2 (1:2, 1.5 mL) and stirred for 30 minutes at room temperature. After concentration, the crude was dissolved in pyridine (1 mL) and acetic anhydride (0.5 mL). After reacting for 1 h at room temperature, extracting with acetate and water, concentrating the aqueous phase and purifying by HPLC in reversed-phase, compound **22** (7 mg, 30%) was afforded as a viscous colorless oil. The elimination product was found in the organic phase. Concentration and purification by column chromatography on silica gel (CH_2Cl_2/MeOH, 95:5) affording compound **22'** (3 mg, 14%) as a viscous colorless oil.

Semi-preparative HPLC gradient (t_R **22**= 16.40)

Time (min)	Flow (mL/min)	H_2O + 0.1% TFA (%)	Acetonitrile (%)
0	10	75	25
30	10	5	95
40	10	75	25
45	10	75	25

Compound **22**: $[a]_D^{20}$= -8.2 (*c* 1.0 in CH_3OH). HRMS (ESI) m/z = 607.2898, calculated for $C_{36}H_{39}N_4O_5^+$ (M^+) = 607.2915. ^{1}H NMR (400 MHz, CD_3OD) δ (ppm): 1.84 (s, 3H, C*H*$_3$), 1.89 (s, 3H, Ac), 2.68-3.03 (m, 3H, C*H*$_2$ of Phe1 and of Phe2), 3.33-3.37 (m, 1H, C*H*$_2$ of Phe2), 3.60 (d, 1H, *J* = 14.8 Hz, NHC*H*$_2$C), 4.03 (d, 1H, *J* = 14.8 Hz, NHC*H*$_2$C), 4.22-4.28 (m, 1H, C*H* of Phe1), 4.78-4.84 (m, 1H, C*H* of Phe2), 5.23 (s, 2H, OC*H*$_2$Ph), 7.12-8.60 (m, 20H, Arom). ^{13}C NMR (100 MHz, CD_3OD) δ (ppm): 19.7 (*C*H_3), 20.9 (Ac), 35.7 (*C*H_2 of Phe2), 36.7 (*C*H_2 of Phe1), 45.8 (NH*C*H_2C), 54.3 (*C*H of Phe2), 55.2 (*C*H of Phe1), 67.1 (O*C*H_2Ph), 76.4 (NHCH_2*C*), 126.6, 126.7, 127.5, 128.2, 128.2, 128.3, 128.4, 128.6, 128.7, 135.6, 136.7, 136.9, 143.4, 146.3 (Arom), 168.6, 170.7, 171.8, 173.4 (*C*O). Compound **22'**: $[a]_D^{20}$= -5.1 (*c* 0.75 in $CHCl_3$). HRMS (ESI) m/z = 550.2304, calculated for $C_{31}H_{33}N_3O_5Na^+$ (Na^+) = 550.2312. ^{1}H NMR (400 MHz, $CDCl_3$) δ (ppm): 1.97 (s, 3H, Ac), 2.98-3.26 (m, 4H, C*H*$_2$ of Phe1 and Phe2), 3.89 (dd, 1H, *J*= 15.3 Hz, *J* = 5.4 Hz, NHC*H*$_2$C), 4.22 (dd, 1H, *J* = 15.3 Hz, *J* = 7.1 Hz, NHC*H*$_2$C), 4.63-4.74 (m, 1H, C*H* of Phe1), 4.85-4.96 (m, 1H, C*H* of Phe2), 5.11-5.26 (m, 2H, OC*H*$_2$Ph), 5.44 (s, 1H, CC*H*$_2$), 5.78 (s, 1H, CC*H*$_2$), 6.31 (d, 1H, *J* = 8.2 Hz, NH of Phe1), 6.35-6.43 (m, 1H, CON*H*CH_2), 6.86 (d, 1H, *J* = 7.6 Hz, NH of Phe2), 7.10-7.46 (m, 15H, Arom). ^{13}C NMR (100 MHz, $CDCl_3$) δ (ppm): 23.1 (Ac), 37.6 (*C*H_2 of Phe2), 37.9 (*C*H_2 of Phe1), 40.8 (NH*C*H_2C), 53.6 (*C*H of Phe2), 54.4 (*C*H of Phe1), 67.4 (O*C*H_2Ph), 77.2 (NHCH_2*C*), 122.7 (C*C*H_2),

127.0, 127.2, 128.5, 128.6, 128.7, 129.2, 129.3, 135.1, 135.8, 136.7 (Arom), 139.7 (*C*CH_2), 166.2, 170.3, 171.3, 171.8 (*C*O).

1-((4*S*,7*S*,11*S*)-11-((1*H*-Indol-3-yl)methyl)-4-benzyl-7-methyl-3,6,10,13-tetraoxo-1-phenyl-2-oxa-5,9,12-triazatetradecan-7-yl)pyridin-1-ium chloride [23] and benzyl (2-(((*S*)-2-acetamido-3-(1*H*-indol-3-yl)propanami-do)methyl)acryloyl)-L-phenylalaninate [23′]

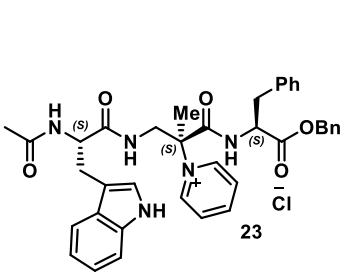

23

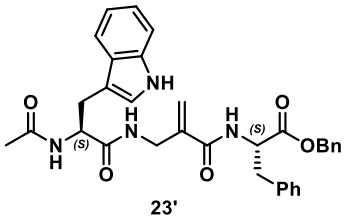

23'

Compound **13** (38 mg, 0.054 mmol) was dissolved in pyridine (1 mL) and stirred at 60 ºC for 12 hours. After concentration, the resulting crude was dissolved in a mixture of CH_2Cl_2 and 2 M HCl aqueous solution (1:1, 1.4 mL) and allowed to react for 30 minutes at room temperature. After concentration, the crude was dissolved in a mixture of TFA and CH_2Cl_2 (1:2, 1.5 mL) and stirred for 30 minutes at room temperature. After concentration, the crude was dissolved in pyridine (1 mL) and acetic anhydride (0.5 mL). After reacting for 1 h at room temperature, extracting with acetate and water, concentrating the aqueous phase and purifying with a reverse phase cartridge Sep-pack C_{18}, compound **23** (10 mg, 33%) was afforded as a viscous colorless oil. The elimination product was found in the organic phase. Concentration and purification by column chromatography on silica gel (CH_2Cl_2/MeOH, 95:5) affording compound **23′** (3 mg, 10%) as a colorless viscous oil. Compound **23**: $[a]_D^{20}$= -18.8 (*c* 1.0 in CH_3OH). HRMS (ESI) m/z = 646.3031, calculated for $C_{38}H_{40}N_5O_5^+$ (M^+) = 646.3024. ^{1}H NMR (400 MHz, CD_3OD) δ (ppm):

1.67 (s, 3H, C*H*$_3$), 1.93 (s, 3H, Ac), 2.89-3.00 (m, 2H, C*H*$_2$ of Phe and C*H*$_2$ of Trp), 3.02-3.11 (m, 1H, C*H*$_2$ of Phe), 3.27-3.31 (m, 1H, C*H*$_2$ of Trp), 3.67 (d, 1H, *J* = 14.9 Hz, NHC*H*$_2$C), 3.86 (d, 1H, *J* = 14.9 Hz, NHC*H*$_2$C), 4.33 (t, 1H, *J* = 7.6 Hz, C*H* of Phe), 4.76 (dd, 1H, *J* = 11.1 Hz, *J* = 5.0 Hz, C*H* of Trp), 5.21 (s, 2H, OC*H*$_2$Ph), 6.99-8.68 (m, 20H, Arom). ^{13}C NMR (100 MHz, CD_3OD) δ (ppm): 19.6 (*C*H_3), 21.0 (Ac), 26.9 (*C*H_2 of Phe), 35.7 (*C*H_2 of Trp), 45.7 (NH*C*H_2C), 54.3 (*C*H of Trp), 54.8 (*C*H of Phe), 67.1 (O*C*H_2Ph), 76.4 (NHCH_2*C*), 109.3, 111.0, 118.0, 118.6, 121.2, 123.4, 126.7, 127.2, 127.5, 128.2, 128.3, 128.4, 128.6, 135.6, 136.6, 136.9, 143.2, 146.2 (Arom), 168.7, 170.7, 171.9, 174.0 (*C*O). Compound ***23'***: $[\alpha]_D^{20}$= -9.0 (*c* 0.75 in $CHCl_3$). HRMS (ESI) m/z = 567.2599, calculated for $C_{33}H_{35}N_4O_5^+$ (H^+) = 567.2602. ^{1}H NMR (400 MHz, $CDCl_3$) δ (ppm): 1.99 (s, 3H, Ac), 3.01-3.25 (m, 3H, C*H*$_2$ of Phe and C*H*$_2$ of Trp), 3.27-3.39 (m, 1H, C*H*$_2$ of Trp), 3.88 (dd, 1H, *J* = 15.2 Hz, *J* = 6.4 Hz, NHC*H*$_2$C), 4.11 (d, 1H, *J* = 15.2 Hz, *J* = 6.4 Hz, NHC*H*$_2$C), 4.74-4.82 (m, 1H, C*H* of Phe), 4.83-4.93 (m, 1H, C*H* of Trp), 5.10-5.25 (m, 2H, OC*H*$_2$Ph), 5.38 (s, 1H, CC*H*$_2$), 5.73 (s, 1H, CC*H*$_2$),), 6.28 (t, *J* = 6.4 Hz, 1H, N*H*CH_2), 6.39 (d, 1H, *J* = 7.9 Hz, N*H*CH of Phe), 6.83 (d, 1H, *J* = 7.7 Hz, N*H*CH of Trp), 6.99-7.75 (m, 15H, Arom), 8.12 (s, 1H, N*H* of Trp). ^{13}C NMR (100 MHz, $CDCl_3$) δ (ppm): 23.3 (Ac), 27.8 (*C*H_2 of Phe), 37.6 (*C*H_2 of Trp), 40.8 (NH*C*H_2C), 53.6 (*C*H of Trp), 53.9 (*C*H of Phe), 67.3 (O*C*H_2Ph), 77.2 (NHCH_2*C*), 122.7 (C*C*H_2), 110.7, 111.2, 118.9, 119.8, 122.3, 123.2, 127.2, 127.6, 128.4, 128.5, 128.6, 128.7, 129.2, 135.1, 135.9, 136.2, 139.7 (Arom), 139.7 (*C*CH_2), 166.2, 170.3, 171.7 (*C*O).

J-Phe-Phe-Asp-NH_2 [24]

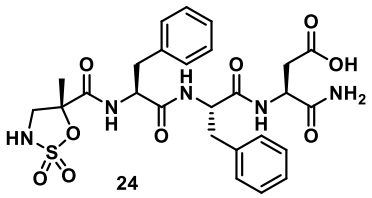

Coupling of α-methylisoserine sulfamidate to peptides by solid phase peptide synthesis (SPPS) is described in *section 10.5*. Natural amino acids were coupling using the standard protocol. Peptide **24** was afforded after cleavage and purification by HPLC (72 % global yield).

Semi-preparative HPLC gradient (t_R 30.33 min):

Time (min)	Flow(mL/min)	Acetonitrile (%)	H_2O + 0.1% TFA (%)
0	10	2	98
10	10	20	80
20	10	40	60
30	10	60	40
40	10	80	20
45	10	2	98

HRMS (ESI) m/z = 612.1740, calculated for $C_{26}H_{31}N_5O_9SNa$ (MNa^+) = 612.1735. ^{1}H NMR (300 MHz, CD_3OD) δ (ppm): 1.38 (s, 3H, C*H*$_3$), 2.72 (dd, 1H, *J* = 16.9 Hz, *J* = 6.7 Hz, C*H*$_2$ of Asp), 2.79-2.92 (m, 2H, C*H*$_2$ of Asp, C*H*$_2$ of Phe1), 3.01 (dd, 1H, *J* = 13.8 Hz, *J* = 8.3 Hz, C*H*$_2$ of Phe2), 3.10-3.24 (m, 2H, C*H*$_2$ of Phe1, C*H*$_2$ of Phe2), 3.38 (d, 1H, *J* = 12.6 Hz, C*H*$_2$ of Sulfamidate), 3.86 (d, 1H, *J* = 12.6 Hz, C*H*$_2$ of Sulfamidate), 4.57-4.63 (m, 1H, C*H*α of Phe2), 4.63-4.72 (m, 2H, C*H*α of Asp, C*H*α of Phe1), 7.12-7.39 (m, 10H, Arom). ^{1}H NMR (400 MHz, H_2O/D_2O 9:1, pH = 5.7, amide region) δ (ppm): 8.0 (d, 1H, *J* = 7.3 Hz, NH of Phe2), 8.18 (d, 1H, *J* = 7.5 Hz, NH of

Asp), 8.42 (d, 1H, *J* = 8.0 Hz, NH of Phe1). ^{13}C NMR (75 MHz, CD_3OD) δ (ppm): 21.9 (*C*H_3), 35.1 (*C*H_2 of Asp), 37.0 (*C*H_2 of Phe2), 37.1 (*C*H_2 of Phe1), 49.6 (*C*Hα of Asp), 51.4 (*C*H_2 of Sulfamidate), 54.5 (*C*Hα of Phe1), 55.1 (*C*Hα of Phe2), 89.3 (NHCH$_2$*C*), 126.5, 126.6, 128.1, 128.3, 129.0, 136.6, 136.7 (Arom), 170.8, 171.8, 172.6, 173.6 (*C*O).

Ring-opening peptide [25]

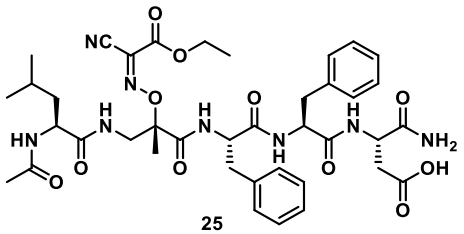

25

Coupling of α-methylisoserine sulfamidate to peptides by solid phase peptide synthesis (SPPS) is described in *section 10.5*. Natural amino acids were coupling using the standard protocol. Peptide **25** was afforded after cleavage and purification by HPLC (21 % global yield).

Semi-preparative HPLC gradient (t_R 30.08 min):

Time (min)	Flow(mL/min)	Acetonitrile (%)	H_2O + 0.1% TFA (%)
0	10	2	98
10	10	20	80
20	10	40	60
30	10	60	40
40	10	80	20
50	10	100	0
60	10	2	98

HRMS (ESI) m/z = 829.3494, calculated for $C_{39}H_{50}N_8O_{11}Na$ (MNa^+) = 829.3491. ^{1}H NMR (400 MHz, CD_3OD) δ (ppm): 0.83-1.01 (m, 6H, 2 *CH*$_3$

of Leu), 1.34-1.40 (m, 3H, *CH₃* of oxyme), 1.48 (s, 3H, C*H*₃), 1.54-1.63 (m, 3H, C*H*γ and C*H₂*β of Leu), 1.97 (s, 3H, Ac), 2.65-2.88 (m, 2H, C*H₂* of Asp), 2.94-3.19 (m, 4H, C*H₂* of Phe2, C*H₂* of Phe1), 3.58 (d, 1H, *J* = 14.7 Hz, NHC*H₂*C), 3.72 (d, 1H, *J* = 14.7 Hz, NHC*H₂*C), 4.30-4.44 (m, 3H, C*H₂* of oxyme, C*H*α of Leu), 4.51-4.61 (m, 2H, C*H*α of Phe2, C*H*α of Phe1), 4.62-4.71 (C*H*α of Asp), 7.17-7.31 (m, 10H, Arom). ^{13}C NMR (100 MHz, CD_3OD) δ (ppm): 11.4 (*C*H₃ of oxyme), 17.7 (*C*H₃), 19.2 (*C*H₃ of Leu), 19.5 (Ac), 20.4 (*C*H₃ of Leu), 23.1 (*C*Hγ of Leu), 33.6 (*C*H₂ of Asp), 35.3 (*C*H₂ of Phe2), 35.5 (*C*H₂ of Phe1), 39.0 (*C*H₂β of Leu), 41.4 (NH*C*H₂C), 48.1 (*C*Hα of Asp), 50.5 (*C*Hα of Leu), 53.5 (*C*Hα of Phe1), 53.6 (*C*Hα of Phe2), 61.6 (*C*H₂ of oxyme), 86.9 (NHCH₂*C*), 87.9 (*C*CN), 106.0, 125.0, 125.1, 125.7, 126.7, 126.8, 127.5, 135.2 (Arom), 156.0, 169.5, 170.1, 170.4, 170.5, 171.1, 172.2, 172.5 (*C*O).

Ring-opening peptide [26]

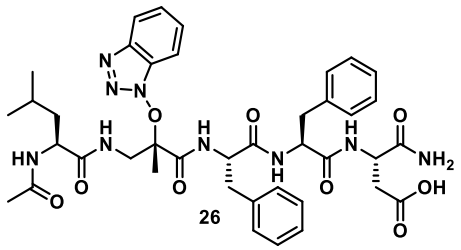

26

Coupling of α-methylisoserine sulfamidate to peptides by solid phase peptide synthesis (SPPS) is described in *section 10.5*. Natural amino acids were coupling using the standard protocol. Peptide **26** was afforded after cleavage and purification by HPLC (5 % global yield).

Semi-preparative HPLC gradient (t_R 31.39 min):

Time (min)	Flow(mL/min)	Acetonitrile (%)	H_2O + 0.1% TFA (%)
0	10	2	98
10	10	20	80
20	10	40	60
30	10	60	40
40	10	80	20
50	10	100	0
60	10	2	98

HRMS (ESI) m/z = 822.3552, calculated for $C_{40}H_{49}N_9O_9Na$ (MNa^+) = 822.3545. ^{1}H NMR (400 MHz, CD_3OD) δ (ppm): 0.93-1.07 (m, 6H, 2 *CH₃* of Leu), 1.19 (s, 3H, C*H₃*), 1.56-1.77 (m, 3H, C*H*γ and C*H₂*β of Leu), 2.04 (s, 3H, Ac), 2.70 (dd, 2H, *J* = 16.9 Hz, *J* = 7.1 Hz, C*H₂* of Asp), 2.80-2.85 (m, 2H, C*H₂* of Asp), 2.99 (dd, 1H, *J* = 14.0 Hz, *J*= 9.6 Hz, C*H₂* of Phe2), 3.18 (dd, 1H, *J* = 14.0 Hz, *J* = 5.9 Hz, C*H₂* of Phe2), 3.34-3.39 (m, 2H, C*H₂* of Phe1), 3.50 (d, 1H, *J* = 14.5 Hz, NHC*H₂*C), 3.68 (d, 1H, *J* = 14.5 Hz, NHC*H₂*C), 4.51 (dd, 1H, *J* = 9.1 Hz, *J* = 5.9 Hz, C*H*α of Leu), 4.61-4.73 (m, 3H, C*H*α of Phe2, C*H*α of Asp, C*H*α of Phe1), 7.12-7.37 (m, 10H, Arom of Ph), 7.48-7.55 (m, 1H, Arom of OBt), 7.61-7.68 (m, 1H, Arom of OBt), 7.74 (d, 1H, *J* = 8.4 Hz, Arom of OBt), 8.05 (d, 1H, *J* = 8.5 Hz, Arom of OBt).
^{13}C NMR (100 MHz, CD_3OD) δ (ppm): 15.7 (*C*H_3), 20.6 (*C*H_3 of Leu), 21.1 (Ac), 22.1 (*C*H_3 of Leu), 24.6 (*C*Hγ of Leu), 35.1 (*C*H_2 of Asp), 36.5 (*C*H_2 of Phe1), 36.8 (*C*H_2 of Phe2), 40.7 (*C*H_2β of Leu), 44.3 (NH*C*H_2C), 49.7 (*C*Hα of Asp), 52.0 (*C*Hα of Leu), 55.6 (*C*Hα of Phe1, *C*Hα of Phe2), 93.1 (NHCH_2*C*), 109.5, 119.6, 125.2, 126.5, 128.1, 128.2, 128.9, 129.0, 129.2, 136.8, 137.2 (Arom), 170.8, 171.8, 172.1, 172.5, 172.5, 173.8, 174.2 (*C*O).

FmocLeu-J-Phe-Phe-Asp-NH_2 [27]

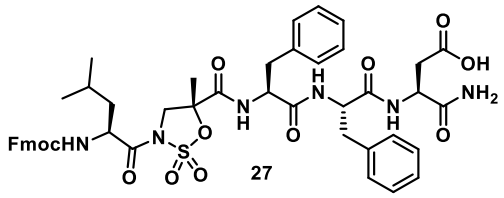

Coupling of α-methylisoserine sulfamidate to peptides by solid phase peptide synthesis (SPPS) is described in *section 10.5*. Natural amino acids were coupling using the standard protocol. Peptide **27** was afforded after cleavage and purification by HPLC (61 % global yield).

Semi-preparative HPLC gradient (t_R 44.58 min):

Time (min)	Flow(mL/min)	Acetonitrile (%)	H_2O + 0.1% TFA (%)
0	10	2	98
10	10	20	80
20	10	40	60
30	10	60	40
40	10	80	20
50	10	100	0
60	10	2	98

HRMS (ESI) m/z = 947.3263, calculated for $C_{47}H_{52}N_6O_{12}SNa$ (MNa^+) = 947.3256. ^1H NMR (300 MHz, CD_3OD) δ (ppm): 0.94 (s, 3H, *CH₃* of Leu), 0.96 (s, 3H, *CH₃* of Leu), 1.43 (s, 3H, C*H₃*), 1.58-1.79 (m, 3H, C*H*γ and C*H₂*β of Leu), 2.66-3.29 (m, 6H, C*H₂* of Asp, C*H₂* of Phe1, C*H₂* of Phe2), 4.03 (d, 1H, *J* = 10.8 Hz, C*H₂* of Sulfamidate), 4.17-4.27 (m, 1H, C*H* of Fmoc), 4.28-4.48 (m, 2H, C*H₂* of Fmoc), 4.55-4.74 (m, 4H, C*H₂* of Sulfamidate, C*H*α of Phe2, C*H*α of Asp, C*H*α of Leu), 4.75-4.84 (m, 1H, C*H*α of Phe1), 7.12-7.43 (m, 14H, Arom of Fmoc and Ph), 7.60-7.72 (m, 2H, Arom of Fmoc), 7.75-

7.86 (m, 2H, Arom of Fmoc). ^{13}C NMR (75 MHz, CD_3OD) δ (ppm): 20.1 (*C*H$_3$ of Leu), 22.1 (*C*H$_3$), 22.3 (*C*H$_3$ of Leu), 24.5 (*C*Hγ of Leu), 35.1 (*C*H$_2$ of Asp), 36.8 (*C*H$_2$ of Phe1), 37.1 (*C*H$_2$ of Phe2), 39.5 (*C*H$_2$β of Leu), 47.0 (*C*Hα of Fmoc), 49.5 (*C*Hα of Asp), 52.0 (*C*H$_2$ of Sulfamidate), 52.3 (*C*Hα of Leu), 54.4 (*C*Hα of Phe1), 55.2 (*C*Hα of Phe2), 66.8 (*C*H$_2$ of Fmoc), 85.8 (NHCH$_2$*C*), 119.5, 124.9, 125.0, 126.4, 126.6, 126.8, 127.4, 128.0, 128.3, 129.0, 136.6, 136.9, 141.2, 143.7, 144.0 (Arom), 157.1(*C*O of Fmoc), 168.4, 170.2, 171.5, 171.6, 172.6, 173.6 (*C*O).

Ac-Leu-J-Phe-Phe-Asp-NH$_2$ [28]

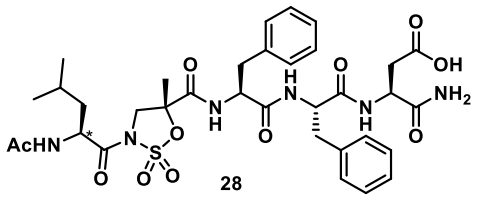

28

Coupling of α-methylisoserine sulfamidate to peptides by solid phase peptide synthesis (SPPS) is described in *section 10.5*. Natural amino acids were coupling using the standard protocol. Ac-Leu-OH was coupled using DIC/DIPEA at room temperature for 16 h. Peptide **30** was afforded after cleavage and purification by HPLC (`43 % global yield).

Semi-preparative HPLC gradient (t_{R1} 60.22 min and t_{R2} 62.13 min):

Time (min)	Flow(mL/min)	Acetonitrile (%)	H_2O + 0.1% TFA (%)
0	10	25	75
15	10	25	75
65	10	45	55
75	10	25	75

t_{R1}: MS (ESI) m/z = 767.2784, calculated for $C_{26}H_{31}N_5O_9SNa$ (MNa^+) = 767.2681. ^{1}H NMR (400 MHz, CD_3OD) δ (ppm): 0.89-0.97 (m, 6H, 2 *CH₃* of Leu), 1.41 (s, 3H, CC*H₃*), 1.55-1.72 (m, 3H, C*H*γ and C*H₂*β of Leu), 1.92 (s, 3H, Ac), 2.67 (dd, 2H, *J* = 16.9 Hz, *J* = 6.5 Hz, C*H₂* of Asp), 2.74-2.91 (m, 2H, C*H₂* of Asp, C*H₂* of Phe1), 2.99 (dd, 1H, *J* = 13.8 Hz, *J* = 7.8 Hz, C*H₂* of Phe2), 3.10 (dd, 1H, *J* = 13.8 Hz, *J* = 6.9 Hz, C*H₂* of Phe2), 3.22 (dd, 1H, *J* = 14.0 Hz, *J* = 5.0 Hz, C*H₂* of Phe1), 4.08 (d, 1H, *J* = 10.4 Hz, C*H₂* of Sulfamidate), 4.49-4.58 (m, 2H, C*H₂* of Sulfamidate, C*H* of Phe2), 4.62 (t, 1H, *J* = 6.3 Hz, C*H* of Asp), 4.65-4.71 (m, 1H, C*H*α of Leu), 4.75 (dd, 1H, *J* = 10.4 Hz, *J* = 4.9 Hz, C*H* of Phe1), 7.11-7.32 (m, 10H, Ar). ^{13}C NMR (100 MHz, CD_3OD) δ (ppm): 20.1 (*C*H_3 of Leu), 20.6 (Ac), 21.9 (C*C*H_3), 22.2 (*C*H_3 of Leu), 24.6 (*C*Hγ of Leu), 35.0 (*C*H_2 of Asp), 36.8 (*C*H_2 of Phe2), 36.9 (*C*H_2 of Phe1), 39.2 (*C*H_2β of Leu), 49.5 (*C*H of Asp), 50.8 (*C*Hα of Leu), 52.0 (*C*H_2 of Sulfamidate), 54.3 (*C*H of Phe1), 55.3 (*C*H of Phe2), 85.4 (*C*CH_3), 126.4, 126.6, 128.0, 128.3, 129.0, 136.7, 136.9 (C_{Ar}), 168.4, 168.7, 170.0, 171.5, 172.1, 172.7, 173.7 (CO). t_{R2}: MS (ESI) m/z = 767.2747, calculated for $C_{26}H_{31}N_5O_9SNa$ (MNa^+) = 767.2681. ^{1}H NMR (400 MHz, CD_3OD) δ (ppm): 0.89-0.96 (m, 6H, 2 *CH₃* of Leu), 1.40 (s, 3H, CC*H₃*), 1.55-1.70 (m, 3H, C*H*γ and C*H₂*β of Leu), 1.94 (s, 3H, Ac), 2.65 (dd, 2H, *J* = 16.9 Hz, *J* = 6.6 Hz, C*H₂* of Asp), 2.75-2.89 (m, 2H, C*H₂* of Asp, C*H₂* of Phe1), 2.96 (dd, 1H, *J* = 13.8 Hz, *J* = 8.0 Hz, C*H₂* of Phe2), 3.09 (dd, 1H, *J* = 13.9 Hz, *J* = 6.9 Hz, C*H₂* of Phe2), 3.21 (dd, 1H, *J* = 14.1 Hz, *J* = 4.8 Hz, C*H₂* of Phe1), 3.97 (d, 1H, *J* = 10.8 Hz, C*H₂* of Sulfamidate), 4.54 (dd, 1H, *J* = 8.0 Hz, *J* = 6.9 Hz, C*H* of Phe2), 4.57-4.63 (m, 2H, C*H₂* of Sulfamidate, C*H* of Asp), 4.73 (dd, 1H, *J* = 10.5 Hz, *J* = 4.7 Hz, C*H* of Phe1), 4.77-4.80 (m, 1H, C*H*α of Leu), 7.10-7.34 (m, 10H, Ar). ^{13}C NMR (100 MHz, CD_3OD) δ (ppm): 20.2 (*C*H_3 of Leu), 20.9 (Ac), 21.9 (C*C*H_3), 22.3 (*C*H_3 of Leu), 24.5 (*C*Hγ of

Leu), 35.1 (*C*H$_2$ of Asp), 36.7 (*C*H$_2$ of Phe1), 37.0 (*C*H$_2$ of Phe2), 39.4 (*C*H$_2$β of Leu), 49.6 (*C*H of Asp), 50.6 (*C*Hα of Leu), 52.0 (*C*H$_2$ of Sulfamidate), 54.5 (*C*H of Phe1), 55.2 (*C*H of Phe2), 86.0 (*C*CH$_3$), 126.4, 126.6, 128.0, 128.3, 128.9, 129.0, 136.6, 136.9 (*C*$_{Ar}$), 168.4, 169.6, 171.6, 171.6, 172.1, 172.7, 173.6 (CO).

Ac-Pro-Phe-Phe-Asp-NH$_2$ [30]

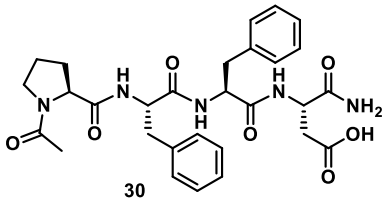

30

Natural amino acids were coupling using the standard protocol. Peptide **29** was afforded after cleavage and purification by HPLC (71 % global yield).

Semi-preparative HPLC gradient (t_R 26.42 min):

Time (min)	Flow(mL/min)	Acetonitrile (%)	H$_2$O + 0.1% TFA (%)
0	10	2	98
10	10	20	80
20	10	40	60
30	10	60	40
40	10	80	20
45	10	2	98

HRMS (ESI) m/z = 588.2412, calculated for $C_{29}H_{35}N_5O_7Na$ (MNa^+) = 588.2429. ^{1}H NMR (300 MHz, DMSO) δ (ppm): 1.39 and 1.97 (s, 3H, Ac), 1.52-1.70 (m, 2H, C*H$_2$*β of Pro, C*H$_2$*δ of Pro), 1.78-2.12 (m, 2 H, C*H$_2$*β of Pro, C*H$_2$*δ of Pro), 2.60-3.31 (m, 8 H, C*H$_2$* of Asp, C*H$_2$* of 2Phe, C*H$_2$*γ of Pro), 4.10-4.25 (m, 1H, C*Hα* of Pro), 4.35-4.69 (m, 3H, C*Hα* of Asp, C*Hα*

of 2Phe), 7.09-7.30 (m, 10H, Arom) 7.79-8.32 (m, 3H, NH). ^{13}C NMR (75 MHz, DMSO) δ (ppm): 22.2, 22.8 (Ac), 22.7, 24.5 (*C*H$_2$γ of Pro) 29.3, 32.0 (*C*H$_2$β of Pro), 36.5 (*C*H$_2$ of Asp), 37.2, 37.5, 37.9 (*C*H$_2$ of 2Phe), 46.6, 48.0 (*C*H$_2$δ of Pro), 49.8, 49.9 (*C*Hα of Asp), 53.9, 54.4, 54.5, 54.8 (*C*Hα of 2Phe), 59.9, 60.6 (*C*Hα of Pro), 126.6, 126.8, 128.4, 128.5, 128.6, 129.6, 129.7, 137.9, 138.1, 138.2, 138.3 (Arom), 169.2, 169.9, 171.2, 171.5, 171.7, 171.8, 172.2, 172.3, 172.7 (*C*O).

Signal splitting is due to proline cis-trans isomerization, which is more acute in solvents such as DMSO.[14]

Ac-J-Phe-Phe-Asp-NH$_2$ [31]

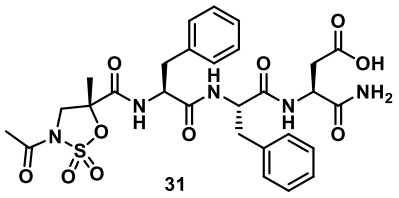

31

Coupling of α-methylisoserine sulfamidate to peptides by solid phase peptide synthesis (SPPS) is described in *section 10.5*. Natural amino acids were coupling using the standard protocol. Peptide **31** was afforded after cleavage and purification by HPLC (51 % global yield).

Semi-preparative HPLC gradient (t_R 30.68 min):

Time (min)	Flow(mL/min)	Acetonitrile (%)	H$_2$O + 0.1% TFA (%)
0	10	2	98
10	10	20	80
20	10	40	60
30	10	60	40
40	10	80	20
45	10	2	98

HRMS (ESI) m/z = 654.1838, calculated for $C_{28}H_{33}N_5O_{10}SNa$ (MNa^+) = 654.1840. ^1H NMR (300 MHz, CD_3OD) δ (ppm): 1.44 (s, 3H, C*H*$_3$), 2.34 (s, 3H, Ac), 2.70 (dd, 1H, *J* = 16.9 Hz, *J* = 6.6 Hz, C*H*$_2$ of Asp), 2.77-2.93 (m, 2H, C*H*$_2$ of Asp, C*H*$_2$ of Phe1), 2.99 (dd, 1H, *J* = 13.9 Hz, *J* = 8.3 Hz, C*H*$_2$ of Phe2), 3.09-3.26 (m, 2H, C*H*$_2$ of Phe1, C*H*$_2$ of Phe2), 3.95 (d, 1H, *J* = 10.7 Hz, C*H*$_2$ of Sulfamidate), 4.53 (d, 1H, *J* = 10.7 Hz, C*H*$_2$ of Sulfamidate), 4.58 (dd, 1H, *J* = 8.2 Hz, *J* = 6.7 Hz, C*H*α of Phe2), 4.64 (t, 1H, *J* = 6.3 Hz, C*H*α of Asp), 4.75 (dd, 1H, *J* = 10.4 Hz, *J* = 4.8 Hz, C*H*α of Phe1), 7.13-7.35 (m, 10H, Arom). ^1H NMR (400 MHz, H_2O/D_2O 9:1, pH = 5.7, amide region) δ (ppm): 7.91 (d, 1H, *J* = 7.5 Hz, NH of Phe2), 8.20 (d, 1H, *J* = 7.7 Hz, NH of Asp), 8.75 (d, 1H, *J* = 8.3 Hz, NH of Phe1). ^{13}C NMR (75 MHz, CD_3OD) δ (ppm): 19.6 (Ac), 20.6 (*C*H$_3$), 33.5 (*C*H$_2$ of Asp), 35.3 (*C*H$_2$ of Phe2), 35.4 (*C*H$_2$ of Phe1), 48.0 (*C*Hα of Asp), 50.6 (*C*H$_2$ of Sulfamidate), 53.1 (*C*Hα of Phe1), 53.6 (*C*Hα of Phe2), 84.1 (NHCH$_2$*C*), 124.9, 125.1, 126.5, 126.6, 126.7, 126.8, 127.5, 135.2, 135.3 (Arom), 167.0, 170.0, 171.1, 172.2 (*C*O).

Ac-Pro-Phe-Phe-Ala-Glu-NH$_2$ [32]

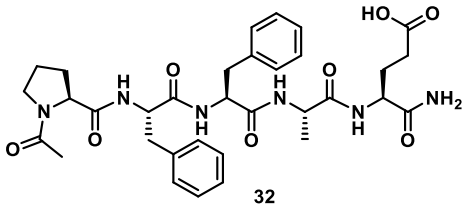

32

Natural amino acids were coupling using the standard protocol. Peptide **32** was afforded after cleavage and purification by HPLC (65 % global yield).

Semi-preparative HPLC gradient (t_R 26.53 min):

Time (min)	Flow(mL/min)	Acetonitrile (%)	H_2O + 0.1% TFA (%)
0	10	2	98
10	10	20	80
20	10	40	60
30	10	60	40
40	10	80	20
45	10	2	98

HRMS (ESI) m/z = 673.2957, calculated for $C_{33}H_{42}N_6O_8Na$ (MNa^+) = 673.2956. ^{1}H NMR (300 MHz, DMSO) δ (ppm): 1.24 (d, 3H, *J* = 7.0 Hz, C*H*$_3$ of Ala), 1.40 and 1.97 (s, 3H, Ac), 1.48-2.08 (m, 6H, C*H*$_2$β of Glu, C*H*$_2$β of Pro, C*H*$_2$δ of Pro), 2.16-2.32 (m, 2H, C*H*$_2$β of Glu), 2.65-2.92 (m, 2H, C*H*$_2$ of Phe), 2.93-3.14 (m, 2H, C*H*$_2$ of Phe), 3.18-3.35 (m, 2H, C*H*$_2$γ of Pro), 4.08-4.35 (m, 3H, C*H*α of Ala, C*H*α of Pro, C*H*α of Glu), 4.36-4.65 (m, 2H, C*H*α of 2Phe), 7.05-7.34 (m, 10H, Arom), 7.69-8.33 (m, 4H, NH). ^{13}C NMR (75 MHz, DMSO) δ (ppm): 18.2, 18.4 (*C*H$_3$ of Ala), 22.2, 22.8 (Ac), 22.7, 24.5 (*C*H$_2$γ of Pro), 27.8, 27.9 (*C*H$_2$β of Glu), 30.5 (*C*H$_2$γ of Glu), 29.3, 32.0 (*C*H$_2$β of Pro), 37.2, 37.5, 37.8, 37.9 (*C*H$_2$ of 2Phe), 46.6, 48.0 (*C*H$_2$δ of Pro), 48.8, 49.0 (*C*Hα of Ala), 52.1 (*C*Hα of Glu), 53.9, 554.2, 54.3, 54.5 (*C*Hα of 2Phe), 59.9, 60.6 (*C*H$_2$α of Pro), 126.6, 126.7, 128.4, 128.5, 128.6, 129.6, 129.7, 138.1, 138.2, 138.3 (Arom), 169.2, 169.9 171.3, 171.4, 171.6, 171.8, 172.1, 172.3, 173.4, 173.5, 174.4 (*C*O). Signal splitting is due to proline cis-trans isomerization, which is more acute in solvents such as DMSO.[14]

Ac-J-Phe-Phe-Ala-Glu-NH_2 [33]

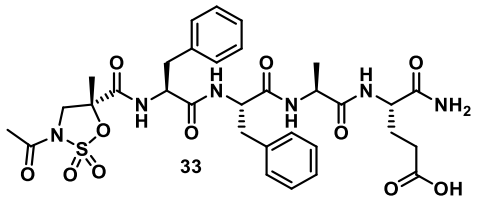

Coupling of α-methylisoserine sulfamidate to peptides by solid phase peptide synthesis (SPPS) is described in *section 10.5*. Natural amino acids were coupling using the standard protocol. Peptide **33** was afforded after cleavage and purification by HPLC (49 % global yield).

Semi-preparative HPLC gradient (t_R 30.03 min):

Time (min)	Flow(mL/min)	Acetonitrile (%)	H_2O + 0.1% TFA (%)
0	10	2	98
10	10	20	80
20	10	40	60
30	10	60	40
40	10	80	20
45	10	2	98

HRMS (ESI) m/z = 739.2369, calculated for $C_{32}H_{40}N_6O_{11}SNa$ (MNa^+) = 739.2368. ^{1}H NMR (300 MHz, CD_3OD) δ (ppm): 1.37 (d, 3H, *J* = 7.2 Hz, C*H*$_3$ of Ala), 1.46 (s, 3H, C*H*$_3$), 1.91-2.07 (m, 1H, C*H*$_2$β of Glu), 2.09-2.24 (m, 1H, C*H*$_2$β of Glu), 2.35 (s, 3H, Ac), 2.39-2.49 (m, 2H, C*H*$_2$γ of Glu), 2.80-3.03 (m, 2H, C*H*$_2$ of Phe1, C*H*$_2$ of Phe2), 3.13-3.25 (m, 2H, C*H*$_2$ of Phe1, C*H*$_2$ of Phe2), 3.97 (d, 1H, *J* = 10.7 Hz, C*H*$_2$ of Sulfamidate), 4.29 (q, 1H, *J* = 7.1 Hz, C*H*α of Ala), 4.34-4.41 (m, 1H, C*H*α of Glu), 4.55 (d, 1H, *J* = 10.7 Hz, C*H*$_2$ of Sulfamidate), 4.58-4.65 (m, 1H, C*H*α of Phe2), 4.68-4.79 (m, 1H, C*H*α of Phe1), 7.13-7.37 (m, 10H, Arom). ^{1}H NMR (400 MHz, H_2O/D_2O

9:1, pH = 5.7, amide region) δ (ppm): 7.84 (d, 1H, *J* = 7.5 Hz, NH of Phe2), 8.07-8.15 (m, 2H, NH of Glu, NH of Ala), 8.74 (d, 1H, *J* = 8.2 Hz, NH of Phe1). ^{13}C NMR (75 MHz, CD_3OD) δ (ppm): 16.2 (*C*H_3 of Ala), 21.1 (Ac), 22.0 (*C*H_3), 26.9 (*C*H_2β of Glu), 29.9 (*C*H_2γ of Glu), 36.7 (*C*H_2 of Phe2), 36.9 (*C*H_2 of Phe1), 49.5 (*C*Hα of Ala), 52.1 (*C*H_2 of Sulfamidate), 52.5 (*C*Hα of Glu), 54.8 (*C*Hα of Phe1), 55.0 (*C*Hα of Phe2), 85.6 (NHCH_2*C*), 126.4, 126.5, 128.0, 128.2, 128.9, 129.0, 136.8, 166.9, 168.6 (Arom), 171.6, 171.9, 173.3, 174.8, 175.1 (*C*O).

J-Phe-Phe-Ala-Glu-NH_2 [34]

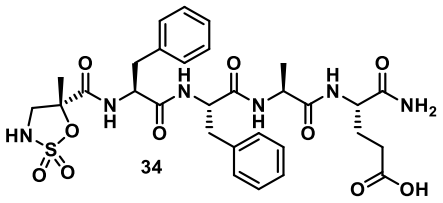

Coupling of α-methylisoserine sulfamidate to peptides by solid phase peptide synthesis (SPPS) is described in *section 10.5*. Natural amino acids were coupling using the standard protocol. Peptide **34** was afforded after cleavage and purification by HPLC (62 % global yield).

Semi-preparative HPLC gradient (t_R 29.57 min):

Time (min)	Flow(mL/min)	Acetonitrile (%)	H_2O + 0.1% TFA (%)
0	10	2	98
10	10	20	80
20	10	40	60
30	10	60	40
40	10	80	20
45	10	2	98

HRMS (ESI) m/z = 697.2259, calculated for $C_{30}H_{38}N_6O_{10}SNa$ (MNa^+) = 697.2262. ^1H NMR (300 MHz, CD_3OD) δ (ppm): 1.32-1.45 (m, 6H, C*H*$_3$ of Ala, C*H*$_3$), 1.90-2.07 (m, 1H, C*H*$_2$β of Glu), 2.08-2.23 (m, 1H, C*H*$_2$β of Glu), 2.39-2.48 (m, 2H, C*H*$_2$γ of Glu), 2.79-3.05 (m, 2H, C*H*$_2$ of Phe1, C*H*$_2$ of Phe2), 3.08-3.26 (m, 2H, C*H*$_2$ of Phe1, C*H*$_2$ of Phe2), 3.38 (d, 1H, *J* = 12.5 Hz, C*H*$_2$ of Sulfamidate), 3.87 (d, 1H, *J* = 12.5 Hz, C*H*$_2$ of Sulfamidate), 4.27-4.43 (m, 2H, C*H*α of Ala, C*H*α of Glu), 4.58-4.70 (m, 2H, C*H*α of Phe2, C*H*α of Phe1), 7.10-7.40 (m, 10H, Arom). ^1H NMR (400 MHz, H_2O/D_2O 9:1, pH = 5.7, amide region) δ (ppm): 7.93 (d, 1H, *J* = 7.5 Hz, NH of Phe2), 8.11 (d, 1H, *J* = 6.7 Hz, NH of Glu), 8.16 (d, 1H, *J* = 6.1 Hz, NH of Ala), 8.40 (d, 1H, *J* = 8.0 Hz, NH of Phe1). ^{13}C NMR (75 MHz, CD_3OD) δ (ppm): 16.3 (*C*H$_3$ of Ala), 21.8 (*C*H$_3$), 27.0 (*C*H$_2$β of Glu), 29.9 (*C*H$_2$γ of Glu), 37.0 (*C*H$_2$ of Phe2, *C*H$_2$ of Phe1), 49.4 (*C*Hα of Ala), 51.4 (*C*H$_2$ of Sulfamidate), 52.4 (*C*Hα of Glu), 54.8 (*C*Hα of Phe1), 54.9 (*C*Hα of Phe2), 89.3 (NHCH$_2$*C*), 126.5, 128.0, 128.1, 128.2, 128.3, 128.9, 129.0, 136.6, 136.9 (Arom), 170.9, 171.8, 172.2, 173.3, 174.8, 175.1 (*C*O).

J-Phe-Phe-NH$_2$

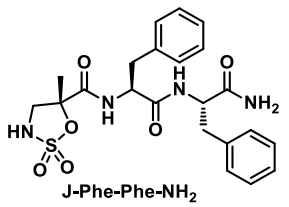

Coupling of α-methylisoserine sulfamidate to peptides by solid phase peptide synthesis (SPPS) is described in *section 10.5*. Natural amino acids were coupling using the standard protocol. No purification was needed. Scale 0.25 mmol of resin. HRMS (ESI) m/z = 475.1648, calculated for $C_{22}H_{26}N_4O_6S$

(MH^+) = 475.1646. ^{1}H NMR (300 MHz, CD_3OD) δ (ppm): 1.39 (s, 3H, C*H*$_3$), 2.77-3.01 (m, 2H, C*H*$_2$ of Phe1, C*H*$_2$ of Phe2), 3.10-3.20 (m, 2H, C*H*$_2$ of Phe1, C*H*$_2$ of Phe2), 3.38 (d, 1H, *J* = 12.5 Hz, C*H*$_2$ of Sulfamidate), 3.87 (d, 1H, *J* = 12.5 Hz, C*H*$_2$ of Sulfamidate), 4.57-4.69 (m, 1H, C*H*α of Phe1, C*H*α of Phe2), 7.12-7.34 (m, 10H, Arom). ^{13}C NMR (100 MHz, CD_3OD) δ (ppm): 21.8 (*C*H$_3$), 37.1 (*C*H$_2$ of Phe2), 37.5 (*C*H$_2$ of Phe1), 51.5 (*C*H$_2$ of Sulfamidate), 54.4 (*C*Hα of Phe1), 54.7 (*C*Hα of Phe2), 89.4 (NHCH$_2$*C*), 126.4, 126.5, 128.1, 129.0, 136.6, 137.0 (Arom), 170.8, 171.4, 174.4 (*C*O).

Ac-J-Ala-Pro-Asp-Thr-Arg-Pro-NH$_2$ [35]

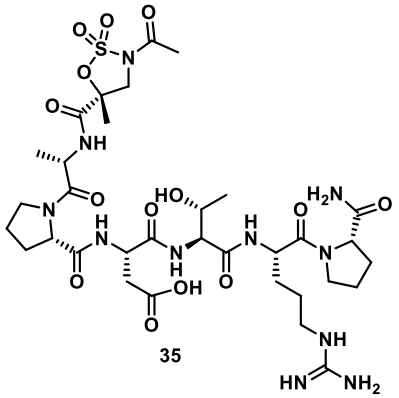

Coupling of α-methylisoserine sulfamidate to peptides by solid phase peptide synthesis (SPPS) is described in *section 10.5*. Natural amino acids were coupling using the standard protocol. Peptide **35** was afforded after cleavage and purification by HPLC (78 % global yield).

Semi-preparative HPLC gradient (t_R 26.92 min):

Time (min)	Flow(mL/min)	Acetonitrile (%)	H2O + 0.1% TFA (%)
0	10	1	99
1	10	1	99
31	10	31	69
32	10	1	99
37	10	1	99

HRMS (ESI) m/z = 860.3561, calculated for $C_{33}H_{54}N_{11}O_{14}S$ (MH^+) = 860.3567. ^{1}H NMR (300 MHz, D_2O) δ (ppm): 1.05 (d, 3H, *J* = 6.4 Hz, C*H*$_3$ of Thr), 1.27 (d, 3H, *J* = 7.0 Hz, C*H*$_3$ of Ala), 1.47-1.63 (m, 3H, C*H*$_2$γ of Arg, C*H*$_2$β of Arg), 1.65-1.93 (m, 10H, C*H*$_3$, C*H*$_2$β of Arg, C*H*$_2$β of Pro1, C*H*$_2$β of Pro2, C*H*$_2$γ of Pro1, C*H*$_2$γ of Pro2), 2.07-2.27 (m, 5H, Ac, C*H*$_2$β of Pro1, C*H*$_2$β of Pro2), 2.71-2.90 (m, 2H, C*H*$_2$ of Asp), 3.01-3.13 (m, 2H, C*H*$_2$δ of Arg), 3.43-3.72 (m, 4H, C*H*$_2$δ of Pro1, C*H*$_2$δ of Pro2), 4.02-4.14 (m, 2H, C*H*$_2$ of Sulfamidate, C*H*β of Thr), 4.16-4.31 (m, 3H, C*H*α of Pro1, C*H*α of Pro2, C*H*α of Thr), 4.47 (d, 1H, *J* = 10.5 Hz, C*H*$_2$ of Sulfamidate), 4.50-4.65 (m, 3H, C*H*α of Ala, C*H*α of Arg, C*H*α of Asp). ^{13}C NMR (75 MHz, D_2O) δ (ppm): 15.1 (*C*H$_3$ of Ala), 18.8 (*C*H$_3$ of Thr), 22.2 (Ac), 22.5 (*C*H$_3$), 23.9 (*C*H$_2$γ of Arg), 24.6 (*C*H$_2$γ of Pro1, *C*H$_2$γ of Pro2), 27.4 (*C*H$_2$β of Arg), 29.2 (*C*H$_2$β of Pro1), 29.5 (*C*H$_2$β of Pro2), 34.9 (*C*H$_2$ of Asp), 40.5 (*C*H$_2$δ of Arg), 47.7 (*C*H$_2$δ of Pro1), 47.8 (*C*H$_2$δ of Pro2), 48.3 (*C*Hα of Ala), 50.1 (*C*Hα of Asp), 51.1 (*C*Hα of Arg), 52.7 (*C*H$_2$ of Sulfamidate), 59.0 (*C*Hα of Thr), 60.2 (*C*Hα of Pro2), 60.7 (*C*Hα of Pro1), 66.9 (*C*Hβ of Thr), 90.1 (NHCH$_2$*C*), 156.6 (HN*C*), 169.2, 171.3, 172.2, 172.3, 172.4, 172.5, 173.9, 173.9, 176.7 (*C*O).

J-Ala-Pro-Asp-Thr-Arg-Pro-NH_2 [36]

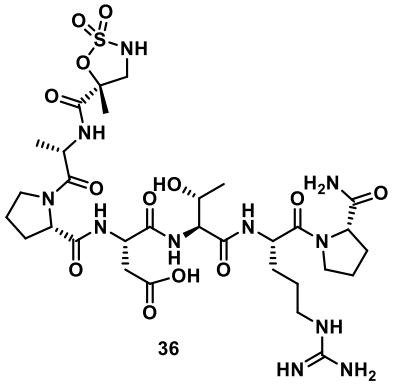

36

Coupling of α-methylisoserine sulfamidate to peptides by solid phase peptide synthesis (SPPS) is described in *section 10.5*. Natural amino acids were coupling using the standard protocol. Peptide **36** was afforded after cleavage and purification by HPLC (62 % global yield).

Semi-preparative HPLC gradient (t_R 25.33 min):

Time (min)	Flow(mL/min)	Acetonitrile (%)	H_2O + 0.1% TFA (%)
0	10	1	99
1	10	1	99
31	10	31	69
32	10	1	99
37	10	1	99

HRMS (ESI) m/z = 840.3290, calculated for $C_{31}H_{51}N_{11}O_{13}SNa$ (MNa^+) = 840.3281. ^1H NMR (300 MHz, D_2O) δ (ppm): 1.08 (d, 3H, *J* = 6.4 Hz, C*H*$_3$ of Thr), 1.31 (d, 3H, *J* = 7.1 Hz, C*H*$_3$ of Ala), 1.51-1.67 (m, 6H, C*H*$_3$, C*H*$_2$γ of Arg, C*H*$_2$β of Arg), 1.68-2.01 (m, 7H, C*H*$_2$β of Arg, C*H*$_2$β of Pro1, C*H*$_2$β of Pro2, C*H*$_2$γ of Pro1, C*H*$_2$γ of Pro2), 2.12-2.28 (m, 2H, C*H*$_2$β of Pro1, C*H*$_2$β of Pro2), 2.71-2.96 (m, 2H, C*H*$_2$ of Asp), 3.04-3.17 (m, 2H, C*H*$_2$δ of Arg), 3.45-3.62 (m, 3H, C*H*$_2$ of Sulfamidate, C*H*$_2$δ of Pro1, C*H*$_2$δ of Pro2), 3.63-

3.76 (m, 2H, C*H*$_2$δ of Pro1, C*H*$_2$δ of Pro2), 3.81 (d, 1H, *J* = 12.8 Hz, C*H*$_2$ of Sulfamidate), 4.05-4.14 (m, 1H, C*H*β of Thr), 4.19-4.35 (m, 3H, C*H*α of Pro1, C*H*α of Pro2, C*H*α of Thr), 4.48-4.66 (m, 3H, C*H*α of Ala, C*H*α of Arg, C*H*α of Asp). ^{13}C NMR (75 MHz, D_2O) δ (ppm): 15.1 (*C*H$_3$ of Ala), 18.8 (*C*H$_3$ of Thr), 22.5 (*C*H$_3$), 24.0 (*C*H$_2$γ of Arg), 24.6 (*C*H$_2$γ of Pro1), 24.7 (*C*H$_2$γ of Pro2), 27.5 (*C*H$_2$β of Arg), 29.2 (*C*H$_2$β of Pro1), 29.5 (*C*H$_2$β of Pro2), 34.9 (*C*H$_2$ of Asp), 40.5 (*C*H$_2$δ of Arg), 47.7 (*C*H$_2$δ of Pro1), 47.9 (*C*H$_2$δ of Pro2), 48.3 (*C*Hα of Ala), 50.1 (*C*Hα of Asp), 51.1 (*C*Hα of Arg), 51.2 (*C*H$_2$ of Sulfamidate), 59.0 (*C*Hα of Thr), 60.2 (*C*Hα of Pro2), 60.7 (*C*Hα of Pro1), 67.1 (*C*Hβ of Thr), 90.2 (NHCH$_2$*C*), 156.7 (HN*C*), 171.3, 171.3, 171.4, 172.4, 172.6, 174.0, 176.8 (*C*O).

Ring-opening peptide with azide [37]

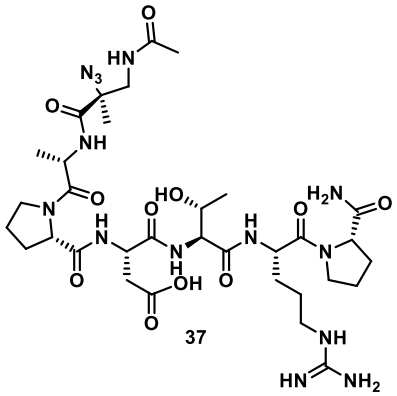

37

Coupling of α-methylisoserine sulfamidate to peptides by solid phase peptide synthesis (SPPS) is described in *section 10.5*. Natural amino acids were coupling using the standard protocol. The ring-opening reaction was carried out on solid phase, using 20 equivalents excess of NaN_3 in DMF at room temperature for 3 hours. Peptide **37** was afforded after cleavage and purification by HPLC (31 % global yield).

Semi-preparative HPLC gradient (t_R 23.39 min):

Time (min)	Flow(mL/min)	Acetonitrile (%)	H_2O + 0.1% TFA (%)
0	10	1	99
1	10	1	99
35	10	35	65
37	10	1	99

HRMS (ESI) m/z = 823.4161, calculated for $C_{33}H_{54}N_{14}O_{11}H$ (MH^+) = 823.4169. ^{1}H NMR (300 MHz, D_2O) δ (ppm): 1.11 (d, 3H, *J* = 6.4 Hz, C*H*$_3$ of Thr), 1.31 (d, 3H, *J* = 7.1 Hz, C*H*$_3$ of Ala), 1.44 (s, 3H, C*H*$_3$), 1.52-2.04 (m, 13H, C*H*$_2$γ of Arg, C*H*$_2$β of Arg, C*H*$_2$β of Pro1, C*H*$_2$β of Pro2, C*H*$_2$γ of Pro1, C*H*$_2$γ of Pro2, Ac), 2.14-2.32 (m, 2H, C*H*$_2$β of Pro1, C*H*$_2$β of Pro2), 2.75-2.98 (m, 2H, C*H*$_2$ of Asp), 3.14 (t, 2H, *J* = 6.8 Hz, C*H*$_2$δ of Arg), 3.40 (d, 1H, *J* = 14.2 Hz, NHC*H*$_2$C), 3.48-3.80 (m, 5H, C*H*$_2$δ of Pro1, C*H*$_2$δ of Pro2, NHC*H*$_2$C), 4.08-4.19 (m, 1H, C*H*β of Thr), 4.20-4.39 (m, 3H, C*H*α of Pro1, C*H*α of Pro2, C*H*α of Thr), 4.43-4.67 (m, 3H, C*H*α of Ala, C*H*α of Arg, C*H*α of Asp). ^{13}C NMR (75 MHz, D_2O) δ (ppm): 15.2 (*C*H$_3$ of Ala), 18.8 (*C*H$_3$ of Thr), 19.0 (*C*H$_3$), 21.8 (Ac), 24.0 (*C*H$_2$γ of Arg), 24.6 (*C*H$_2$γ of Pro1), 24.7 (*C*H$_2$γ of Pro2), 27.4 (*C*H$_2$β of Arg), 29.3 (*C*H$_2$β of Pro1), 29.6 (*C*H$_2$β of Pro2), 35.0 (*C*H$_2$ of Asp), 40.5 (*C*H$_2$δ of Arg), 45.4 (NHC*H*$_2$C), 47.8 (*C*H$_2$δ of Pro1), 47.9 (*C*H$_2$δ of Pro2), 48.2 (*C*Hα of Ala), 50.1 (*C*Hα of Asp), 51.1 (*C*Hα of Arg), 59.0 (*C*Hα of Thr), 60.3 (*C*Hα of Pro2), 60.6 (*C*Hα of Pro1), 67.0 (*C*Hβ of Thr), 118.2 (NHCH$_2$*C*), 156.7 (HN*C*), 171.3, 171.4, 172.4, 172.5, 173.0, 174.0, 174.4, 176.8 (*C*O).

Click peptide with ciclooctine [38 and 38']

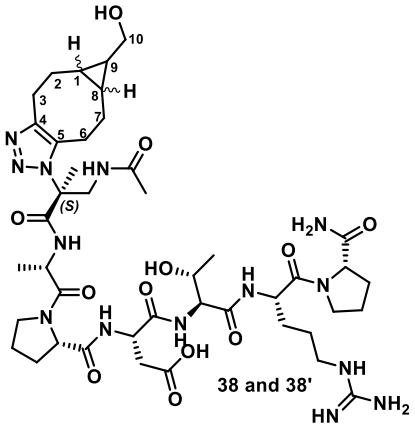

Peptide **37** (1 equivalent) and a bicyclo[6.1.0]non-4-yn-9-ylmethanol (cyclooctine) (2 equivalents) were dissolved in H_2O/CH_3CN (1:3) and allowed to react at 25 ºC for 2 hours. The reaction underwent with high yield (77 %), but two diasteoisomers, **38** and **38'**, were detected and separated by HPLC, due to the mixture of diastereoisomer of the commercially available cyclooctine. ^{13}C NMR could not obtain.

Semi-preparative HPLC gradient (t_{R1} 18.60 min, t_{R2} 20.00 min):

Time (min)	Flow(mL/min)	Acetonitrile (%)	H_2O + 0.1% TFA (%)
0	10	1	99
1	10	1	99
3	10	10	90
43	10	40	60
44	10	1	99
50	10	1	99

t_{R1}: HRMS (ESI) m/z = 973.5200, calculated for $C_{43}H_{68}N_{14}O_{12}$ (MH^+) = 973.5214. ^1H NMR (300 MHz, D_2O) δ (ppm): 1.02-1.13 (m, 5H, CH_3 of Thr, CH^1, CH^8), 1.16-1.31 (m, 4H, CH_3 of Ala, CH^9), 1.46-2.33 (m, 22H, C$H_2\gamma$ of

Arg, CH_2β of Arg, CH_3, CH_2β of Pro1, CH_2β of Pro2, CH_2γ of Pro1, CH_2γ of Pro2, Ac, CH_2^2, CH_2^7), 2.57-2.97 (m, 6H, CH_2 of Asp, CH_2^3, CH_2^6), 3.12 (t, 2H, J = 7.1 Hz, CH_2δ of Arg), 3.50-3.81 (m, 7H, CH_2δ of Pro1, CH_2δ of Pro2, , CH_2^{10}, NHCH_2C), 3.98 (d, 1H, J = 14.4 Hz, NHCH_2C), 4.05-4.13 (m, 1H, CHβ of Thr), 4.18-4.36 (m, 3H, CHα of Pro1, CHα of Pro2, CHα of Thr), 4.42-4.67 (m, 3H, CHα of Ala, CHα of Arg, CHα of Asp). t_{R2}: HRMS (ESI) m/z = 973.5211, calculated for $C_{43}H_{68}N_{14}O_{12}$ (MH^+) = 973.5214. ^{1}H NMR (300 MHz, D_2O) δ (ppm): 0.71-0.90 (CH^1, CH^8), 0.95-1.12 (m, 4H, CH_3 of Thr, CH^9), 1.22 (d, 3H, J = 7.1Hz, CH_3 of Ala), 1.43-2.29 (m, 22H, CH_2γ of Arg, CH_2β of Arg, CH_3, CH_2β of Pro1, CH_2β of Pro2, CH_2γ of Pro1, CH_2γ of Pro2, Ac, CH_2^2, CH_2^7), 2.51-2.96 (m, 6H, CH_2 of Asp, CH_2^3, CH_2^6), 3.12 (t, 2H, J = 6.8 Hz, CH_2δ of Arg), 3.48-3.83 (m, 7H, CH_2δ of Pro1, CH_2δ of Pro2, CH_2^{10}, NHCH_2C), 3.99 (d, 1H, J = 14.5 Hz, NHCH_2C), 4.05-4.14 (m, 1H, CHβ of Thr), 4.17-4.37 (m, 3H, CHα of Pro1, CHα of Pro2, CHα of Thr), 4.50-4.64 (m, 3H, CHα of Ala, CHα of Arg, CHα of Asp).

Ring-opening peptide with thiocumarine [39]

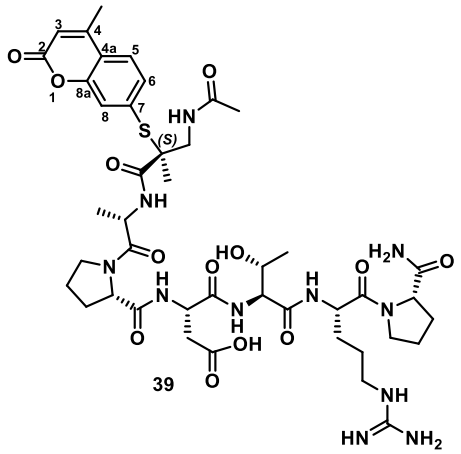

Coupling of α-methylisoserine sulfamidate to peptides by solid phase peptide synthesis (SPPS) is described in *section 10.5*. Natural amino acids were coupling using the standard protocol. The ring-opening reaction was carried out on solid phase, using 10 equivalents excess of 7-mercapto-4-methylcoumarin (Coum) in DMF and 9 equivalents excess of DIPEA in DMF at 25 ºC for 1.5 hours. Peptide **39** was afforded after cleavage and purification by HPLC (45 % global yield).

Semi-preparative HPLC gradient (t_R 16.47 min):

Time (min)	Flow(mL/min)	Acetonitrile (%)	H_2O + 0.1% TFA (%)
0	10	1	99
1	10	1	99
3	10	18	82
25	10	40	60
26	10	80	20
30	10	80	20
31	10	1	99
37	10	1	99

HRMS (ESI) m/z = 972.4240, calculated for $C_{43}H_{61}N_{11}O_{13}SH$ (MH^+) = 972.4244. ^{1}H NMR (300 MHz, D_2O) δ (ppm): 1.09 (d, 3H, *J* = 6.4 Hz, C*H*$_3$ of Thr), 1.27 (d, 3H, *J* = 7.0 Hz, C*H*$_3$ of Ala), 1.35 (s, 3H, C*H*$_3$), 1.45-2.04 (m, 13H, C*H*$_2$γ of Arg, C*H*$_2$β of Arg, C*H*$_2$β of Pro1, C*H*$_2$β of Pro2, C*H*$_2$γ of Pro1, C*H*$_2$γ of Pro2, Ac), 2.13-2.30 (m, 2H, C*H*$_2$β of Pro1, C*H*$_2$β of Pro2), 2.36 (s, 3H, C*H*$_3$ of Coum), 2.77-2.96 (m, 2H, C*H*$_2$ of Asp), 3.00-3.14 (m, 2H, C*H*$_2$δ of Arg), 3.46-3.75 (m, 6H, C*H*$_2$δ of Pro1, C*H*$_2$δ of Pro2, NHC*H*$_2$C), 4.05-4.17 (m, 1H, C*H*β of Thr), 4.21-4.67 (m, 6H, C*H*α of Pro1, C*H*α of Pro2, C*H*α of Thr, C*H*α of Ala, C*H*α of Arg, C*H*α of Asp), 6.30 (s, 1H, C*H*^{3}), 7.24-7.40 (m, 2H, C*H*^{6}, C*H*^{8}), 7.62 (d, 1H, *J* = 8.1 Hz, C*H*^{5}). ^{13}C NMR (75

MHz, D_2O) δ (ppm): 15.3 (*C*H_3 of Ala), 17.9 (*C*H_3 of Coum), 18.8 (*C*H_3 of Thr), 21.0 (*C*H_3), 21.8 (Ac), 24.0 (*C*H_2γ of Arg), 24.6 (*C*H_2γ of Pro1), 24.7 (*C*H_2γ of Pro2), 27.5 (*C*H_2β of Arg), 29.3 (*C*H_2β of Pro1), 29.6 (*C*H_2β of Pro2), 34.9 (*C*H_2 of Asp), 40.5 (*C*H_2δ of Arg), 45.5 (NHC*H*$_2$C), 47.8 (*C*H_2δ of Pro1), 47.9 (*C*H_2δ of Pro2), 48.3 (*C*Hα of Ala), 50.2 (*C*Hα of Asp), 51.0 (*C*Hα of Arg), 55.9 (NHCH_2*C*), 59.1 (*C*Hα of Thr), 60.2 (*C*Hα of Pro2), 60.6 (*C*Hα of Pro1), 67.1 (*C*Hβ of Thr), 114.4 (*C*H^3), 120.5 (*C*^{4a}), 122.8 (*C*H^8), 125.6 (*C*H^5), 131.4 (*C*H^6), 134.5 (*C*^{7}), 152.1 (*C*^{8a}), 155.4 (*C*^{4}), 156.6 (HN*C*), 163.5 (*C*^{2}), 171.2, 171.3, 172.5, 172.9, 173.5, 174.0, 174.3, 176.7 (*C*O).

Ring-opening peptide with thiocarbohydrate [40]

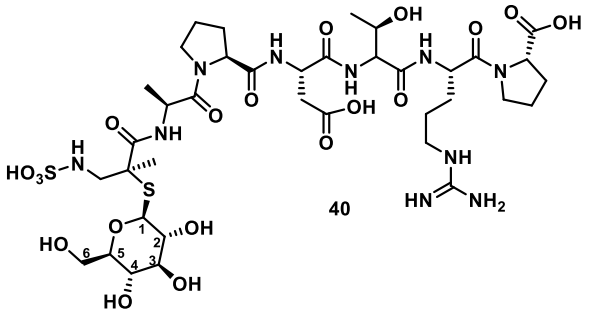

40

Coupling of α-methylisoserine sulfamidate to peptides by solid phase peptide synthesis (SPPS) is described in *section 10.5*. Natural amino acids were coupling using the standard protocol. The ring-opening reaction was carried out on solid phase, using 10 equivalents excess of Tetra-*O*-acetyl-β-thioglucose and 9 equivalents excess of DIPEA in DMF for 1.5 h at room temperature. After deprotection of the Ac groups using 70% hydrazine in methanol, cleavage and purification, we obtained a glycosylated peptide **40** with moderated global yields (16 %).

Semi-preparative HPLC gradient (t_R 19.77 min):

Time (min)	Flow(mL/min)	Acetonitrile (%)	H_2O + 0.1% TFA (%)
0	10	1	99
3	10	1	99
33	10	31	69
35	10	1	99
40	10	1	99

HRMS (ESI) m/z 1014.3829, calculated for $C_{37}H_{63}N_{11}O_{18}S_2H$ (MH^+) = 1014.3867. ^{1}H NMR (400 MHz, D_2O) δ (ppm): 1.08 (d, 3H, *J* = 6.4 Hz, C*H*$_3$ of Thr), 1.29 (d, 3H, *J* = 7.1 Hz, C*H*$_3$ of Ala), 1.46 (s, 3H, C*H*$_3$), 1.50-2.00 (m, 10H, C*H*$_2$γ of Arg, C*H*$_2$β of Arg, C*H*$_2$β of Pro1, C*H*$_2$β of Pro2, C*H*$_2$γ of Pro1, C*H*$_2$γ of Pro2), 2.12-2.23 (m, 2H, C*H*$_2$β of Pro1, C*H*$_2$β of Pro2), 2.74-2.92 (m, 2H, C*H*$_2$ of Asp), 3.04-3.32 (m, 7H, C*H*$_2$δ of Arg, H_{2S}, H_{4S}, H_{5S}, H_{6S}), 3.36-3.44 (m, 1H, H_{3S}), 3.46-3.79 (m, 6H, C*H*$_2$δ of Pro1, C*H*$_2$δ of Pro2, NHC*H*$_2$C), 4.05-4.16 (m, 1H, C*H*β of Thr), 4.17-4.34 (m, 3H, C*H*α of Pro1, C*H*α of Pro2, C*H*α of Thr), 4.40-4.64 (m, 4H, C*H*α of Ala, C*H*α of Arg, C*H*α of Asp, H_{1S}). ^{13}C NMR (75 MHz, D_2O) δ (ppm): 15.0 (*C*H$_3$ of Ala), 18.8 (*C*H$_3$ of Thr), 22.1 (*C*H$_3$), 24.0 (*C*H$_2$γ of Arg), 24.6 (*C*H$_2$γ of Pro1, *C*H$_2$γ of Pro2), 27.3 (*C*H$_2$β of Arg), 29.2 (*C*H$_2$β of Pro1), 29.5 (*C*H$_2$β of Pro2), 35.0 (*C*H$_2$ of Asp), 40.4 (*C*H$_2$δ of Arg), 47.7 (*C*H$_2$δ of Pro1), 47.8 (*C*H$_2$δ of Pro2), 48.5 (*C*Hα of Ala), 49.4 (C_{H6S}), 50.2 (*C*Hα of Asp), 51.1 (*C*Hα of Arg), 52.8 (NHCH$_2$*C*), 59.0 (*C*Hα of Thr), 60.2 (*C*Hα of Pro1, *C*Hα of Pro2), 60.6 (NHC*H*$_2$C), 66.9 (*C*Hβ of Thr), 69.1 (C_{H4S}), 72.2 (C_{H2S}), 77.1 (C_{H3S}), 79.7 (C_{H5S}), 83.0 (C_{H1S}), 156.6 (HN*C*), 171.3, 171.4, 172.6, 173.3, 174.1, 174.5, 176.8 (*C*O).

FmocAla-J-Ala-Pro-Asp-Thr-Arg-Pro-NH$_2$ [41]

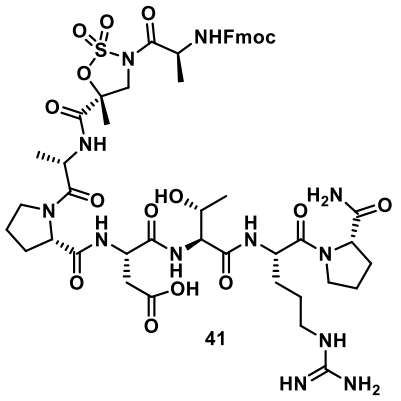

Coupling of α-methylisoserine sulfamidate to peptides by solid phase peptide synthesis (SPPS) is described in *section 10.5*. Natural amino acids were coupling using the standard protocol. Peptide **41** was afforded after cleavage and purification by HPLC (72 % global yield).

Semi-preparative HPLC gradient (t_R 47.38 min):

Time (min)	Flow(mL/min)	Acetonitrile (%)	H_2O + 0.1% TFA (%)
0	10	1	99
1	10	1	99
61	10	61	39
65	10	1	99

HRMS (ESI) m/z = 1111.4511, calculated for $C_{49}H_{67}N_{12}O_{16}S$ (MH^+) = 1111.4513. ^{1}H NMR (300 MHz, CD_3OD) δ (ppm): 1.20 (d, 3H, *J* = 6.4 Hz, C*H*$_3$ of Thr), 1.34-1.50 (m, 6H, C*H*$_3$ of Ala1, C*H*$_3$ of Ala2), 1.63-1.85 (m, 6H, C*H*$_3$, C*H*$_2$γ of Arg, C*H*$_2$β of Arg), 1.86-2.11 (m, 7H, C*H*$_2$β of Arg, C*H*$_2$β of Pro1, C*H*$_2$β of Pro2, C*H*$_2$γ of Pro1, C*H*$_2$γ of Pro2), 2.14-2.32 (m, 2H, C*H*$_2$β of Pro1, C*H*$_2$β of Pro2), 2.84-3.01 (m, 2H, C*H*$_2$ of Asp), 3.13-3.28 (m, 2H, C*H*$_2$δ of Arg), 3.56-3.88 (m, 4H, C*H*$_2$δ of Pro1, C*H*$_2$δ of Pro2), 4.16 (d, 1H,

J = 10.8 Hz, , C*H*$_2$ of Sulfamidate), 4.20-4.49 (m, 7H, C*H*β of Thr, C*H*α of Pro1, C*H*α of Pro2, C*H*α of Thr, C*H* of Fmoc, C*H*$_2$ of Fmoc), 4.56-4.78 (m, 5H, C*H*$_2$ of Sulfamidate, C*H*α of Ala1, C*H*α of Ala2, C*H*α of Arg, C*H*α of Asp), 7.26-7.45 (m, 4H, Arom), 7.62-7.73 (m, 2H, Arom), 7.76-7.85 (m, 2H, Arom). ^{13}C NMR (75 MHz, CD_3OD) δ (ppm): 15.5 (*C*H$_3$ of Ala1), 15.6 (*C*H$_3$ of Ala2), 18.9 (*C*H$_3$ of Thr), 22.2 (*C*H$_3$), 24.2 (*C*H$_2$γ of Arg), 24.6 (*C*H$_2$γ of Pro1, *C*H$_2$γ of Pro2), 27.9 (*C*H$_2$β of Arg), 29.0 (*C*H$_2$β of Pro1), 29.6 (*C*H$_2$β of Pro2), 34.4 (*C*H$_2$ of Asp), 40.7 (*C*H$_2$δ of Arg), 46.9 (*C*H of Fmoc), 47.5 (*C*H$_2$δ of Pro1, *C*H$_2$δ of Pro2), 47.8 (*C*Hα of Ala2), 49.7 (*C*Hα of Ala1), 50.3 (*C*Hα of Asp), 50.6 (*C*Hα of Arg), 52.0 (*C*H$_2$ of Sulfamidate), 59.0 (*C*Hα of Thr), 60.0 (*C*Hα of Pro2), 61.2 (*C*Hα of Pro1), 66.8 (*C*H$_2$ of Fmoc), 67.0 (*C*Hβ of Thr), 85.8 (NHCH$_2$*C*), 119.5, 124.9, 126.8, 127.4, 141.2, 143.7, 143.8 (Arom), 157.2 (HN*C*), 156.7 (*C*O of Fmoc), 168.1, 170.3, 170.5, 170.9, 171.4, 171.7, 172.9, 173.1, 175.7 (*C*O).

Biotin-J-Ala-Pro-Asp-Thr-Arg-Pro-NH$_2$ [42]

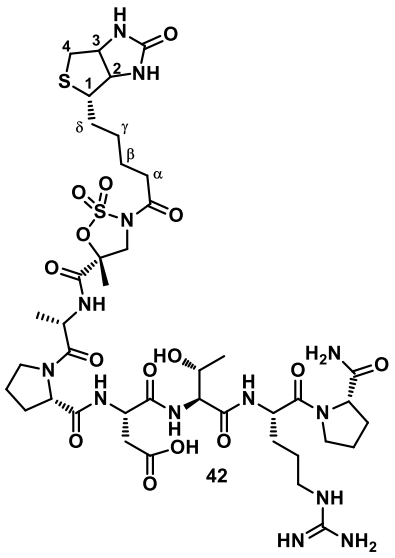

Coupling of α-methylisoserine sulfamidate and biotin to peptides by solid phase peptide synthesis (SPPS) are described in *section 10.5*. Natural amino acids were coupling using the standard protocol. Peptide **42** was afforded after cleavage and purification by HPLC (62 % global yield).

Semi-preparative HPLC gradient (t_R 31.49 min):

Time (min)	Flow(mL/min)	Acetonitrile (%)	H_2O + 0.1% TFA (%)
0	10	1	99
1	10	1	99
61	10	61	39
65	10	1	99

HRMS (ESI) m/z = 1044.4221, calculated for $C_{41}H_{66}N_{13}O_{15}S_2$ (MH^+) = 1044.4237. ^{1}H NMR (300 MHz, D_2O) δ (ppm): 1.06 (d, 3H, *J* = 6.4 Hz, C*H*$_3$ of Thr), 1.24-1.37 (m, 6H, C*H*$_3$ of Ala, C*H*$_2$γ of Biotin, C*H*$_2$β of Biotin), 1.49-1.63 (m, 7H, C*H*$_2$β of Biotin, C*H*$_2$δ of Biotin, C*H*$_2$γ of Arg, C*H*$_2$β of Arg), 1.68-1.97 (m, 10H, C*H*$_3$, C*H*$_2$β of Arg, C*H*$_2$β of Pro1, C*H*$_2$β of Pro2, C*H*$_2$γ of Pro1, C*H*$_2$γ of Pro2), 2.11-2.26 (m, 2H, C*H*$_2$β of Pro1, C*H*$_2$β of Pro2), 2.46-2.57 (m, 2H, C*H*$_2$α of Biotin), 2.65 (d, 1H, *J* = 13.0 Hz, C*H*$_2$*4* of Biotin), 2.73-2.93 (m, 3H, C*H*$_2$ of Asp, C*H*$_2$*4* of Biotin), 3.03-3.15 (m, 2H, C*H*$_2$δ of Arg), 3.16-3.25 (m, 2H, C*H*$_2$*1* of Biotin), 3.47-3.74 (m, 4H, C*H*$_2$δ of Pro1, C*H*$_2$δ of Pro2), 4.05-4.14 (m, 2H, C*H*$_2$ of Sulfamidate, C*H*β of Thr), 4.17-4.37 (m, 4H, C*H*α of Pro1, C*H*α of Pro2, C*H*α of Thr, C*H*$_2$*2* of Biotin), 4.46-4.65 (m, 5H, C*H*$_2$ of Sulfamidate, C*H*α of Ala, C*H*α of Arg, C*H*α of Asp, C*H*$_2$*3* of Biotin). ^{13}C NMR (75 MHz, D_2O) δ (ppm): 15.2 (*C*H$_3$ of Ala), 18.8 (*C*H$_3$ of Thr), 22.3 (*C*H$_3$), 24.0 (*C*H$_2$γ of Arg), 24.6 (*C*H$_2$γ of Pro1, *C*H$_2$γ of Pro2), 27.4 (*C*H$_2$β of Arg), 27.5 (*C*H$_2$δ of Biotin), 27.6 (*C*H$_2$β of Biotin), 27.8 (*C*H$_2$γ of Biotin), 29.2 (*C*H$_2$β of Pro1), 29.5 (*C*H$_2$β of Pro2), 34.3 (*C*H$_2$α of

Biotin), 34.8 (*C*H_2 of Asp), 39.6 (*C*H_2*4* of Biotin), 40.5 (*C*H_2δ of Arg), 47.7 (*C*H_2δ of Pro1), 47.9 (*C*H_2δ of Pro2), 48.3 (*C*Hα of Ala), 50.1 (*C*Hα of Asp), 51.1 (*C*Hα of Arg), 52.3 (*C*H_2 of Sulfamidate), 55.2 (*C*H_2*1* of Biotin), 59.1 (*C*Hα of Thr), 60.2 (*C*Hα of Pro2), 60.7 (*C*Hα of Pro1), 60.8 (*C*H_2*3* of Biotin), 62.0 (*C*H_2*2* of Biotin), 67.0 (*C*Hβ of Thr), 86.3 (NHCH_2*C*), 156.6 (HN*C*), 165.2, 169.1, 171.3, 171.4, 172.1, 172.4, 172.6, 173.9, 174.0, 176.7, 178.8 (*C*O).

Chlorambucil-J-Ala-Pro-Asp-Thr-Arg-Pro-NH_2 [43]

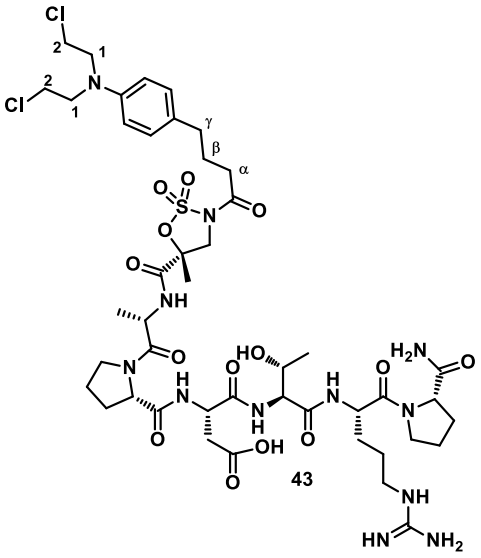

Coupling of α-methylisoserine sulfamidate and chlorambucil to peptides by solid phase peptide synthesis (SPPS) are described in *section 10.5*. Natural amino acids were coupling using the standard protocol. Peptide **43** was afforded after cleavage and purification by HPLC (33 % global yield).

Semi-preparative HPLC gradient (t_R 52.07 min):

Time (min)	Flow(mL/min)	Acetonitrile (%)	H_2O + 0.1% TFA (%)
0	10	1	99
1	10	1	99
61	10	61	39
65	10	1	99

HRMS (ESI) m/z = 1103.4147, calculated for $C_{45}H_{69}Cl_2N_{12}O_{14}S$ (MH^+) = 1103.4148. ^{1}H NMR (300 MHz, D_2O) δ (ppm): 1.08 (d, 3H, *J* = 6.3 Hz, C*H*$_3$ of Thr), 1.31 (d, 3H, *J* = 7.0 Hz, C*H*$_3$ of Ala), 1.51-2.01 (m, 15H, C*H*$_3$, C*H*$_2$γ of Arg, C*H*$_2$β of Arg, C*H*$_2$β of Pro1, C*H*$_2$β of Pro2, C*H*$_2$γ of Pro1, C*H*$_2$γ of Pro2, C*H*$_2$β of Chlorambucil), 2.08-2.31 (m, 2H, C*H*$_2$β of Pro1, C*H*$_2$β of Pro2), 2.45-2.58 (m, 2H, C*H*$_2$α of Chlorambucil), 2.60-2.73 (m, 2H, C*H*$_2$γ of Chlorambucil), 2.74-2.96 (m, 2H, C*H*$_2$ of Asp), 3.05-3.15 (m, 2H, C*H*$_2$δ of Arg), 3.45-3.77 (m, 8H, C*H*$_2$δ of Pro1, C*H*$_2$δ of Pro2, 2C*H*$_2$*1* of Chlorambucil), 3.92-4.02 (m, 4H, , 2C*H*$_2$*2* of Chlorambucil), 4.03-4.16 (m, 2H, C*H*$_2$ of Sulfamidate, C*H*β of Thr), 4.17-4.35 (m, 3H, C*H*α of Pro1, C*H*α of Pro2, C*H*α of Thr), 4.43-4.66 (m, 4H, C*H*$_2$ of Sulfamidate, C*H*α of Ala, C*H*α of Arg, C*H*α of Asp), 7.36-7.50 (m, 4H, Arom). ^{13}C NMR (75 MHz, D_2O) δ (ppm): 15.2 (*C*H$_3$ of Ala), 18.8 (*C*H$_3$ of Thr), 22.4 (*C*H$_3$), 24.0 (*C*H$_2$γ of Arg), 24.6 (*C*H$_2$γ of Pro1, *C*H$_2$γ of Pro2), 25.5 (*C*H$_2$β of Chlorambucil), 27.4 (*C*H$_2$β of Arg), 29.2 (*C*H$_2$β of Pro1), 29.5 (*C*H$_2$β of Pro2), 32.9 (*C*H$_2$α of Chlorambucil), 33.5 (*C*H$_2$γ of Chlorambucil), 34.9 (*C*H$_2$ of Asp), 37.2 (2*C*H$_2$*1* of Chlorambucil), 40.5 (*C*H$_2$δ of Arg), 47.7 (*C*H$_2$δ of Pro1), 47.9 (*C*H$_2$δ of Pro2), 48.3 (*C*Hα of Ala), 50.1 (*C*Hα of Asp), 51.1 (*C*Hα of Arg), 52.2 (*C*H$_2$ of Sulfamidate), 58.9 (2*C*H$_2$*2* of Chlorambucil), 59.1 (*C*Hα of Thr),

60.2 (*C*Hα of Pro2), 60.7 (*C*Hα of Pro1), 67.0 (*C*Hβ of Thr), 86.3 (NHCH$_2$*C*), 122.1, 122.3, 130.7, 130.8, 133.0, 144.8 (Arom), 156.7 (HN*C*), 169.1, 171.1, 172.1, 172.4, 173.9, 174.0, 176.7 (*C*O).

FmocAla-J-Ala-His-Asn-Cys-Gly-NH$_2$ [44]

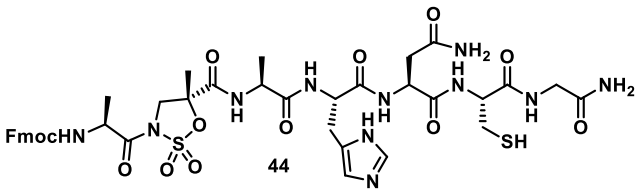

Coupling of α-methylisoserine sulfamidate to peptides by solid phase peptide synthesis (SPPS) is described in *section 10.5*. Natural amino acids were coupling using the standard protocol. Peptide **44** was afforded after cleavage and purification by HPLC (40 % global yield).

Semi-preparative HPLC gradient (t_R 25.39 min):

Time (min)	Flow(mL/min)	Acetonitrile (%)	H$_2$O + 0.1% TFA (%)
0	10	5	95
1	10	5	95
5	10	25	75
30	10	50	50
31	10	75	25
34	10	75	25
35	10	5	95
40	10	5	95

HRMS (ESI) m/z = 956.3012, calculated for $C_{40}H_{50}N_{11}O_{13}S_2$ (MH^+) = 956.3025. ^{1}H NMR (300 MHz, CD_3CN/D_2O (95:5)) δ (ppm): 1.18-1.47 (m, 6H, 2C*H*$_3$ of 2Ala), 1.79 (s, 3H, C*H*$_3$), 2.71-2.74 (m, 2H, C*H*$_2$ of His), 2.86-2.98 (m, 2H, C*H*$_2$ of Cys), 3.01-3.28 (m, 2H, C*H*$_2$ of Asn), 3.66-3.89 (m, 2H, C*H*$_2$ of Gly), 4.15 (d, 1H, *J* = 10.4 Hz, C*H*$_2$ of Sulfamidate), 4.20-4.53 (m,

6H, C*H*α of Cys, C*H*$_2$ of Fmoc, C*H* of Fmoc, 2C*H*α of 2Ala), 4.54-4.68 (m, 2H, C*H*α of His, C*H*α of Asn), 4.74 (d, 1H, J = 10.4 Hz, C*H*$_2$ of Sulfamidate), 7.21 (s, 1H, Arom of His), 7.32-7.52 (m, 4H, Arom), 7.60-7.71 (m, 2H, Arom), 7.79-7.90 (m, 2H, Arom), 8.43 (s, 1H, Arom of His). ^{13}C NMR (75 MHz, CD_3CN/D_2O (95:5)) δ (ppm): 15.8, 16.6 (*C*H$_3$ of 2Ala), 22.5 (*C*H$_3$), 25.3 (*C*H$_2$ of Cys), 26.2 (*C*H$_2$ of Asn), 35.9 (*C*H$_2$ of His), 42.1 (*C*H$_2$ of Gly), 46.9 (*C*H of Fmoc), 49.8 (2*C*Hα of 2 Ala), 50.6 (*C*H$_α$ of His), 52.2 (*C*H$_2$ of Sulfamidate), 52.5 (*C*Hα of Asn), 56.0 (*C*Hα of Cys), 66.9 (*C*H$_2$ of Fmoc), 85.9 (NHCH$_2$*C*), 120.0, 125.3, 127.2, 127.8, 128.9, 133.5, 141.1, 143.9, 144.0 (Arom), 156.3 (*C*O of Fmoc), 168.1, 170.4, 170.8, 171.7, 172.5, 173.0 (*C*O).

J-Ala-His-Asn-Cys-Gly-NH$_2$ [45]

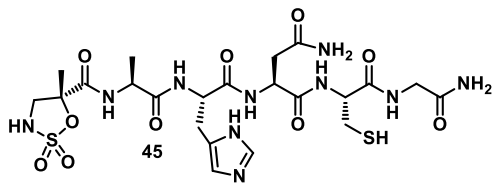

Coupling of α-methylisoserine sulfamidate to peptides by solid phase peptide synthesis (SPPS) is described in *section 10.5*. Natural amino acids were coupling using the standard protocol. Peptide **45** was afforded after cleavage and purification by HPLC (72 % global yield).

Semi-preparative HPLC gradient (t_R 17.28 min):

Time (min)	Flow(mL/min)	Acetonitrile (%)	H_2O + 0.1% TFA (%)
0	10	5	95
1	10	5	95
26	10	30	70
27	10	50	50
30	10	50	50
31	10	5	95
35	10	5	95

HRMS (ESI) m/z = 663.1681, calculated for $C_{22}H_{35}N_{10}O_{10}S_2$ (MH^+) = 663.1974. ^{1}H NMR (300 MHz, CD_3CN/D_2O (95:5)) δ (ppm): 1.35 (d, 3H, *J* = 7.2 Hz, C*H*$_3$ of Ala), 1.66 (s, 3H, C*H*$_3$), 2.72-2.81 (m, 2H, C*H*$_2$ of His), 2.87-2.98 (m, 2H, C*H*$_2$ of Cys), 3.03-3.33 (m, 2H, C*H*$_2$ of Asn), 3.48 (d, 1H, *J* = 12.7 Hz, C*H*$_2$ of Sulfamidate), 3.69-3.91 (m, 2H, C*H*$_2$ of Gly), 3.99 (d, 1H, *J* = 12.7 Hz, C*H*$_2$ of Sulfamidate), 4.29-4.37 (m, 1H, C*Hα* of Ala), 4.41-4.50 (m, 1H, C*Hα* of Cys), 4.58-4.72 (m, 2H, C*Hα* of His, C*Hα* of Asn), 7.28 (s, 1H, Arom of His), 8.51 (s, 1H, Arom of His). ^{13}C NMR (75 MHz, CD_3CN/D_2O (95:5)) δ (ppm): 16.6 (*C*H_3 of Ala), 22.4 (C*C*H_3), 25.3 (*C*H_2 of Cys), 26.4 (*C*H_2 of Asn), 36.0 (*C*H_2 of His), 42.1 (*C*H_2 of Gly), 49.9 (2*C*Hα of 2Ala), 50.7 (*C*Hα of His), 51.8 (*C*H_2 of Sulfamidate), 52.4 (*C*Hα of Asn), 56.0 (*C*Hα of Cys), 90.2 (NHCH_2*C*), 128.9, 133.6 (Arom), 170.5, 170.6, 171.7, 172.2, 173.1 (*C*O).

FmocAla-J-Ala-His-Cys-Asn-Gly-NH_2 [47]

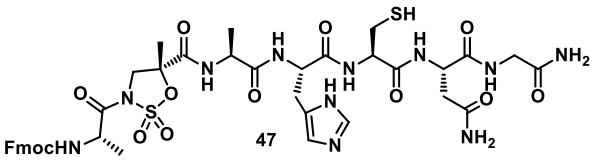

Coupling of α-methylisoserine sulfamidate to peptides by solid phase peptide synthesis (SPPS) is described in *section 10.5*. Natural amino acids were coupling using the standard protocol. Peptide **47** was afforded after cleavage and purification by HPLC (31 % global yield).

Semi-preparative HPLC gradient (t_R 26.00 min):

Time (min)	Flow(mL/min)	Acetonitrile (%)	H_2O + 0.1% TFA (%)
0	10	5	95
1	10	5	95
5	10	25	75
30	10	50	50
31	10	75	25
34	10	75	25
35	10	5	95
40	10	5	95

HRMS (ESI) m/z = 956.3029, calculated for $C_{40}H_{50}N_{11}O_{13}S_2$ (MH^+) = 956.3025. ^{1}H NMR (300 MHz, CD_3CN/D_2O (95:5)) δ (ppm): 1.29-1.40 (m, 6H, 2C*H*$_3$ of 2Ala), 1.79 (s, 3H, C*H*$_3$), 2.73-2.76 (m, 2H, C*H*$_2$ of His), 2.83-2.89 (m, 2H, C*H*$_2$ of Cys), 3.03-3.30 (m, 2H, C*H*$_2$ of Asn), 3.69-3.90 (m, 2H, C*H*$_2$ of Gly), 4.14 (d, 1H, *J* = 10.4 Hz, C*H*$_2$ of Sulfamidate), 4.20-4.54 (m, 6H, C*Hα* of Cys, C*H*$_2$ of Fmoc, C*H* of Fmoc, 2C*Hα* of 2Ala), 4.62-4.75 (m, 3H, C*Hα* of His, C*Hα* of Asn, C*H*$_2$ of Sulfamidate), 7.23 (s, 1H, Arom of His), 7.30-7.46 (m, 4H, Arom), 7.57-7.70 (m, 2H, Arom), 7.78-7.89 (m, 2H, Arom), 8.47 (s, 1H, Arom of His). ^{13}C NMR (75 MHz, CD_3CN/D_2O (95:5))

δ (ppm): 15.9, 16.7 (*C*H$_3$ of 2Ala), 22.5 (*C*H$_3$), 25.2 (*C*H$_2$ of Cys), 26.5 (*C*H$_2$ of Asn), 36.1 (*C*H$_2$ of His), 42.2 (*C*H$_2$ of Gly), 46.9 (*C*H of Fmoc), 49.8 (2*C*Hα of 2 Ala), 50.3 (*C*Hα of His), 52.3 (*C*H$_2$ of Sulfamidate and *C*Hα of Asn), 56.0 (*C*Hα of Cys), 66.8 (*C*H$_2$ of Fmoc), 86.0 (NHCH$_2$*C*), 120.0, 125.3, 127.2, 127.8, 129.0, 133.6, 141.1, 143.9, 144.0 (Arom), 156.2 (*C*O of Fmoc), 168.1, 168.3, 170.5, 170.8, 171.3, 172.3, 173.5 (*C*O).

FmocAla-J-Ala-His-Asn-Gly-Cys-NH$_2$ [48]

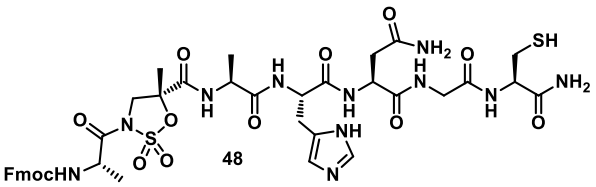

Coupling of α-methylisoserine sulfamidate to peptides by solid phase peptide synthesis (SPPS) is described in *section 10.5*. Natural amino acids were coupling using the standard protocol. Peptide **48** was afforded after cleavage and purification by HPLC (31 % global yield).

Semi-preparative HPLC gradient (t_R 26.14 min):

Time (min)	Flow(mL/min)	Acetonitrile (%)	H_2O + 0.1% TFA (%)
0	10	5	95
1	10	5	95
5	10	25	75
30	10	50	50
31	10	75	25
34	10	75	25
35	10	5	95
40	10	5	95

HRMS (ESI) m/z = 956.3006, calculated for $C_{40}H_{50}N_{11}O_{13}S_2$ (MH^+) = 956.3025. ^{1}H NMR (300 MHz, CD_3CN/D_2O (95:5)) δ (ppm): 1.20-1.40 (m,

6H, 2C*H*$_3$ of 2Ala), 1.79 (s, 3H, CC*H*$_3$), 2.80-2.93 (m, 4H, C*H*$_2$ of His, C*H*$_2$ of Cys), 3.00-3.27 (m, 2H, C*H*$_2$ of Asn), 3.69-3.99 (m, 2H, C*H*$_2$ of Gly), 4.15 (d, 1H, J = 10.4 Hz, C*H*$_2$ of Sulfamidate), 4.19-4.52 (m, 6H, C*H*α of Cys, C*H*$_2$ of Fmoc, C*H* of Fmoc, 2C*H*α of 2Ala), 4.53-4.65 (m, 2H, C*H*α of His, C*H*$_\alpha$ of Asn), 4.73 (d, 1H, J = 10.4 Hz, C*H*$_2$ of Sulfamidate), 7.20 (s, 1H, Arom of His), 7.31-7.50 (m, 4H, Arom), 7.62-7.74 (m, 2H, Arom), 7.81-7.85 (m, 2H, Arom), 8.42 (s, 1H, Arom of His). ^{13}C NMR (75 MHz, CD_3CN/D_2O (95:5)) δ (ppm): 15.8, 16.6 (*C*H$_3$ of 2Ala), 22.5 (*C*H$_3$), 25.5 (*C*H$_2$ of Cys), 26.1 (*C*H$_2$ of Asn), 35.9 (*C*H$_2$ of His), 42.8 (*C*H$_2$ of Gly), 46.9 (*C*H of Fmoc), 49.8 (2*C*Hα of 2 Ala), 50.3 (*C*Hα of His), 52.2 (*C*H$_2$ of Sulfamidate and *C*Hα of Asn), 55.5 (*C*Hα of Cys), 66.9 (*C*H$_2$ of Fmoc), 85.9 (NHCH$_2$*C*), 120.0, 125.3, 127.2, 127.8, 128.9, 133.5, 141.1, 143.9 (Arom), 156.4 (*C*O of Fmoc), 168.2, 170.0, 170.5, 170.8, 172.1, 172.6, 172.9, 173.3 (*C*O).

FmocAla-J-His-Asn-Cys-Gly-NH$_2$ [49]

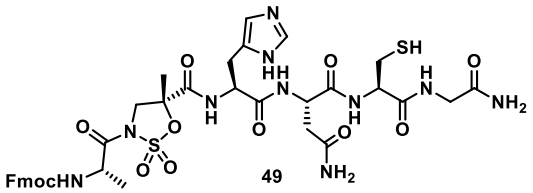

Coupling of α-methylisoserine sulfamidate to peptides by solid phase peptide synthesis (SPPS) is described in *section 10.5*. Natural amino acids were coupling using the standard protocol. Peptide **49** was afforded after cleavage and purification by HPLC (32 % global yield).

Semi-preparative HPLC gradient (t_R 25.83 min):

Time (min)	Flow(mL/min)	Acetonitrile (%)	H_2O + 0.1% TFA (%)
0	10	5	95
1	10	5	95
5	10	25	75
30	10	50	50
31	10	75	25
34	10	75	25
35	10	5	95
40	10	5	95

HRMS (ESI) m/z = 885.2623, calculated for $C_{37}H_{45}N_{10}O_{12}S_2$ (MH^+) = 885.2654. ^{1}H NMR (300 MHz, CD_3CN/D_2O (95:5)) δ (ppm): 1.36 (d, 3H, *J* = 7.0 Hz, C*H*$_3$ of Ala), 1.69 (s, 3H, C*H*$_3$), 2.71-2.75 (m, 2H, C*H*$_2$ of His), 2.87-2.94 (m, 2H, C*H*$_2$ of Cys), 3.11-3.43 (m, 2H, C*H*$_2$ of Asn), 3.66-3.91 (m, 2H, C*H*$_2$ of Gly), 4.10 (d, 1H, *J* = 10.4 Hz, C*H*$_2$ of Sulfamidate), 4.21-4.49 (m, 5H, C*Hα* of Cys, C*H*$_2$ of Fmoc, C*H* of Fmoc, C*Hα* of Ala), 4.61-4.80 (m, 3H, C*Hα* of His, C*Hα* of Asn, C*H*$_2$ of Sulfamidate), 7.24 (s, 1H, Arom of His), 7.29-7.53 (m, 4H, Arom), 7.60-7.69 (m, 2H, Arom), 7.79-7.90 (m, 2H, Arom), 8.48 (s, 1H, Arom of His). ^{13}C NMR (75 MHz, CD_3CN/D_2O (95:5)) δ (ppm): 15.9 (*C*H$_3$ of Ala), 22.5 (*C*H$_3$), 25.2 (*C*H$_2$ of Cys), 26.1 (*C*H$_2$ of Asn), 35.9 (*C*H$_2$ of His), 42.1 (*C*H$_2$ of Gly), 46.9 (*C*H of Fmoc), 49.7 (*C*Hα of Ala), 50.8 (*C*Hα of His), 52.2 (*C*H$_2$ of Sulfamidate), 52.5 (*C*Hα of Asn), 55.9 (*C*Hα of Cys), 66.8 (*C*H$_2$ of Fmoc), 85.9 (NHCH$_2$*C*), 120.0, 125.3, 127.2, 127.8, 129.1, 133.7, 141.1, 143.9, 144.0, (Arom), 156.2 (*C*O of Fmoc), 168.4, 169.8, 170.2, 170.4, 170.6, 171.7, 172.2, 173.0 (*C*O).

FmocAla-J-Ala-His-Asn-Ser-Gly-NH_2 [53]

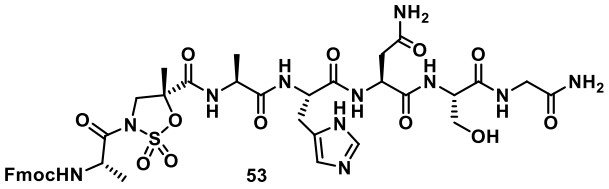

53

Coupling of α-methylisoserine sulfamidate to peptides by solid phase peptide synthesis (SPPS) is described in *section 10.5*. Natural amino acids were coupling using the standard protocol. Peptide **53** was afforded after cleavage and purification by HPLC (30 % global yield).

Semi-preparative HPLC gradient (t_R 24.14 min):

Time (min)	Flow(mL/min)	Acetonitrile (%)	H_2O + 0.1% TFA (%)
0	10	5	95
1	10	5	95
5	10	25	75
30	10	50	50
31	10	75	25
34	10	75	25
35	10	5	95
40	10	5	95

HRMS (ESI) m/z = 940.3217, calculated for $C_{40}H_{50}N_{11}O_{14}S$ (MH^+) = 940.3254. ^{1}H NMR (300 MHz, CD_3CN/D_2O (95:5)) δ (ppm): 1.29-1.40 (m, 6H, 2C*H*$_3$ of 2Ala), 1.79 (s, 3H, C*H*$_3$), 2.66-2.78 (m, 2H, C*H*$_2$ of His), 3.02-3.26 (m, 2H, C*H*$_2$ of Asn), 3.71-3.93 (m, 4H, C*H*$_2$ of Gly, C*H*$_2$ of Ser), 4.14 (d, 1H, *J* = 10.4 Hz, C*H*$_2$ of Sulfamidate), 4.21-4.54 (m, 6H, C*Hα* of Ser, C*H*$_2$ of Fmoc, C*H* of Fmoc, 2C*Hα* of 2Ala), 4.57-4.67 (m, 2H, C*Hα* of His, C*Hα* of Asn), 4.72 (d, 1H, *J* = 10.4 Hz, C*H*$_2$ of Sulfamidate), 7.21 (s, 1H, Arom of His), 7.31-7.46 (m, 4H, Arom), 7.62-7.70 (m, 2H, Arom), 7.82-7.88 (m, 2H,

Arom), 8.44 (s, 1H, Arom of His). ^{13}C NMR (75 MHz, CD_3CN/D_2O (95:5)) δ (ppm): 15.8, 16.6 (*C*H_3 of 2Ala), 22.5 (*C*H_3), 26.2 (*C*H_2 of Asn), 36.1 (*C*H_2 of His), 42.0 (*C*H_2 of Gly), 46.9 (*C*H of Fmoc), 49.7 (2*C*Hα of 2Ala), 50.4 (*C*Hα of His), 52.2 (*C*H_2 of Sulfamidate), 52.4 (*C*Hα of Asn), 55.9 (*C*Hα of Ser), 61.3 (*C*H_2 of Ser), 66.9 (*C*H_2 of Fmoc), 85.9 ($NHCH_2C$), 120.0, 125.3, 127.2, 127.8, 128.7, 133.5, 141.1, 143.9, 144.0, (Arom), 156.4 (*C*O of Fmoc), 168.2, 170.4, 170.8, 171.0, 171.8, 172.5, 172.6 (*C*O).

FmocAla-J-Ala-His-Asn-Thr-Gly-NH_2 [54]

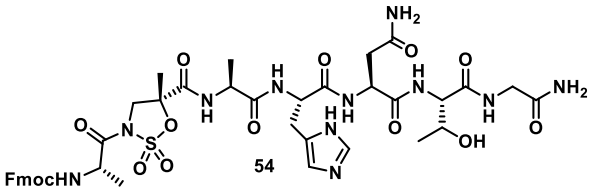

Coupling of α-methylisoserine sulfamidate to peptides by solid phase peptide synthesis (SPPS) is described in *section 10.5*. Natural amino acids were coupling using the standard protocol. Peptide **54** was afforded after cleavage and purification by HPLC (40 % global yield).

Semi-preparative HPLC gradient (t_R 23.70 min):

Time (min)	Flow(mL/min)	Acetonitrile (%)	H_2O + 0.1% TFA (%)
0	10	5	95
1	10	5	95
5	10	25	75
30	10	50	50
31	10	75	25
34	10	75	25
35	10	5	95
40	10	5	95

HRMS (ESI) m/z = 954.3418, calculated for $C_{41}H_{52}N_{11}O_{14}S$ (MH^+) = 954.3410. ^1H NMR (300 MHz, CD_3CN/D_2O (95:5)) δ (ppm): 1.13 (d, 3H, *J*= 6.6 Hz, C*H*$_3$ of Thr), 1.29-1.41 (m, 6H, 2C*H*$_3$ of 2Ala), 1.79 (s, 3H, C*H*$_3$), 2.68-2.79 (m, 2H, C*H*$_2$ of His), 3.02-3.30 (m, 2H, C*H*$_2$ of Asn), 3.69-3.93 (m, 2H, C*H*$_2$ of Gly), 4.15 (d, 1H, *J* = 10.3 Hz, C*H*$_2$ of Sulfamidate), 4.21-4.55 (m, 7H, C*Hα* of Thr, C*Hβ* of Thr, C*H*$_2$ of Fmoc, C*H* of Fmoc, 2C*Hα* of 2Ala), 4.61-4.79 (m, 3H, C*Hα* of His, C*Hα* of Asn, C*H*$_2$ of Sulfamidate), 7.22 (s, 1H, Arom of His), 7.28-7.49 (m, 4H, Arom), 7.61-7.72 (m, 2H, Arom), 7.78-7.89 (m, 2H, Arom), 8.46 (s, 1H, Arom of His). ^{13}C NMR (75 MHz, CD_3CN/D_2O (95:5)) δ (ppm): 15.9, 16.6 (*C*H$_3$ of 2Ala), 18.9 (*C*H$_3$ of Thr), 22.5 (*C*H$_3$), 26.3 (*C*H$_2$ of Asn), 36.1 (*C*H$_2$ of His), 42.1 (*C*H$_2$ of Gly), 46.9 (*C*H of Fmoc), 49.7, 49.8 (2*C*Hα of 2Ala), 50.6 (*C*Hα of His), 52.2 (*C*H$_2$ of Sulfamidate), 52.5 (*C*Hα of Asn), 59.1 (*C*Hα of Thr), 66.8 (*C*H$_2$ of Fmoc, *C*Hβ of Thr), 85.9 (NHCH$_2$*C*), 120.0, 125.3, 127.2, 127.8, 128.8, 133.6, 141.1, 143.9, 144.0, (Arom), 156.3 (*C*O of Fmoc), 168.1, 170.5, 170.8, 171.3, 171.9, 172.6, 173.2 (*C*O).

FmocAla-J-Ala-His-Asn-Lys-Gly-NH$_2$ [55]

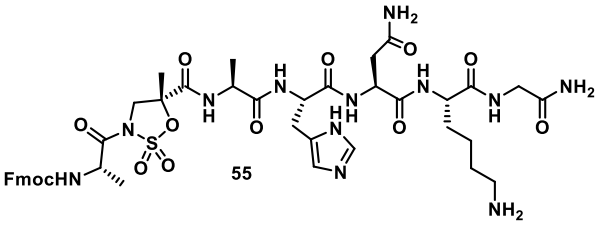

Coupling of α-methylisoserine sulfamidate to peptides by solid phase peptide synthesis (SPPS) is described in *section 10.5*. Natural amino acids were coupling using the standard protocol. Peptide **55** was afforded after cleavage and purification by HPLC (49 % global yield).

Semi-preparative HPLC gradient (t_R 20.67 min):

Time (min)	Flow(mL/min)	Acetonitrile (%)	H_2O + 0.1% TFA (%)
0	10	5	95
1	10	5	95
5	10	25	75
30	10	50	50
31	10	75	25
34	10	75	25
35	10	5	95
40	10	5	95

HRMS (ESI) m/z = 981.3849, calculated for $C_{43}H_{57}N_{12}O_{13}S$ (MH^+) = 981.3883. ^{1}H NMR (300 MHz, CD_3CN/D_2O (95:5)) δ (ppm): 1.25-1.48 (m, 8H, 2C*H*$_3$ of 2Ala, C*H*$_2$γ of Lys), 1.52-1.91 (m, 7H, C*H*$_3$, C*H*$_2$δ of Lys, C*H*$_2$β of Lys), 2.65-2.76 (m, 2H, C*H*$_2$ of His), 2.86-2.94 (m, 2H, C*H*$_2$ε of Lys), 3.07-3.30 (m, 2H, C*H*$_2$ of Asn), 3.70-3.88 (m, 2H, C*H*$_2$ of Gly), 4.15 (d, 1H, *J* = 10.4 Hz, C*H*$_2$ of Sulfamidate), 4.18-4.53 (m, 6H, C*H*α of Lys, C*H*$_2$ of Fmoc, C*H* of Fmoc, 2C*H*α of 2Ala), 4.56-4.67 (m, 2H, C*H*α of His, C*H*α of Asn), 4.72 (d, 1H, *J* = 10.4 Hz, C*H*$_2$ of Sulfamidate), 7.23 (s, 1H, Arom of His), 7.29-7.50 (m, 4H, Arom), 7.62-7.71 (m, 2H, Arom), 7.78-7.89 (m, 2H, Arom), 8.48 (s, 1H, Arom of His). ^{13}C NMR (75 MHz, CD_3CN/D_2O (95:5)) δ (ppm): 15.8, 16.6 (*C*H$_3$ of 2Ala), 21.9 (*C*H$_2$γ of Lys), 22.5 (*C*H$_3$), 26.0 (*C*H$_2$ of Asn, *C*H$_2$δ of Lys), 30.0 (*C*H$_2$β of Lys), 35.9 (*C*H$_2$ of His), 39.2 (*C*H$_2$ε of Lys), 42.0 (*C*H$_2$ of Gly), 46.9 (*C*H of Fmoc), 49.8 (2*C*Hα of 2Ala), 50.5 (*C*Hα of His), 52.2 (*C*H$_2$ of Sulfamidate), 52.6 (*C*Hα of Asn), 53.3 (*C*Hα of Lys), 66.9 (*C*H$_2$ of Fmoc), 86.0 (NHCH$_2$*C*), 120.0, 125.3, 127.2, 127.8, 128.9, 133.5, 141.1, 143.9, (Arom), 156.4 (*C*O of Fmoc), 168.2, 170.7, 170.9, 171.9, 172.6, 172.7, 172.9, 173.4 (*C*O).

Dansyl-J-Ala-His-Asn-Cys-Gly-NH_2 [59]

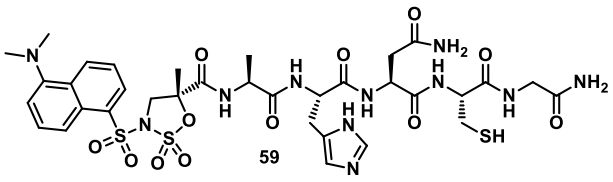

59

Coupling of α-methylisoserine sulfamidate and dansyl group to peptides by solid phase peptide synthesis (SPPS) are described in *section 10.5*. Natural amino acids were coupling using the standard protocol. Peptide **59** was afforded after cleavage and purification by HPLC (42 % global yield).

Semi-preparative HPLC gradient (t_R 19.40 min):

Time (min)	Flow(mL/min)	Acetonitrile (%)	H_2O + 0.1% TFA (%)
0	10	5	95
1	10	5	95
5	10	25	75
30	10	50	50
31	10	75	25
34	10	75	25
35	10	5	95
40	10	5	95

HRMS (ESI) m/z = 896.2478, calculated for $C_{34}H_{46}N_{11}O_{12}S_3$ (MH^+) = 896.2484. ^{1}H NMR (300 MHz, CD_3CN/D_2O (95:5)) δ (ppm): 1.25 (d, 3H, *J* = 7.1 Hz, C*H*$_3$ of Ala), 1.60 (s, 3H, C*H*$_3$), 2.71-2.79 (m, 2H, C*H*$_2$ of His), 2.86-2.97 (m, 8H, C*H*$_2$ of Cys, 2 C*H*$_3$ of Dansyl), 3.06-3.30 (m, 2H, C*H*$_2$ of Asn), 3.69-3.91 (m, 3H, C*H*$_2$ of Sulfamidate, C*H*$_2$ of Gly), 4.14-4.26 (m, 1H, C*Hα* of Ala), 4.36 (d, 1H, *J* = 10.3 Hz, C*H*$_2$ of Sulfamidate), 4.39-4.47 (m, 1H, C*Hα* of Cys), 4.56-4.67 (m, 2H, C*Hα* of His, C*Hα* of Asn), 7.25 (s, 1H, Arom of His), 7.31-7.37 (m, 1H, Arom of Dansyl), 7.63-7.76 (m, 2H, Arom

of Dansyl), 8.31-8.43 (m, 2H, Arom of Dansyl), 8.50 (s, 1H, Arom of His), 8.71-8.79 (m, 1H, Arom of Dansyl). ^{13}C NMR (75 MHz, CD_3CN/D_2O (95:5)) δ (ppm): 16.6 (*C*H_3 of Ala), 22.2 (*C*H_3), 25.3 (*C*H_2 of Cys), 26.2 (*C*H_2 of Asn), 36.0 (*C*H_2 of His), 42.1 (*C*H_2 of Gly), 44.8 (2*C*H_3 of Dansyl), 49.6 (*C*Hα of Ala), 50.7 (*C*Hα of His), 52.7 (*C*Hα of Asn), 53.9 (*C*H_2 of Sulfamidate), 56.0 (*C*Hα of Cys), 86.3 (NHCH$_2$*C*), 116.0, 118.1, 123.6, 128.9, 129.5, 129.6, 130.6, 132.7, 133.4, 133.5, 151.9 (Arom), 167.6, 170.4, 171.7, 172.1, 172.3, 173.0 (*C*O).

Intramolecular ring-opening peptide [60]

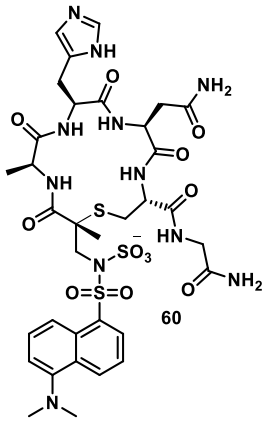

60

Peptide **59** (11 mg, 0.012 mmol) was dissolved in CD_3CN/D_2O (96:4) in a quartz NMR tube and Et_3N (1.6 equiv.) was added. The reaction became cloudy immediately after addition, affording, after HPLC purification, peptide **60** (9 mg, 0.010 mmol) with a good yield (84%).

Semi-preparative HPLC gradient (t_R 21.45 min):

Time (min)	Flow(mL/min)	Acetonitrile (%)	H_2O + 0.1% TFA (%)
0	10	5	95
1	10	5	95
26	10	30	70
27	10	50	50
30	10	50	50
31	10	5	95
35	10	5	95

HRMS (ESI) m/z = 894.2341, calculated for $C_{34}H_{44}N_{11}O_{12}S_3$ (M^-) = 894.2339. ^{1}H NMR (400 MHz, D_2O) δ (ppm): 1.49 (d, 3H, *J* = 7.1 Hz, C*H*$_3$ of Ala), 1.73 (s, 3H, C*H*$_3$), 2.71-2.91 (m, 2H, C*H*$_2$ of His, C*H*$_2$ of Asn), 2.97-3.08 (m, 1H, C*H*$_2$ of His), 3.23 (s. 6H, 2C*H*$_3$ of Dansyl), 3.26-3.47 (m, 3H, C*H*$_2$ of "Cys", C*H*$_2$ of Asn), 3.86-3.98 (m, 2H, C*H*$_2$ of Gly), 4.10-4.24 (m, 2H, C*H*$_2$ of Sulfamidate, C*Hα* of Ala), 4.39-4.47 (m, 1H, C*Hα* of Asn), 4.49-4.57 (m, 2H, C*Hα* of "Cys", C*H*$_2$ of Sulfamidate), 4.69-4.77 (m, 1H, C*Hα* of His), 7.37 (s, 1H, Arom of His), 7.71-7.90 (m, 3H, Arom of Dansyl), 8.26-8.35 (m, 1H, Arom of Dansyl), 8.36-8.44 (m, 1H, Arom of Dansyl), 8.46-8.55 (m, 1H, Arom of Dansyl), 8.65 (s, 1H, Arom of His). ^{13}C NMR (100 MHz, D_2O) δ (ppm): 14.7 (*C*H$_3$ of Ala), 21.4 (*C*H$_3$), 25.2 (*C*H$_2$ of "Cys"), 30.8 (*C*H$_2$ of Asn), 35.8 (*C*H$_2$ of His), 42.2 (*C*H$_2$ of Gly), 45.9 (2*C*H$_3$ of Dansyl), 51.0 (*C*Hα of Ala, *C*Hα of His), 52.4 (*C*Hα of Asn), 53.9 (NHCH$_2$*C*), 54.8 (*C*H$_2$ of Sulfamidate), 55.0 (*C*Hα of "Cys"), 117.3, 117.8, 122.8, 125.3, 127.1, 128.1, 128.4, 129.1, 130.8, 133.7, 135.1 (Arom), 171.9, 172.4, 172.8, 173.9, 174.0, 174.7, 176.3 (*C*O).

Methyl *N*-(((9H-fluoren-9-yl)methoxy)carbonyl)-*O*-tosyl-D-threoninate [61]

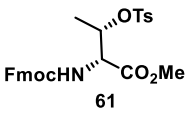

61

Fmoc-Thr-CO_2Me (5.5 g, 15.5 mmol) was dissolved in pyridine (57 mL) at 0 ºC, and then TsCl (7.4 g, 38.7 mmol) was added. The mixture was stirred at 0 ºC for 2 days. After that, the mixture was extracted with AcOEt (540 mL) and washed with 5% aqueous $KHSO_4$ (160 mL). The organic phase was dried with Na_2SO_4 and concentrated. Purification by column chromatography on silica gel (AcOEt/Hex, 3:7) affording compound **61** (5.0 g, 67%) as a sticky white foam. $[\alpha]_D^{20}$ =+17.1 (*c* 1.0 in $CHCl_3$). HRMS (ESI) m/z = 510.1575, calculated for $C_{27}H_{27}NO_7S$ (MH^+) = 510.1581. ^{1}H NMR (300 MHz, $CDCl_3$) δ (ppm): 1.38 (d, 3H, *J* = 6.4 Hz, C*H*$_3$ of Thr), 2.48 (s, 3H, C*H*$_3$ of Ts), 3.62 (s, 3H, C*H*$_3$ of CO_2CH_3), 4.19-4.31 (m, 1H, C*H* of Fmoc), 4.36-4.46 (m, 2H, C*H*$_2$ of Fmoc), 4.47-4.56 (m, 1H, C*H*α), 5.112-5.24 (m, 1H, C*H*β), 5.53 (d, 1H, *J*= 9.7 Hz, N*H*), 7.29-7.48 (m, 7H, Arom), 7.58-7.68 (m, 4H, Arom), 7.74-7.81 (m, 2H, Arom). ^{13}C NMR (75 MHz, $CDCl_3$) δ (ppm): 18.2 (*C*H_3 of Thr), 21.7 (*C*H_3 of Ts), 47.1 (*C*H of Fmoc), 52.8 (CO_2CH_3), 58.0 (*C*Hα), 67.5 (*C*H_2 of Fmoc), 78.4 (*C*Hβ), 120.0, 125.1, 127.1, 127.8, 127.9, 129.9, 133.5, 141.3, 143.6, 143.7, 145.1 (Arom), 156.5 (*C*O of Fmoc), 169.2 (CO_2CH_3).

Methyl (2*S*,3*S*)-2-((((9H-fluoren-9-yl)methoxy)carbonyl)amino)-3-(phenylselanyl)butanoate [62]

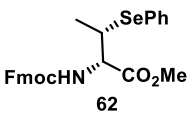

62

KOH (408 mg, 7.2 mmol) was dissolved in methanol (5.6 mL) and PhSeH (888 μL, 8.3 mmol) was added under argon atmosphere. The mixture was stirred at room temperature for 10 minutes. After that, the crude was concentrated affording a white yellow

solid. Compound **61** (1.75 g, 3.63 mmol) is dissolved in DMF and cooled to 0 ºC and transferred to the above solid. The orange mixture was stirred at room temperature for 4 h. Ice-cold 5% aqueous $KHSO_4$ (56 mL) was added, and the mixture was extracted with AcOEt (141 mL). The organic phase was washed with sat. $NaHCO_3$ (28 mL), brine (28 mL), dried with Na_2SO_4 and concentrated. Purification by column chromatography on silica gel (AcOEt/Hex, 3:7) affording compound **62** (2.36 g, 70%) as a white solid. $[\alpha]_D^{20}$ =+6.1 (*c* 1.0 in $CHCl_3$). Mp= 97.4 ºC. HRMS (ESI) m/z = 496.1015, calculated for $C_{26}H_{26}NO_4Se$ (MH^+)= 496.1023. ^1H NMR (300 MHz, $CDCl_3$) δ (ppm): 1.50 (d, 3H, *J* = 7.2 Hz, C*H*$_3$ of Sec), 3.59-3.72 (m, 1H, C*H*α), 3.78 (s, 3H, C*H*$_3$ of CO_2CH_3), 4.20-4.31 (m, 1H, C*H* of Fmoc), 4.36-4.48 (m, 2H, C*H*$_2$ of Fmoc), 4.60-4.71 (m, 1H, C*H*β), 5.56 (d, 1H, *J* = 9.0 Hz, N*H*), 7.26-7.47 (m, 7H, Arom), 7.58-7.68 (m, 4H, Arom), 7.75-7.86 (m, 2H, Arom). ^{13}C NMR (75 MHz, CD_3CN) δ (ppm): 18.3 (*C*H_3 of Sec), 41.1 (*C*Hβ), 47.1 (*C*H of Fmoc), 52.5 (CO_2CH_3), 58.5 (*C*Hα), 67.3 (*C*H_2 of Fmoc), 120.0, 125.2, 127.1, 127.8, 128.1, 128.2, 129.2, 135.4, 141.3, 143.8 (Arom), 155.9 (*C*O of Fmoc), 170.9 (CO_2CH_3).

(2S,3S)-2-((((9H-Fluoren-9-yl)methoxy)carbonyl)amino)-3-(phenylselanyl)butanoic acid [63]

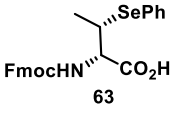

63

A 1 M aqueous solution of NaOH (1.2 mL) was added to a solution of $CaCl_2$ (1.3 g, 11.75 mmol) in a mixture 7:3 of ^iPrOH:H_2O (23 mL). The resulting cloudy reaction was cooled to 0 ºC and transferred to compound **62** (363 mg, 0.73 mmol). After stirring at room temperature for 24 hours, the ^iPrOH was evaporated and the aqueous phase was acidified with 1M HCl. Then, it was extracted with

CH_2Cl_2. The organic phase was dried with Na_2SO_4 and concentrated, affording compound **63** (292 mg, 83%) as a white solid.

The proprieties of this compound is described in the bibliography.[15–17]

Ns-J-63-Pro-Ala-Cys-NH_2 [64]

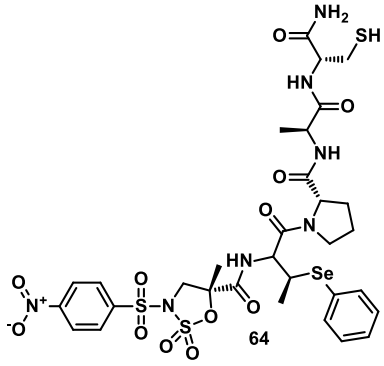

64

To couple compound **63**, we followed the conditions of the van der Donk's group.[15,17] HOAT (27 mg, 0.2 mmol), DIC (31 μL, 0.2 mmol) and compound **63** (96.2 mg, 0.2 mmol) was dissolved in DMF (2 mL) and added to the resin. After 2 h at room temperature, the coupling was completed. Fmoc group was removed with 20% piperidine in DMF (three times for one minute each). Coupling of α-methylisoserine sulfamidate and nosyl group to peptides by solid phase peptide synthesis (SPPS) is described in *section 10.5*. Natural amino acids were coupling using the standard protocol. Peptide **64** was afforded after cleavage and purification by HPLC (18 % global yield).

Semi-preparative HPLC gradient (t_R 27.62 min):

Time (min)	Flow(mL/min)	Acetonitrile (%)	H_2O + 0.1% TFA (%)
0	10	40	60
3	10	40	60
28	10	65	35
29	10	40	60
34	10	40	60

HRMS (ESI) m/z = 878.1060, calculated for $C_{31}H_{39}N_7O_{12}S_3Se$ (MH^+) = 878.1057. ^{1}H NMR (400 MHz, CD_3CN) δ (ppm): 1.18-1.30 (m, 6H, C*H*$_3$ of Ala, C*H*$_3$ of Sec), 1.57 (s, 3H, C*H*$_3$), 1.76-1.82 (m, 1H, C*H*$_2$δ of Pro), 1.87-1.94 (m, 2H, C*H*$_2$δ of Pro, C*H*$_2$β of Pro), 2.08-2.16 (m, 1H, C*H*$_2$β of Pro), 2.74-2.83 (m, 1H, C*H*$_2$ of Cys), 2.89-2.98 (m, 1H, C*H*$_2$ of Cys), 3.23-3.33 (m, 1H, C*H*$_2$γ of Pro), 3.34-3.45 (m, 1H, C*H*$_2$γ of Pro), 3.55-3.65 (m, 1H, C*H*α of Sec), 3.85 (d, 1H, *J* = 10.1 Hz, C*H*$_2$ of Sulfamidate), 3.98-4.07 (m, 1 H, C*H*$_\alpha$ of Ala), 4.08-4.16 (m, 1H, C*H*$_2$α of Pro), 4.19-4.27 (m, 1H, C*H*$_2$α of Cys), 4.40 (d, 1H, *J* = 10.1 Hz, C*H*$_2$ of Sulfamidate), 4.67-4.74 (m, 1H, C*Hβ* of Sec), 5.73 (s, 1H, CON*H*$_2$), 6.60 (s, 1H, CON*H*$_2$), 6.90 (d, 1H, *J* = 5.5 Hz, CON*H* of Ala), 7.20-7.35 (m, 5H, Arom of SePh, CON*H* of Cys, CON*H* of Sec), 7.51-7.58 (m, 2H, Arom of SePh), 8.08-8.17 (m, 2H, Arom of Ns), 8.28-8.38 (m, 2H, Arom of Ns). ^{13}C NMR (75 MHz, CD_3CN) δ (ppm): 16.4, 16.8 (*C*H$_3$ of Ala, *C*H$_3$ of Sec), 22.3 (*C*H$_3$), 24.6 (*C*H$_2$δ of Pro), 25.8 (*C*H$_2$ of Cys), 28.9 (*C*H$_2$β of Pro), 39.1 (*C*H$_2$α of Ala), 47.6 (*C*H$_2$γ of Pro), 50.7 (*C*H$_2$α of Sec), 54.1 (*C*H$_2$ of Sulfamidate), 54.6 (*C*H$_2$β of Sec), 55.7 (*C*Hα of Cys), 61.9 (*C*Hα of Pro), 87.0 (NHCH$_2$*C*), 124.8, 127.2, 128.6, 129.3, 130.4, 135.9, 140.5, 151.7 (Arom), 166.9, 169.2, 172.1, 172.3, 172.6 (*C*O).

Peptide 65

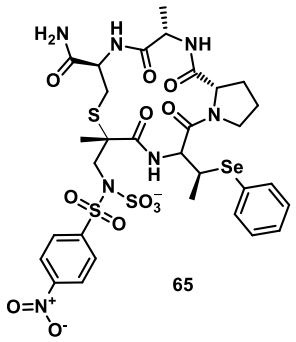

65

Peptide **64** was dissolved in CD_3CN/D_2O (96:4) in a quartz NMR tube and Et_3N (1.6 equiv.) was added. The reaction became cloudy immediately after addition, affording peptide **65**, which was purified by SPE C18-cartridge (t_R= 42.88 min in analytical HPLC). HRMS (ESI) m/z = 876.0887, calculated for $C_{31}H_{38}N_7O_{12}S_3Se$ (M^-) = 876.0912.

Peptide 66

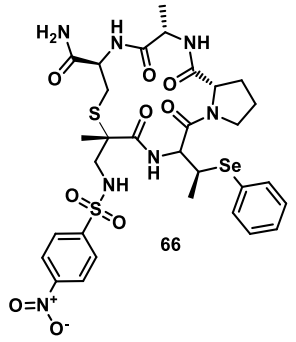

66

Peptide **65** was dissolved in a mixture (1:1) of 2 M HCl in CH_3CN. After 30 minutes at room temperature, the crude was lyophilized, affording the cycle peptide **66**, confirmed by ESI-MS and HPLC (t_R= 45.23 min in analytical HPLC). HRMS (ESI) m/z = 798.1491, calculated for $C_{31}H_{39}N_7O_9S_2Se$ (MH^+) = 798.1490.

Peptide 67

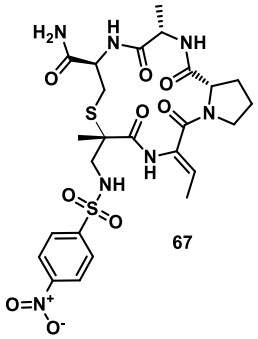

67

The phenyl selenium group of peptide **66** was oxidized using $NaIO_4$ (8 equiv.) in H_2O/CH_3CN (1:1) at room temperature for 3h. Elimination of the selenoxide group to form the Dhb into the peptide, afforded peptide **67** (t_R=36.79 min in analytical HPLC). HRMS (ESI) m/z = 640.1864, calculated for $C_{25}H_{33}N_7O_9S_2$ (MH^+) = 640.1854.

Peptide 72

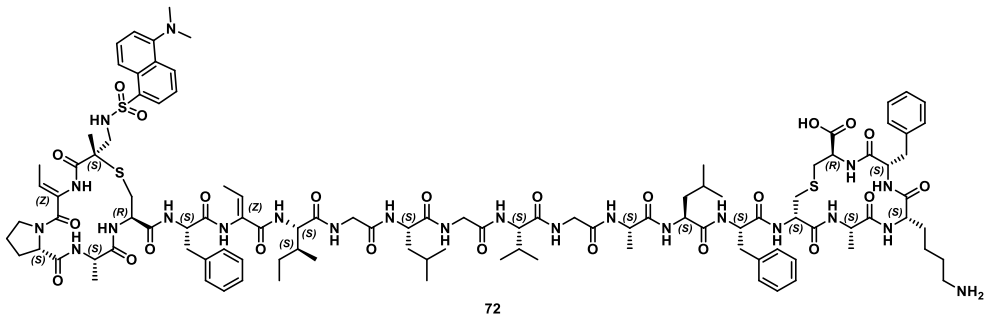

72

HMPB ChemMatrix® resin (0.05 mmol) was swelled with DMF (5 mL) for 30 min. Building block **69** (1.5 mmol) was coupled using DIC (2.0 mmol) and DMAP (0.005 mmol) in DMF (1 mL) for 50 min. This process was repeated with freshly prepared solution to maximize the coupling yield.[18–20] Natural Fmoc-protected amino acids (0.25 mmol) were coupled using HATU (0.245 mmol) and DIPEA (0.4 mmol) in DMF (2 mL) for 30 min. The

deprotection of allyl ester and allyl carbamate and ring-closure to obtain cycle B was performed following the conditions described by van der Donk.[21] A small fraction of the resin was treated with TFA:TIS:H_2O (95:2.5:2.5) and the resulting peptide was analyzed by ESI-MS to confirm that the cyclization reaction took place. The sequence IGLGVGALF was coupled in a Liberty Microwave (CEM Corporation, Mathews, NC) synthesizer using DIC/Oxyma Pure standard protocol. Building block **63** was manually coupled following the conditions described for peptide **64**. Sulfamidate **J** and dansyl chloride were coupled using the methodology described in *section 10.5*. Final cleavage and deprotection was performed using TFA:TIS:H_2O:DODT (94:1:2.5:2.5) at room temperature for 1 hour. The resulting crude mixture was precipitated with cold Et_2O, centrifuged, washed twice with more Et_2O, suspended in 70% aqueous MeCN and lyophilized to obtain peptide **70** (30 mg, 0.011 mmol), which was used without further purification. Sulfamidate ring-opening reaction was performed by dissolving peptide **70** in DMSO (1 mL) and adding Et_3N (6 μL). After 30 min, the solution was frozen and lyophilized to obtain peptide **71**, which dissolved in a mixture (1 mL) of DMSO and concentrated HCl (final HCl concentration 0.6 M). After 3 h, the mixture was frozen, lyophilized and purified by SPE C18-cartridge to obtain $CylL_S$ analog **72** (1 mg, 1% global yield, 90% per reaction step, 45 steps). MS (MALDI) m/z =756.0604, calculated for $C_{25}H_{33}N_7O_9S_2$ ($[M+3H]^{3+}$) = 755.6874.

Semi-preparative HPLC gradient (t_R 22.90 min):

Time (min)	Flow(mL/min)	Acetonitrile (%)	H_2O + 0.1% TFA (%)
0	10	5	95
3	10	5	95
33	10	95	5
34	10	5	95
39	10	5	95

10.14 References

(1) Frisch, M. J.; Trucks, G. W.; Schlegel, H. B.; Scuseria, G. E.; Robb, M. A.; Cheeseman, J. R.; Scalmani, G.; Barone, V.; Mennucci, B.; Petersson, G. A.; Nakatsuji, H.; Caricato, M.; Li, X.; Hratchian, H. P.; Izmaylov, A. F. .; Bloino, J. .; Zheng, G. .; Sonnenberg, J. L. .; Hada, M. .; Ehara, M. .; Toyota, K. .; Fukuda, R. .; Hasegawa, J. .; Ishida, M. .; Nakajima, T. .; Honda, Y. .; Kitao, O. .; Nakai, H. .; Vreven, T. .; Montgomery Jr., J. A. .; Peralta, J. E. .; Ogliaro, F. .; Bearpark, M. .; Heyd, J. J. .; Brothers, E. .; Kudin, K. N. .; Staroverov, V. N. .; Kobayashi, R. .; Normand, J. .; Raghavachari, K. .; Rendell, A. .; Burant, J. C. .; Iyengar, S. S. .; Tomasi, J. .; Cossi, M. .; Rega, N. .; Millam, J. M. .; Klene, M. .; Knox, J. E. .; Cross, J. B. .; Bakken, V. .; Adamo, C. .; Jaramillo, J. .; Gomperts, R. .; Stratmann, R. E. .; Yazyev, O. .; Austin, A. J. .; Cammi, R. .; Pomelli, C. .; Ochterski, J. W. .; Martin, R. L. .; Morokuma, K. .; Zakrzewski, V. G. .; Voth, G. A. .; Salvador, P. .; Dannenberg, J. J. .; Dapprich, S. .; Daniels, A. D. .; Farkas, Ö. .; Foresman, J. B. .; Ortiz, J. V. .; Cioslowski, J. .; Fox, D. J. . *Gaussian 09*; Wallingford, CT, 2009.

(2) Zhao, Y.; Truhlar, D. G. *Theor. Chem. Acc.* **2008**, *120*, 215–241.

(3) Scalmani, G.; Frisch, M. J. *J. Chem. Phys.* **2010**, *132*, 114110.

(4) Ribeiro, R. F.; Marenich, A. V.; Cramer, C. J.; Truhlar, D. G. *J. Phys. Chem. B* **2011**, *115*, 14556–14562.

(5) Gonzalez, C.; Bernhard Schlegel, H. *J. Chem. Phys.* **1989**, *90*, 2154–2161.

(6) Gonzalez, C.; Schlegel, H. B. *J. Phys. Chem.* **1990**, *94*, 5523–5527.

(7) Bayly, C. I.; Cieplak, P.; Cornell, W. D.; Kollman, P. A. *J. Phys. Chem.* **1993**, *97*, 10269–10280.

(8) Jorgensen, W. L.; Chandrasekhar, J.; Madura, J. D.; Impey, R. W.; Klein, M. L. *J. Chem. Phys.* **1983**, *79*, 926–935.

(9) Duan, Y.; Wu, C.; Chowdhury, S.; Lee, M. C.; Xiong, G.; Zhang, W.; Yang, R.; Cieplak, P.; Luo, R.; Lee, T.; Caldwell, J.; Wang, J.; Kollman, P. *J.*

Comput. Chem. **2003**, *24*, 1999–2012.

(10) Andrea, T. A.; Swope, W. C.; Andersen, H. C. *J. Chem. Phys.* **1983**, *79*, 4576–4584.

(11) Darden, T.; York, D.; Pedersen, L. *J. Chem. Phys.* **1993**, *98*, 10089–10092.

(12) Navo, C. D.; Mazo, N.; Avenoza, A.; Busto, J. H.; Peregrina, J. M.; Jiménez-Osés, G. *J. Org. Chem.* **2017**, *82*, 13250–13255.

(13) NIST Computational Chemistry Comparison and Benchmark Database NIST Standard Reference Database Number 101 Release 19, April 2018, Editor: Russell D. Johnson III DOI:10.18434/T47C7Z.

(14) Sugawara, M.; Tonan, K.; Ikawa, S. I. *Spectrochim. Acta Part A* **2001**, *57*, 1305–1316.

(15) Zhou, H.; van der Donk, W. A. *Org. Lett.* **2002**, *4*, 1335–1338.

(16) Okeley, N. M.; Zhu, Y.; van der Donk, W. A. *Org. Lett.* **2000**, *2*, 3603–3606.

(17) Levengood, M. R.; van der Donk, W. A. *Nat. Protoc.* **2007**, *1*, 3001–3010.

(18) Knerr, P. J.; van der Donk, W. A. *J. Am. Chem. Soc.* **2012**, *134*, 7648–7651.

(19) Mukherjee, S.; Huo, L.; Thibodeaux, G. N.; van der Donk, W. A. *Org. Lett.* **2016**, *18*, 6188–6191.

(20) Knerr, P. J.; Tzekou, A.; Ricklin, D.; Qu, H.; Chen, H.; van der Donk, W. A.; Lambris, J. D. *ACS Chem. Biol.* **2011**, *6*, 753–760.

(21) Mukherjee, S.; Huo, L.; Thibodeaux, G. N.; van der Donk, W. A. *Org. Lett.* **2016**, *18*, 6188–6191.

Chapter 11.
Supplementary Information

Supplementary Information I: NMR spectra

Supplementary Information II: Tables & Figures

Supplementary Information III: HPLC Chromatograms

Supplementary Information I: NMR spectra

NMR spectra for the compounds described throughout *Chapter 10: Experimental section* are collected in the following pages. 2D COSY and HSQC experiments performed for describing the following compounds have been omitted in this section.

^{1}H NMR 400 MHz in D_2O

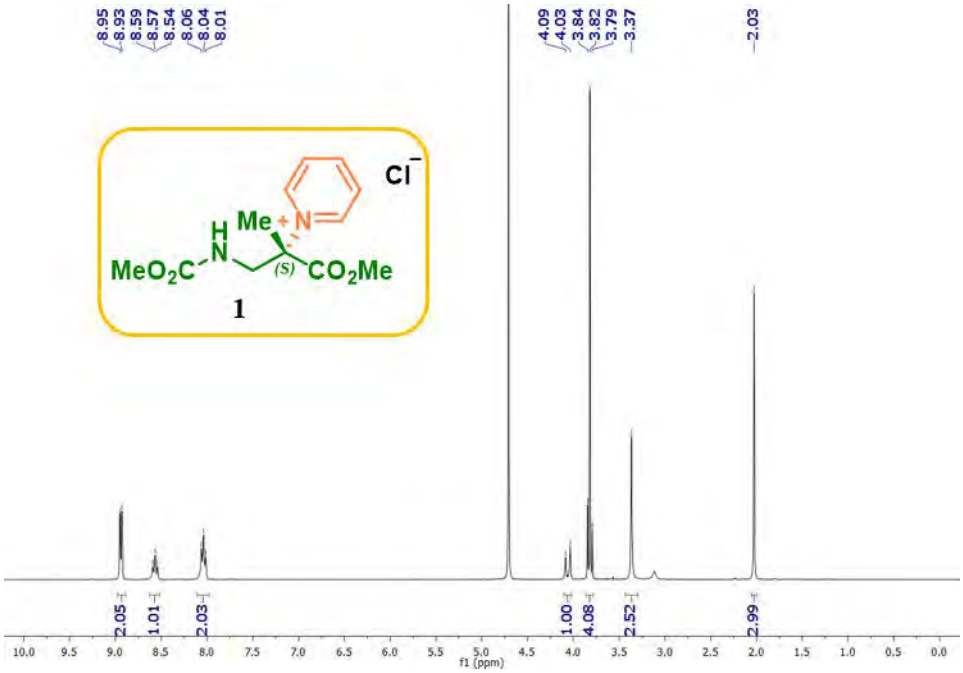

^{3}C NMR 100 MHz in D_2O

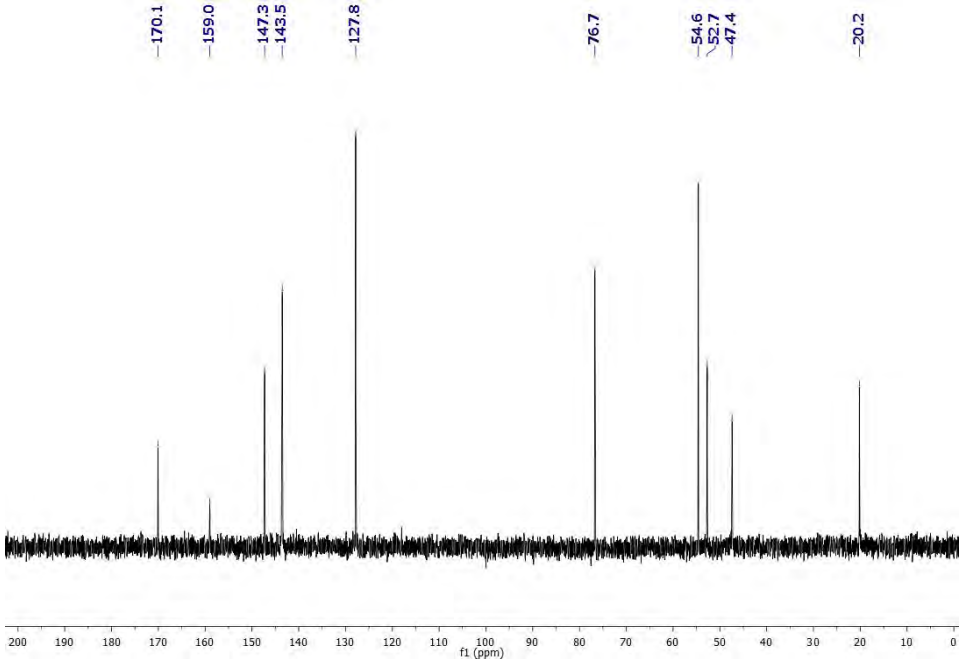

^{1}H NMR 400 MHz in D_2O

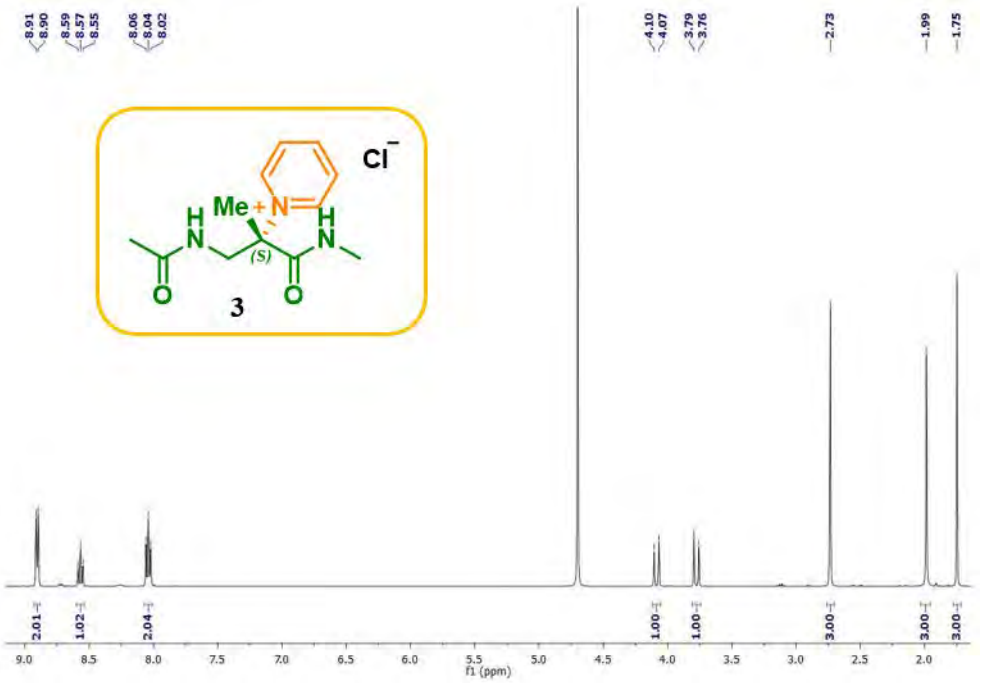

^{13}C NMR 100 MHz in D_2O

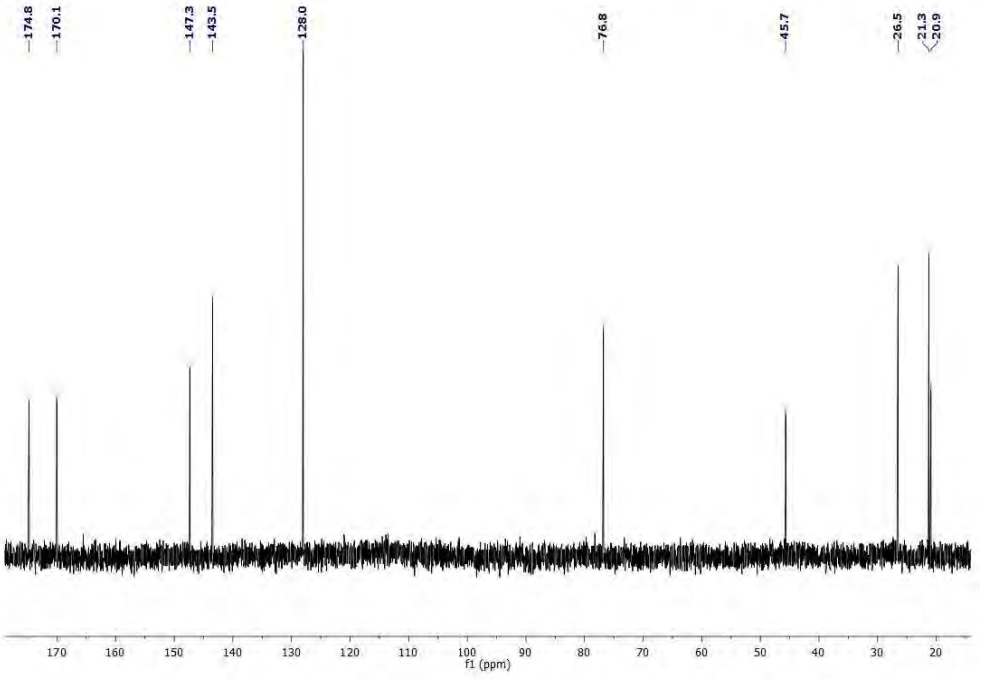

^{1}H NMR 400 MHz in D_2O

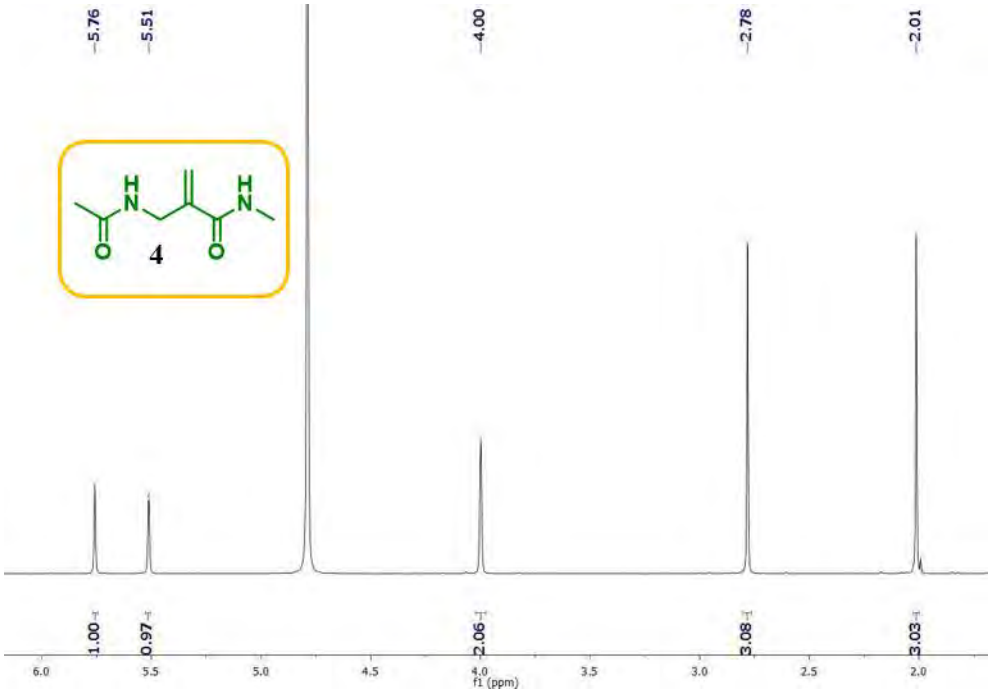

^{13}C NMR 100 MHz in D_2O

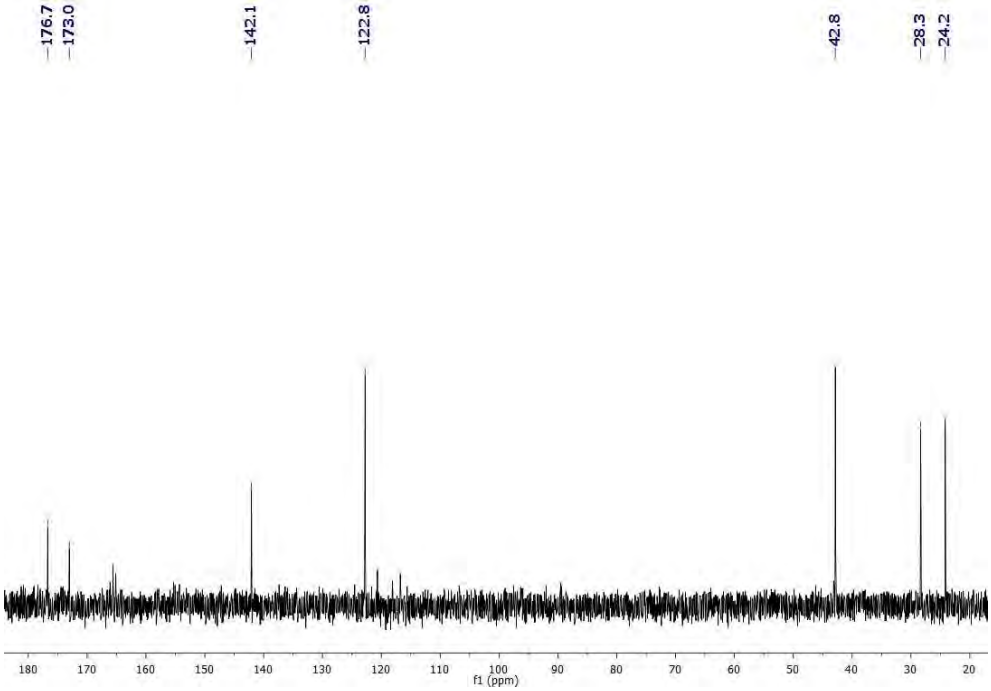

^{1}H NMR 400 MHz in $CDCl_3$

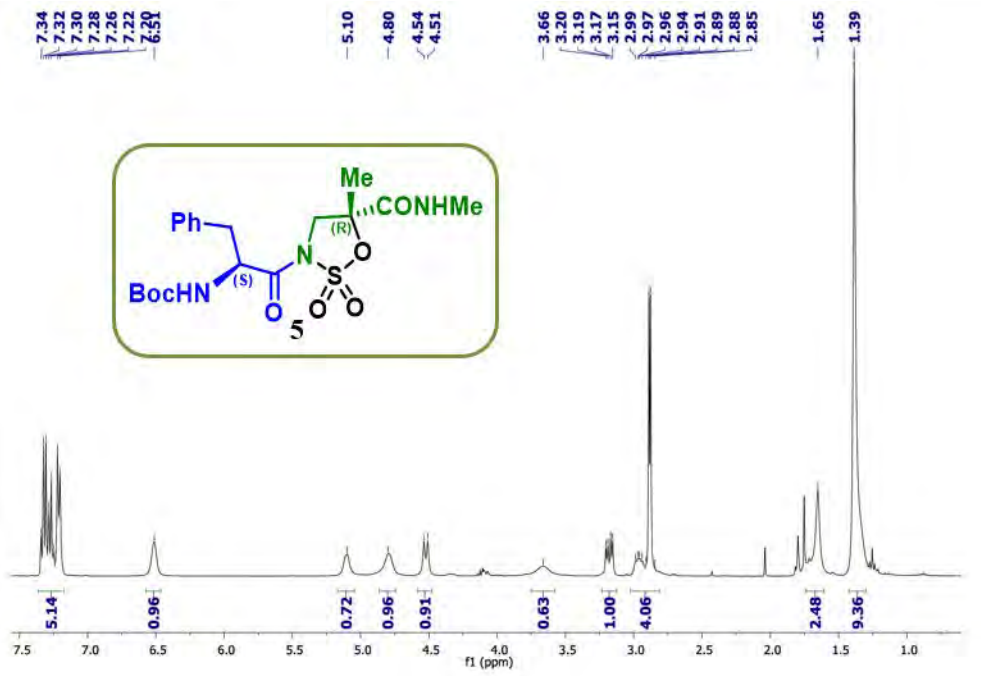

^{13}C NMR 100 MHz in $CDCl_3$

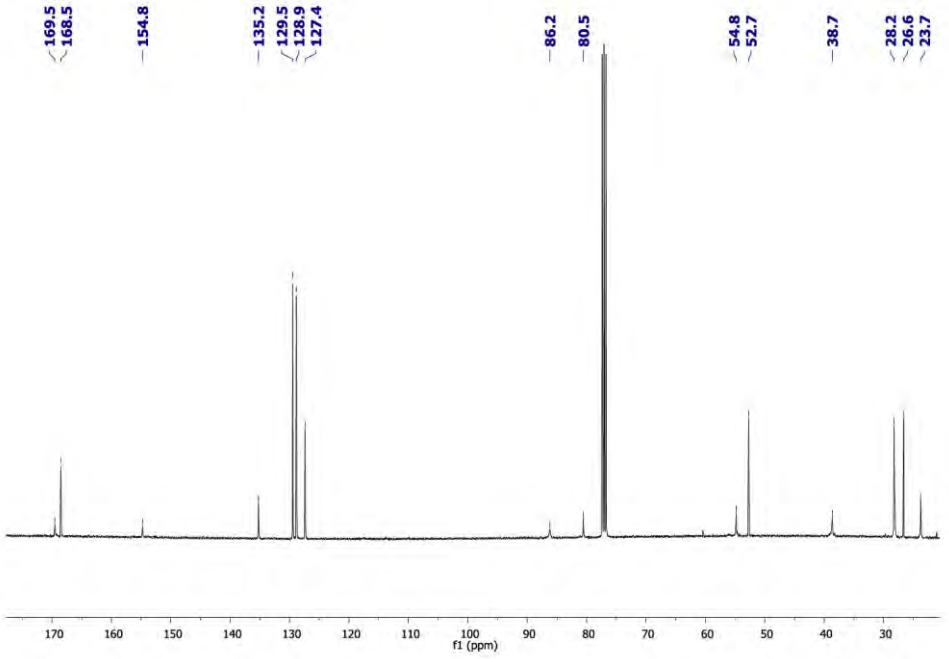

^{1}H NMR 400 MHz in $CDCl_3$

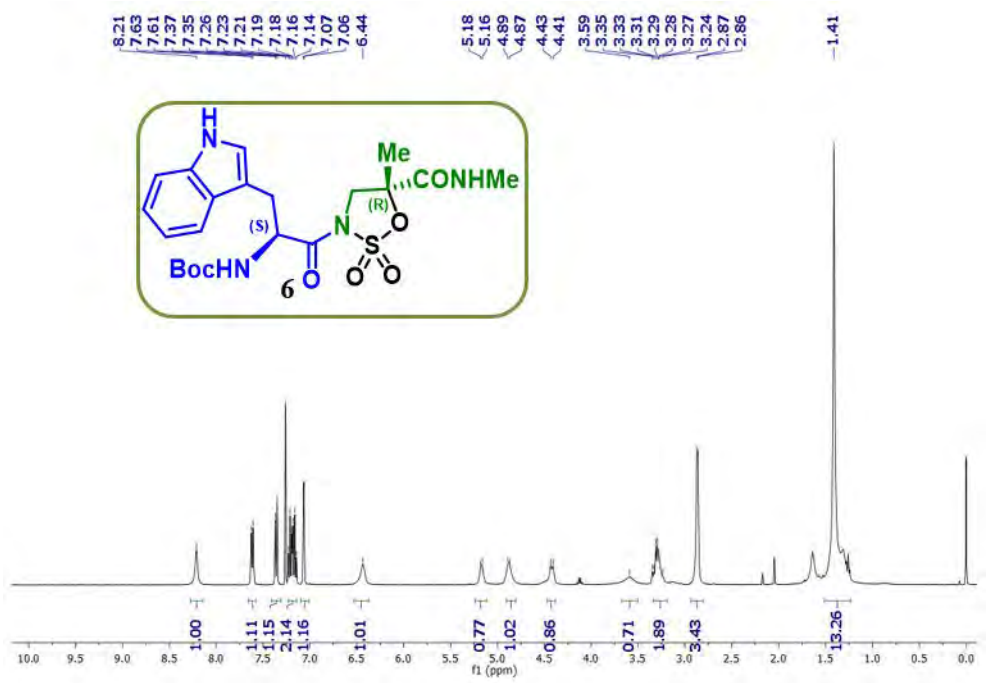

^{13}C NMR 100 MHz in $CDCl_3$

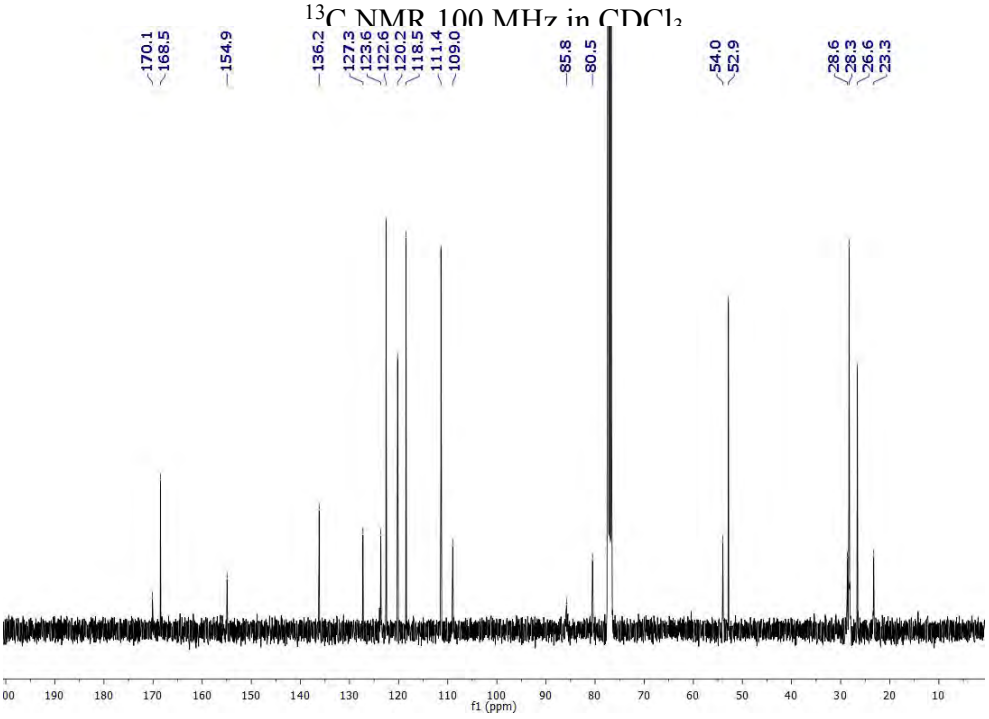

^{1}H NMR 400 MHz in $CDCl_3$

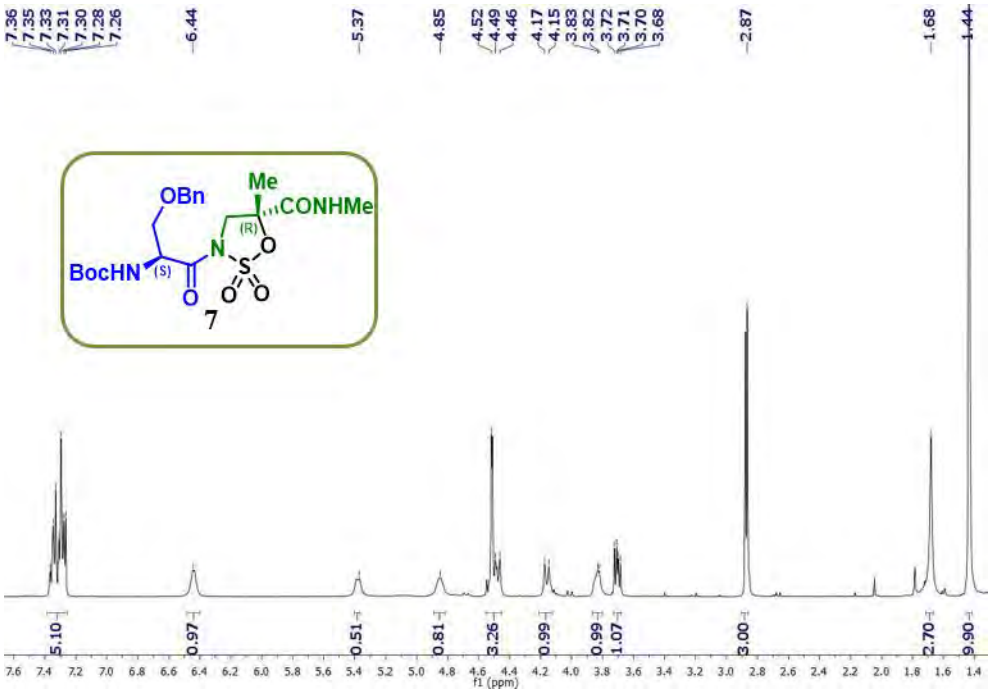

^{13}C NMR 100 MHz in $CDCl_3$

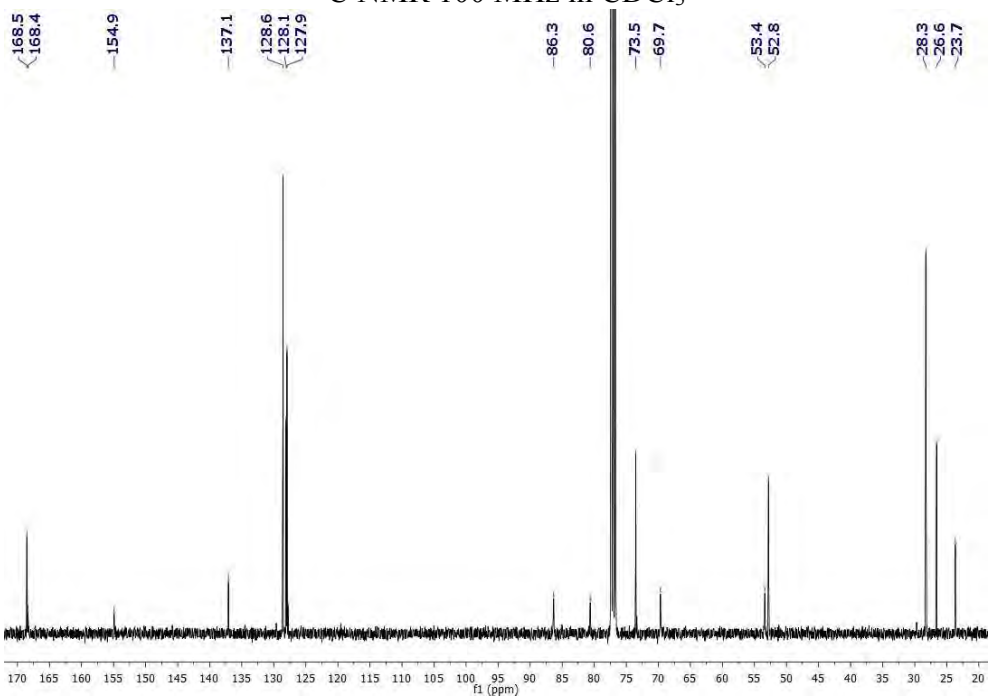

^{1}H NMR 400 MHz in $CDCl_3$

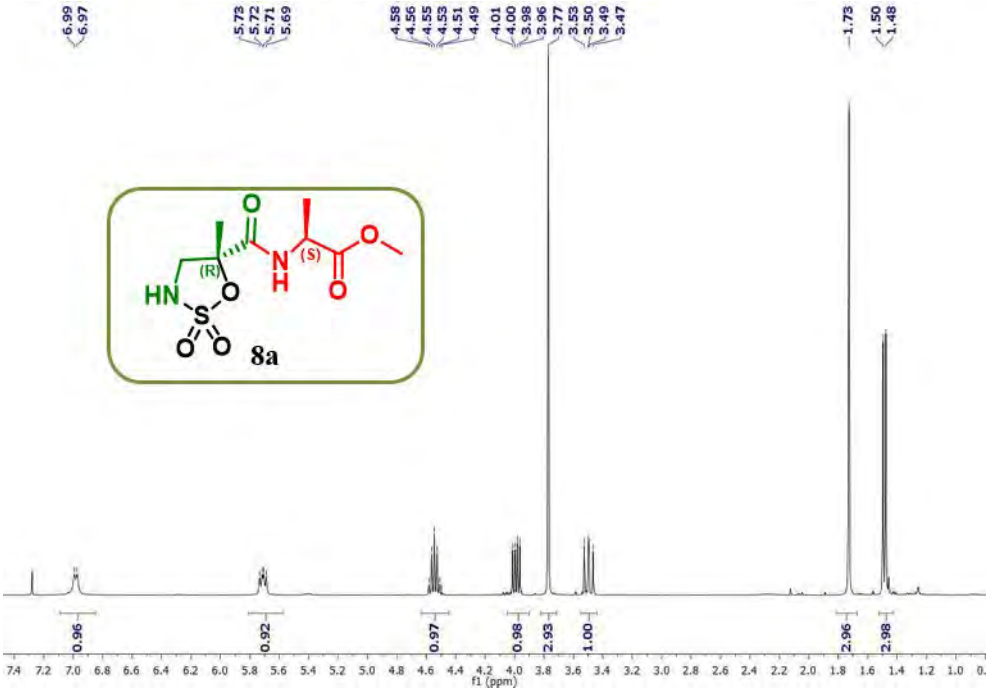

^{13}C NMR 100 MHz in $CDCl_3$

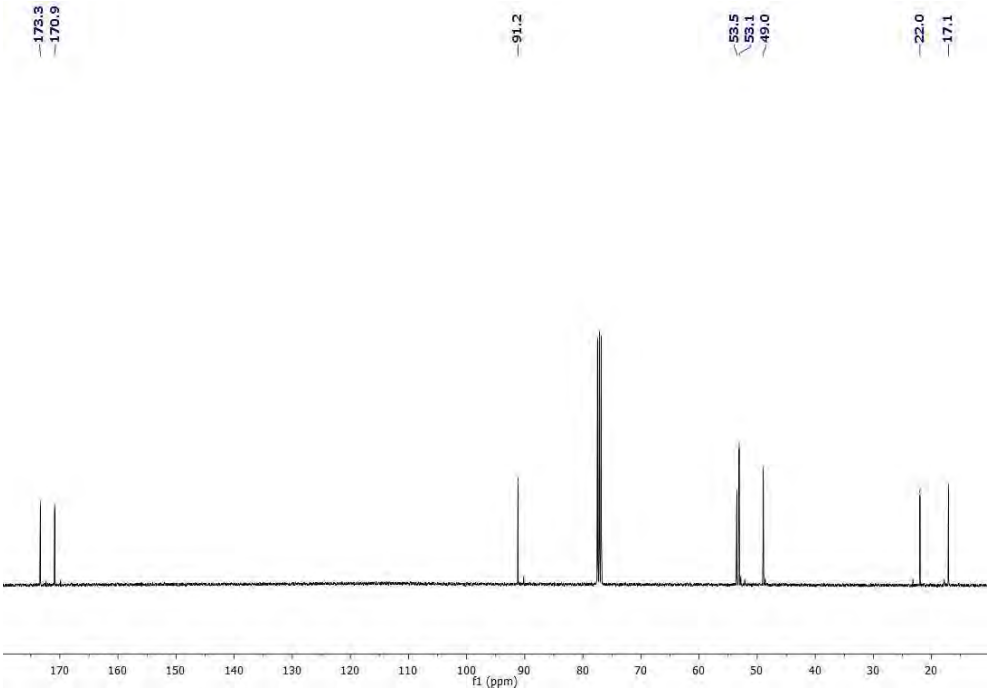

^{1}H NMR 400 MHz in $CDCl_3$

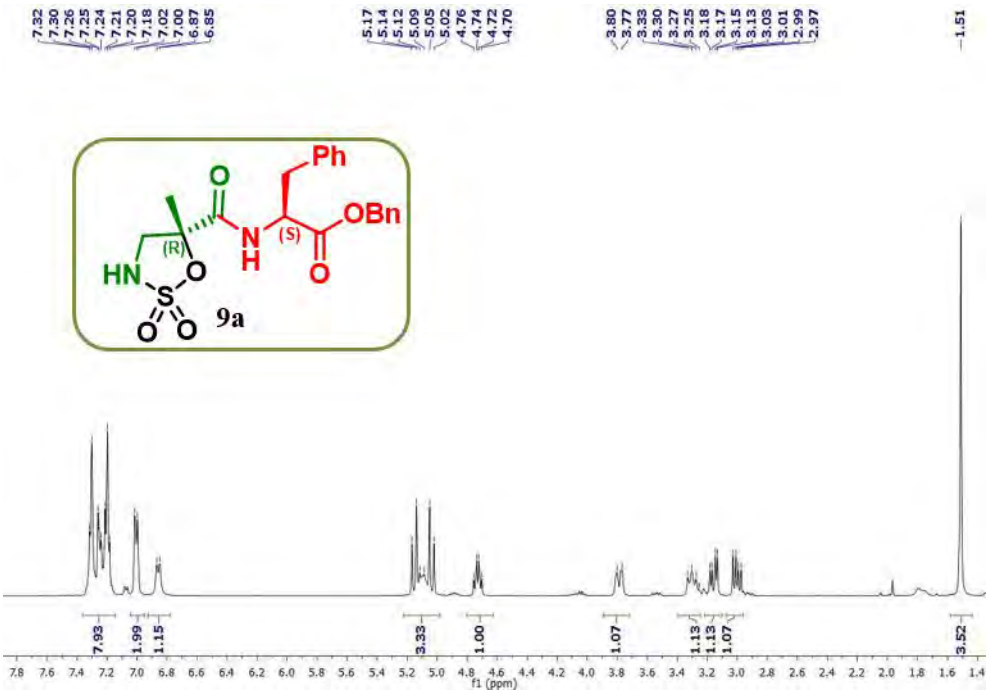

^{13}C NMR 100 MHz in $CDCl_3$

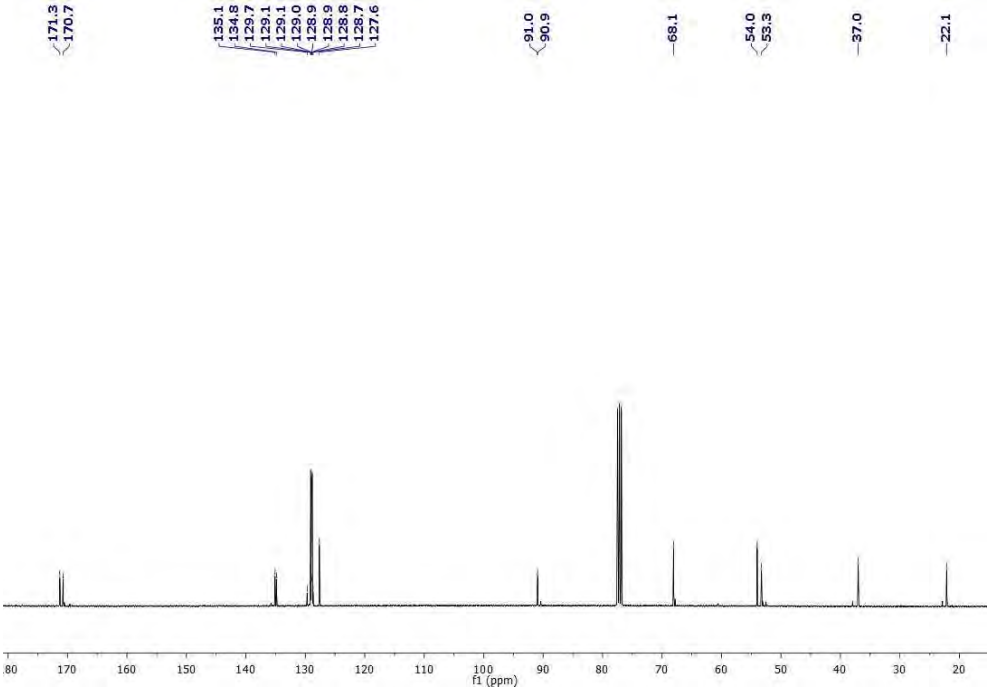

^{1}H NMR 400 MHz in $CDCl_3$

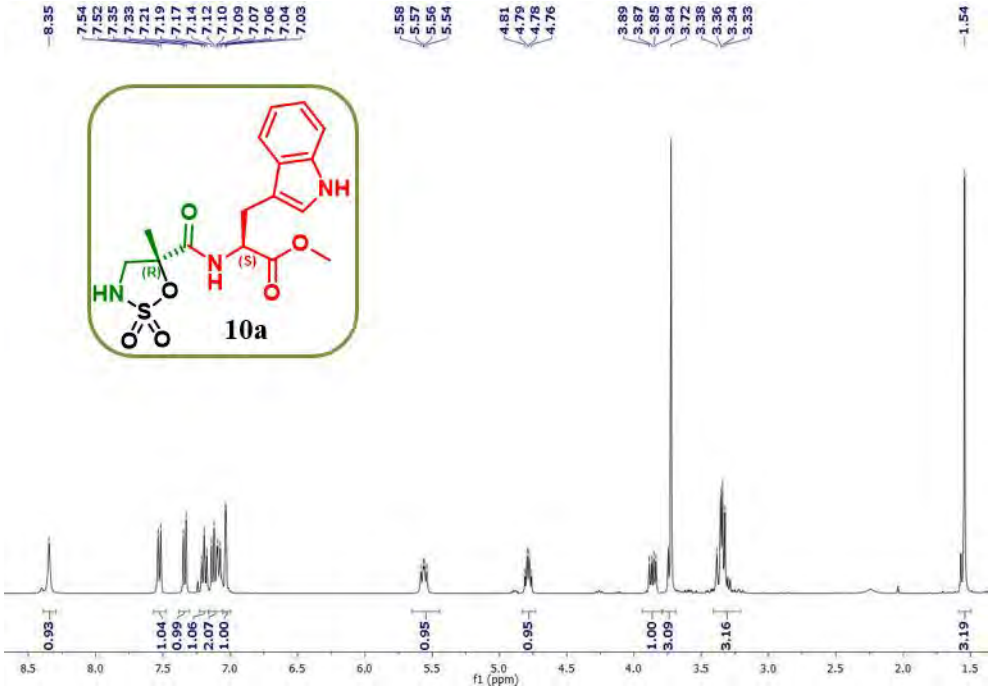

^{13}C NMR 100 MHz in $CDCl_3$

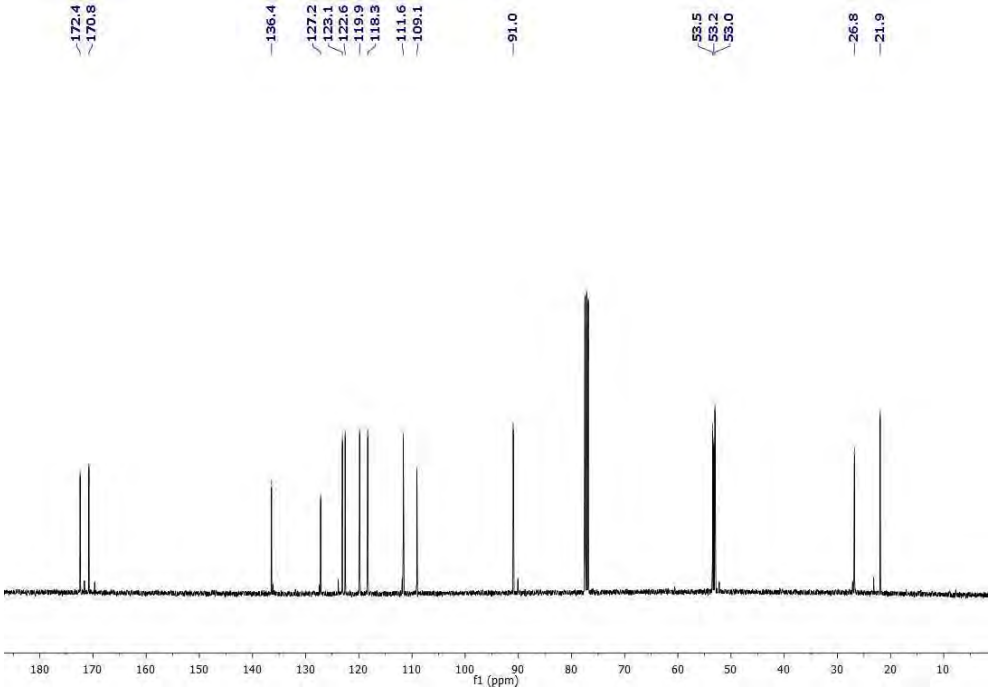

^{1}H NMR 400 MHz in $CDCl_3$

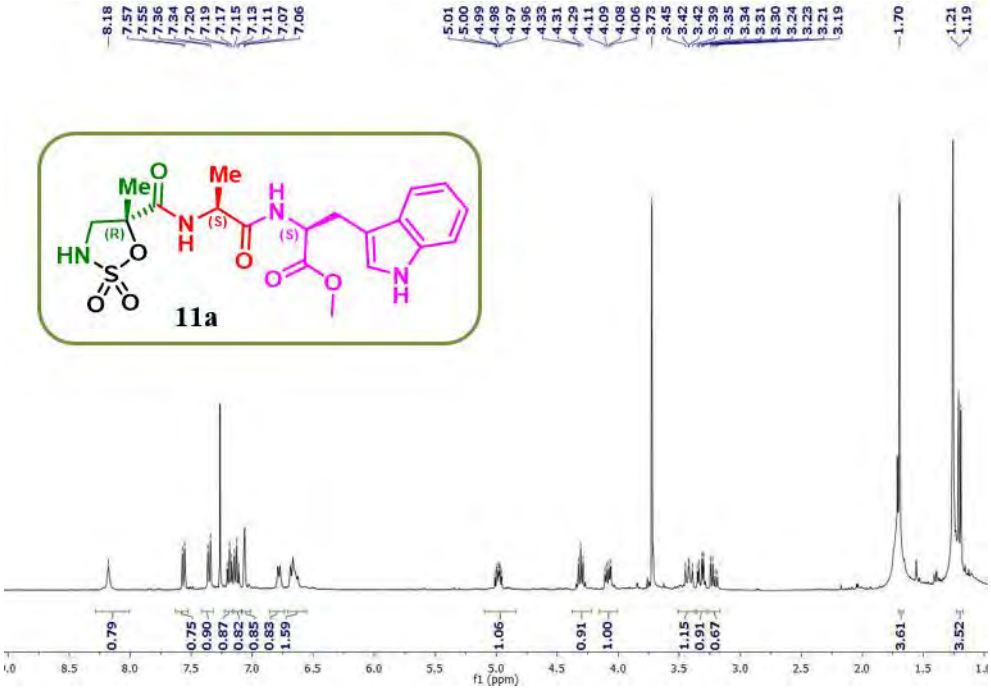

^{13}C NMR 100 MHz in $CDCl_3$

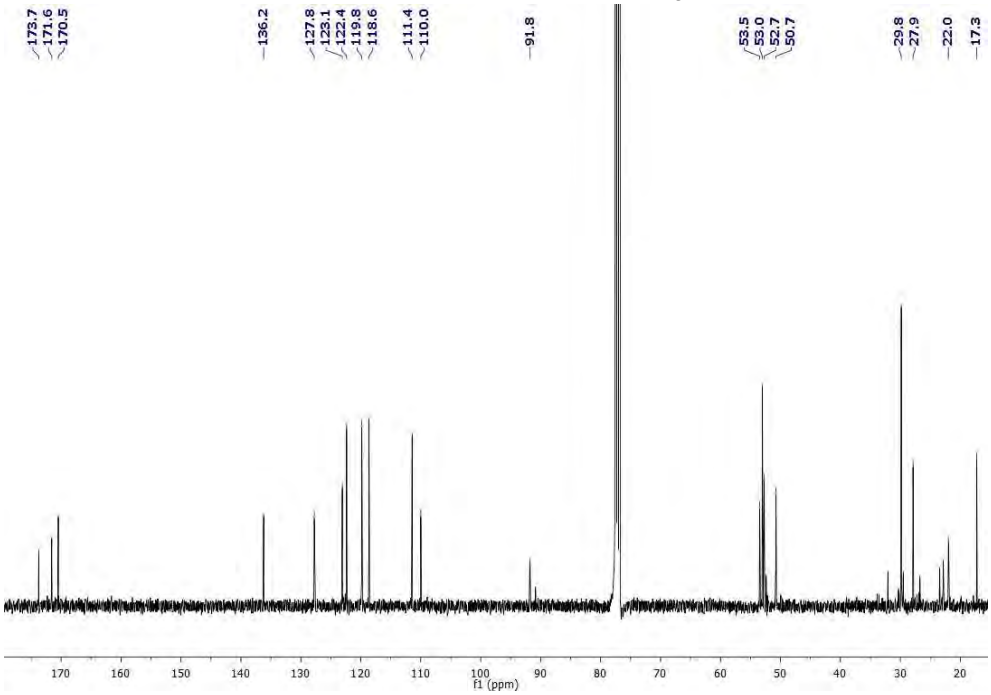

^{1}H NMR 400 MHz in $CDCl_3$

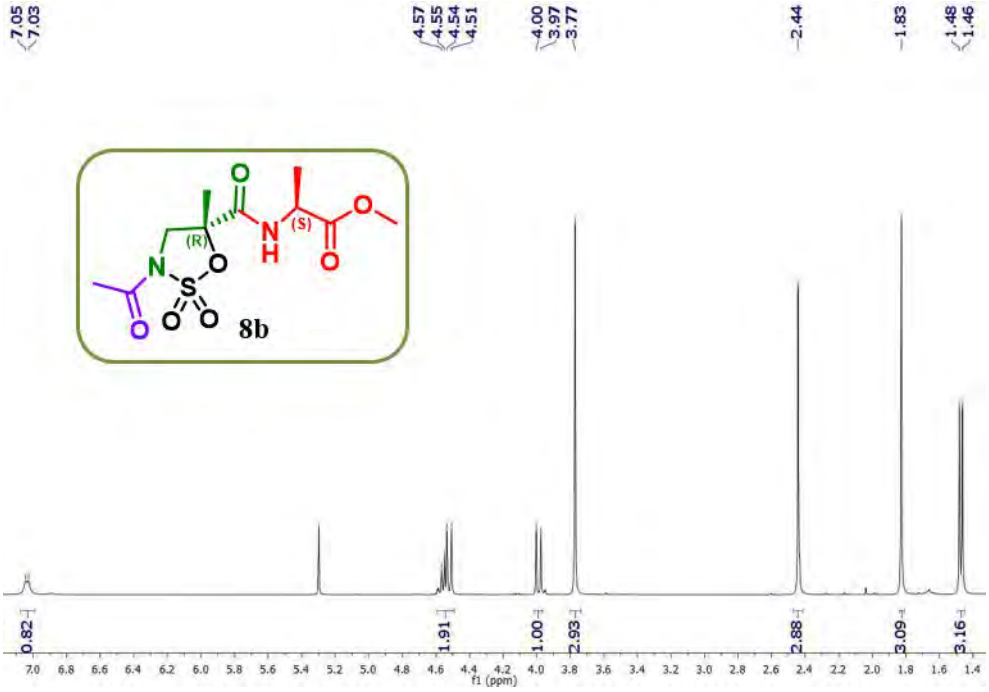

^{13}C NMR 100 MHz in $CDCl_3$

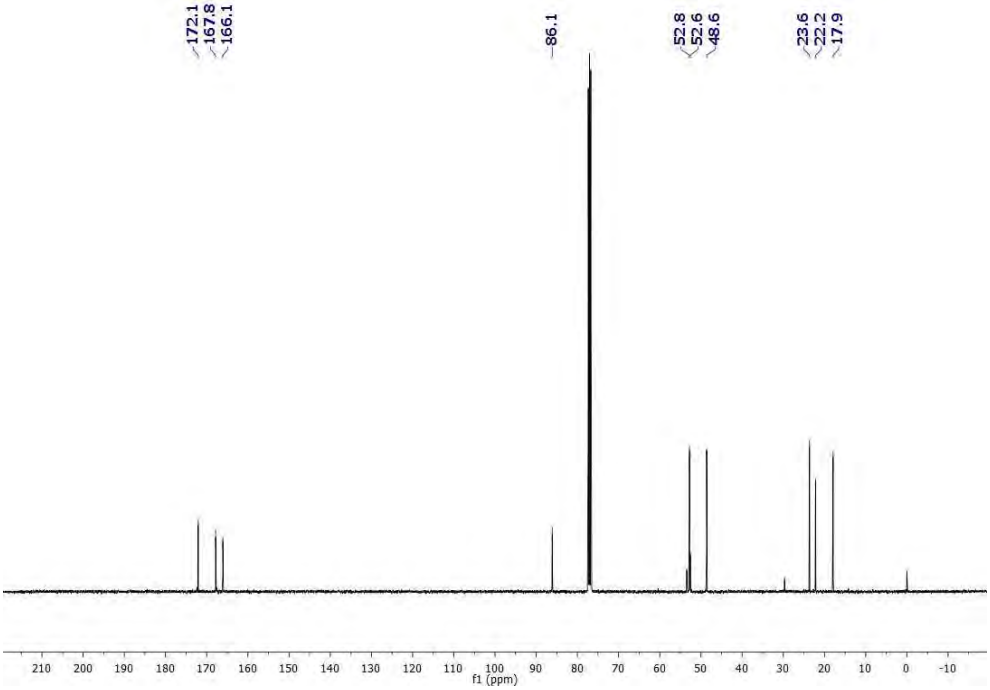

^{1}H NMR 400 MHz in $CDCl_3$

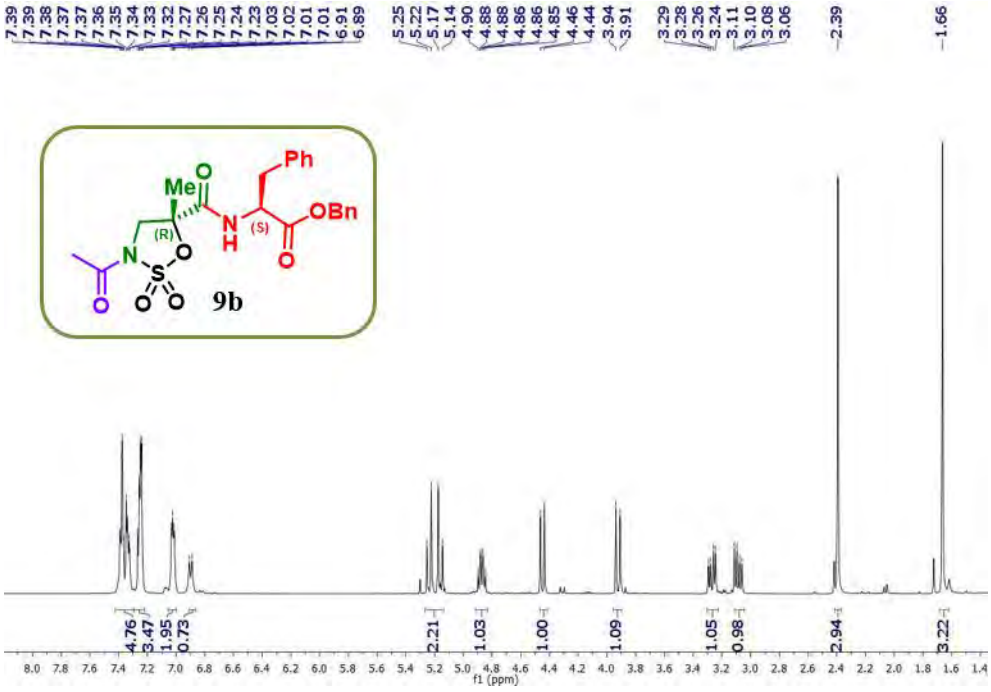

^{13}C NMR 100 MHz in $CDCl_3$

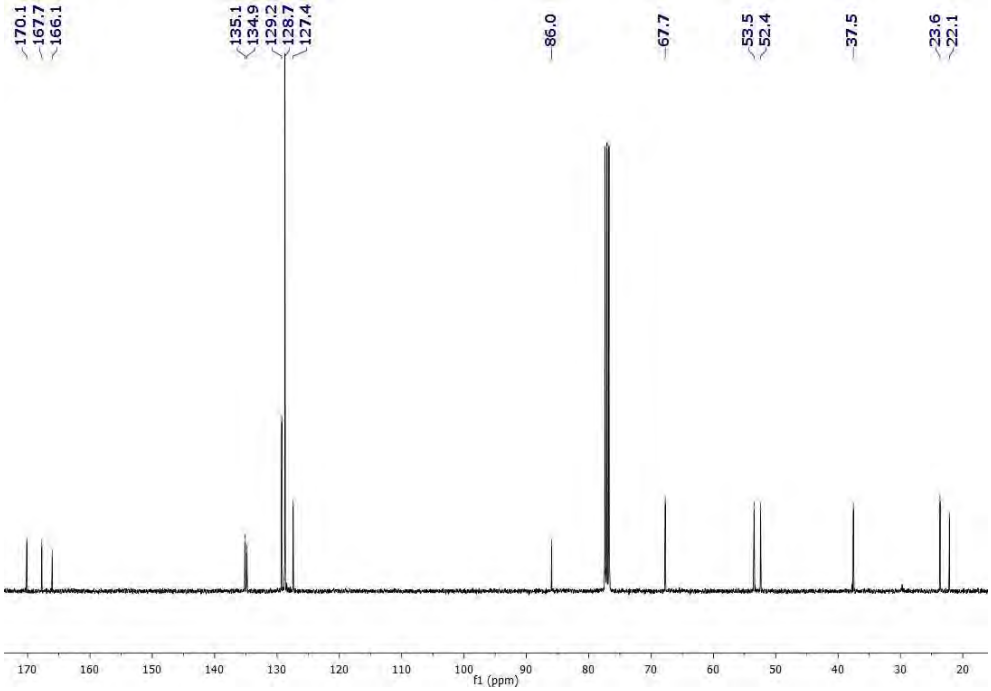

^{1}H NMR 400 MHz in $CDCl_3$

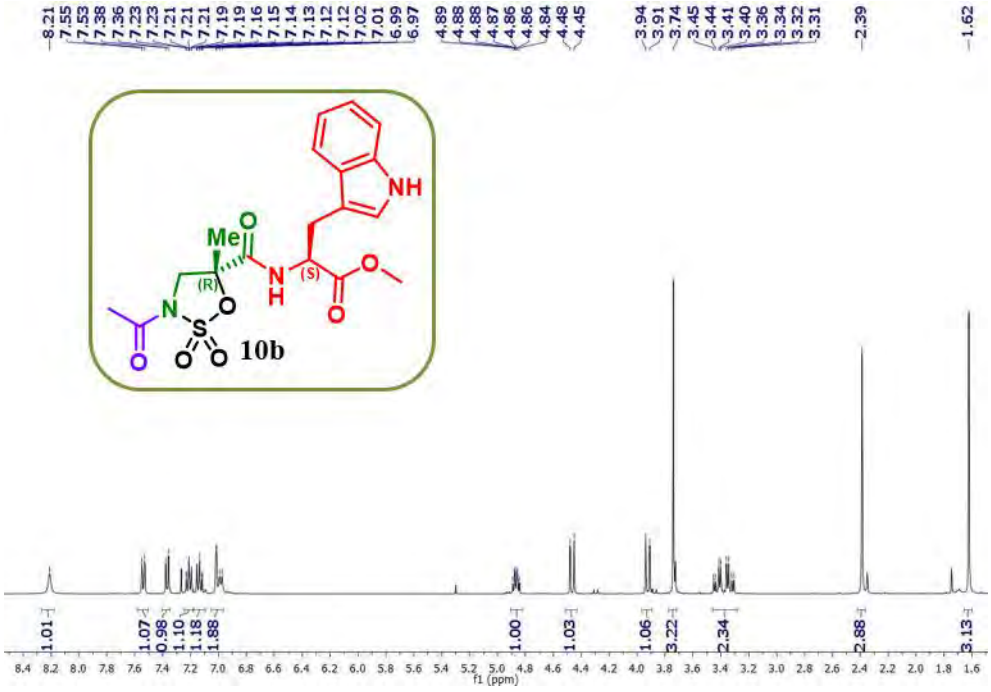

^{13}C NMR 100 MHz in $CDCl_3$

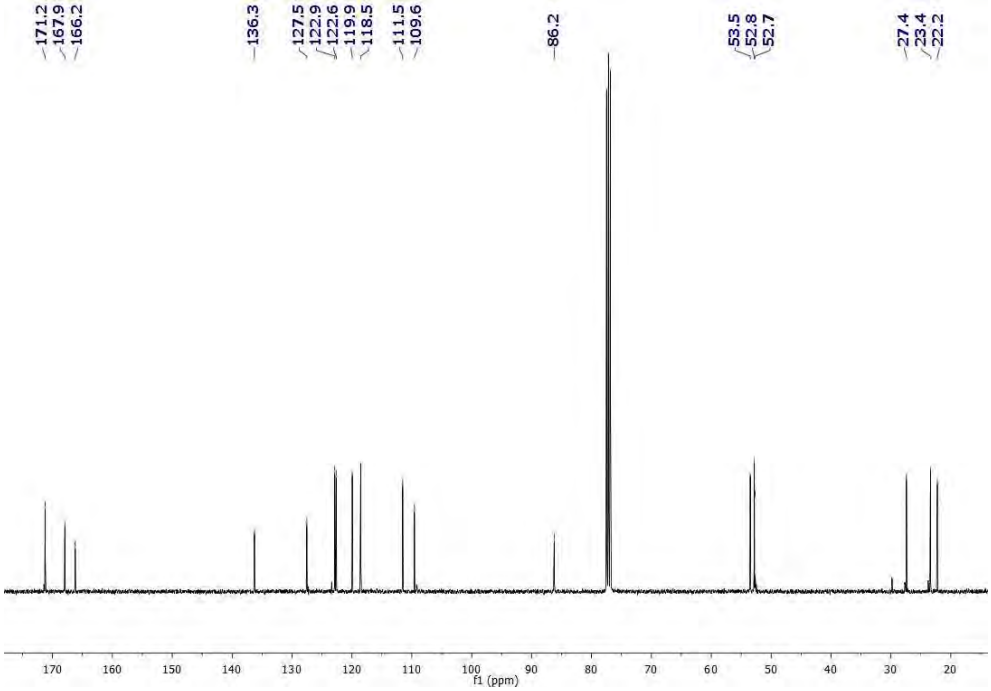

^{1}H NMR 400 MHz in $CDCl_3$

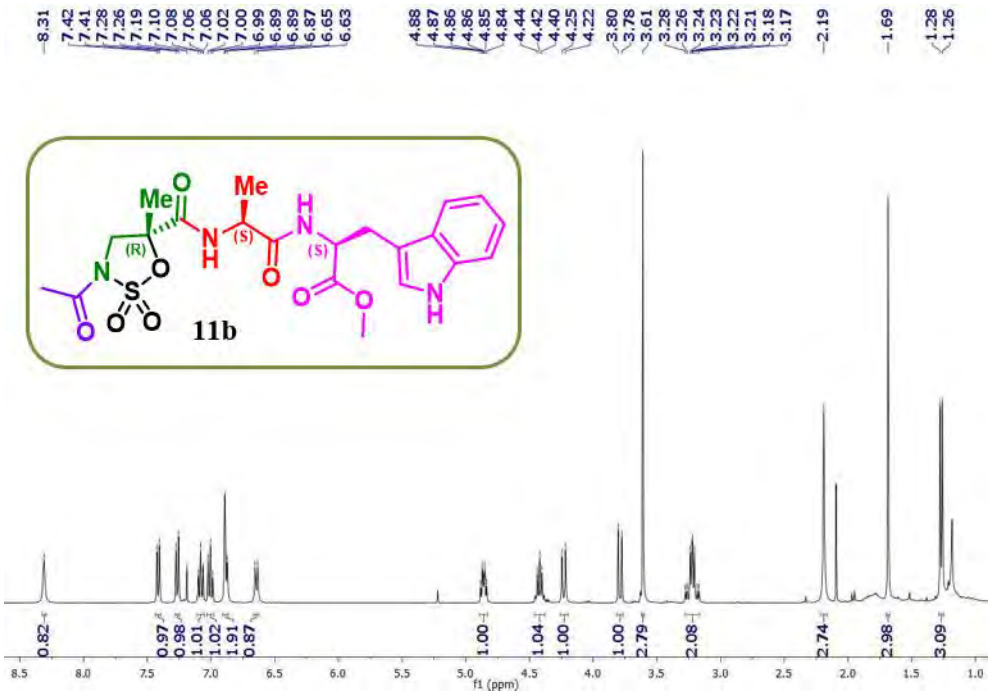

^{13}C NMR 100 MHz in $CDCl_3$

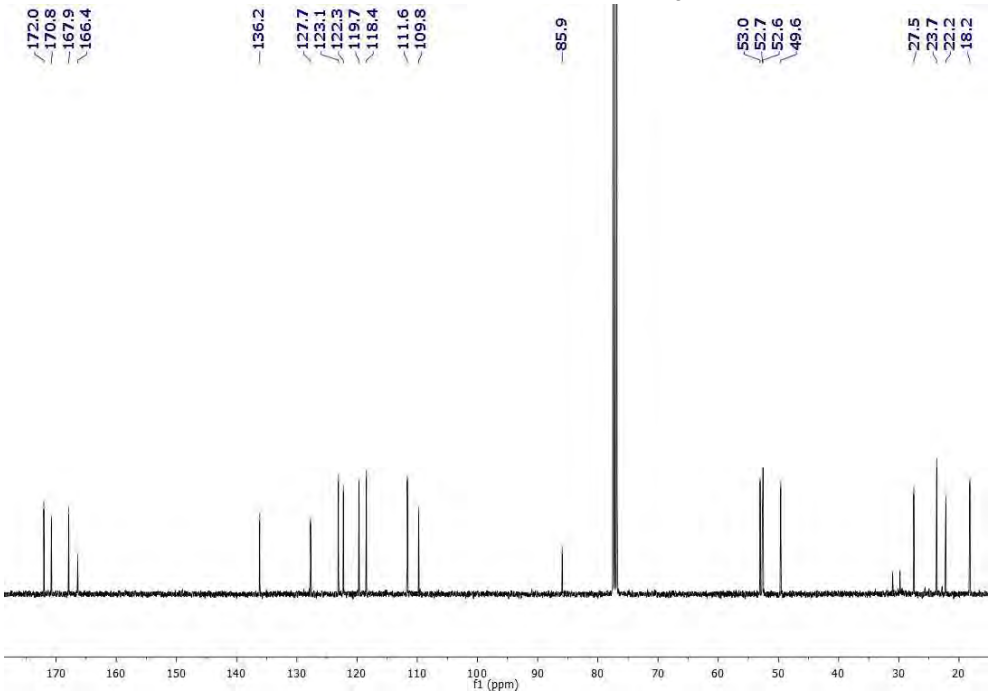

^{1}H NMR 400 MHz in $CDCl_3$

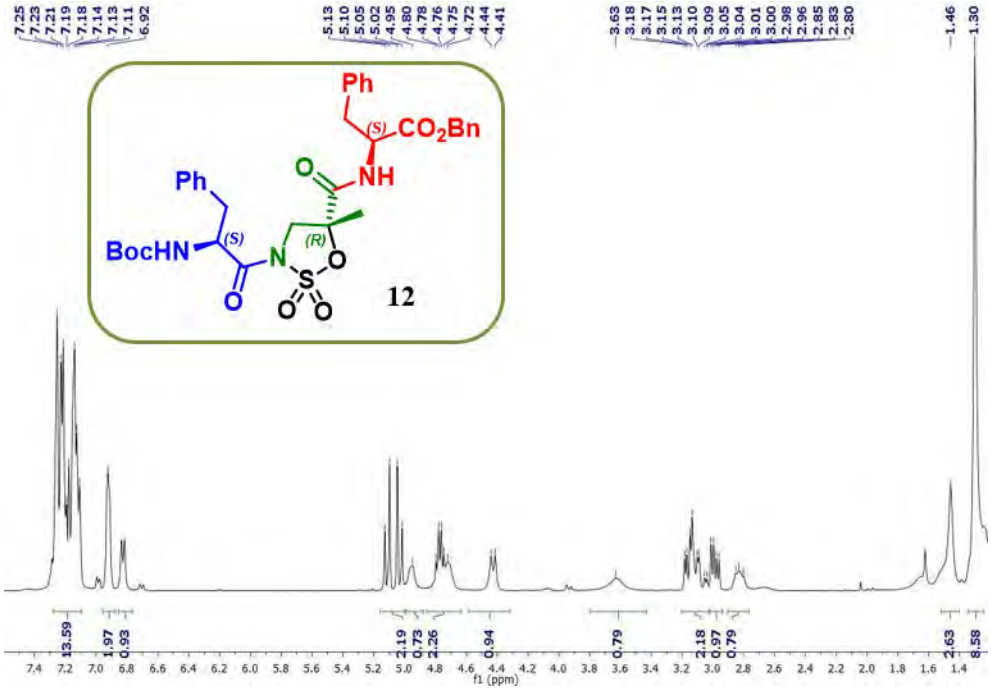

^{13}C NMR 100 MHz in $CDCl_3$

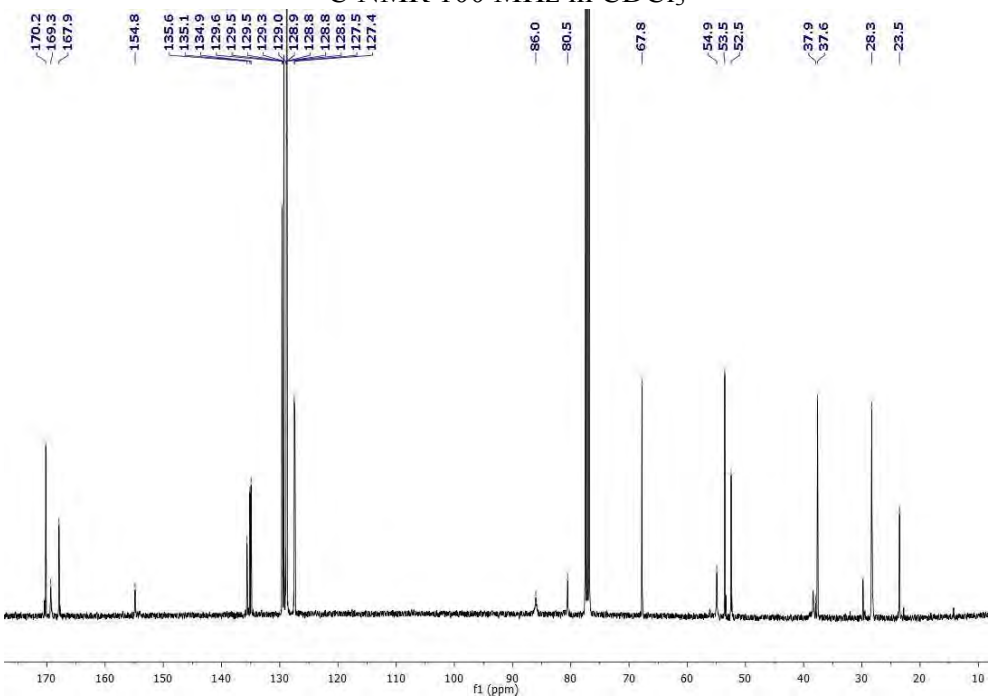

^{1}H NMR 400 MHz in $CDCl_3$

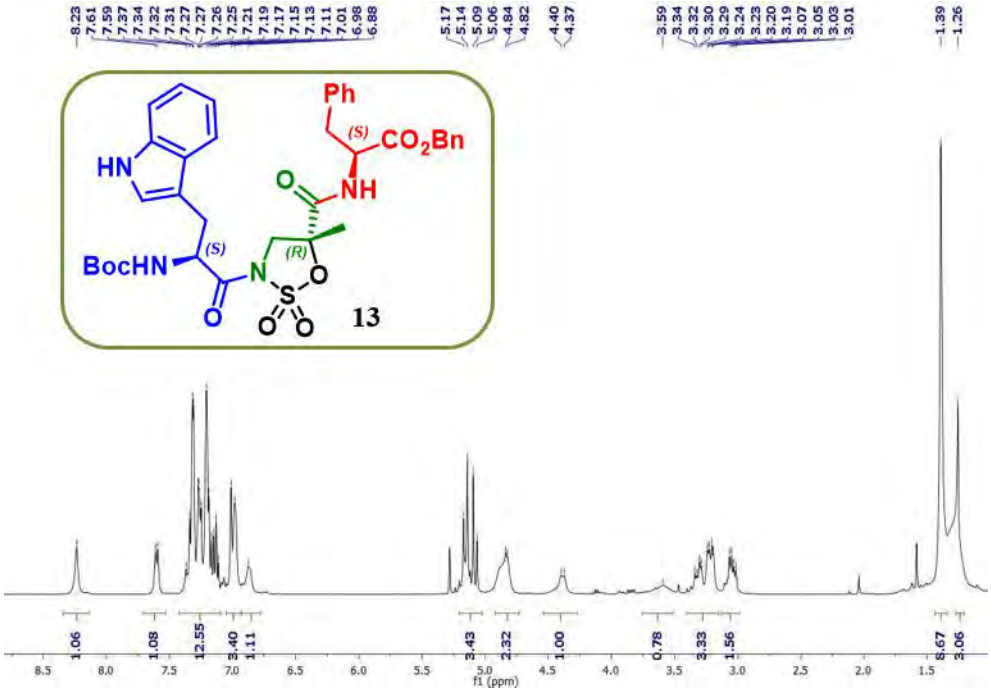

^{13}C NMR 100 MHz in $CDCl_3$

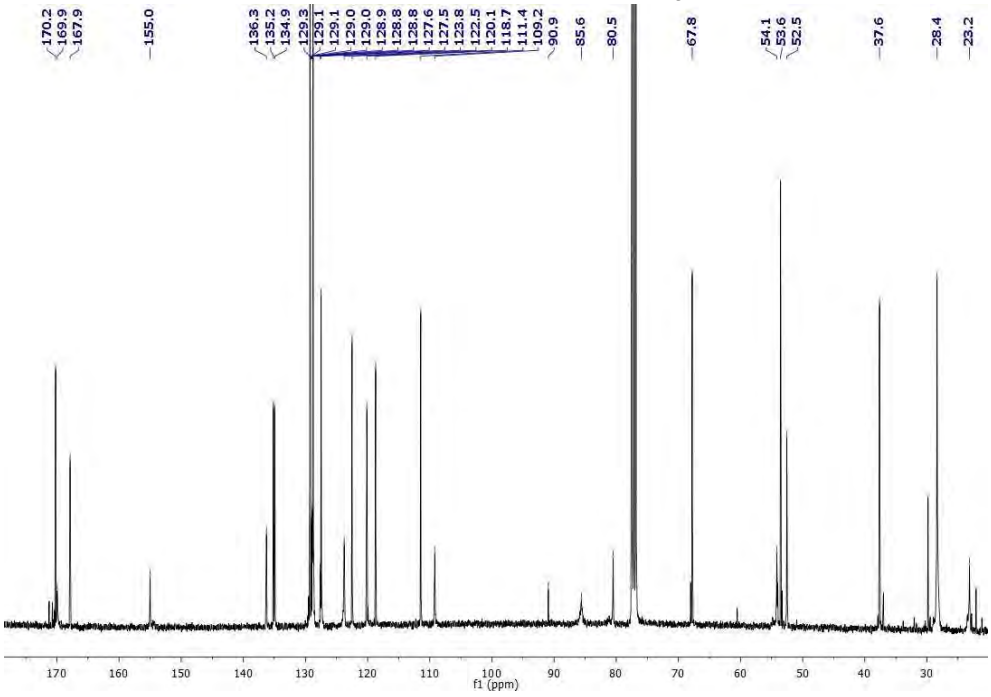

^{1}H NMR 400 MHz in D_2O

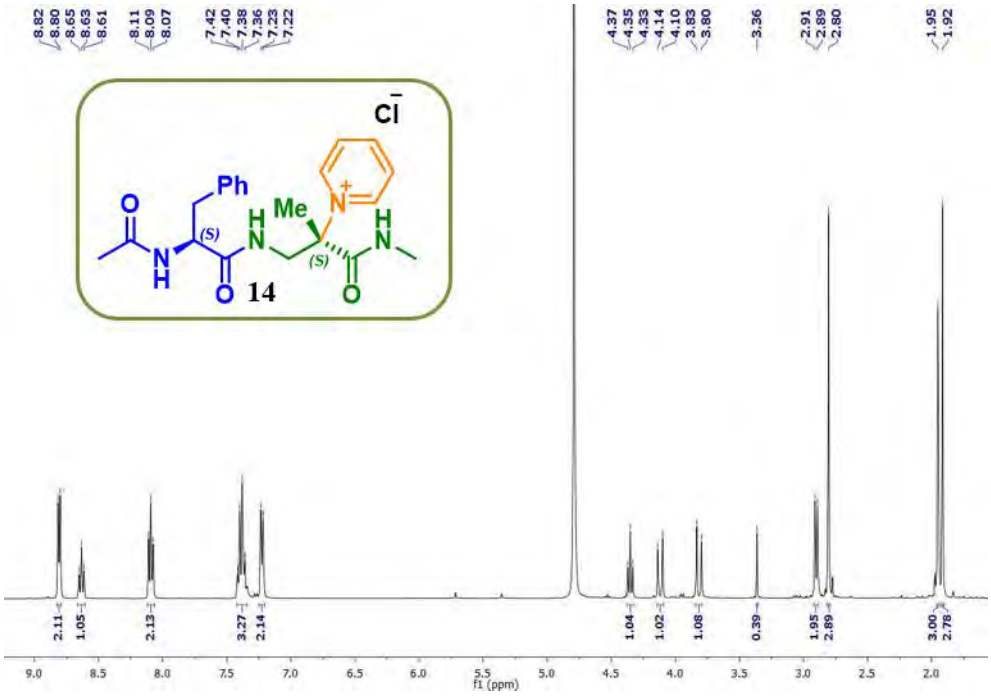

^{13}C NMR 100 MHz in D_2O

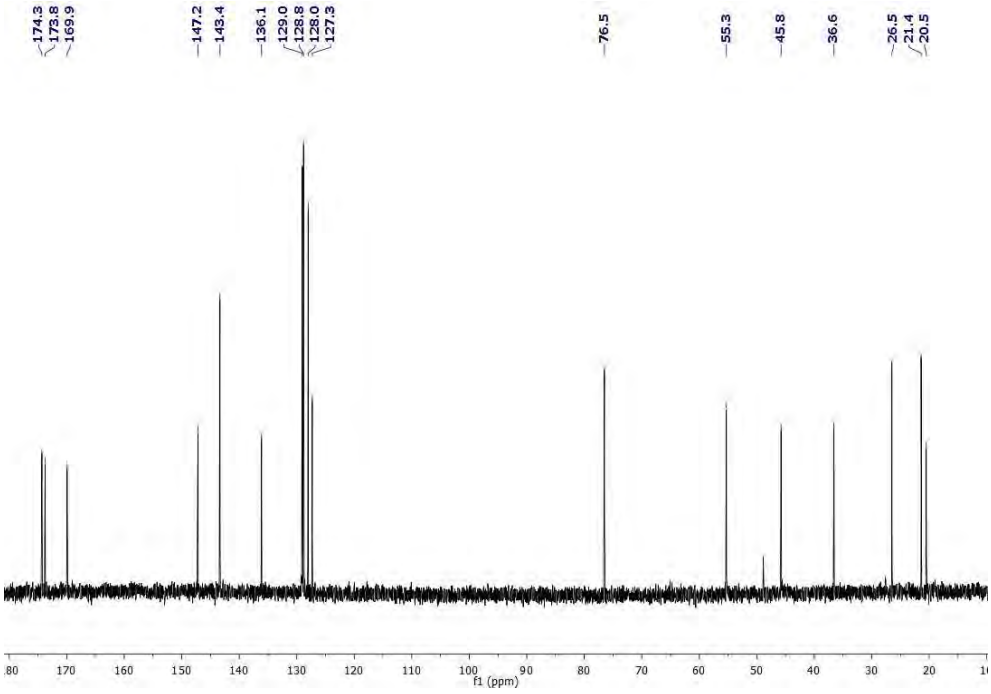

NOESY 400 MHz in H_2O/D_2O

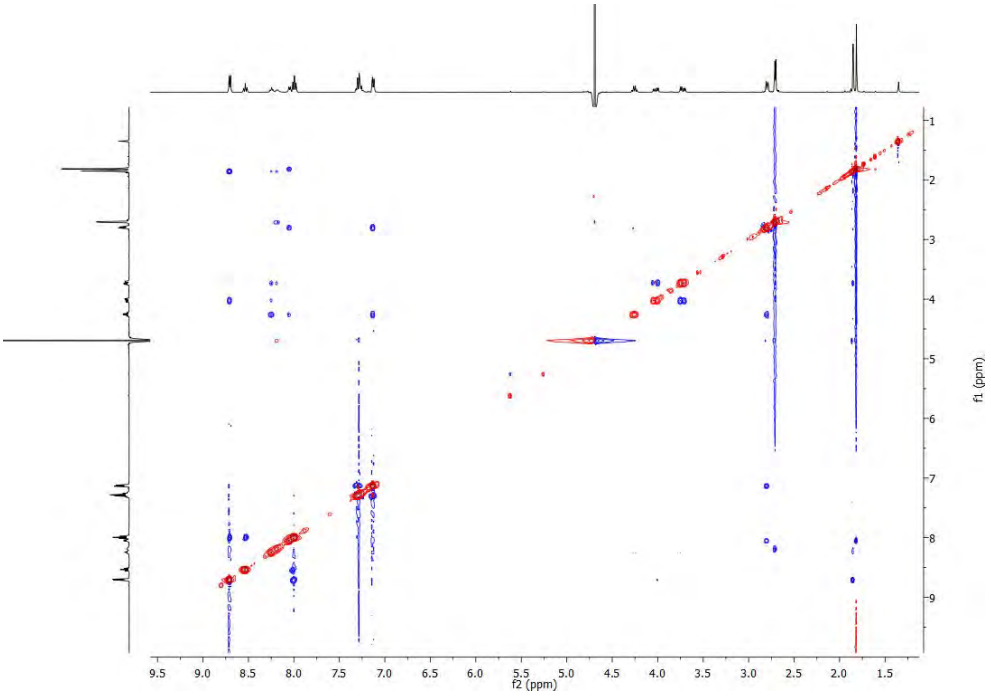

^{1}H NMR 400 MHz in D_2O

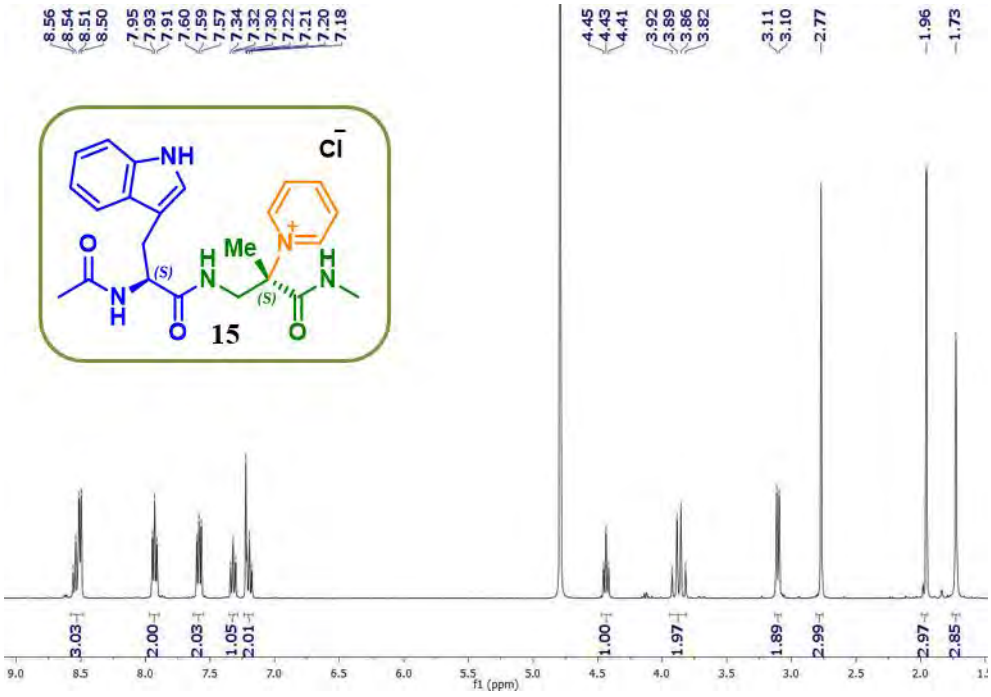

^{13}C NMR 100 MHz in D_2O

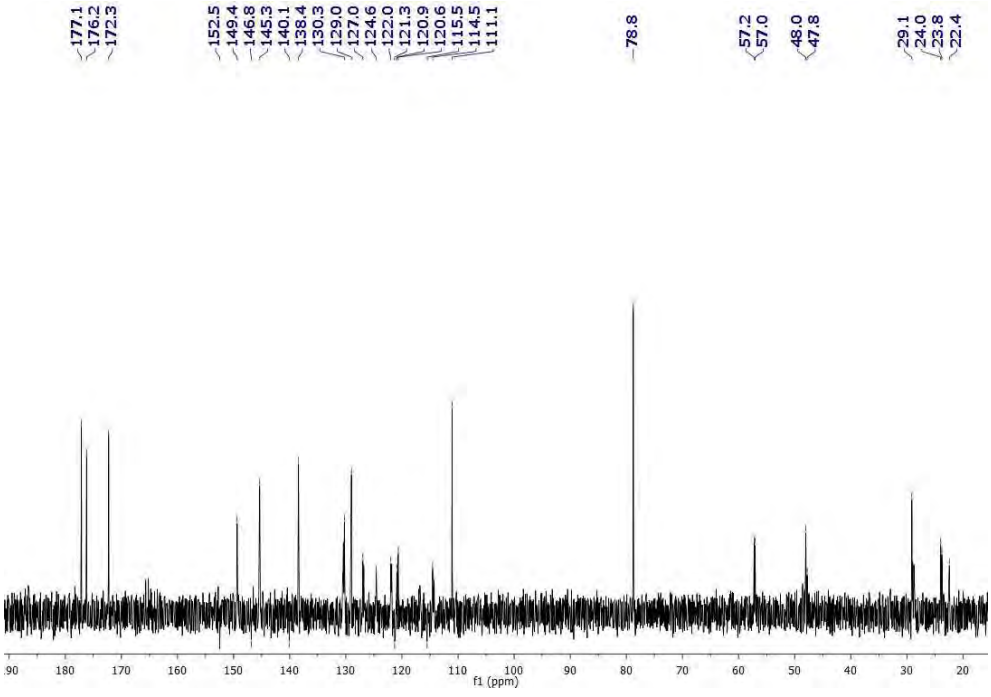

NOESY 400 MHz in H_2O/D_2O

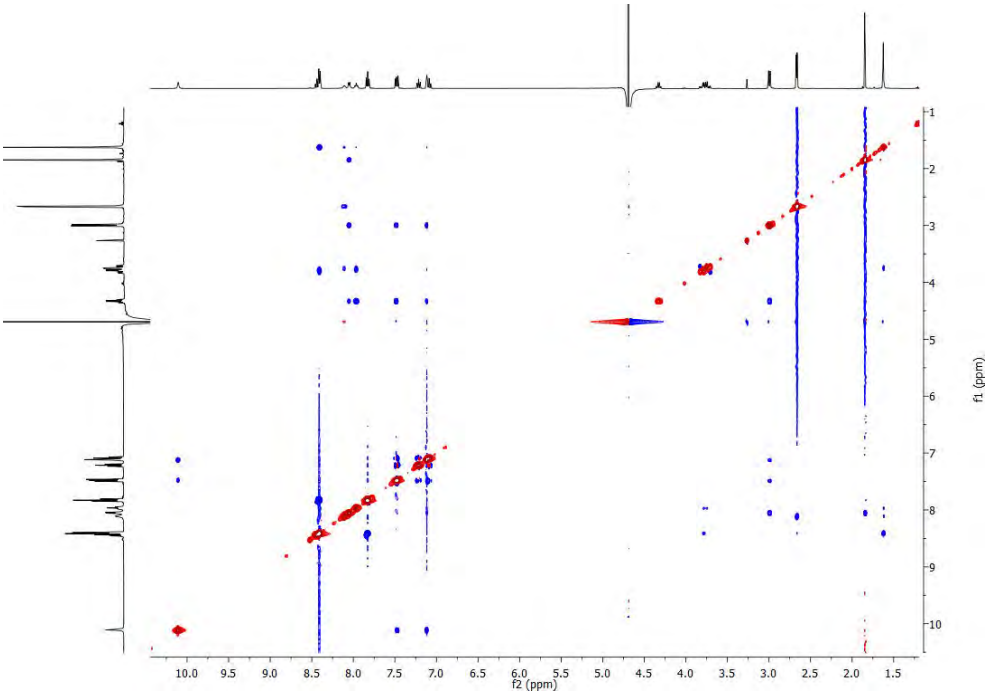

^{1}H NMR 400 MHz in D_2O

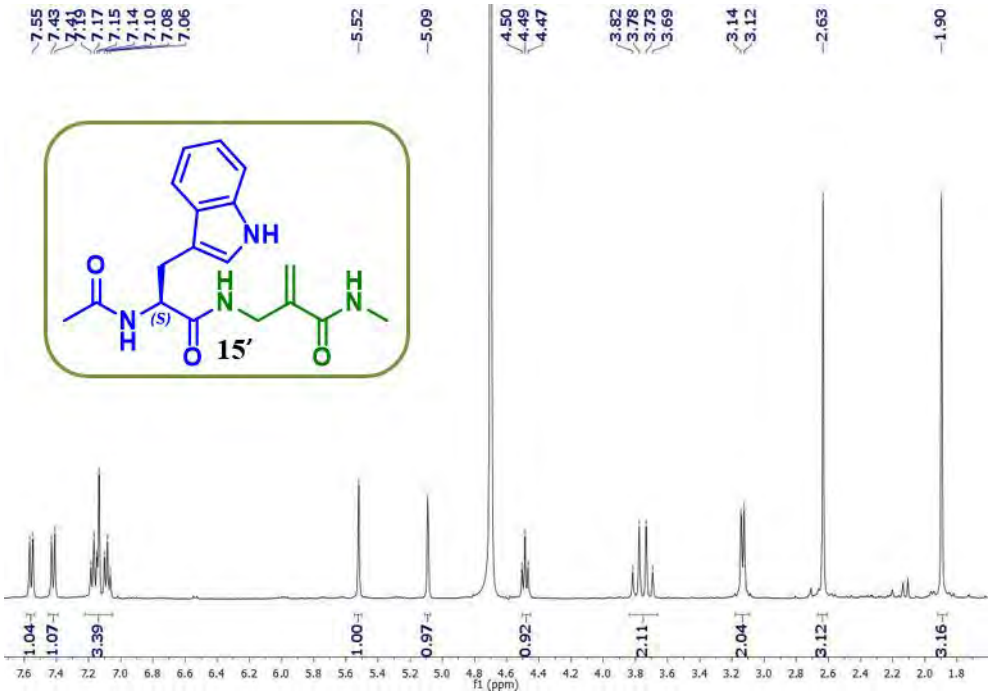

^{13}C NMR 100 MHz in D_2O

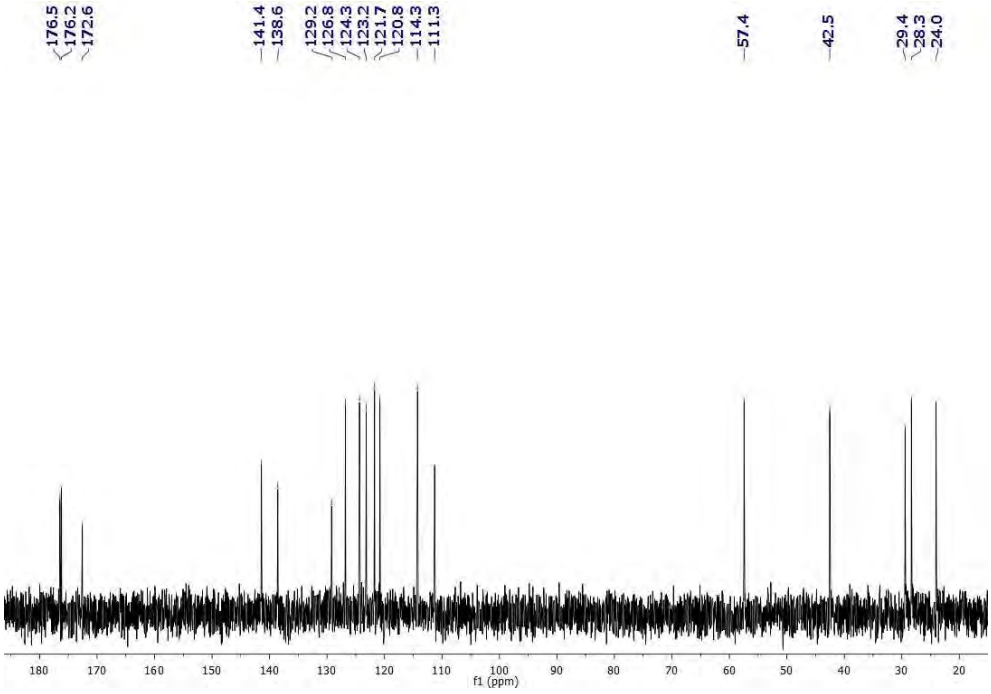

^{1}H NMR 400 MHz in D_2O

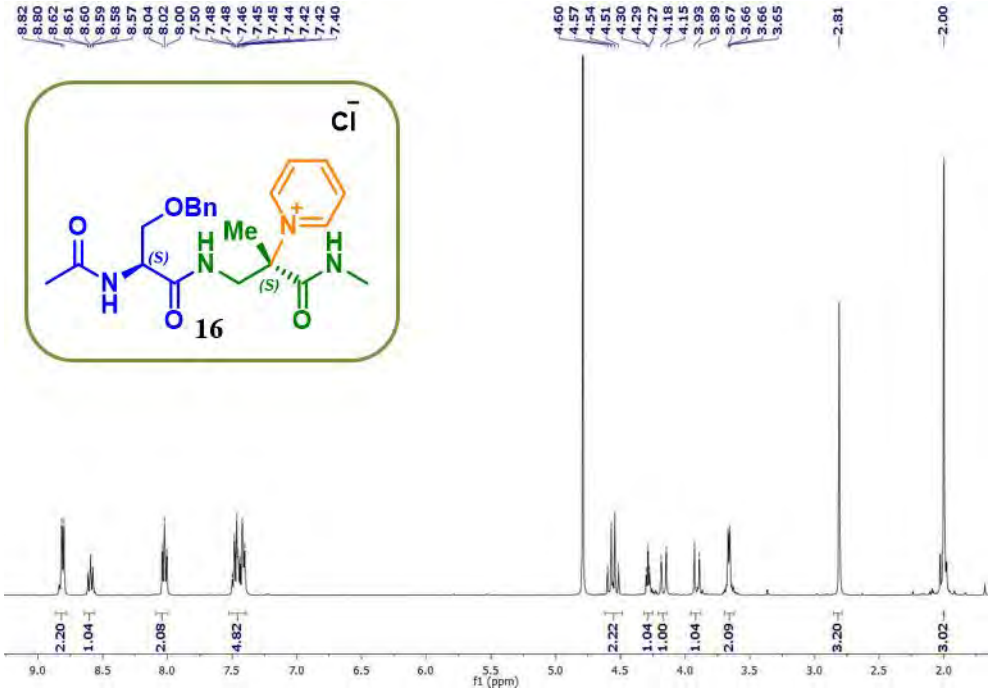

^{13}C NMR 100 MHz in D_2O

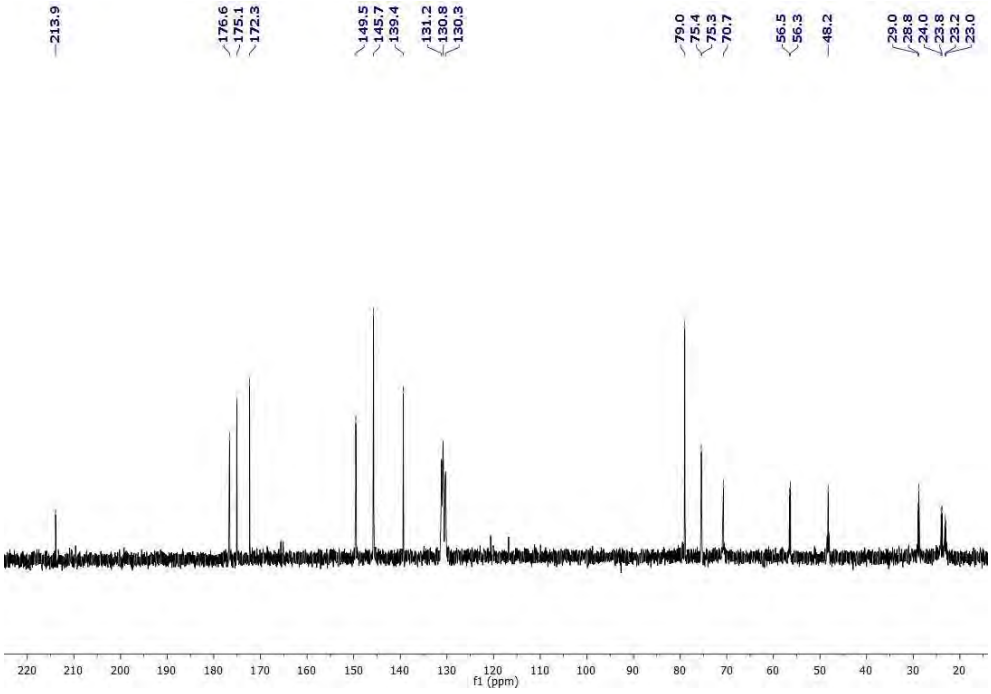

^{1}H NMR 400 MHz in D_2O

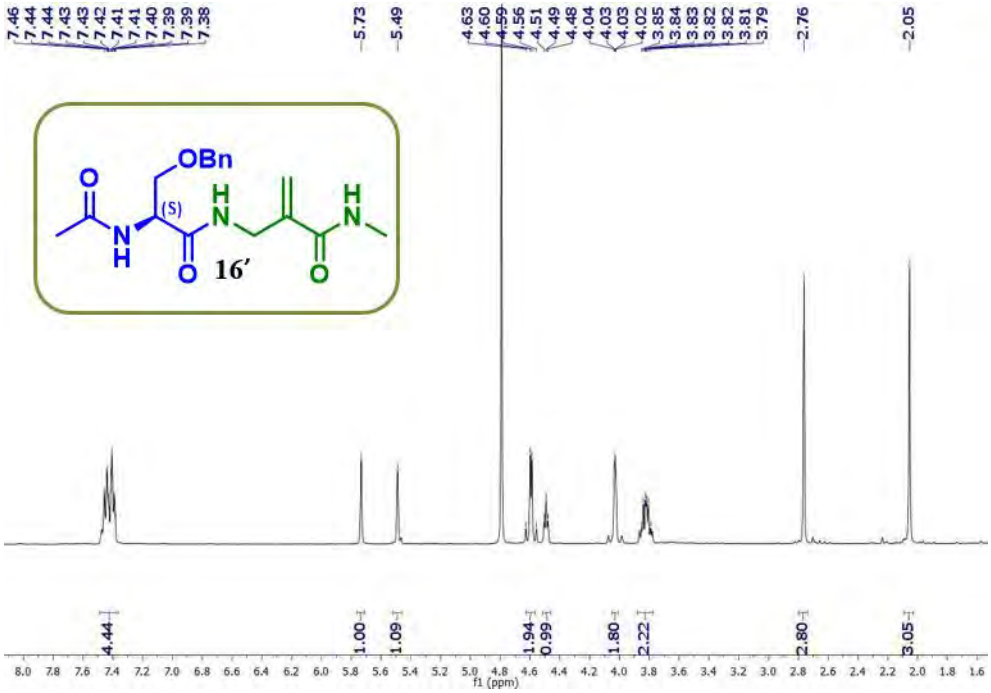

^{13}C NMR 100 MHz in D_2O

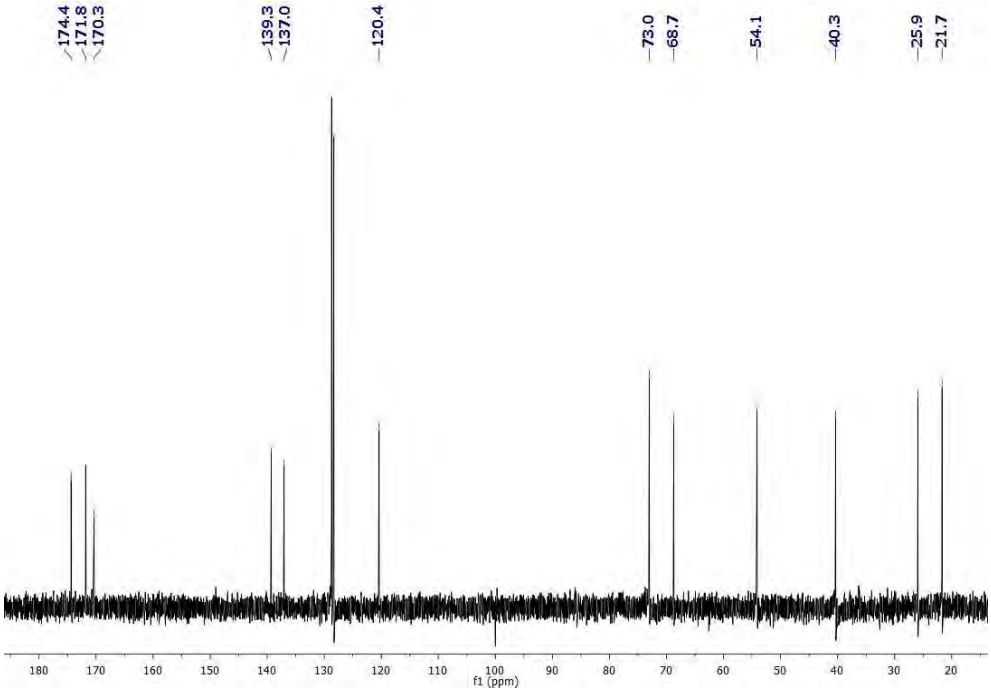

^{1}H NMR 400 MHz in D_2O

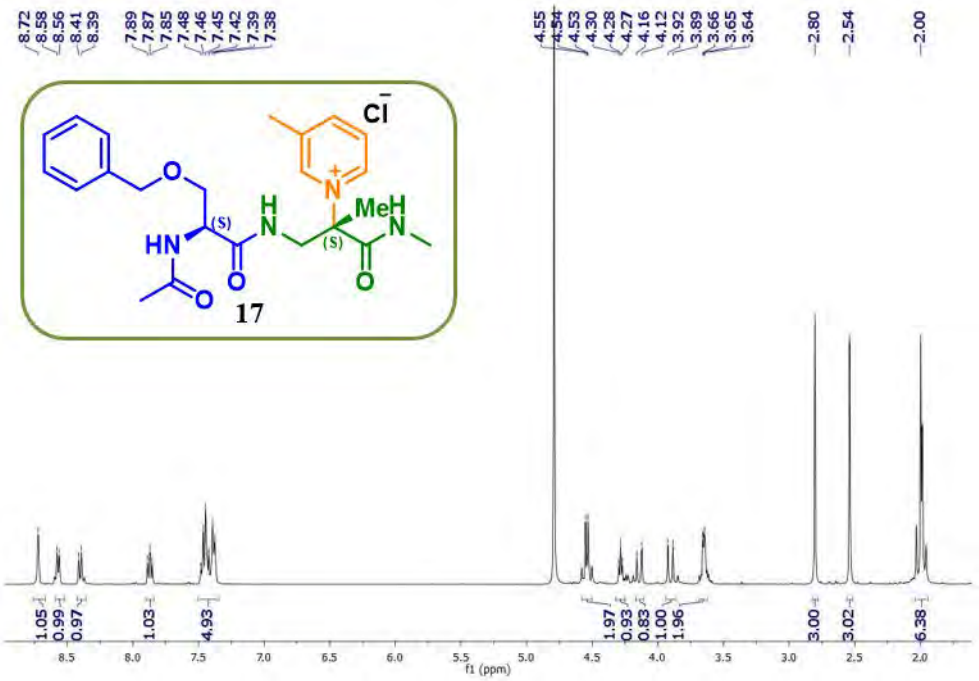

^{13}C NMR 100 MHz in D_2O

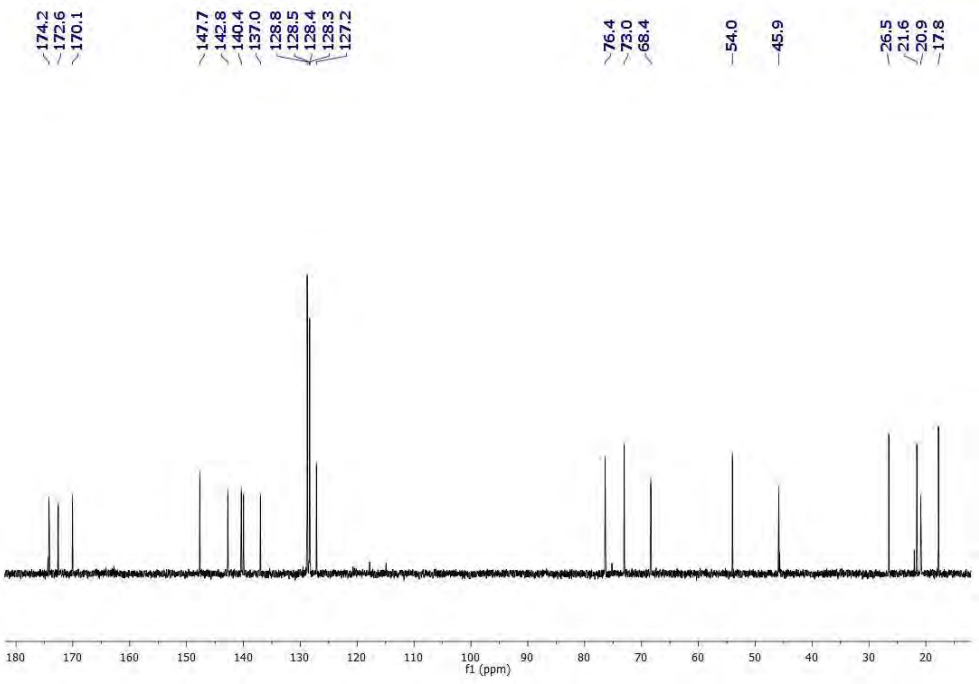

^{1}H NMR 400 MHz in D_2O

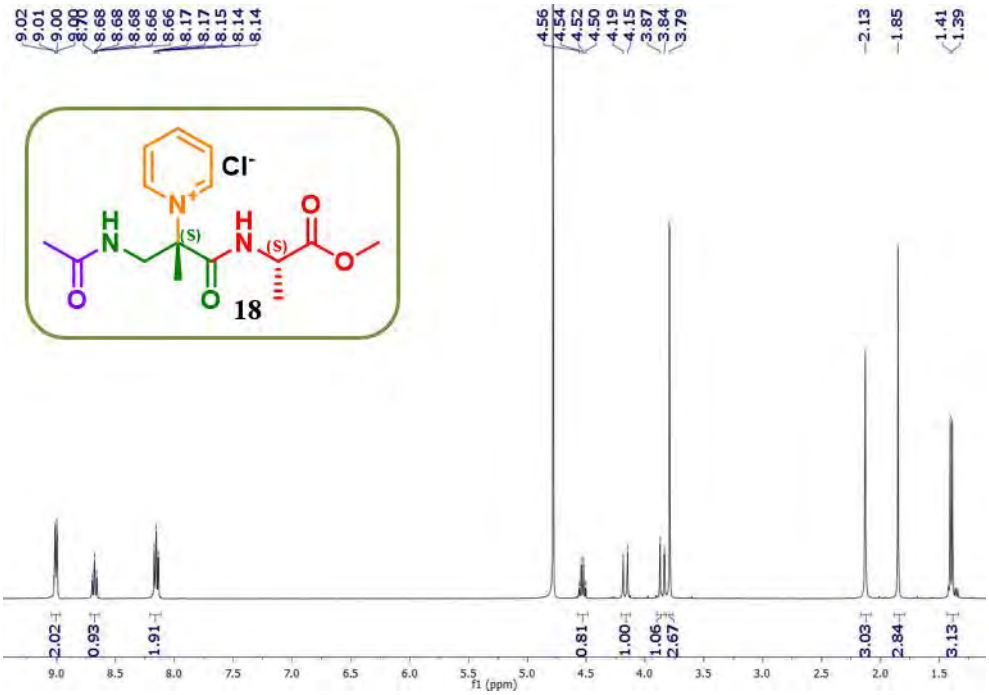

^{13}C NMR 100 MHz in D_2O

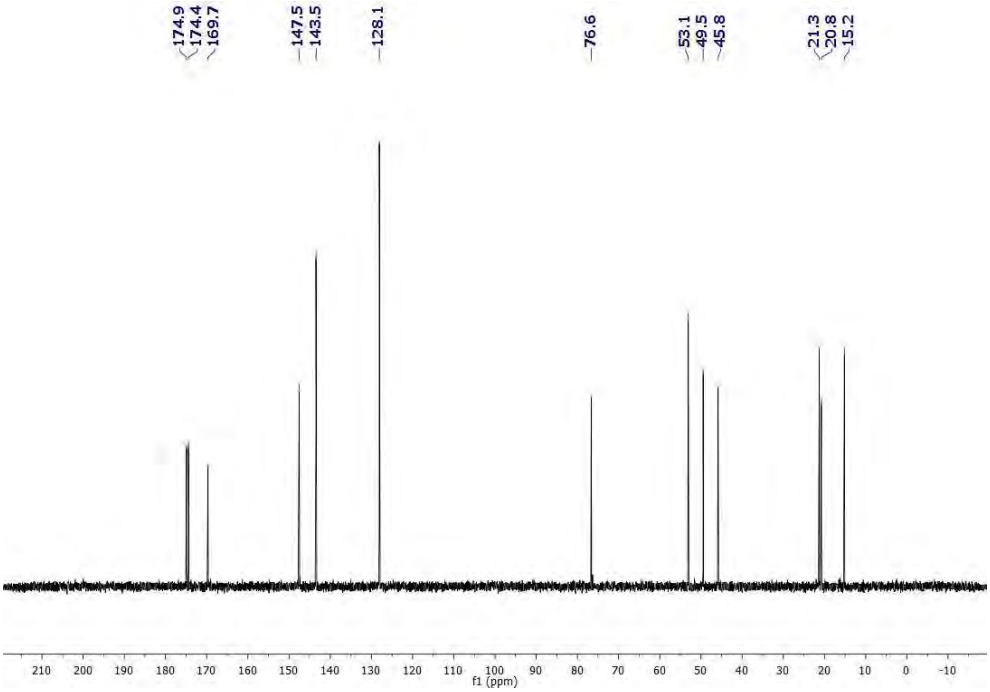

^{1}H NMR 400 MHz in D_2O

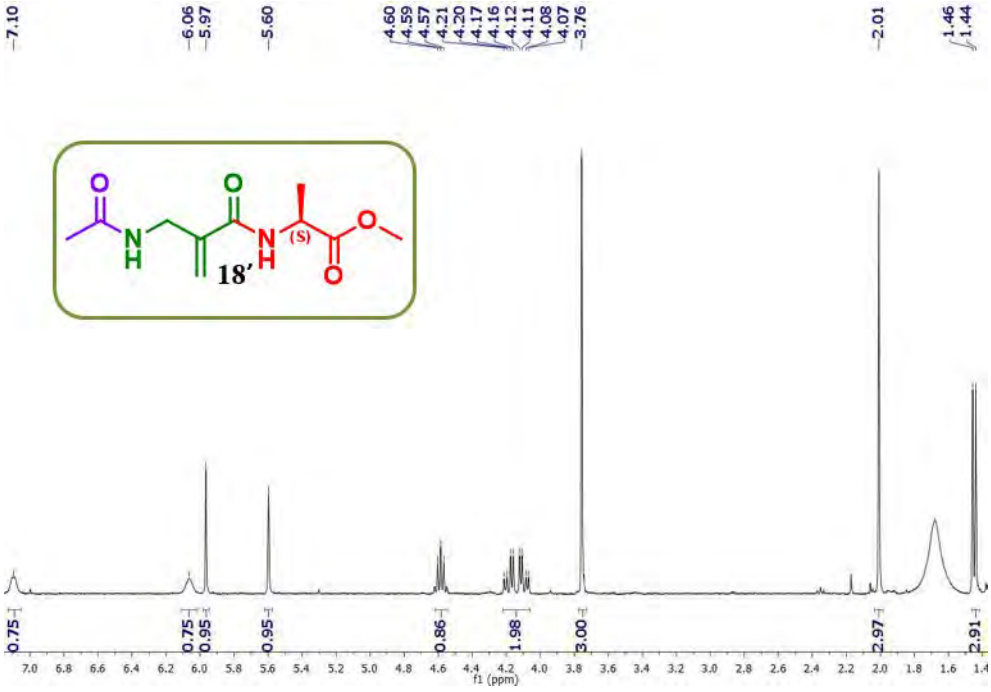

^{13}C NMR 100 MHz in D_2O

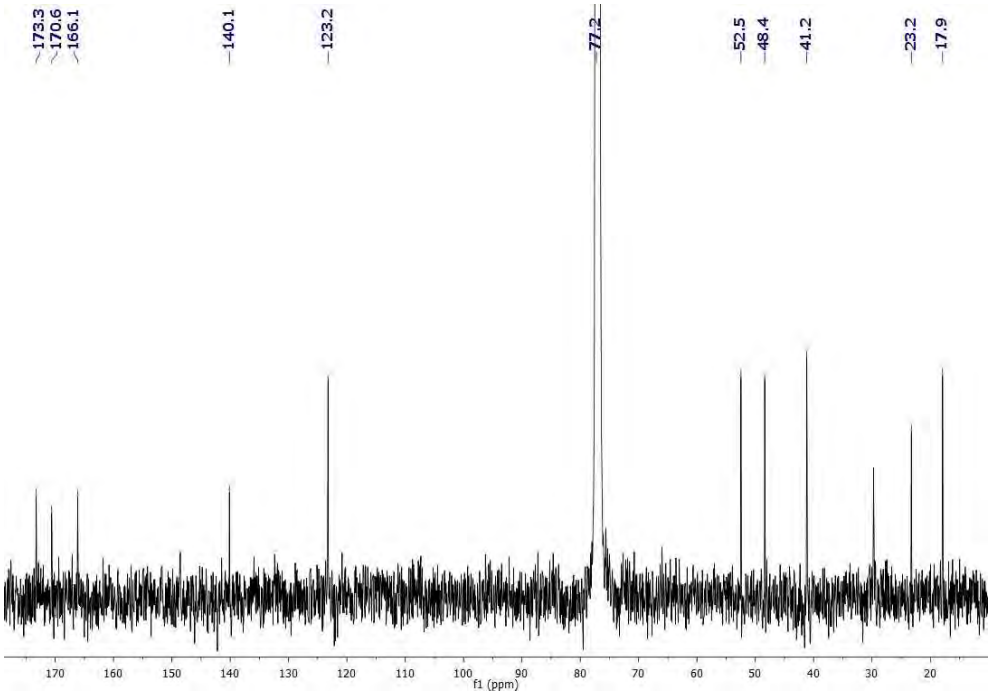

^{1}H NMR 400 MHz in D_2O

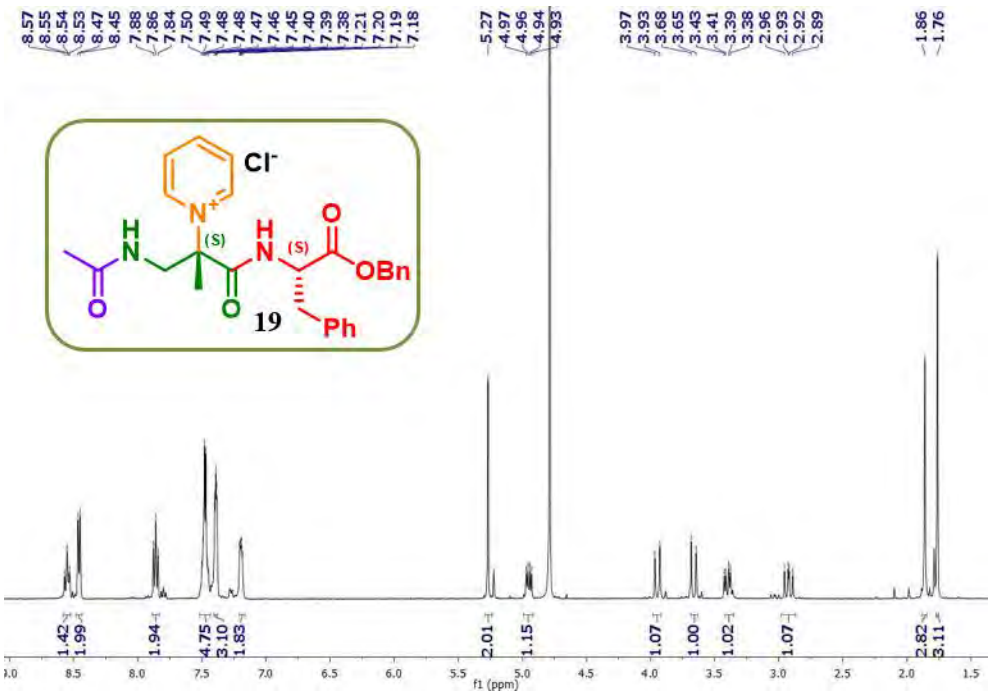

^{13}C NMR 100 MHz in D_2O

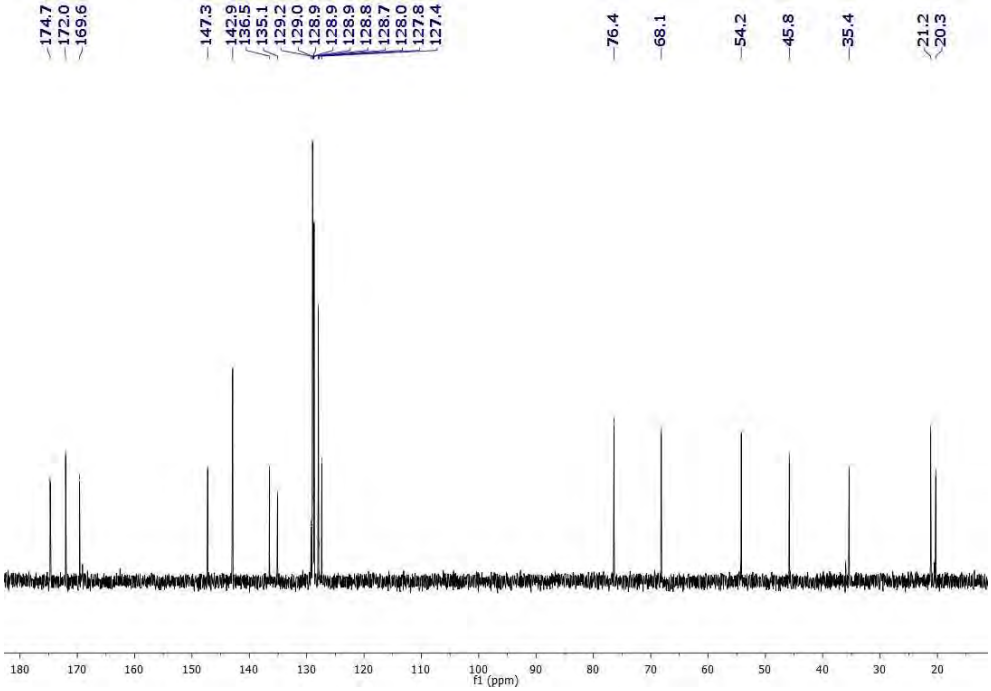

^{1}H NMR 400 MHz in D_2O

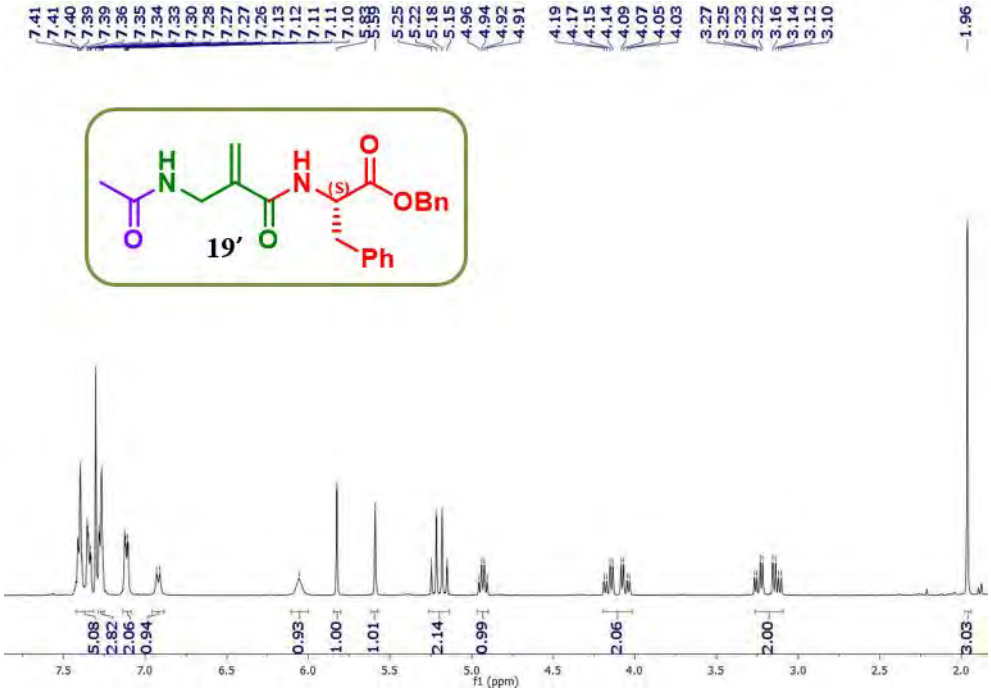

^{13}C NMR 100 MHz in D_2O

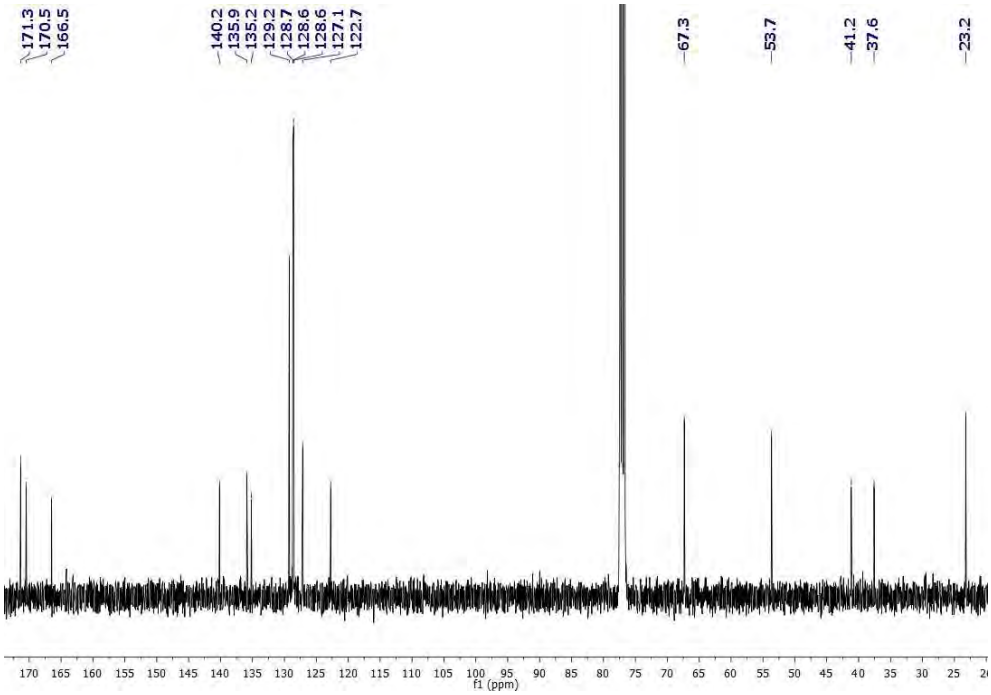

^{1}H NMR 400 MHz in D_2O

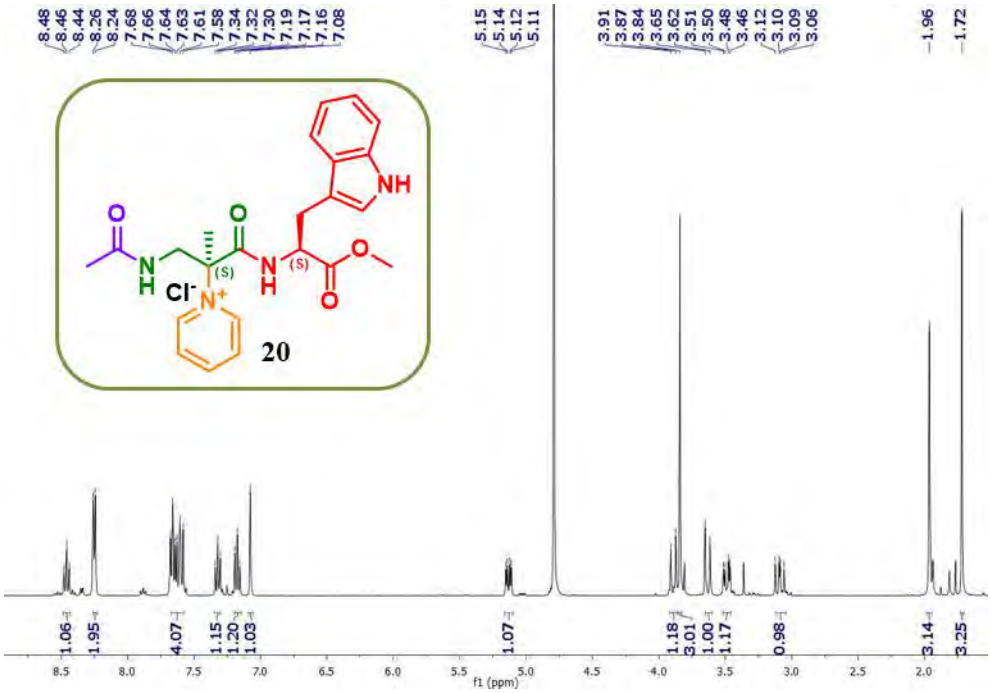

^{13}C NMR 100 MHz in D_2O

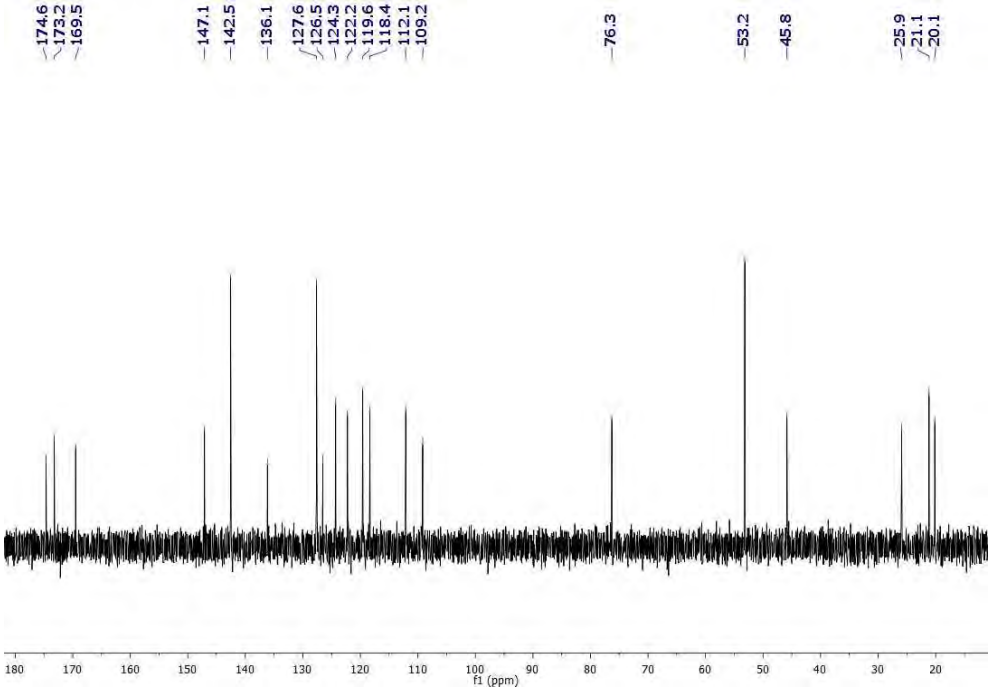

^{1}H NMR 400 MHz in D_2O

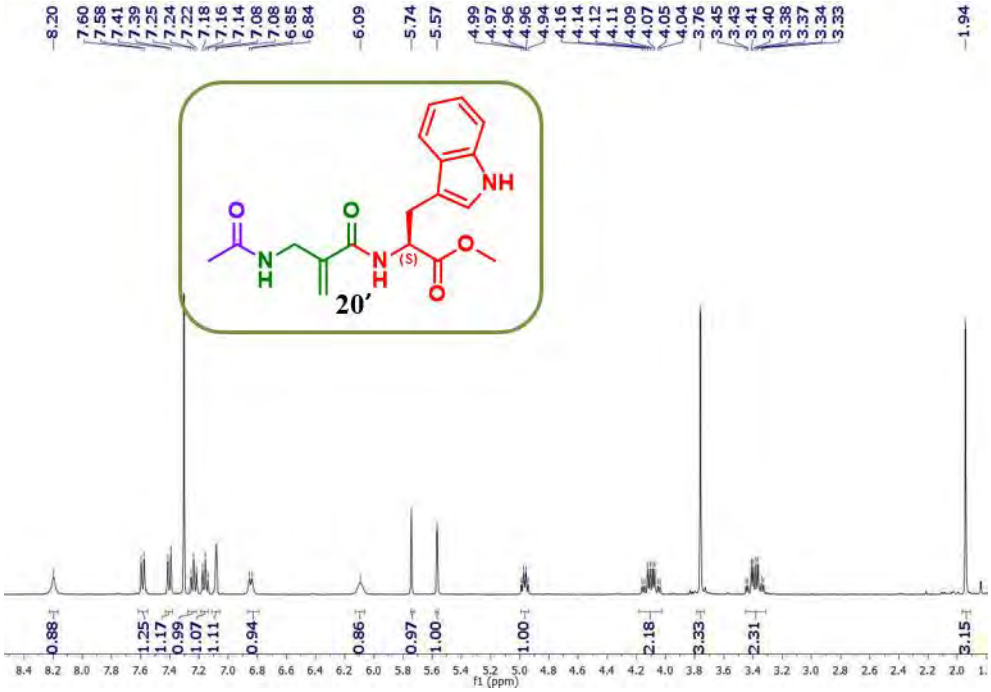

^{13}C NMR 100 MHz in D_2O

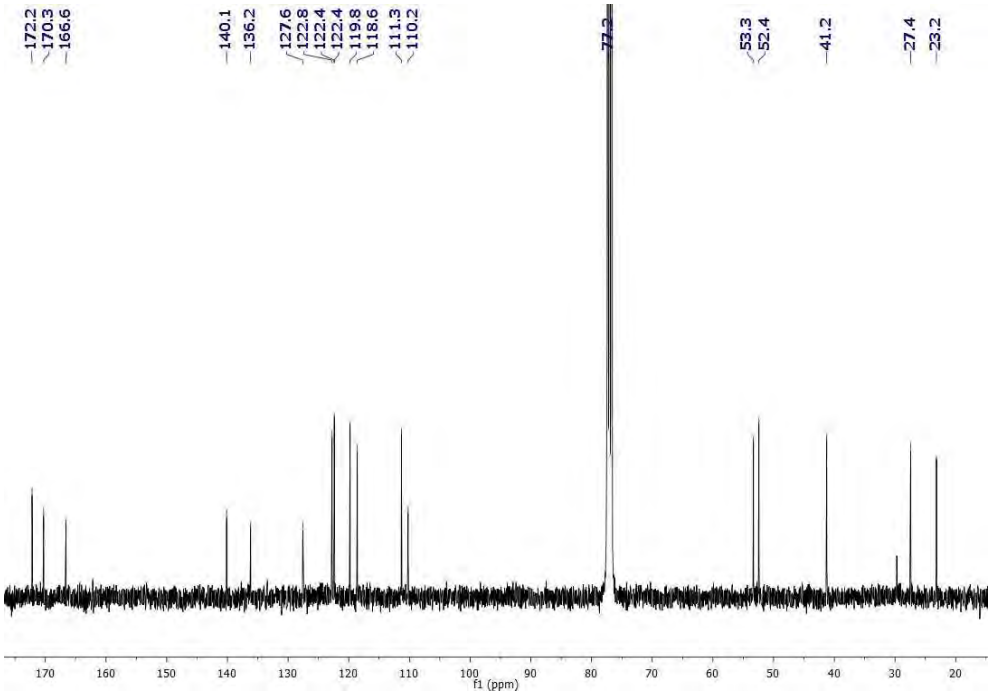

^{1}H NMR 400 MHz in D_2O

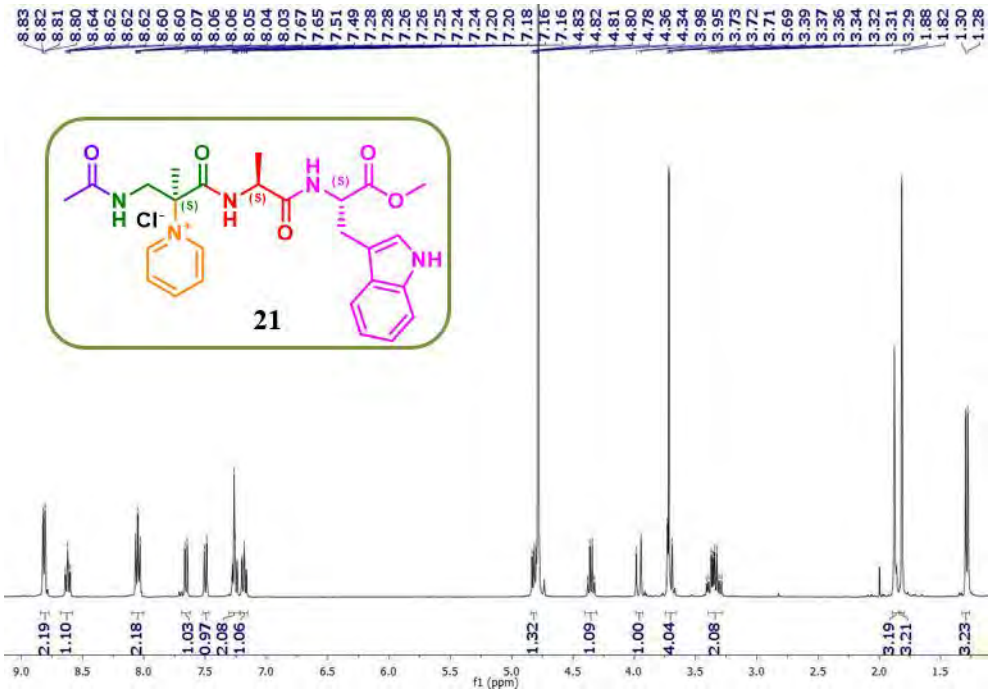

^{13}C NMR 100 MHz in D_2O

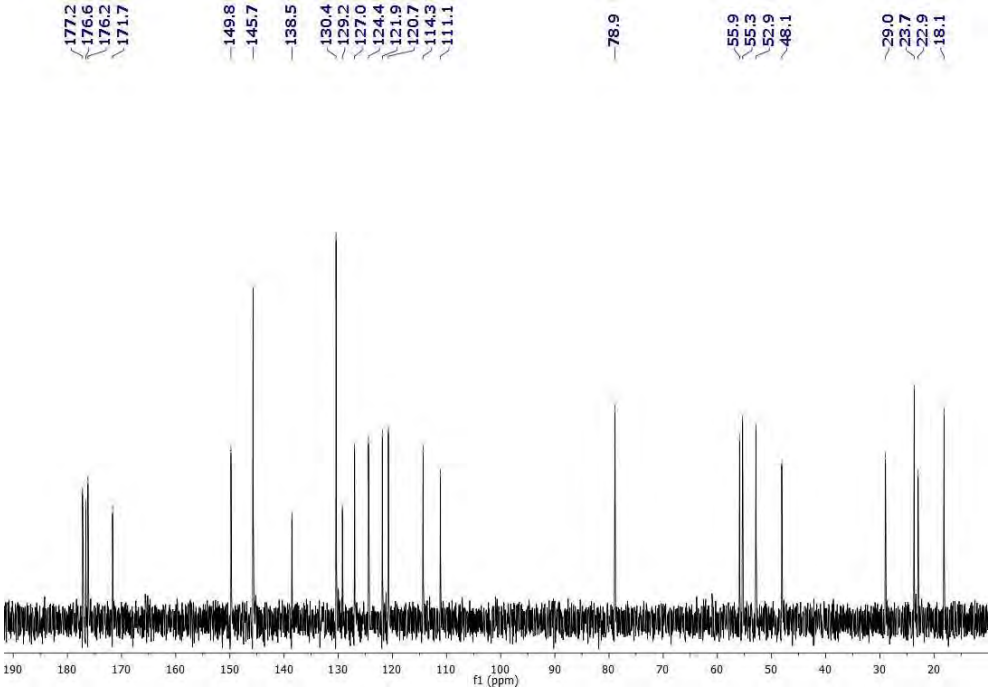

^{1}H NMR 400 MHz in D_2O

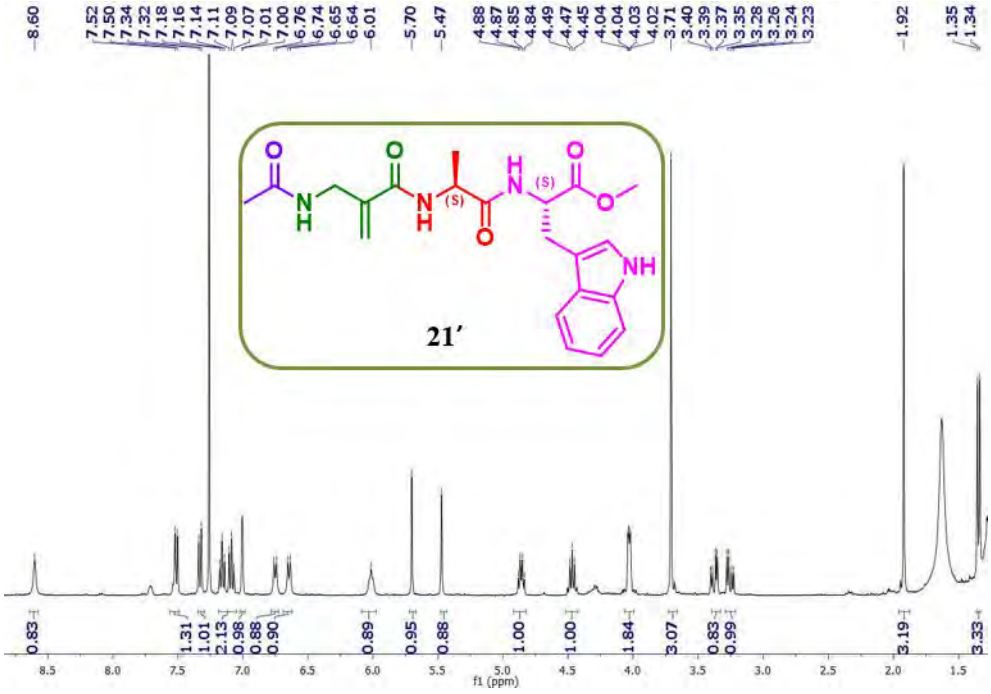

^{13}C NMR 100 MHz in D_2O

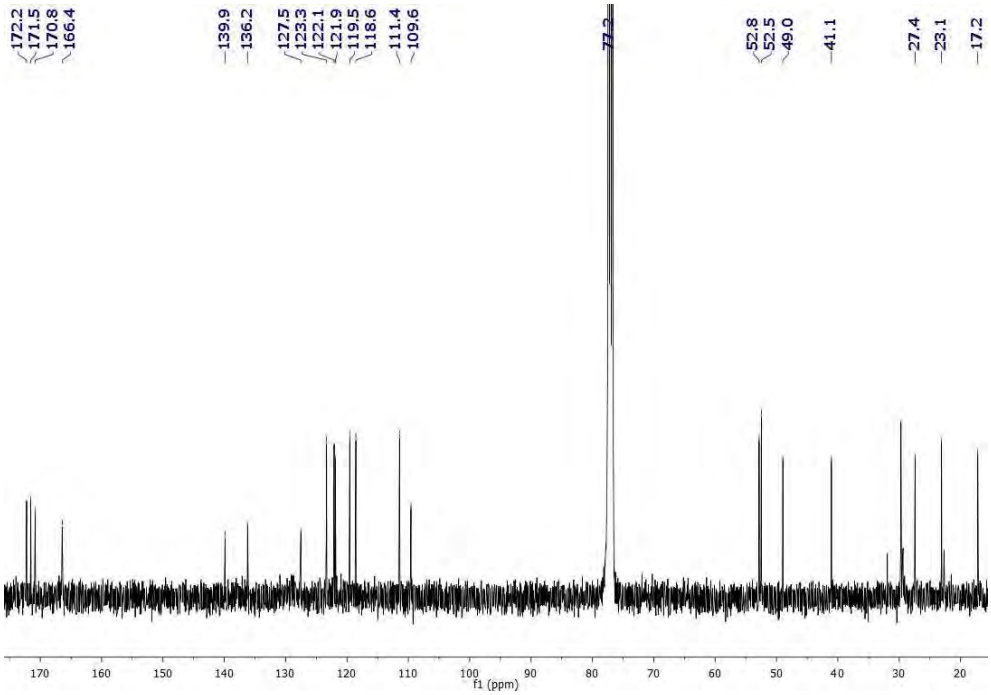

^{1}H NMR 400 MHz in D_2O

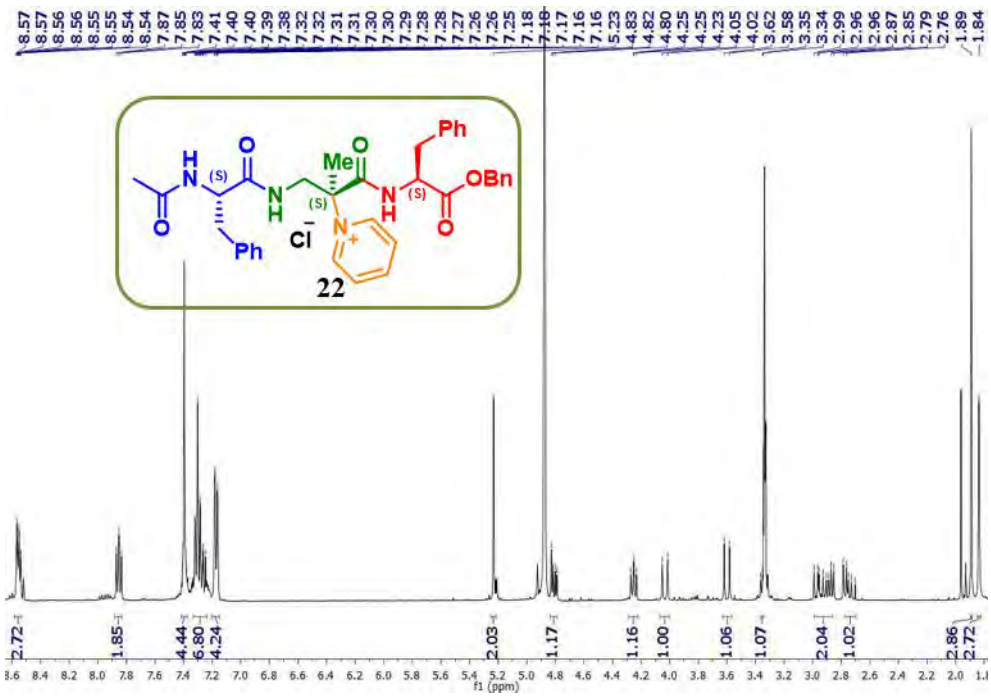

^{13}C NMR 100 MHz in D_2O

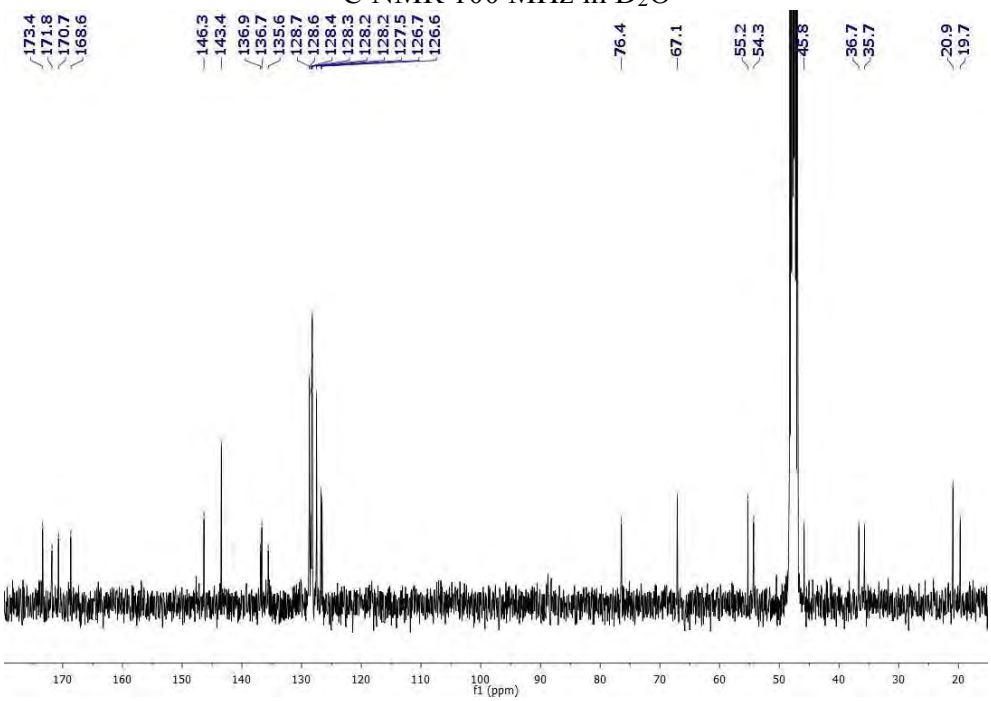

^{1}H NMR 400 MHz in D_2O

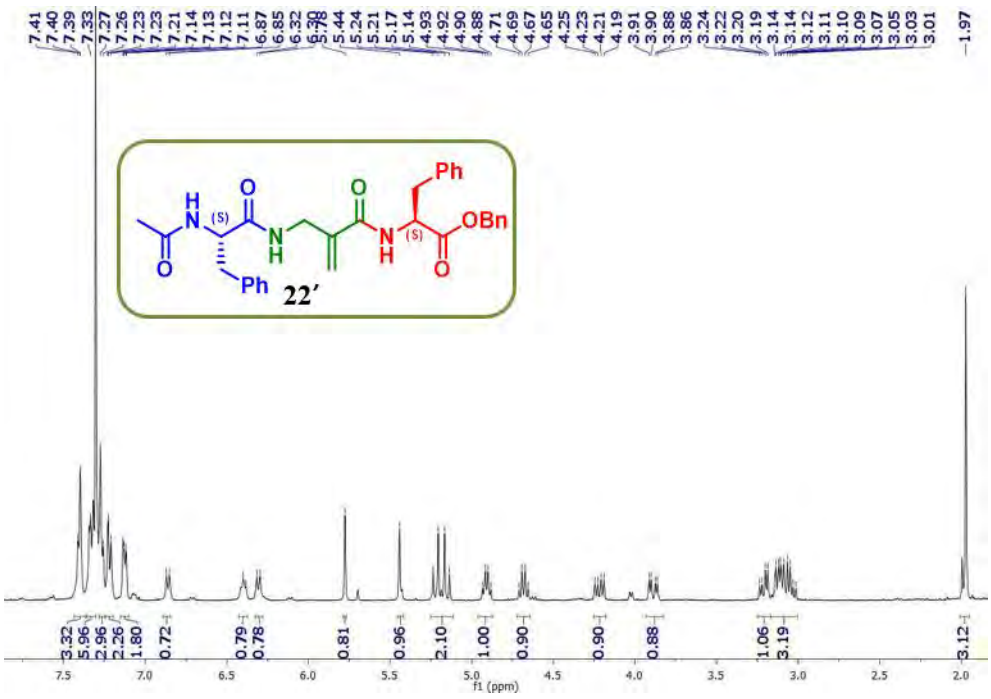

^{13}C NMR 100 MHz in D_2O

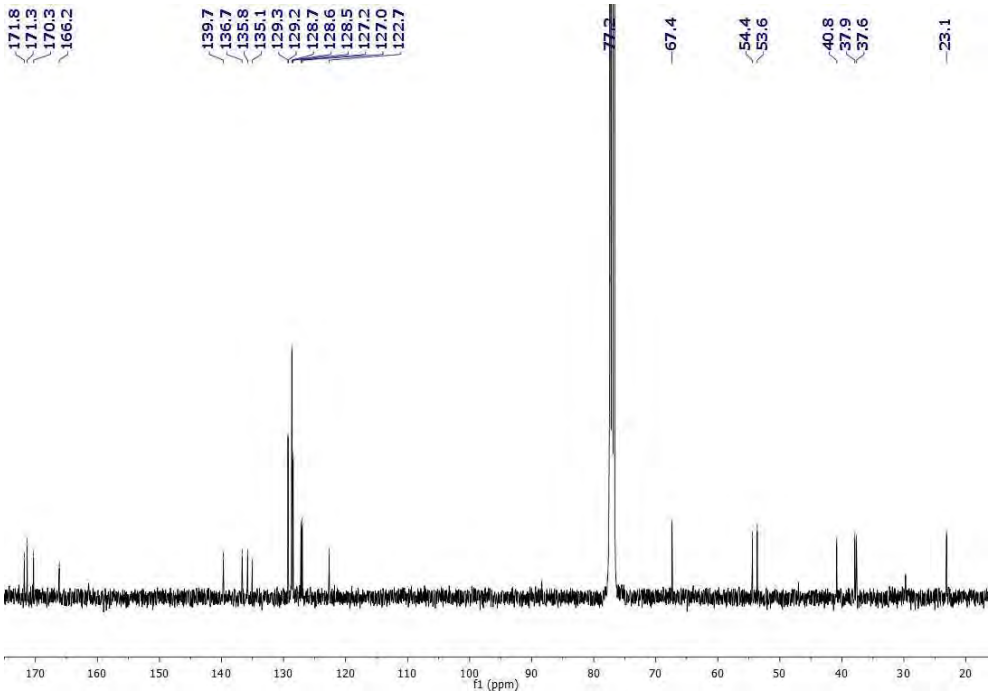

^{1}H NMR 400 MHz in D_2O

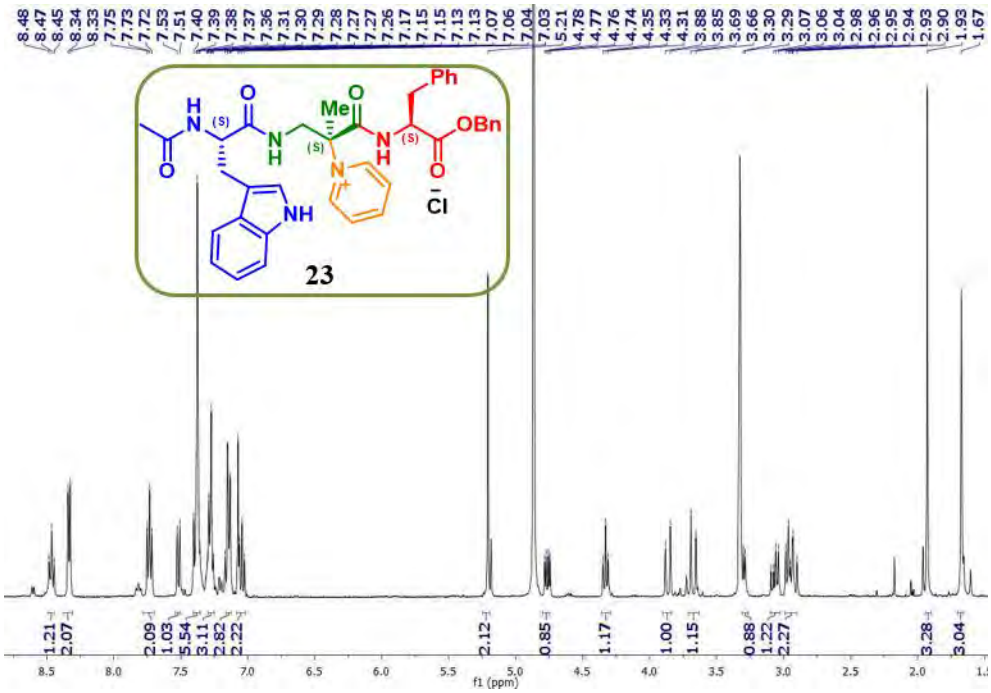

^{13}C NMR 100 MHz in D_2O

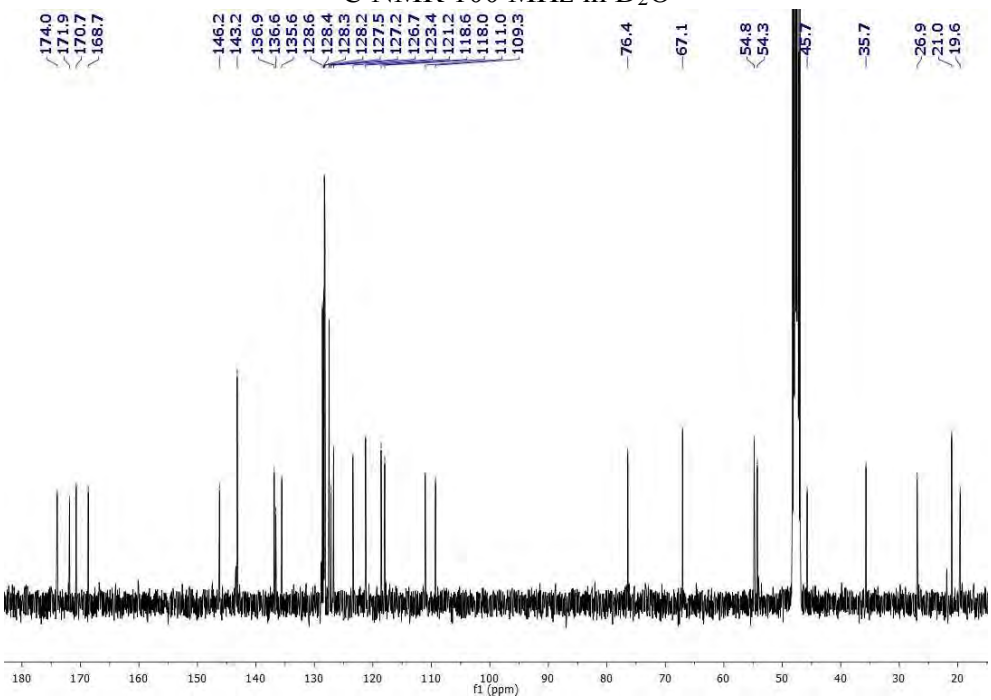

^{1}H NMR 400 MHz in D_2O

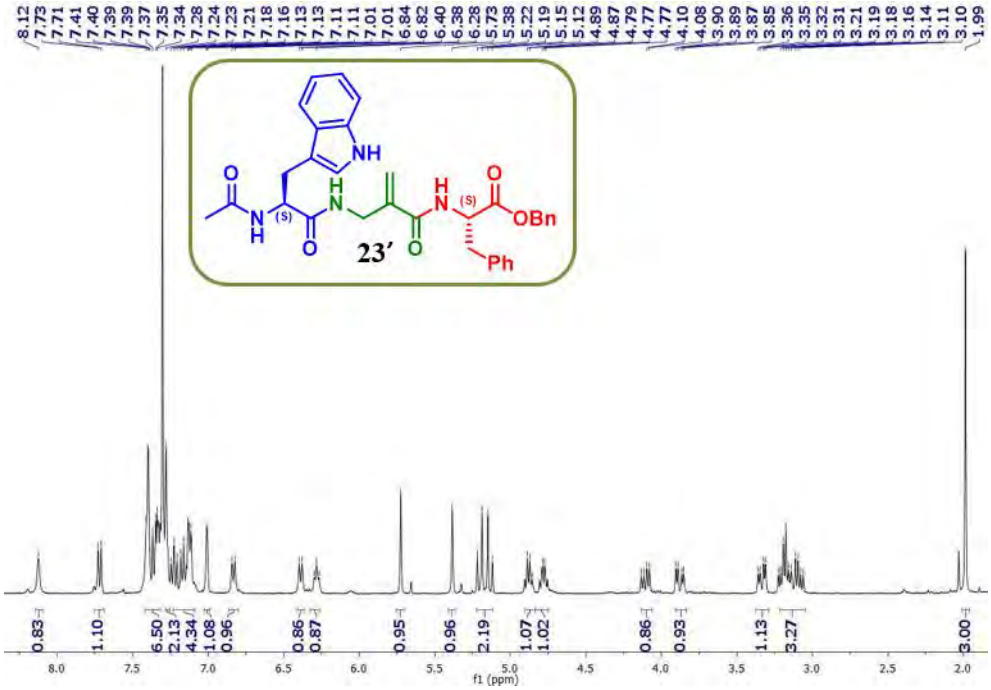

^{13}C NMR 100 MHz in D_2O

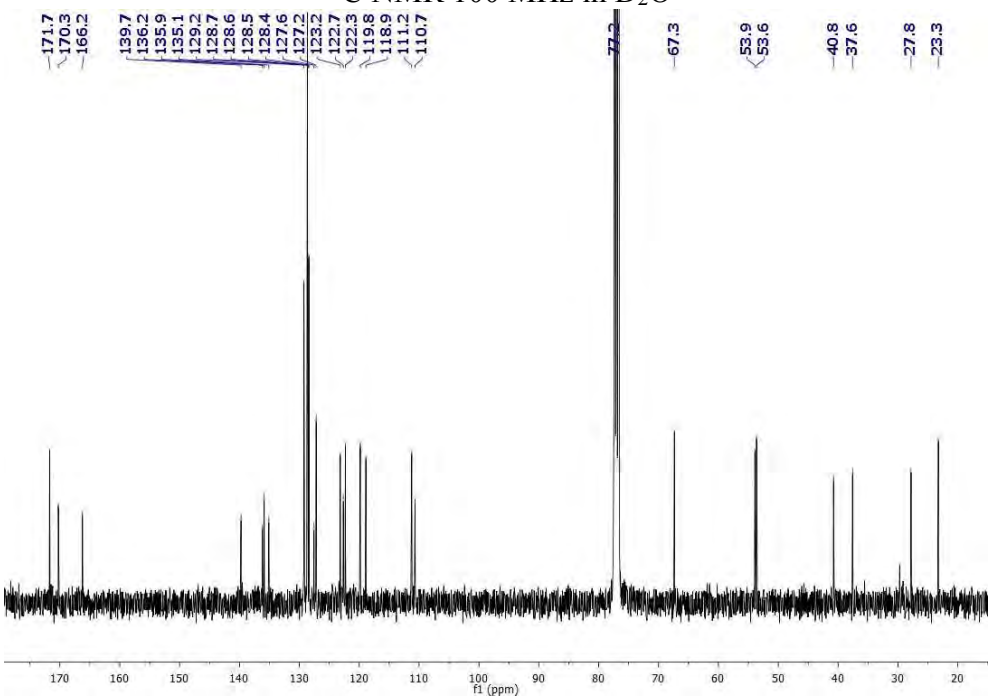

^{1}H NMR 300 MHz in CD_3OH

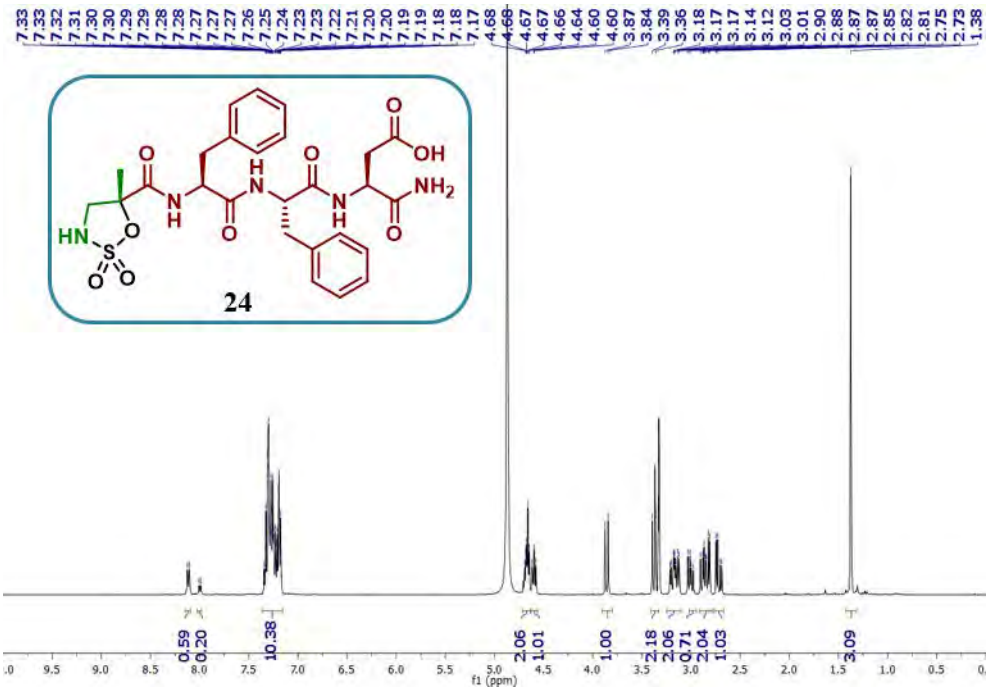

^{13}C NMR 75 MHz in CD_3OH

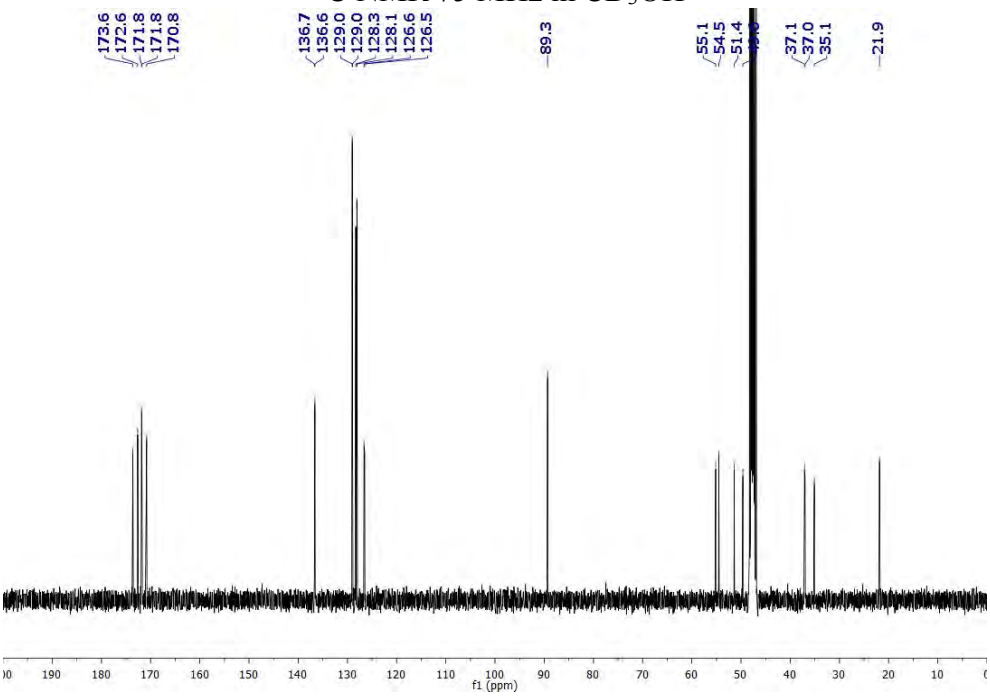

NOESY 400 MHz in H_2O/D_2O

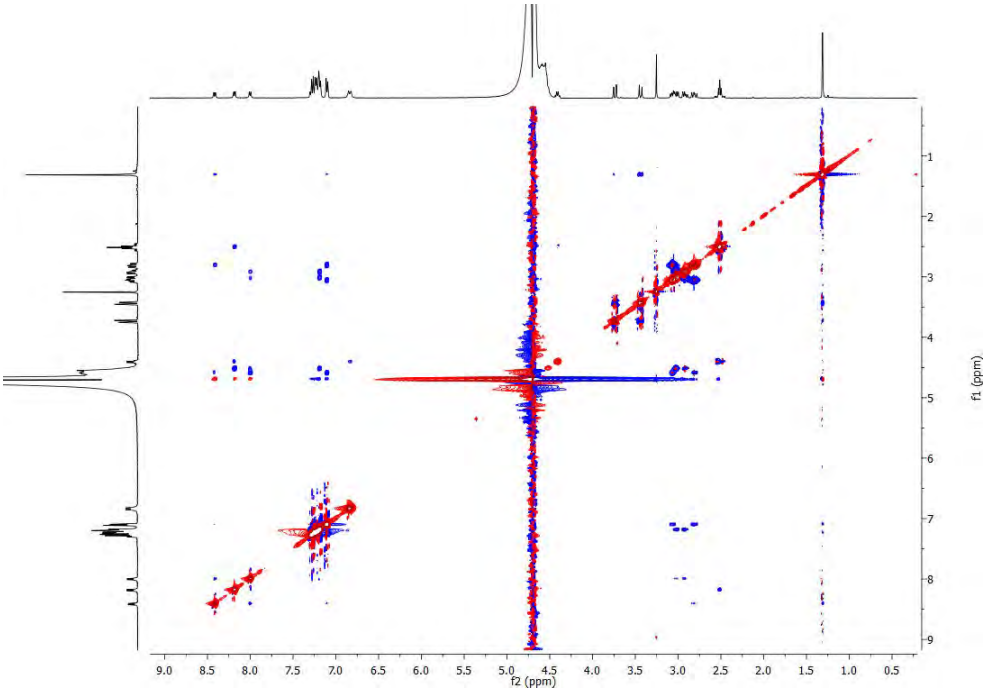

^1H NMR 400 MHz in H_2O/D_2O amide region

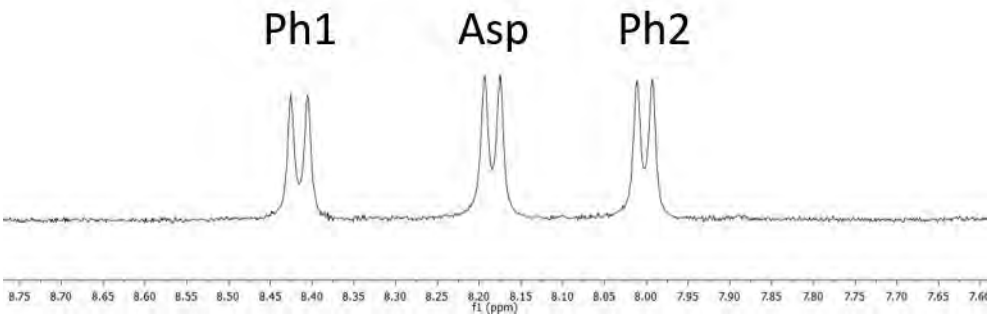

^{1}H NMR 400 MHz in CD_3OH

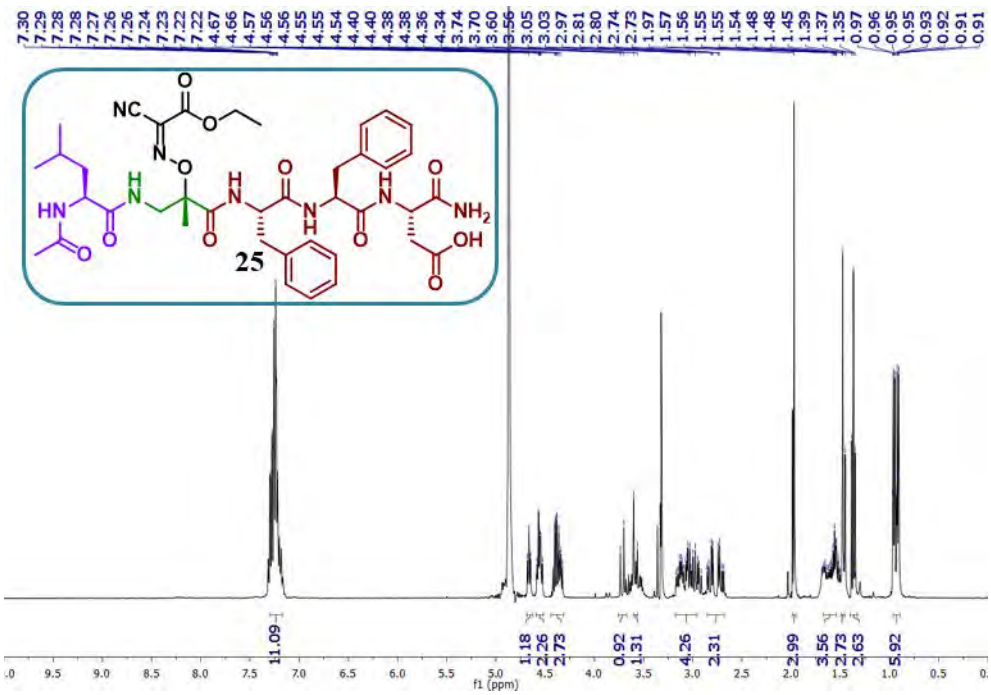

^{13}C NMR 100 MHz in CD_3OH

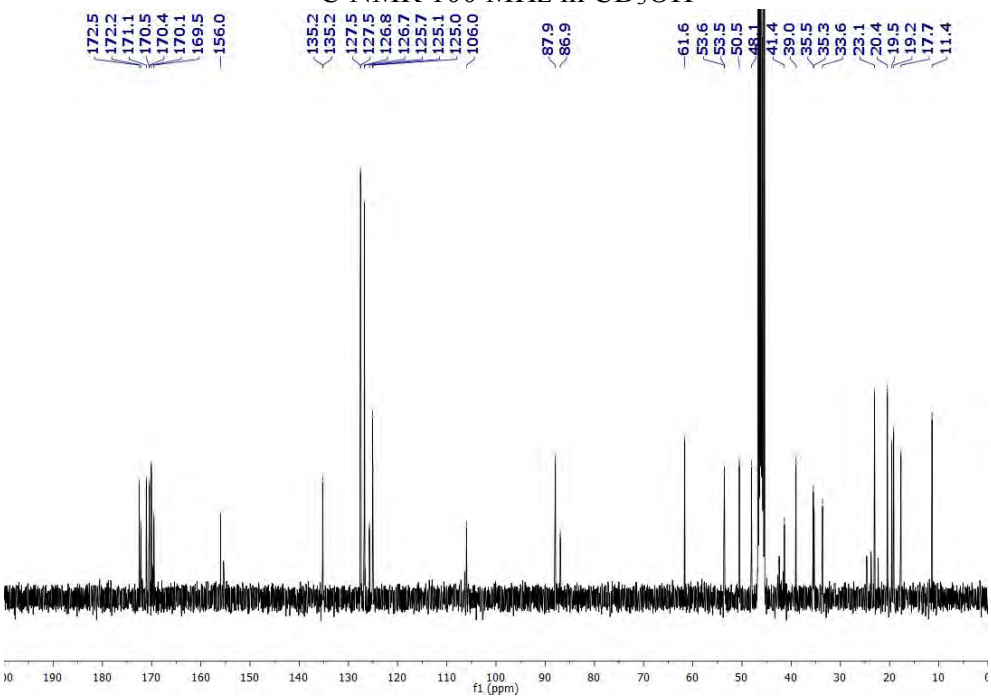

^{1}H NMR 400 MHz in CD_3OH

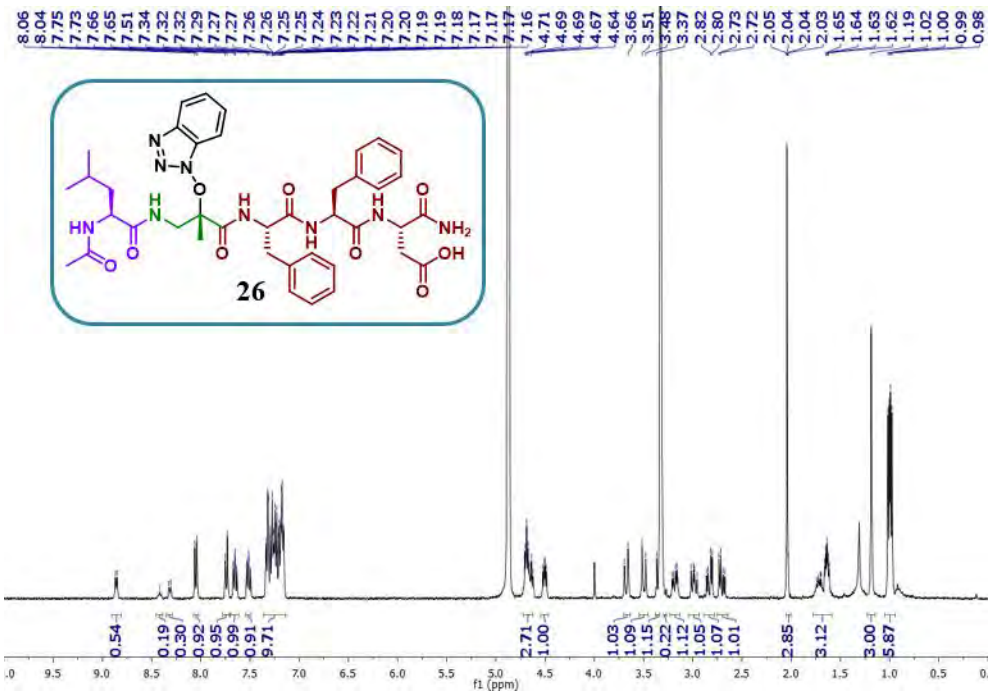

^{13}H NMR 100 MHz in CD_3OH

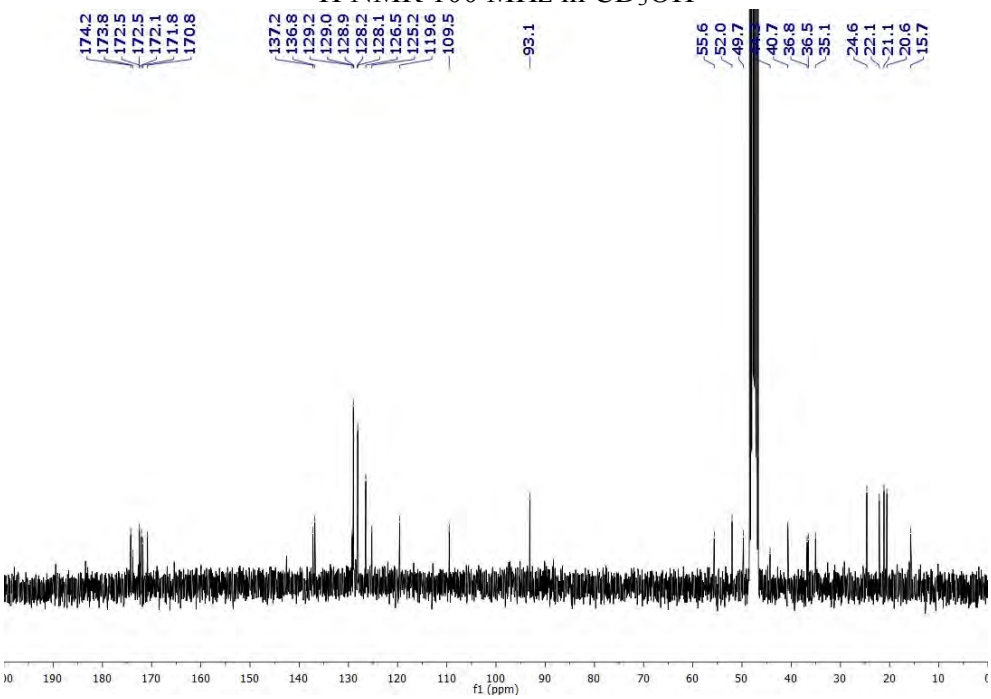

^{1}H NMR 300 MHz in CD_3OH

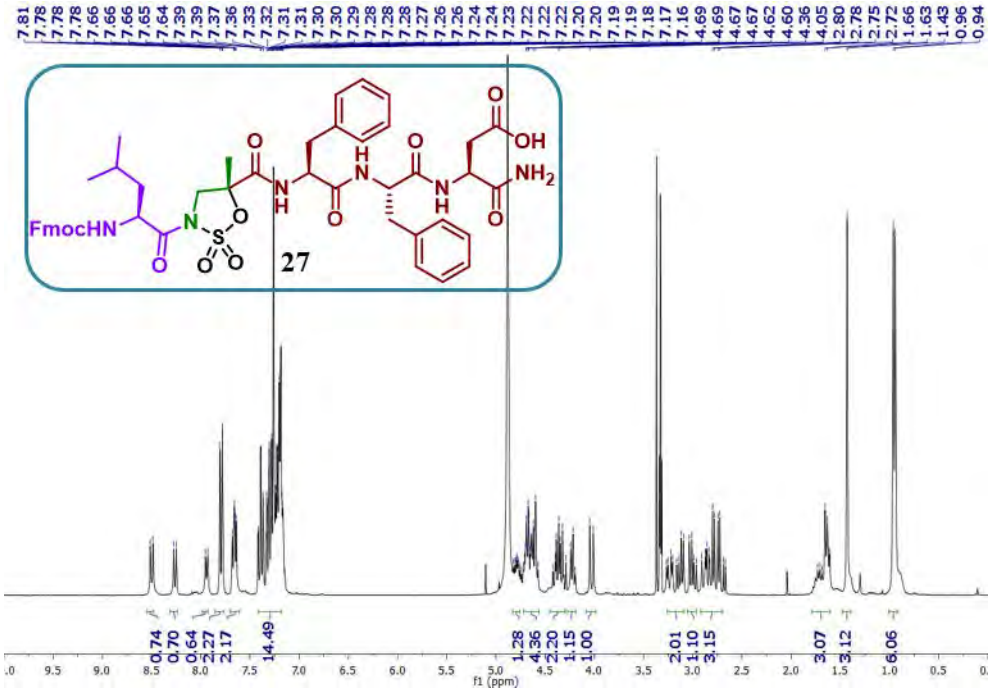

^{13}C NMR 75 MHz in CD_3OH

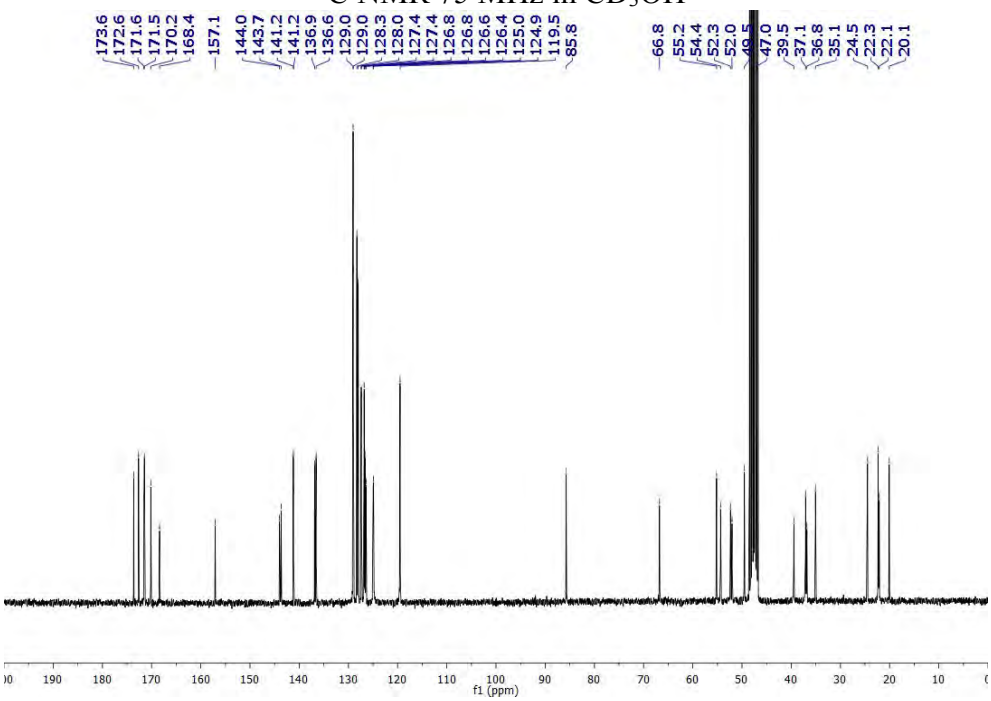

^{1}H NMR 400 MHz in CD_3OH

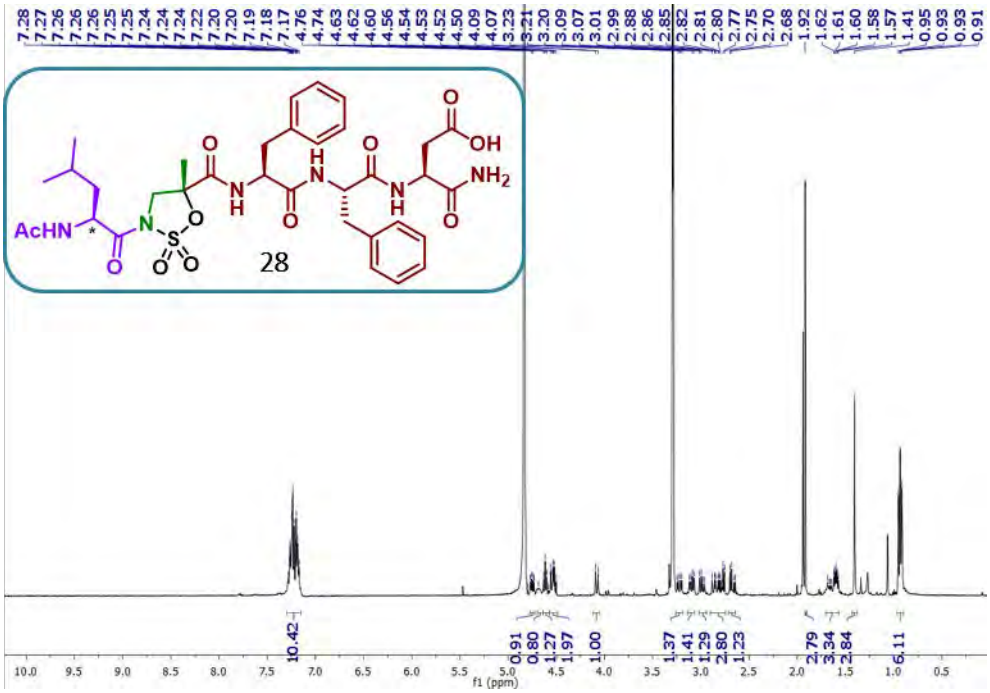

^{13}C NMR 100 MHz in CD_3OH

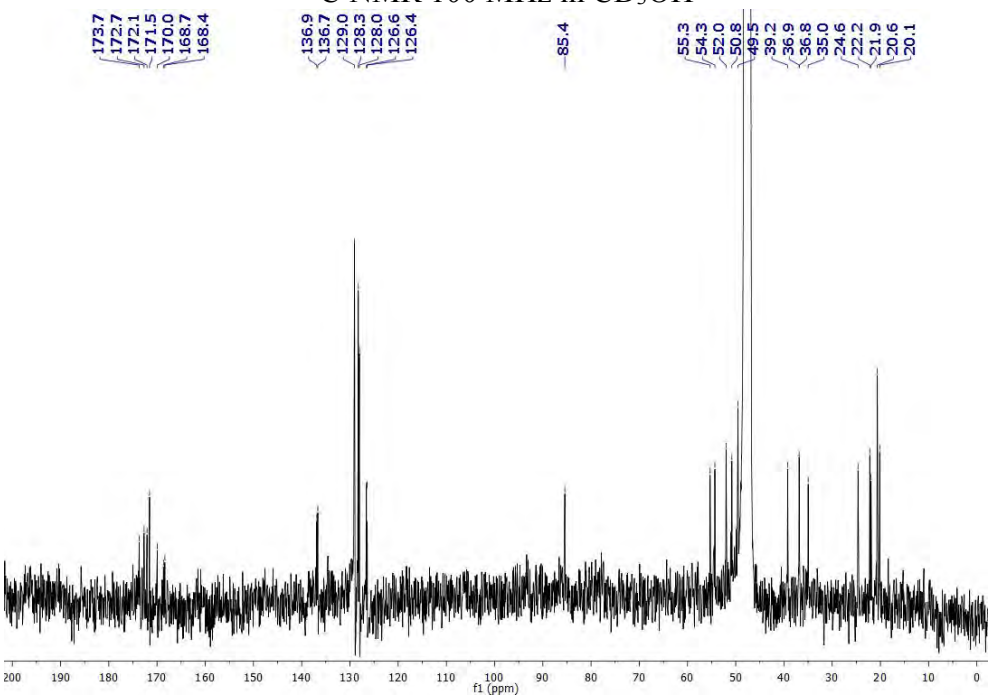

^{1}H NMR 400 MHz in CD_3OH

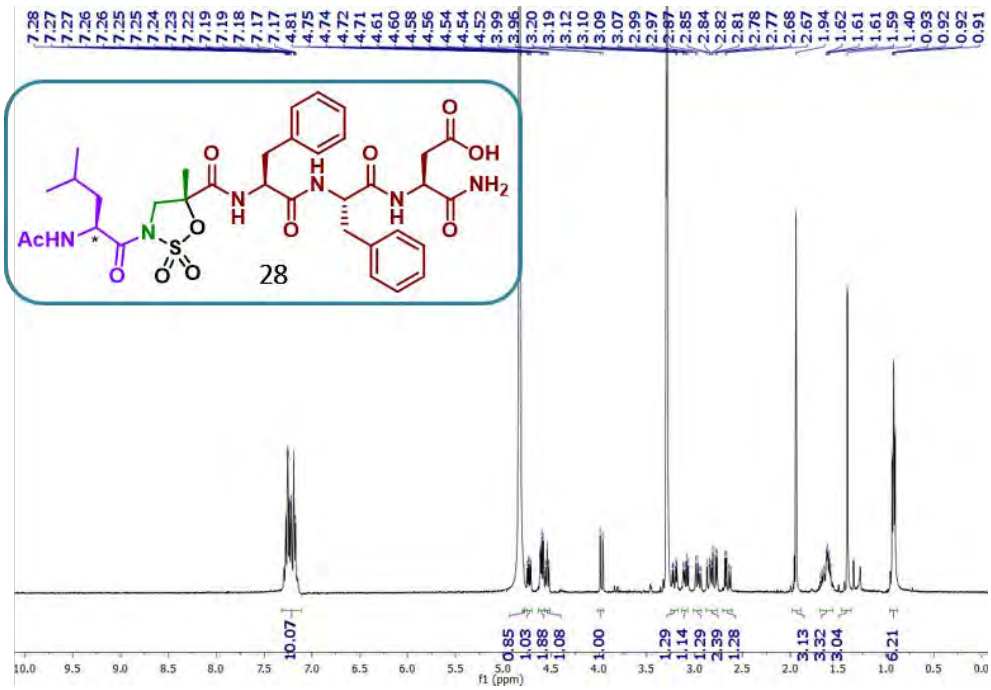

^{13}C NMR 100 MHz in CD_3OH

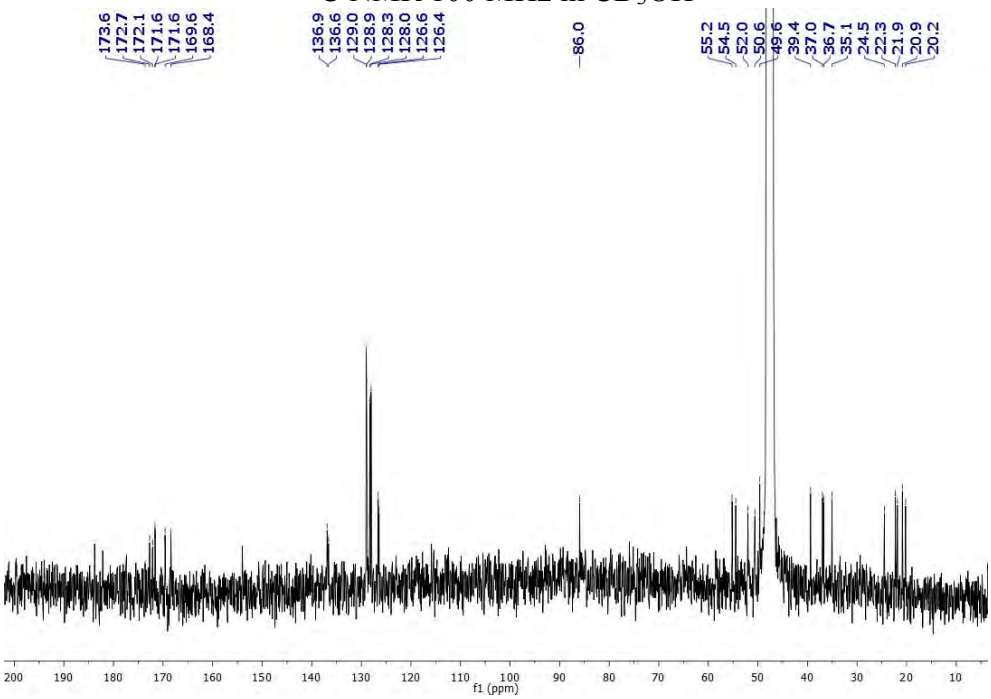

^{1}H NMR 300 MHz in DMSO

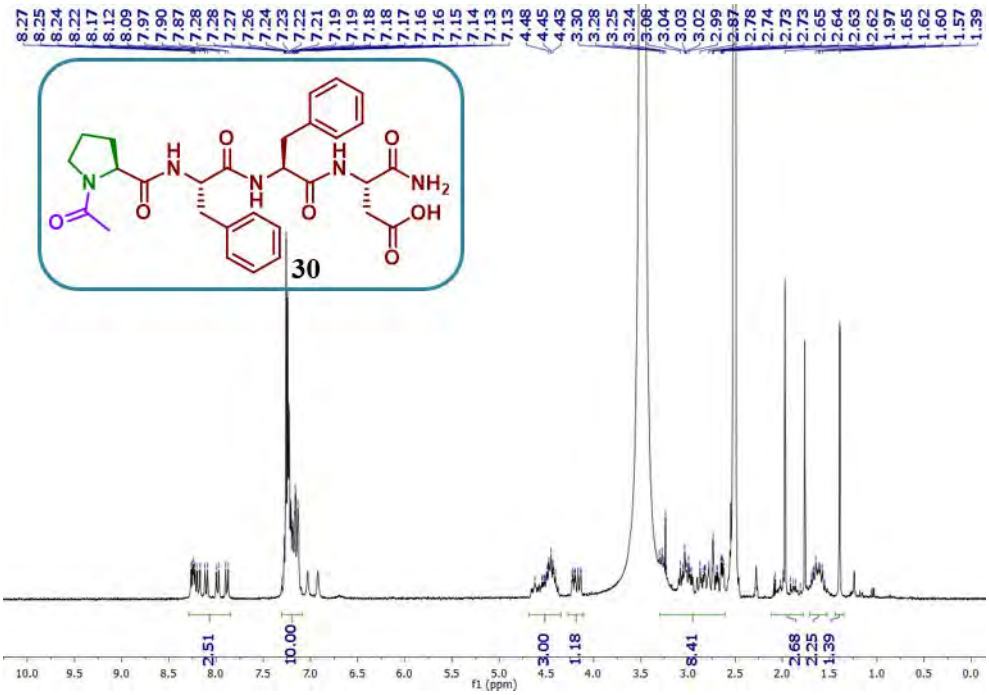

^{13}C NMR 75 MHz in DMSO

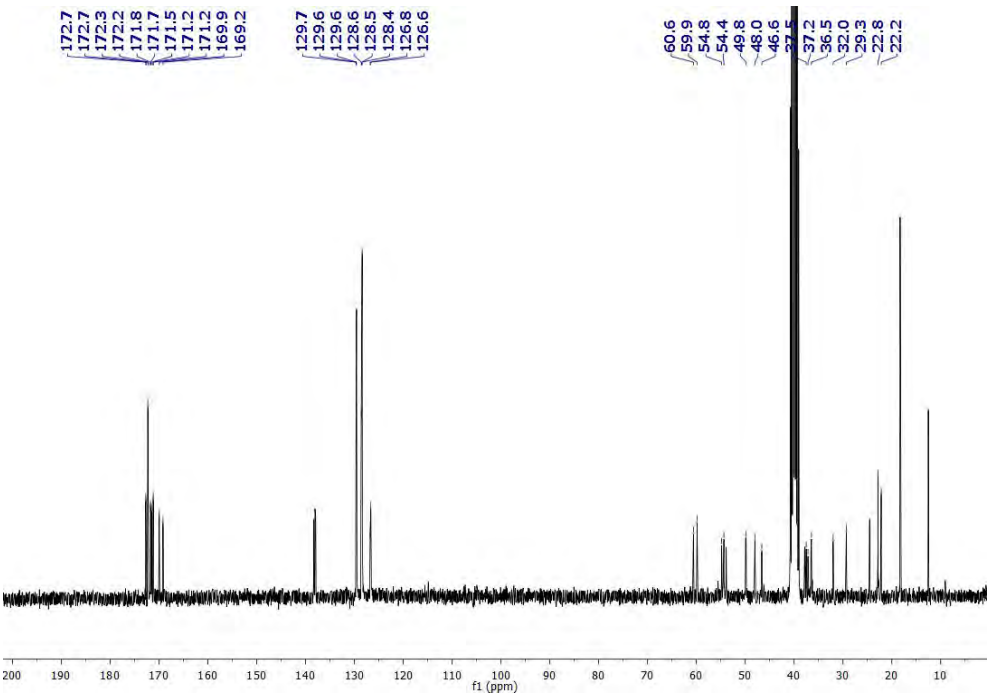

^{1}H NMR 300 MHz in CD_3OH

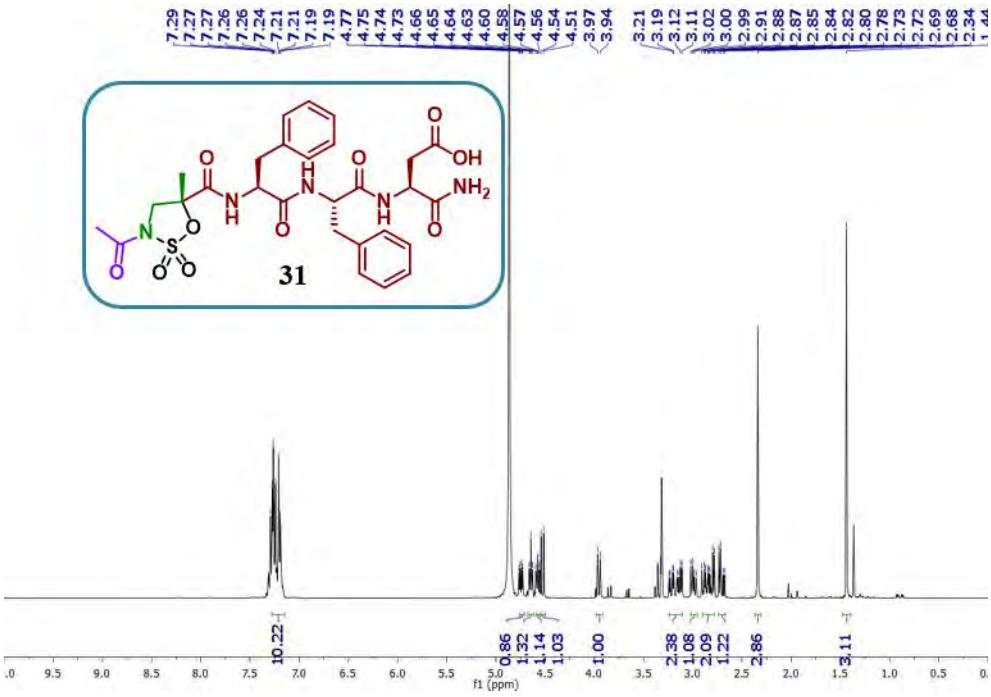

^{13}C NMR 75 MHz in CD_3OH

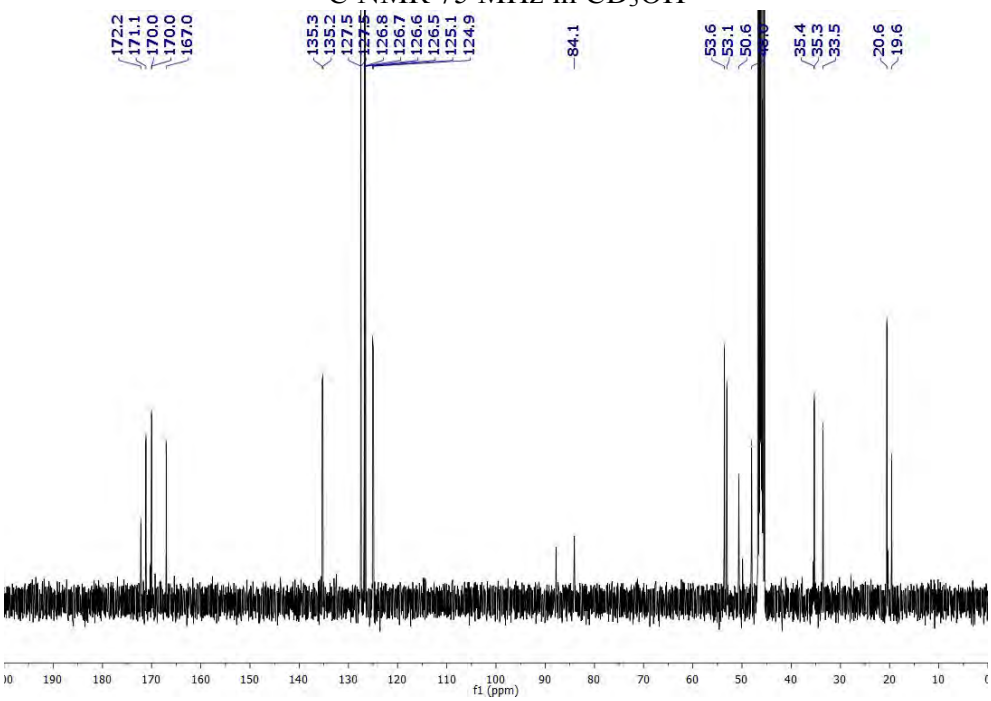

NOESY 400 MHz in H_2O/D_2O

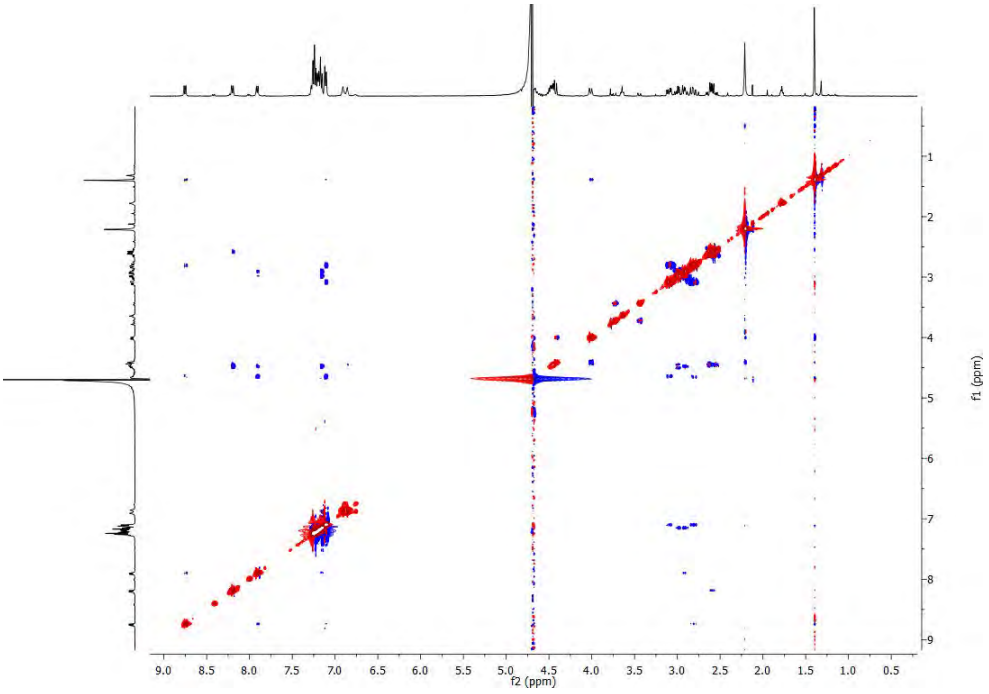

^1H NMR 400 MHz in H_2O/D_2O amide region

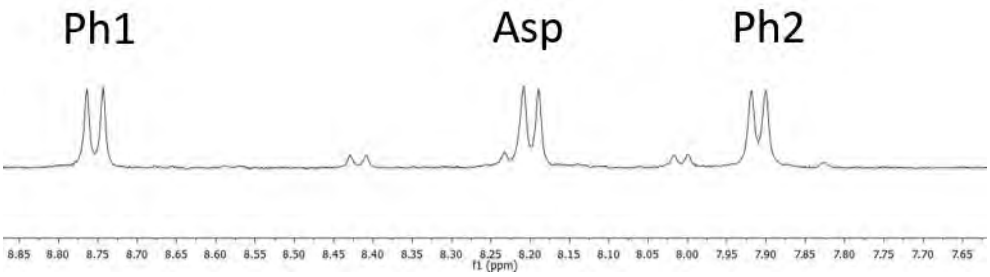

^{1}H NMR 300 MHz in DMSO

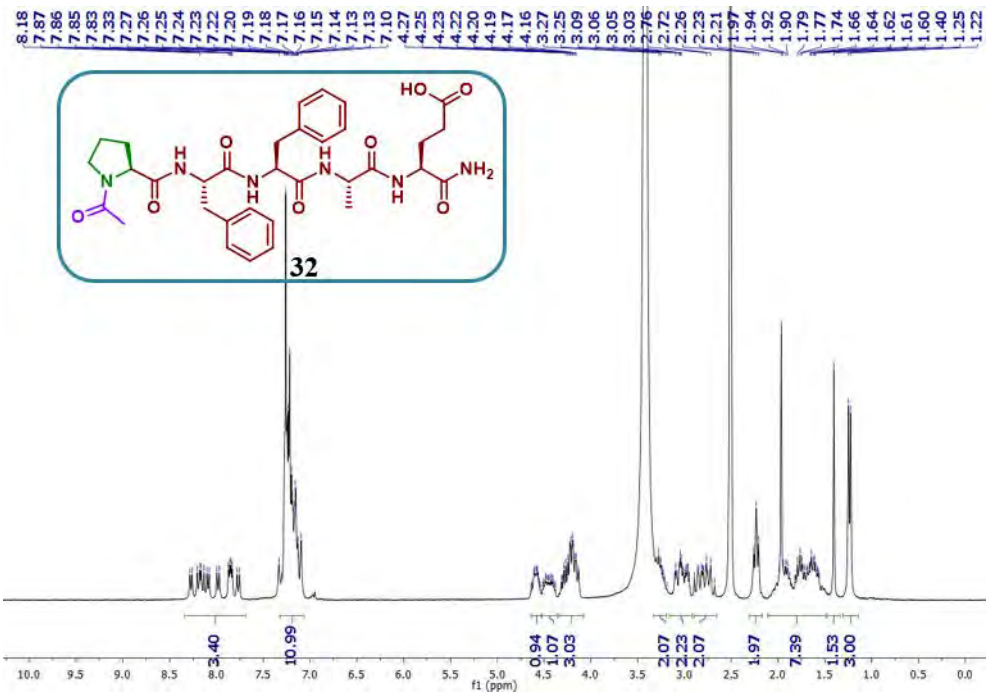

^{13}C NMR 75 MHz in DMSO

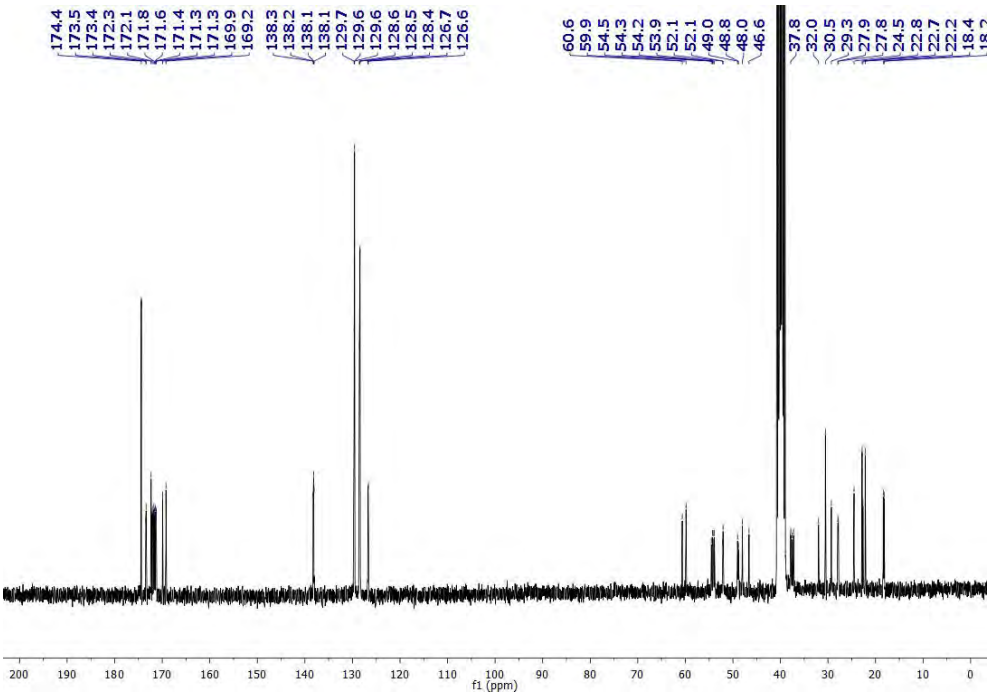

^{1}H NMR 300 MHz in CD_3OH

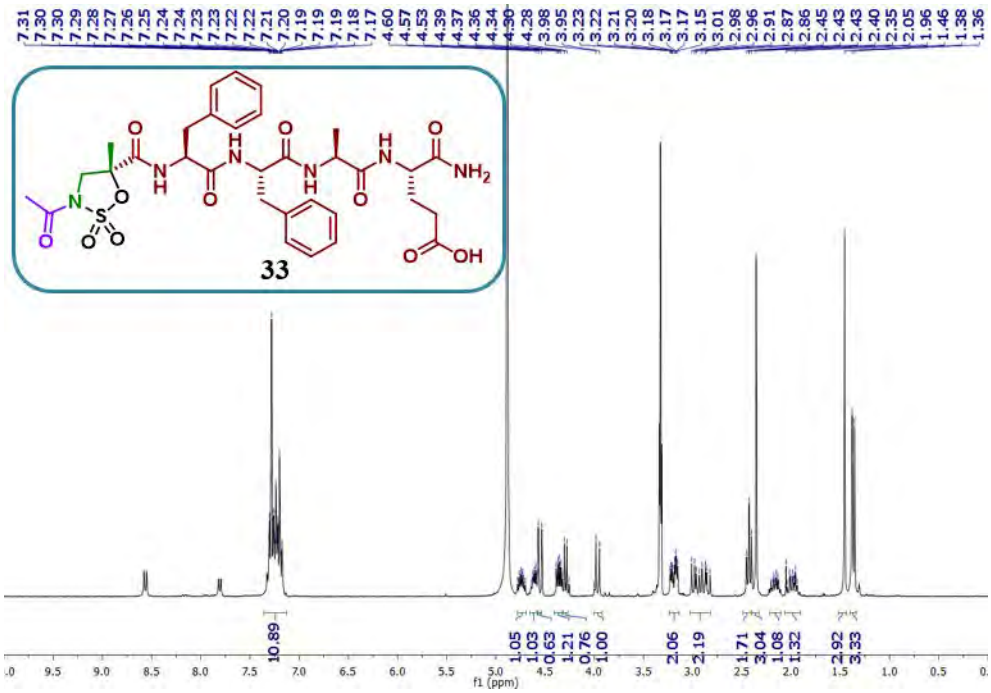

^{13}C NMR 75 MHz in CD_3OH

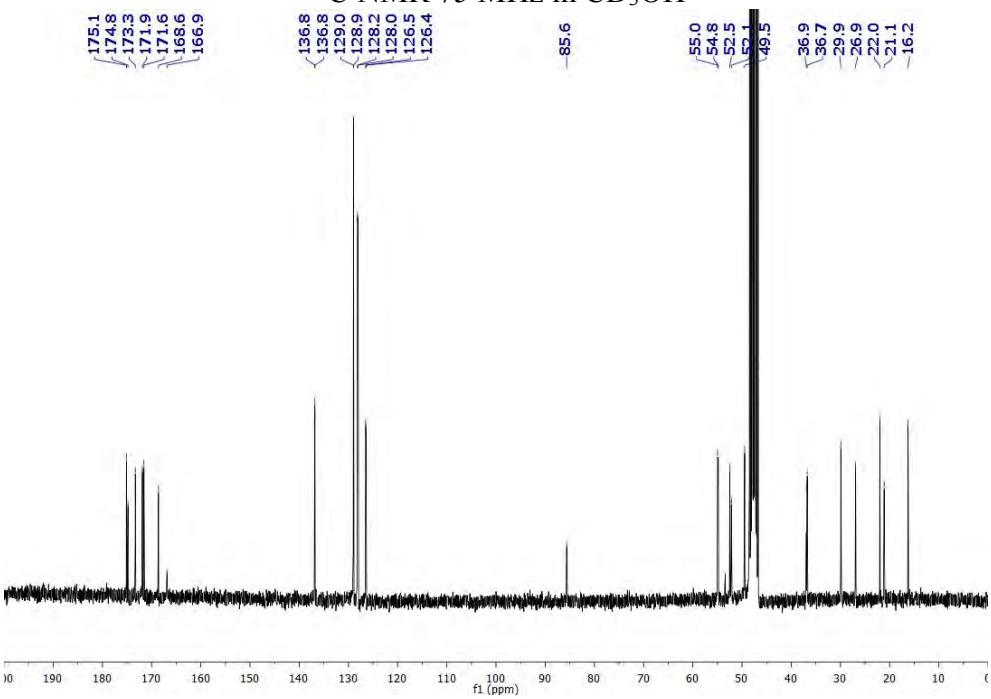

NOESY 400 MHz in H_2O/D_2O

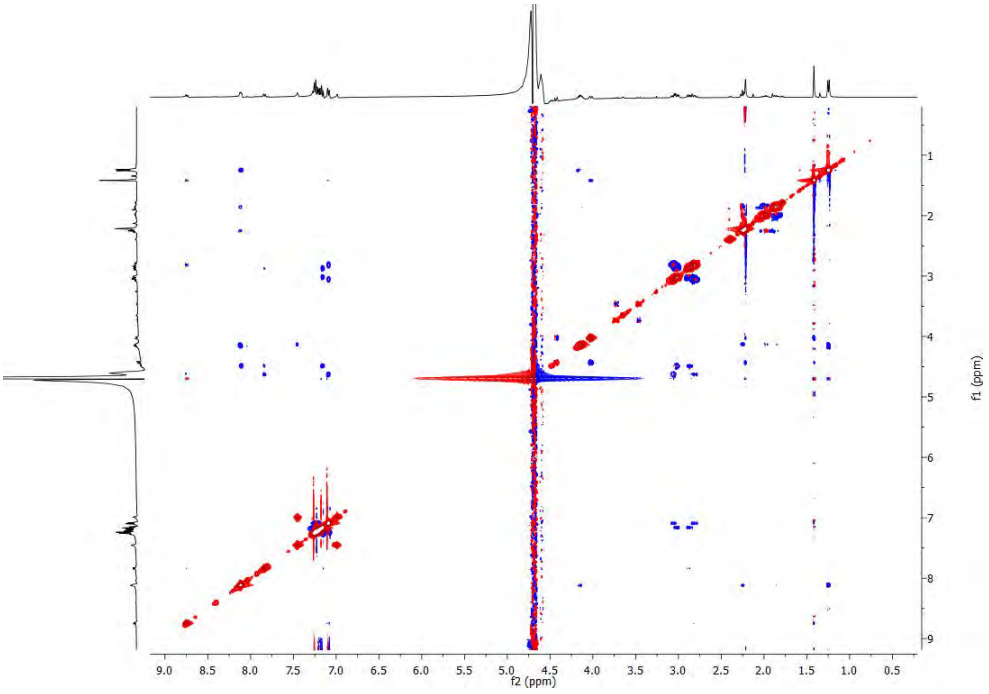

^1H NMR 400 MHz in H_2O/D_2O amide region

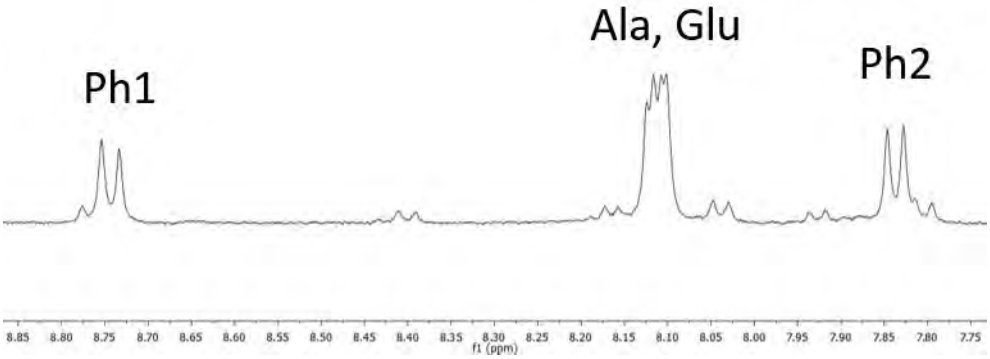

^{1}H NMR 300 MHz in CD_3OH

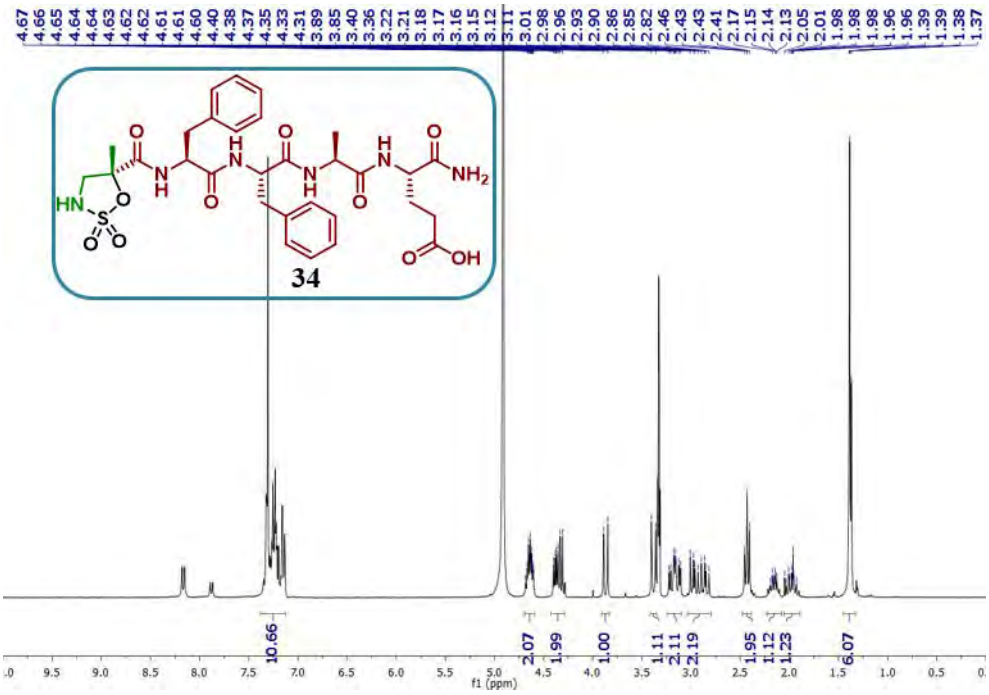

^{13}C NMR 300 MHz in CD_3OH

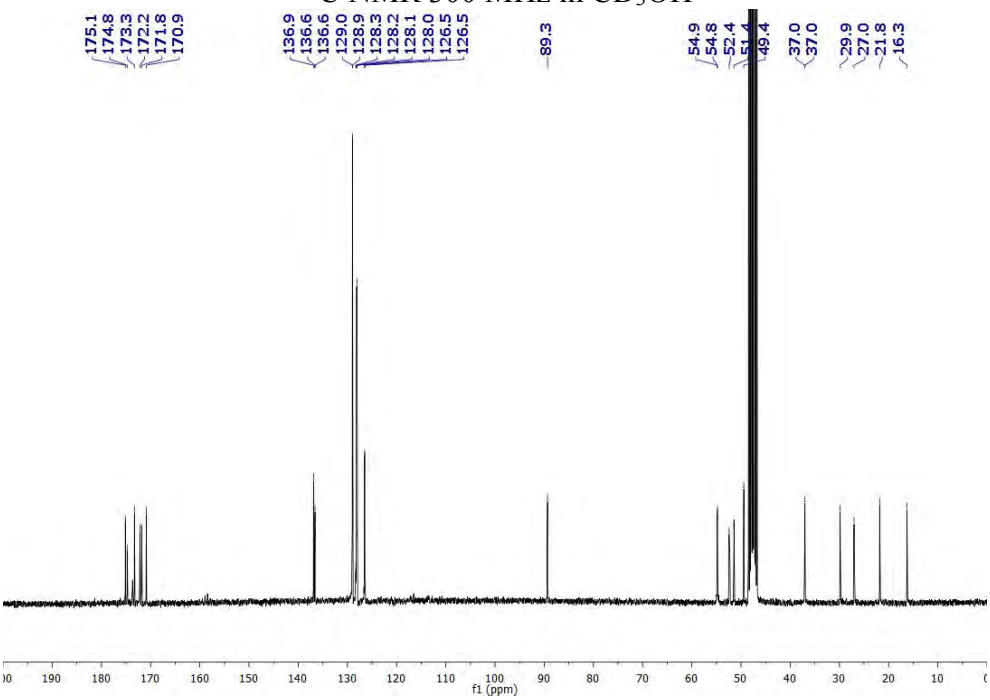

NOESY 400 MHz in H_2O/D_2O

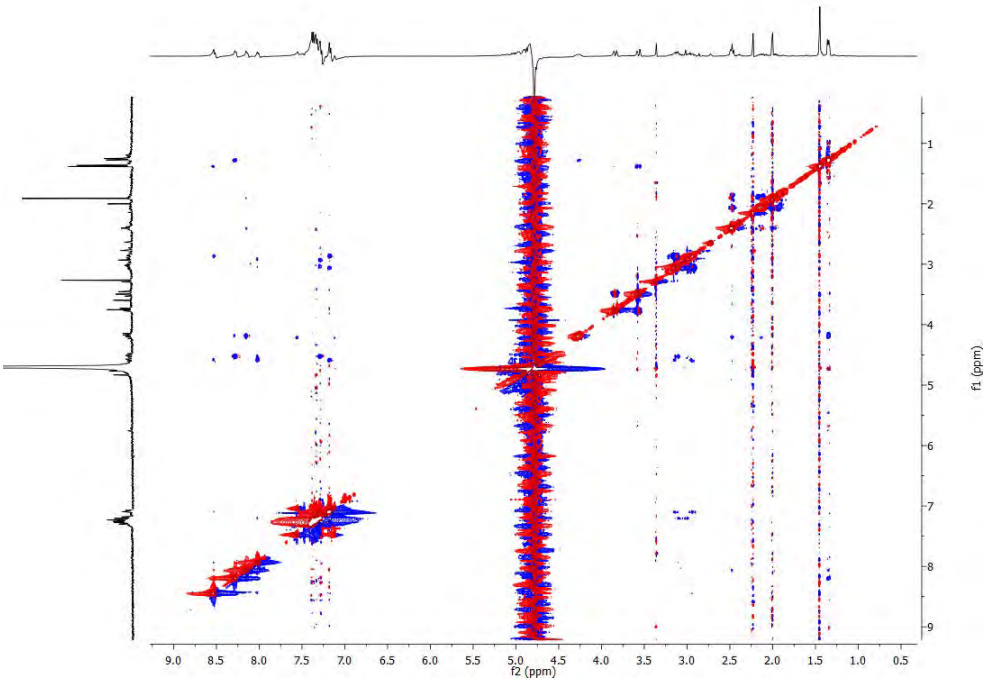

^1H NMR 400 MHz in H_2O/D_2O amide region

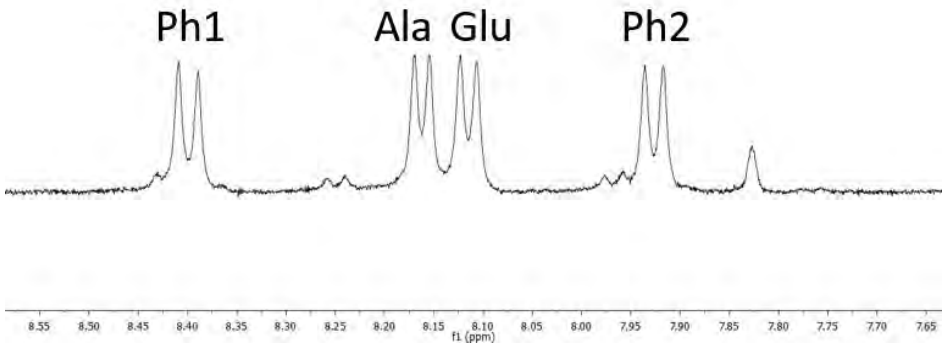

^{1}H NMR 300 MHz in CD_3OH

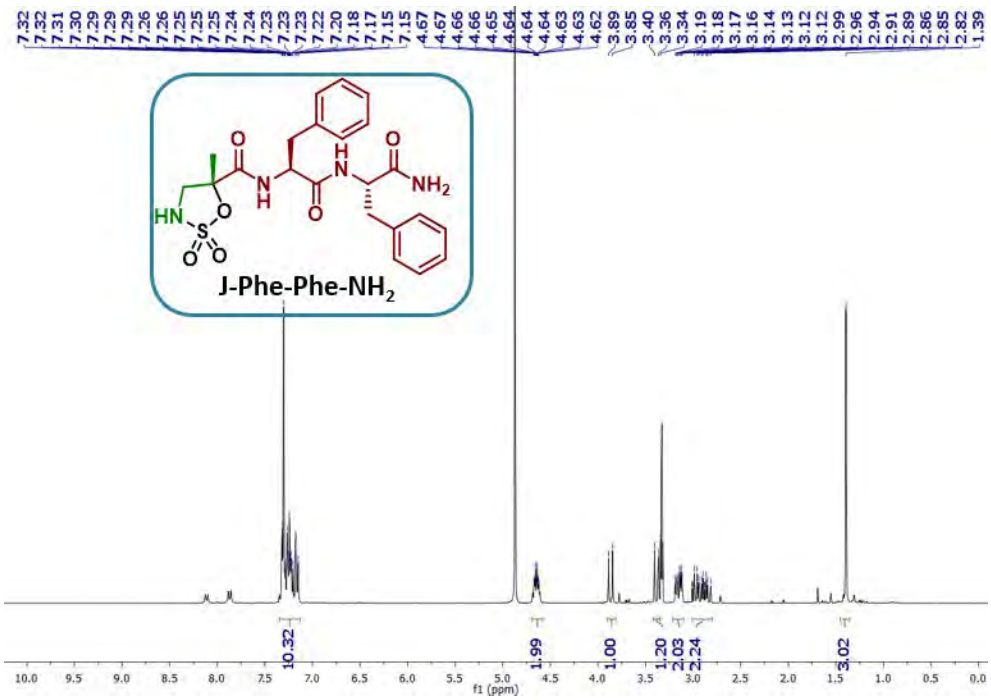

^{13}C NMR 100 MHz in CD_3OH

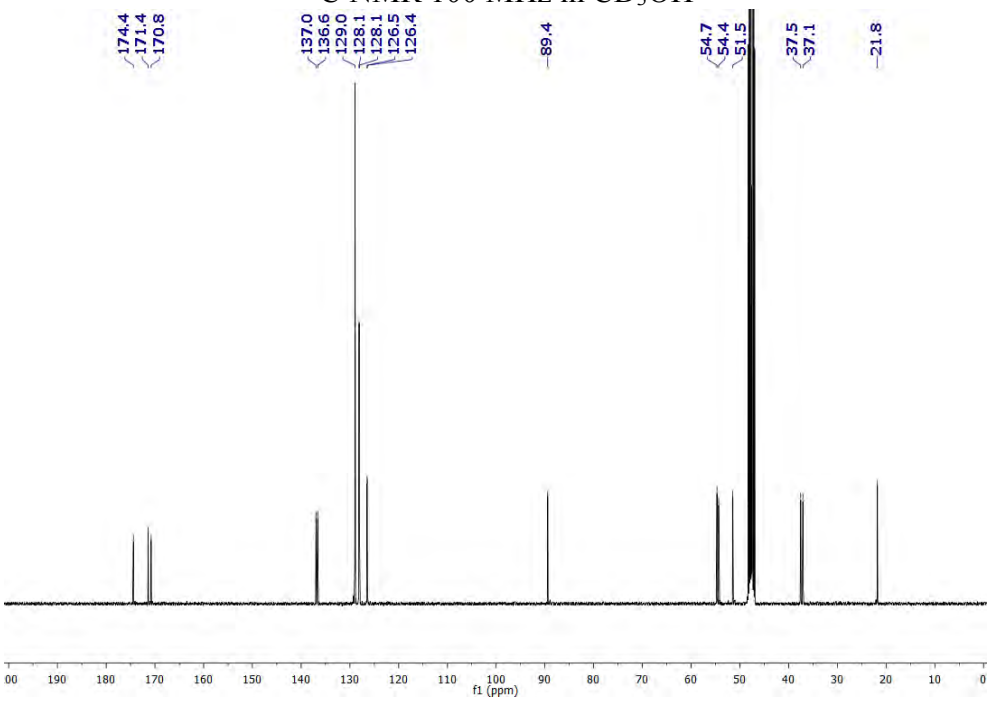

^{1}H NMR 300 MHz in D_2O

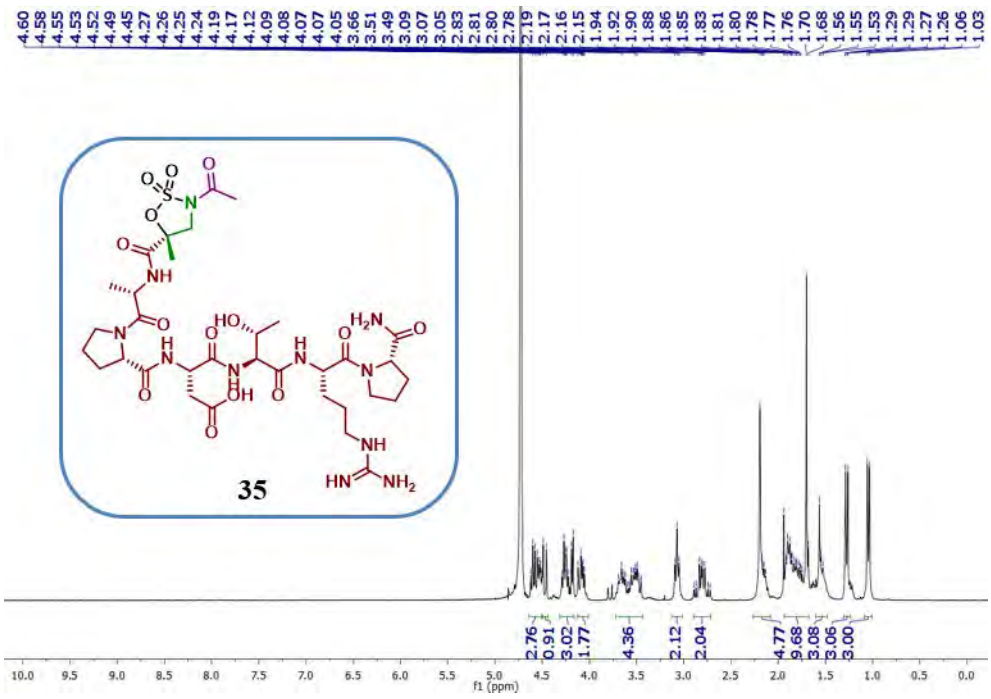

^{13}C NMR 75 MHz in D_2O

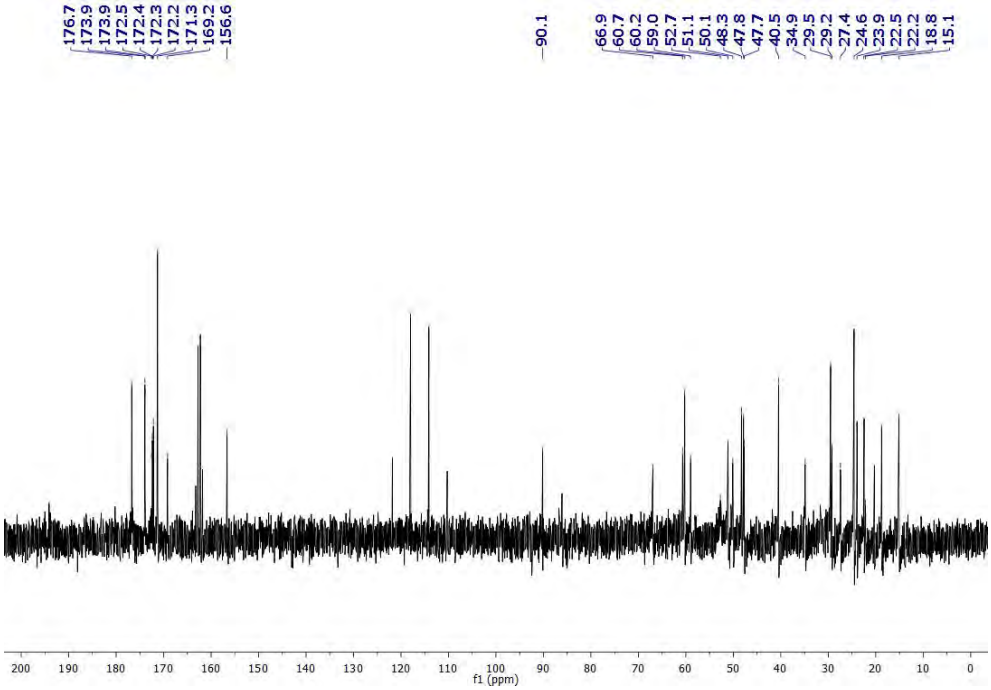

^{1}H NMR 300 MHz in D_2O

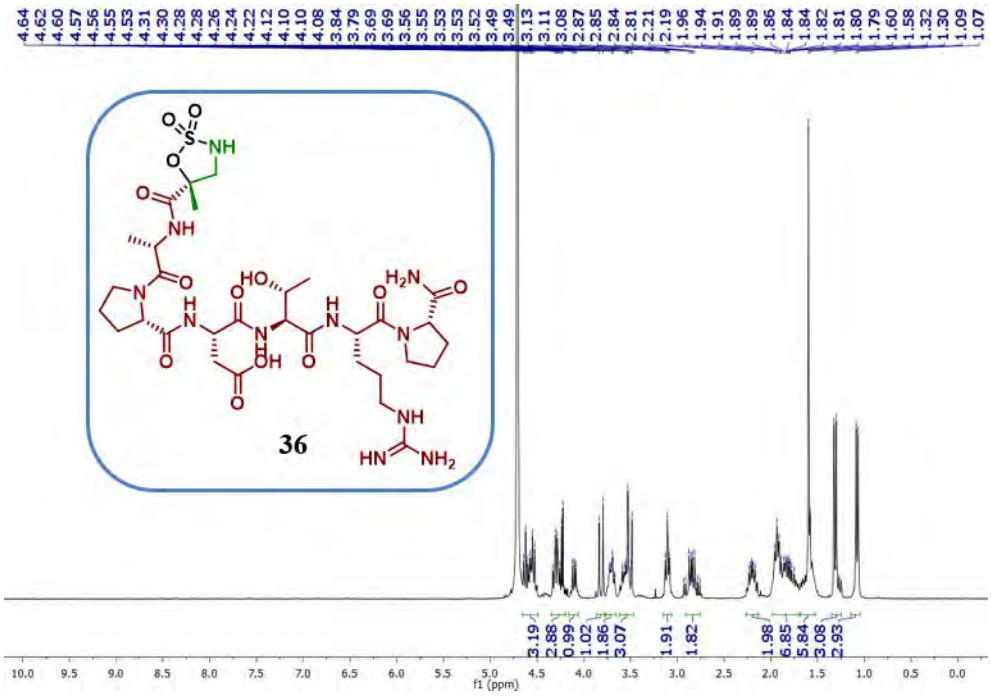

^{13}C NMR 75 MHz in D_2O

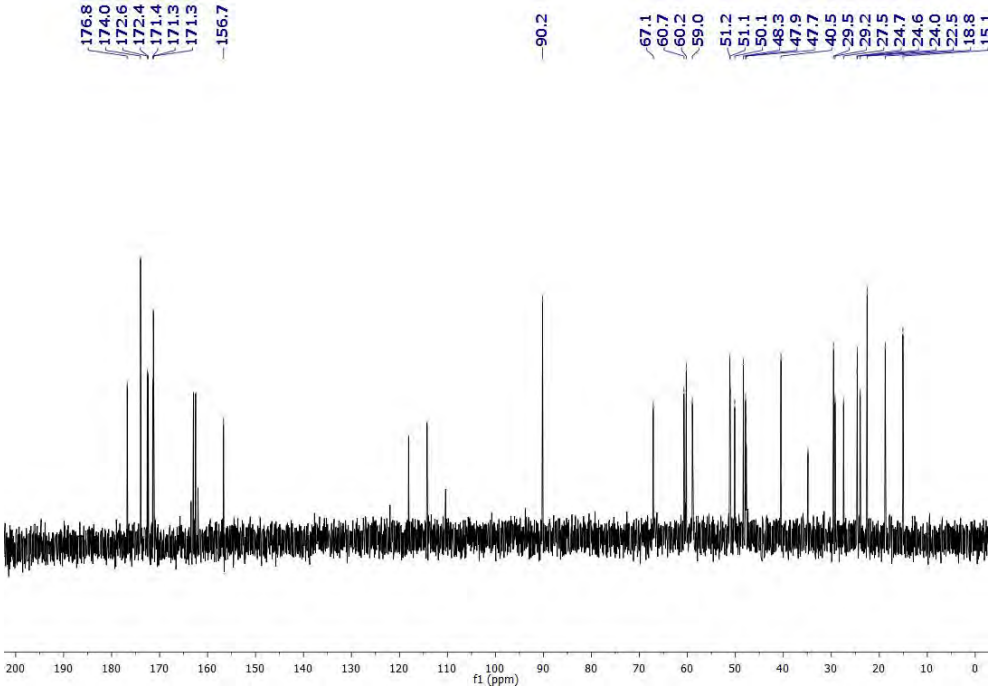

^{1}H NMR 300 MHz in D_2O

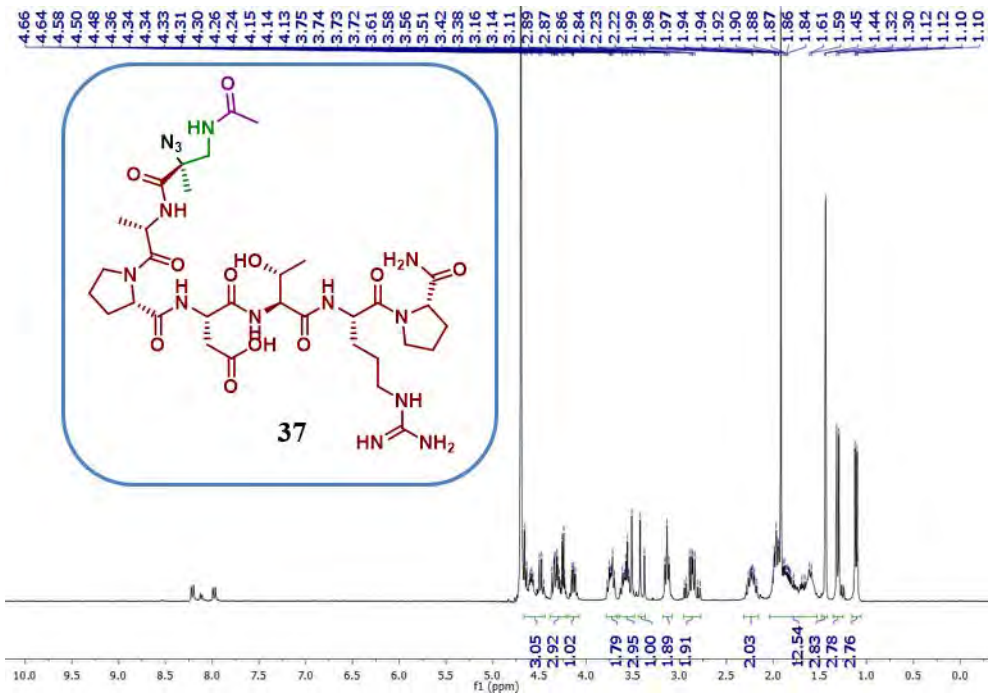

^{13}C NMR 75 MHz in D_2O

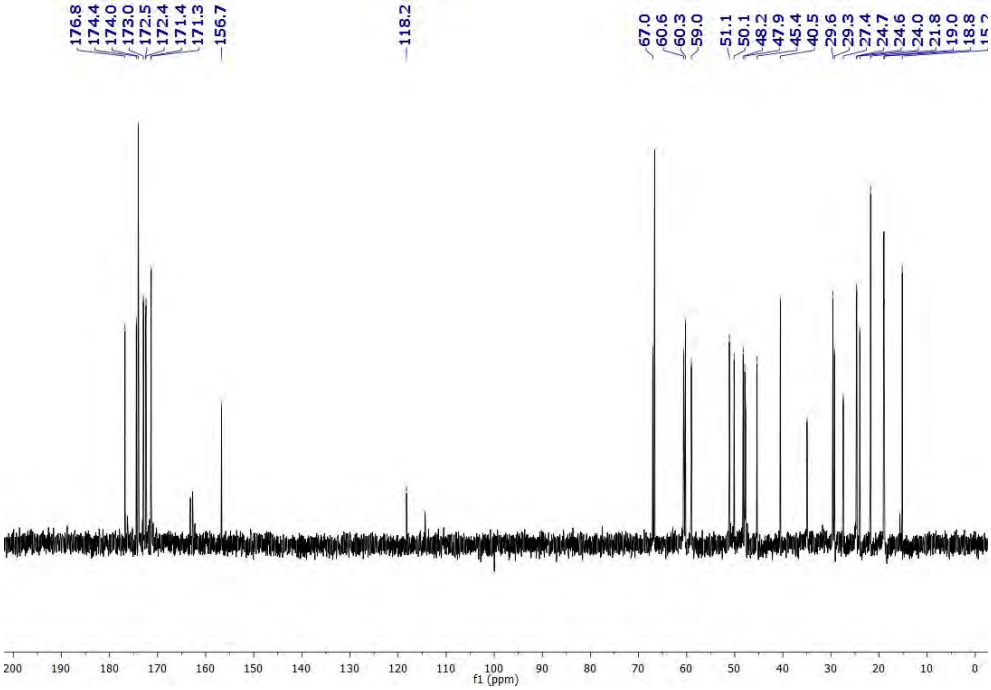

^{1}H NMR 300 MHz in D_2O

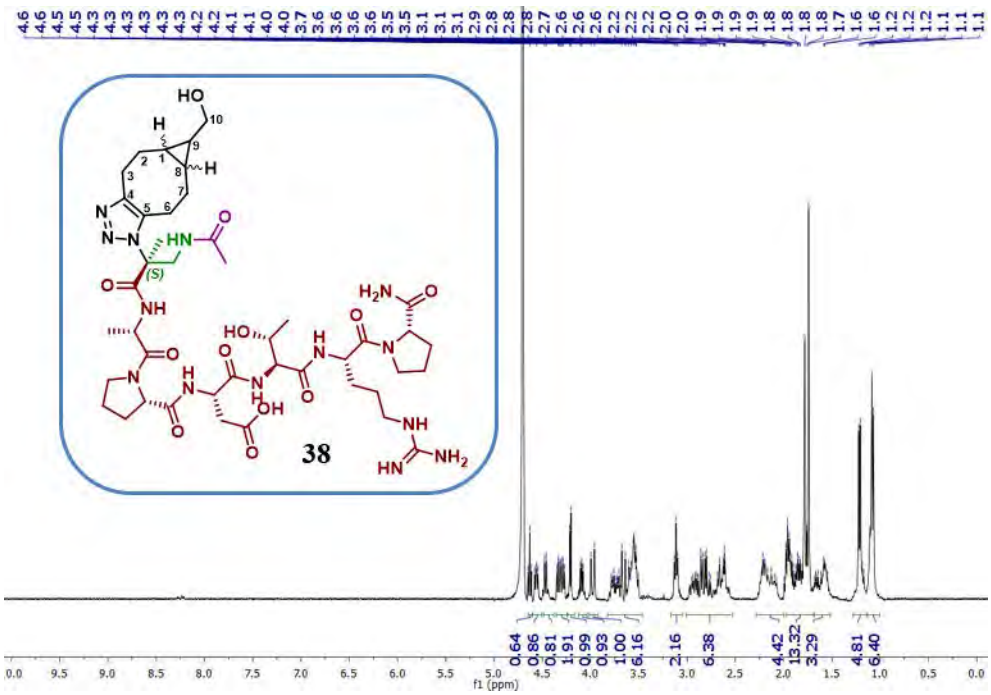

^{1}H NMR 300 MHz in D_2O

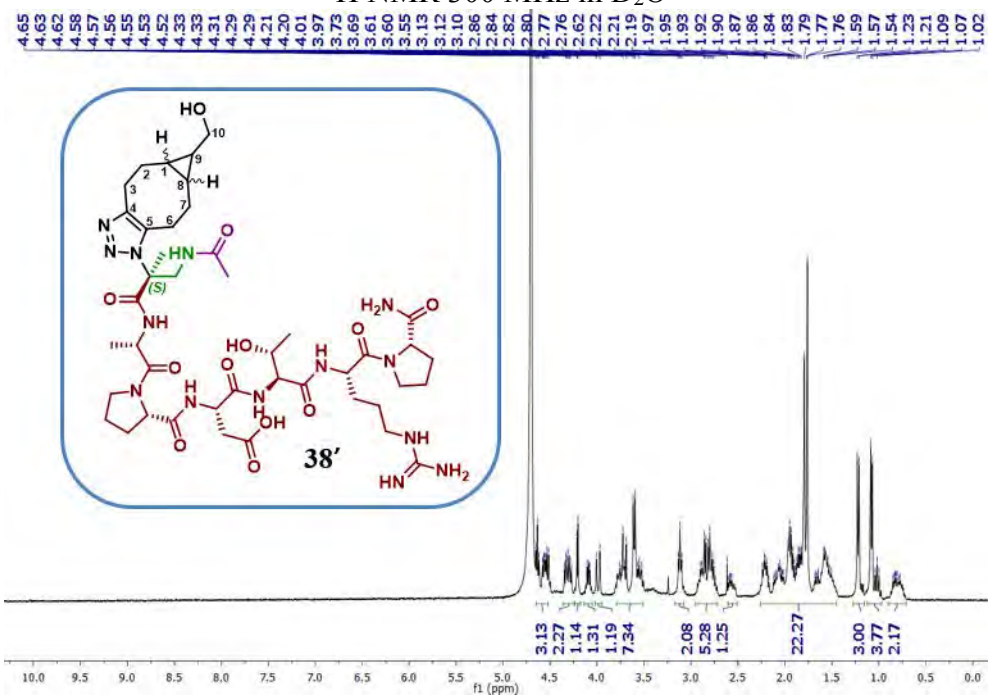

^{1}H NMR 300 MHz in D_2O

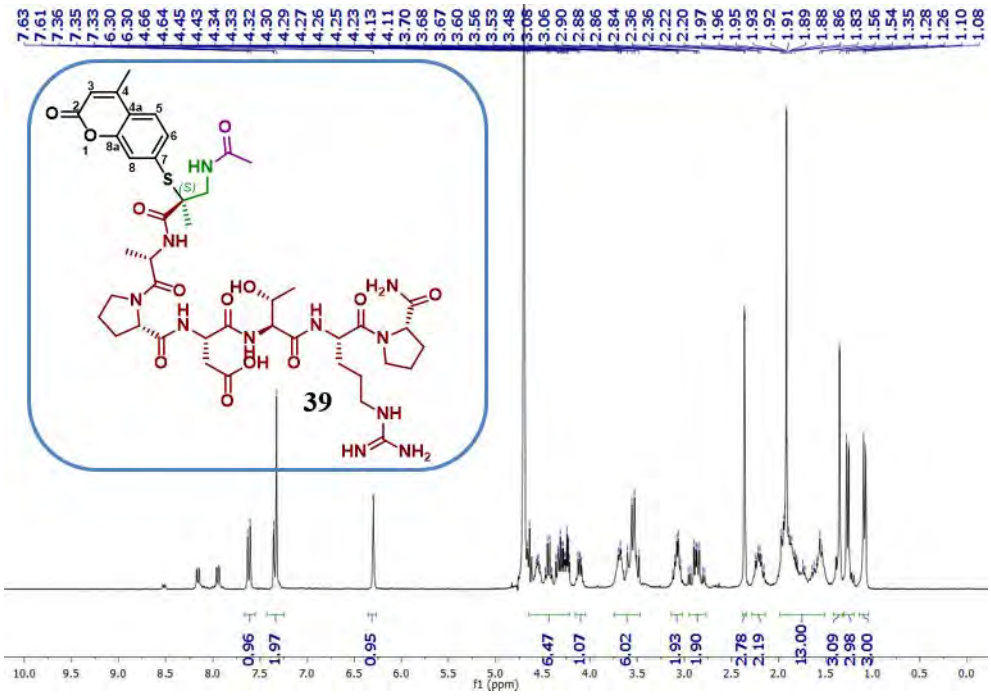

^{13}C NMR 75 MHz in D_2O

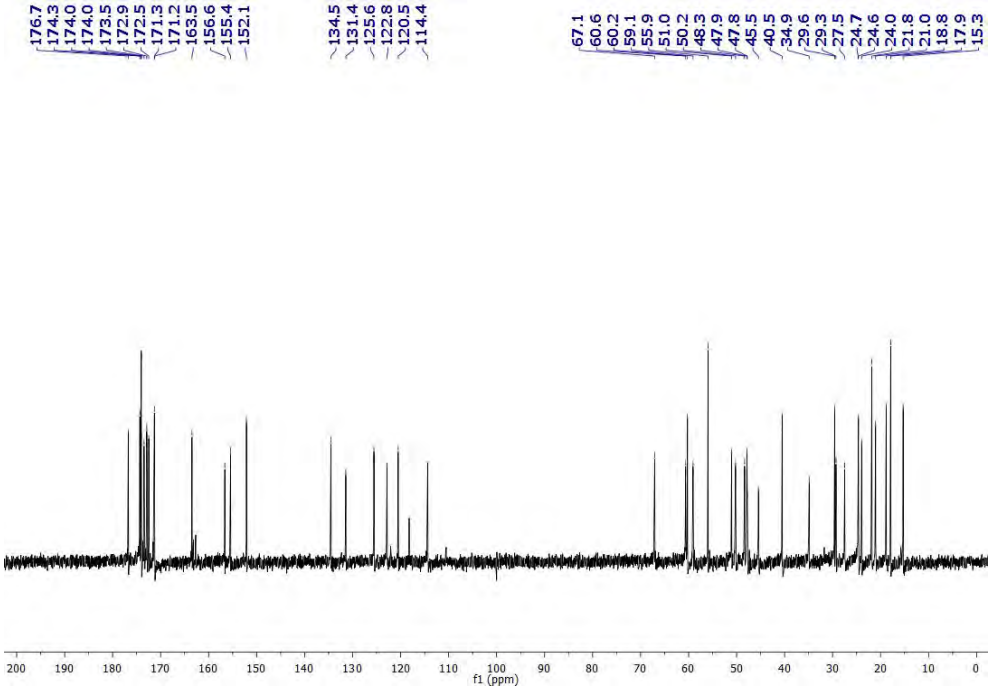

^{1}H NMR 400 MHz in D_2O

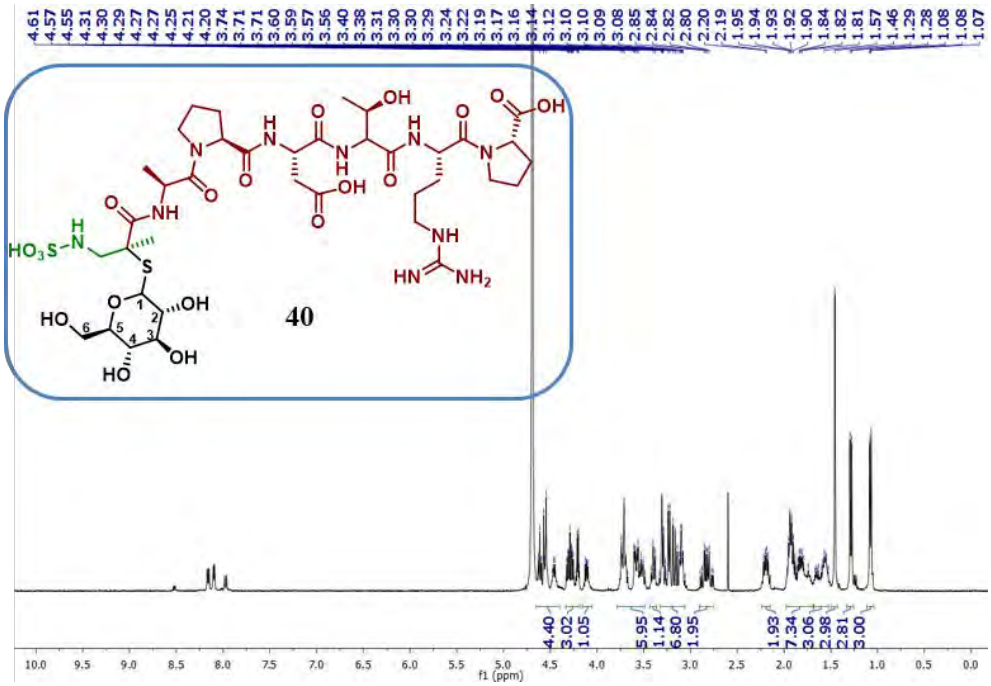

^{13}C NMR 75 MHz in D_2O

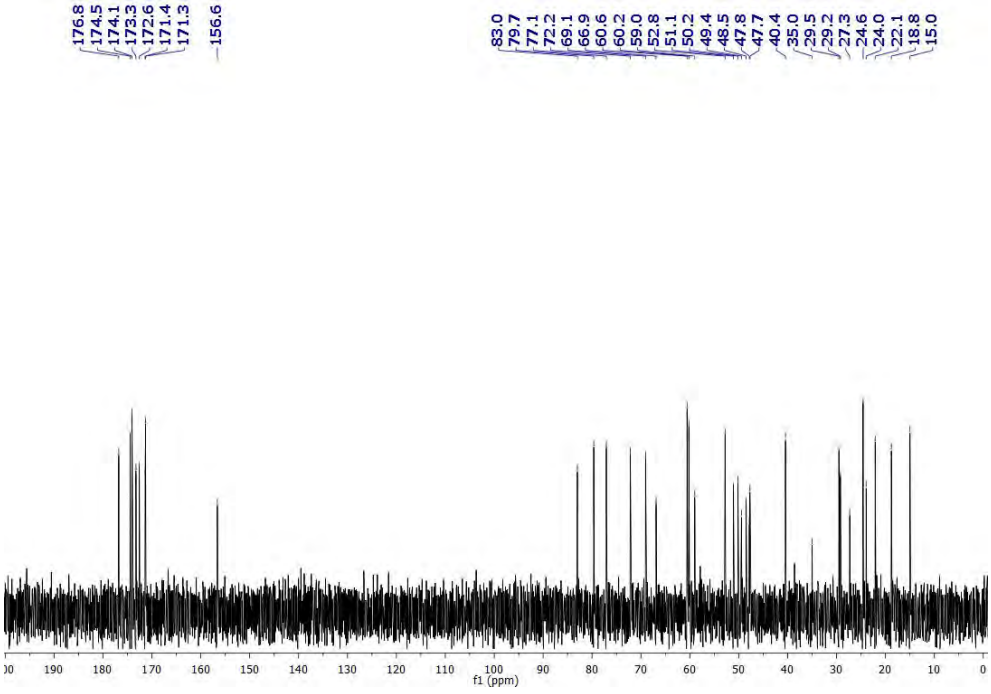

HMBC 400 MHz in D_2O

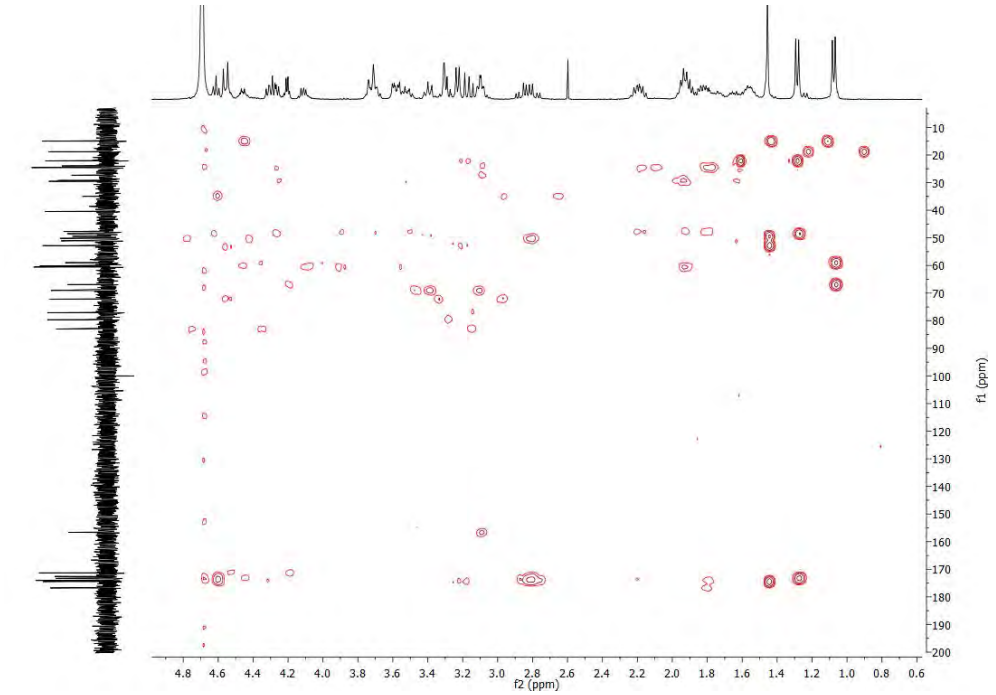

NOESY 400 MHz in H_2O/D_2O

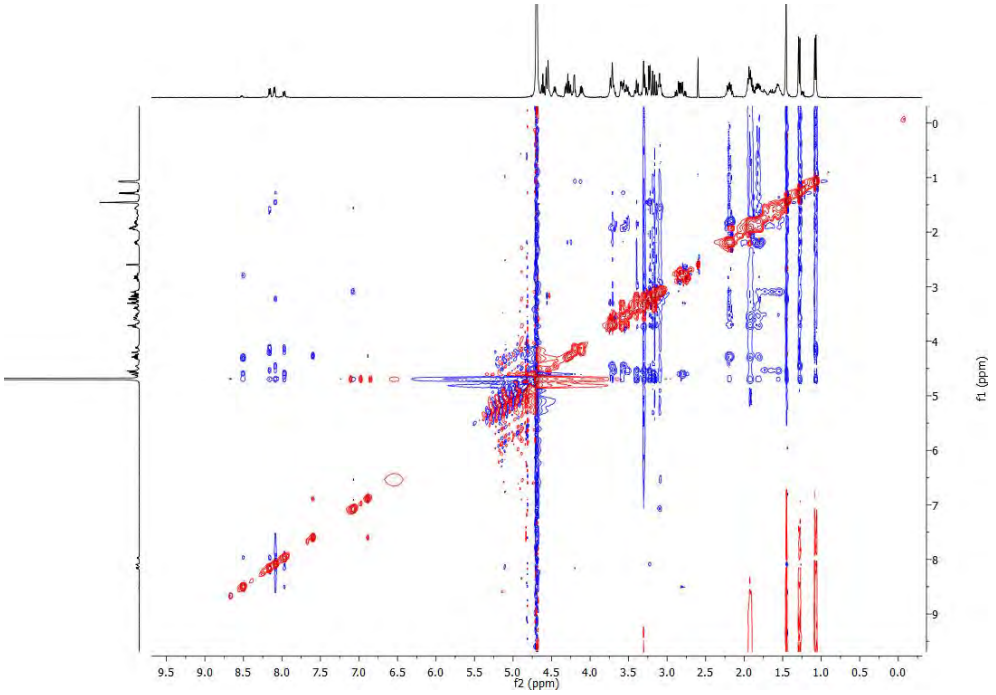

^{1}H NMR 300 MHz in CD_3OH

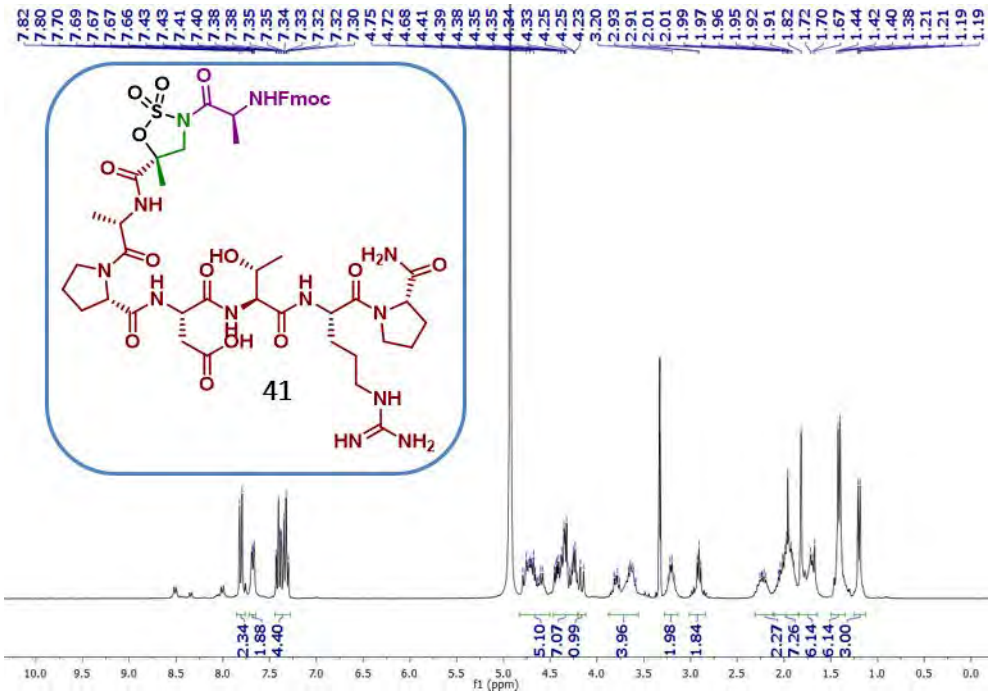

^{13}C NMR 300 MHz in CD_3OH

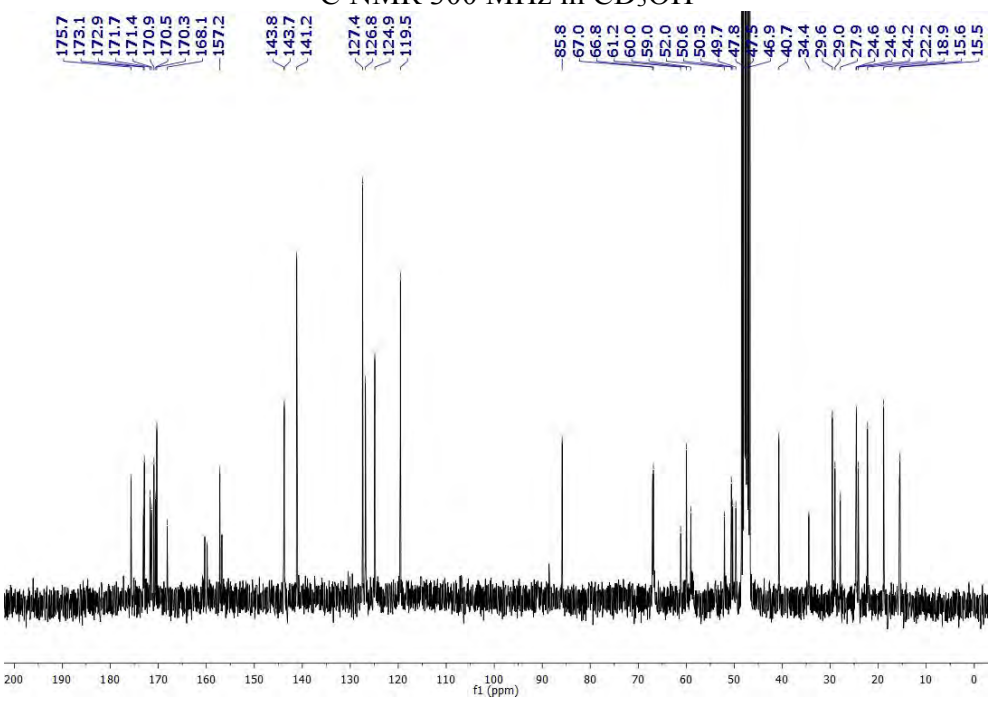

^{1}H NMR 300 MHz in D_2O

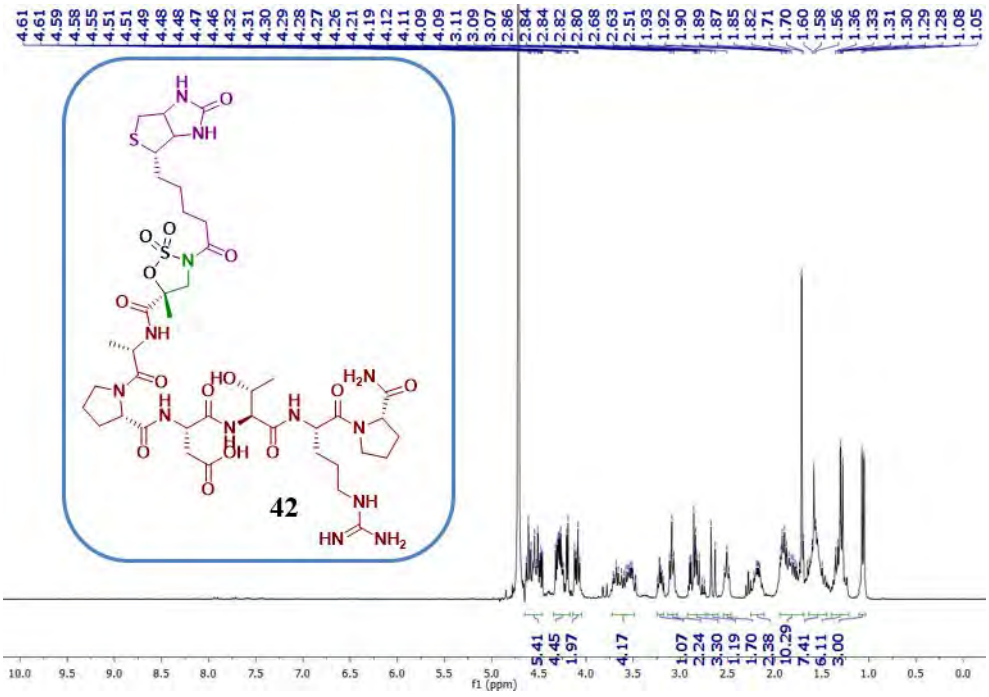

^{13}C NMR 75 MHz in D_2O

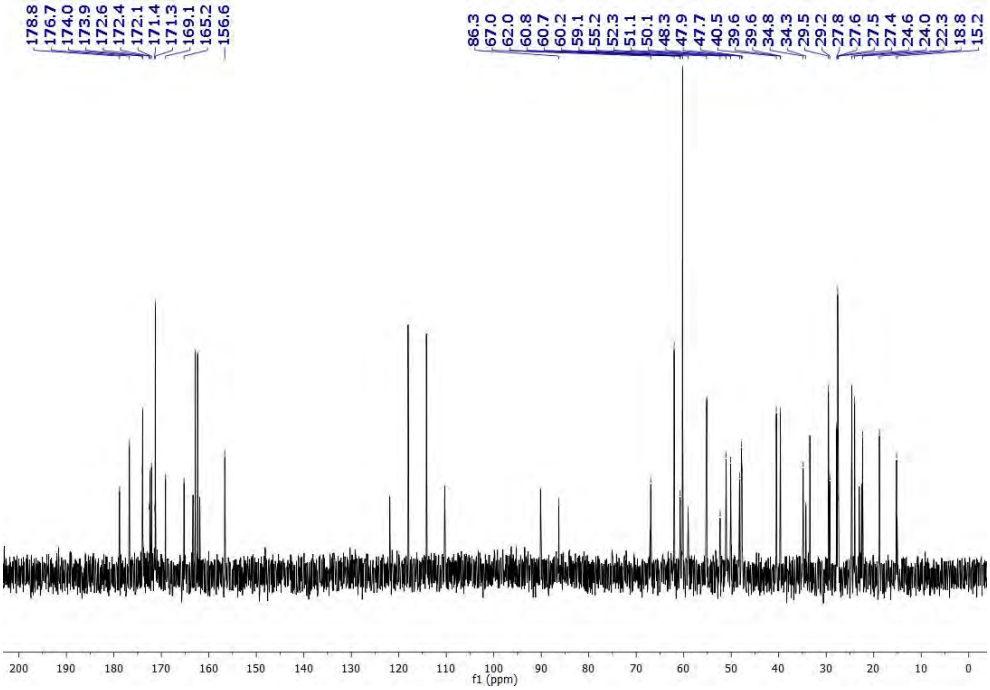

^{1}H NMR 300 MHz in D_2O

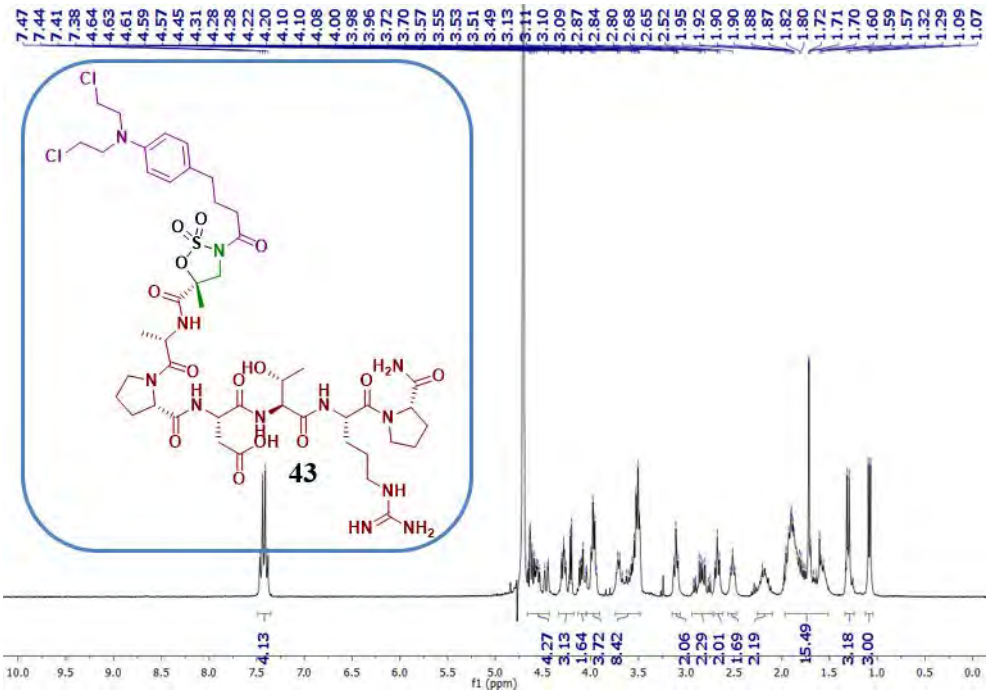

^{13}C NMR 75 MHz in D_2O

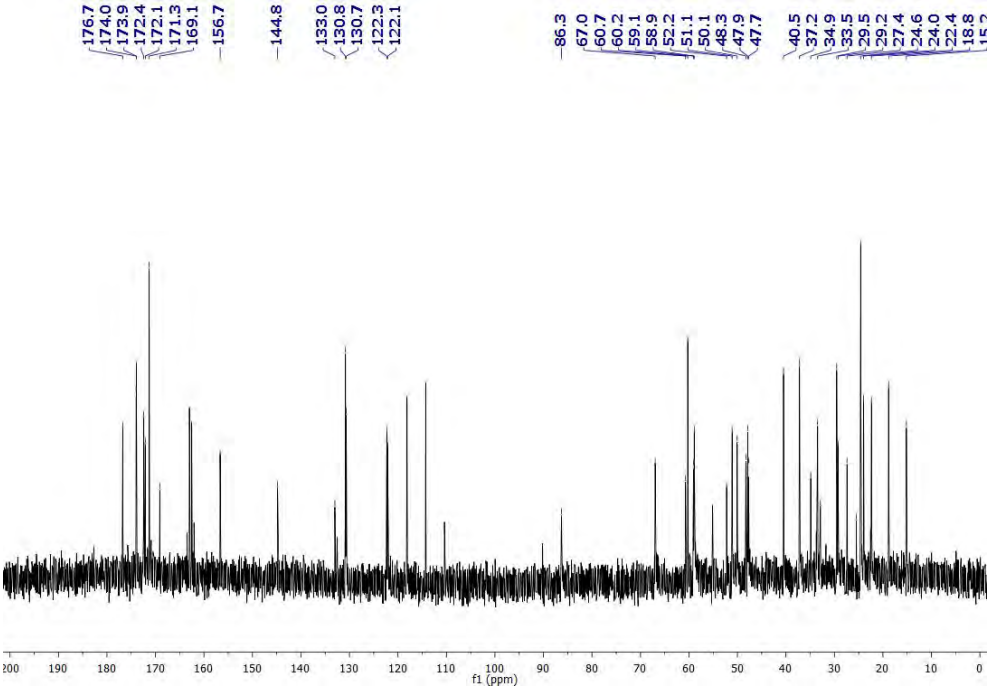

^{1}H NMR 300 MHz in CD_3CN/D_2O (95:5)

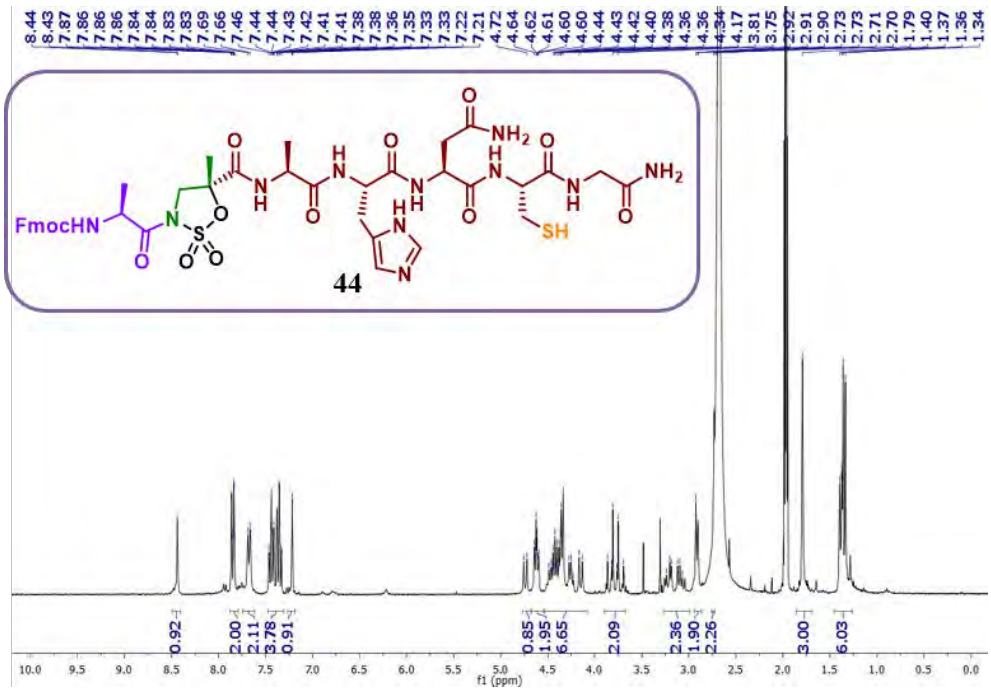

^{13}C NMR 75 MHz in CD_3CN/D_2O (95:5)

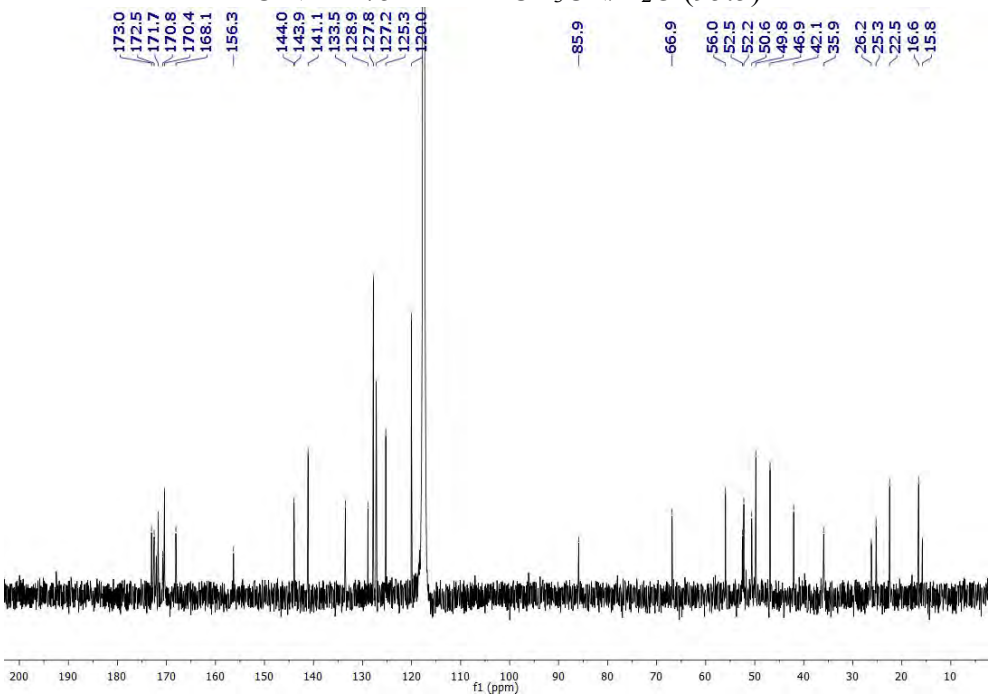

^{1}H NMR 300 MHz in CD_3CN/D_2O (95:5)

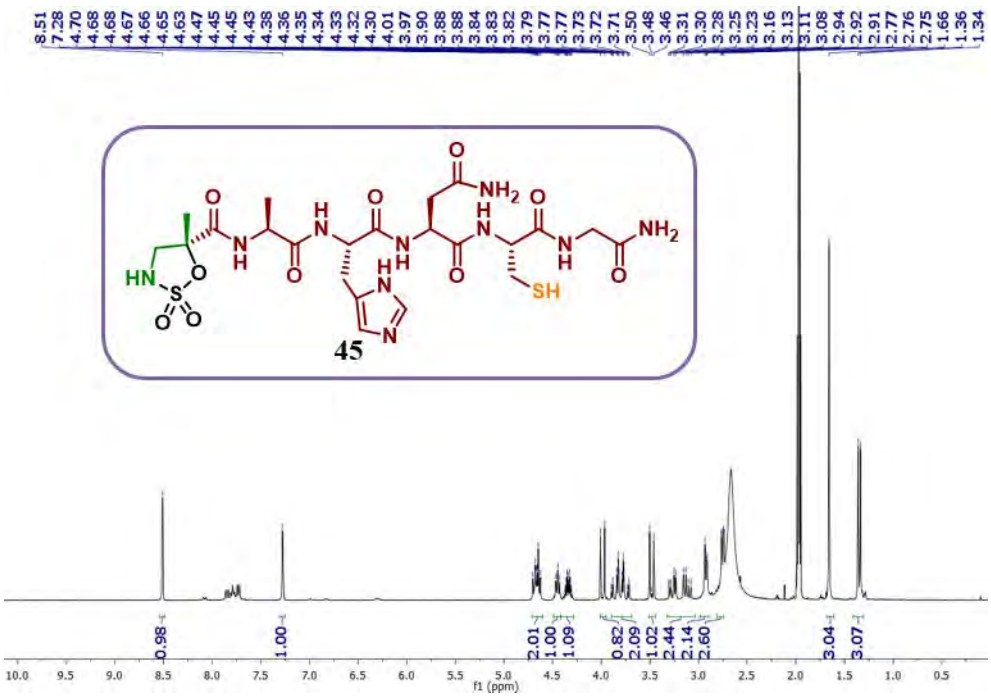

^{13}C NMR 75 MHz in CD_3CN/D_2O (95:5)

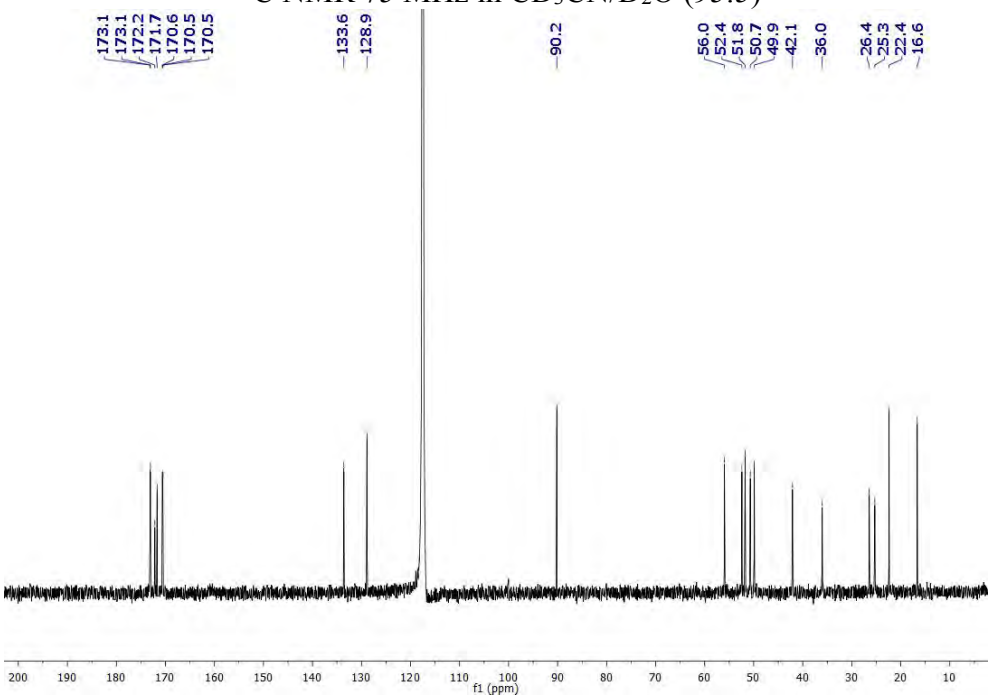

^{1}H NMR 300 MHz in CD_3CN/D_2O (95:5)

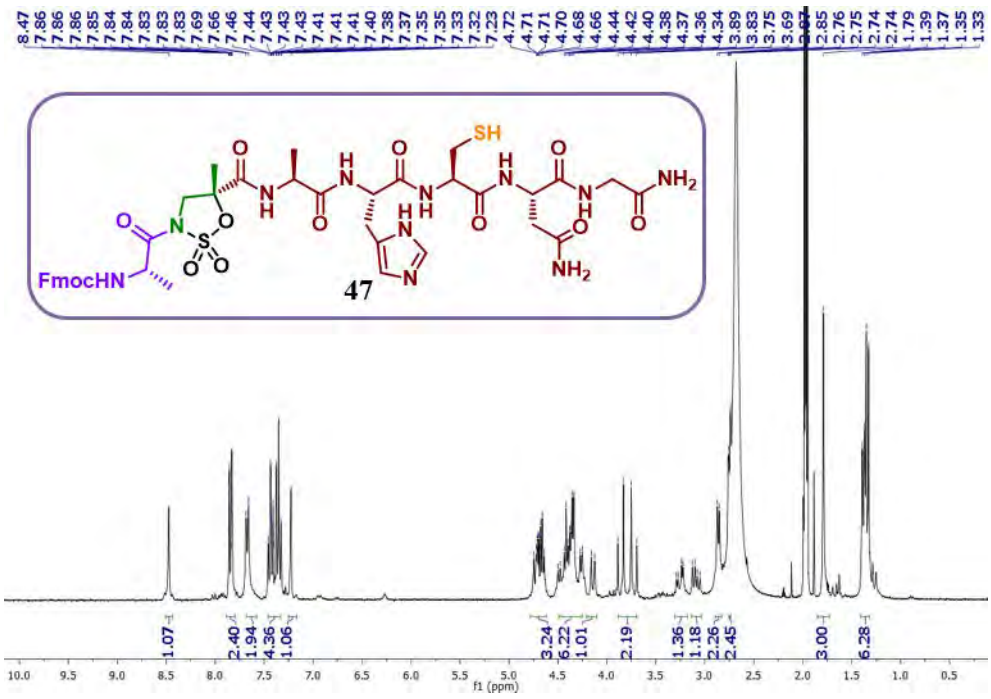

^{13}C NMR 75 MHz in CD_3CN/D_2O (95:5)

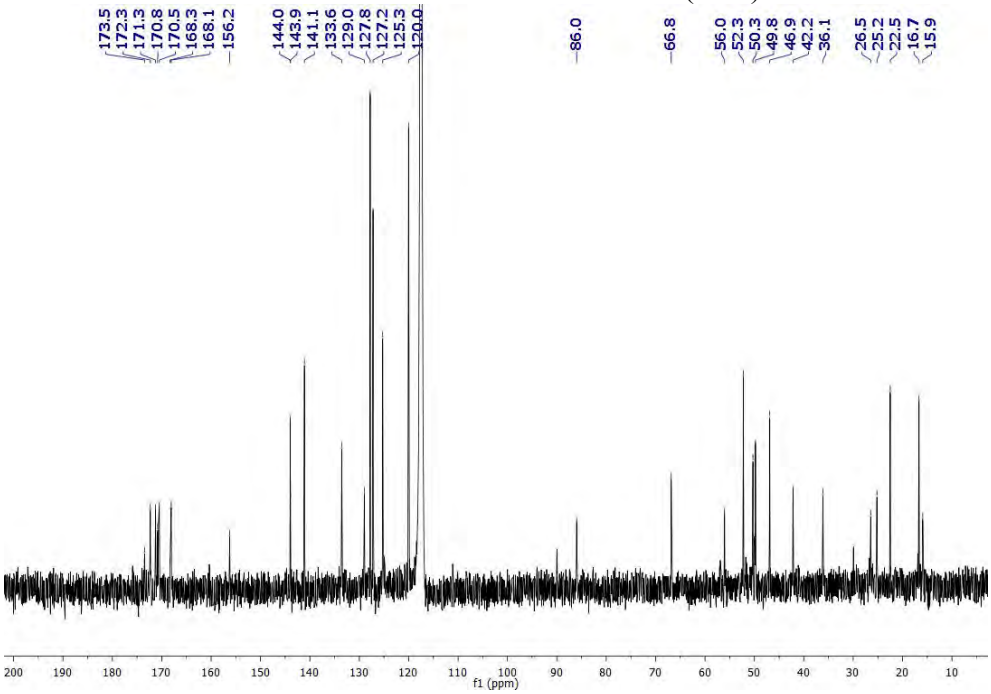

^{1}H NMR 300 MHz in CD_3CN/D_2O (95:5)

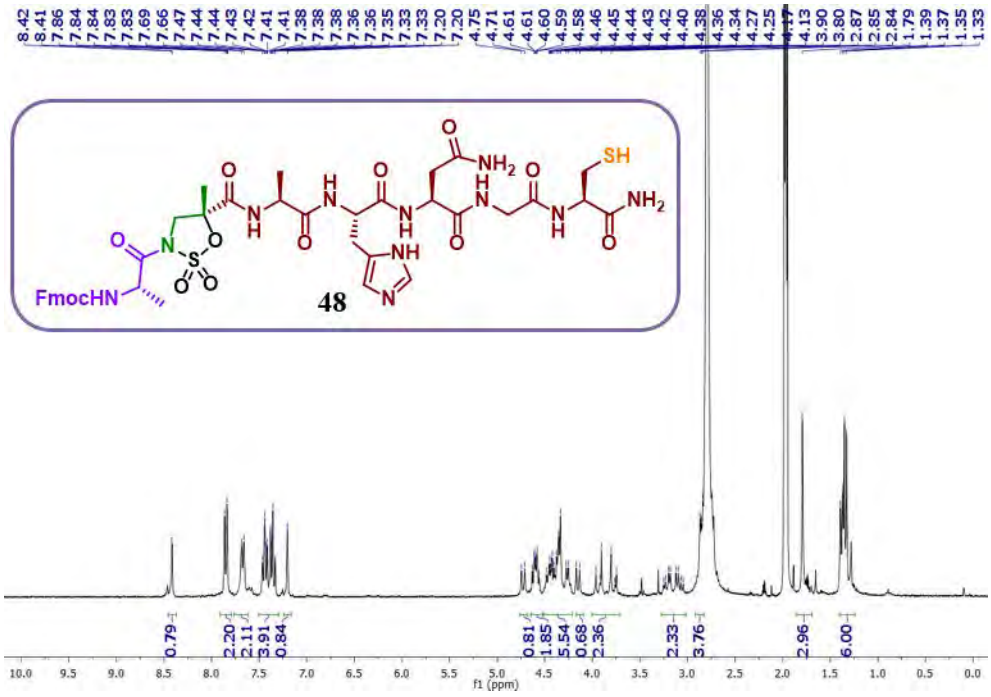

^{13}C NMR 75 MHz in CD_3CN/D_2O (95:5)

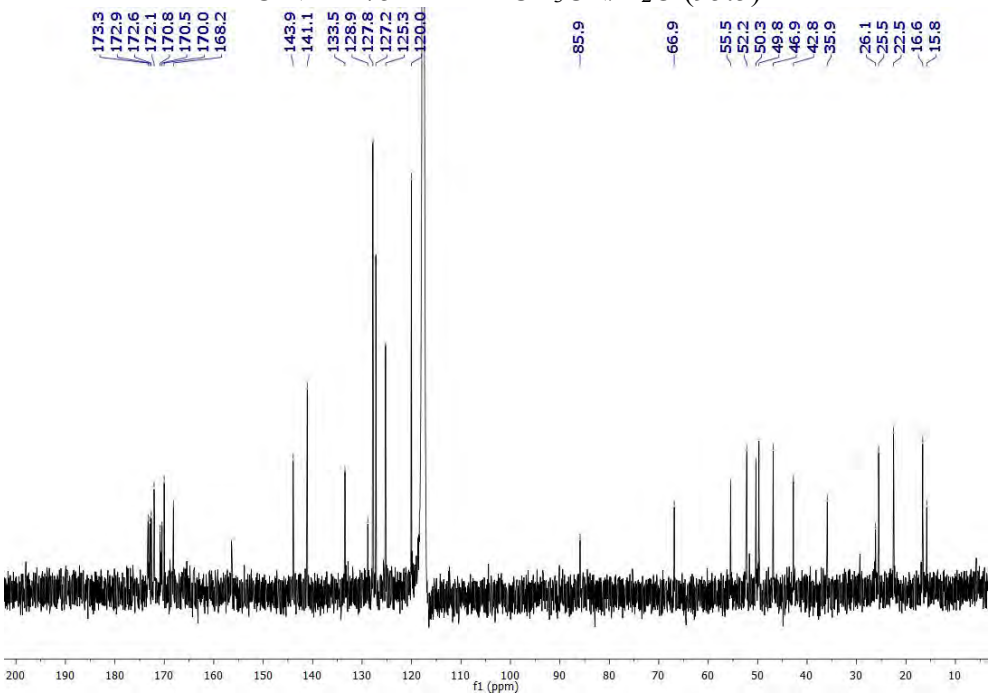

^{1}H NMR 300 MHz in CD_3CN/D_2O (95:5)

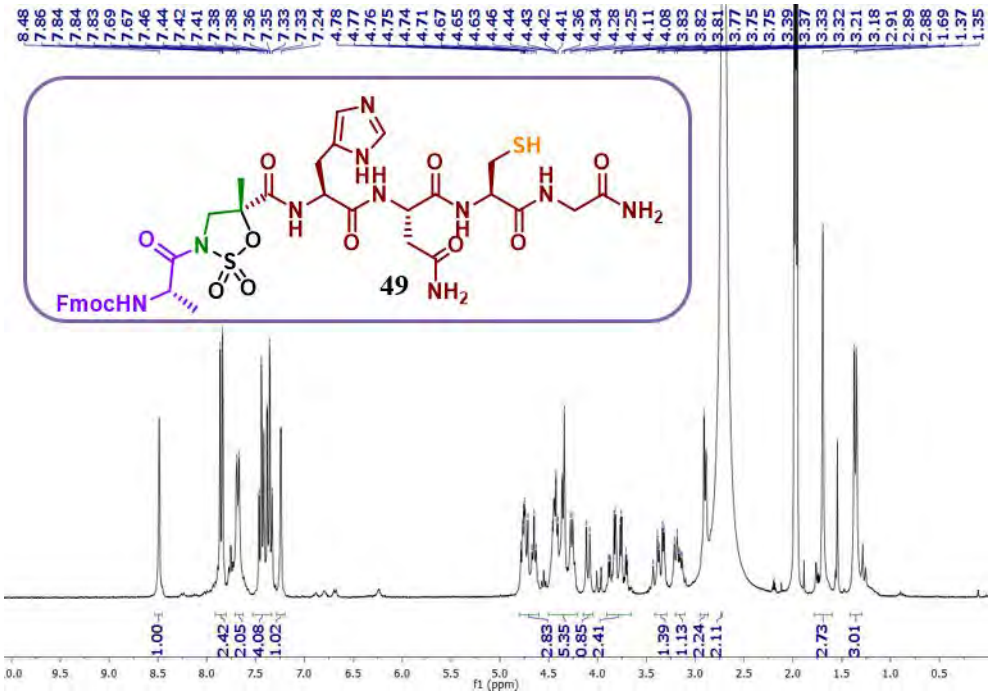

^{13}C NMR 75 MHz in CD_3CN/D_2O (95:5)

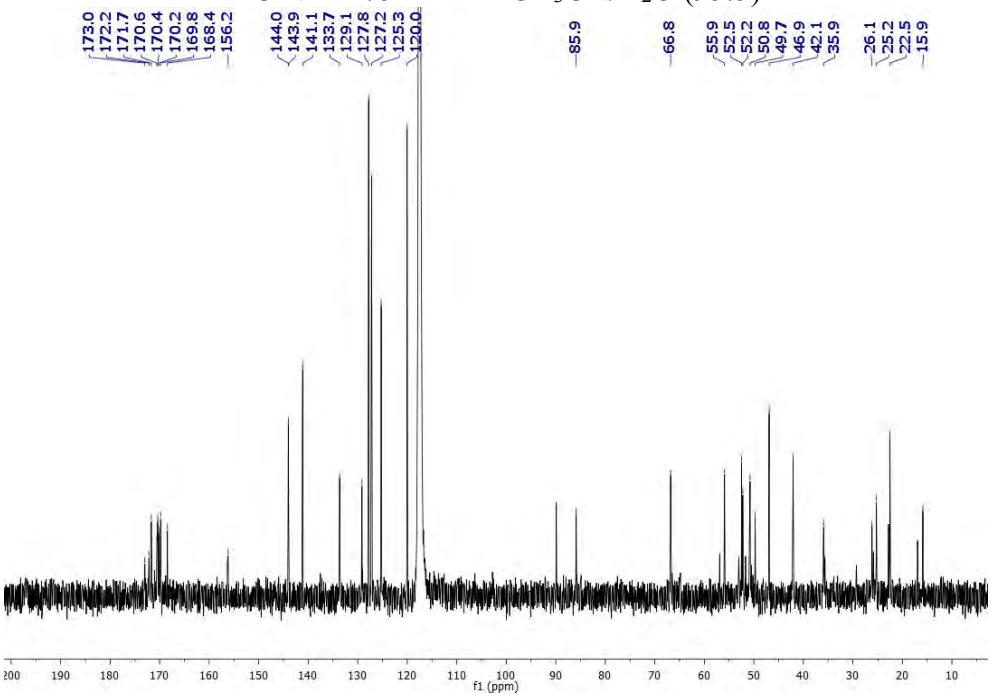

^{1}H NMR 300 MHz in CD_3CN/D_2O (95:5)

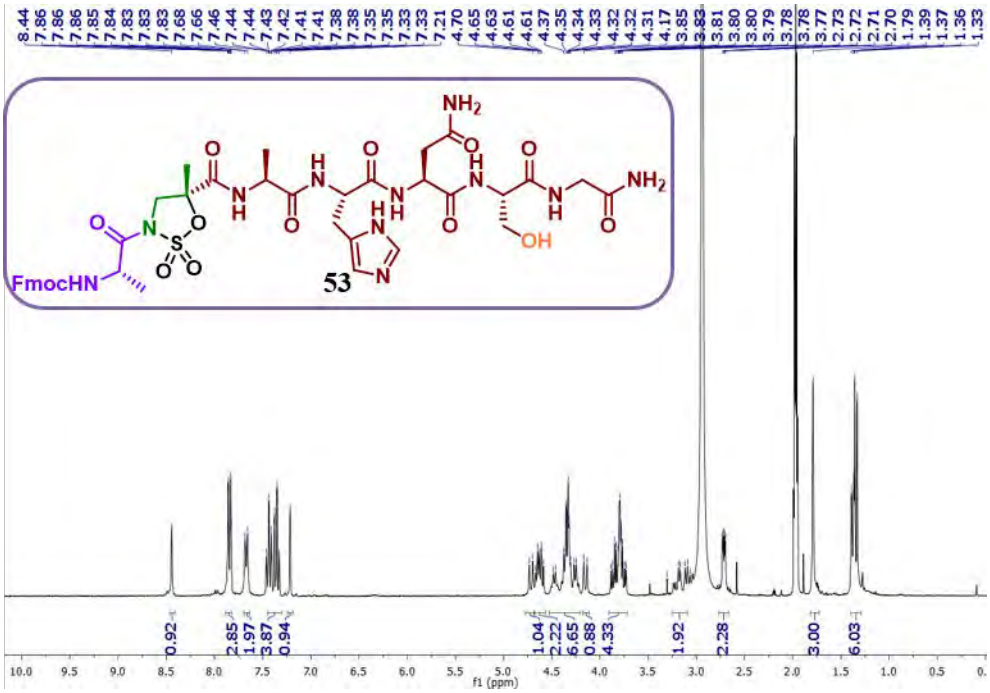

^{13}C NMR 75 MHz in CD_3CN/D_2O (95:5)

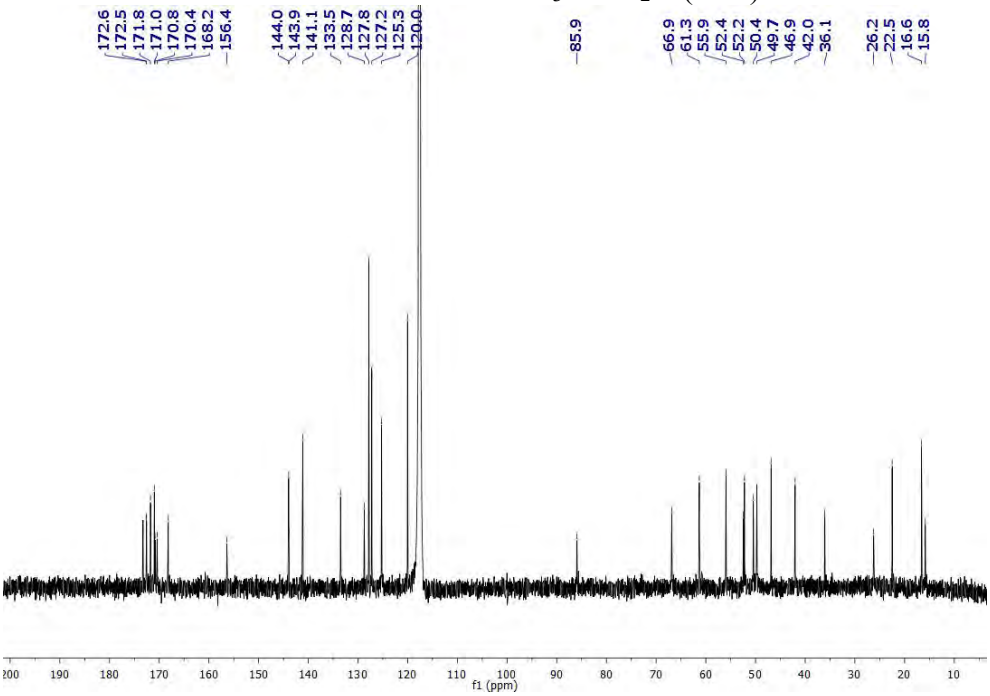

^{1}H NMR 300 MHz in CD_3CN/D_2O (95:5)

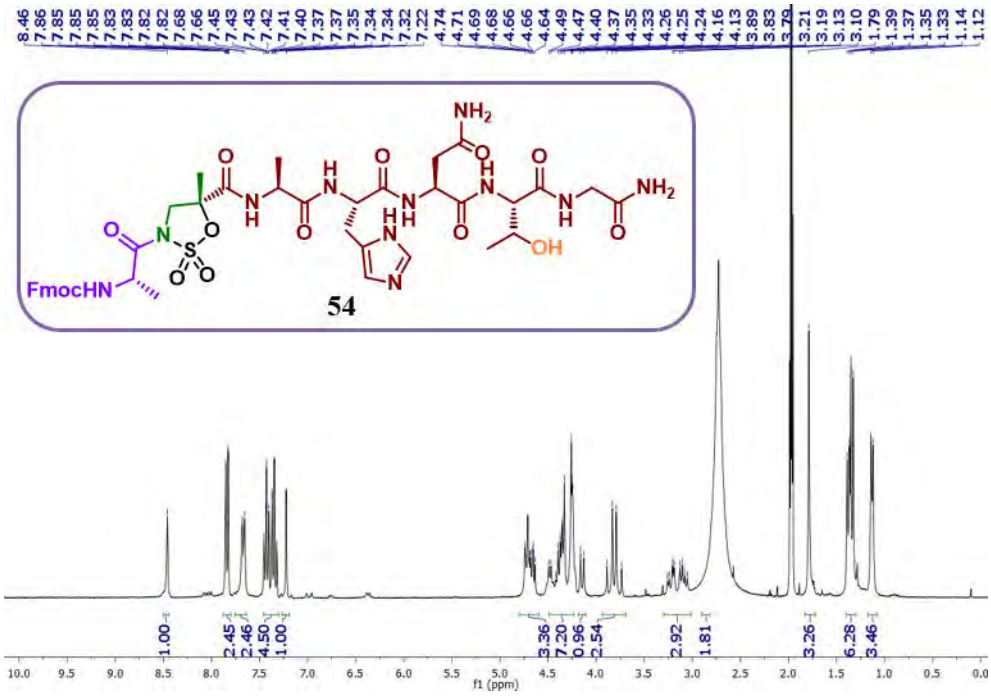

^{13}C NMR 75 MHz in CD_3CN/D_2O (95:5)

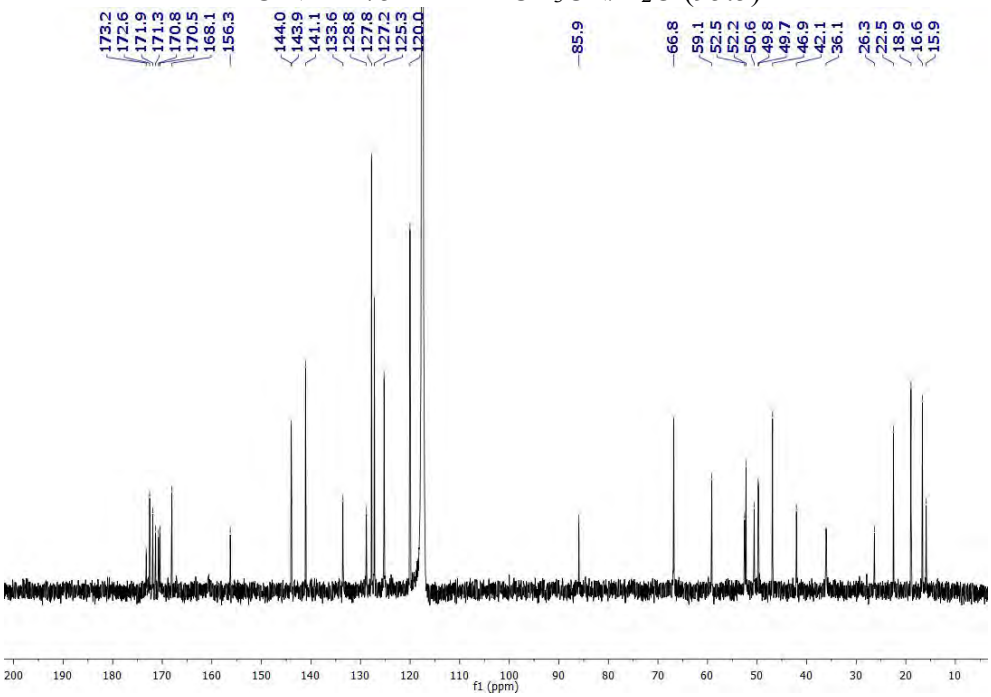

^{1}H NMR 300 MHz in CD_3CN/D_2O (95:5)

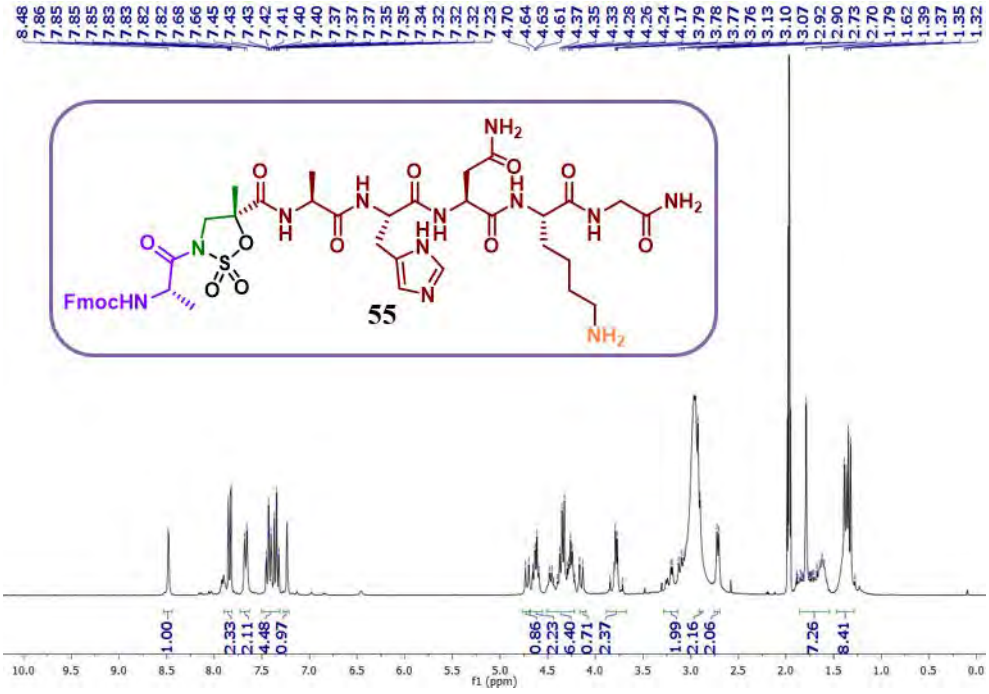

^{13}C NMR 75 MHz in CD_3CN/D_2O (95:5)

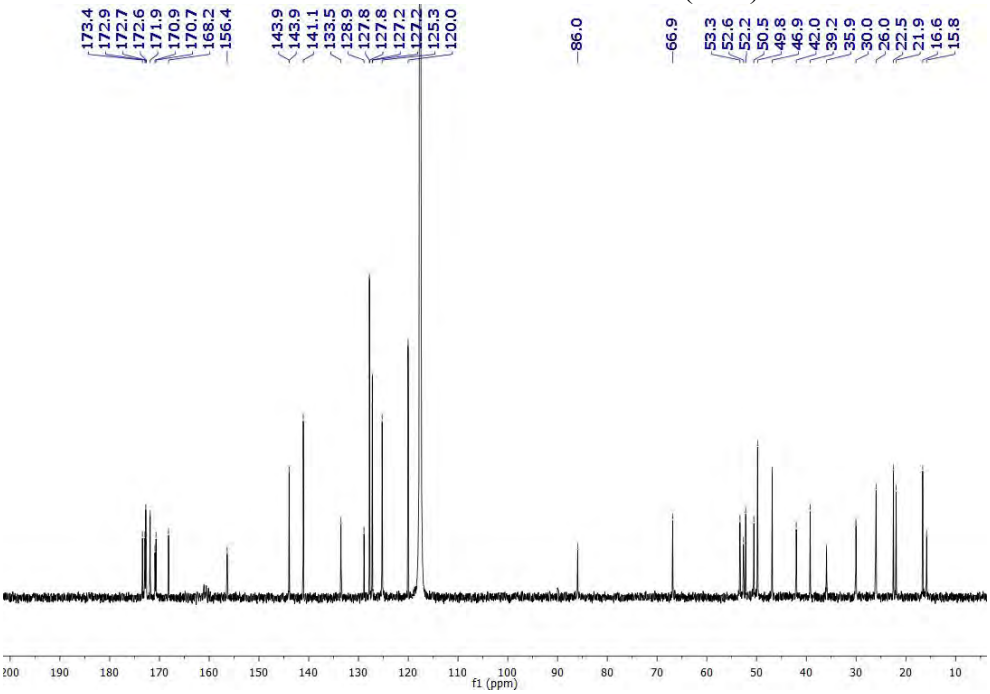

^{1}H NMR 300 MHz in CD_3CN/D_2O (95:5)

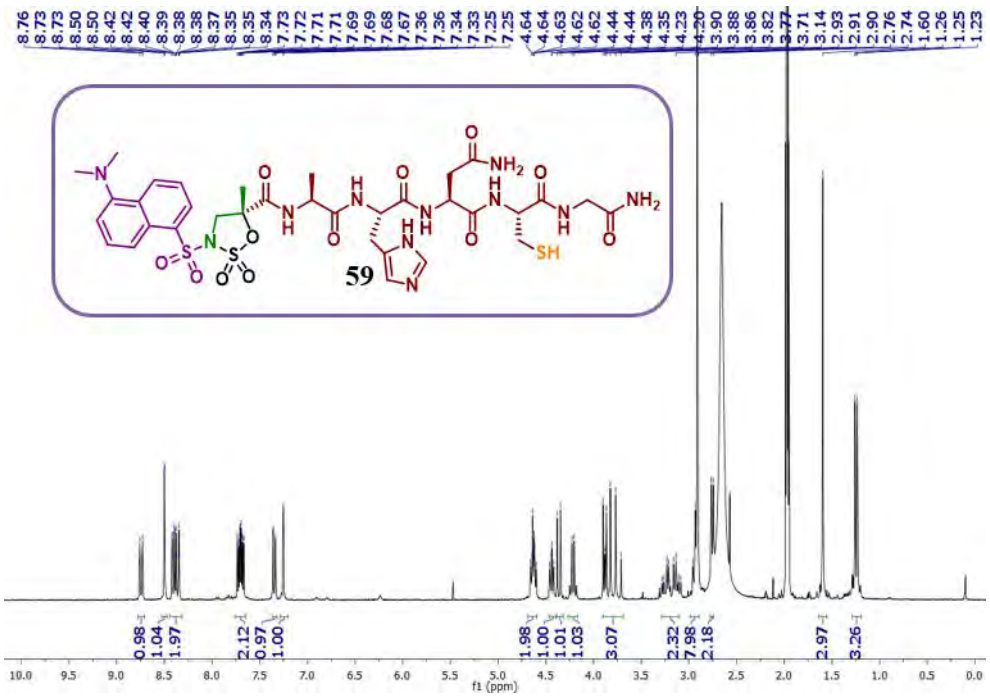

^{13}C NMR 75 MHz in CD_3CN/D_2O (95:5)

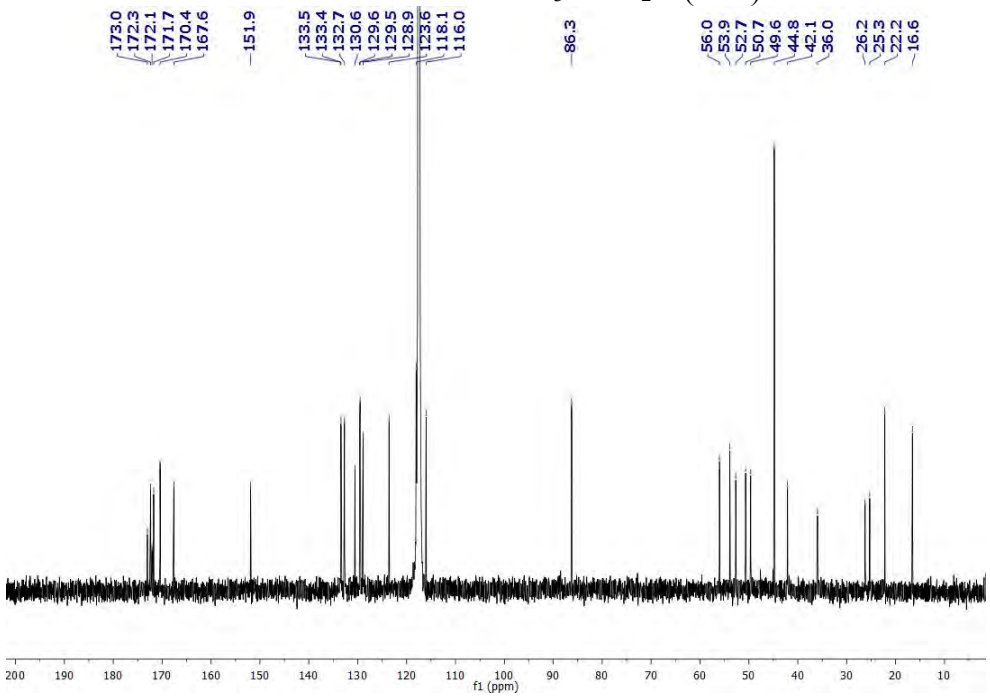

^{1}H NMR 400 MHz in D_2O

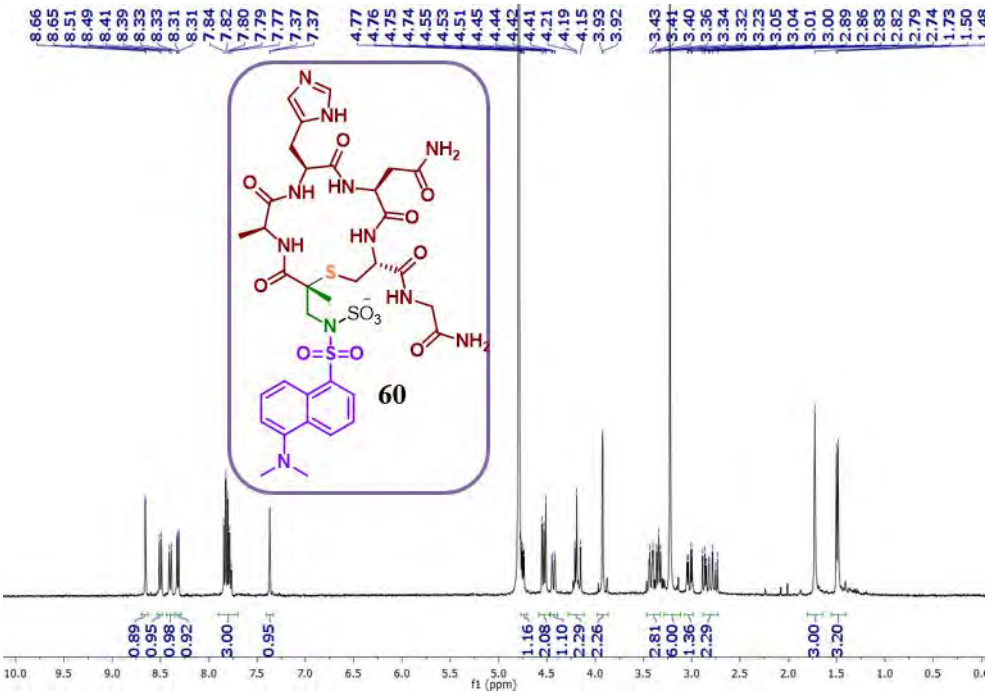

^{13}C NMR 100 MHz in D_2O

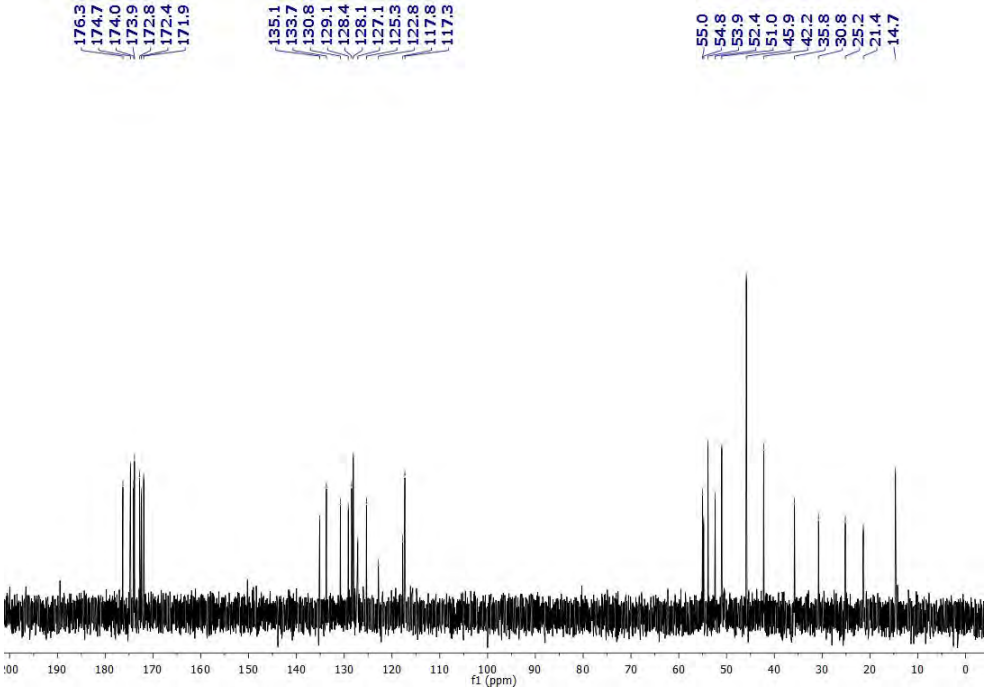

^{1}H NMR 300 MHz in CD_3Cl

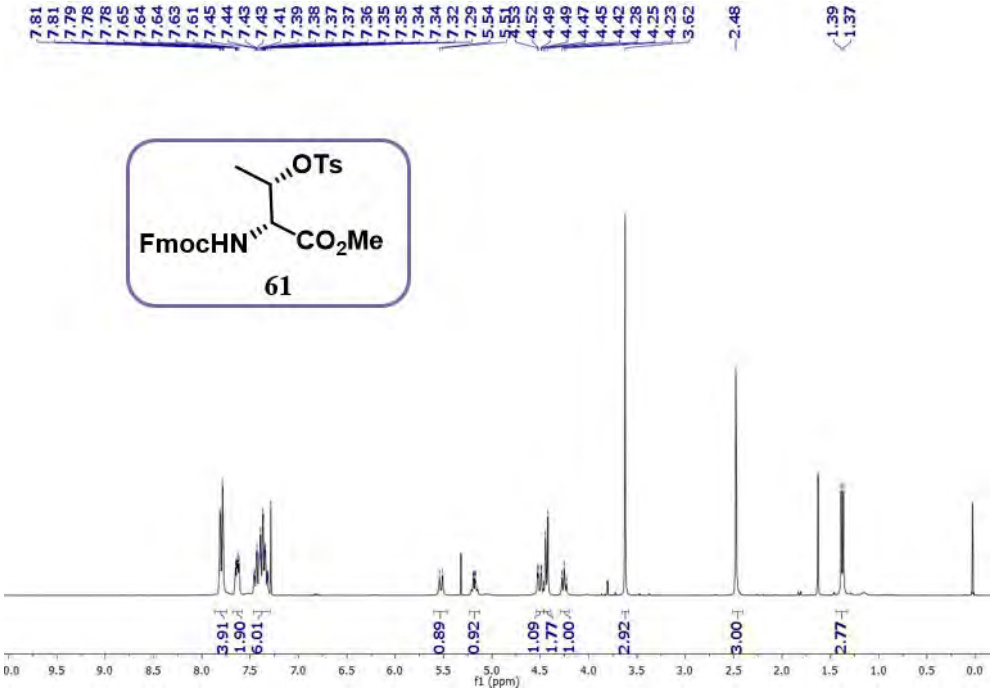

^{13}C NMR 75 MHz in CD_3Cl

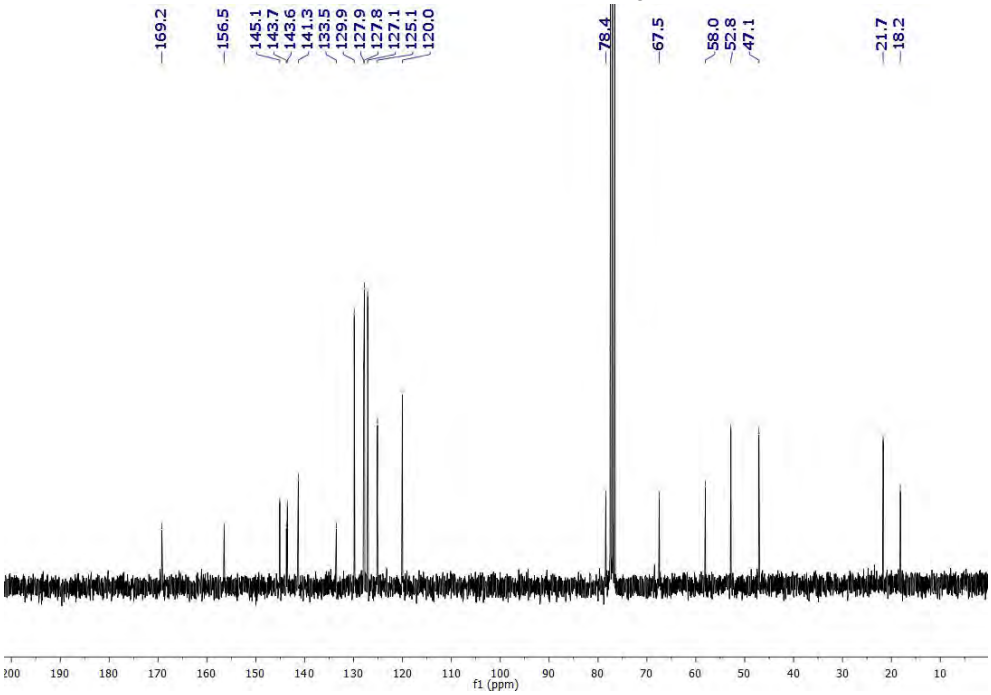

^{1}H NMR 300 MHz in CD_3Cl

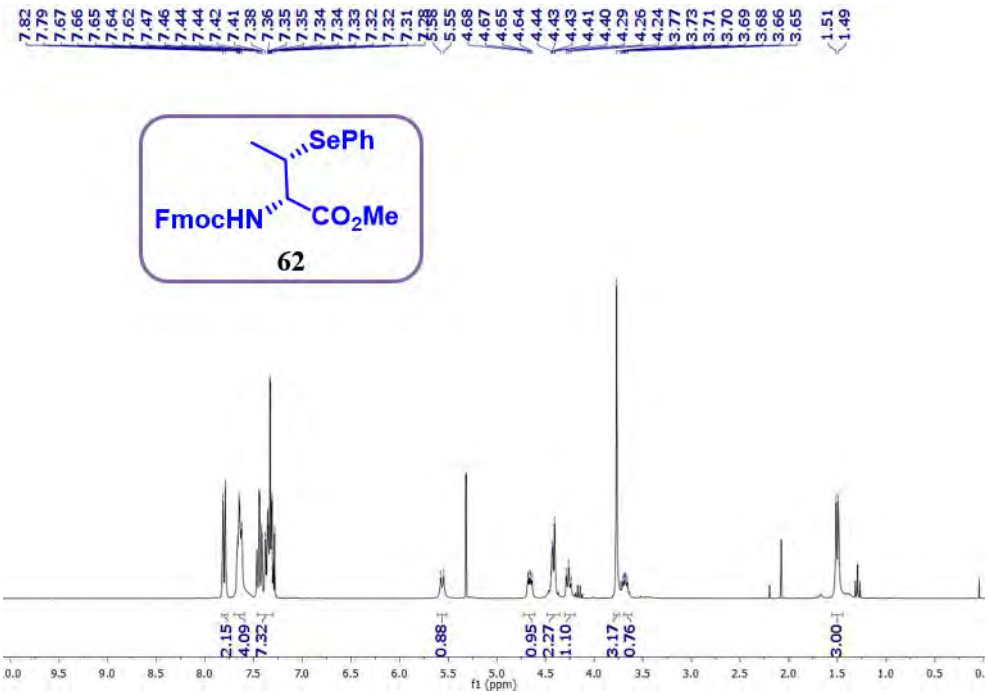

^{13}C NMR 75 MHz in CD_3Cl

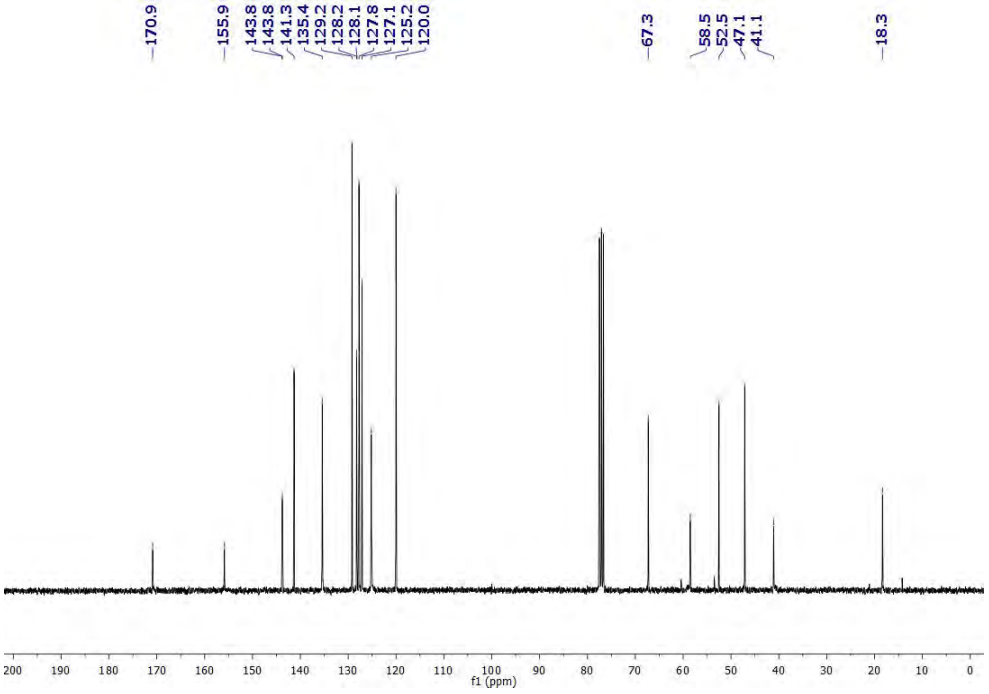

^{1}H NMR 400 MHz in CD_3CN

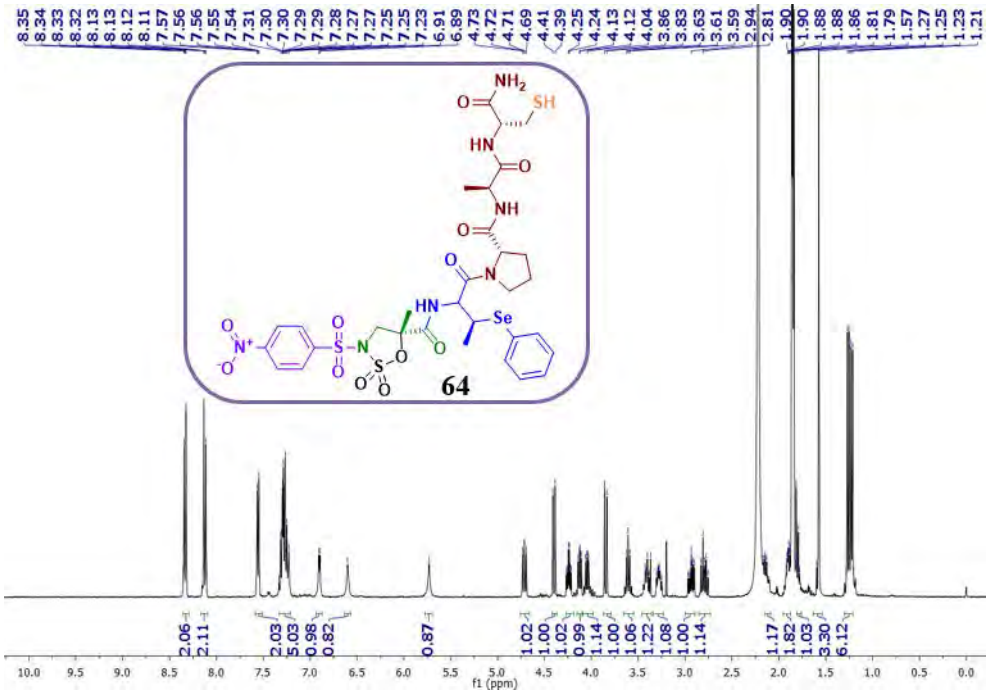

^{13}C NMR 75 MHz in CD_3CN

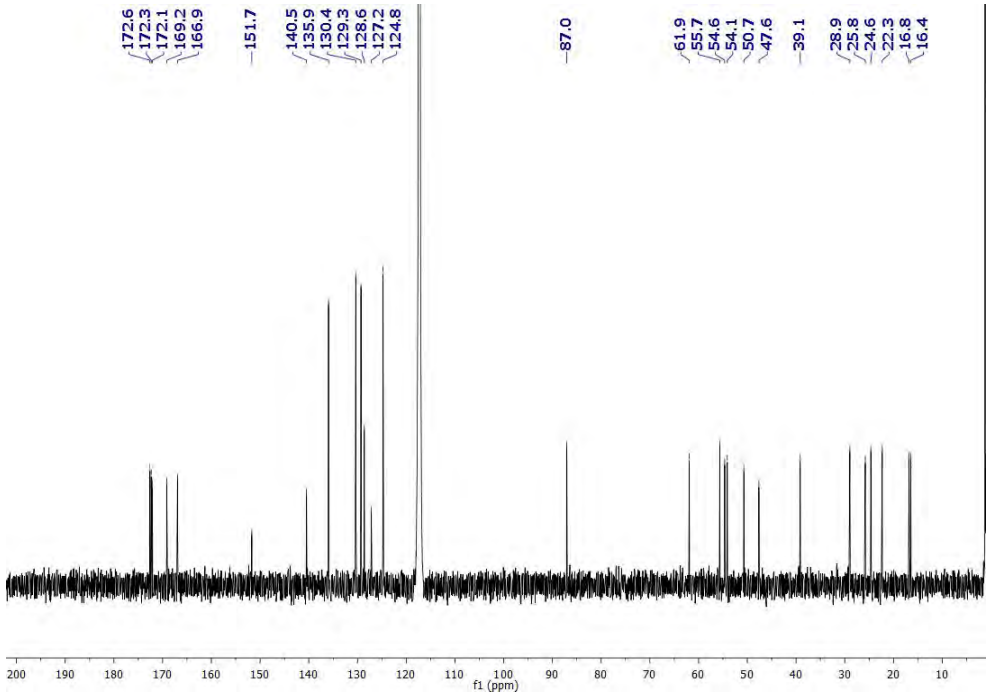

HMBC 400 MHz in CD_3CN

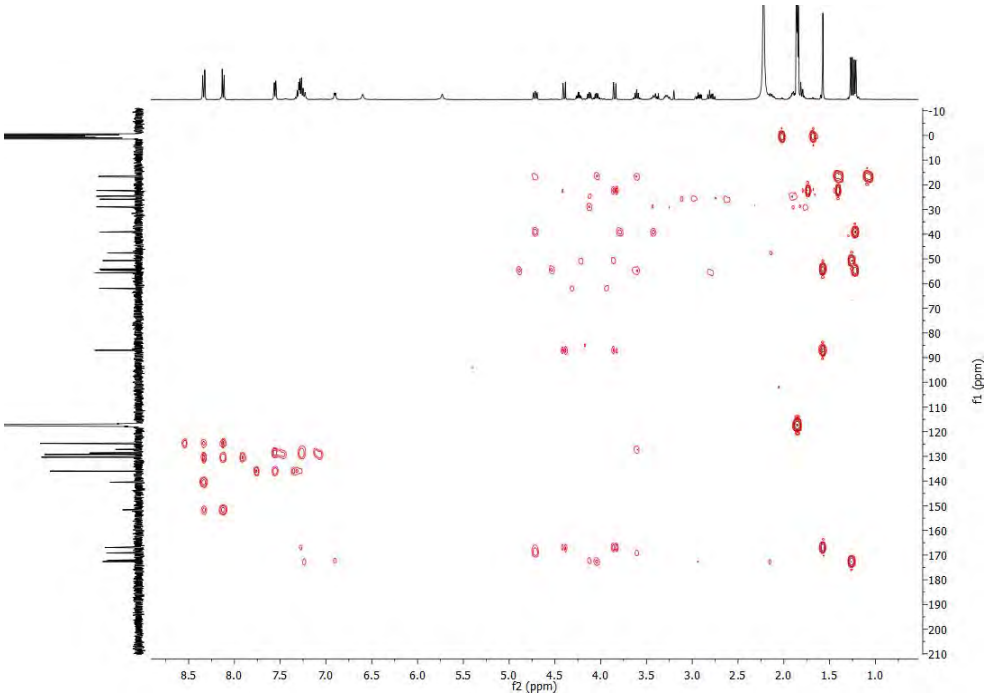

Supplementary Information II: Tables & Figures

Chapter 3

Table S1. Energies, enthalpies, free energies, and entropies of the lowest energy structures calculated at the PCM(Pyridine)/M06-2X/6-31+G(d,p) level.

Compound	E0	E0+ZPE	E0+DH	E0+DG	S	E0+DG_corr	Freq1
	(Hartree)[a]	(Hartree)[a]	(Hartree)[a]	(Hartree)[a]	(cal mol^{-1} K^{-1})[b]	(Hartree)[a]	(cm^{-1})
Pyridine	–248.191435	–248.101816	–248.095535	–248.133104	70.8	–248.133104	386.4
E	–1177.302210	–1177.105495	–1177.085420	–1177.157524	135.8	–1177.153855	20.1
E-TS_{SN2}	–1425.465079	–1425.178056	–1425.151465	–1425.238394	163.7	–1425.233597	–540.1
E-TS_{E2}	–1425.451263	–1425.169603	–1425.142632	–1425.233195	170.6	–1425.225535	–1307.9
F	–1252.504173	–1252.301424	–1252.280341	–1252.354435	139.6	–1252.351259	25.8
F-TS_{SN2}	–1500.665332	–1500.372878	–1500.344976	–1500.435752	171.0	–1500.430120	–542.7
F-TS_{E2}	–1500.651927	–1500.364637	–1500.336454	–1500.430088	176.4	–1500.422145	–1293.5
G	–1024.703760	–1024.543845	–1024.528388	–1024.588651	113.5	–1024.586867	37.1
G-TS_{SN2}	–1272.860245	–1272.610532	–1272.588299	–1272.664505	143.5	–1272.661434	–542.6
G-TS_{E2}	–1272.848201	–1272.603554	–1272.581034	–1272.661029	150.7	–1272.654907	–1295.1
H	–1157.453084	–1157.243961	–1157.223517	–1157.296224	136.9	–1157.292471	25.1
H-TS_{SN2}	–1405.610215	–1405.310960	–1405.283892	–1405.371963	165.9	–1405.366860	–531.4
H-TS_{E2}	–1405.604506	–1405.310568	–1405.283241	–1405.373990	170.9	–1405.367074	–1276.5
I	–1004.855002	–1004.682857	–1004.666877	–1004.728625	116.3	–1004.726383	38.1
I-TS_{SN2}	–1253.007143	–1252.744682	–1252.722333	–1252.798272	143.0	–1252.795977	–532.4
I-TS_{E2}	–1252.999377	–1252.742776	–1252.719735	–1252.800294	151.7	–1252.794969	–1287.0

[a] 1 Hartree = 627.5 kcal mol^{-1}. [b] Thermal corrections at 333.15 K.

Chapter 5

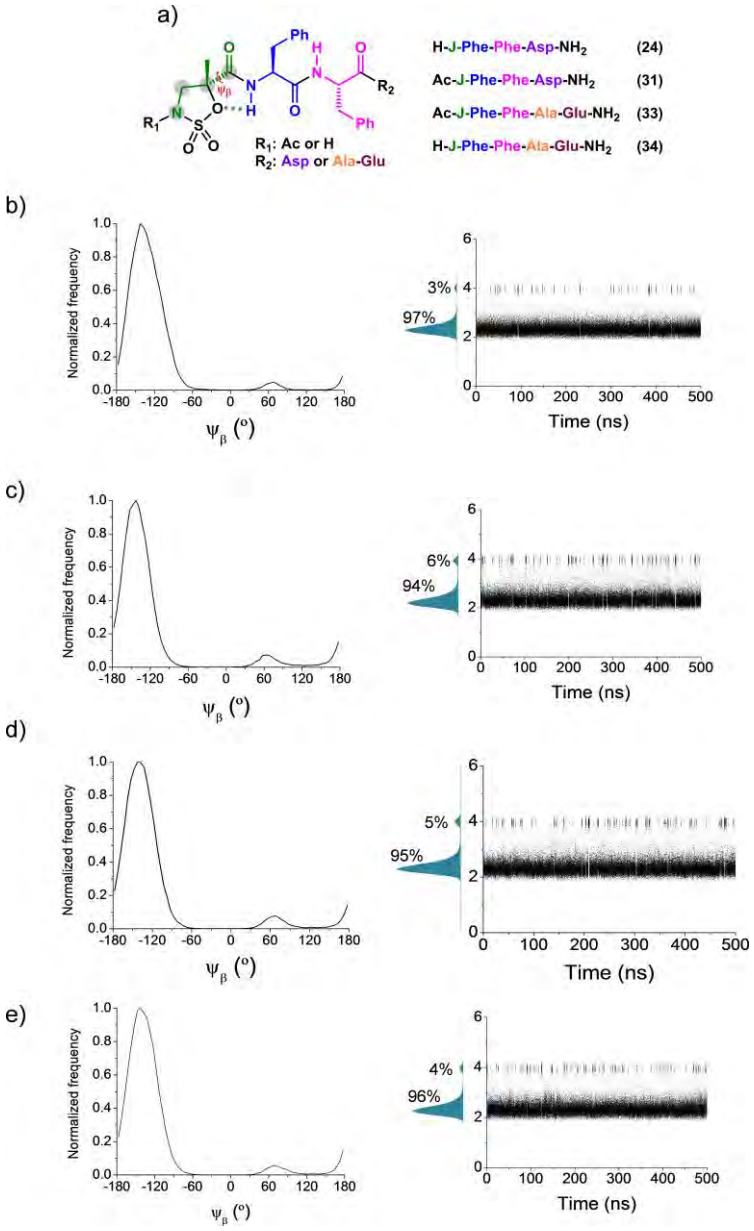

Figure S1. a) Chemical structure for peptides **24, 31, 33** and **34** highlighting the dihedral angle ψβ . b-e) Relative population of the ψβ angle (left) obtained from the 500 ns MD-tar simulation in explicit water for peptides **24, 31, 33** and **34**, respectively, and NH*Phe2*–Oendo***J*** distance distribution (right) derived from the 500 ns MD-tar simulation in explicit water for peptides **24, 31, 33** and **34**, respectively.

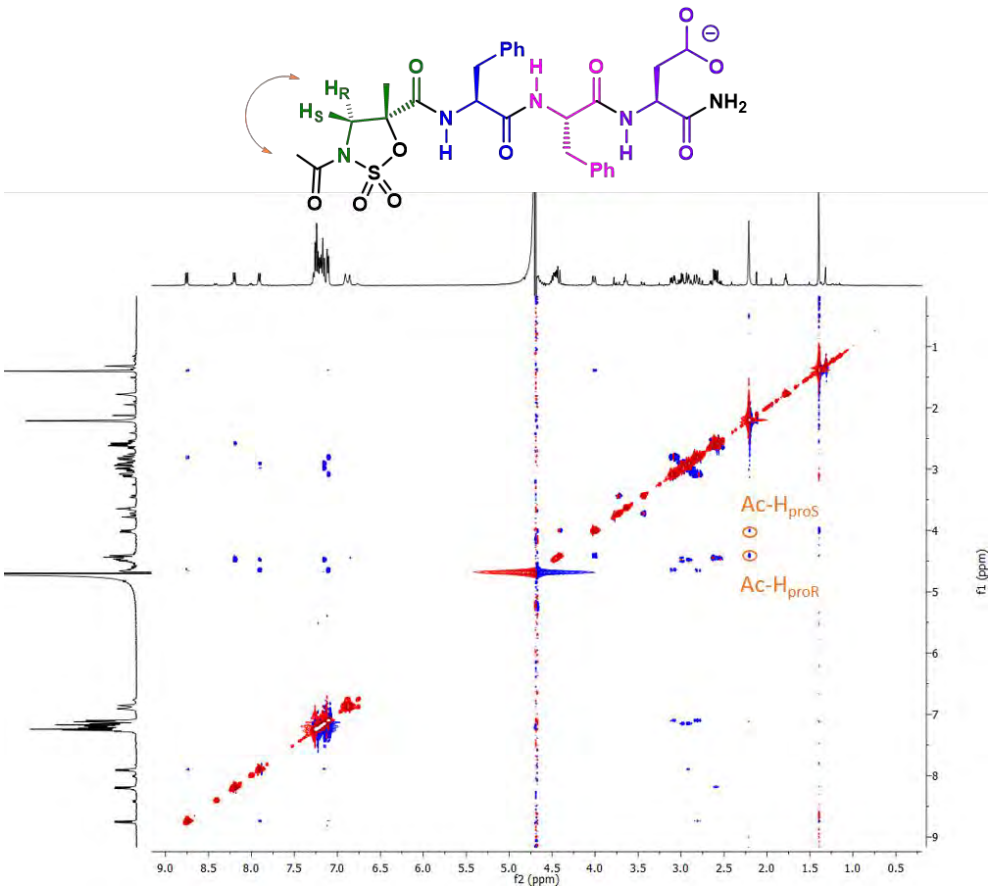

Figure S2. NOESY spectrum for compound **31** in H_2O/D_2O (9:1), PBS buffer pH 5.7, at room temperature (mixing time 0.3 s). The cross-peaks corresponding to the Ac–HproR and Ac–HproS are highlighted in orange.

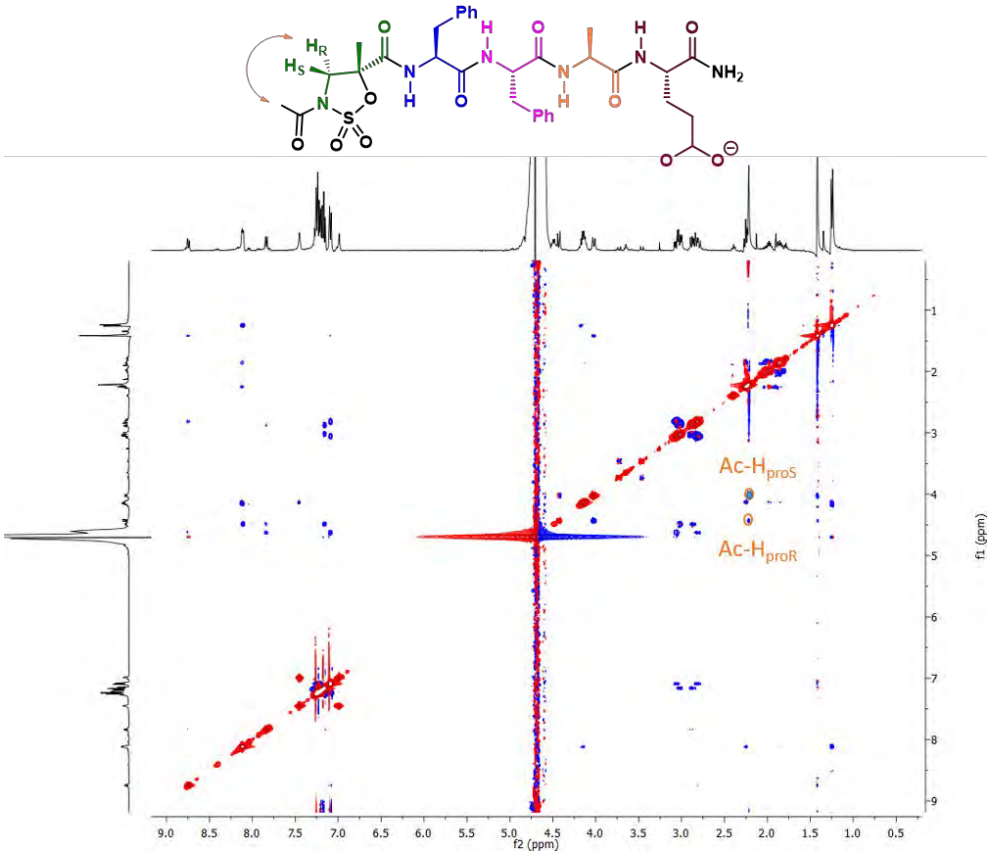

Figure S3. NOESY spectrum for compound **33** in in H_2O/D_2O (9:1), PBS buffer pH 5.7, at room temperature (mixing time 0.3 s). The cross-peaks corresponding to the Ac–HproR and Ac–HproS are highlighted in orange.

Supplementary Information III: HPLC Chromatograms

Analytical HPLC for peptides used for biological assays in *chapter 5*:

HPLC methods were performed using a linear gradient 0% to 100 % of solvent B in 60 min. Solvent A: H_2O containing 0.1% TFA (v/v); solvent B: acetonitrile.

Peptide **24**

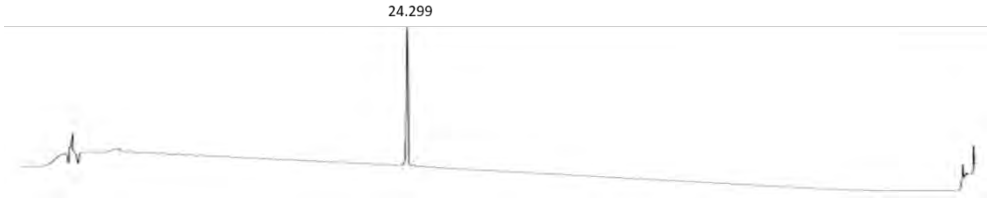

Peptide **29**

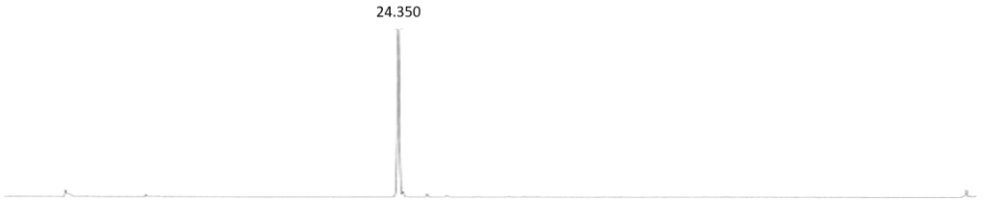

Peptide **30**

Peptide **31**

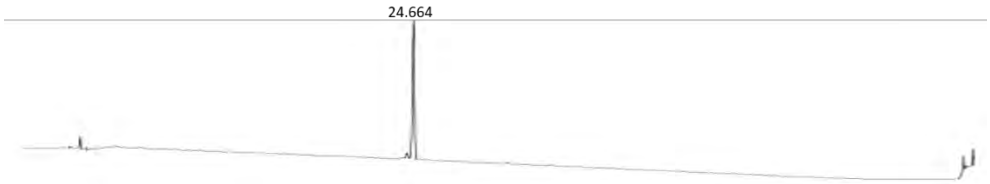

Peptide **32**

Peptide **33**

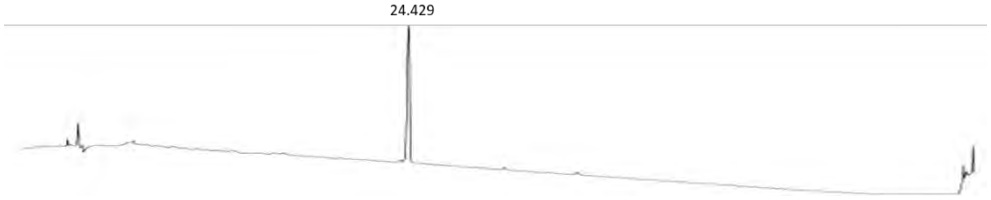

Peptide **34**

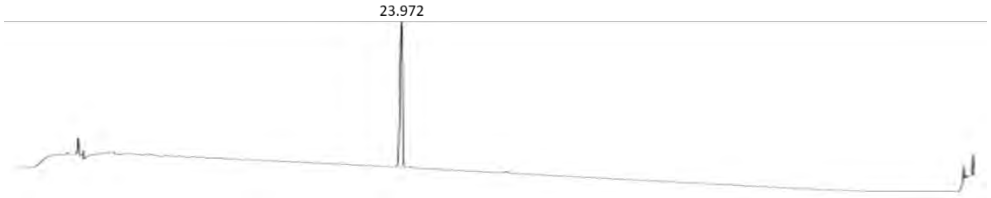

Peptide: **J-Phe-Phe-NH_2**

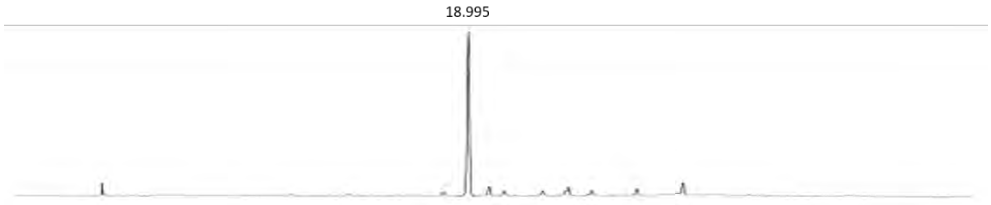

Analytical HPLC for peptide used for biological assays in *chapter 6*:

HPLC method for peptide **43** was performed using a linear gradient of 5% to 95 % of solvent B in 37 min. Solvent A: H_2O containing 0.1% TFA (v/v); solvent B: acetonitrile.

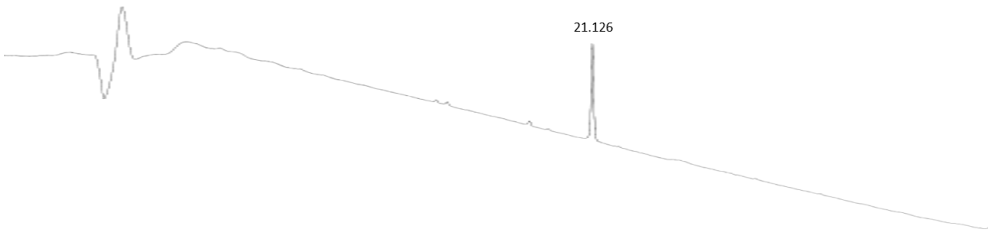

Analytical HPLC for peptides used for transacylation in *chapter 7*:

HPLC methods were performed using a linear gradient 1% to 71 % of solvent B in 35 min. Solvent A: H_2O containing 0.1% TFA (v/v); solevent B: acetonitrile.

Peptide **44** (top) and transacylation peptide **46** (bottom)

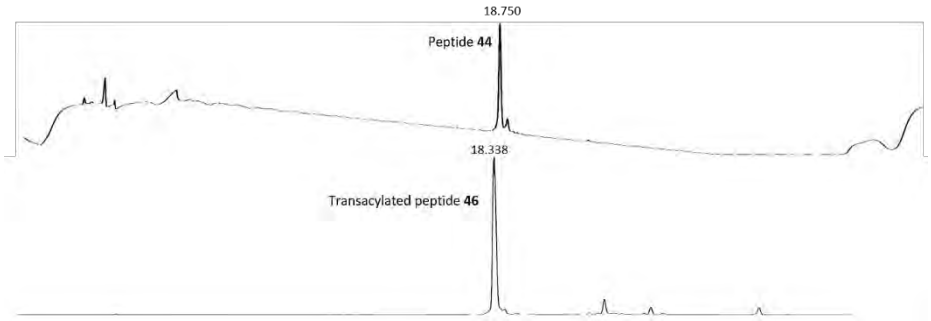

Peptide **47** (top) and transacylation peptide **50** (bottom)

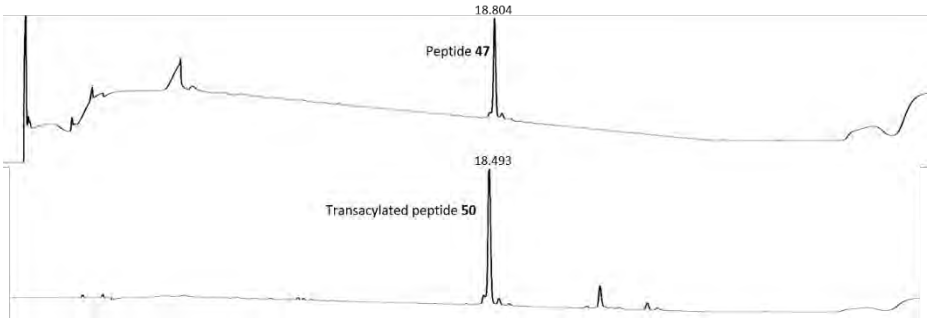

Peptide **48** (top) and transacylation peptide **51** (bottom)

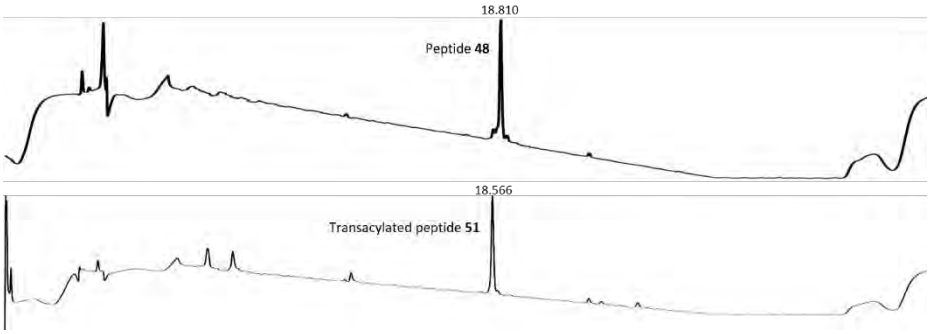

Peptide **49** (top) and transacylation peptide **52** (bottom)

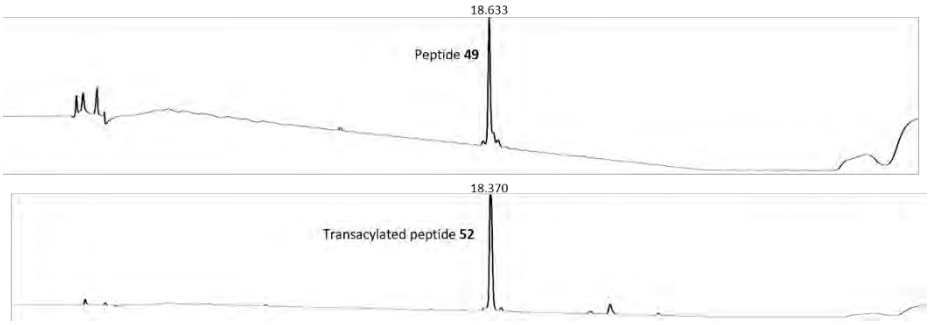

Peptide **53** (top) and transacylation peptide **56** (bottom)

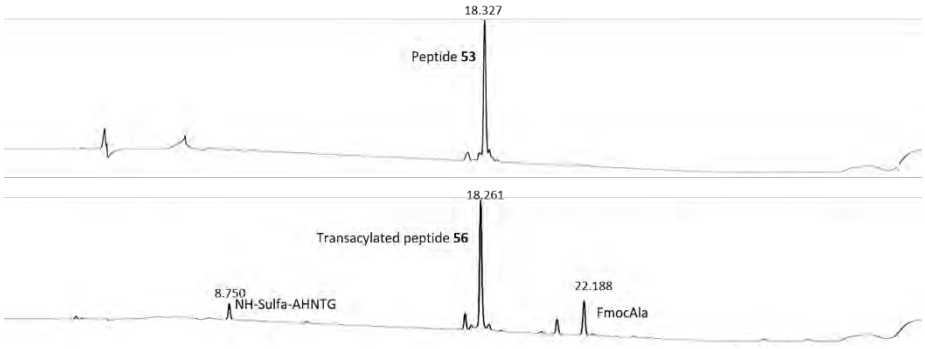

Peptide **54** (top) and transacylation peptide **57** (bottom)

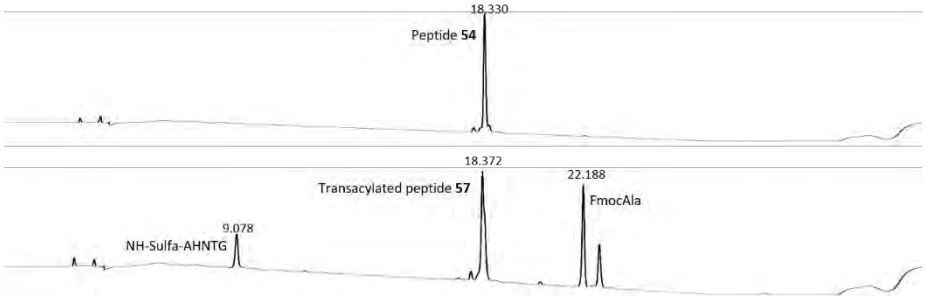

Peptide **55** (top) and transacylation peptide **58** (bottom)